

DYNAMICS AND CONTROL OF
**ROBOTIC
SYSTEMS**

ANDREW J. KURDILA | PINHAS BEN-TZVI

WILEY

Andrew J. Kurdila and Pinhas Ben-Tzvi

Dynamics and Control of Robotic Systems

– Draft Monograph –

January 7, 2019

Springer

*This book is dedicated to Patrick, Hannah
and Justin, and to Timor, Jonathan, Daniel,
and Sara*

Preface

The goal of this book is to provide a modern, systematic, and thorough theoretical background for the study of the dynamics and control of robotic systems. The presentation of the material emphasizes the underlying principles of dynamics and control that can be employed in a host of contemporary applications. Consequently, at its core, the goal of this book is quite ambitious. Not only do we seek to give a detailed presentation of the precepts of robotics, but also we aim to provide methodologies that are applicable to realistic robotic systems. These robotic systems include the following well-known examples: classical industrial manipulators, humanoid robots, autonomous ground vehicles, autonomous air vehicles, autonomous marine vehicles, robotic surgical assistants, space vehicles and computer controlled milling machines. Modern robotic systems are inherently complex, and the representation of their dynamics and the synthesis of their control can be unavoidably complicated.

One of the principal reasons for creating this book has been to show how modern computational and analytical tools expand and enhance our ability to address problems in robotics. Even a few years ago, the complexity of modern robotic systems rendered intractable the solutions by hand of all but the most simple examples. The formulation of dynamic models of common robotic systems was once too tedious for the classroom. The advent of symbolic, numeric and general purpose computational engines over the past few decades is particularly relevant to the problems addressed in this book. With higher level computing environments such as MATLAB, Mathematica, Maple or similar programs, the envelope of problems that can be addressed by undergraduate and graduate students has expanded dramatically. These tools enable students to focus on principles and theory, and free them from tedious exercises in algebraic gymnastics which merely distract from the technical foundations. It is critical, in our opinion, that the student concentrate on the systematic application of the underlying principles.

This text evolved from class notes and problem assignments for courses in dynamics, control, and robotics taught by the authors over a period of several years. These courses have been taught at several top-tier universities in the United States, and our approach in presenting the material has continuously evolved during this time. This material is suitable for a two semester sequence in dynamics, control,

and robotics at the senior undergraduate or first year graduate student level. A course intended for the senior year of an undergraduate curriculum can focus on the fundamentals of kinematics and dynamics as applied to robotic systems. This first semester can be built primarily from topics extracted from Chapters (2), (3), and (4), and to a lesser degree Chapter (5). A second semester can concentrate on the techniques of analytical mechanics in Chapter (5) and control theory in Chapter (6). Specific advanced topics such as the recursive order N formulation in Chapters (3) and (4), or the vision-based control methodologies in Chapter (7) can also be covered in the second semester.

The authors have worked hard to demonstrate that a wide array of design and analysis problems for robotic systems are made tractable through the use of modern computational and analytical tools. To this end, an extensive collection of examples and problems are included in the text. The solutions of many of the examples or problems have been carried out using either MATLAB, Simulink or Mathematica, or a combination of both. It is important that the students who use this book realize that the authors are not advocating the use of a particular computational tool, but rather espousing a common philosophy. For nearly every problem in this book, the computational tools are interchangeable: a student can use whatever software package with which he or she is most familiar. The theoretical foundations, however, are irreplaceable and constitute the common language for addressing any specific problem.

Andrew J. Kurdila

Pinhas Ben-Tzvi

March, 2017

Contents

1	Introduction	1
1.1	Motivation	2
1.2	Origins of Robotic Systems	5
1.3	General Structure of Robotic Systems	7
1.4	Robotic Manipulators	8
1.4.1	Typical Structure of Robotic Manipulators	10
1.4.2	Classification of Robotic Manipulators	13
1.4.2.1	Classification by Motion Characteristics	13
1.4.2.2	Classification by Degrees of Freedom	13
1.4.2.3	Classification by Driver Technology and Drive Power	13
1.4.2.4	Classification by Kinematic Structure	14
1.4.2.5	Classification by Workspace Geometry	16
1.4.3	Examples of Robotic Manipulators	16
1.4.3.1	Cartesian Robotic Manipulator	17
1.4.3.2	Cylindrical Robotic Manipulator	17
1.4.3.3	SCARA Robotic Manipulator	18
1.4.3.4	Spherical Robotic Manipulator	20
1.4.3.5	PUMA Robotic Manipulator	20
1.4.4	Spherical Wrist	21
1.4.5	Articulated Robot	22
1.5	Mobile Robotics	23
1.5.1	Humanoid Robots	23
1.5.2	Autonomous Ground Vehicles	25
1.5.3	Autonomous Air Vehicles	27
1.5.4	Autonomous Marine Vehicles	28
1.6	An Overview of Robotics Dynamics and Control Problems	29
1.6.1	Forward Kinematics	31
1.6.2	Inverse Kinematics	33
1.6.3	Forward Dynamics	33
1.6.4	Inverse Dynamics and Feedback Control	34

1.6.5	Dynamics and Control of Robotic Vehicles	35
1.7	Organization of the Book	36
1.8	Problems for Chapter (1), Introduction	38
2	Fundamentals of Kinematics	41
2.1	Bases and Coordinate Systems	41
2.1.1	N -Tuples and $M \times N$ Arrays	42
2.1.2	Vectors, Bases and Frames	46
2.1.2.1	Vectors	47
2.1.2.2	Bases and Frames	48
2.2	Rotation Matrices	55
2.3	Parameterizations of Rotation Matrices	59
2.3.1	Single Axis Rotations	59
2.3.2	Cascades of Rotation Matrices	63
2.3.2.1	Cascade Rotations about Moving Axes	63
2.3.2.2	Cascade Rotations about Fixed Axes	64
2.3.3	Euler Angles	65
2.3.3.1	The 3–2–1 Yaw-Pitch-Roll Euler Angles	66
2.3.3.2	The 3–1–3 Precession-Nutation-Spin Euler Angles	70
2.3.4	Axis-Angle Parameterization	73
2.4	Position, Velocity, and Acceleration	77
2.5	Angular Velocity and Angular Acceleration	86
2.5.1	Angular Velocity	86
2.5.2	Angular Acceleration	92
2.6	Theorems of Kinematics	92
2.6.1	Addition of Angular Velocities	93
2.6.2	Relative Velocity	96
2.6.3	Relative Acceleration	97
2.6.4	Common Coordinate Systems	100
2.6.4.1	Cartesian Coordinates	101
2.6.4.2	Cylindrical Coordinates	101
2.6.4.3	Spherical Coordinates	103
2.7	Problems for Chapter 2, Kinematics	106
2.7.1	Problems on N -tuples and $M \times N$ Arrays	106
2.7.2	Problems on Vectors, Bases, Frames	107
2.7.3	Problems on Rotation Matrices	108
2.7.4	Problems on Position, Velocity, Acceleration	113
2.7.5	Problems on Angular Velocity	115
2.7.6	Problems on the Theorems of Kinematics	115
2.7.6.1	Problems on the Addition of Angular Velocities	115
2.7.7	Problems on Relative Velocity and Acceleration	116
2.7.8	Problems on Common Coordinate Systems	119

Contents	xi
3 Kinematics of Robotic Systems	121
3.1 Homogeneous Transformations and Rigid Motion	121
3.2 Ideal Joints	127
3.2.1 The Prismatic Joint	128
3.2.2 The Revolute Joint	130
3.2.3 Other Ideal Joints	131
3.3 The Denavit-Hartenberg (DH) Convention	134
3.3.1 Kinematic Chains, Numbering in the DH Convention	134
3.3.2 Definition of Frames in the DH Convention	136
3.3.3 Homogeneous Transforms in the Denavit-Hartenberg Convention	137
3.3.4 The DH Procedure	139
3.3.5 Angular Velocity and Velocity in the DH Convention	147
3.4 Recursive $O(N)$ Formulation of Forward Kinematics	151
3.4.1 Recursive Calculation of Velocity and Angular Velocity	154
3.4.2 Efficiency and Computational Cost	157
3.4.3 Recursive Calculation of Acceleration and Angular Acceleration	161
3.5 Inverse Kinematics	175
3.5.1 Solvability	176
3.5.2 Analytical Methods	179
3.5.2.1 Algebraic Methods	179
3.5.2.2 Geometric Methods	190
3.5.3 Optimization Methods	194
3.5.4 Inverse Velocity Kinematics	202
3.5.4.1 Singularity	202
3.6 Problems for Chapter 3, Kinematics of Robotic Systems	203
3.6.1 Problems on Homogeneous Transformations	203
3.6.2 Problems on Ideal Joints and Constraints	206
3.6.3 Problems on Denavit-Hartenberg Convention	207
3.6.4 Problems on Angular Velocity and Velocity for Kinematic Chains	208
3.6.5 Problems on Inverse Kinematics	212
4 Newton-Euler Formulations	215
4.1 Linear Momentum of Rigid Bodies	215
4.2 Angular Momentum of Rigid Bodies	222
4.2.1 First Principles	222
4.2.2 Angular Momentum and Inertia	228
4.2.3 Calculation of the Inertia Matrix	234
4.2.3.1 The Inertia Rotation Transformation Law	235
4.2.3.2 Principal Axes of Inertia	238
4.2.3.3 The Parallel Axis Theorem	241
4.2.3.4 Symmetry and Inertia	245
4.3 The Newton-Euler Equations	250

4.4	Euler's Equation for a Rigid Body	255
4.5	Equations of Motion for Mechanical Systems	257
4.5.1	The General Strategy	257
4.5.2	Free Body Diagrams	258
4.6	Structure of Governing Equations: Newton-Euler Formulations	281
4.6.1	Differential-Algebraic Equations (DAEs)	281
4.6.2	Ordinary Differential Equations (ODEs)	283
4.7	Recursive Newton-Euler Formulations	285
4.7.1	Recursive Calculation of Forces and Moments	285
4.8	Recursive Derivation of the Equations of Motion	293
4.9	Problems for Chapter 4, Newton-Euler Equations	296
4.9.1	Problems on Linear Momentum	296
4.9.2	Problems on the Center of Mass	300
4.9.3	Problems on the Inertia matrix	302
4.9.4	Problems on Angular Momentum	304
4.9.5	Problems on the Newton-Euler Equations	305
5	Analytical Mechanics	309
5.1	Hamilton's Principle	309
5.1.1	Generalized Coordinates	309
5.1.2	Functionals and the Calculus of Variations	312
5.1.3	Hamilton's Principle for Conservative Systems	316
5.1.4	Kinetic Energy for Rigid Bodies	324
5.2	Lagrange's Equations for Conservative Systems	329
5.3	Hamilton's Extended Principle	333
5.3.1	Virtual Work Formulations	333
5.4	Lagrange's Equations for Robotic Systems	349
5.4.1	Natural Systems	350
5.4.2	Lagrange's Equations and the Denavit-Hartenberg Convention	354
5.5	Constrained Systems	357
5.6	Problems for Chapter 5, Analytical Mechanics	362
5.6.1	Problems on Hamilton's Principle	362
5.6.2	Problems on Lagrange's Equations	366
5.6.3	Problems on Hamilton's Extended Principle	368
5.6.4	Problems on Constrained Systems	374
6	Control of Robotic Systems	377
6.1	The Structure of Control Problems	377
6.1.1	Setpoint and Tracking Feedback Control Problems	378
6.1.2	Open Loop and Closed Loop Control	379
6.1.3	Linear and Nonlinear Control	379
6.2	Fundamentals of Stability Theory	381
6.3	Advanced Techniques of Stability Theory	388
6.4	Lyapunov's Direct Method	389

Contents	xiii
6.5 The Invariance Principle	392
6.6 Dynamic Inversion or Computed Torque Control	398
6.7 Approximate Dynamic Inversion and Uncertainty	407
6.8 Controllers Based on Passivity	421
6.9 Actuator Models	426
6.9.1 Electric Motors	426
6.9.2 Linear Actuators	433
6.10 Backstepping Control and Actuator Dynamics	438
6.11 Problems for Chapter (6), control of Robotic Systems	442
6.11.1 Problems on Gravity Compensation and PD setpoint control	442
6.11.2 Problems on Computed Torque Tracking Control	446
6.11.3 Problems on Dissipativity Based Tracking Control	447
7 Image-Based Control of Robotic Systems	451
7.1 The Geometry of Camera Measurements	451
7.1.1 Perspective Projection and Pinhole Camera Models	452
7.1.2 Pixel Coordinates and CCD Cameras	454
7.1.3 The Interaction Matrix	456
7.2 Image-Based Visual Servo Control	460
7.2.1 Control Synthesis and Closed Loop Equations	460
7.2.2 Calculation of Initial Conditions	464
7.3 Task Space Control	472
7.4 Task Space and Visual Control	479
7.5 Problems for Chapter (7)	498
8 Appendices	505
8.1 Fundamentals of Linear Algebra	505
8.1.1 Solution of Matrix Equations	507
8.1.2 Linear Independence and Rank	509
8.1.3 Invertibility and Rank	510
8.1.4 Least Squares Approximation	511
8.1.5 Rank Conditions and the Interaction Matrix	516
8.2 The Algebraic Eigenvalue Problem	516
8.2.1 Self-Adjoint Matrices	517
8.2.2 Jordan Canonical Form	520
8.3 Gauss Transformations and LU Factorizations	521
References	527

Chapter 1

Introduction

Abstract In this chapter the collection of *robotic systems* that are studied in this book are introduced. The field of robotics embraces topics requiring expertise in a number of technical disciplines including mechanical engineering, electrical engineering, computer science, applied mathematics, industrial engineering, cognitive science, psychology, biology, bio-inspired design and software engineering. Moreover, the family of robotic systems that can be designed and fabricated today is growing rapidly. Reasons for this trend are based in economics and the maturity of the technological infrastructure supporting robotics. A wide variety of sensing and actuation technologies that are portable, compact and inexpensive are now readily available. These building blocks can be used to construct a plethora of robotic systems using commercial-off-the-shelf technology. The broad scope of the robotics field precludes a comprehensive theoretical summary of the disciplines relevant to all of these diverse systems being given. Instead, this text specifically deals with the construction of models of the kinematics and dynamics of typical robotic systems, and the derivation of control strategies for these systems.Upon completion of this chapter, the student should be able to:

- Discuss a variety of definitions of a robotic system and explain their key attributes.
- Discuss the general structure and components of robotic systems.
- Describe a variety of methods for classifying robotic systems.
- Describe the classical robotic manipulators, including the Cartesian, cylindrical, spherical, SCARA, PUMA and articulated robotic manipulators.
- Describe other common, contemporary robotic systems.
- Describe the fundamental problems of *forward kinematics*, *inverse kinematics*, *forward dynamics*, and *control synthesis* for robotic systems.

1.1 Motivation

Over the past few decades, the robotic systems that undergraduate and graduate students are expected to be able to design and analyze has expanded dramatically. It is now commonplace in varying engineering disciplines to ask relatively inexperienced engineers and researchers to design, analyze and construct prototypical robotic systems. Students may encounter such challenges in either undergraduate or graduate design projects, or immediately upon taking a job in industry or at a national laboratory. Projects may be as varied as the development of a computer-controlled, multi-axis stage for positioning of laser Doppler vibration measurements, the development of a flapping wing autonomous flight vehicle, the modification of a commercial vehicle for autonomous operation, or the development of a humanoid robot. The diversity and complexity of this list continues to grow every year.

While the study of robotics has been popular for several decades, the recent rapid expansion of robotic systems in commercial markets can be attributed in part to the fact that sensors and actuators have become increasingly cost effective, modular, and portable. This trend has lead to the emergence of the field of *mechatronics*, which has played a key role in the spread of robotics technologies. Mechatronics is a multidisciplinary field of study that integrates aspects of mechanisms, electronics, computer hardware/software, systems theory, and information technologies into a unified practical design methodology. The fusion of these topical areas that define the study of mechatronics is depicted in Figure (1.1). A key feature of mechatronic systems is that they often feature built-in intelligence that is applied to the task for which they are designed.

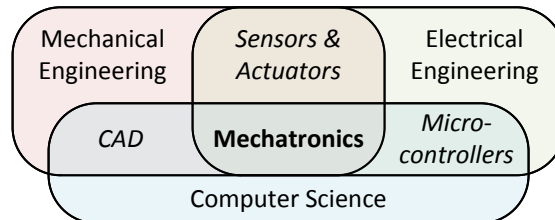


Fig. 1.1: Fields of Expertise Associated with Mechatronics

Although the range of mechatronic systems is vast, there are features common to most, if not all, such systems. Figure (1.2) illustrates a schematic drawing of signal flow for a typical mechatronic system. The Computer Systems connect the mechatronic system to sources of intelligence, be it user inputs/outputs to include humans in the operation and/or algorithms to interpret sensor data and make decisions for the mechatronic systems. The Electrical System conditions signals passing between the Computer and Mechanical Systems, along with regulating the electrical power provided to the mechatronic system. The Mechanical Systems consists

of the physical system(s) that interact with its environment. Commands from the digital Computer Systems to the analog Electrical Systems pass through a *digital-to-analog* converter, and these commands are implemented on actuators connecting the Electrical and Mechanical Systems. Sensors integrated into the Mechanical Systems generate signals passed to the Electrical Systems, and these signals (after conditioning) are communicated to the Computer Systems through an *analog-to-digital* converter.

Mechatronics is elevated to a field distinct from its contributing fields by the need to balance consideration of mechanical, electrical and information technology factors when designing an overall systems. Assessing the signal processing and algorithmic requirements for operating a physical system, and meeting these requirements intelligently and efficiently distinguishes mechatronics as a unique discipline and not simply an exercise in hardware connectivity. While some systems may require complex multi-core processors to operate in real-time, others may simply require a simple embedded controller. Interested readers can refer to the following textbooks for more in-depth study of Mechatronics as an integrating approach to engineering design [1, 8, 11].

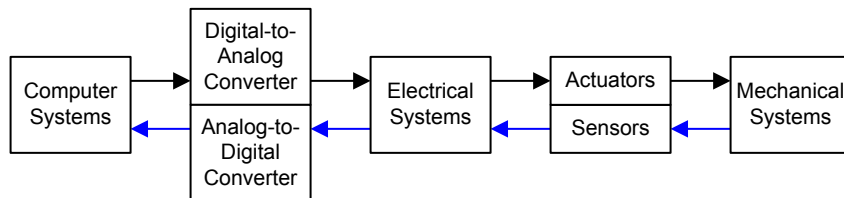


Fig. 1.2: Structure of a Typical Mechatronic System

As the robotics infrastructure has matured, expectations of students in the field of robotics has correspondingly increased. A decade ago a beginning student might have been asked to create a simple two-dimensional model of a robotic system. Older textbooks are filled with such introductory problems that serve to familiarize students with the fundamentals. However, technical tools and analytical skills are now required that facilitate modeling of robot kinematics and dynamics in three spatial dimensions.

Fortunately, the tools that are applicable throughout the design and analysis process have also evolved and matured. A few years ago, the computational tools available for the systematic design, analysis, and study of complex robotic systems were limited in number. At that time a student faced with the creation of a detailed model of a realistic robotic system was confronted with a daunting task. The determination of the kinematics and dynamics of robotic systems via hand calculation was a lengthy and tedious job for all but the simplest cases. Once the heroic effort of deriving a formulation was complete, the student was faced with coding the governing equations in a low-level programming language such as C or Fortran. It is no exag-

geration that the time involved in this task could be measured in months, or worse, years, of effort.

Now, two separate and complementary collections of commercial software packages make this problem much more manageable. First, there is an ever expanding list of specialized three dimensional modeling programs such as

- Autodesk Inventor
- SolidWorks
- Pro Engineer
- MSC Adams
- LabView

that are available for building highly detailed and general models of the kinematics, dynamics and control of robotic systems. These packages vary in the generality of their simulation capabilities, but all allow numerical approximation of the solutions of the forward kinematics and dynamics problems. Some also incorporate programming interfaces for the introduction of user-defined controls. These software packages can be expensive to purchase. However, most universities have software contracts with the vendors of these packages. Most large engineering firms or government laboratories also have licenses for a portfolio of these analysis programs. Many of the more complex examples in this book have been modeled by students under an academic license for Autodesk Inventor.

As useful as the programs above can be, sometimes greater flexibility is needed in formulating the governing equations of dynamics or in deriving a control architecture for a robotic system. As an example, a model is created for the purpose of constructing a controller for a specific robot system, a symbolic set of equations for hardware implementation is often required. Some programs have the option of explicitly generating symbolic code that is suitable for hardware implementation. It should be noted that the packages listed above vary dramatically in the ways that they handle code generation. There is currently a highly competitive market of software tools to download controller equations to specific hardware platforms. Still, it is often the case that a standard commercially available software simulation tool, such as those listed above, does not allow the flexibility that a practicing control engineer requires. It can also be the case that an analyst wants to implement a controller in terms of a highly efficient algorithm, like the recursive formulations discussed in Chapters (3) or (4). These algorithms may not be supported by a specific commercial software package. It should come as no surprise that no matter how well a commercial package is designed, a user will often desire some functionality that is not available.

In such cases, the software packages that support symbolic computation can be used to great advantage. These are general purpose, object-oriented, high-level programs that define their own computing languages. Examples include:

- MATLAB
- Mathematica
- Mathcad
- Maple

Each of these software programs has developed its own object-oriented, high-level language that performs calculations on a large number of different types of mathematical objects. For example, they usually have a large library of operators based on linear algebra, signal processing, and calculus. The mathematical objects may be matrices and vectors, or they can be discrete dynamical systems, or they might take the form of systems of ordinary differential equations. A few lines of code in the language of these packages can replace thousands of lines of code in a low-level programming language like C, C++ or Fortran. Perhaps most importantly for this text, each of these programs has a syntax that enables symbolic computation. This is a computing engine that incorporates most well-known operations defined in differential or integral calculus. For the most part, tedious operations can be performed using these symbolic variables with minimal input from the analyst. Both public domain and commercial packages designed expressly for the study of robotic systems have been written in several of these computing languages. This text makes extensive use of some of these packages in solving the examples in the text and the problems at the end of each chapter. In many cases the solutions of the problems are carried out by writing general purpose programs that address fundamental robotics problems; a family of high level functions that solve core robotics problems are provided with the solutions for this text.

1.2 Origins of Robotic Systems

Robotic systems have been traced historically to efforts by early artists, artisans, craftsmen, engineers and scientists to create machines that mimic humans in action or reasoning. The modern notion of a robotic system emerged as society sought to create surrogates that can replace human labor in jobs that are menial, tiresome or even dangerous. Even before industrial robots became commonplace, the potentially transformative role of automatons in the workplace was imagined. The role of robots as factory workers has been noted repeatedly over the years. The word 'robot' was coined by the Czech writer Karel Capek in the play *Rossum's Universal Robots*, published in 1920. Capek wanted to describe the repetitive and boring nature of robotic tasks. The word 'robot' originates from the Czech word 'roboť' which means 'work' or 'forced labor'. The play studied moral questions arising in the creation and use of digitally programmed slaves. This has been a reoccurring theme in novels, plays, and movies. For example, the novelist Kurt Vonnegut explores the angst and disillusionment of a society with the displacement of human workers by automation in the more recent novel *Player Piano*.

Despite these cautionary tales, robots have proliferated as a means of replacing human labor in adverse environments. The first reprogrammable digitally controlled robot was created in 1954 by George Devol. This robot, *Unimate*, was an industrial manipulator having a spherical workspace and was used to lift and move heavy production parts in a factory setting. It was purchased by General Motors in 1960 and was the forerunner of the large collection of industrial robots that are now common-

place along modern factory assembly lines. Demands on performance have been a driving force in the use of robotics in industry. The load capacity, repeatability, precision and speed afforded by modern robotic systems far exceed the capabilities of man.

Current definitions of what constitutes a robotic system vary dramatically, but all definitions convey the idea that robots perform menial or repetitive tasks. *Merriam-Webster's Dictionary* defines a robot as

- *a machine that looks like a human being and performs various complex tasks, or*
- *a device that automatically performs complicated often repetitive tasks.*

The first definition above requires that robots appear to be humanoid, and while some robotic systems do indeed have a humanoid appearance, this definition would exclude many of the robotic systems in this book. A critical attribute of robotic systems that this definition omits, one that is important to engineers and scientists who actually build robotic systems, is that robots are controlled by computers. This fact is made explicit in the *Cambridge Dictionary* which defines a robot as

- *a machine used to perform jobs automatically, which is controlled by a computer.*

Some definitions of robots have arisen in view of the historical concentration of robots in factories and along assembly lines. The *Robotics Institute of America* defines a robot as

- *a reprogrammable, multifunctional manipulator designed to move material, parts, tools or specialized devices through various programmed motions for the performance of a variety of tasks.*

This definition focuses on the robot as a *multifunctional manipulator* or *robotic arm*, but neglects a wide range of mobile robots designed to explore and map environments without the need for a manipulator to interact with these environments.

All of the definitions of robots above are accurate in some contexts, but do not describe the breadth of systems that will be considered in this book. The definition of a robotic system that will be used in this book is given below.

Definition 1.1 (Robotic System). A robotic system is a reprogrammable, computer-controlled mechanical system that may sense and react to attributes of its surroundings as it performs assigned tasks with some degree of autonomy.

This definition expands those previously introduced and is broad enough to encompass the examples encountered in this book. A robot need not have humanoid form, and it does not necessarily have the form of a multifunctional manipulator. The above definition emphasizes that robotic systems exhibit some level of autonomy. They operate, to varying degrees, independent of human intervention. They have sensors such as cameras, laser ranging sensors, acoustic proximity sensors, or force transducers that allow them to sense their environment via measurements. This data is subsequently used by the robot to react to its environment. For example, an

autonomous ground, air, marine or space vehicle may change course to avoid obstructions or debris; a dexterous manipulator may change the pressure with which a tool is gripped based on force transducer measurements; a robotic manipulator may use camera measurements to position a tool in the workspace. Finally, the definition makes explicit that a robot is a mechanical system, one that is built from the interconnection of components.

In summary, a robotic system is made possible through the synthesis of theory and techniques from many fields, perhaps most notably mechanical engineering, electrical engineering, and information technology. The field of mechatronics facilitates and enables the development of complex robotic systems from standard subsystems and has accelerated the maturation of the robotics field in recent years. This relationship among some of the primary fields contributing to robotics is depicted in Figure (1.3).

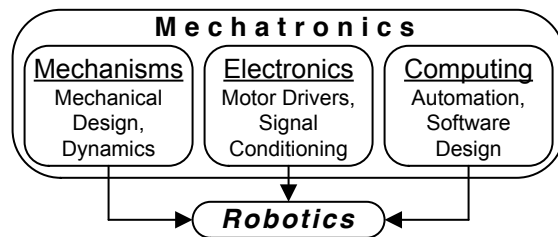


Fig. 1.3: Fields Contributing to Robotics

1.3 General Structure of Robotic Systems

As will be discussed in the following sections, there are a diverse population of robotics that have been developed over the years, ranging from robotic manipulators to mobile robots that traverse the air, land or sea. These robots may emulate humans or animals, or have novel topologies to accomplish desired tasks. However, despite these differences, there are some common features that many robots share that are discussed in this section.

Figure (1.4) depicts several components of a typical robotic system. Nearly all robotic systems feature *actuators*. The actuators serve as the muscles of the system and produce motion. Their power is usually supplied electrically, pneumatically, or by hydraulics. Since many robots are either controlled remotely or make provision for interruptions to their autonomous operation from outside agents, many robots include a *communicator* of some sort. The communicator is a unit that transmits information to a host and/or receives instructions from a remote operator. As noted

earlier, an essential feature of any robot is that it exhibit some level of autonomy or intelligence. A *control unit* is a vital component of nearly all robotic systems. It may consist of a single processor, or may be a central computer that integrates the activities of several microprocessors. Many robotic manipulator systems, underwater autonomous vehicles, or space robots must directly mechanically manipulate their environment. An *end-effector* that consists of a *gripping device* at the end of a manipulator arm can therefore be essential to the operation of the robot. The end effector can be used to make intentional contact with an object or to produce the robot's final effect on its surroundings. In some cases there may be several manipulator arms or gripping mechanisms. Since a robot must interact with its environment, and usually lacks much information about its surroundings, many robots also include *sensor suites* that include a variety of sensing modalities. Each *sensor* is usually a transducer of some kind whose inputs are physical phenomena and whose outputs consist of electronic signals. Finally, since mobility, sensing, and actuation require energy expenditure, a robot must have a *power supply* of some type. Most frequently this is an energy storage device such as a battery. In some instances the robot may be tethered to a fixed power supply. For example, a military or industrial exoskeleton may require so much power that it is only feasible to connect to a remote local power supply while the suit is worn in a warehouse to move heavy payloads.

Any particular robotic system may include many of these components, or simply a few in each category. An autonomous military ground vehicle will usually host a wide variety of vision sensors, motion sensors including GPS and compass, thermal sensors, and chemical sensors. A simple table top robotic manipulator in a laboratory might only have joint encoders to sense motion. Figure (1.5) illustrates a typical robotic manipulator that might be suitable for a laboratory benchtop. The figure emphasizes the data flow within the robotic system. In this system, the robot is usually equipped with rotary encoders that return measurements of angular motion at the joints to the controller and computer. In this particular system, a vision or laser tracking sensor is also configured to provide measurements of the end-effector position and velocity. This measurement is returned to the computer to assist controlling the position tracking of the end-effector along a desired trajectory. It should also be noted that this figure, while giving a general picture of the topology and connectivity of a robotic system, lacks many details that are necessary for a real robotic system. For example, the motor controllers are not shown in the figure, nor are the amplifiers or signal conditioners that may be required between the primary components.

1.4 Robotic Manipulators

An important type of robotic system that is studied often in this text is the *robotic manipulator* or *robotic arm*. Robotic systems of this kind were some of the first to achieve widespread use in industry. As noted in the previous section, robotic ma-

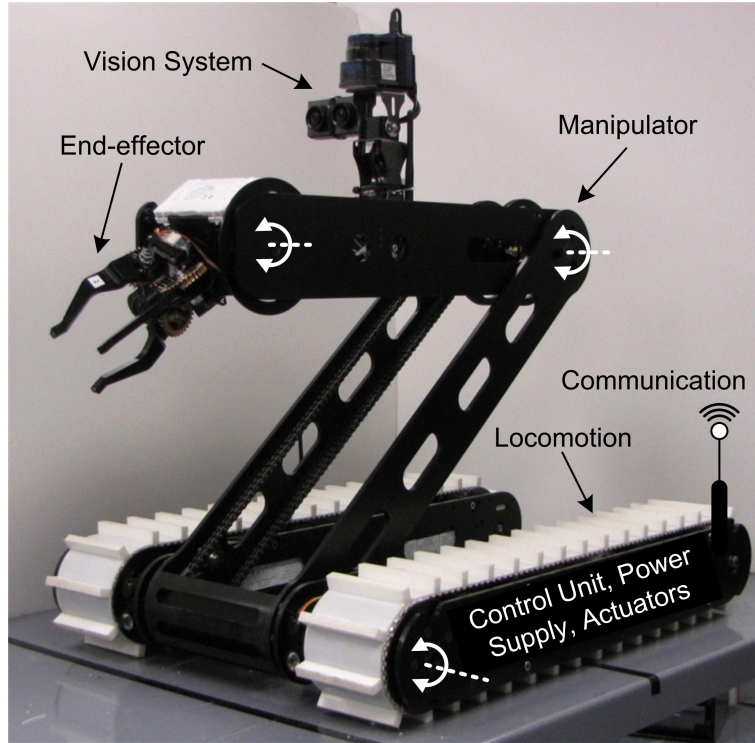


Fig. 1.4: Typical Mobile Robotic System Components [5, 4, 6]

nipulators have become a standard feature of modern assembly lines. They perform a host of tasks including welding, spraying, pick and place operations, drilling, cutting, and lifting. Many of the analytical techniques, modeling methodologies and control strategies introduced in this text are demonstrated on examples that treat robotic manipulators. The reasons for this choice are numerous. Robotic manipulators are some of the simplest examples of practical robotic systems. Their study helps clarify the underlying principles and problems encountered when studying more complex systems. Although an autonomous marine vehicle may not resemble a robot on an assembly line, the general form of the mathematical problem that must be solved to control these two types of systems can be surprisingly similar. The same is true for modeling and control of autonomous ground or air vehicles. General methodologies applicable to one system can often be a starting point for the development of models and controllers for others. Moreover, it is often the case that a subsystem of an autonomous robotic system can be modeled or controlled using techniques developed for robotic manipulators. For example, the arms or legs of a humanoid robot or an imaging payload that actively controls the line of sight

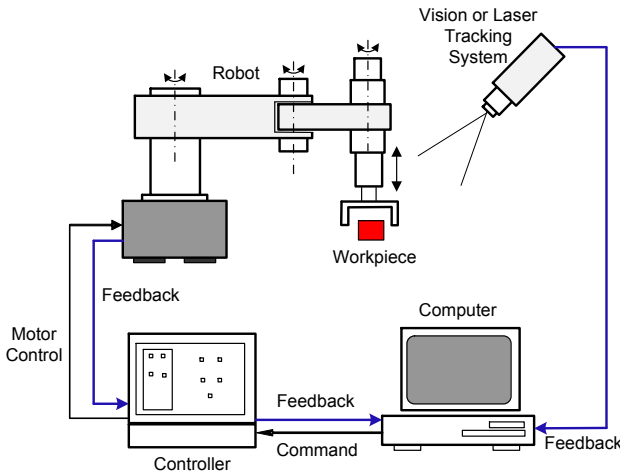


Fig. 1.5: Typical Robotic Manipulator System Components

of a camera on an autonomous air vehicle may be modeled using techniques from robotic manipulators.

1.4.1 Typical Structure of Robotic Manipulators

Many robots consist of a number individual bodies or *links* that are connected by *joints*. The individual bodies that make up the robot are often treated as rigid bodies, and that is the assumption throughout this text. However, for high-speed or highly loaded mechanisms, elastic effects of the material body become significant and should be taken into consideration. The joints that connect the links in the robot can be quite complex and may themselves exhibit highly nontrivial mechanics including flexibility, hysteresis, backlash, or friction. An ideal joint is an interconnection between rigid bodies of a robotic system that allows only specific, predefined relative motions such as translation or rotation. Mathematically, an ideal joint imposes a kinematic constraint on the motion between rigid bodies that is based on the joint geometry. Common types of ideal joints include *revolute*, *prismatic*, *universal*, *spherical* or *screw joints*. Figure (1.6) depicts a few of these ideal joints and summarizes some of their properties.

The two simplest types are the prismatic joint or revolute joint. Nearly all of the robotic systems studied in this text consist of these two types. Many of the other types of ideal joints can be modeled by combining these two. For example, a universal joint consists of a pair of revolute joints with their joint axes orthogonal

Name of Pair	Geometric Form	Schematic Representation	Degrees of Freedom
Revolute			1
Prismatic			1
Cylindrical			2

Fig. 1.6: Ideal Joints and Their Properties

to one another. A prismatic joint allows only relative translation between two links along a prescribed axis, while the revolute joint permits only relative rotation about a prescribed axis.

An independent variable that is used to describe the motion of a robot, or the relative motion allowed by an ideal joint, is often called a *degree of freedom*. The number of degrees of freedom of an ideal joint is the number of independent variables required to model the relative motion that the joint permits. A robot has N *degrees of freedom* if it requires N independent variables to describe all of its possible configurations. The revolute and prismatic joints are consequently *single degree of freedom joints*. If the joint constraints are independent of one another, the number of degrees of freedom N for a general mechanism can be calculated as

$$N = \lambda(n - 1) - \sum_{i=1}^k (\lambda - f_i) \quad (1.4.1)$$

where n is then number of links, k is the number of joints, and f_i is the number of degrees of freedom for joint i . For planar mechanisms $\lambda = 3$ and for spatial mechanisms $\lambda = 6$.

Example 1.4.1. Consider the *pantograph* mechanism depicted in Figure (1.7).

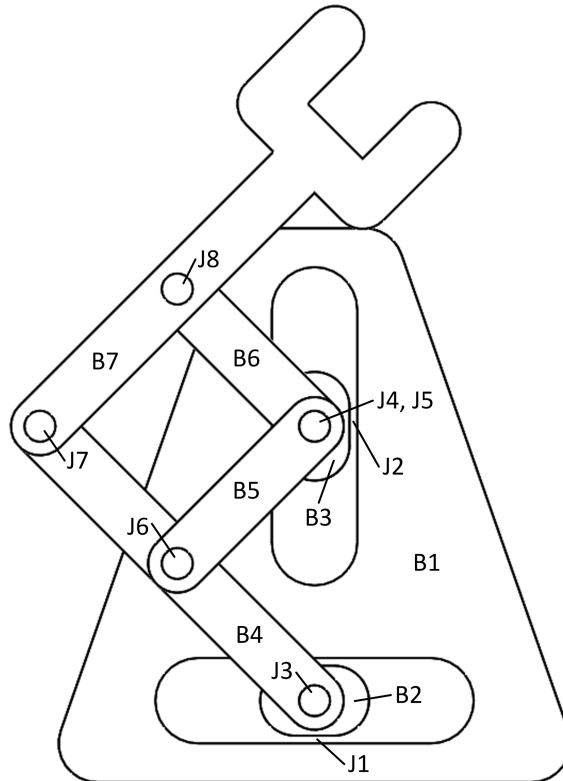


Fig. 1.7: Pantograph Mechanism

When Equation 1.4.1 is applied to the pantograph in Figure (1.7), the values $\lambda = 3$, $n = 7$ (including the ground link), $k = 8$, and $f_i = 1$ for $i = 1, \dots, 8$ are determined. It follows that the number of degrees of freedom $N = 2$.

More details on the properties of the ideal joints are presented in Chapters (3) and (4). Precise mathematical definitions of the degrees of freedom for mechanical systems, and robots in particular, are discussed in Chapter (5).

1.4.2 Classification of Robotic Manipulators

Now that the basic definitions of links, joints, and degrees of freedom for typical robotic manipulators have been defined, a summary of different ways in which robots are classified is provided. Again, although this discussion focuses on robotic manipulators, some of the classifications are pertinent to other classes of robots. For example, classification of robots by driver technology and drive power applies equally well to all types of mobile robots whether they operate in the air, on land, under water, or on the water's surface.

1.4.2.1 Classification by Motion Characteristics

One of the most common means of differentiating among different robot architectures considers motion characteristics. A *planar manipulator* is one in which all the moving links in the mechanism perform planar motions that are parallel to one another. In contrast, a *spatial manipulator* is one in which at least one of the moving links demonstrates a general spatial motion. In other words $\lambda = 6$ in Equation 1.4.1. In some cases the manipulator is constructed so that only very specific kinds of motion are possible. A *spherical manipulator* is constructed so that the moving links perform spherical motions about a common stationary point. A *cylindrical manipulator* is constructed so that the end effector travels on the surface of a cylinder. More details of these two types of manipulators are discussed in Sections 1.4.3.2 and 1.4.3.4.

1.4.2.2 Classification by Degrees of Freedom

Another means for classifying robots does so based on their number and type of degrees of freedom. A *general purpose robot* possesses $\lambda = 3$ degrees of freedom if it is a planar robot or $\lambda = 6$ degrees of freedom if it is spatial robot. A robot is *redundant* if it posses more than λ degrees of freedom. A redundant robot can be used to move around obstacles and operate in tightly confined spaces. A robot is *deficient* if it has less than λ degrees of freedom.

1.4.2.3 Classification by Driver Technology and Drive Power

Robots are often characterized by the nature and type of their drive technology. An *electric robot* employs DC servo motors or stepper motors. These robots have the advantage that they are clean and relatively easy to control. A *hydraulic robot* is preferred for tasks that require a large load carrying capacity. Care and maintenance is required to handle leaks and fluid compressibility problems. For high speed applications, a *pneumatic robot* is often preferred. These robots are generally clean, but can be hard to control due to challenges associated with air compressibility.

A *direct drive manipulator* is one in which each joint is driven directly by an actuator without any torque transmission mechanism. These drives can be bulky and heavy, but do not exhibit backlash or drive flexibility which can render robotic control more difficult. Finally, a *conventional manipulator* generates a driver torque that is magnified by a transmission mechanism. Usually this is achieved via gear reduction or by a harmonic drive unit. This design allows the use of smaller actuators. However, the gear mechanisms suffer from backlash, and the harmonic drives inherently exhibit flexibility effects.

1.4.2.4 Classification by Kinematic Structure

Kinematic structure is a topic of great importance to robotics and is yet another means that can be used to classify different types of robots. The kinematic structure of a robot results from its *system connectivity*. This topic has been studied extensively in multibody dynamics and has had profound impact on robotics. The study of *multibody dynamics* is closely related to robotics, and strong references for the basic theory can be found in [14, 46, 24]. Many of the results discussed in this book can be considered as special cases within the general study of multibody dynamics. Generally speaking, the field of robotics is usually more concerned with problems of forward kinematics, inverse kinematics, or control synthesis, and the field of multibody dynamics tends to focus more on the study of numerical methods for approximations of the solution of the forward dynamics problem. It has been known for some time in the field of multibody dynamics that the *connectivity topology* of a system can have a dramatic influence on the complexity of simulating or deriving a control strategy for a system.

A robotic system is said to have the connectivity of a *kinematic chain* if there is one and only one connected path that traverses a system from the first to the last link. Such a robot is also often referred to as a *serial manipulator* or as a *open-loop manipulator* in the robotics literature. A single arm or leg of a humanoid robot is a good example of a kinematic chain. Multibody systems that form a kinematic chain have the simplest connectivity topology. It is this class of robotic systems for which the richest collection of formulations and control strategies have been derived. The kinematics of chains is studied carefully in Chapters (3), their dynamics is studied in Chapters (4) and (5), and their control is the topic of Chapters (6) and (7).

A multibody system is said to have *tree topology connectivity* when it is built from an assembly of kinematic chains and no closed loops are formed by their interconnection. A full body humanoid robot or a space station in orbit are two familiar examples of systems having a tree topology connectivity. It is relatively straightforward to extend the techniques for modeling and control of kinematic chains to treat systems that have tree topology connectivity, although such methods must often be extended to account for the rigid body motion of the robotic system as a whole.

Finally, a robotic system is said to have *closed loop connectivity* whenever it is possible to construct a continuous path that starts at one link, traverses several other links, and finally connects to the original link. The multibody model of an autonomous ground vehicle can be an example of a system that has closed loop topology if its suspension system has closed loops. Two robotic manipulators that cooperate in the task of lifting a large payload also form a system that has closed loop topology. The Stewart platform depicted in Figure (1.8) is a common robotic platform that has closed loop connectivity.

Robotic manipulator systems with closed loop connectivity are commonly referred to as *parallel manipulators* in the field of robotics. General robotic systems that have closed loop topology are not addressed in this introductory book.

Of course, some systems are constructed from subsystems that constitute both open and closed loop chains. In some industrial manipulators, such as the Fanuc S-900W, a four-bar push-rod linkage is used to drive the intermediate joints, which in turn are mounted on the robot base or waist. This design reduces the inertia of the manipulator. Such a system, that contains both open and closed loop chains as subsystems, is known as a *hybrid manipulator*.



Fig. 1.8: Industrial Stewart Platforms

In summary, robotic systems that have the form of a kinematic chain are the most basic; other more complicated robotic systems can be assembled from them. Methods for analyzing, simulating, or synthesizing a controller for kinematic chains can

be applied to subsystems having more complex connectivity. Robotic manipulators serve as prototypical examples of robots that form kinematic chains.

1.4.2.5 Classification by Workspace Geometry

The last method for classifying robots discussed looks at their *workspace geometry*. The *manipulator workspace* is the volume of space that the end effector can reach. The set of points where every point can be reached by the end effector in at least one orientation or pose is the *reachable workspace*. The set of points where every point can be reached by the end effector in all possible orientations or poses is called the *dexterous workspace*. By definition, it follows that the dexterous workspace is a subset of the reachable workspace. It should be noted that most industrial serial manipulators are designed with their first three moving links longer than the remaining links. These inner links are used primarily for controlling the end effector position. The remaining outboard links are used typically for controlling the end effector pose or orientation. Often, the subassembly associated with the first three links is denoted the arm, and the remaining outboard links constitute the wrist. Figure (1.9) shows four common types of workspaces.

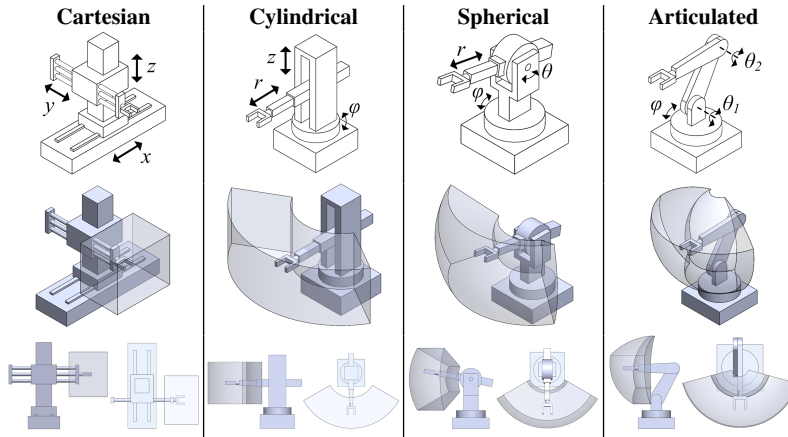


Fig. 1.9: Various Workspace Geometries

1.4.3 Examples of Robotic Manipulators

In the next few sections a few of the most common robotic manipulators are described. All of these examples consist of a few links joined by either prismatic joints or revolute joints. These joints can be either *driven* or *passive*.

A driven joint is one in which an actuator directly generates motion, either translation (prismatic joint) or rotation (revolute joint). In a driven joint, a linear or rotational motor is connected to each link constrained by the joint. If a joint is not driven by an actuator, it is said to be a passive joint. For example, in the pantograph shown in Figure (1.7), assume the two prismatic joints (J1 and J2) are controlled by linear actuators. These are thus driven joints. The remaining revolute joints (J3-J8) are now passive joints, as the motion between the bodies at these joints is prescribed by the motion of the two active joints.

Usually, the manipulators are designated by a sequence such as PPP or RPP that indicate the type and ordering of the prismatic (P) and revolute (R) joints that make up the robot. For example, a PPP robotic manipulator is constructed from three prismatic joints, while an RPP robot is built from a revolute joint that is followed by two successive prismatic joints. This designation is often a good indicator, in broad terms, of the general geometry and functionality of a robotic manipulator.

1.4.3.1 Cartesian Robotic Manipulator

A *Cartesian robot* is a *PPP manipulator* defined by three mutually orthogonal prismatic joints. Figure (1.10) depicts a typical example. The PPP arm is one of the simplest robotic manipulators. This type of multi-functional arm is sometimes called a gantry or a traverse, depending on the context in which it is used. A gantry is usually a suspended version of a Cartesian robot used for positioning large industrial payloads. A traverse is often used for positioning optical experiments or surgical tools. A PPP manipulator has several advantages owing to its simple geometry. Models for PPP robots are easy to derive, as are the control laws that are used to position and move these robots. The simplest models for PPP manipulators have equations of translational motion along three perpendicular directions that are decoupled. Since no rotational degrees of freedom are included in a Cartesian robot, these systems tend to be rigid or structurally stiff. They can sustain and deliver large loads and achieve high precision in positioning. One drawback of this robot is that it requires a large area in which to operate, and the workspace is smaller than the robot itself (Fig. (1.9)). Another drawback is that the guides for the prismatic joints must be sealed from foreign substances, which can complicate maintenance.

1.4.3.2 Cylindrical Robotic Manipulator

Suppose the first prismatic joint in the Cartesian robot is replaced with a revolute joint. By making a judicious choice of the direction of the axis of rotation, the re-



Fig. 1.10: Cartesian Robot by Sepro America
<http://www.sepro-america.com/>

sulting RPP robot is an example of a cylindrical robot. One example of a cylindrical robot that is analyzed in this text is depicted in Figure (1.11). It is easy to see that the location of the end of the horizontal arm in the cylindrical robot can be expressed in terms of cylindrical coordinates, which gives this robot its name. Its workspace takes the form of a hollow cylinder. Again, this manipulator has several advantages owing to its structural simplicity. While the kinematic and dynamic models of a cylindrical manipulator are more complex than that of a Cartesian robot, they are still simple to derive. The associated control laws are likewise quite straightforward to determine. The topology of the RPP manipulator makes it well-suited for reaching into work pieces that have cavities or other similar complex geometries. It can achieve high precision and is used for pick and place operations on an assembly line. One disadvantage of this type of robot is that the back of the robot can protrude into the workspace in some configurations. This can cause interference with the workspace and complicates path planning and control. As in any robot that uses prismatic joints with external guides, the guide surfaces must be clean and free of debris. This can make upkeep and maintenance more difficult.

1.4.3.3 SCARA Robotic Manipulator

The SCARA (Selective Compliance Articulated Robot Arm) RRP robot was introduced as a compromise between highly rigid robots such as the Cartesian robotic manipulator and robots that can access geometrically complex workspaces such



Fig. 1.11: Cylindrical Robot by ST Robotics
<http://www.strobotics.com/index.htm>

as the spherical manipulator. Since the axes of the two revolute joints are parallel in a SCARA robot, this robot is relatively compliant in motion that occurs in the horizontal plane and relatively stiff in motion normal to this plane. The variation in compliance between these two modes of motion gives this robot its name. The workspace of this robot is highly structured. The SCARA manipulator can be an attractive robot for precision pick and place operations, for example.

1.4.3.4 Spherical Robotic Manipulator

The RRP spherical robotic manipulator is formed from two perpendicular revolute joints and a prismatic joint. For some choices of the fixed offset dimensions between the joints, the motion of the tool or tip of the manipulator arm can be expressed in terms of spherical coordinates, which gives this robot its name. Some of the most famous robotic manipulators that have appeared over the years have been of this type. The *Unimate* robot discussed in Section 1.2 and shown in Figure (1.13) is an example of a spherical manipulator.

The primary advantage of this robot architecture is its suitability to a wide range of tasks that must be carried out over complex geometries. The spherical workspace accessible by this robot is large compared to the robot size. Unfortunately, this flexibility comes at a cost. The kinematic and dynamic models of the spherical robot are



Fig. 1.12: SCARA Robot by Epson
<http://robots.epson.com/>



Fig. 1.13: Unimate Spherical Robot

more complicated than those for Cartesian or cylindrical manipulators, which leads to control laws that are likewise more complex. The introduction of an additional perpendicular axis of rotation yields a robot that is less rigid and more compliant than the Cartesian manipulator. The result is that the spherical robot can be less precise in positioning. Generally speaking, a spherical robot can be more appropriate

for tasks such as welding or painting that require somewhat less precision than pick and place operations, but require accessibility over a large and complex workspace.

1.4.3.5 PUMA Robotic Manipulator

Historically, one of the most widely used robotic manipulators on assembly lines is the PUMA (Programmable Universal Machine for Assembly) RRR robot. An example of a PUMA robot is depicted in Figure (1.14). The first revolute joint of this robot is about the vertical axis, and the next two parallel revolute joints are perpendicular to the vertical axis. The widespread use of the PUMA robot can be attributed to the fact that it has a rich kinematics and can access a large hemispherical workspace. With the introduction of three rotational axes along two perpendicular directions, however, the PUMA is less rigid than the Cartesian robot. It is well-suited to applications that require a large and highly reconfigurable workspace.



Fig. 1.14: PUMA Robot

1.4.4 Spherical Wrist

The previous section presented variants of the PPP, RPP, RRP and RRR robotic arms and given an overview of some of their advantages. The spherical wrist is an RRR robotic component that often appears as a subsystem that is attached to these more complex manipulators. Figure (1.15) illustrates the spherical wrist in detail. The wrist is built from three revolute joints whose axes of rotation intersect at a common point, the wrist center. The anthropomorphic arm in Figure (1.16) is similar: a spherical wrist subsystem is connected to the end of the arm. Not only does this design resemble human anatomy, it has an important pragmatic implication for control design. This common geometry is attractive in that it makes it possible to decouple the task of positioning the wrist center and orienting the tool at the end of the spherical wrist. This topic is discussed in Chapter (3) when inverse kinematics is covered.

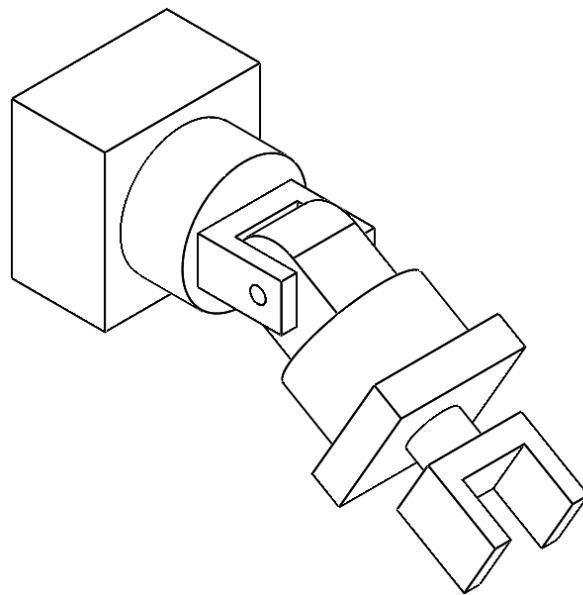


Fig. 1.15: Spherical Wrist

1.4.5 Articulated Robot

The articulated robot arm or anthropomorphic robot arm is a manipulator that is able to achieve motions that resemble those of the human arm. All anthropomorphic robot arms have at least three revolute joints, and it is common that they have five, six, or more, revolute joints. A typical configuration is depicted in Figure (1.16) where a spherical wrist has been attached to an RRR robotic arm. Note that the first three degrees of freedom resemble that of the PUMA robot studied in Section (1.4.3.5). The first, vertical revolute joint permits the motion that is sometimes known as the arm sweep. The next two joints are referred to as the shoulder and elbow joints, respectively. The result is an arm that can access a large workspace, and it can pose the tool located at its tip at an arbitrary orientation. The anthropomorphic arm finds widespread use in welding and spraying on assembly lines. In comparison to the other robotic manipulators discussed, this arm does have a complicated geometry. The corresponding equations that describe the kinematics and dynamics of this robotic system are complicated in form, as are the control laws derived from these models.



Fig. 1.16: Articulated Robotic Arm
<http://www.kuka-robotics.com/>

1.5 Mobile Robotics

In the last section several of the most common multifunctional robotic arms were described. It was noted that they can vary dramatically in form, operation, and application. This section summarizes another major subset of robotics: mobile robots, including humanoid or full-body anthropomorphic robot and autonomous air/ground/marine vehicles.

1.5.1 Humanoid Robots

It was shown in Section (1.4.5) that anthropomorphic or humanoid arms have reached a point of maturity in the robotics field: they are ubiquitous in factories throughout the world. The creation of full-body humanoid robots, in comparison, remains an area of active research. From the earliest stages in the emergence of the robotics field, designers have dreamed of creating robots that resemble humans in both appearance and function. Early craftsmen and artisans, as well as artists and inventors, sought to create mechanical systems that would emulate human actions. These early researchers included such notables as Leonardo Da Vinci. His and others' early efforts, while visionary, met with limited success due to the lack of technological infrastructure. Today, the infrastructure has evolved to the point where current anthropomorphic robots are evaluated in the performance of sometimes surprisingly complex tasks. A good example is the RoboCup international autonomous soccer competition. Since the inception of the humanoid league in 2002, teams that create humanoid robots have come from all over the world to this annual event. Figure (1.17) illustrates one such robot created by student researchers at Virginia Tech under the direction of Professor Dennis Hong, who is now a professor at the University of California, Los Angeles (UCLA).

The complexity of these humanoid soccer players is impressive. Each robotic player must be able to run, walk, kick, and block shots, which are difficult mobility challenges for two legged robots. Each robot must also be capable of image-based perception and feature recognition during the course of a match. Finally, the robots must have the onboard processing hardware and software that enables them to predict and react to the play of the game in a strategic and coordinated fashion. Full-scale humanoid robots are also currently under development by researchers around the world. While the potential applications are diverse, it is hoped that these full-scale robots will have roles in the care of the elderly or in the design and testing of prosthetics. Figure (1.18) shows *CHARLI*, a full scale humanoid robot also created by students under the supervision of Dr. Dennis Hong.

The full complexity of humanoid robot design, analysis, and fabrication far exceeds the scope of this text. This text does show how to develop kinematic models, dynamic models and control schemes that are applicable to typical subsystems that make up such a humanoid robot. Examples and problems related to the arm or leg assemblies of humanoid robots can be found in Chapters (2), (3), (4), (5), (6),

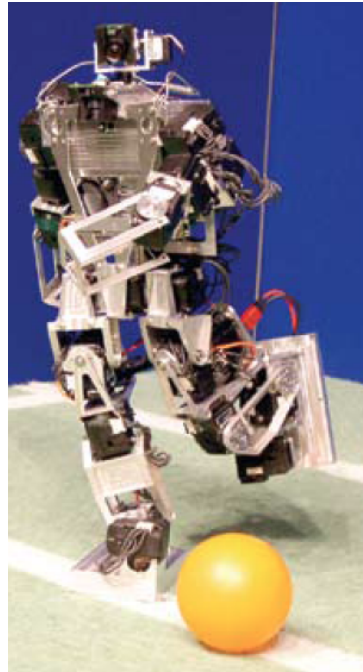


Fig. 1.17: Humanoid Robot for RoboCup Soccer Competition
Created by students at Virginia Tech under the direction of Professor Dennis Hong, currently of UCLA



Fig. 1.18: Humanoid Robot *CHARLI*
Created by students at Virginia Tech under the direction of Professor Dennis Hong, currently of UCLA

and (7). Typical research topics for this class of robot that continues to fascinate researchers include the study of the dynamics and control of bipedal locomotion, perception, vision-based control, vision-based perception, dexterous manipulation, and human-machine interaction.

1.5.2 Autonomous Ground Vehicles

The design, analysis and fabrication of robotic ground vehicles, or autonomous ground vehicles (AGV) has been carried out in this country and around the world for several years. Most of the autonomous ground vehicles that have appeared over the years fall within the class of *research vehicles* that have been designed to establish the feasibility of a solution for some specific technical problem in the field of mobile robotics.

Only recently has it become clear that the field of AGV robotics has matured to the point where it is reasonable to expect the appearance of reliable, high-performance commercial and military robots in the near future. One reason for optimism is the spectacular success of the DARPA (Defense Advanced Research Projects Agency) Grand Challenge and Urban Challenge competitions that were held between 2004 and 2008. The DARPA Grand Challenge was first held in 2004. After a series of qualification events, robot developers from across the country met at a 142 mile test track in the California desert. While no team completed the entire course in the first year that the event was held, four teams finished the race in 2005. In 2007 the DARPA Urban Challenge was held. This contest required that entry vehicles operate autonomously in an urban environment, reacting to other vehicles in traffic. Figure (1.19) illustrates the AGV *Odin*. This vehicle was created by students under the direction of Dr. Al Wicks of Virginia Tech and full time researchers at TORC, a company specializing in the creation of autonomous ground vehicles. The vehicle *Odin* was one of three robotic cars that successfully completed the DARPA Urban Challenge.

Figure (1.20) depicts examples of military ground vehicles, also created by Dr. Al Wicks and TORC, that evolved from the technology derived from the vehicle *Odin*. The use of autonomous ground vehicles by the military reduces the risk to troops. Contemporary research topics pertinent to AGVs can include autonomous guidance, navigation and control (GNC), autonomous exploration and mapping, sensor fusion, estimation and filtering techniques, hybrid AGV design, and active energy management for increased endurance.

1.5.3 Autonomous Air Vehicles

Over the past five years, it has become commonplace to encounter news on the radio, television or Internet that describes military operations that feature the use of



Fig. 1.19: Autonomous Ground Vehicle *Odin*
Created by students directed by Dr. Alfred Wicks of Virginia Tech
and researchers from TORC, www.torctech.com



Fig. 1.20: The Autonomous Remote-Controlled HMMWV, *ARCH*
Created by students directed by Dr. Alfred Wicks of Virginia Tech
and researchers from TORC, www.torctech.com

autonomous air vehicles (AAVs). Since, as noted earlier, robots have proliferated historically in jobs that are dirty, dull or dangerous, it should come as no surprise that they have become a critical part of the military air vehicle inventory.

While present generation drones are remotely piloted and do not make decisions to engage targets autonomously, they do exhibit some autonomy. They react to their environment, for example, as they sense their orientation, heading and position, and

as they correct for navigational errors via an autopilot. In this sense, every commercial or military aircraft with an autopilot can be considered a robotic system. By convention, however, AAVs are usually classified as those air vehicles that do not contain a pilot and exhibit some level of mission-level autonomy. The degree of autonomy exhibited by AAVs increases with each passing year. Current strategic plans make provision for AAVs that engage targets autonomously in the next few decades.

By their nature, autonomous air vehicles are necessarily more complex than their ground based counterparts. With this complexity comes an increased cost that limits the routine use of autonomous flight vehicles, at least presently. Most examples of AAVs have been fielded by the military of governments all over the world. Despite their expense, applications of robotic air vehicles continue to expand in the commercial sector. Many applications have been identified by government agencies other than the military. Autonomous flight vehicles have been proposed for applications in agriculture, disaster relief, police surveillance, and border security. Figure (1.21) depicts an autonomous helicopter that is being used to conduct geophysical mapping of radioactive sources. This research effort is under the direction of Dr. Kevin Kochersberger of the Unmanned System Laboratory at Virginia Tech.



Fig. 1.21: Autonomous Rotorcraft for Radiation Sensing
Created by students under the direction of Professor Kevin Kochersberger of Virginia Tech

One noteworthy trend in this segment of the robotic industry is the increasing number of small air vehicles, or even *micro air vehicles*, that have been introduced over the past few years. It is now common to find examples of small, fixed-wing robotic air vehicles that have a wing span measuring from a few inches to a few feet in length. Figure (1.22) shows the fleet of SPAARO autonomous aircraft that Professor Craig Woolsey at Virginia Tech uses in a variety of research activities. These vehicles support research in applications ranging from automation of commercial agriculture and remote sensing of airborne pathogens to coordinated control of autonomous vehicle teams.



Fig. 1.22: Fleet of SPAARO Autonomous Air Vehicles (AAV)
Used in the research program of Professor Craig Woolsey of Virginia Tech

1.5.4 Autonomous Marine Vehicles

Just as there are significant differences in the design and fabrication of AGVs and AAVs, the development of an autonomous marine vehicle poses its own special challenges. The nature of these obstacles is illustrated in a number of the autonomous surface vehicles (ASV) and autonomous underwater vehicles (AUV) that have been developed over the past few years. Consider the task of operating a robotic surface marine vehicle along a river or a coastal region.

Often, some notion of the overall path to be taken is known, but littoral waters can have numerous unforeseen hazards. They must be sensed and avoided during any mission. Obstacles and hazards can be on the surface, at the waterline, or under the surface. For military vehicles, the ability to attack or flee at high speeds is an important capability to have. The task of navigating a vehicle along a partially unknown course, at high speed, defines a control problem of exceptional difficulty. As difficult as is the control of an AAV such as the Predator, it does not have to operate routinely in close proximity to collision hazards. The reaction time and computational time for deciding contingent actions is very short when obstacles loom immediately ahead or below a marine vehicle. Figure (1.23) depicts one example of an ASV that was created by student researchers under the direction of Dr. Dan Stilwell of Virginia Tech. These researchers have concentrated on the creation of robotic marine vehicles that operate autonomously, potentially at high speeds, in riverine environments. Of course, the deployment of autonomous marine vehicles is further complicated by the fact that the vehicles may be limited to travel on the surface of a body of water, or they can be designed for undersea travel. Figure (1.24) depicts an AUV created at Virginia Tech by Professor Dan Stilwell.



Fig. 1.23: Autonomous Surface Vehicle (ASV)
Created by students under the direction of Dr. Dan Stilwell of Virginia Tech



Fig. 1.24: Autonomous Underwater Vehicle (AUV) *Javelin*
Created by students under the direction of Professor Dan Stilwell of Virginia Tech

1.6 An Overview of Robotics Dynamics and Control Problems

The overview in Sections (1.2), (1.4), and (1.5) mentions some of the disciplines that influence the study of robotic systems. This book studies several classical problems that arise in the dynamics and control of nearly all robotic systems. These are the problems of forward kinematics, inverse kinematics, forward dynamics and inverse dynamics/feedback control of robotic systems. The essential features of these problems will be described in Sections (1.6.1), (1.6.2), (1.6.3) and (1.6.4) and discuss how they arise for typical robotic systems. The presentation uses the flapping wing

robot depicted in Figure (1.25) as a case study to illustrate the underlying principles. Section (1.6.5) discusses how, despite their apparent dissimilarity, these same problems arise in the control of mobile robots.

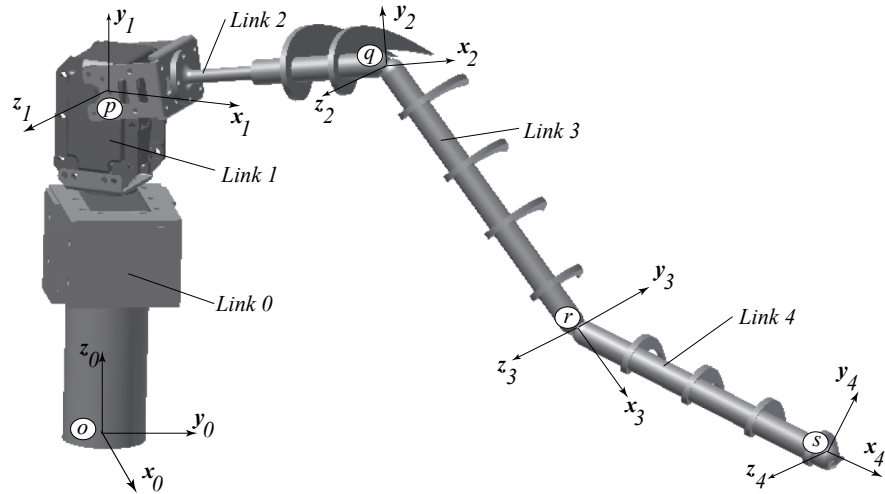


Fig. 1.25: Flapping Wing Robot

1.6.1 Forward Kinematics

Just as researchers have sought to design and build robots that mimic humans in form and action, so too have designers strived to build robots that resemble animals. Efforts to create bio-inspired flapping wing robots are one particularly challenging example. These designs represent a significant departure from that of most existing commercial flying vehicles. A successful design of a flapping wing robot is difficult in part due to a lack of understanding of the inherently complex nonlinear and unsteady aerodynamics surrounding the vehicle. This area continues to be an active topic of research. The task of building a flapping wing vehicle, while exceptionally difficult, provides an excellent example of how the classical problems of forward kinematics, inverse kinematics, forward dynamics and feedback control can arise in applications.

One of the first considerations in building a model of a robot of the type depicted in Figure (1.25) is the choice of the variables that will be used in its representation. This topic is discussed in general terms in Chapter (2), and a summary of the more common representations for articulated robotic systems is presented in Chapter (3). While there are exceptions, the most popular choice of variables for articulated me-

chanical systems is joint variables that define how the bodies of a robotic system move relative to one another. If the entire robotic system also undergoes rigid body motion with respect to a defined ground reference (instead of being fixed to that reference), as seen in the study of the space robotics or full-body humanoids, the joint variables must be supplemented with additional variables to represent the net motion.

In Figure (1.26), the robot is fixed rigidly to the ground. Therefore, the use of joint variables alone suffices to represent the dynamics. The joint variables in this example are the joint angles $\theta_1, \theta_2, \theta_3$ and θ_4 that determine the relative rotations of the bodies at individual revolute joints. It is also frequently the case that joint variables are selected to be the relative displacements between the bodies when a robot includes prismatic joints that permit translation. In general, a generic set of joint variables is denoted by $q_i(t)$ for $i = 1, \dots, N$ where N is the number of degrees of freedom. The problem of forward kinematics studies how the configuration of the robot changes as the joint variables are varied. For example, for the flapping wing robot, it is desired to design a system such that the wings trace out motions that resemble as closely as possible the motion of actual birds. The problem of forward kinematics seeks to find the position, velocity, and acceleration of typical points like s on the robot in Figure (1.25) given the time histories $q_i(t)$ of the joint variables for $i = 1, \dots, N$.

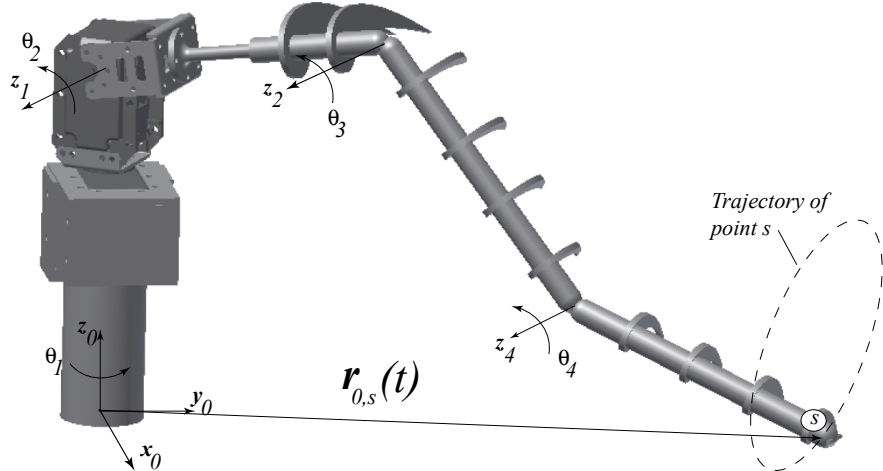


Fig. 1.26: Robotic flapping using robot and joint variables $\theta_1, \theta_2, \theta_3, \theta_4$

This problem can be stated succinctly: let $\mathbf{r}_{0,s}(t), \mathbf{v}_{0,s}(t)$ and $\mathbf{a}_{0,s}(t)$ be the position, velocity and acceleration of the point s relative to the ground, or 0, frame; find the mapping from the joint variables and their derivatives to the position, velocity and acceleration of point s on the robot

$$\mathbf{q}(t), \dot{\mathbf{q}}(t), \ddot{\mathbf{q}}(t) \mapsto \mathbf{r}_{0,s}(t), \mathbf{v}_{0,s}(t), \mathbf{a}_{0,s}(t)$$

It is important to realize that this problem must be solved as part of nearly all modeling or control tasks. The specific choice of joint angles used in Figure (1.26) are defined using the Denavit-Hartenberg Convention, one of the most commonly used general strategies for describing articulated robots that form kinematic chains. This topic is covered in detail in Chapter (3).

1.6.2 Inverse Kinematics

While solving the problem of forward kinematics is an important first step in many modeling and control problems, it does not answer all the important questions regarding the motion of a given robot. In the case at hand of the flapping wing robot, the wings should be able to trace out trajectories that mimic those of real birds, or as close as possible given the robot geometry. By taking video recordings of birds in flight, it is possible to generate estimates of the trajectories that certain points on the wings trace out as a function of time. Suppose these experimentally collected trajectories of point s on the wings are treated as input data. That is, suppose the position, velocity and acceleration of the point s as a function of time are given. The problem of inverse kinematics seeks to find the joint variables and their derivatives given the position, velocity and acceleration of a point s on the robotic system. In other words the mapping from the positions, velocities and accelerations of point s on the robot to the joint variables and their derivatives should be found.

$$\mathbf{r}_{0,s}(t), \mathbf{v}_{0,s}(t), \mathbf{a}_{0,s}(t) \mapsto \mathbf{q}(t), \dot{\mathbf{q}}(t), \ddot{\mathbf{q}}(t)$$

It is evident that this problem seeks to find the inverse of the mapping studied in the forward kinematics problem. It is well-known that the inverse kinematics problem can be much more difficult to solve than the forward kinematics problem. The inverse kinematics problem can have no solutions or multiple solutions, depending on the robot geometry and design objectives. Chapter (3) discusses some of the difficulties encountered in the solution of inverse kinematic problems.

1.6.3 Forward Dynamics

The problems of forward kinematics and inverse kinematics are purely geometric in nature. There is no provision for or consideration of the forces or moments that must be applied to achieve a specific motion. For many of the robotic systems studied in this book, the governing equations can be written in the form

$$\mathbf{M}(\mathbf{q}(t))\ddot{\mathbf{q}}(t) = \mathbf{n}(\mathbf{q}(t), \dot{\mathbf{q}}(t)) + \boldsymbol{\tau}(t)$$

where $\mathbf{M}(\mathbf{q})$ is an $N \times N$ nonlinear generalized mass or inertia matrix, $\mathbf{n}(\mathbf{q}, \dot{\mathbf{q}})$ is an $N \times 1$ vector of nonlinear functions including Coriolis and centripetal terms, and $\boldsymbol{\tau}$ is an $N \times 1$ vector of forces or torques applied to the robot by actuators. This is a nonlinear, second-order system of coupled ordinary differential equations (ODEs). The most common general strategy for studying these equations introduces the state variables \mathbf{x} that stacks the generalized coordinates \mathbf{q} and their derivatives $\dot{\mathbf{q}}$ in the form

$$\mathbf{x}(t) := \begin{Bmatrix} \mathbf{x}_1(t) \\ \mathbf{x}_2(t) \end{Bmatrix} := \begin{Bmatrix} \mathbf{q}(t) \\ \dot{\mathbf{q}}(t) \end{Bmatrix}$$

and rewrites the governing system of equations as

$$\dot{\mathbf{x}}(t) = \mathbf{f}(\mathbf{x}(t), \mathbf{u}(t)) := \begin{Bmatrix} \mathbf{x}_2(t) \\ \mathbf{M}^{-1}(\mathbf{x}_1(t))(\mathbf{n}(\mathbf{x}_1(t), \mathbf{x}_2(t)) + \mathbf{u}(t)) \end{Bmatrix} \quad (1.6.1)$$

where $\mathbf{u}(t) := \boldsymbol{\tau}(t)$ is the set of control inputs.

The problem of forward dynamics seeks to solve these equations for the state $\mathbf{x}(t)$, thereby obtaining the joint variables $\mathbf{q}(t)$ and their derivatives $\dot{\mathbf{q}}(t)$, given the input forces and torques in $\boldsymbol{\tau}(t)$. The solution procedure may be analytic or numerical, but the models of most practical robots are so complex that analytic solutions are not usually feasible. The numerical approximate solution of these equations utilizes the rich and well-developed collection of time stepping numerical algorithms for nonlinear ordinary differential equations. Specific algorithms that are commonly used to generate numerical approximations of the solutions include the popular family of Runge-Kutta techniques, linear multistep methods, and specialized schemes that are tailored to stiff systems. The solution of the forward dynamics problem can be used in many facets of robotic design and analysis.

1.6.4 Inverse Dynamics and Feedback Control

The problem of forward dynamics can be solved to understand how a specific set of input forces and torques in $\boldsymbol{\tau}(t)$ induce a corresponding time history of the joint variables $\mathbf{q}(t)$ for $t \geq 0$. The solution of the forward dynamics problem can be described as finding the dynamic behavior of the system given an input actuation time history $\boldsymbol{\tau}(t)$, $t \geq 0$. Similar to the relationship between forward and inverse kinematics, the problem of inverse dynamics of a robotic system can be thought of as asking a converse question: what must the control input history $\boldsymbol{\tau}(t)$, $t \geq 0$, be as a function of the generalized coordinates $\boldsymbol{\tau}(t) := \boldsymbol{\tau}(q_1(t), \dots, q_n(t), t)$ to yield a specific dynamic behavior?

However, when considering practical systems, there is often a disconnect between the prescribed desired state vector \mathbf{q}_d and the estimated state vector \mathbf{q}_e from sensors associated with the robotic system, internal (e.g., joint encoders) or external (e.g., workspace cameras). By incorporating techniques from control theory alongside inverse dynamic analysis, feedback control laws may be designed to calculate

appropriate actuation inputs trajectories $\tau(t)$ as a function of the desired and estimated states \mathbf{q}_d and \mathbf{q}_e .

While there are numerous specific control problems that make sense for a robotic system, a tracking control problem is easy to pose for the flapping wing robot. Suppose again that video post-processing methods have been used to identify the trajectories of points on the wings of actual birds in flight. One example of a trajectory tracking problem seeks to find the input torques and forces $\tau(t)$ as a function of time that will drive the robot so that the points on the wing approach the experimentally collected trajectories as time t increases. Many variants of this problem can be defined depending on the type of measurements and the metric used to define how closely the robot follows the desired trajectories. Mathematically, many of these control problems can be interpreted as a constrained optimization problem where some cost or performance functional J is minimized. The optimization problem is solved for the best input \mathbf{u}^* in the set of admissible control \mathcal{U} in the sense that

$$\mathbf{u}^* = \underset{\mathbf{u} \in \mathcal{U}}{\operatorname{argmin}} J(\mathbf{x}, \mathbf{u}) \quad (1.6.2)$$

subject to the constraint that the state \mathbf{x} satisfies the equations of motion in Equation (1.6.1).

1.6.5 Dynamics and Control of Robotic Vehicles

The fundamental dynamics and control problems for robotics, and their role in the study of a typical flapping wing robot, have been discussed in Sections (1.6.1), (1.6.2), (1.6.3), and (1.6.4). The example used for illustration in these sections could just as well have been selected to be any of the robotic manipulators. The structural similarity among these systems is striking. Perhaps surprisingly, each of the fundamental problems of robotics and dynamics – forward kinematics, inverse kinematics, forward dynamics, and feedback control synthesis – can also be stated when robotic systems that are autonomous vehicles are considered. In many cases the language used to describe the variants of these problems is different depending on the type of vehicle, even though the underlying problems are structurally similar in form. For example, the trajectory tracking or path following problem that seeks to position a tool mounted on a robotic arm is mathematically similar to that of guidance and navigation of autonomous vehicles. In addition, it is also common that robotic manipulators are mounted on autonomous vehicles as shown in Figure (1.27). Another example of this latter type includes the combined space shuttle and remote manipulator system. It is possible to speak of the guidance and navigation of the vehicle and the control of the robotic manipulator. These problems are in fact coupled, and the solution of dynamics and control problems for the coupled system can be substantially more difficult than that associated with only the base vehicle or only the manipulator.

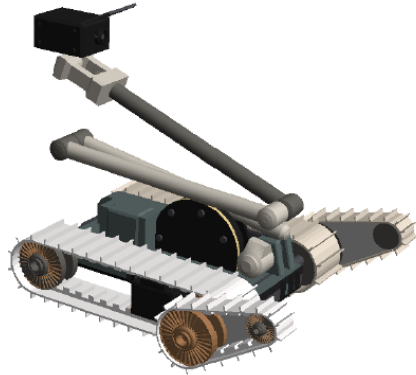


Fig. 1.27: Autonomous Ground Vehicle, iRobot PackBot, with Manipulator Arm

While the study of robotic manipulators provides a foundation that can be used to help formulate and solve dynamics and control problems for autonomous systems, there remain many substantial differences to methodologies for autonomous vehicles. One of the principal differences between formulations of the dynamics of AGV, AAV, ASV, or AUV is that the set of variables used to describe motion must be capable of representing rigid body motion. While the general study of kinematics in Chapter (2) covers many of the topics needed to study this problem, the specific methodologies for robots having the form of kinematic chains in Chapter (3) are not sufficient to represent the rigid body motion of an autonomous vehicle. Fortunately, for many of the different types of autonomous vehicles, it is the case that governing equations have the form shown Equation (1.6.1). Many problems of vehicle control are solved by casting the control problem as one of optimization, as summarized in Equation (1.6.2).

1.7 Organization of the Book

This study of robotic systems with an exposition of the fundamental principles of kinematics in Chapter (2). The chapter constitutes a self-contained introduction to the field of kinematics in three spatial dimensions and establishes notation and conventions for common mathematical expressions used throughout the book. Particular emphasis is placed on the foundations of kinematics in three spatial dimensions, including the study of vectors, coordinate systems, and rotation matrices. General definitions of linear position, velocity, and acceleration with respect to different frames of reference are introduced, as well as angular velocity and angular acceleration. The chapter concludes with a collection of some of the most commonly used theorems of kinematics. These include the theorems that introduce relative velocity

[2.16](#) and relative acceleration [2.17](#), the Derivative Theorem [2.12](#) and the Addition Theorem [2.15](#) for angular velocity.

Chapter (3) introduces refinements of the principles of kinematics that are tailored to specific types of robotic systems. The chapter introduces homogenous transformations that are used to relate rigid body motions of links in a robotic system. Mathematical models of ideal joints between the links that comprise the system are discussed. In addition to these general topics in kinematics of robotic systems, the chapter discusses two popular methods (Denavit Hartenberg and recursive) for the representation of robotic systems that form kinematic chains. In the presentation of the Denavit-Hartenberg convention, explicit constructions of the homogeneous transforms associated with the bodies in a kinematic chain are derived. A general procedure is detailed for defining the link parameters that determine the kinematics of a serial chain. The recursive formulation of the forward kinematics problem, in contrast to the Denavit-Hartenberg formulation, has been specifically based on efficiency in calculation. This formulation notes the highly structured nature of the kinematic relationship between successive bodies in a kinematic chain, and it exploits this structure to derive algorithms for recursive calculation of the kinematics. The chapter closes with a discussion of inverse kinematics.

Chapter (4) discusses the strategy for deriving the equations of motion of robotic systems using Newton-Euler formulations. General definitions of linear and angular momentum of rigid bodies are introduced. The inertia matrix of a rigid body is introduced to facilitate the calculation of angular momentum of components in a robotic system. The Newton-Euler equations are introduced as a means for deriving the equations of motion of general robotic systems. This chapter further extends the recursive formulation first studied in Chapter (3), and the resulting approach is used for the derivation of the equations of motion of robotic systems. It is demonstrated that the equations of motion of kinematic chains can be derived recursively by exploiting the structure of the same matrices that arise in the kinematics formulation. The equations of motion derived via the Newton-Euler formulation have the form of nonlinear differential-algebraic equations, or DAEs. It is demonstrated in the chapter that these equations can be re-cast as a set of nonlinear ordinary differential equations, or ODEs.

Methods of analytical mechanics, as they are used to derive the equations of motion of robotic systems, are introduced in Chapter (5). The chapter begins with the statement of Hamilton's Principle and explains how it can be interpreted as a problem of variational calculus. Its solution yields the equations of motion for the robotic system. Since the kinetic energy and potential energy of many robotic systems have the same functional form, it is possible to derive Lagrange's equations from the variational calculus problem generated by Hamilton's Principle. Hamilton's Extended Principle is presented as a means of incorporating contributions due to the presence of nonconservative forces in the equations of motion. A standard form for the governing equations for a large class of robotic systems is derived using Lagrange's Equations. Finally, the chapter presents the method of Lagrange's Equations with Lagrange multipliers that is appropriate for deriving governing equations in terms

of redundant collections of variables. This approach results in a system of nonlinear DAEs, in general.

Methods of feedback control of robotic systems are presented in Chapter (6). The general form and structure of control problems are discussed, and an overview of stability theory is given. The fundamental principles of stability theory are presented, and the use of the Lyapunov functions to establish stability for practical robotic systems is discussed. These techniques are critical to modern approaches of control synthesis for robotic systems. Lyapunov's Direct Method and LaSalle's Invariance Principle are applied to establish stability and convergence of typical set point and tracking controllers. Feedback controllers based on exact feedback linearization or computed torque control, approximate dynamic inversion and passivity principles are derived. The chapter finishes with an introduction to actuator models, emphasizing electric motors and electromechanical linear actuators.

The final chapter of this book, Chapter (7), discusses techniques of image-based control for robotic systems. The ideal pinhole camera model is discussed in detail, which enables a succinct presentation of image-based visual servo (IBVS) control strategies. Stability and asymptotic stability of IBVS control methods is established, as well as the role of singular configurations in the performance of these methods. The general approach of task space control formulations, in contrast to the joint space methods described in Chapter (6), is presented. Task space formulations of visual control objectives is the final topic in Chapter (7).

1.8 Problems for Chapter (1), Introduction

Problem 1.1. Briefly summarize the origins of the word 'robot.'

Problem 1.2. Define what is meant by a robotic system in this book. How does this definition differ from other common definitions?

Problem 1.3. Define the following terms that commonly appear in the study of robotics:

- actuator
- sensor
- workspace
- ideal joint
- joint variable
- passive joint
- driven joint
- precision, accuracy, and resolution
- repeatability
- tool frame
- end effector

Problem 1.4. Define the following robotic manipulators, describe their general features, and find commercially available examples of each:

- Cartesian robot
- Cylindrical robot
- Spherical robot
- SCARA robot
- PUMA robot
- Anthropomorphic arm

Problem 1.5. Define the fundamental problems of

- forward kinematics
- inverse kinematics
- forward dynamics
- feedback control

for robotic systems. Find and describe an explicit example of each problem for a commercially available robotic system.

Problem 1.6. Discuss examples of how the fundamental problems of the dynamics and control of robots (forward kinematics, inverse kinematics, forward dynamics and feedback control) may arise in the development of humanoid robots. Describe specific subproblems for each of the fundamental problems in this application area.

Problem 1.7. Discuss examples of how the fundamental problems of the dynamics and control of robots (forward kinematics, inverse kinematics, forward dynamics and feedback control) may arise in the development of autonomous ground vehicles. Describe specific subproblems for each of the fundamental problems in this application area.

Problem 1.8. Discuss examples of how the fundamental problems of the dynamics and control of robots (forward kinematics, inverse kinematics, forward dynamics and feedback control) may arise in the development of autonomous air vehicles. Describe specific subproblems for each of the fundamental problems in this application area.

Chapter 2

Fundamentals of Kinematics

Abstract The study of dynamics is comprised of the fields of *kinematics* and *kinetics*. *Kinematics* is the study of the geometry of motion and does not consider the forces and moments that give rise to that motion. *Kinetics* studies the causality between the applied forces or moments and the motion that they generate. This chapter focuses on kinematics, while Chapters (4) and (5) introduce kinetics. Chapter (3) applies the general results of this chapter to obtain formulations specific to robotic systems. Upon the completion of this chapter, the student should be able to

- Define different frames of reference or coordinate systems.
- Define rotation matrices and use them to change coordinate representations.
- Parameterize rotation matrices in terms of angles that measure rotation.
- Calculate the angular velocity and acceleration of frames in mechanical systems.
- Calculate the position, velocity and acceleration of points in mechanical systems.

2.1 Bases and Coordinate Systems

It is now commonplace to employ a number of *bases*, or *frames of reference*, or *coordinate systems*, to describe the motion of engineering systems. The Remote Manipulator System in Figure (2.1), the autonomous vehicle in Figure (2.2), or the humanoid robot in Figure (2.3) are just a few of the robotic systems that require numerous *frames of reference* to describe their motion. To aid in definition of these frames and the rotation matrices defined between these frames for mechanical systems, a few preliminaries are in order.



Fig. 2.1: Space Station with Remote Manipulator System

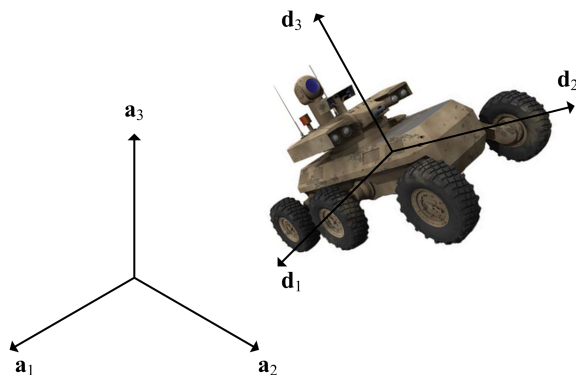


Fig. 2.2: MULE Autonomous Vehicle, Orientation

2.1.1 *N*-Tuples and $M \times N$ Arrays

First, a few comments on notation. Throughout this text the notation \mathbb{R} will be used to denote the set of real numbers, and \mathbb{C} will be used to denote the set of complex numbers. Integers will typically be referred to using the lower-case letters $i, j, k, l, m, n\dots$ when the integer is an *index* and capital letters $I, J, K, L, M, N\dots$ when the integer is the *upper limit* or *lower limit* of sequence of integers. An *N*-tuple is defined as an ordered collection of *N* real or complex numbers; no other properties are implied when referring to an *N*-tuple of numbers. The domain of an *N*-tuple of



Fig. 2.3: Humanoid Robot

real numbers is \mathbb{R}^N , and N -tuples will be denoted by lowercase bold letters, such as \mathbf{u} , and, by chosen convention, will be arranged in columns:

$$\mathbf{u} := \begin{pmatrix} u_1 \\ u_2 \\ \vdots \\ u_N \end{pmatrix}$$

where u_n is the n^{th} element of the N -tuple \mathbf{u} . In addition, $:=$ should be read as “is defined to be” and not simply as “equals.” The *norm* $\|\mathbf{u}\|$ of an N -tuple \mathbf{u} is given by the square root of the sum of the squares of its elements, such that

$$\|\mathbf{u}\| := \left\{ \sum_{n=1}^N u_n^2 \right\}^{1/2}.$$

This definition of the norm $\|\bullet\|$ is actually a specific example of a more general group of operations: it is the 2-norm or Euclidean norm of the N -tuple. In later chapters, for example, when numerical methods are addressed, or Chapter (5) when methods of analytical mechanics are introduced, the more general p -norm for $p = 1, \dots, \infty$ will be introduced. If \mathbf{u}, \mathbf{v} are two N -tuples, their *dot product* is defined as

$$\mathbf{u} \cdot \mathbf{v} := \sum_{n=1}^N u_n v_n.$$

By definition, $\|\mathbf{u}\|^2 = \mathbf{u} \cdot \mathbf{u}$.

The set of $M \times N$ real matrices, that is, arrays of real numbers having M rows and N columns, will be denoted by $\mathbb{R}^{M \times N}$. Uppercase bold letters such as \mathbf{A} are used to represent arrays, while the *matrix element* in the i^{th} row and j^{th} column of \mathbf{A} is denoted by the lowercase a_{ij} . For an $M \times N$ matrix \mathbf{A} , the *transpose* \mathbf{A}^T is defined to be the $N \times M$ array obtained by interchanging rows and columns, such that

$$\mathbf{A}^T = \mathbf{B} \Leftrightarrow a_{mn} = b_{nm} \quad 1 \leq m \leq M, \quad 1 \leq n \leq N. \quad (2.1.1)$$

Suppose that $\mathbf{A} \in \mathbb{R}^{I \times J}$, $\mathbf{B} \in \mathbb{R}^{J \times K}$ and $\mathbf{C} \in \mathbb{R}^{I \times K}$. Recall that *matrix multiplication* is defined for the matrices $\mathbf{A}, \mathbf{B}, \mathbf{C}$ via

$$\mathbf{C} := \mathbf{AB},$$

where the entry c_{ik} of \mathbf{C} is given by the formula

$$c_{ik} := \sum_{j=1}^J a_{ij} b_{jk}$$

for $i = 1 \dots I$, $k = 1 \dots K$. This definition is meaningful only if the number of columns of \mathbf{A} is equal to the number of rows of \mathbf{B} . The result of multiplying matrices \mathbf{A} and \mathbf{B} is a matrix \mathbf{C} that has the same number of rows as \mathbf{A} and the same number of columns as \mathbf{B} .

The previously stated convention that N -tuples are interpreted as columns means that an N -tuple may also be interpreted as an $N \times 1$ array. This fact has many implications. In particular, it means that the product $\mathbf{v} := \mathbf{Au}$ sensible whenever the number of columns of the $M \times N$ array \mathbf{A} is equal to the length of the N -tuple \mathbf{u} . By definition, the vector \mathbf{v} is an M -tuple,

$$\mathbf{v} := \mathbf{Au} \Leftrightarrow v_m = \sum_{n=1}^N a_{mn} u_n \quad \text{for } m = 1, \dots, M.$$

An array is said to be a *sparse matrix* if the number of zero elements overwhelmingly exceeds the number of nonzero elements. Otherwise, it is called a *full matrix*. An array is a *square matrix* if it has the same number of rows and columns. The *main diagonal* or *principal diagonal* of a matrix $\mathbf{A} \in \mathbb{R}^{N \times N}$ is the collection of elements a_{jj} for $j = 1 \dots N$. An array is a *diagonal matrix* if its elements are equal to zero except on the main diagonal.

The *identity matrix* is the unique matrix denoted \mathbb{I} such that $\mathbf{AI} = \mathbb{I}\mathbf{A} = \mathbf{A}$ for every square matrix \mathbf{A} . The identity matrix is a diagonal matrix with ones for each element of its diagonal. The identity matrix will be used to help describe the *matrix inverse* in the following definition.

Definition 2.1 (Matrix Inverse). A square matrix $\mathbf{A} \in \mathbb{R}^{M \times M}$ is invertible if and only if there is a matrix \mathbf{B} such that

$$\mathbf{AB} = \mathbf{BA} = \mathbb{I}$$

where \mathbb{I} is the *identity matrix*. When such a matrix \mathbf{B} exists, the inverse matrix is unique and denoted as

$$\mathbf{A}^{-1} := \mathbf{B}$$

The *matrix inverse* arises in a natural way when solving a set of *linear matrix equations*. Given a set of equations having the matrix form

$$\mathbf{Au} = \mathbf{v},$$

and the matrix \mathbf{A} is invertible, both sides of the above equation can be multiplied by \mathbf{A}^{-1} to obtain a solution for \mathbf{u} :

$$\mathbf{A}^{-1}\mathbf{Au} = \mathbb{I}\mathbf{u} = \mathbf{u} = \mathbf{A}^{-1}\mathbf{v}.$$

A discussion of the existence and uniqueness of solutions to such systems of linear matrix equations can be found in Appendix (8). This inverse \mathbf{A}^{-1} may be calculated in closed form analytically or iteratively using a numerical solver. Both cases are important in the dynamics and control of autonomous systems. Another consequence of identifying an M -tuple as an $M \times 1$ array is the ability to partition an $M \times N$ array \mathbf{A} into its columns

$$\mathbf{A} := [\mathbf{a}_1 \ \mathbf{a}_2 \ \mathbf{a}_3 \ \dots \ \mathbf{a}_N]. \quad (2.1.2)$$

By definition, each of the columns \mathbf{a}_n for $n = 1 \dots N$ is an M -tuple, or $M \times 1$ array. It is also possible to partition a matrix by rows by observing that the transpose of an $M \times 1$ array is a $1 \times M$ array. Since the convention is that any M -tuple \mathbf{u} corresponds to a column, the $1 \times M$ array is denoted by \mathbf{u}^T . As a result, the $N \times M$ matrix obtained by taking the transpose \mathbf{A}^T of the matrix \mathbf{A} in (2.1.2) is just

$$\mathbf{A}^T = \begin{bmatrix} \mathbf{a}_1^T \\ \mathbf{a}_2^T \\ \vdots \\ \mathbf{a}_N^T \end{bmatrix}.$$

Finally, suppose that $\mathbf{A}^T \in \mathbb{R}^{I \times J}$ and $\mathbf{B} \in \mathbb{R}^{J \times K}$, so that the product $\mathbf{A}^T\mathbf{B}$ is valid. This matrix product can be calculated by the *conformal partition* of the matrices \mathbf{A}^T and \mathbf{B} into rows, and columns, respectively.

$$\mathbf{A}^T \mathbf{B} = \begin{bmatrix} \mathbf{a}_1^T \\ \mathbf{a}_2^T \\ \vdots \\ \mathbf{a}_I^T \end{bmatrix} \begin{bmatrix} \mathbf{b}_1 & \mathbf{b}_2 & \mathbf{b}_3 & \dots & \mathbf{b}_K \end{bmatrix} = \begin{bmatrix} \mathbf{a}_1^T \mathbf{b}_1 & \mathbf{a}_1^T \mathbf{b}_2 & \dots & \mathbf{a}_1^T \mathbf{b}_K \\ \mathbf{a}_2^T \mathbf{b}_1 & \mathbf{a}_2^T \mathbf{b}_2 & \dots & \mathbf{a}_2^T \mathbf{b}_K \\ \vdots & \ddots & \dots & \vdots \\ \mathbf{a}_I^T \mathbf{b}_1 & \mathbf{a}_I^T \mathbf{b}_2 & \dots & \mathbf{a}_I^T \mathbf{b}_K \end{bmatrix}. \quad (2.1.3)$$

Each of the entries $\mathbf{a}_i^T \mathbf{b}_k = \mathbf{a}_i \cdot \mathbf{b}_k$ is the dot product of the J -tuples \mathbf{a}_i and \mathbf{b}_k , for $i = 1 \dots I$ and $k = 1 \dots K$. Other examples of *conformal partitions* of products of matrices are discussed in the problems.

2.1.2 Vectors, Bases and Frames

In the previous section, N -tuples and $M \times N$ arrays were defined, and techniques for manipulating them were discussed. In this section, *vectors* in \mathbb{R}^3 are introduced. While not every 3-tuple is a vector in \mathbb{R}^3 , all vectors in \mathbb{R}^3 are 3-tuples. As a result, the methods for organizing and manipulating 3-tuples discussed in the Section (2.1.1) will be applied to the representation of vectors.

However, a vector is a much more general construct than an N -tuple. A vector is defined to be an element of a vector space, which can contain abstract mathematical objects. For example, in the discussion of analytical mechanics in Chapter (5), more general notions of vectors are introduced. The directions or variations that arise in statements of variational calculus can be construed as vectors that exist in a suitably defined vector space. Section (8.1) of the appendix summarizes some of the most fundamental properties of *vector spaces*. Some texts do not distinguish between N -tuples of numbers and vectors. See for example [18]. However, the distinction between N -tuples and vectors in a general setting can be considerably more abstract, and the interested reader can study [34] or [9] for details.

The level of rigor and abstraction introduced in [9] is an important tool in graduate treatments of dynamics and control: topics including differential geometry or Lie algebra can provide important insights into the structure of different problems. These topics require substantially more preparation in the mathematics that underlie *vector spaces*, *tensor analysis* and the foundations of *manifolds*. An example of the applications of these foundations in robotics can be found in [36].

In this text, only those properties of vectors that will aid in solving specific problems in the dynamics and control of robotic systems at an undergraduate or beginning graduate level are introduced. In this chapter, it is important to note the following differences between an N -tuple and vector in \mathbb{R}^N .

- Vectors are mathematical entities characterized by a direction and length. An N -tuple is just an ordered collection of numbers.
- Physically observable, or measurable, quantities such as velocity, angular velocity, and momentum are idealized as vectors.
- Vectors obey *transformation laws* or *change of basis* formulae. The physically observable quantities they represent also transform according to these rules.

- A vector has an infinite number of different yet equivalent *representations*.
- Each *representation* of a vector specifies the *coordinates* or *components* of the *vector* with respect to a specific *basis* or *frame*.

This presentation of vectors will proceed with a review of their basic properties in Section (2.1.2.1), followed by a discussion of the transformation laws used in the change of basis formulae in Sections (2.1.2.2) and (2.2).

2.1.2.1 Vectors

A *vector* \mathbf{v} in \mathbb{R}^3 is represented by a 3-tuple and is characterized by its direction and length. The length of a vector $\mathbf{v} \in \mathbb{R}^3$ is given by the norm of the 3-tuple

$$\text{length}(\mathbf{v}) = \|\mathbf{v}\| = \left\{ \sum_{i=1}^3 |v_i|^2 \right\}^{\frac{1}{2}},$$

while its direction is given by the *unit vector* \mathbf{u}

$$\text{direction}(\mathbf{v}) = \mathbf{u} = \frac{\mathbf{v}}{\|\mathbf{v}\|}.$$

It is immediate that the length of a unit vector $\text{length}(\mathbf{u}) = 1$. In Section (2.1.1) the dot product of two N -tuples \mathbf{u}, \mathbf{v} is defined to be

$$\mathbf{u} \cdot \mathbf{v} = u_1 v_1 + u_2 v_2 + u_3 v_3. \quad (2.1.4)$$

It is well known from introductory calculus that the dot product of \mathbf{u} and \mathbf{v} can also be written as

$$\mathbf{u} \cdot \mathbf{v} = \|\mathbf{u}\| \|\mathbf{v}\| \cos \theta_{\mathbf{u}, \mathbf{v}} \quad (2.1.5)$$

where $\cos \theta_{\mathbf{u}, \mathbf{v}}$ is the cosine of the angle $\theta_{\mathbf{u}, \mathbf{v}}$ between the vectors \mathbf{u} and \mathbf{v} . Finally, the *cross product* \mathbf{w} of two vectors \mathbf{u}, \mathbf{v} in \mathbb{R}^3 is defined by

$$\mathbf{w} = \mathbf{u} \times \mathbf{v} \quad (2.1.6)$$

where

$$\mathbf{w} = \begin{Bmatrix} w_1 \\ w_2 \\ w_3 \end{Bmatrix} = \begin{Bmatrix} u_2 v_3 - u_3 v_2 \\ u_3 v_1 - u_1 v_3 \\ u_1 v_2 - v_1 u_2 \end{Bmatrix}.$$

Note that the dot product yields a scalar, whereas the cross product defines a vector. The length of the cross product of two vectors satisfies a formula similar to Equation (2.1.5).

$$\|\mathbf{u} \times \mathbf{v}\| = \|\mathbf{u}\| \|\mathbf{v}\| \sin \theta_{\mathbf{u}, \mathbf{v}}$$

There are many alternatives that are commonly used to represent the cross product in Equation (2.1.6). One that will be used frequently in this text, particularly in

applications to robotics, makes use of the *skew operator* $\mathbf{S}(\cdot)$. The skew operator $\mathbf{S}(\cdot)$ assigns to a vector \mathbf{u} the matrix

$$\mathbf{S}(\mathbf{u}) := \begin{bmatrix} 0 & -u_3 & u_2 \\ u_3 & 0 & -u_1 \\ -u_2 & u_1 & 0 \end{bmatrix}.$$

The cross product $\mathbf{w} = \mathbf{u} \times \mathbf{v}$ is then expressed as the action of a matrix on the vector \mathbf{v} in

$$\begin{aligned} \mathbf{w} &= \mathbf{u} \times \mathbf{v}, \\ &= \mathbf{S}(\mathbf{u})\mathbf{v}, \\ &= \begin{bmatrix} 0 & -u_3 & u_2 \\ u_3 & 0 & -u_1 \\ -u_2 & u_1 & 0 \end{bmatrix} \begin{Bmatrix} v_1 \\ v_2 \\ v_3 \end{Bmatrix}. \end{aligned}$$

2.1.2.2 Bases and Frames

A *coordinate system* or *frame* \mathbb{X} for a vector in \mathbb{R}^3 is defined by a *right-handed (dextral)*, *orthonormal* collection of three vectors $\mathbf{x}_i \in \mathbb{R}^3$ where $i = 1, 2, 3$. The set of vectors \mathbf{x}_i for $i = 1, 2, 3$ is called the *basis* for the *frame* \mathbb{X} .

Saying $\mathbf{x}_1, \mathbf{x}_2, \mathbf{x}_3$ is a *dextral, orthonormal* collection of vectors is a compact way of describing three properties of this set of vectors:

- each is a unit vector,
- each vector is perpendicular to the other two, and
- the vectors permute cyclically under the cross product.

The first property enforces three independent constraints on the magnitude of the three basis vectors \mathbf{x}_i , such that

$$\|\mathbf{x}_i\| = 1 \quad i = 1, 2, 3.$$

The second property enforces three additional independent constraints on the dot products of pairs of the three basis vectors, such that

$$\mathbf{x}_i \cdot \mathbf{x}_j = 0 \quad \text{when } i \neq j,$$

The third property dictates the relative directions of the vectors (positive or negative) along the axes specified by the first two properties.

Sets of vectors that satisfy the first two of these conditions (mutually orthogonal unit vectors) are said to be *orthonormal*. A more concise way of stating the orthonormality condition is

$$\mathbf{x}_i \cdot \mathbf{x}_j = \delta_{ij} \tag{2.1.7}$$

where δ_{ij} is the Kronecker Delta function,

$$\delta_{ij} = \begin{cases} 0 & \text{if } i \neq j, \\ 1 & \text{if } i = j. \end{cases} \quad (2.1.8)$$

This definition takes advantage of the fact that the norm of a unit vector is the same as the dot product of the unit vector with itself.

Saying these vectors define a *right-handed* or *dextral* basis means that the basis vectors permute cyclically under the cross product. Vectors that permute cyclically under the cross product satisfy

$$\mathbf{x}_i \times \mathbf{x}_j = \mathbf{x}_k$$

where $\{i, j, k\} = \{1, 2, 3\}, \{2, 3, 1\}$ or $\{3, 1, 2\}$. Since the sign of the cross product changes if the order of the vectors in the cross product is changed, it follows that $\mathbf{x}_i \times \mathbf{x}_j = -\mathbf{x}_k$ whenever $\{i, j, k\} = \{2, 1, 3\}, \{3, 2, 1\}$ or $\{1, 3, 2\}$. Figure (2.4) is a graphic representation of how vectors permute cyclically under the cross product.

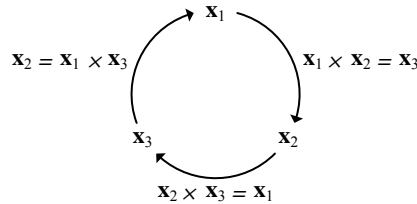


Fig. 2.4: Cyclic Permutations for Vectors $\mathbf{x}_1, \mathbf{x}_2, \mathbf{x}_3$

These observations are summarized in the following definition.

Definition 2.2 (Vector Basis/Frame). A *basis* or *frame* \mathbb{X} in \mathbb{R}^3 is defined by a set $\{\mathbf{x}_1, \mathbf{x}_2, \mathbf{x}_3\}$ of *orthonormal* vectors that permute cyclically under the cross product according to the right hand rule.

Another common approach used both in this textbook and the broader literature is to denote the three orthogonal basis vectors as $\mathbf{x}_i, \mathbf{y}_i$ and \mathbf{z}_i for frame i . In this notation, the vector denotes the specific basis vector, and the subscript denotes the associated frame (as opposed to the vector specifying the frame, and the subscript specifying the basis vector as defined earlier in this section). This approach is particularly useful when using numbers to name frames, as in Example 2.4.1.

The next example shows the need models for practical robotic systems have for numerous frames of reference and emphasizes the need for systematic techniques to model these systems.

Example 2.1.1. Consider the humanoid robot depicted in Figure (2.3). Create a detailed figure of one leg and its connectivity to the pelvis. Define a collection of

frames or bases, each of which moves with a particular rigid body in the leg sub-assembly. This set is a collection of body fixed frames for the mechanical system. Describe how each pair of adjacent frames in the leg assembly move relative to one another as the leg undergoes general motion.

Solution: Figures (2.5) and (2.6) depict the model representing the humanoid robot. There are many choices of individual frames that make sense for this problem. Specific conventions for defining frames for robotic systems are studied in Chapter (3). The detailed definitions of the body fixed frames in this example are shown in Figure (2.6).

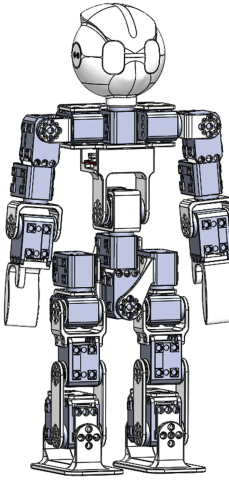


Fig. 2.5: Detailed model of humanoid robot

The frames are denoted as \mathbb{A} through \mathbb{G} , having bases $(\mathbf{a}_1, \mathbf{a}_2, \mathbf{a}_3)$ through $(\mathbf{g}_1, \mathbf{g}_2, \mathbf{g}_3)$, respectively. Each frame is fixed in a particular rigid body. In this example,

Frame	Description	Frame Color
\mathbb{A}	Fixed in rigid body \mathbb{A} that models the pelvis	Red
\mathbb{B}	Fixed in rigid body \mathbb{B} that models the upper hip	Blue
\mathbb{C}	Fixed in rigid body \mathbb{C} that models the lower hip	Orange
\mathbb{D}	Fixed in rigid body \mathbb{C} that models the thigh	Green
\mathbb{E}	Fixed in rigid body \mathbb{E} that models the shin	Red
\mathbb{F}	Fixed in rigid body \mathbb{F} that models the ankle	Blue
\mathbb{G}	Fixed in rigid body \mathbb{G} that models the foot	Orange

For this set of frames, there is a single frame fixed to each rigid body. However, this need not be the case. It is often convenient to have multiple frames fixed to a single body. For example, a frame may be included for each joint, along with a frame at the center of mass. This portion of the robot is constructed of eight rigid

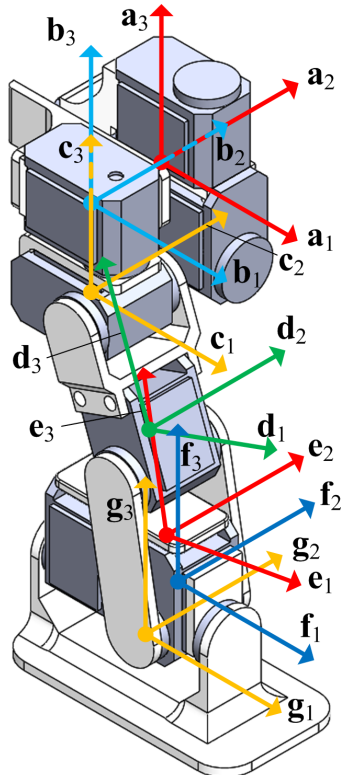


Fig. 2.6: Detailed model of leg assembly

bodies that connected to each other by seven *revolute joints*. Each pair of frames that are fixed to adjacent rigid bodies rotate relative to one another about a common axis. While the net motion of the leg assembly can be complex, the relative motion of each pair of adjacent frames is simple. The seven joints between adjacent pairs of rigid bodies are detailed below, including the axes in each frame parallel to the revolute joint axis

Rigid Body 1	Rigid Body 2	Axes Parallel to Revolute Joint Axis
A	B	a_1 and b_1
B	C	b_3 and c_3
C	D	c_2 and d_2
D	E	d_2 and e_2
D	F	e_2 and f_2
F	G	f_1 and g_1

Given a basis $\{\mathbf{x}_1, \mathbf{x}_2, \mathbf{x}_3\}$, any *vector* \mathbf{v} in \mathbb{R}^3 can be expressed *uniquely* in terms of the basis vectors,

$$\mathbf{v} = v_1^{\mathbb{X}} \mathbf{x}_1 + v_2^{\mathbb{X}} \mathbf{x}_2 + v_3^{\mathbb{X}} \mathbf{x}_3 = \sum_{i=1}^3 v_i^{\mathbb{X}} \mathbf{x}_i, \quad (2.1.9)$$

where the coefficients $\mathbf{v}^{\mathbb{X}} := \{v_1^{\mathbb{X}}, v_2^{\mathbb{X}}, v_3^{\mathbb{X}}\}^T$ are the *components* or *coordinates* of the vector \mathbf{v} with respect to the $\{\mathbf{x}_1, \mathbf{x}_2, \mathbf{x}_3\}$ basis vectors. If $\mathbf{u} = \sum_{i=1}^3 u_i^{\mathbb{X}} \mathbf{x}_i$ is another vector expressed in the same basis \mathbb{X} , then the dot product is defined to be

$$\mathbf{u} \cdot \mathbf{v} = \mathbf{u}^T \mathbf{v} = \mathbf{v}^T \mathbf{u} = \sum_{i=1}^3 u_i^{\mathbb{X}} v_i^{\mathbb{X}}.$$

Using the orthonormality of the basis vector \mathbb{X} , a direct calculation shows that

$$v_i^{\mathbb{X}} = \mathbf{v} \cdot \mathbf{x}_i \quad \text{and} \quad u_i^{\mathbb{X}} = \mathbf{u} \cdot \mathbf{x}_i.$$

These facts are summarized in the following theorem.

Theorem 2.1 (Vector Coordinates). Let $\mathbf{x}_1, \mathbf{x}_2, \mathbf{x}_3$ be the basis for the frame \mathbb{X} in \mathbb{R}^3 . For any vector $\mathbf{v} \in \mathbb{R}^3$, there is a unique expansion $\mathbf{v} = \sum_{i=1}^3 v_i^{\mathbb{X}} \mathbf{x}_i$. The coefficients $v_1^{\mathbb{X}}, v_2^{\mathbb{X}}, v_3^{\mathbb{X}}$ are the coordinates or components of the vector \mathbf{v} with respect to the \mathbb{X} -frame. The coordinates $\mathbf{v}^{\mathbb{X}}$ of the vector \mathbf{v} with respect to the \mathbb{X} frame are defined as

$$\mathbf{v}^{\mathbb{X}} := \begin{Bmatrix} v_1^{\mathbb{X}} \\ v_2^{\mathbb{X}} \\ v_3^{\mathbb{X}} \end{Bmatrix} = \begin{Bmatrix} \mathbf{v} \cdot \mathbf{x}_1 \\ \mathbf{v} \cdot \mathbf{x}_2 \\ \mathbf{v} \cdot \mathbf{x}_3 \end{Bmatrix}$$

Suppose that the vectors \mathbf{u} and \mathbf{v} are defined as above and that $\mathbf{w} = \sum_{i=1}^3 w_i^{\mathbb{X}} \mathbf{x}_i$. The vector \mathbf{w} is the cross product of \mathbf{u} and \mathbf{v} , that is $\mathbf{w} = \mathbf{u} \times \mathbf{v}$, if the components of these vectors satisfy the equation

$$\begin{Bmatrix} w_1^{\mathbb{X}} \\ w_2^{\mathbb{X}} \\ w_3^{\mathbb{X}} \end{Bmatrix} = \begin{bmatrix} 0 & -u_3^{\mathbb{X}} & u_2^{\mathbb{X}} \\ u_3^{\mathbb{X}} & 0 & -u_1^{\mathbb{X}} \\ -u_2^{\mathbb{X}} & u_1^{\mathbb{X}} & 0 \end{bmatrix} \begin{Bmatrix} v_1^{\mathbb{X}} \\ v_2^{\mathbb{X}} \\ v_3^{\mathbb{X}} \end{Bmatrix} \quad \iff \quad \mathbf{w}^{\mathbb{X}} = \mathbf{S}(\mathbf{u}^{\mathbb{X}})\mathbf{v}^{\mathbb{X}}.$$

There is an infinite number of bases or frames for \mathbb{R}^3 . Suppose two frames with different sets of basis vectors in \mathbb{R}^3 are given: frame \mathbb{X} with basis $\{\mathbf{x}_1, \mathbf{x}_2, \mathbf{x}_3\}$, and frame \mathbb{Y} with basis $\{\mathbf{y}_1, \mathbf{y}_2, \mathbf{y}_3\}$. For any arbitrary vector $\mathbf{v} \in \mathbb{R}^3$ there is a unique expansion having the form in Equation (2.1.9). There is also a unique expansion for the vector \mathbf{v} in terms of the basis $\{\mathbf{y}_1, \mathbf{y}_2, \mathbf{y}_3\}$

$$\mathbf{v} = v_1^{\mathbb{Y}} \mathbf{y}_1 + v_2^{\mathbb{Y}} \mathbf{y}_2 + v_3^{\mathbb{Y}} \mathbf{y}_3 = \sum_{i=1}^3 v_i^{\mathbb{Y}} \mathbf{y}_i. \quad (2.1.10)$$

Given the orthonormality of the two sets of basis vectors, a matrix relationship between the two vector representations, and by extension, the two frames, may be defined. The following theorem provides a concise solution to the problem of relating $\mathbf{v}^{\mathbb{X}}$ and $\mathbf{v}^{\mathbb{Y}}$.

Theorem 2.2 (Changing Vector Frame). Let \mathbb{X} and \mathbb{Y} be two frames in \mathbb{R}^3 and let $\mathbf{v}^{\mathbb{X}}$ and $\mathbf{v}^{\mathbb{Y}}$ be the coordinate representations of a fixed vector \mathbf{v} with respect to the frames \mathbb{X} and \mathbb{Y} , respectively. The coordinate representations $\mathbf{v}^{\mathbb{X}}$ and $\mathbf{v}^{\mathbb{Y}}$ are related by the matrix equations

$$\mathbf{v}^{\mathbb{X}} = \mathbf{R}_{\mathbb{Y}}^{\mathbb{X}} \mathbf{v}^{\mathbb{Y}} \quad (2.1.11)$$

$$\mathbf{v}^{\mathbb{Y}} = \mathbf{R}_{\mathbb{X}}^{\mathbb{Y}} \mathbf{v}^{\mathbb{X}} \quad (2.1.12)$$

where the matrices $\mathbf{R}_{\mathbb{Y}}^{\mathbb{X}}$ and $\mathbf{R}_{\mathbb{X}}^{\mathbb{Y}}$ are defined as

$$\mathbf{R}_{\mathbb{Y}}^{\mathbb{X}} = \begin{bmatrix} (\mathbf{x}_1 \cdot \mathbf{y}_1) & (\mathbf{x}_1 \cdot \mathbf{y}_2) & (\mathbf{x}_1 \cdot \mathbf{y}_3) \\ (\mathbf{x}_2 \cdot \mathbf{y}_1) & (\mathbf{x}_2 \cdot \mathbf{y}_2) & (\mathbf{x}_2 \cdot \mathbf{y}_3) \\ (\mathbf{x}_3 \cdot \mathbf{y}_1) & (\mathbf{x}_3 \cdot \mathbf{y}_2) & (\mathbf{x}_3 \cdot \mathbf{y}_3) \end{bmatrix}$$

$$\mathbf{R}_{\mathbb{X}}^{\mathbb{Y}} = \begin{bmatrix} (\mathbf{y}_1 \cdot \mathbf{x}_1) & (\mathbf{y}_1 \cdot \mathbf{x}_2) & (\mathbf{y}_1 \cdot \mathbf{x}_3) \\ (\mathbf{y}_2 \cdot \mathbf{x}_1) & (\mathbf{y}_2 \cdot \mathbf{x}_2) & (\mathbf{y}_2 \cdot \mathbf{x}_3) \\ (\mathbf{y}_3 \cdot \mathbf{x}_1) & (\mathbf{y}_3 \cdot \mathbf{x}_2) & (\mathbf{y}_3 \cdot \mathbf{x}_3) \end{bmatrix}$$

Proof. Given that Equations (2.1.9) and (2.1.10) are both equal to \mathbf{v} , they may be set equal to one another. By taking the dot product of both sides of these equations with \mathbf{x}_1 , \mathbf{x}_2 and \mathbf{x}_3 , the following three equations are obtained

$$\begin{aligned} & \left\{ \begin{array}{l} v_1^{\mathbb{X}}(\mathbf{x}_1 \cdot \mathbf{x}_1) + v_2^{\mathbb{X}}(\mathbf{x}_1 \cdot \mathbf{x}_2) + v_3^{\mathbb{X}}(\mathbf{x}_1 \cdot \mathbf{x}_3) \\ v_1^{\mathbb{X}}(\mathbf{x}_2 \cdot \mathbf{x}_1) + v_2^{\mathbb{X}}(\mathbf{x}_2 \cdot \mathbf{x}_2) + v_3^{\mathbb{X}}(\mathbf{x}_2 \cdot \mathbf{x}_3) \\ v_1^{\mathbb{X}}(\mathbf{x}_3 \cdot \mathbf{x}_1) + v_2^{\mathbb{X}}(\mathbf{x}_3 \cdot \mathbf{x}_2) + v_3^{\mathbb{X}}(\mathbf{x}_3 \cdot \mathbf{x}_3) \end{array} \right\} \\ &= \left\{ \begin{array}{l} v_1^{\mathbb{Y}}(\mathbf{x}_1 \cdot \mathbf{y}_1) + v_2^{\mathbb{Y}}(\mathbf{x}_1 \cdot \mathbf{y}_2) + v_3^{\mathbb{Y}}(\mathbf{x}_1 \cdot \mathbf{y}_3) \\ v_1^{\mathbb{Y}}(\mathbf{x}_2 \cdot \mathbf{y}_1) + v_2^{\mathbb{Y}}(\mathbf{x}_2 \cdot \mathbf{y}_2) + v_3^{\mathbb{Y}}(\mathbf{x}_2 \cdot \mathbf{y}_3) \\ v_1^{\mathbb{Y}}(\mathbf{x}_3 \cdot \mathbf{y}_1) + v_2^{\mathbb{Y}}(\mathbf{x}_3 \cdot \mathbf{y}_2) + v_3^{\mathbb{Y}}(\mathbf{x}_3 \cdot \mathbf{y}_3) \end{array} \right\}. \end{aligned}$$

By orthonormality of the \mathbb{X} basis, all of the dot products on the left hand side of these equations are either zero or one. These equations can be written as a matrix relationship between the \mathbb{X} basis and \mathbb{Y} basis coefficients:

$$\begin{Bmatrix} v_1^{\mathbb{X}} \\ v_2^{\mathbb{X}} \\ v_3^{\mathbb{X}} \end{Bmatrix} = \begin{bmatrix} (\mathbf{x}_1 \cdot \mathbf{y}_1) & (\mathbf{x}_1 \cdot \mathbf{y}_2) & (\mathbf{x}_1 \cdot \mathbf{y}_3) \\ (\mathbf{x}_2 \cdot \mathbf{y}_1) & (\mathbf{x}_2 \cdot \mathbf{y}_2) & (\mathbf{x}_2 \cdot \mathbf{y}_3) \\ (\mathbf{x}_3 \cdot \mathbf{y}_1) & (\mathbf{x}_3 \cdot \mathbf{y}_2) & (\mathbf{x}_3 \cdot \mathbf{y}_3) \end{bmatrix} \begin{Bmatrix} v_1^{\mathbb{Y}} \\ v_2^{\mathbb{Y}} \\ v_3^{\mathbb{Y}} \end{Bmatrix}. \quad (2.1.13)$$

Alternatively, the dot product on both sides of these equations may be taken with \mathbf{y}_1 , \mathbf{y}_2 and \mathbf{y}_3 to construct a matrix expression that explicitly solves for the \mathbb{Y} -frame coefficients:

$$\begin{Bmatrix} v_1^{\mathbb{Y}} \\ v_2^{\mathbb{Y}} \\ v_3^{\mathbb{Y}} \end{Bmatrix} = \begin{bmatrix} (\mathbf{y}_1 \cdot \mathbf{x}_1) & (\mathbf{y}_1 \cdot \mathbf{x}_2) & (\mathbf{y}_1 \cdot \mathbf{x}_3) \\ (\mathbf{y}_2 \cdot \mathbf{x}_1) & (\mathbf{y}_2 \cdot \mathbf{x}_2) & (\mathbf{y}_2 \cdot \mathbf{x}_3) \\ (\mathbf{y}_3 \cdot \mathbf{x}_1) & (\mathbf{y}_3 \cdot \mathbf{x}_2) & (\mathbf{y}_3 \cdot \mathbf{x}_3) \end{bmatrix} \begin{Bmatrix} v_1^{\mathbb{X}} \\ v_2^{\mathbb{X}} \\ v_3^{\mathbb{X}} \end{Bmatrix}. \quad (2.1.14)$$

Equations (2.1.13) and (2.1.14) give a complete description of how the coefficients of any vector that is expressed with respect to the two different frames \mathbb{X} and \mathbb{Y} can be related. \square

Note that the above definitions of $\mathbf{R}_{\mathbb{Y}}^{\mathbb{X}}$ and $\mathbf{R}_{\mathbb{X}}^{\mathbb{Y}}$ satisfy the equation

$$(\mathbf{R}_{\mathbb{Y}}^{\mathbb{X}})^T = \mathbf{R}_{\mathbb{X}}^{\mathbb{Y}}.$$

As discussed in the next section, this property that the matrix associated with an inverse transformation is simply the transpose of the original transformation matrix is of fundamental importance in kinematics. Sections 2.2 will show that $\mathbf{R}_{\mathbb{Y}}^{\mathbb{X}}$ and $\mathbf{R}_{\mathbb{X}}^{\mathbb{Y}}$ are examples of *rotation matrices* or *direction cosine matrices* and play a key role in spatial robot kinematics.

Example 2.1.2. Consider a pair of frames \mathbb{A} and \mathbb{B} that share a common origin and have a single common basis vector $\mathbf{a}_3 = \mathbf{b}_3$. From an initial alignment with frame \mathbb{A} , the \mathbb{B} frame is rotated 30° counter-clockwise about the \mathbf{a}_3 axis in relation to the \mathbb{A} frame, as shown in Figure (2.7). The vector \mathbf{v} relative to the \mathbb{A} frame is defined as $\mathbf{v}^{\mathbb{A}} = \begin{Bmatrix} 1 & 1.2 & 1.5 \end{Bmatrix}^T$. Calculate the representation of vector \mathbf{v} in relation to frame \mathbb{B} , or $\mathbf{v}^{\mathbb{B}}$.

Solution: The matrix $\mathbf{R}_{\mathbb{A}}^{\mathbb{B}}$ is used to change the basis from the \mathbb{A} frame to the \mathbb{B} frame using the equation $\mathbf{v}^{\mathbb{B}} = \mathbf{R}_{\mathbb{A}}^{\mathbb{B}} \mathbf{v}^{\mathbb{A}}$. This matrix $\mathbf{R}_{\mathbb{A}}^{\mathbb{B}}$ may be constructed using the expression in Theorem (2.2)

$$\mathbf{R}_{\mathbb{A}}^{\mathbb{B}} = \begin{bmatrix} \mathbf{b}_1 \cdot \mathbf{a}_1 & \mathbf{b}_1 \cdot \mathbf{a}_2 & \mathbf{b}_1 \cdot \mathbf{a}_3 \\ \mathbf{b}_2 \cdot \mathbf{a}_1 & \mathbf{b}_2 \cdot \mathbf{a}_2 & \mathbf{b}_2 \cdot \mathbf{a}_3 \\ \mathbf{b}_3 \cdot \mathbf{a}_1 & \mathbf{b}_3 \cdot \mathbf{a}_2 & \mathbf{b}_3 \cdot \mathbf{a}_3 \end{bmatrix}.$$

The basis vectors are unit vectors which implies that the dot products reduce to the cosine of the angle between each pair of unit vectors. For the geometry described in this problem,

$$\mathbf{R}_{\mathbb{A}}^{\mathbb{B}} = \begin{bmatrix} \cos 30^\circ & \cos 60^\circ & 0 \\ \cos 120^\circ & \cos 30^\circ & 0 \\ 0 & 0 & 1 \end{bmatrix},$$

which may be further simplified into a form that only utilized the rotation angle 30° as the trigonometric argument

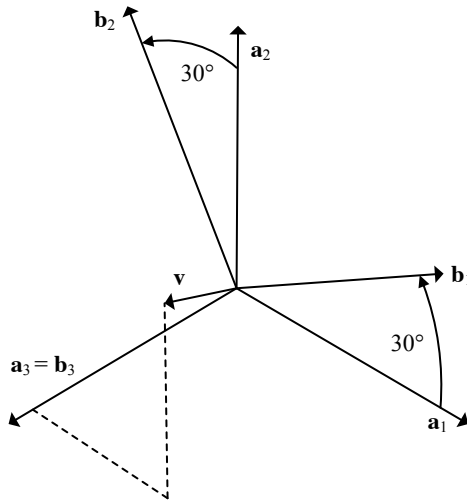


Fig. 2.7: Frames A and B and vector v for Example (2.1.2)

$$\mathbf{R}_A^B = \begin{bmatrix} \cos 30^\circ & \sin 30^\circ & 0 \\ -\sin 30^\circ & \cos 30^\circ & 0 \\ 0 & 0 & 1 \end{bmatrix}.$$

Using this form of \mathbf{R}_A^B , \mathbf{v}^B may be calculated as

$$\mathbf{v}^B = \mathbf{R}_A^B \mathbf{v}^A = \begin{bmatrix} 0.866 & .5 & 0 \\ -.5 & .866 & 0 \\ 0 & 0 & 1 \end{bmatrix} \begin{Bmatrix} 1 \\ 1.2 \\ 1.5 \end{Bmatrix} = \begin{Bmatrix} 1.466 \\ .538 \\ 1.5 \end{Bmatrix}.$$

2.2 Rotation Matrices

In the last section equations were derived that relate the components v^X and v^Y of a vector v expressed in frames X and Y, respectively. In this section, the relationships in Equations (2.1.13) and (2.1.14) will be demonstrated as *rotation matrices*. Since these are used extensively throughout the book, they will be studied in detail.

Definition 2.3 (Rotation Matrix). A rotation matrix, or orthogonal matrix, is a matrix \mathbf{R} for which its inverse \mathbf{R}^{-1} is equal to its transpose \mathbf{R}^T , that is

$$\mathbf{R}^{-1} = \mathbf{R}^T$$

A rotation matrix \mathbf{R} corresponds to a right-hand, or dextral, basis if $\det(\mathbf{R}) = +1$. A rotation matrix \mathbf{R} corresponds to a left-hand, or sinister, basis if $\det(\mathbf{R}) = -1$.

Recalling the notation introduced in Theorem (2.2), if \mathbb{X} and \mathbb{Y} are frames, then the coordinate representations $\mathbf{v}^{\mathbb{X}}$ and $\mathbf{v}^{\mathbb{Y}}$ of a vector \mathbf{v} with respect to these two frames are related via the formulae

$$\mathbf{v}^{\mathbb{X}} = \mathbf{R}_{\mathbb{Y}}^{\mathbb{X}} \mathbf{v}^{\mathbb{Y}}, \quad (2.2.1)$$

$$\mathbf{v}^{\mathbb{Y}} = \mathbf{R}_{\mathbb{X}}^{\mathbb{Y}} \mathbf{v}^{\mathbb{X}}. \quad (2.2.2)$$

The matrix $\mathbf{R}_{\mathbb{Y}}^{\mathbb{X}}$ maps the vector \mathbf{v} \mathbb{Y} -frame components into the \mathbb{X} -frame components. Conversely, the matrix $\mathbf{R}_{\mathbb{X}}^{\mathbb{Y}}$ maps the vector \mathbf{v} \mathbb{X} -frame components into the \mathbb{Y} -frame components. Thus, this pair of equations defines a *change of basis formula*.

Theorem 2.3 (Rotation Matrix as Change of Basis).

The matrices $\mathbf{R}_{\mathbb{Y}}^{\mathbb{X}}$ and $\mathbf{R}_{\mathbb{X}}^{\mathbb{Y}}$ in the change of basis formulae (2.1.11) and (2.1.12) are rotation matrices, such that

$$(\mathbf{R}_{\mathbb{X}}^{\mathbb{Y}})^{-1} = (\mathbf{R}_{\mathbb{X}}^{\mathbb{Y}})^T = \mathbf{R}_{\mathbb{Y}}^{\mathbb{X}}$$

Proof. Begin by substituting Equation (2.2.1) into (2.2.2), and factor out $\mathbf{v}^{\mathbb{Y}}$.

$$(\mathbb{I} - \mathbf{R}_{\mathbb{X}}^{\mathbb{Y}} \mathbf{R}_{\mathbb{Y}}^{\mathbb{X}}) \mathbf{v}^{\mathbb{Y}} = \mathbf{0}.$$

Since this equation must hold for arbitrary $\mathbf{v}^{\mathbb{Y}}$, it must be true that

$$\mathbb{I} = \mathbf{R}_{\mathbb{X}}^{\mathbb{Y}} \mathbf{R}_{\mathbb{Y}}^{\mathbb{X}}. \quad (2.2.3)$$

By the same reasoning, substitute Equation (2.2.2) into (2.2.1), and factor out $\mathbf{v}^{\mathbb{X}}$,

$$(\mathbb{I} - \mathbf{R}_{\mathbb{Y}}^{\mathbb{X}} \mathbf{R}_{\mathbb{X}}^{\mathbb{Y}}) \mathbf{v}^{\mathbb{X}} = \mathbf{0}$$

from which it likewise follows that

$$\mathbb{I} = \mathbf{R}_{\mathbb{Y}}^{\mathbb{X}} \mathbf{R}_{\mathbb{X}}^{\mathbb{Y}}. \quad (2.2.4)$$

Equations (2.2.3) and (2.2.4) yield

$$\mathbb{I} = \mathbf{R}_{\mathbb{Y}}^{\mathbb{X}} \mathbf{R}_{\mathbb{X}}^{\mathbb{Y}} = \mathbf{R}_{\mathbb{X}}^{\mathbb{Y}} \mathbf{R}_{\mathbb{Y}}^{\mathbb{X}}$$

from which it may be observed that the matrices are inverses of one another,

$$\mathbf{R}_{\mathbb{Y}}^{\mathbb{X}} = (\mathbf{R}_{\mathbb{X}}^{\mathbb{Y}})^{-1}.$$

By inspection of Equations (2.1.13) and (2.1.14), these matrices are also transposes of one another. These two properties

$$(\mathbf{R}_{\mathbb{Y}}^{\mathbb{X}})^{-1} = (\mathbf{R}_{\mathbb{Y}}^{\mathbb{X}})^T, \quad (\mathbf{R}_{\mathbb{X}}^{\mathbb{Y}})^{-1} = (\mathbf{R}_{\mathbb{X}}^{\mathbb{Y}})^T,$$

together show that the two matrices under consideration are rotation matrices. \square

The definition of a rotation matrix in Definition (2.3) might not be intuitive at first glance, but the columns (or rows) of a rotation matrix have a simple interpretation. The columns (or rows) of an orthogonal matrix form a basis for \mathbb{R}^3 . If they permute cyclically under the cross product, the rotation matrix corresponds to a right-handed basis.

Theorem 2.4 (Rotation Matrix Properties).

Suppose that $\mathbf{R} = [\mathbf{r}_1 \ \mathbf{r}_2 \ \mathbf{r}_3]$ is a rotation matrix. Then

- (1) The columns $\{\mathbf{r}_i\}_{i=1,2,3}$ are a basis for \mathbb{R}^3 .
- (2) The determinant $\det(\mathbf{R}) = \det(\mathbf{R}^T) = \pm 1$.
- (3) The cross product $\mathbf{r}_1 \times \mathbf{r}_2 = \pm \mathbf{r}_3$.
- (4) The following statements are equivalent:
 - (4.1) The cross product $\mathbf{r}_1 \times \mathbf{r}_2 = +\mathbf{r}_3$.
 - (4.2) The determinant $\det(\mathbf{R}) = +1$.
 - (4.3) The columns (or rows) of \mathbf{R} form a right-handed basis.

Proof. First, partition \mathbf{R} as $\mathbf{R} = [\mathbf{r}_1 \ \mathbf{r}_2 \ \mathbf{r}_3]$ and its transpose \mathbf{R}^T as

$$\mathbf{R}^T = \begin{bmatrix} \mathbf{r}_1^T \\ \mathbf{r}_2^T \\ \mathbf{r}_3^T \end{bmatrix}.$$

The product $\mathbf{R}^T \mathbf{R}$ can then be written (see Equation (2.1.3)) as

$$\mathbf{R}^T \mathbf{R} = \begin{bmatrix} \mathbf{r}_1^T \\ \mathbf{r}_2^T \\ \mathbf{r}_3^T \end{bmatrix} \begin{bmatrix} \mathbf{r}_1 & \mathbf{r}_2 & \mathbf{r}_3 \end{bmatrix} = \begin{bmatrix} \mathbf{r}_1^T \mathbf{r}_1 & \mathbf{r}_1^T \mathbf{r}_2 & \mathbf{r}_1^T \mathbf{r}_3 \\ \mathbf{r}_2^T \mathbf{r}_1 & \mathbf{r}_2^T \mathbf{r}_2 & \mathbf{r}_2^T \mathbf{r}_3 \\ \mathbf{r}_3^T \mathbf{r}_1 & \mathbf{r}_3^T \mathbf{r}_2 & \mathbf{r}_3^T \mathbf{r}_3 \end{bmatrix} = \begin{bmatrix} 1 & 0 & 0 \\ 0 & 1 & 0 \\ 0 & 0 & 1 \end{bmatrix}. \quad (2.2.5)$$

The last equality on the right hand side follows from the definition of an orthogonal matrix. Recall that for any i, j , the product $\mathbf{r}_i^T \mathbf{r}_j$ is just the matrix multiplication of a 1×3 vector and a 3×1 vector. That is, $\mathbf{r}_i^T \mathbf{r}_j = \mathbf{r}_i \cdot \mathbf{r}_j$ for $i, j = 1, 2, 3$. The off-diagonal entries of the matrix equation in (2.2.5) yield $\mathbf{r}_1 \cdot \mathbf{r}_2 = \mathbf{r}_2 \cdot \mathbf{r}_3 = \mathbf{r}_3 \cdot \mathbf{r}_1 = 0$. This shows that each of the columns is orthogonal to the others. The diagonal entries of this matrix equation yield the scalar equations $\mathbf{r}_1 \cdot \mathbf{r}_1 = \mathbf{r}_2 \cdot \mathbf{r}_2 = \mathbf{r}_3 \cdot \mathbf{r}_3 = 1$. Hence,

each of the columns is a unit vector. Moreover, recall that the determinant $\det(\mathbf{R})$ is given by

$$\det(\mathbf{R}) = \mathbf{r}_1 \times \mathbf{r}_2 \cdot \mathbf{r}_3,$$

the scalar triple product (see Problem (2.12)). It is already established that the columns are mutually orthogonal. Hence, $\sin(\theta_{\mathbf{r}_1, \mathbf{r}_2}) = 1$ where $\theta_{\mathbf{r}_1, \mathbf{r}_2}$ is the angle between \mathbf{r}_1 and \mathbf{r}_2 . From the identity $\|\mathbf{r}_1 \times \mathbf{r}_2\| = \|\mathbf{r}_1\| \|\mathbf{r}_2\| \sin(\theta_{\mathbf{r}_1, \mathbf{r}_2}) = 1$, it is seen that $\mathbf{r}_1 \times \mathbf{r}_2$ is a unit vector. Since the direction of $\mathbf{r}_1 \times \mathbf{r}_2$ is always perpendicular to the plane spanned by \mathbf{r}_1 and \mathbf{r}_2 , it follows that $\mathbf{r}_1 \times \mathbf{r}_2$ must equal $\pm \mathbf{r}_3$. The dot product of $\mathbf{r}_1 \times \mathbf{r}_2$ with \mathbf{r}_3 will be +1 if the vectors permute cyclically under the cross product, and -1 otherwise. \square

Now consider the structure of the matrices $\mathbf{R}_{\mathbb{Y}}^{\mathbb{X}}$ and $\mathbf{R}_{\mathbb{X}}^{\mathbb{Y}}$ in light of Theorem (2.4). The columns of $\mathbf{R}_{\mathbb{Y}}^{\mathbb{X}}$ are precisely the representations of the basis $\mathbf{x}_1, \mathbf{x}_2, \mathbf{x}_3$ in terms of the \mathbb{Y} -basis. The columns of $\mathbf{R}_{\mathbb{X}}^{\mathbb{Y}}$ are precisely the representations of the basis $\mathbf{y}_1, \mathbf{y}_2, \mathbf{y}_3$ in terms of the \mathbb{X} -basis.

Theorem 2.5 (Rotation Matrices From Basis Vectors). *Let $\{\mathbf{x}_1, \mathbf{x}_2, \mathbf{x}_3\}$ be a basis for the frame \mathbb{X} and $\{\mathbf{y}_1, \mathbf{y}_2, \mathbf{y}_3\}$ be a basis for the frame \mathbb{Y} . The rotation matrices $\mathbf{R}_{\mathbb{Y}}^{\mathbb{X}}$ and $\mathbf{R}_{\mathbb{X}}^{\mathbb{Y}}$ are given by*

$$\mathbf{R}_{\mathbb{Y}}^{\mathbb{X}} = \begin{bmatrix} \mathbf{y}_1^{\mathbb{X}} & \mathbf{y}_2^{\mathbb{X}} & \mathbf{y}_3^{\mathbb{X}} \end{bmatrix}$$

$$\mathbf{R}_{\mathbb{X}}^{\mathbb{Y}} = \begin{bmatrix} \mathbf{x}_1^{\mathbb{Y}} & \mathbf{x}_2^{\mathbb{Y}} & \mathbf{x}_3^{\mathbb{Y}} \end{bmatrix}$$

Proof. For any vector \mathbf{v} , based on the construction of the matrix $\mathbf{R}_{\mathbb{Y}}^{\mathbb{X}}$, it is true that

$$\mathbf{v}^{\mathbb{X}} = \mathbf{R}_{\mathbb{Y}}^{\mathbb{X}} \mathbf{v}^{\mathbb{Y}} \quad (2.2.6)$$

where $\mathbf{v}^{\mathbb{X}}$ is the representation \mathbf{v} with respect to the \mathbb{X} -frame, and $\mathbf{v}^{\mathbb{Y}}$ is the representation of \mathbf{v} with respect to the \mathbb{Y} -frame. Assume $\mathbf{v} = \mathbf{y}_1$. By definition, this vector \mathbf{y}_1 has a straightforward expansion in terms of the \mathbb{Y} -basis:

$$\mathbf{y}_1^{\mathbb{Y}} = \begin{Bmatrix} 1 \\ 0 \\ 0 \end{Bmatrix}.$$

When this representation is substituted into Equation (2.2.6), it results in

$$\mathbf{y}_1^{\mathbb{X}} = \mathbf{R}_{\mathbb{Y}}^{\mathbb{X}} \mathbf{y}_1^{\mathbb{Y}} = \mathbf{R}_{\mathbb{Y}}^{\mathbb{X}} \begin{Bmatrix} 1 \\ 0 \\ 0 \end{Bmatrix}$$

Since multiplication of the matrix \mathbf{R}_Y^X by the vector $\begin{pmatrix} 1 & 0 & 0 \end{pmatrix}^T$ isolates the first column of \mathbf{R}_Y^X , the first column of \mathbf{R}_Y^X must be equal to \mathbf{y}_1^X . This process may be repeated for columns 2 and 3 for \mathbf{R}_Y^X , and a similar argument can be made for \mathbf{R}_X^Y . \square

2.3 Parameterizations of Rotation Matrices

For the next step, the definition of a general rotation matrix will be connected to physically meaningful quantities such as angles of rotation that define the relative orientation between two frames. This is the problem of determining *rotation matrix parameterizations*. The parameters that define the rotation matrix are usually selected to be different angles that measure rotation; however, the choice of the type of rotation angle can be made in a variety of ways.

Each rotation matrix contains 9 entries which are the direction cosines that relate the bases of the two frames that are associated with the rotation matrix. By definition, these entries are not independent; there are 6 constraints that are implied in the definition of any rotation matrix. The dot product of any column/row of the rotation matrix with itself must be equal to 1 since each column/row is a unit vector. The dot product of any column/row with a different column/row must equal zero since they constitute an orthogonal set of basis vectors. This means that in the most general case $3 = 9 - 6$ independent variables are required to parameterize a given rotation matrix.

There do exist parameterizations of a general rotation matrix that use more than three variables. One example is the Axis-Angle Parameterization that utilizes a unit vector along the direction of rotation and a rotation angle about that axis. A total of four scalar variables are therefore used in this case. However, they are not independent variables. There is a single constraint equation that relates these four variables, the requirement that the norm of the unit vector entries is equal to one. Any parameterization of a rotation matrix using more than 3 variables is necessarily redundant, and there must be constraint equations that imply the variables are dependent.

In summary, a minimal parameterization of a general rotation matrix defines 3 independent variables. For some important special geometries, a rotation matrix can be parameterized with fewer than 3 parameters. For example, the relative pose between two bodies connected by a universal joint may be defined by only 2 rotation angles. However, the simplest examples of rotation matrix parameterizations are those associated with *single-axis rotations*.

2.3.1 Single Axis Rotations

Single axis rotations play a central role in the study of kinematics. Not only are they of interest in their own right in a variety of problems, they are also used as the building blocks for more general constructions in three dimensions. Figures (2.8a),

(2.8b) and (2.8c) depict the canonical single axis rotations about the 1, 2 and 3 axes, respectively.

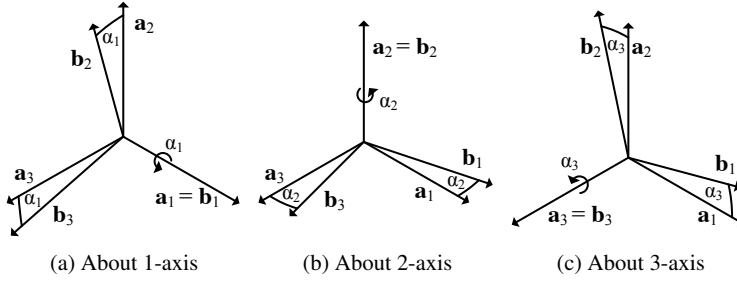


Fig. 2.8: Canonical Single Axis Rotations

In the i^{th} single axis rotation, the frame rotates by angle α_i about the axis $\mathbf{x}_i = \mathbf{y}_i$. The frame \mathbb{X} is interpreted as the initial frame which is mapped into the final frame \mathbb{Y} . The following theorem establishes the structure of the single axis rotation matrices.

Theorem 2.6 (Single Axis Rotations). *The single axis rotation matrices associated with rotation α_i as shown in Figures (2.8a), (2.8b) and (2.8c), respectively, are*

$$\mathbf{R}_{\mathbb{Y}}^{\mathbb{X}} = \mathbf{R}_1(\alpha_1) = \begin{bmatrix} 1 & 0 & 0 \\ 0 \cos \alpha_1 & -\sin \alpha_1 & 0 \\ 0 \sin \alpha_1 & \cos \alpha_1 & 0 \end{bmatrix}$$

$$\mathbf{R}_{\mathbb{Y}}^{\mathbb{X}} = \mathbf{R}_2(\alpha_2) = \begin{bmatrix} \cos \alpha_2 & 0 & \sin \alpha_2 \\ 0 & 1 & 0 \\ -\sin \alpha_2 & 0 & \cos \alpha_2 \end{bmatrix}$$

$$\mathbf{R}_{\mathbb{Y}}^{\mathbb{X}} = \mathbf{R}_3(\alpha_3) = \begin{bmatrix} \cos \alpha_3 & -\sin \alpha_3 & 0 \\ \sin \alpha_3 & \cos \alpha_3 & 0 \\ 0 & 0 & 1 \end{bmatrix}$$

Proof. The case for $i = 3$ will be proven, and the other cases will be left as exercises. Begin by projecting the basis vectors for frame \mathbb{Y} onto the basis vectors for frame \mathbb{X} , such that

$$\begin{aligned} \mathbf{y}_1 &= \cos \alpha_3 \mathbf{x}_1 + \sin \alpha_3 \mathbf{x}_2, \\ \mathbf{y}_2 &= -\sin \alpha_3 \mathbf{x}_1 + \cos \alpha_3 \mathbf{x}_2, \\ \mathbf{y}_3 &= \mathbf{x}_3. \end{aligned}$$

These equations lead to definitions for the representations $\mathbf{y}_1^X, \mathbf{y}_2^X, \mathbf{y}_3^X$:

$$\mathbf{y}_1^X = \begin{Bmatrix} \cos \alpha_3 \\ \sin \alpha_3 \\ 0 \end{Bmatrix}, \quad \mathbf{y}_2^X = \begin{Bmatrix} -\sin \alpha_3 \\ \cos \alpha_3 \\ 0 \end{Bmatrix}, \quad \mathbf{y}_3^X = \begin{Bmatrix} 0 \\ 0 \\ 1 \end{Bmatrix}.$$

Theorem (2.5) gives the rotation matrix \mathbf{R}_Y^X in terms of these representations

$$\mathbf{R}_Y^X(\alpha_3) = [\mathbf{y}_1^X \ \mathbf{y}_2^X \ \mathbf{y}_3^X] = \begin{bmatrix} \cos \alpha_3 & -\sin \alpha_3 & 0 \\ \sin \alpha_3 & \cos \alpha_3 & 0 \\ 0 & 0 & 1 \end{bmatrix}. \quad (2.3.1)$$

Alternatively, from Theorem (2.2)

$$\mathbf{R}_Y^X = \begin{bmatrix} \mathbf{x}_1 \cdot \mathbf{y}_1 & \mathbf{x}_1 \cdot \mathbf{y}_2 & \mathbf{x}_1 \cdot \mathbf{y}_3 \\ \mathbf{x}_2 \cdot \mathbf{y}_1 & \mathbf{x}_2 \cdot \mathbf{y}_2 & \mathbf{x}_2 \cdot \mathbf{y}_3 \\ \mathbf{x}_3 \cdot \mathbf{y}_1 & \mathbf{x}_3 \cdot \mathbf{y}_2 & \mathbf{x}_3 \cdot \mathbf{y}_3 \end{bmatrix}.$$

But since the single axis rotation about the 3 axis is under consideration, by definition $\mathbf{x}_3 \cdot \mathbf{y}_3 = 1$ and $\mathbf{x}_1 \cdot \mathbf{y}_3 = \mathbf{x}_2 \cdot \mathbf{y}_3 = \mathbf{x}_3 \cdot \mathbf{y}_1 = \mathbf{x}_3 \cdot \mathbf{y}_2 = 0$. Moreover, $\mathbf{x}_1 \cdot \mathbf{y}_1 = \mathbf{x}_2 \cdot \mathbf{y}_2 = \cos \alpha_3$. Finally, trigonometric identities yield

$$\mathbf{x}_1 \cdot \mathbf{y}_2 = \cos(90^\circ + \alpha_3) = \cos 90^\circ \cos \alpha_3 - \sin 90^\circ \sin \alpha_3 = -\sin \alpha_3,$$

$$\mathbf{x}_2 \cdot \mathbf{y}_1 = \cos(90^\circ - \alpha_3) = \cos 90^\circ \cos \alpha_3 + \sin 90^\circ \sin \alpha_3 = \sin \alpha_3.$$

□

Example 2.3.1. The form of the rotation matrices derived in Theorem (2.6) has been determined by drawing the two dimensional rotation of bases and using the geometry to express one set of bases in terms of another. In Theorem (2.3) the change of basis formulae are expressed in terms of rotation matrices that satisfy

$$(\mathbf{R}_X^Y)^{-1} = (\mathbf{R}_X^Y)^T = \mathbf{R}_Y^X.$$

Show that the rotation matrices in Theorem (2.6) satisfy the conditions of Theorem (2.3).

Solution: $\mathbf{R}_Y^X(\alpha_1)$ will be considered, since the other matrices associated with single axis rotations can be treated in a similar way. Recall that the inverse of a general, invertible 2×2 matrix is

$$\begin{bmatrix} a & b \\ c & d \end{bmatrix} = \frac{1}{(ad - bc)} \begin{bmatrix} d & -b \\ -c & a \end{bmatrix}$$

where $(ad - bc)$ is the determinant of the matrix. This formula can be used to calculate the inverse of a 3×3 matrix that has the special form

$$\begin{bmatrix} 1 & 0 & 0 \\ 0 & a & b \\ 0 & c & d \end{bmatrix}^{-1} = \begin{bmatrix} 1 & 0 & 0 \\ 0 & \frac{d}{ad-bc} & \frac{-b}{ad-bc} \\ 0 & \frac{-c}{ad-bc} & \frac{a}{ad-bc} \end{bmatrix}.$$

The rotation matrix $\mathbf{R}_{\mathbb{Y}}^{\mathbb{X}}(\alpha_1)$ in Theorem (2.3) has the form

$$\mathbf{R}_{\mathbb{Y}}^{\mathbb{X}}(\alpha_1) = \begin{bmatrix} 1 & 0 & 0 \\ 0 & \cos \alpha_1 & -\sin \alpha_1 \\ 0 & \sin \alpha_1 & \cos \alpha_1 \end{bmatrix},$$

and the inverse is calculated using the expression above, resulting in

$$(\mathbf{R}_{\mathbb{Y}}^{\mathbb{X}}(\alpha_1))^{-1} = \begin{bmatrix} 1 & 0 & 0 \\ 0 & \frac{\cos \alpha_1}{\cos^2 \alpha_1 + \sin^2 \alpha_1} & \frac{\sin \alpha_1}{\cos^2 \alpha_1 + \sin^2 \alpha_1} \\ 0 & \frac{-\sin \alpha_1}{\cos^2 \alpha_1 + \sin^2 \alpha_1} & \frac{\cos \alpha_1}{\cos^2 \alpha_1 + \sin^2 \alpha_1} \end{bmatrix} = \begin{bmatrix} 1 & 0 & 0 \\ 0 & \cos \alpha_1 & \sin \alpha_1 \\ 0 & -\sin \alpha_1 & \cos \alpha_1 \end{bmatrix} = (\mathbf{R}_{\mathbb{Y}}^{\mathbb{X}}(\alpha_1))^T.$$

When using principal or canonical rotation matrices in Theorem 2.6 in applications, the product of two or more of these matrices is often needed. If a rotation matrix \mathbf{R}_1 is followed by the rotation \mathbf{R}_2 , the resulting matrix \mathbf{R} given by

$$\mathbf{R} = \mathbf{R}_2 \mathbf{R}_1$$

is always a rotation matrix. This is evident from the fact that $\det(\mathbf{AB}) = \det(\mathbf{A})\det(\mathbf{B})$ for any two matrices \mathbf{A} and \mathbf{B} . Since the determinants of \mathbf{R}_1 and \mathbf{R}_2 are both +1 as orthonormal, dextral matrices by definition, so too is the determinant of \mathbf{R} . This line of reasoning can be extended to show that the product of any finite number of rotation matrices is itself a rotation matrix.

However, for the general case, the product of rotation matrices does not commute. If \mathbf{R}_1 and \mathbf{R}_2 are two rotation matrices, then the products $\mathbf{R}_1 \mathbf{R}_2$ and $\mathbf{R}_2 \mathbf{R}_1$ do not in general represent the same change in pose or relative orientation. The following example illustrates this fact.

Example 2.3.2. Consider a pair of canonical rotations: a rotation \mathbf{R}_A about the x_1 axis through angle 90° , and a rotation \mathbf{R}_B about the x_3 axis through angle 90° . Show the product of the rotations does not commute.

Solution: Figure (2.9) illustrate the two sequences of rotations under consideration: $\mathbf{R}_B \mathbf{R}_A$ (top pair) and $\mathbf{R}_A \mathbf{R}_B$ (bottom pair). As the final configurations do not match for this specific sequence of rotations, rotations matrices do not commute.

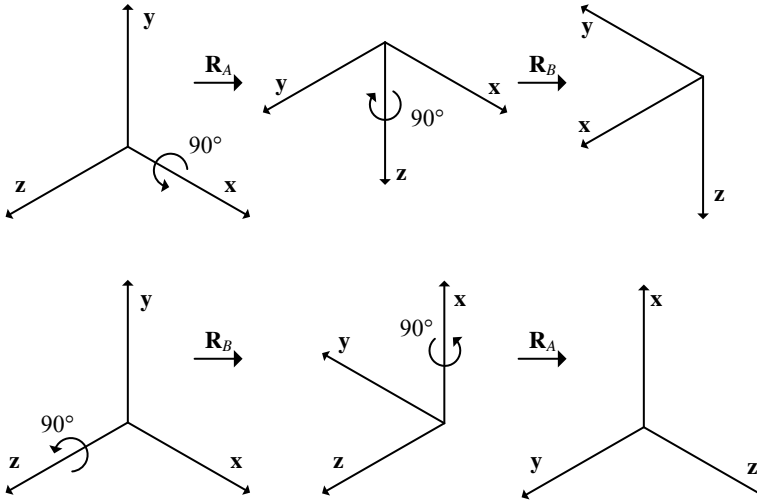


Fig. 2.9: General Non-Commutation of Rotation Matrix Multiplication

2.3.2 Cascades of Rotation Matrices

While the geometries to which the principal or canonical rotations in Theorem 2.6 are applicable are limited, standard methods are available to combine these rotation matrices to construct more general rotation matrices. These techniques are known as cascade rotations or concatenated rotations.

2.3.2.1 Cascade Rotations about Moving Axes

First, the construction of cascades of rotation matrices about moving axes will be considered. Starting from an initial frame \mathbb{A} , an axis \mathbf{a}_i is selected and the associated canonical rotation $\mathbf{R}_i(\alpha_i)$ in Theorem 2.6 is applied to map the original \mathbb{A} frame into the new \mathbb{B} frame. As a result

$$\mathbf{b} = \mathbf{R}_i^T(\alpha_i)\mathbf{a},$$

where $\mathbf{a} := [\mathbf{a}_1 \ \mathbf{a}_2 \ \mathbf{a}_3]^T$ and $\mathbf{b} := [\mathbf{b}_1 \ \mathbf{b}_2 \ \mathbf{b}_3]^T$. Next, choose an axis \mathbf{b}_j of the \mathbb{B} frame and apply the associated canonical rotation $\mathbf{R}_j(\alpha_j)$ to the \mathbb{B} frame to generate a new frame \mathbb{C} so that

$$\mathbf{c} = \mathbf{R}_j^T(\alpha_j)\mathbf{b} = \mathbf{R}_j^T(\alpha_j)\mathbf{R}_i^T(\alpha_i)\mathbf{a}.$$

This process can be repeated an arbitrary number of times, but often it is applied three times to create a general rotation matrix in three dimensions defined by the chosen axes of rotation and parameterized by the three rotation angles. With a final rotation $\mathbf{R}_k(\alpha_k)$ applied about the \mathbf{c}_k axis, the mapping from the original \mathbb{A} to the final \mathbb{D} frame is

$$\mathbf{d} = \underbrace{\mathbf{R}_k^T(\alpha_k) \mathbf{R}_j^T(\alpha_j) \mathbf{R}_i^T(\alpha_i) \mathbf{a}}_{\mathbf{R}_{\mathbb{A}}^{\mathbb{D}}}.$$

In robotics applications (particularly autonomous vehicles), the \mathbb{D} frame is often fixed to the moving body and the \mathbb{A} frame is fixed to the ground. The \mathbb{B} and \mathbb{C} frames are used only for intermediate calculations and often do not appear explicitly in a problem formulation. Conversely, the rotation matrix $\mathbf{R}_{\mathbb{D}}^{\mathbb{A}}$ that maps the vehicle fixed frame into the ground frame is given by

$$\mathbf{R}_{\mathbb{D}}^{\mathbb{A}} = \mathbf{R}_i(\alpha_i) \mathbf{R}_j(\alpha_j) \mathbf{R}_k(\alpha_k). \quad (2.3.2)$$

2.3.2.2 Cascade Rotations about Fixed Axes

Another strategy for building cascades of rotation matrices applies a sequence of rotations defined with reference to the original, fixed frame \mathbb{A} .

Recall that in the last section, the frame first rotated by the angle α_i about \mathbf{a}_i , then the second frame by α_j about \mathbf{b}_j , and then the third frame by α_k about \mathbf{c}_k . In this section, the sequence of rotations is applied *in the reverse order* about basis vectors of the original \mathbb{A} frame. First, the \mathbb{B} frame is created by rotating by α_k about the \mathbf{a}_k axis,

$$\mathbf{b} = \mathbf{R}_k^T(\alpha_k) \mathbf{a}.$$

Next, a rotation matrix is created for a rotation by angle α_j about the \mathbf{a}_j axis and maps the \mathbb{B} frame into the \mathbb{C} frame:

$$\mathbf{c} = \mathbf{R}_j^T(\alpha_j) \mathbf{b}.$$

Finally, a rotation matrix is created for a rotation by angle α_i about the \mathbf{a}_i axis and maps the \mathbb{C} frame into the \mathbb{D} frame:

$$\mathbf{d} = \mathbf{R}_i^T(\alpha_i) \mathbf{c}.$$

As in the last section, this process can be repeated any number of times, but three rotations is sufficient to construct a general spatial rotation defined by three parameters. The rotation matrix that maps the original \mathbb{A} frame into the final \mathbb{D} frame is given by the formula

$$\mathbf{d} = \underbrace{\mathbf{R}_k^T(\alpha_k) \mathbf{R}_j^T(\alpha_j) \mathbf{R}_i^T(\alpha_i)}_{\mathbf{R}_{\mathbb{A}}^{\mathbb{D}}} \mathbf{a}. \quad (2.3.3)$$

Equations 2.3.2 and 2.3.3 result in the same final rotation matrix. In other words, when rotations about moving axis are applied in the sequence

$$\alpha_i \text{ about } \mathbf{a}_i \implies \alpha_j \text{ about } \mathbf{b}_j \implies \alpha_k \text{ about } \mathbf{c}_k,$$

the same overall rotation matrix is obtained when rotations about the fixed frame \mathbb{A} are applied in the sequence

$$\alpha_k \text{ about } \mathbf{a}_k \implies \alpha_j \text{ about } \mathbf{a}_j \implies \alpha_i \text{ about } \mathbf{a}_i$$

2.3.3 Euler Angles

To define a general spatial rotation matrix that maps the frame \mathbb{A} into the frame \mathbb{D} , as shown in Figures (2.10) or (2.11), section (2.3) noted that three parameters are required. A common method to define these three parameters *concatenates* three single-axis rotations about a known sequence of basis vectors to generate a spatial rotation matrix. This approach is the family of *Euler angle* methods.

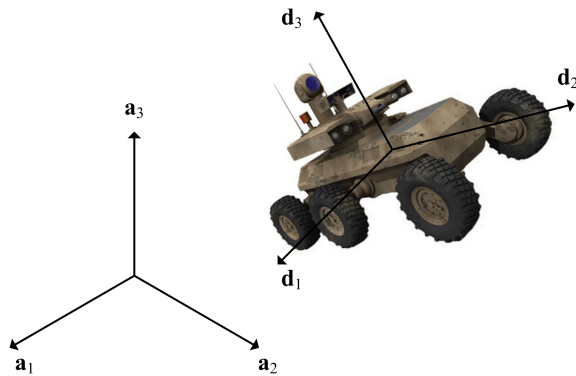


Fig. 2.10: Orientation of an Autonomous Ground Vehicle

The *Euler angle* approach defines three parameters, such as α, β, γ , to be single-axis rotation angles applied in succession. A first axis i_1 is selected, and the original frame \mathbb{A} is rotated about the i_1 axis by the angle α . A new axis $i_2 (\neq i_1)$ is selected from the *rotated frame*, and the frame is rotated about this axis i_2 by the angle β . This process is repeated a final time by choosing a third axis $i_3 (\neq i_1, i_2)$ from the *second rotated frame*, and rotating the frame about this axis by angle γ . The above construction defines the $(i_1 - i_2 - i_3)$ Euler angles α, β, γ . The order of the axis in this notation is critical; for example, the $(3 - 2 - 1)$ Euler angles are not the same as the $(2 - 1 - 3)$ Euler angles.

For a mathematically precise definition, let \mathbb{A} denote the original frame, \mathbb{B} denote the frame resulting from the α angle rotation of frame \mathbb{A} , \mathbb{C} denote the frame resulting from the β angle rotation of frame \mathbb{B} , and \mathbb{D} denote the frame resulting from the γ angle rotation of frame \mathbb{C} . Introduce the single axis rotation matrices $\mathbf{R}_{\mathbb{B}}^{\mathbb{A}}(\alpha)$, $\mathbf{R}_{\mathbb{C}}^{\mathbb{B}}(\beta)$ and $\mathbf{R}_{\mathbb{D}}^{\mathbb{C}}(\gamma)$ corresponding to the rotations associated with angles α, β , and γ that map one frame into the next. For an arbitrary vector \mathbf{v} , its representations

$\mathbf{v}^A, \mathbf{v}^B, \mathbf{v}^C, \mathbf{v}^D$ may be related in terms of these frames by

$$\mathbf{v}^A = \mathbf{R}_B^A(\alpha)\mathbf{v}^B, \quad (2.3.4)$$

$$\mathbf{v}^B = \mathbf{R}_C^B(\beta)\mathbf{v}^C, \quad (2.3.5)$$

$$\mathbf{v}^C = \mathbf{R}_D^C(\gamma)\mathbf{v}^D. \quad (2.3.6)$$

The desired rotation matrix \mathbf{R}_D^A that relates the frames A and D is obtained by substituting (2.3.5) into (2.3.4), and subsequently substituting (2.3.6) into that result. This sequence of substitutions yields

$$\mathbf{v}^A = \mathbf{R}_B^A(\alpha)\mathbf{R}_C^B(\beta)\mathbf{R}_D^C(\gamma)\mathbf{v}^D.$$

Since this equation holds for an arbitrary vector \mathbf{v} , the desired matrix \mathbf{R}_D^A is given by the equation

$$\mathbf{R}_D^A(\alpha, \beta, \gamma) = \mathbf{R}_B^A(\alpha)\mathbf{R}_C^B(\beta)\mathbf{R}_D^C(\gamma). \quad (2.3.7)$$

The most common sequences of *Euler angles* utilized in applications are discussed in the next few sections.

2.3.3.1 The 3 – 2 – 1 Yaw-Pitch-Roll Euler Angles

One of the most common sequences of Euler angles is the *(3-2-1) Euler angles*, more commonly known as the *Yaw-Pitch-Roll angles* and sometimes as *Tait-Bryan angles*. The yaw angle ψ , pitch angle θ and roll angle ϕ are illustrated in Figure (2.11) for an autonomous air vehicle. In this figure, the final frame D is fixed rigidly to the air vehicle, and the initial frame A is fixed to Earth. Often in navigation problems, the ground fixed basis vectors $\mathbf{a}_1, \mathbf{a}_2$ and \mathbf{a}_3 are aligned with true north, true east and point toward the center of gravity of the earth, respectively, but this is not necessary. See Problem (2.27) for a related problem. For the vechicle-fixed frame D , the \mathbf{d}_1 axis points out the nose of the aircraft, the \mathbf{d}_2 axis is oriented along the right wing, and the \mathbf{d}_3 axis completes the right-handed frame.

First, the intermediate frame B will be defined. As a starting point, assume frames B and A are aligned. For all time, the vectors \mathbf{a}_3 and \mathbf{b}_3 will remain coincident, but vectors \mathbf{b}_1 and \mathbf{b}_2 may rotate in the $\mathbf{a}_1, \mathbf{a}_2$ plane while preserving their dextral orthogonality. The yaw angle ψ is defined as the rotation about the axis $\mathbf{a}_3 = \mathbf{b}_3$ that maps the \mathbf{a}_1 basis vector into the \mathbf{b}_1 basis vector. An isometric view of the yaw angle and frames A and B is shown in Figure (2.12). The single-axis rotation matrix associated with yaw ψ is given in (2.6) and is

$$\mathbf{R}_B^A(\psi) = \begin{bmatrix} \cos\psi & -\sin\psi & 0 \\ \sin\psi & \cos\psi & 0 \\ 0 & 0 & 1 \end{bmatrix}. \quad (2.3.8)$$

Next, the second intermediate frame C will be defined. Assuming the frames B and D are known, let $\mathbf{c}_2 = \mathbf{b}_2$ and $\mathbf{c}_1 = \mathbf{d}_1$. Complete the right-handed frame by

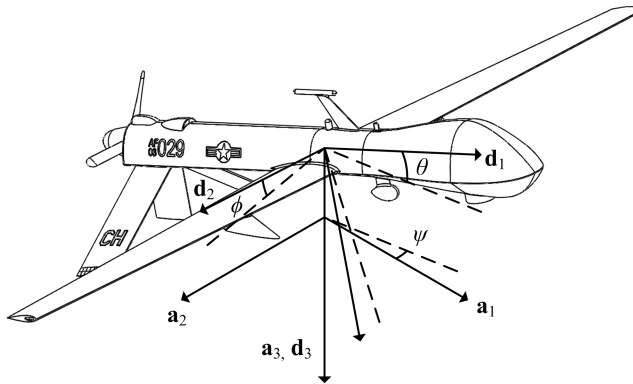


Fig. 2.11: Orientation of an Autonomous Air Vehicle, Yaw-Pitch-Roll Euler Angles

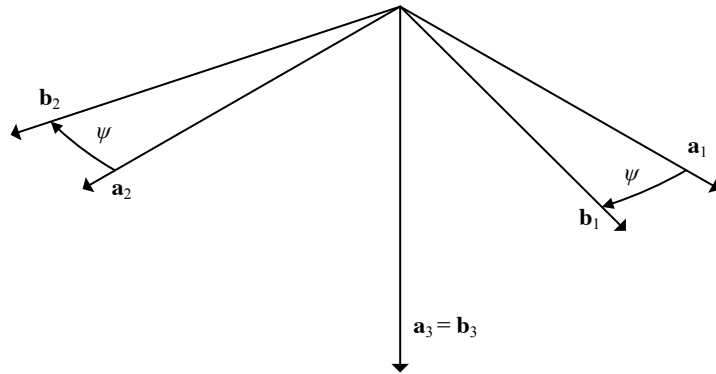


Fig. 2.12: Yaw Angle Definition

defining $\mathbf{c}_3 = \mathbf{c}_1 \times \mathbf{c}_2$. The pitch angle θ is defined as the rotation about axis $\mathbf{c}_2 = \mathbf{b}_2$ that maps the \mathbf{b}_1 basis vector into the \mathbf{c}_1 basis vector. An isometric view of the pitch angle and frames \mathbb{B} and \mathbb{C} is shown in Figure (2.13). The single-axis rotation matrix associated with the pitch angle θ is defined in theorem (2.6) to be

$$\mathbf{R}_{\mathbb{C}}^{\mathbb{B}}(\theta) = \begin{bmatrix} \cos \theta & 0 & \sin \theta \\ 0 & 1 & 0 \\ -\sin \theta & 0 & \cos \theta \end{bmatrix}. \quad (2.3.9)$$

The roll angle ϕ is the angle about the $\mathbf{c}_1 = \mathbf{d}_1$ axis that maps the \mathbf{c}_2 basis vector onto the \mathbf{d}_2 basis vector, and by orthogonality, the \mathbf{c}_3 basis vector onto the \mathbf{d}_3 vector. An isometric view of the roll angle and frames \mathbb{C} and \mathbb{D} is shown in Figure (2.14). The single-axis rotation matrix associated with the pitch angle θ is defined in theorem (2.6) to be

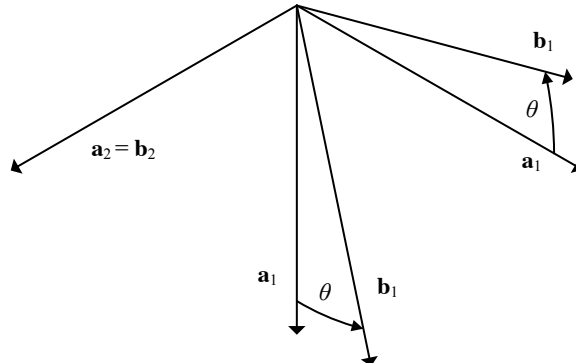


Fig. 2.13: Pitch Angle Definition

$$\mathbf{R}_{\mathbb{D}}^{\mathbb{C}}(\phi) = \begin{bmatrix} 1 & 0 & 0 \\ 0 & \cos \phi & -\sin \phi \\ 0 & \sin \phi & \cos \phi \end{bmatrix}. \quad (2.3.10)$$

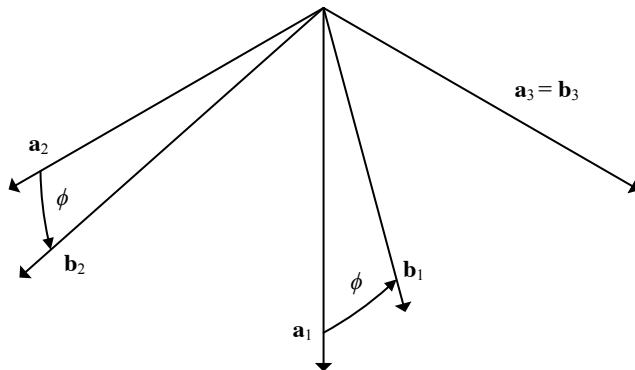


Fig. 2.14: Roll Angle Definitions, 3D and 2D

The single axis rotations in Equations (2.3.8), (2.3.9) and (2.3.10) are combined to obtain the general rotation matrix in Equation (2.3.7).

$$\begin{aligned}
\mathbf{R}_{\mathbb{D}}^{\mathbb{A}}(\psi, \theta, \phi) &= \mathbf{R}_{\mathbb{B}}^{\mathbb{A}}(\psi) \mathbf{R}_{\mathbb{C}}^{\mathbb{B}}(\theta) \mathbf{R}_{\mathbb{D}}^{\mathbb{C}}(\phi), \\
&= \begin{bmatrix} \cos \psi & -\sin \psi & 0 \\ \sin \psi & \cos \psi & 0 \\ 0 & 0 & 1 \end{bmatrix} \begin{bmatrix} \cos \theta & 0 & \sin \theta \\ 0 & 1 & 0 \\ -\sin \theta & 0 & \cos \theta \end{bmatrix} \begin{bmatrix} 1 & 0 & 0 \\ 0 & \cos \phi & -\sin \phi \\ 0 & \sin \phi & \cos \phi \end{bmatrix}, \\
&= \begin{bmatrix} \cos \theta \cos \psi & (\cos \psi \sin \theta \sin \phi - \cos \phi \sin \psi) & (\sin \phi \sin \psi + \cos \phi \cos \psi \sin \theta) \\ \cos \theta \sin \psi & (\cos \phi \cos \psi + \sin \theta \sin \phi \sin \psi) & (\cos \phi \sin \theta \sin \psi - \cos \psi \sin \phi) \\ -\sin \theta & \cos \theta \sin \phi & \cos \theta \cos \phi \end{bmatrix}.
\end{aligned}$$

See Examples ?? and ?? of the MATLAB Workbook for DCRS.

Example 2.3.3. It has been stated that the order in which the finite rotations are defined in an Euler angle sequence is critical to the definition. If the order of the axes about which the rotations are defined is changed, the resulting rotation matrices can be different. Show that this is true even in a simple case.

Suppose that the yaw angle $\psi = 0$, but that the order of the pitch rotation about the 2 axis and the roll rotation about the 1 axis are switched. Sometimes it is observed that a rotation matrix associated with (infinitesimally) small yaw ψ , pitch θ and roll ϕ angles does not depend on the order in which the rotations are carried out. This conflicts with the situation where the rotations are finite. Linearize the derived 3 – 2 – 1 Euler angle rotation matrices but now assume that θ and ϕ are small. Linearize the rotation matrix obtained when the order in which the rotation are performed is reversed. Show that the linearized rotation matrices are the same.

Solution: The rotation matrix for pitch and roll, if performed in the order described in Section (2.3.3.1) is

$$\begin{aligned}
\mathbf{R}_{\mathbb{D}}^{\mathbb{A}} &= \begin{bmatrix} \cos \theta & 0 & \sin \theta \\ 0 & 1 & 0 \\ -\sin \theta & 0 & \cos \theta \end{bmatrix} \begin{bmatrix} 1 & 0 & 0 \\ 0 & \cos \phi & -\sin \phi \\ 0 & \sin \phi & \cos \phi \end{bmatrix}, \\
&= \begin{bmatrix} \cos \theta & \sin \theta \sin \phi & \sin \theta \cos \phi \\ 0 & \cos \phi & -\sin \phi \\ -\sin \theta \cos \phi & \sin \phi & \cos \theta \cos \phi \end{bmatrix}.
\end{aligned}$$

If the order is reversed, the rotation matrix relating the \mathbb{A} and \mathbb{D} frames is

$$\begin{aligned}
(\mathbf{R}_{\mathbb{D}}^{\mathbb{A}})_{reversed} &= \begin{bmatrix} 1 & 0 & 0 \\ 0 & \cos \phi & -\sin \phi \\ 0 & \sin \phi & \cos \phi \end{bmatrix} \begin{bmatrix} \cos \theta & 0 & \sin \theta \\ 0 & 1 & 0 \\ -\sin \theta & 0 & \cos \theta \end{bmatrix}, \\
&= \begin{bmatrix} \cos \theta & 0 & \sin \theta \\ \sin \theta \sin \phi & \cos \phi & -\cos \theta \sin \phi \\ -\sin \theta \cos \phi & \sin \phi & \cos \theta \cos \phi \end{bmatrix}.
\end{aligned}$$

Obviously, these two matrices are not the same. If the matrices are linearized above for small angles using the approximations $\sin \theta \approx \theta$, $\sin \phi \approx \phi$, $\cos \theta \approx 1$, $\cos \phi \approx 1$, the matrices simplify to

$$\mathbf{R}_{\mathbb{D}}^{\mathbb{A}} = \begin{bmatrix} 1 & \theta\phi & \theta \\ 0 & 1 & -\phi \\ -\theta & \phi & 1 \end{bmatrix}, \quad (\mathbf{R}_{\mathbb{D}}^{\mathbb{A}})_{reversed} = \begin{bmatrix} 1 & 0 & \theta \\ \theta\phi & 1 & -\phi \\ -\theta & \phi & 1 \end{bmatrix}.$$

Given that θ and ϕ are assumed to be small angles, their product may be approximated as $\phi\theta \approx 0$. As a result, the final approximation of both matrices for small angles θ and ϕ are both

$$\mathbf{R}_{\mathbb{D}}^{\mathbb{A}} = (\mathbf{R}_{\mathbb{D}}^{\mathbb{A}})_{reversed} = \begin{bmatrix} 1 & 0 & \theta \\ 0 & 1 & -\phi \\ -\theta & \phi & 1 \end{bmatrix}.$$

2.3.3.2 The 3 – 1 – 3 Precession-Nutation-Spin Euler Angles

Another well-known sets of *Euler angles* are the 3 – 1 – 3 *Euler angles* that define precession α , nutation β and spin γ in the study of gyroscopic. These were originally defined by Leonhard Euler (1707-1783) in the study of rigid body kinematics. Figures (2.15a), (2.15b), (2.15c) depicts one common, compact way of visualizing this set of Euler angles. The initial frame \mathbb{A} is, as in the last section, fixed to ground (i.e., Earth), and the final frame \mathbb{D} is fixed to the body under consideration. For this sequence of Euler angles, the $\mathbf{a}_1 = \mathbf{b}_1$ axis is given a special name: the *line of nodes*.

The first intermediate frame \mathbb{B} initially aligns with the \mathbb{A} frame and is rotated by the angle α about the $\mathbf{a}_3 = \mathbf{b}_3$ axis. The second intermediate frame \mathbb{C} initially aligns with the \mathbb{B} frame and is rotated about the $\mathbf{b}_1 = \mathbf{c}_1$ axis through the angle β until the \mathbf{c}_3 basis vector is aligned with the body-fixed \mathbf{d}_3 basis vector. The final frame \mathbb{D} is reached by rotating about the $\mathbf{c}_3 = \mathbf{d}_3$ axis by the angle γ until the \mathbf{c}_1 and \mathbf{c}_2 basis vectors are mapped onto the \mathbf{d}_1 and \mathbf{d}_2 basis vectors. The three single-axis rotation matrices $\mathbf{R}_{\mathbb{B}}^{\mathbb{A}}(\alpha)$, $\mathbf{R}_{\mathbb{C}}^{\mathbb{B}}(\beta)$, and $\mathbf{R}_{\mathbb{D}}^{\mathbb{C}}(\gamma)$, associated with the precession α , nutation β and spin γ , are

$$\mathbf{R}_{\mathbb{B}}^{\mathbb{A}}(\alpha) = \begin{bmatrix} \cos\alpha & -\sin\alpha & 0 \\ \sin\alpha & \cos\alpha & 0 \\ 0 & 0 & 1 \end{bmatrix}, \quad \mathbf{R}_{\mathbb{C}}^{\mathbb{B}}(\beta) = \begin{bmatrix} 1 & 0 & 0 \\ 0 & \cos\beta & -\sin\beta \\ 0 & \sin\beta & \cos\beta \end{bmatrix}, \quad \mathbf{R}_{\mathbb{D}}^{\mathbb{C}}(\gamma) = \begin{bmatrix} \cos\gamma & -\sin\gamma & 0 \\ \sin\gamma & \cos\gamma & 0 \\ 0 & 0 & 1 \end{bmatrix}.$$

These rotation matrices may be verified using Theorem (2.6). The rotation matrix $\mathbf{R}_{\mathbb{D}}^{\mathbb{A}}(\alpha, \beta, \gamma)$ is given by the product

$$\begin{aligned}
 & \mathbf{R}_{\mathbb{D}}^{\mathbb{A}}(\alpha, \beta, \gamma) \\
 &= \begin{bmatrix} \cos \alpha & -\sin \alpha & 0 \\ \sin \alpha & \cos \alpha & 0 \\ 0 & 0 & 1 \end{bmatrix} \begin{bmatrix} 1 & 0 & 0 \\ 0 & \cos \beta & -\sin \beta \\ 0 & \sin \beta & \cos \beta \end{bmatrix} \begin{bmatrix} \cos \gamma & -\sin \gamma & 0 \\ \sin \gamma & \cos \gamma & 0 \\ 0 & 0 & 1 \end{bmatrix}, \\
 &= \begin{bmatrix} (\cos \alpha \cos \gamma - \cos \beta \sin \alpha \sin \gamma) & (-\cos \alpha \sin \gamma - \cos \beta \cos \gamma \sin \alpha) & \sin \beta \sin \alpha \\ (\cos \gamma \sin \alpha + \cos \beta \cos \alpha \sin \gamma) & (\cos \beta \cos \alpha \cos \gamma - \sin \alpha \sin \gamma) & -\cos \alpha \sin \beta \\ \sin \beta \sin \gamma & \cos \gamma \sin \beta & \cos \beta \end{bmatrix}.
 \end{aligned}$$

See Example ?? of the MATLAB Workbook for DCRS for an example of MATLAB function to calculate the rotation matrix generated by the 3 – 1 – 3 Euler angles.

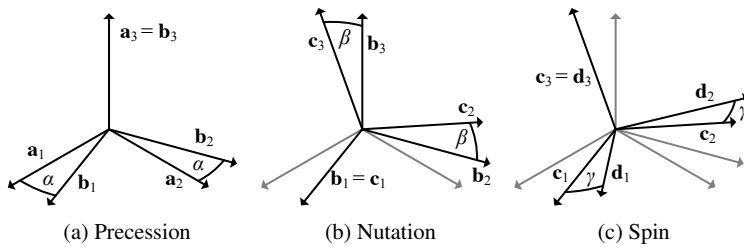


Fig. 2.15: Euler Angles: Precession, Nutation, Spin

Example 2.3.4. Figures (2.16a), (2.16b) and (2.16c) depict the geometry that can be used to define the kinematics of an autonomous satellite system. It will be shown that the frames used in this example correspond to a set of 3 – 1 – 3 Euler Angles. The \mathbb{E} frame is fixed at the center of the Earth, and the $\mathbf{e}_1 - \mathbf{e}_2$ plane coincides with the equatorial plane. The orientation of an orbit of the satellite is defined in terms of the *inclination* ψ and the right ascension ϕ of the orbit.

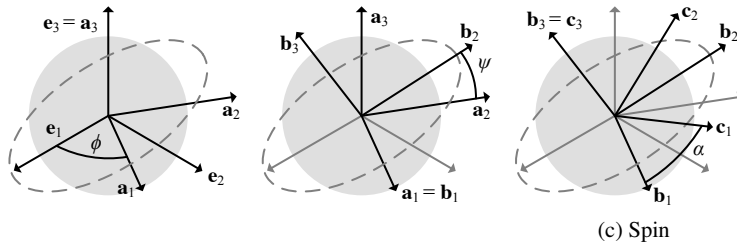


Fig. 2.16: Kinematic Model of a Satellite Orbit around Earth

The orbital plane of the satellite around the Earth intersects the $\mathbf{e}_1 - \mathbf{e}_2$ plane along the line of nodes, which coincides with the vector \mathbf{a}_1 . The \mathbb{A} frame is defined with a single-axis rotation by the angle ϕ about the \mathbf{e}_3 axis. The *right ascension* ϕ measures this angle between the \mathbf{e}_1 and \mathbf{a}_1 axes. A second frame \mathbb{B} is introduced using a single-axis rotation by angle ψ about the \mathbf{a}_1 axis from an initial alignment with the \mathbb{A} frame. The angle ψ is the *inclination* of the orbital plane relative to the equatorial plane. The \mathbb{C} frame corresponding to the satellite's orientation relative to Earth is obtained from the \mathbb{B} frame by rotating by the angle α about the \mathbf{b}_3 axis. The \mathbf{c}_1 axis is along the position vector from the Earth to the satellite/frame \mathbb{C} origin, and \mathbf{c}_3 is perpendicular to the orbital plane.

Calculate the rotation matrix that maps the basis for the Earth frame \mathbb{E} to the basis for the \mathbb{C} frame.

Solution: As before, the rotation matrix $\mathbf{R}_{\mathbb{E}}^{\mathbb{C}}$ is a composition of three single-axis rotation matrices

$$\mathbf{R}_{\mathbb{E}}^{\mathbb{C}} = \mathbf{R}_{\mathbb{B}}^{\mathbb{C}} \mathbf{R}_{\mathbb{A}}^{\mathbb{B}} \mathbf{R}_{\mathbb{E}}^{\mathbb{A}}.$$

By inspection of geometry, the basis for \mathbb{A} can be written in terms of the basis for \mathbb{E} as

$$\begin{aligned}\mathbf{a}_1 &= \cos \phi \mathbf{e}_1 + \sin \phi \mathbf{e}_2, \\ \mathbf{a}_2 &= -\sin \phi \mathbf{e}_1 + \cos \phi \mathbf{e}_2, \\ \mathbf{a}_3 &= \mathbf{e}_3.\end{aligned}$$

Similarly, the basis for \mathbb{B} can be written in terms of the basis for \mathbb{A} as

$$\begin{aligned}\mathbf{b}_1 &= \mathbf{a}_1, \\ \mathbf{b}_2 &= \cos \psi \mathbf{a}_2 + \sin \psi \mathbf{a}_3, \\ \mathbf{b}_3 &= -\sin \psi \mathbf{a}_2 + \cos \psi \mathbf{a}_3.\end{aligned}$$

The basis for \mathbb{C} is expressed in terms of the basis for \mathbb{B} in the equations

$$\begin{aligned}\mathbf{c}_1 &= \cos \alpha \mathbf{b}_1 + \sin \alpha \mathbf{b}_2, \\ \mathbf{c}_2 &= -\sin \alpha \mathbf{b}_1 + \cos \alpha \mathbf{b}_2, \\ \mathbf{c}_3 &= \mathbf{b}_3.\end{aligned}$$

The corresponding rotation matrices are

$$\mathbf{R}_{\mathbb{E}}^{\mathbb{A}} = \begin{bmatrix} \cos \phi & \sin \phi & 0 \\ -\sin \phi & \cos \phi & 0 \\ 0 & 0 & 1 \end{bmatrix}, \quad \mathbf{R}_{\mathbb{A}}^{\mathbb{B}} = \begin{bmatrix} 1 & 0 & 0 \\ 0 & \cos \psi & \sin \psi \\ 0 & -\sin \psi & \cos \psi \end{bmatrix}, \quad \mathbf{R}_{\mathbb{B}}^{\mathbb{C}} = \begin{bmatrix} \cos \alpha & \sin \alpha & 0 \\ -\sin \alpha & \cos \alpha & 0 \\ 0 & 0 & 1 \end{bmatrix}.$$

The final expression for the composite rotation matrix is $\mathbf{R}_{\mathbb{E}}^{\mathbb{C}} = \mathbf{R}_{\mathbb{B}}^{\mathbb{C}} \mathbf{R}_{\mathbb{A}}^{\mathbb{B}} \mathbf{R}_{\mathbb{E}}^{\mathbb{A}}$, and we can write

$$\mathbf{R}_{\mathbb{B}}^{\mathbb{C}} = \begin{bmatrix} \cos \alpha & \sin \alpha & 0 \\ -\sin \alpha & \cos \alpha & 0 \\ 0 & 0 & 1 \end{bmatrix} \begin{bmatrix} 1 & 0 & 0 \\ 0 & \cos \psi & \sin \psi \\ 0 & -\sin \psi & \cos \psi \end{bmatrix} \begin{bmatrix} \cos \phi & \sin \phi & 0 \\ -\sin \phi & \cos \phi & 0 \\ 0 & 0 & 1 \end{bmatrix}.$$

The transpose $\mathbf{R}_{\mathbb{C}}^{\mathbb{B}} = (\mathbf{R}_{\mathbb{B}}^{\mathbb{C}})^T$ of this rotation matrix is identical to that generated by the 3–1–3 Euler angles. See Example ?? in the MATLAB Workbook.

2.3.4 Axis-Angle Parameterization

Sections (2.3.3.1) and (2.3.3.2) address two of the most common examples of concatenated, body-fixed rotations that define particular *Euler angles* sequences. This section focuses on another common approach to represent general rotation matrices in three dimensions, the *Axis-Angle Parameterization*. This technique differs substantially from the family of *Euler angle* methods discussed in Section (2.3.3). This case utilizes the property of rotation matrices that states that any generalized rotation matrix may be reached by a single rotation by angle ϕ about an axis of rotation \mathbf{u} . The geometry and definition of the variables ϕ and \mathbf{u} are shown in Figure (2.17). The following theorems give a concise description of the rotation matrix $\mathbf{R}_{\mathbb{A}}^{\mathbb{B}}$ for the transformation shown in Figure (2.17) parameterized by ϕ and \mathbf{u} .

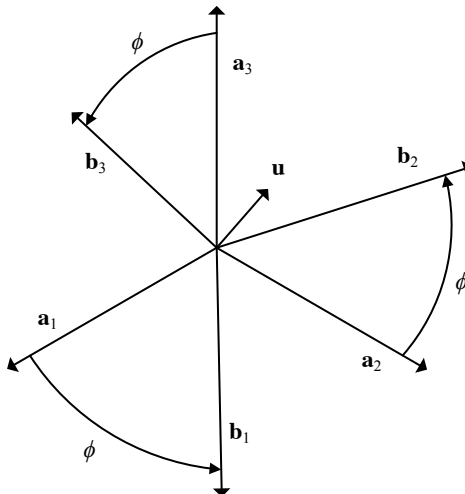


Fig. 2.17: Definition of Direction of Rotation \mathbf{u} and Angle of Rotation ϕ

Theorem 2.7 (Rotation Matrix Exponential). *The matrix exponential $e^{\mathbf{S}(\phi\mathbf{u})}$ is a rotation matrix for any scalar ϕ and unit vector \mathbf{u} and is given by*

$$\begin{aligned} e^{\mathbf{S}(\phi\mathbf{u})} &= \cos \phi (\mathbb{I} - \mathbf{u}\mathbf{u}^T) + \sin \phi \mathbf{S}(\mathbf{u}) + \mathbf{u}\mathbf{u}^T, \\ &= \mathbb{I} + (1 - \cos \phi) \mathbf{S}^2(\mathbf{u}) + \sin \phi \mathbf{S}(\mathbf{u}). \end{aligned} \quad (2.3.11)$$

Conversely, any rotation matrix can be written as $e^{\mathbf{S}(\phi\mathbf{u})}$ for some choice of ϕ and unit vector \mathbf{u} .

Theorem 2.8 (Axis-Angle Parameterization). *Suppose the frame \mathbb{A} is mapped to the frame \mathbb{B} in Figure (2.17) via rotation ϕ about the unit vector \mathbf{u} . The rotation matrix $\mathbf{R}_{\mathbb{A}}^{\mathbb{B}}$ is given by the matrix exponential*

$$\mathbf{R}_{\mathbb{A}}^{\mathbb{B}} = e^{\mathbf{S}(\phi\mathbf{u})} \quad (2.3.12)$$

where $\mathbf{S}(\cdot)$ is the skew operator.

Proof. The proof of these two theorems is lengthy; as such, it will only be shown that the formula in Equation (2.3.11) holds for any scalar ϕ and unit vector \mathbf{u} . The proof that the matrix exponential $e^{\mathbf{S}(\phi\mathbf{u})}$ is a rotation matrix addressed in Problem (2.34). The proof that $e^{\mathbf{S}(\phi\mathbf{u})}$ is the rotation matrix associated specifically with rotation through an angle ϕ about the \mathbf{u} direction is addressed in Problem (2.29). The derivation of a few of the identities used in the proof that follows are addressed in Problems (2.15) and (2.16).

The matrix exponential for any matrix \mathbf{A} is defined via the infinite series

$$e^{\mathbf{A}} = \sum_{i=0}^{\infty} \frac{\mathbf{A}^i}{i!} = \mathbb{I} + \mathbf{A} + \frac{1}{2!} \mathbf{A}^2 + \frac{1}{3!} \mathbf{A}^3 + \dots,$$

and for the axis-angle parameterization, $e^{\mathbf{S}(\phi\mathbf{u})}$ expands as

$$\begin{aligned} e^{\mathbf{S}(\phi\mathbf{u})} &= \mathbb{I} + \mathbf{S}(\phi\mathbf{u}) + \frac{1}{2!} \mathbf{S}^2(\phi\mathbf{u}) + \frac{1}{3!} \mathbf{S}^3(\phi\mathbf{u}) + \dots, \\ &= \mathbb{I} + \phi \mathbf{S}(\mathbf{u}) + \frac{1}{2!} \phi^2 \mathbf{S}^2(\mathbf{u}) + \frac{1}{3!} \phi^3 \mathbf{S}(\mathbf{u}) + \dots, \end{aligned}$$

since $\mathbf{S}(\phi\mathbf{u}) = \phi \mathbf{S}(\mathbf{u})$ for any scalar ϕ . Problems (2.16) and (2.17) show that for any $\boldsymbol{\omega}$ in \mathbb{R}^3

$$\begin{aligned} \mathbf{S}^2(\boldsymbol{\omega}) &= -\|\boldsymbol{\omega}\|^2 \mathbb{I} + \boldsymbol{\omega} \boldsymbol{\omega}^T, \\ \mathbf{S}^3(\boldsymbol{\omega}) &= -\|\boldsymbol{\omega}\|^2 \mathbf{S}(\boldsymbol{\omega}). \end{aligned}$$

Using these identities, it is determined that

$$\begin{aligned}\mathbf{S}^2(\mathbf{u}) &= -(\mathbb{I} - \mathbf{u}\mathbf{u}^T), \\ \mathbf{S}^3(\mathbf{u}) &= -\mathbf{S}(\mathbf{u}), \\ \mathbf{S}^4(\mathbf{u}) &= (\mathbb{I} - \mathbf{u}\mathbf{u}^T)(\mathbb{I} - \mathbf{u}\mathbf{u}^T) = \mathbb{I} - \mathbf{u}\mathbf{u}^T, \\ \mathbf{S}^5(\mathbf{u}) &= \mathbf{S}(\mathbf{u})(\mathbb{I} - \mathbf{u}\mathbf{u}^T) = \mathbf{S}(\mathbf{u}),\end{aligned}$$

since $(\mathbf{u}\mathbf{u}^T)\mathbf{S}(\mathbf{u}) = \mathbf{S}(\mathbf{u})\mathbf{u}\mathbf{u}^T = 0$. The following expression is obtained when these identities are substituted into the series expression for the matrix exponential

$$\begin{aligned}e^{\mathbf{S}(\phi\mathbf{u})} &= \mathbb{I} + \phi\mathbf{S}(\mathbf{u}) - \frac{1}{2!}\phi^2(\mathbb{I} - \mathbf{u}\mathbf{u}^T) - \frac{1}{3!}\phi^3\mathbf{S}(\mathbf{u}) \\ &\quad + \frac{1}{4!}\phi^4(\mathbb{I} - \mathbf{u}\mathbf{u}^T) + \frac{1}{5!}\phi^5\mathbf{S}(\mathbf{u}) + \dots, \\ &= \mathbb{I} + \left(1 - \frac{\phi^2}{2!} + \frac{\phi^4}{4!} - \frac{\phi^6}{6!} + \dots\right)(\mathbb{I} - \mathbf{u}\mathbf{u}^T) - (\mathbb{I} - \mathbf{u}\mathbf{u}^T) \\ &\quad + \left(\phi - \frac{1}{3!}\phi^3 + \frac{1}{5!}\phi^5 + \dots\right)\mathbf{S}(\mathbf{u}), \\ &= \cos\phi(\mathbb{I} - \mathbf{u}\mathbf{u}^T) + \sin\phi\mathbf{S}(\mathbf{u}) + \mathbf{u}\mathbf{u}^T.\end{aligned}$$

□

Example 2.3.5. Let the rotation matrix \mathbf{R} be given by

$$\mathbf{R} = \begin{bmatrix} \cos\theta & \sin\theta & 0 \\ -\sin\theta & \cos\theta & 0 \\ 0 & 0 & 1 \end{bmatrix}$$

Use the equation

$$\mathbf{e}^{\phi\mathbf{u}} := \mathbb{I} + (1 - \cos\phi)\mathbf{S}^2(\mathbf{u}) + \sin\phi\mathbf{S}(\mathbf{u})$$

derived in Theorem (2.8) to show that this rotation matrix corresponds to rotation about the 3 axis through the angle θ .

Solution: For this solution, the rotation matrix \mathbf{R} and unit vector \mathbf{u} will be parameterized by r_{ij} and u_i , respectively. First, the expression for $\mathbf{S}^2(\mathbf{u})$ will be expanded in terms of u_i , such that

$$\mathbf{S}^2(\mathbf{u}) = -\mathbb{I} + \mathbf{u}\mathbf{u}^T = \begin{bmatrix} -(u_2^2 + u_3^2) & u_1u_2 & u_1u_3 \\ u_2u_1 & -(u_1^2 + u_3^2) & u_2u_3 \\ u_3u_1 & u_3u_2 & -(u_1^2 + u_2^2) \end{bmatrix}.$$

Using this expression to expand $\mathbf{e}^{\phi\mathbf{u}}$ results in

$$\mathbf{e}^{\phi\mathbf{u}} = \begin{bmatrix} 1 & 0 & 0 \\ 0 & 1 & 0 \\ 0 & 0 & 1 \end{bmatrix} + (1 - \cos \phi) \begin{bmatrix} -(u_2^2 + u_3^2) & u_1 u_2 & u_1 u_3 \\ u_2 u_1 & -(u_1^2 + u_3^2) & u_2 u_3 \\ u_3 u_1 & u_3 u_2 & -(u_1^2 + u_2^2) \end{bmatrix} + \sin \phi \begin{bmatrix} 0 & -u_3 & u_2 \\ u_3 & 0 & -u_1 \\ -u_2 & u_1 & 0 \end{bmatrix}.$$

In parallel, the rotation matrix may be expanded such that

$$\mathbf{R} = \begin{bmatrix} r_{11} & r_{12} & r_{13} \\ r_{21} & r_{22} & r_{23} \\ r_{31} & r_{32} & r_{33} \end{bmatrix} = \begin{bmatrix} \cos \theta & \sin \theta & 0 \\ -\sin \theta & \cos \theta & 0 \\ 0 & 0 & 1 \end{bmatrix}. \quad (2.3.13)$$

An equation for ϕ may be found by taking the traces of $\mathbf{e}^{\phi\mathbf{u}}$ and \mathbf{R} and setting them equal to one another, resulting in

$$\begin{aligned} 3 - 2(1 - \cos \phi) &= 2 \cos \theta + 1, \\ 1 + 2 \cos \phi &= 2 \cos \theta + 1, \\ \cos \theta &= \cos \phi. \end{aligned}$$

This equation is true provided $\theta = \pm \phi$. By convention, it is assumed that $\theta = \phi$; if the converse assumption was made, the resulting axis of rotation would be $-\mathbf{u}$. Next, expand the off-diagonal entries r_{12} and r_{21} to see that

$$\sin \theta = r_{12} = (1 - \cos \phi)u_1 u_2 + \sin \phi(-u_3),$$

$$-\sin \theta = r_{21} = (1 - \cos \phi)u_2 u_1 + \sin \phi(u_3),$$

and subtract the first equation from the second to obtain

$$2 \sin \theta = -2 \sin \phi u_3,$$

$$u_3 = -\frac{\sin \theta}{\sin \phi} = -1.$$

Because \mathbf{u} is a unit vector, $u_1 = u_2 = 0$. Substituting the expressions for ϕ and \mathbf{u} into the expression for $\mathbf{e}^{\phi\mathbf{u}}$ results in the expected form of the rotation matrix.

$$\mathbf{e}^{\phi\mathbf{u}} = \begin{bmatrix} 1 & 0 & 0 \\ 0 & 1 & 0 \\ 0 & 0 & 1 \end{bmatrix} + (1 - \cos \theta) \begin{bmatrix} -1 & 0 & 0 \\ 0 & -1 & 0 \\ 0 & 0 & 0 \end{bmatrix} + \sin \theta \begin{bmatrix} 0 & 1 & 0 \\ 1 & 0 & 0 \\ 0 & 0 & 0 \end{bmatrix} = \begin{bmatrix} \cos \theta & \sin \theta & 0 \\ -\sin \theta & \cos \theta & 0 \\ 0 & 0 & 1 \end{bmatrix}.$$

See Example ?? in the MATLAB Workbook for DCRS for an m-file that can be used to construct the rotation matrix $\mathbf{e}^{\phi\mathbf{u}}$ for any rotation angle ϕ and unit vector \mathbf{u} .

2.4 Position, Velocity, and Acceleration

This study of kinematics is based on the definitions of position, velocity, and accelerations of points on rigid bodies that make up mechanical systems. As already discussed, in applications related to robotics, there can be numerous frames of reference in a single mechanical system. As a result, a systematic methodology is required for utilizing these numerous frames of reference. This framework for a systematic treatment of complex systems, one that accommodates numerous frames of reference, distinguishes the approach in this text from an introductory account. As a starting point, definitions are presented that capture the behavior of one frame varying with respect to another, and subsequently define the *total time derivative* of a vector.

Definition 2.4 (Time-Varying Representation). Suppose \mathbb{X} and \mathbb{Y} are frames with bases $\mathbf{x}_1, \mathbf{x}_2, \mathbf{x}_3$, and $\mathbf{y}_1, \mathbf{y}_2, \mathbf{y}_3$, respectively. \mathbb{Y} is time varying with respect to \mathbb{X} if the representation $\mathbf{y}_1^{\mathbb{X}}, \mathbf{y}_2^{\mathbb{X}}, \mathbf{y}_3^{\mathbb{X}}$ has the form

$$\mathbf{y}_1^{\mathbb{X}} = \mathbf{y}_1^{\mathbb{X}}(t), \quad \mathbf{y}_2^{\mathbb{X}} = \mathbf{y}_2^{\mathbb{X}}(t), \quad \mathbf{y}_3^{\mathbb{X}} = \mathbf{y}_3^{\mathbb{X}}(t).$$

When the background frame \mathbb{X} is understood, the frame \mathbb{Y} may be written with *time-varying bases* $\mathbf{y}_1(t), \mathbf{y}_2(t), \mathbf{y}_3(t)$.

The above definition agrees with intuition. In addition, this definition is symmetric in the sense that if \mathbb{Y} varies with respect to \mathbb{X} , \mathbb{X} also varies with respect to \mathbb{Y} , since $\mathbf{R}_{\mathbb{Y}}^{\mathbb{X}}(t) = (\mathbf{R}_{\mathbb{X}}^{\mathbb{Y}}(t))^T$.

In addition, the fact that one frame varies with respect to another is often implicit, rather than explicit, in the description of a problem. It is often simply stated that the frame \mathbb{Y} has a time varying basis $\mathbf{y}_1(t), \mathbf{y}_2(t), \mathbf{y}_3(t)$ without explicitly discussing the representations $\mathbf{y}_1^{\mathbb{X}}(t), \mathbf{y}_2^{\mathbb{X}}(t), \mathbf{y}_3^{\mathbb{X}}(t)$.

Example 2.4.1. A cylindrical robotic manipulator is depicted in Figures (2.18), along with frames chosen for each of its rigid bodies.

Frame 0 is fixed to the ground link, frame 1 is fixed in the vertical link, frame 2 is fixed in the horizontal link, and frame 3 is attached to the tool. Using Definition (2.4), determine whether the following pairs of frames vary with respect to one another: (i) frames 0 and 1, (ii) frames 1 and 2, (iii) frames 2 and 3.

Solution: From inspection of Figure (2.18), the basis vectors of frame 1 can be represented with respect to the basis vectors of frame 0, such that

$$\begin{aligned}\mathbf{x}_1 &= \cos \theta_1 \mathbf{x}_0 + \sin \theta_1 \mathbf{y}_0, \\ \mathbf{y}_1 &= -\sin \theta_1 \mathbf{x}_0 + \cos \theta_1 \mathbf{y}_0, \\ \mathbf{z}_1 &= \mathbf{z}_0,\end{aligned}$$

which implies that the rotation matrix \mathbf{R}_0^1 is given as

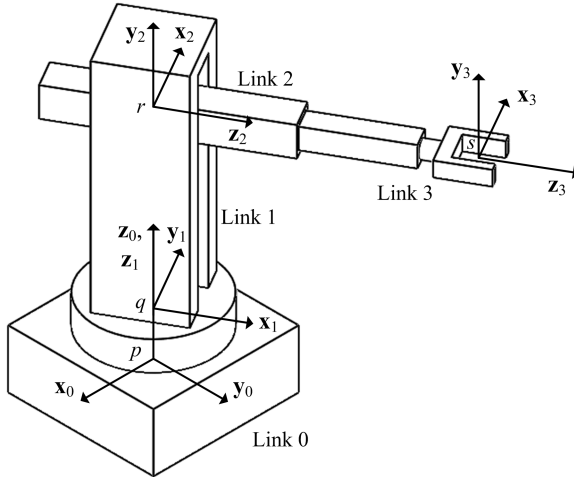


Fig. 2.18: Cylindrical Robot, Frames

$$\mathbf{R}_0^1 = \begin{bmatrix} \cos\theta_1 & \sin\theta_1 & 0 \\ -\sin\theta_1 & \cos\theta_1 & 0 \\ 0 & 0 & 1 \end{bmatrix} = [\mathbf{x}_0^1 \ \mathbf{y}_0^1 \ \mathbf{z}_0^1].$$

In other words, when the joint angles are written as explicit functions of time

$$\mathbf{x}_0^1(t) = \begin{Bmatrix} \cos\theta_1(t) \\ -\sin\theta_1(t) \\ 0 \end{Bmatrix}, \quad \mathbf{y}_0^1(t) = \begin{Bmatrix} \sin\theta_1(t) \\ \cos\theta_1(t) \\ 0 \end{Bmatrix}, \quad \mathbf{z}_0^1(t) = \begin{Bmatrix} 0 \\ 0 \\ 1 \end{Bmatrix},$$

and since the inverse relationship may be found by taking the transpose of \mathbf{R}_0^1 and isolating the columns

$$\mathbf{x}_1^0(t) = \begin{Bmatrix} \cos\theta_1(t) \\ \sin\theta_1(t) \\ 0 \end{Bmatrix}, \quad \mathbf{y}_1^0(t) = \begin{Bmatrix} -\sin\theta_1(t) \\ \cos\theta_1(t) \\ 0 \end{Bmatrix}, \quad \mathbf{z}_1^0(t) = \begin{Bmatrix} 0 \\ 0 \\ 1 \end{Bmatrix},$$

the frames 0 and 1 are shown to vary with respect to one another, according to Definition (2.4). However, for frames 1 and 2, for all time t

$$\begin{aligned} \mathbf{x}_2 &= \mathbf{y}_1, \\ \mathbf{y}_2 &= \mathbf{z}_1, \\ \mathbf{z}_2 &= \mathbf{x}_1 \end{aligned}$$

or equivalently

$$\mathbf{R}_1^2 = \begin{bmatrix} 0 & 1 & 0 \\ 0 & 0 & 1 \\ 1 & 0 & 0 \end{bmatrix}.$$

The following unit vectors can be extracted from the columns of \mathbf{R}_1^2

$$\mathbf{x}_1^2 = \begin{Bmatrix} 0 \\ 0 \\ 1 \end{Bmatrix}, \quad \mathbf{y}_1^2 = \begin{Bmatrix} 1 \\ 0 \\ 0 \end{Bmatrix}, \quad \mathbf{z}_1^2 = \begin{Bmatrix} 0 \\ 1 \\ 0 \end{Bmatrix},$$

and the columns of \mathbf{R}_2^1 can likewise be written as

$$\mathbf{x}_2^1 = \begin{Bmatrix} 0 \\ 1 \\ 0 \end{Bmatrix}, \quad \mathbf{y}_2^1 = \begin{Bmatrix} 0 \\ 0 \\ 1 \end{Bmatrix}, \quad \mathbf{z}_2^1 = \begin{Bmatrix} 1 \\ 0 \\ 0 \end{Bmatrix}.$$

These representations are constant with respect to time, so by Definition (2.5), frame 2 does not vary with respect to frame 1. By a similar argument, since the rotation matrix

$$\mathbf{R}_2^3 = \begin{bmatrix} 1 & 0 & 0 \\ 0 & 0 & 1 \\ 0 & -1 & 0 \end{bmatrix}$$

is constant, frames 2 and 3 do not vary with respect to one another.

For the definitions of velocity and acceleration, vector derivatives are required. This task is made more difficult by the fact that there may be many frames of reference in a given system. The derivative of a vector \mathbf{v} must always be defined, either explicitly or implicitly, with respect to some background frame, as the following theorem makes clear.

Definition 2.5 (Total Time Derivative). Suppose that the frame \mathbb{Y} is time-varying relative to the frame \mathbb{X} , and denote the basis for the frame \mathbb{Y} as $\mathbf{y}_1(t), \mathbf{y}_2(t), \mathbf{y}_3(t)$. The *total time derivative* with respect to the frame \mathbb{X} of a vector $\mathbf{v}(t) = v_1(t)\mathbf{y}_1(t) + v_2(t)\mathbf{y}_2(t) + v_3(t)\mathbf{y}_3(t)$ is given by the chain rule

$$\frac{d}{dt} \Big|_{\mathbb{X}} (\mathbf{v}(t)) = \dot{v}_1(t)\mathbf{y}_1(t) + \dot{v}_2(t)\mathbf{y}_2(t) + \dot{v}_3(t)\mathbf{y}_3(t) \quad (2.4.1)$$

$$+ v_1(t) \frac{d}{dt} \Big|_{\mathbb{X}} (\mathbf{y}_1(t)) + v_2(t) \frac{d}{dt} \Big|_{\mathbb{X}} (\mathbf{y}_2(t)) + v_3(t) \frac{d}{dt} \Big|_{\mathbb{X}} (\mathbf{y}_3(t)). \quad (2.4.2)$$

There is a common structure to the total time derivative of the vector $\mathbf{v}(t)$ in Definition (2.5) that occurs in many of the problems discussed in this book. The first three terms in the total derivative involve the derivatives of the coefficients that multiply the unit vectors $\mathbf{y}_1(t), \mathbf{y}_2(t), \mathbf{y}_3(t)$. These three terms constitute the *basis-fixed*

derivative in frame \mathbb{Y} or the *derivative with respect to an observer* fixed in the \mathbb{Y} frame. The last three terms in the total time derivative involve the *derivative of unit vectors*; it will be shown that these three terms can be expressed in terms of *angular velocity* in Section (2.5) in Theorem (2.12).

Definition 2.6 (Basis-Fixed Derivative). Let \mathbb{Y} and \mathbf{v} be as in Definition (2.5). The *basis-fixed derivative* in frame \mathbb{Y} is defined as

$$\frac{d}{dt} \Big|_{\mathbb{Y}} (\mathbf{v}(t)) := \dot{v}_1(t)\mathbf{y}_1(t) + \dot{v}_2(t)\mathbf{y}_2(t) + \dot{v}_3(t)\mathbf{y}_3(t). \quad (2.4.3)$$

The derivative in Equation (2.4.3) is also known as the *derivative with respect to an observer* fixed in the \mathbb{Y} frame.

If the direction and length of a coordinate vector with respect to a particular basis is constant, then the derivative of the vector while holding that basis fixed is equal to zero. Because this property is used so frequently, the following theorem is introduced.

Theorem 2.9 (Derivative of Fixed-Basis Frame). Let $\mathbf{y}_1, \mathbf{y}_2, \mathbf{y}_3$ be a basis for the \mathbb{Y} frame and suppose that

$$\mathbf{v}(t) = v_1\mathbf{y}_1(t) + v_2\mathbf{y}_2(t) + v_3\mathbf{y}_3(t)$$

where v_1, v_2 and v_3 are constants. By definition

$$\frac{d}{dt} \Big|_{\mathbb{Y}} (\mathbf{v}(t)) = 0.$$

In particular, it is always the case that

$$\frac{d}{dt} \Big|_{\mathbb{Y}} (\mathbf{y}_i(t)) = 0$$

for $i = 1, 2, 3$.

Proof. This theorem follows directly from Definition (2.6). \square

The next example illustrates how Definitions (2.5) and (2.6) and Theorem (2.9) are used directly in problems.

Example 2.4.2. Consider again the cylindrical robot studied in Example (2.4.1) and depicted in Figure (2.18). Let the vector $\mathbf{u}(t)$ be defined as

$$\mathbf{u}(t) = \ln t \mathbf{x}_1(t) + e^t \mathbf{y}_1(t) + (t^3 + \sin \Omega t) \mathbf{z}_1(t) \quad (2.4.4)$$

where $\mathbf{x}_1(t), \mathbf{y}_1(t), \mathbf{z}_1(t)$ are the basis vectors of the frame 1. What is the derivative of $\mathbf{u}(t)$ with respect to the 0 frame?

Solution: By Definition (2.5),

$$\begin{aligned} \frac{d}{dt}\Big|_0 (\mathbf{u}(t)) &= \dot{u}_1(t)\mathbf{x}_1(t) + \dot{u}_2(t)\mathbf{y}_1(t) + \dot{u}_3(t)\mathbf{z}_1(t) \\ &\quad + u_1(t) \frac{d}{dt}\Big|_0 (\mathbf{x}_1(t)) + u_2(t) \frac{d}{dt}\Big|_0 (\mathbf{y}_1(t)) + u_3(t) \frac{d}{dt}\Big|_0 (\mathbf{z}_1(t)). \end{aligned}$$

The first three terms on the right are obtained by differentiating the coefficients of $\mathbf{x}_1(t), \mathbf{x}_2(t)$ and $\mathbf{x}_3(t)$ in Equation (2.4.4).

$$\dot{u}_1\mathbf{x}_1(t) + \dot{u}_2\mathbf{y}_1(t) + \dot{u}_3\mathbf{z}_1(t) = \frac{1}{t}\mathbf{x}_1(t) + e^t\mathbf{y}_1(t) + (3t^2 + \Omega \cos \Omega t)\mathbf{z}_1(t).$$

The time derivatives of $\mathbf{x}_1(t), \mathbf{y}_1(t)$ and $\mathbf{z}_1(t)$ relative to the 0 frame are calculated by expanding the basis vectors that define the 0 frame and differentiating the resulting expressions

$$\begin{aligned} \frac{d}{dt}\Big|_0 (\mathbf{x}_1(t)) &= \frac{d}{dt}\Big|_0 (\cos \theta_1(t)\mathbf{x}_0 + \sin \theta_1(t)\mathbf{y}_0) = \dot{\theta}(t)(-\sin \theta_1(t)\mathbf{x}_0 + \cos \theta_1(t)\mathbf{y}_0) = \dot{\theta}\mathbf{y}_1(t), \\ \frac{d}{dt}\Big|_0 (\mathbf{y}_1(t)) &= \frac{d}{dt}\Big|_0 (-\sin \theta_1(t)\mathbf{x}_0 + \cos \theta_1(t)\mathbf{y}_0) = -\dot{\theta}(t)(\cos \theta_1(t)\mathbf{x}_0 + \sin \theta_1(t)\mathbf{y}_0) = -\dot{\theta}\mathbf{x}_1(t), \\ \frac{d}{dt}\Big|_0 \mathbf{z}_1 &= \frac{d}{dt}\Big|_0 \mathbf{z}_0 = 0. \end{aligned}$$

Implicit in the above differentiation is that

$$\frac{d}{dt}\Big|_0 (\mathbf{x}_0) = \frac{d}{dt}\Big|_0 (\mathbf{y}_0) = \frac{d}{dt}\Big|_0 (\mathbf{z}_0) = 0$$

from Theorem (2.9) above. Combining these two halves of the total time derivative results in

$$\begin{aligned} \frac{d}{dt}\Big|_0 (\mathbf{u}(t)) &= \frac{1}{t}\mathbf{x}_1(t) + e^t\mathbf{y}_1(t) + (3t^2 + \Omega \cos \Omega t)\mathbf{z}_1(t) + \ln t \dot{\theta}\mathbf{y}_1(t) - e^t \dot{\theta}\mathbf{x}_1(t), \\ &= \left(\frac{1}{t} - e^t \dot{\theta}\right)\mathbf{x}_1(t) + (e^t + \ln t \dot{\theta})\mathbf{y}_1(t) + (3t^2 + \Omega \cos \Omega t)\mathbf{z}_1(t). \end{aligned}$$

See Example ?? of the MATLAB Workbook for DCRS for this problem.

Finally, the primary focus of this section: the definition of the position, velocity, and acceleration of points p in a mechanical system that contains multiple frames of reference.

Definition 2.7 (Position, Velocity and Acceleration). Suppose that frame \mathbb{X} has basis $\mathbf{x}_1, \mathbf{x}_2, \mathbf{x}_3$. The *position vector* $\mathbf{r}_{\mathbb{X},p}(t)$ of particle p in the \mathbb{X} frame is the vector that connects the origin of the \mathbb{X} frame to the particle p for all time t . The velocity $\mathbf{v}_{\mathbb{X},p}(t)$ of particle p with respect to the \mathbb{X} frame is the derivative of the position $\mathbf{r}_{\mathbb{X},p}(t)$ of the point p with the \mathbb{X} basis held fixed

$$\mathbf{v}_{\mathbb{X},p}(t) = \frac{d}{dt} \Big|_{\mathbb{X}} (\mathbf{r}_{\mathbb{X},p}(t))$$

The acceleration $\mathbf{a}_{\mathbb{X},p}(t)$ of the point p with respect to the frame \mathbb{X} is the derivative of the velocity $\mathbf{v}_{\mathbb{X},p}(t)$ of the point p with the \mathbb{X} basis held fixed

$$\mathbf{a}_{\mathbb{X},p}(t) = \frac{d}{dt} \Big|_{\mathbb{X}} (\mathbf{v}_{\mathbb{X},p}(t))$$

Example 2.4.3. Return again to the robotic system studied in Examples (2.4.1) and (2.4.2), and depicted in Figure (2.18). What is the position vector in frame 0 of the point s ? Express your answer in terms of the basis for frames 2, 1 and 0. What is the position vector in frame 1 of the point s ? Express your answer in terms of the basis for frames 1 and 0.

Solution: The position vector $\mathbf{r}_{0,s}$ of the point s in frame 0 is the vector that connects the origin of frame 0 to the point s . This vector can be written

$$\mathbf{r}_{0,s} = \underbrace{d_{p,q}\mathbf{z}_0}_{\text{from } p \text{ to } q} + \underbrace{d_{q,r}(t)\mathbf{z}_0}_{\text{from } q \text{ to } r} + \underbrace{d_{r,s}(t)\mathbf{z}_2}_{\text{from } r \text{ to } s}.$$

This expression can be recast in any of a number of equivalent ways by a simple change of basis. The representations relative to the 2 frame and 1 frame are, respectively,

$$\begin{aligned} \mathbf{r}_{0,s} &= (d_{p,q} + d_{q,r}(t))\mathbf{y}_2 + d_{r,s}(t)\mathbf{z}_2, \\ &= d_{r,s}(t)\mathbf{x}_1 + (d_{p,q} + d_{q,r}(t))\mathbf{z}_1. \end{aligned}$$

The representation in terms of the basis for the 0 frame is given by

$$\mathbf{r}_{0,s}^0 = \mathbf{R}_1^0 \begin{Bmatrix} d_{r,s}(t) \\ 0 \\ d_{p,q} + d_{q,r}(t) \end{Bmatrix} = \begin{bmatrix} \cos \theta_1 & -\sin \theta_1 & 0 \\ \sin \theta_1 & \cos \theta_1 & 0 \\ 0 & 0 & 1 \end{bmatrix} \begin{Bmatrix} d_{r,s}(t) \\ 0 \\ d_{p,q} + d_{q,r}(t) \end{Bmatrix} = \begin{Bmatrix} d_{r,s}(t) \cos \theta_1 \\ d_{r,s}(t) \sin \theta_1 \\ d_{p,q} + d_{q,r}(t) \end{Bmatrix}.$$

The position vector $\mathbf{r}_{1,s}$ of the point s in frame 1 is the vector that connects the origin of frame 1 to the point s . This vector is written in terms of the basis for frame 1 as

$$\mathbf{r}_{1,s} = d_{r,s}(t)\mathbf{x}_1 + d_{q,r}(t)\mathbf{z}_1.$$

In terms of the basis for frame 0, its components are given by

$$\begin{aligned}\mathbf{r}_{1,s}^0 &= \mathbf{R}_1^0 \mathbf{r}_{1,s}^1 = \begin{bmatrix} \cos \theta_1 & -\sin \theta_1 & 0 \\ \sin \theta_1 & \cos \theta_1 & 0 \\ 0 & 0 & 1 \end{bmatrix} \begin{Bmatrix} d_{r,s}(t) \\ 0 \\ d_{q,r}(t) \end{Bmatrix}, \\ &= d_{r,s}(t) \begin{Bmatrix} \cos \theta_1 \\ \sin \theta_1 \\ 0 \end{Bmatrix} + d_{q,r}(t) \begin{Bmatrix} 0 \\ 0 \\ 1 \end{Bmatrix}.\end{aligned}$$

This example can be found in the MATLAB Workbook for DCRS in Example ??.

Example 2.4.4. Consider the robot depicted in Figure (2.18). What is the velocity in the 0 frame of point s ? What is the acceleration in the 0 frame of point s ?

Solution: By definition, the velocity in the 0 frame of point s is given by

$$\mathbf{v}_{0,s} = \frac{d}{dt} \Big|_0 (\mathbf{r}_{0,s}).$$

In Example (2.4.3), the position vector $\mathbf{r}_{0,s}$ is determined to be

$$\mathbf{r}_{0,s} = d_{r,s}(t) \cos \theta_1 \mathbf{x}_0 + d_{r,s}(t) \sin \theta_1 \mathbf{y}_0 + (d_{p,q} + d_{q,r}(t)) \mathbf{z}_0.$$

Direct application of the definition yields

$$\begin{aligned}\mathbf{v}_{0,s} &= \frac{d}{dt} \Big|_0 (\mathbf{r}_{0,s}), \\ &= (\dot{d}_{r,s} \cos \theta_1 - d_{r,s} \dot{\theta}_1 \sin \theta_1) \mathbf{x}_0 + (\dot{d}_{r,s} \sin \theta_1 + d_{r,s} \dot{\theta}_1 \cos \theta_1) \mathbf{y}_0 + \dot{H} \mathbf{z}_0 \\ &\quad + d_{r,s} \cos \theta_1 \underbrace{\frac{d}{dt} \Big|_0 (\mathbf{x}_0)}_0 + d_{r,s} \sin \theta_1 \underbrace{\frac{d}{dt} \Big|_0 (\mathbf{y}_0)}_0 + (d_{p,q} + d_{q,r}(t)) \underbrace{\frac{d}{dt} \Big|_0 (\mathbf{z}_0)}_0, \\ &= (\dot{d}_{r,s} \cos \theta_1 - d_{r,s} \dot{\theta}_1 \sin \theta_1) \mathbf{x}_0 + (\dot{d}_{r,s} \sin \theta_1 + d_{r,s} \dot{\theta}_1 \cos \theta_1) \mathbf{y}_0 + \dot{d}_{q,r} \mathbf{z}_0.\end{aligned}$$

The acceleration $\mathbf{a}_{0,s}$ is obtained in a similar manner:

$$\begin{aligned}\mathbf{a}_{0,s} &= \frac{d}{dt} \Big|_0 (\mathbf{v}_{0,s}), \\ &= (\ddot{d}_{r,s} \cos \theta_1 - \dot{d}_{r,s} \dot{\theta}_1 \sin \theta_1 - d_{r,s} \ddot{\theta} \sin \theta_1 - \dot{d}_{r,s} \dot{\theta}_1^2 \cos \theta_1) \mathbf{x}_0 \\ &\quad + (\ddot{d}_{r,s} \sin \theta_1 + \dot{d}_{r,s} \dot{\theta}_1 \cos \theta_1 + \dot{d}_{r,s} \dot{\theta}_1 \cos \theta_1 + d_{r,s} \ddot{\theta}_1 \cos \theta_1 - \dot{d}_{r,s} \dot{\theta}_1^2 \sin \theta_1) \mathbf{y}_0 \\ &\quad + \ddot{d}_{q,r} \mathbf{z}_0.\end{aligned}$$

It should be noted that the components of the velocity and acceleration expressions above can also be rewritten in terms of the cylindrical coordinate system, as described in Theorem (2.18),

$$\mathbf{v}_{0,s}^0 = \dot{d}_{r,s} \begin{Bmatrix} \cos \theta_1 \\ \sin \theta_1 \\ 0 \end{Bmatrix} + d_{r,s} \dot{\theta}_1 \begin{Bmatrix} -\sin \theta_1 \\ \cos \theta_1 \\ 0 \end{Bmatrix} + \dot{d}_{q,r} \begin{Bmatrix} 0 \\ 0 \\ 1 \end{Bmatrix},$$

$$\mathbf{a}_{0,s}^0 = (\ddot{d}_{r,s} - d_{r,s} \dot{\theta}_1^2) \begin{Bmatrix} \cos \theta_1 \\ \sin \theta_1 \\ 0 \end{Bmatrix} + (d_{r,s} \ddot{\theta}_1 + 2\dot{d}_{r,s} \dot{\theta}_1) \begin{Bmatrix} -\sin \theta_1 \\ \cos \theta_1 \\ 0 \end{Bmatrix} + \ddot{d}_{q,r} \begin{Bmatrix} 0 \\ 0 \\ 1 \end{Bmatrix}.$$

The velocity $\mathbf{v}_{0,s}$ and acceleration $\mathbf{a}_{0,s}$ are calculated using MATLAB in Example ?? of the MATLAB Workbook for DCRS.

Example 2.4.5. Consider the robot depicted in Figure (2.18) again. What is the velocity in the 1 frame of point s ? What is the acceleration in the 1 frame of point s ?

Solution: The definition of the velocity $\mathbf{v}_{1,s}$ in the 1 frame of point s asserts that

$$\mathbf{v}_{1,s} = \frac{d}{dt} \Big|_1 (\mathbf{r}_{1,s})$$

where $\mathbf{r}_{1,s}$ is the position in the 1 frame of point s . From Example (2.4.3), $\mathbf{r}_{1,s}$ is defined as

$$\mathbf{r}_{1,s} = d_{r,s}(t)\mathbf{x}_1 + d_{q,r}(t)\mathbf{z}_1,$$

and the velocity $\mathbf{v}_{1,s}$ is

$$\begin{aligned} \mathbf{v}_{1,s} &= \dot{d}_{r,s}\mathbf{x}_1 + \dot{d}_{q,r}\mathbf{z}_1 = \frac{d}{dt} \Big|_1 (d_{r,s}(t)\mathbf{x}_1 + d_{q,r}(t)\mathbf{z}_1), \\ &= \dot{d}_{r,s}\mathbf{x}_1 + d_{r,s} \underbrace{\frac{d}{dt} \Big|_1 (\mathbf{x}_1)}_0 + \dot{d}_{q,r}\mathbf{z}_1 + d_{q,r} \underbrace{\frac{d}{dt} \Big|_1 (\mathbf{z}_1)}_0, \\ &= \dot{d}_{r,s}\mathbf{x}_1 + \dot{d}_{q,r}\mathbf{z}_1. \end{aligned}$$

For the acceleration $\mathbf{a}_{1,s}$,

$$\begin{aligned} \mathbf{a}_{1,s} &= \frac{d}{dt} \Big|_1 (\mathbf{v}_{1,s}) = \frac{d}{dt} \Big|_1 (\dot{d}_{r,s}\mathbf{x}_1 + \dot{d}_{q,r}\mathbf{z}_1), \\ &= \ddot{d}_{r,s}\mathbf{x}_1 + \dot{d}_{r,s} \underbrace{\frac{d}{dt} \Big|_1 (\mathbf{x}_1)}_0 + \ddot{d}_{q,r}\mathbf{z}_1 + \dot{d}_{q,r} \underbrace{\frac{d}{dt} \Big|_1 (\mathbf{z}_1)}_0, \\ &= \ddot{d}_{r,s}\mathbf{x}_1 + \ddot{d}_{q,r}\mathbf{z}_1. \end{aligned}$$

Note that the velocities and acceleration above are not obtained from the velocity and acceleration in the 0 frame as calculated in Example (2.4.4) and subsequently changing basis. The position vectors that are used to define $\mathbf{v}_{1,s}$ and $\mathbf{v}_{0,s}$ are not the same.

This calculation is also carried out in Example ?? of the MATLAB Workbook for DCRS.

In many problems the notation $(\cdot)|_{\mathbb{X}}$ is omitted since the background frame should be clear. However, it is crucial to note that $\mathbf{r}_{\mathbb{X},p}$ and $\mathbf{r}_{\mathbb{Y},p}$ are not representations of the same vector in different frames; they are different vectors from different frame origins to the same point. The following definition emphasizes this fact by introducing the notion of the *relative position* $\mathbf{d}_{\mathbb{X},\mathbb{Y}}$ of the frames \mathbb{X} and \mathbb{Y} .

Definition 2.8 (Relative Position). Suppose that frame \mathbb{X} has basis $\mathbf{x}_1, \mathbf{x}_2, \mathbf{x}_3$, and suppose that frame \mathbb{Y} with basis $\mathbf{y}_1(t), \mathbf{y}_2(t), \mathbf{y}_3(t)$ varies with respect to \mathbb{X} as depicted in Figure (2.19). The *relative position* $\mathbf{d}_{\mathbb{X},\mathbb{Y}}(t)$ of frame \mathbb{Y} with respect to frame \mathbb{X} is the vector from the origin of the \mathbb{X} frame to the origin of the \mathbb{Y} frame. The position $\mathbf{r}_{\mathbb{X},p}(t)$ of the particle p with respect to the \mathbb{X} frame, the position $\mathbf{r}_{\mathbb{Y},p}(t)$ of the particle p with respect to the \mathbb{Y} frame, and the relative position $\mathbf{d}_{\mathbb{X},\mathbb{Y}}(t)$ of the frame \mathbb{Y} with respect to the frame \mathbb{X} satisfy the equation

$$\mathbf{r}_{\mathbb{X},p}(t) = \mathbf{d}_{\mathbb{X},\mathbb{Y}}(t) + \mathbf{r}_{\mathbb{Y},p}(t).$$

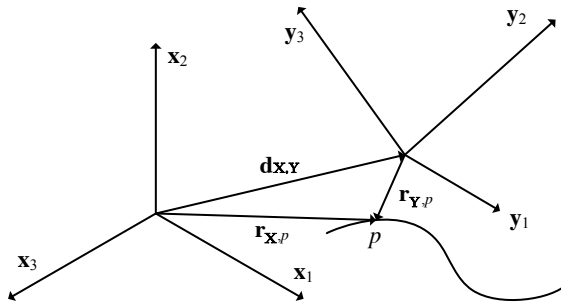


Fig. 2.19: Position Vectors

2.5 Angular Velocity and Angular Acceleration

The calculation of velocity and acceleration in Definition (2.7) often requires *differentiation of unit vectors* or *differentiation of rotation matrices*. These two topics are closely related and are often defined using the *angular velocity* between two different frames of reference. If the expressions for the velocity in Definition (2.7) are further differentiated to obtain the acceleration, the derivative of angular velocity, or *angular acceleration* is also required. Angular velocity is defined in Section (2.5.1), while Section (2.5.2) discusses angular acceleration.

2.5.1 Angular Velocity

Angular velocity is a fundamental quantity in kinematics. Its definition for two-dimensional or planar motion is trivial, as shown in Theorem (2.13), and is easy to interpret geometrically. However, the definition of angular velocity in three dimensions does not lend itself to a simple geometric interpretation. The definition that follows shows that at a fundamental level the definition of angular velocity is connected to the calculation of the time derivative of rotation matrices.

Definition 2.9 (Angular Velocity). Let frame \mathbb{Y} rotate relative to frame \mathbb{X} and suppose that the rotation matrix $\mathbf{R}_{\mathbb{Y}}^{\mathbb{X}}(t)$ is a differentiable function of time t . The angular velocity vector $\boldsymbol{\omega}_{\mathbb{X},\mathbb{Y}}$ of the \mathbb{Y} frame with respect to the \mathbb{X} frame is the unique vector such that the linear operator $\boldsymbol{\omega}_{\mathbb{X},\mathbb{Y}} \times (\bullet)$ has the matrix representation $\dot{\mathbf{R}}_{\mathbb{Y}}^{\mathbb{X}}(\mathbf{R}_{\mathbb{Y}}^{\mathbb{X}})^T$ with respect to the basis for the \mathbb{X} frame.

Before proceeding to some applications and problems, this definition should be shown to be self-consistent. At least a few points should be noted about Definition (2.9). For any possible angular velocity vector $\boldsymbol{\omega}_{\mathbb{X},\mathbb{Y}}$, the operator $\boldsymbol{\omega}_{\mathbb{X},\mathbb{Y}} \times (\bullet)$ acts on *vectors* in \mathbb{R}^3 . Since this operator is a linear operator on vectors, it has a representation that depends on the basis chosen for \mathbb{R}^3 . If $\mathbf{x}_1, \mathbf{x}_2, \mathbf{x}_3$ are chosen for the vectors in \mathbb{R}^3 , the action of the operator $\boldsymbol{\omega}_{\mathbb{X},\mathbb{Y}} \times (\bullet)$ on vectors *expanded in this basis* is given by the usual expression

$$\mathbf{S}(\boldsymbol{\omega}_{\mathbb{Y},\mathbb{X}}^{\mathbb{X}}) \quad (2.5.1)$$

where, again, $\mathbf{S}(\bullet)$ is the skew operator.

This last expression can be expanded to emphasize the point. Suppose that the components of the angular velocity $\boldsymbol{\omega}_{\mathbb{X},\mathbb{Y}}$ are abbreviated in terms of the basis for the \mathbb{X} frame as $\omega_1, \omega_2, \omega_3$. That is, the following shorthand is introduced

$$\boldsymbol{\omega}_{\mathbb{X},\mathbb{Y}}^{\mathbb{X}} = \begin{Bmatrix} \omega_1 \\ \omega_2 \\ \omega_3 \end{Bmatrix} \quad (2.5.2)$$

for the explicit expression

$$\boldsymbol{\omega}_{\mathbb{X},\mathbb{Y}}^{\mathbb{X}} = \omega_1 \mathbf{x}_1 + \omega_2 \mathbf{x}_2 + \omega_3 \mathbf{x}_3. \quad (2.5.3)$$

With these conventions and assumptions, the matrix representation of the operator $\boldsymbol{\omega}_{\mathbb{X},\mathbb{Y}} \times (\bullet)$ acting on vectors *that have been expanded in terms of the basis for the \mathbb{X} frame* is

$$\mathbf{S}(\boldsymbol{\omega}_{\mathbb{Y},\mathbb{X}}^{\mathbb{X}}) = \begin{bmatrix} 0 & -\omega_3 & \omega_2 \\ \omega_3 & 0 & -\omega_1 \\ -\omega_2 & \omega_1 & 0 \end{bmatrix}. \quad (2.5.4)$$

As a result, this matrix is given by the relationship

$$\mathbf{S}(\boldsymbol{\omega}_{\mathbb{X},\mathbb{Y}}^{\mathbb{X}}) = \dot{\mathbf{R}}_{\mathbb{Y}}^{\mathbb{X}} (\mathbf{R}_{\mathbb{Y}}^{\mathbb{X}})^T. \quad (2.5.5)$$

These comments are summarized in the following theorem.

Theorem 2.10 (Rotation Matrix Derivative). Let \mathbb{X} and \mathbb{Y} be two frames, and let the rotation matrix that relates them be time-varying, $\mathbf{R}_{\mathbb{Y}}^{\mathbb{X}}(t)$. The time derivative $\frac{d}{dt}(\mathbf{R}_{\mathbb{Y}}^{\mathbb{X}}(t))$ is given by

$$\frac{d}{dt}(\mathbf{R}_{\mathbb{Y}}^{\mathbb{X}}(t)) = \mathbf{S}(\boldsymbol{\omega}_{\mathbb{X},\mathbb{Y}}^{\mathbb{X}}(t)) \mathbf{R}_{\mathbb{Y}}^{\mathbb{X}}(t)$$

where $\mathbf{S}(\bullet)$ is the skew-symmetric operator and $\boldsymbol{\omega}_{\mathbb{X},\mathbb{Y}}^{\mathbb{X}}$ is the representation with respect to the \mathbb{X} -basis of the angular velocity vector $\boldsymbol{\omega}_{\mathbb{X},\mathbb{Y}}$ of the frame \mathbb{Y} with respect to the frame \mathbb{X} .

Proof. This theorem follows from Definition (2.9) and the preceding comments after noting that

$$(\boldsymbol{\omega}_{\mathbb{X},\mathbb{Y}} x(\cdot))^{\mathbb{X}} = S(\boldsymbol{\omega}_{\mathbb{X},\mathbb{Y}}^{\mathbb{X}}) = \dot{\mathbf{R}}_{\mathbb{Y}}^{\mathbb{X}} (\dot{\mathbf{R}}_{\mathbb{Y}}^{\mathbb{X}})^T.$$

□

While Definition (2.9) is not intuitive, it has a host of applications to practical problems. Considerable effort can sometimes be saved in particular examples through the careful use of angular velocity. The definition of the angular velocity is motivated by considering the velocity of a point that is fixed on a rigid body.

Theorem 2.11 (Velocity of Point-Fixed Bodies). Suppose that the point p is fixed in frame \mathbb{B} with basis $\mathbf{b}_1, \mathbf{b}_2, \mathbf{b}_3$ that moves relative to the \mathbb{X} frame. As shown in Figure (2.20), assume that the origin of the \mathbb{B} and \mathbb{X} frames coincide for all time. The velocity $\mathbf{v}_{\mathbb{X},p}$ of the point p in the \mathbb{X} frame is given by

$$\mathbf{v}_{\mathbb{X},p} = \boldsymbol{\omega}_{\mathbb{X},\mathbb{B}} \times \mathbf{r}_{\mathbb{X},p} \quad (2.5.6)$$

where $\boldsymbol{\omega}_{\mathbb{X},\mathbb{B}}$ is the angular velocity of the \mathbb{B} frame relative to the \mathbb{X} frame.

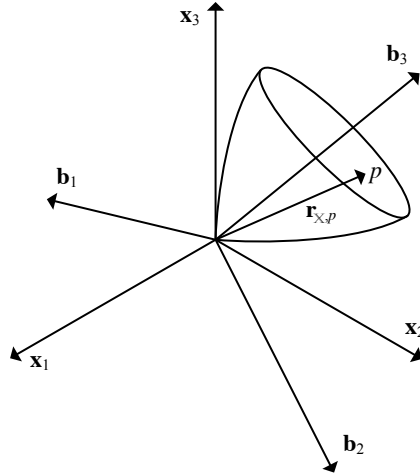


Fig. 2.20: A Point p Fixed in Frame \mathbb{B}

Proof. First note that the position vector $\mathbf{r}_{\mathbb{X},p}$ with respect to the frame \mathbb{X} is identical to the position vector $\mathbf{r}_{\mathbb{B},p}$ with respect to the frame \mathbb{B} because the origins of the two frames coincide for all time. The velocity of the point p in the frame \mathbb{X} is defined to be the derivative of the position vector $\mathbf{r}_{\mathbb{X},p}$ with the basis for the frame \mathbb{X} held fixed,

$$\mathbf{v}_{\mathbb{X},p} = \frac{d}{dt} \Big|_{\mathbb{X}} (\mathbf{r}_{\mathbb{X},p}). \quad (2.5.7)$$

The fact that the basis for the frame \mathbb{X} is held constant is noted by omitting time dependence when writing $\mathbf{x}_1, \mathbf{x}_2, \mathbf{x}_3$, whereas the basis for frame \mathbb{B} is written as $\mathbf{b}_1(t), \mathbf{b}_2(t), \mathbf{b}_3(t)$ to emphasize that it changes with respect to frame \mathbb{X} . The vector $\mathbf{r}_{\mathbb{X},p}$ can be expressed in either the \mathbb{B} -basis as

$$\mathbf{r}_{\mathbb{X},p} = a_1^{\mathbb{B}} \mathbf{b}_1(t) + a_2^{\mathbb{B}} \mathbf{b}_2(t) + a_3^{\mathbb{B}} \mathbf{b}_3(t), \quad (2.5.8)$$

or the \mathbb{X} -basis,

$$\mathbf{r}_{\mathbb{X},p} = \alpha_1^{\mathbb{X}}(t)\mathbf{x}_1 + \alpha_2^{\mathbb{X}}(t)\mathbf{x}_2 + \alpha_3^{\mathbb{X}}(t)\mathbf{x}_3. \quad (2.5.9)$$

There are two important observations to be made regarding the expansions in Equations (2.5.8) and (2.5.9). Since the point p is fixed with respect to frame \mathbb{B} , it does not move relative to the frame \mathbb{B} . This means that the coefficients $\alpha_1^{\mathbb{B}}, \alpha_2^{\mathbb{B}}, \alpha_3^{\mathbb{B}}$ in Equation (2.5.8) are constants: they do not depend on time. By contrast, the coefficients $\alpha_1^{\mathbb{X}}(t), \alpha_2^{\mathbb{X}}(t), \alpha_3^{\mathbb{X}}(t)$ of the point p with respect to the frame \mathbb{X} do vary with time. In fact, the relationship between these two sets of coefficients is known to be

$$\begin{Bmatrix} \alpha_1^{\mathbb{X}}(t) \\ \alpha_2^{\mathbb{X}}(t) \\ \alpha_3^{\mathbb{X}}(t) \end{Bmatrix} = \mathbf{R}_{\mathbb{B}}^{\mathbb{X}}(t) \begin{Bmatrix} \alpha_1^{\mathbb{B}} \\ \alpha_2^{\mathbb{B}} \\ \alpha_3^{\mathbb{B}} \end{Bmatrix}. \quad (2.5.10)$$

This equation can also be written as

$$\mathbf{r}_{\mathbb{X},p}^{\mathbb{X}} = \mathbf{R}_{\mathbb{B}}^{\mathbb{X}} \mathbf{r}_{\mathbb{X},p}^{\mathbb{B}}.$$

Both sides of the 3-tuples of coordinates in the above equation can be differentiated to obtain

$$\begin{Bmatrix} \dot{\alpha}_1^{\mathbb{X}}(t) \\ \dot{\alpha}_2^{\mathbb{X}}(t) \\ \dot{\alpha}_3^{\mathbb{X}}(t) \end{Bmatrix} = \frac{d}{dt}(\mathbf{R}_{\mathbb{B}}^{\mathbb{X}}) \begin{Bmatrix} \alpha_1^{\mathbb{B}} \\ \alpha_2^{\mathbb{B}} \\ \alpha_3^{\mathbb{B}} \end{Bmatrix} \quad (2.5.11)$$

and by the orthogonality of the rotation matrix, the product $(\mathbf{R}_{\mathbb{B}}^{\mathbb{X}})^T \mathbf{R}_{\mathbb{B}}^{\mathbb{X}}$ may be inserted into the equation

$$\begin{Bmatrix} \dot{\alpha}_1^{\mathbb{X}}(t) \\ \dot{\alpha}_2^{\mathbb{X}}(t) \\ \dot{\alpha}_3^{\mathbb{X}}(t) \end{Bmatrix} = \frac{d}{dt}(\mathbf{R}_{\mathbb{B}}^{\mathbb{X}})(\mathbf{R}_{\mathbb{B}}^{\mathbb{X}})^T \mathbf{R}_{\mathbb{B}}^{\mathbb{X}} \begin{Bmatrix} \alpha_1^{\mathbb{B}} \\ \alpha_2^{\mathbb{B}} \\ \alpha_3^{\mathbb{B}} \end{Bmatrix}. \quad (2.5.12)$$

Next, the definition of the angular velocity vector is introduced, resulting in

$$\begin{Bmatrix} \dot{\alpha}_1^{\mathbb{X}}(t) \\ \dot{\alpha}_2^{\mathbb{X}}(t) \\ \dot{\alpha}_3^{\mathbb{X}}(t) \end{Bmatrix} = \mathbf{S}(\boldsymbol{\omega}_{\mathbb{X},\mathbb{B}}^{\mathbb{X}}) \mathbf{R}_{\mathbb{B}}^{\mathbb{X}} \begin{Bmatrix} \alpha_1^{\mathbb{B}} \\ \alpha_2^{\mathbb{B}} \\ \alpha_3^{\mathbb{B}} \end{Bmatrix} = \mathbf{S}(\boldsymbol{\omega}_{\mathbb{X},\mathbb{B}}^{\mathbb{X}}) \begin{Bmatrix} \alpha_1^{\mathbb{X}}(t) \\ \alpha_2^{\mathbb{X}}(t) \\ \alpha_3^{\mathbb{X}}(t) \end{Bmatrix}. \quad (2.5.13)$$

This last equation provides the desired result: the left hand side of the equality contains the coefficients of the velocity vector $\mathbf{v}_{\mathbb{X},p}$ with respect to the \mathbb{X} basis, while the right hand side of the equality is the matrix representation for $\boldsymbol{\omega}_{\mathbb{X},\mathbb{B}} \times \mathbf{r}_{\mathbb{X},p}$ with respect to the \mathbb{X} basis. \square

Theorem (2.11) provides a physical interpretation for the *angular velocity* definition in three dimensions. The velocity of a point on a rigid body that has a single point fixed in the inertial frame can be expressed in terms of the cross product of the angular velocity of the body and a vector that connects the point fixed in the inertial frame to the point p .

The following theorem shows that the *angular velocity* for two frames \mathbb{X} and \mathbb{Y} can also be used to relate derivatives $\frac{d}{dt}|_{\mathbb{X}}(\cdot)$ and $\frac{d}{dt}|_{\mathbb{Y}}(\cdot)$. In addition, this theorem is equivalent to Theorem (2.10); theorem (2.12) can be derived from Theorem (2.10), or vice versa.

Theorem 2.12 (Derivative Theorem). *Let \mathbb{X} and \mathbb{Y} be two frames of reference, and let \mathbf{a} be an arbitrary vector. The derivative of \mathbf{a} holding the basis for the frame \mathbb{X} fixed and the derivative of \mathbf{a} holding the basis for the frame \mathbb{Y} fixed satisfy the equation*

$$\frac{d}{dt}|_{\mathbb{X}}(\mathbf{a}) = \frac{d}{dt}|_{\mathbb{Y}}(\mathbf{a}) + \boldsymbol{\omega}_{\mathbb{X},\mathbb{Y}} \times \mathbf{a}. \quad (2.5.14)$$

Proof. The vector \mathbf{a} can be written in terms of either the basis for the \mathbb{X} frame, or the basis for the \mathbb{Y} frame, as shown below.

$$\begin{aligned} \mathbf{a} &= a_1^{\mathbb{X}} \mathbf{x}_1 + a_2^{\mathbb{X}} \mathbf{x}_2 + a_3^{\mathbb{X}} \mathbf{x}_3, \\ &= a_1^{\mathbb{Y}} \mathbf{y}_1 + a_2^{\mathbb{Y}} \mathbf{y}_2 + a_3^{\mathbb{Y}} \mathbf{y}_3. \end{aligned}$$

By definition,

$$\left\{ \begin{array}{l} \dot{a}_1^{\mathbb{X}} \\ \dot{a}_2^{\mathbb{X}} \\ \dot{a}_3^{\mathbb{X}} \end{array} \right\} = \left(\frac{d}{dt}|_{\mathbb{X}} \right)^{\mathbb{X}} (\mathbf{a})$$

and

$$\left\{ \begin{array}{l} \dot{a}_1^{\mathbb{Y}} \\ \dot{a}_2^{\mathbb{Y}} \\ \dot{a}_3^{\mathbb{Y}} \end{array} \right\} = \left(\frac{d}{dt}|_{\mathbb{Y}} \right)^{\mathbb{Y}} (\mathbf{a}).$$

The coordinates $\mathbf{a}^{\mathbb{X}}$ and $\mathbf{a}^{\mathbb{Y}}$ relative to these two frames are related by the change of basis formula

$$\mathbf{a}^{\mathbb{X}} = \left\{ \begin{array}{l} a_1^{\mathbb{X}} \\ a_2^{\mathbb{X}} \\ a_3^{\mathbb{X}} \end{array} \right\} = \mathbf{R}_{\mathbb{Y}}^{\mathbb{X}} \mathbf{a}^{\mathbb{Y}} = \mathbf{R}_{\mathbb{Y}}^{\mathbb{X}} \left\{ \begin{array}{l} a_1^{\mathbb{Y}} \\ a_2^{\mathbb{Y}} \\ a_3^{\mathbb{Y}} \end{array} \right\}.$$

When the coordinates above are differentiated,

$$\begin{aligned} \left\{ \begin{array}{l} \dot{a}_1^{\mathbb{X}} \\ \dot{a}_2^{\mathbb{X}} \\ \dot{a}_3^{\mathbb{X}} \end{array} \right\} &= \mathbf{R}_{\mathbb{Y}}^{\mathbb{X}} \left\{ \begin{array}{l} \dot{a}_1^{\mathbb{Y}} \\ \dot{a}_2^{\mathbb{Y}} \\ \dot{a}_3^{\mathbb{Y}} \end{array} \right\} + \frac{d}{dt} (\mathbf{R}_{\mathbb{Y}}^{\mathbb{X}}) \mathbf{a}^{\mathbb{Y}}, \\ &= \mathbf{R}_{\mathbb{Y}}^{\mathbb{X}} \left\{ \begin{array}{l} \dot{a}_1^{\mathbb{Y}} \\ \dot{a}_2^{\mathbb{Y}} \\ \dot{a}_3^{\mathbb{Y}} \end{array} \right\} + \mathbf{S}(\boldsymbol{\omega}_{\mathbb{X},\mathbb{Y}}^{\mathbb{X}}) \mathbf{R}_{\mathbb{Y}}^{\mathbb{X}} \mathbf{a}^{\mathbb{Y}}, \\ &= \mathbf{R}_{\mathbb{Y}}^{\mathbb{X}} \left\{ \begin{array}{l} \dot{a}_1^{\mathbb{Y}} \\ \dot{a}_2^{\mathbb{Y}} \\ \dot{a}_3^{\mathbb{Y}} \end{array} \right\} + \mathbf{S}(\boldsymbol{\omega}_{\mathbb{X},\mathbb{Y}}^{\mathbb{X}}) \mathbf{a}^{\mathbb{X}}. \end{aligned}$$

The left hand side of the expression above is just the derivative of the vector \mathbf{a} holding the basis for \mathbb{X} fixed, expressed in terms of the \mathbb{X} basis. The first term on the right above is the derivative of the vector \mathbf{a} holding the basis for \mathbb{Y} fixed, expressed in terms of the \mathbb{X} basis. The second term on the right above is $\boldsymbol{\omega}_{\mathbb{X},\mathbb{Y}} \times \mathbf{a}$ expressed in terms of the \mathbb{X} basis. In other words, this equation can be rewritten

$$\begin{aligned}\left(\frac{d}{dt}\Big|_{\mathbb{X}} (\mathbf{a})\right)^{\mathbb{X}} &= \mathbf{R}_{\mathbb{Y}}^{\mathbb{X}} \left(\frac{d}{dt}\Big|_{\mathbb{Y}} (\mathbf{a})\right)^{\mathbb{Y}} + (\boldsymbol{\omega}_{\mathbb{X},\mathbb{Y}} \times \mathbf{a})^{\mathbb{X}}, \\ \left(\frac{d}{dt}\Big|_{\mathbb{X}} (\mathbf{a})\right)^{\mathbb{X}} &= \left(\frac{d}{dt}\Big|_{\mathbb{Y}} (\mathbf{a})\right)^{\mathbb{X}} + (\boldsymbol{\omega}_{\mathbb{X},\mathbb{Y}} \times \mathbf{a})^{\mathbb{X}}.\end{aligned}$$

which shows the expected relationship between these two derivatives. \square

Several important theorems that are used frequently in applications follow from these definitions. Some of the most important are summarized in Section (2.6), and particularly in Theorems (2.16) and (2.17). This section is closed by focusing on the study of two-dimensional, single-axis rotations. For example, the angular velocity vector for a single-axis rotation can be viewed as the rate of rotation about a unit vector determined by the right hand rule.

Theorem 2.13 (Axis-Angle Rotation Angular Velocity). Suppose that the frame \mathbb{B} and the frame \mathbb{X} have a common origin, and that the frame \mathbb{B} rotates relative to the frame \mathbb{X} through the angle $\theta(t)$ about the unit vector \mathbf{u} . The angular velocity $\boldsymbol{\omega}_{\mathbb{X},\mathbb{B}}$ of the \mathbb{B} -frame relative to the \mathbb{X} -frame is given by

$$\boldsymbol{\omega}_{\mathbb{X},\mathbb{B}} = \dot{\theta}(t)\mathbf{u}.$$

The following theorem shows that it is particularly easy to verify the structure of the matrices in Theorem (2.10) in the event that the motion corresponds to a single-axis rotation.

Theorem 2.14 (Time Derivative of Rotation Matrix). Let $\mathbf{R}_{\mathbb{Y}}^{\mathbb{X}}(\alpha_i(t))$ be the single-axis rotation matrix associated with a rotation of $\alpha_i(t)$ about the $\mathbf{x}_i = \mathbf{y}_i$ axis for $i = 1, 2$ or 3 . The time-derivative $\frac{d}{dt}(\mathbf{R}_{\mathbb{Y}}^{\mathbb{X}}(\alpha_i(t)))$ is given by the product

$$\frac{d}{dt}(\mathbf{R}_{\mathbb{Y}}^{\mathbb{X}}(\alpha_i(t))) = \mathbf{S}\left(\frac{d\alpha_i(t)}{dt}\mathbf{e}_i\right)\mathbf{R}_{\mathbb{Y}}^{\mathbb{X}}$$

where $\mathbf{S}(\bullet)$ is the 3×3 skew operator and \mathbf{e}_i is the ground-frame i -direction unit vector (e.g., $\mathbf{e}_3 := [0 \ 0 \ 1]$).

Proof. It will be shown that this identify holds when $i = 3$, and the other cases will be left for exercises. For $i = 3$, Theorem (2.6) gives an explicit formula for $\mathbf{R}_{\mathbb{Y}}^{\mathbb{X}}$, such that

$$\mathbf{R}_{\mathbb{Y}}^{\mathbb{X}}(\alpha_3(t)) = \begin{bmatrix} \cos \alpha_3(t) & -\sin \alpha_3(t) & 0 \\ \sin \alpha_3(t) & \cos \alpha_3(t) & 0 \\ 0 & 0 & 1 \end{bmatrix}.$$

Differentiating this matrix explicitly results in the expected form of the equation.

$$\begin{aligned} \frac{d}{dt}(\mathbf{R}_{\mathbb{Y}}^{\mathbb{X}}(\alpha_3(t))) &= \begin{bmatrix} -\sin \alpha_3(t) \frac{d\alpha_3}{dt} & -\cos \alpha_3(t) \frac{d\alpha_3}{dt} & 0 \\ \cos \alpha_3(t) \frac{d\alpha_3}{dt} & -\sin \alpha_3(t) \frac{d\alpha_3}{dt} & 0 \\ 0 & 0 & 1 \end{bmatrix}, \\ &= \begin{bmatrix} 0 & -\frac{d\alpha_3}{dt} & 0 \\ \frac{d\alpha_3}{dt} & 0 & 0 \\ 0 & 0 & 0 \end{bmatrix} \begin{bmatrix} \cos \alpha_3(t) & -\sin \alpha_3(t) & 0 \\ \sin \alpha_3(t) & \cos \alpha_3(t) & 0 \\ 0 & 0 & 1 \end{bmatrix}, \\ &= \mathbf{S}\left(\frac{d\alpha_3}{dt} \mathbf{e}_3\right) \mathbf{R}_{\mathbb{Y}}^{\mathbb{X}}(\alpha_3(t)). \end{aligned}$$

□

2.5.2 Angular Acceleration

In Definition (2.7), the velocity and acceleration of a point p in the \mathbb{X} frame was introduced. The acceleration of the point p in the \mathbb{X} frame is the time derivative of the velocity with respect to the \mathbb{X} frame with the basis for the \mathbb{X} frame held fixed. Similarly, the angular acceleration of the \mathbb{Y} frame with respect to the \mathbb{X} frame is the derivative of the angular velocity $\omega_{\mathbb{X},\mathbb{Y}}$ with the basis \mathbb{X} held fixed.

Definition 2.10 (Angular Acceleration). Suppose that \mathbb{X} and \mathbb{Y} are two frames. The *angular acceleration* of the \mathbb{Y} frame with respect to the \mathbb{X} frame is defined to be the time derivative of the angular velocity $\omega_{\mathbb{X},\mathbb{Y}}$ with respect to an observer in the \mathbb{X} frame.

$$\alpha_{\mathbb{X},\mathbb{Y}} := \frac{d}{dt} \Big|_{\mathbb{X}} (\omega_{\mathbb{X},\mathbb{Y}}).$$

2.6 Theorems of Kinematics

The definitions of velocity, acceleration, angular velocity and angular acceleration are sufficient to solve any problem of three dimensional kinematics. Still, considerable work can be avoided in some problems by using one or more of the theorems discussed in this section.

2.6.1 Addition of Angular Velocities

One of the most powerful theorems studied in this chapter is the *Addition Theorem for Angular Velocities*.

Theorem 2.15 (Addition Theorem for Angular Velocities). Let $\mathbb{X}, \mathbb{Y}, \mathbb{Z}$ be three arbitrary frames:

$$\boldsymbol{\omega}_{\mathbb{X},\mathbb{Z}} = \boldsymbol{\omega}_{\mathbb{X},\mathbb{Y}} + \boldsymbol{\omega}_{\mathbb{Y},\mathbb{Z}} \quad (2.6.1)$$

Proof. The proof of this theorem follows from the identity

$$\mathbf{S}(\boldsymbol{\omega}_{\mathbb{X},\mathbb{Z}}^{\mathbb{X}}) = \dot{\mathbf{R}}_{\mathbb{Z}}^{\mathbb{X}} (\mathbf{R}_{\mathbb{Z}}^{\mathbb{X}})^T.$$

Since $\mathbf{R}_{\mathbb{Z}}^{\mathbb{X}} = \mathbf{R}_{\mathbb{Y}}^{\mathbb{X}} \mathbf{R}_{\mathbb{Z}}^{\mathbb{Y}}$,

$$\mathbf{S}(\boldsymbol{\omega}_{\mathbb{X},\mathbb{Z}}^{\mathbb{X}}) = \frac{d}{dt} (\mathbf{R}_{\mathbb{Y}}^{\mathbb{X}} \mathbf{R}_{\mathbb{Z}}^{\mathbb{Y}}) (\mathbf{R}_{\mathbb{Y}}^{\mathbb{X}} \mathbf{R}_{\mathbb{Z}}^{\mathbb{Y}})^T.$$

Expanding the derivative on the right hand side results in the expected form of the equation

$$\begin{aligned} \mathbf{S}(\boldsymbol{\omega}_{\mathbb{X},\mathbb{Z}}^{\mathbb{X}}) &= \dot{\mathbf{R}}_{\mathbb{Y}}^{\mathbb{X}} \mathbf{R}_{\mathbb{Z}}^{\mathbb{Y}} (\mathbf{R}_{\mathbb{Z}}^{\mathbb{Y}})^T (\mathbf{R}_{\mathbb{Y}}^{\mathbb{X}})^T + \mathbf{R}_{\mathbb{Y}}^{\mathbb{X}} \dot{\mathbf{R}}_{\mathbb{Z}}^{\mathbb{Y}} (\mathbf{R}_{\mathbb{Z}}^{\mathbb{Y}})^T (\mathbf{R}_{\mathbb{Y}}^{\mathbb{X}})^T, \\ &= \dot{\mathbf{R}}_{\mathbb{Y}}^{\mathbb{X}} (\mathbf{R}_{\mathbb{Y}}^{\mathbb{X}})^T + \mathbf{R}_{\mathbb{Y}}^{\mathbb{X}} \mathbf{S}(\boldsymbol{\omega}_{\mathbb{Z},\mathbb{Y}}^{\mathbb{Y}}) (\mathbf{R}_{\mathbb{Y}}^{\mathbb{X}})^T, \\ &= \mathbf{S}(\boldsymbol{\omega}_{\mathbb{X},\mathbb{Y}}^{\mathbb{X}}) + \mathbf{R}_{\mathbb{Y}}^{\mathbb{X}} \mathbf{S}(\boldsymbol{\omega}_{\mathbb{Y},\mathbb{Z}}^{\mathbb{Y}}) (\mathbf{R}_{\mathbb{Y}}^{\mathbb{X}})^T, \\ &= \mathbf{S}(\boldsymbol{\omega}_{\mathbb{X},\mathbb{Y}}^{\mathbb{X}}) + \mathbf{S}(\boldsymbol{\omega}_{\mathbb{Y},\mathbb{Z}}^{\mathbb{X}}), \end{aligned}$$

where the last line follows since $\mathbf{S}(\mathbf{R}\mathbf{w}) = \mathbf{R}\mathbf{S}(\mathbf{w})\mathbf{R}^T$ for any rotation matrix \mathbf{R} and arbitrary vector \mathbf{w} (See Problem (2.33)). \square

Example 2.6.1. In this example the angular velocities of the links that make up the leg assembly of the humanoid robot first discussed in Example (2.1.1) are studied. As depicted in Figure (2.21), frames are fixed in the links corresponding to the pelvis (\mathbb{A} , red), upper hip (\mathbb{B} , blue), lower hip (\mathbb{C} , orange), upper leg (\mathbb{D} , green), lower leg (\mathbb{E} , red), ankle (\mathbb{F} , blue), and foot (\mathbb{G} , orange). The upper hip \mathbb{B} rotates relative to the pelvis \mathbb{A} through the angle $\theta_{\mathbb{B}}$ about an axis parallel to the \mathbf{a}_1 and \mathbf{b}_1 axes, where $\theta_{\mathbb{B}}$ is measured from the \mathbf{a}_2 to the \mathbf{b}_2 axis. The lower hip \mathbb{C} rotates relative to the upper hip \mathbb{B} through the angle $\theta_{\mathbb{C}}$ about an axis parallel to the \mathbf{b}_3 and \mathbf{c}_3 axes, where $\theta_{\mathbb{C}}$ is measured from the \mathbf{b}_1 to the \mathbf{c}_1 axis. Find the angular velocity $\boldsymbol{\omega}_{\mathbb{A},\mathbb{C}}$ and angular acceleration $\boldsymbol{\alpha}_{\mathbb{A},\mathbb{C}}$ of the upper leg \mathbb{C} relative to hips \mathbb{A} of the leg assembly. Express these answers first in terms of the basis for the \mathbb{A} frame, and then in terms of the basis for the \mathbb{B} frame.

Solution: The Addition Theorem (2.15) relates the $\boldsymbol{\omega}_{\mathbb{A},\mathbb{C}}$ to the sum of $\boldsymbol{\omega}_{\mathbb{A},\mathbb{B}}$ and

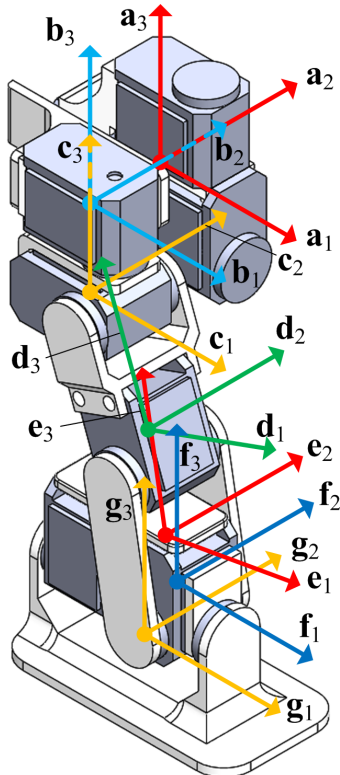


Fig. 2.21: Definition of frames for leg assembly

$$\boldsymbol{\omega}_{B,C},$$

$$\begin{aligned}\boldsymbol{\omega}_{A,C} &= \boldsymbol{\omega}_{A,B} + \boldsymbol{\omega}_{B,C}, \\ &= \dot{\theta}_B \mathbf{a}_1 + \dot{\theta}_C \mathbf{b}_3, \\ &= \dot{\theta}_B \mathbf{b}_1 + \dot{\theta}_C \mathbf{c}_3.\end{aligned}$$

The rotation matrices that relate the A, B and C frames are

$$\mathbf{R}_A^B = \begin{bmatrix} 1 & 0 & 0 \\ 0 & \cos \theta_B & \sin \theta_B \\ 0 & -\sin \theta_B & \cos \theta_B \end{bmatrix}, \quad \mathbf{R}_B^C = \begin{bmatrix} \cos \theta_C & \sin \theta_C & 0 \\ -\sin \theta_C & \cos \theta_C & 0 \\ 0 & 0 & 1 \end{bmatrix}.$$

The expression for the angular velocity $\boldsymbol{\omega}_{A,C}$ in terms of the basis for the A frame is

$$\begin{aligned}\boldsymbol{\omega}_{A,C}^A &= \begin{Bmatrix} \dot{\theta}_B \\ 0 \\ 0 \end{Bmatrix} + \mathbf{R}_B^A \begin{Bmatrix} 0 \\ 0 \\ \dot{\theta}_C \end{Bmatrix}, \\ &= \begin{Bmatrix} \dot{\theta}_B \\ 0 \\ 0 \end{Bmatrix} + \begin{bmatrix} 1 & 0 & 0 \\ 0 & \cos \theta_B & -\sin \theta_B \\ 0 & \sin \theta_B & \cos \theta_B \end{bmatrix} \begin{Bmatrix} 0 \\ 0 \\ \dot{\theta}_C \end{Bmatrix} = \begin{Bmatrix} \dot{\theta}_B \\ -\dot{\theta}_C \sin \theta_B \\ \dot{\theta}_C \cos \theta_B \end{Bmatrix}.\end{aligned}$$

The expression for the angular velocity $\boldsymbol{\omega}_{A,C}$ in terms of the C basis is

$$\begin{aligned}\boldsymbol{\omega}_{A,C}^C &= \mathbf{R}_B^C \begin{Bmatrix} \dot{\theta}_B \\ 0 \\ 0 \end{Bmatrix} + \begin{Bmatrix} 0 \\ 0 \\ \dot{\theta}_C \end{Bmatrix}, \\ &= \begin{bmatrix} \cos \theta_C & \sin \theta_C & 0 \\ -\sin \theta_C & \cos \theta_C & 0 \\ 0 & 0 & 1 \end{bmatrix} \begin{Bmatrix} \dot{\theta}_B \\ 0 \\ \dot{\theta}_C \end{Bmatrix} + \begin{Bmatrix} 0 \\ 0 \\ \dot{\theta}_C \end{Bmatrix} = \begin{Bmatrix} \dot{\theta}_B \cos \theta_C \\ -\dot{\theta}_B \sin \theta_C \\ \dot{\theta}_C \end{Bmatrix}.\end{aligned}$$

Shifting to considering the angular acceleration, by definition, the angular acceleration $\boldsymbol{\alpha}_{A,C}$ is calculated using the identity

$$\boldsymbol{\alpha}_{A,C} = \frac{d}{dt} \Big|_{\mathbb{A}} (\boldsymbol{\omega}_{A,C}).$$

Since

$$\boldsymbol{\omega}_{A,C}^A = \begin{Bmatrix} \dot{\theta}_B \\ \dot{\theta}_C \sin \theta_B \\ \dot{\theta}_C \cos \theta_B \end{Bmatrix},$$

these coordinates can be differentiated to see

$$\boldsymbol{\alpha}_{A,C}^A = \begin{Bmatrix} \ddot{\theta}_B \\ -\ddot{\theta}_C \sin \theta_B - \dot{\theta}_B \dot{\theta}_C \cos \theta_B \\ \ddot{\theta}_C \cos \theta_B - \dot{\theta}_B \dot{\theta}_C \sin \theta_B \end{Bmatrix}.$$

Alternatively, the Derivative Theorem (2.12) can be applied directly to the definition to compute

$$\begin{aligned}\boldsymbol{\alpha}_{A,C} &= \frac{d}{dt} \Big|_{\mathbb{A}} (\boldsymbol{\omega}_{A,C}), \\ &= \frac{d}{dt} \Big|_{\mathbb{A}} (\dot{\theta}_B \mathbf{a}_1) + \frac{d}{dt} \Big|_{\mathbb{A}} (\dot{\theta}_C \mathbf{b}_3), \\ &= \ddot{\theta}_B \mathbf{a}_3 + \frac{d}{dt} \Big|_{\mathbb{B}} (\dot{\theta}_C \mathbf{b}_3) + \underbrace{\boldsymbol{\omega}_{A,B} \times}_{\dot{\theta}_B \mathbf{b}_1} (\dot{\theta}_C \mathbf{b}_3), \\ &= \ddot{\theta}_B \mathbf{a}_1 + \ddot{\theta}_C \mathbf{b}_3 - \dot{\theta}_B \dot{\theta}_C \mathbf{b}_2.\end{aligned}$$

This result is identical to the first calculation.

$$\alpha_{A,C}^A = \begin{Bmatrix} \ddot{\theta}_B \\ 0 \\ 0 \end{Bmatrix} + \begin{Bmatrix} 0 \\ -\sin \theta_B \\ \cos \theta_B \end{Bmatrix} \dot{\theta}_C - \begin{Bmatrix} 0 \\ \cos \theta_B \\ \sin \theta_B \end{Bmatrix} \dot{\theta}_B \dot{\theta}_C.$$

As demonstrated, the algebraic manipulations become complicated in even this relatively simple case where only the first few frames A, B, C are considered. In Example ?? of the MATLAB Workbook for DCRS, these calculations are carried out efficiently using a symbolic manipulation program.

2.6.2 Relative Velocity

The following theorem relates the velocity of two points in the X frame when these two points are fixed in a frame B that moves in X.

Theorem 2.16 (Velocities of Two Points on Single Body). Let p and q be two points fixed in a frame B which moves in the frame X. The velocity of the point p in the frame X and the velocity of the point q in the frame X satisfy

$$\mathbf{v}_{X,p} = \mathbf{v}_{X,q} + \boldsymbol{\omega}_{X,B} \times \mathbf{d}_{q,p}$$

where $\boldsymbol{\omega}_{X,B}$ is the angular velocity of the frame B in the frame X. The term $\boldsymbol{\omega}_{X,B} \times \mathbf{d}_{q,p}$ is referred to as the relative velocity of the point p with respect to the point q.

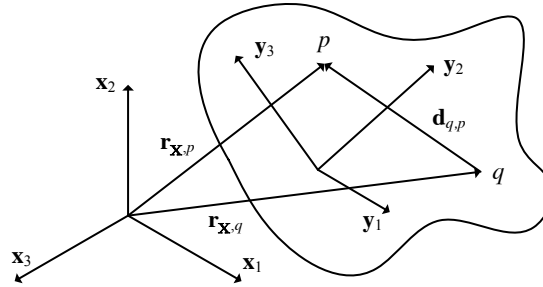
Proof. As shown in Figure (2.22) the positions of points p and point q in the frame X can be related to one another according to

$$\mathbf{r}_{X,p} = \mathbf{r}_{X,q} + \mathbf{d}_{q,p}.$$

When the derivative of both sides of this equation are taken with respect to an observer in the X frame

$$\begin{aligned} \frac{d}{dt} \Big|_X (\mathbf{r}_{X,p}) &= \frac{d}{dt} \Big|_X (\mathbf{r}_{X,q}) + \frac{d}{dt} \Big|_X (\mathbf{d}_{q,p}), \\ \mathbf{v}_{X,p} &= \mathbf{v}_{X,q} + \frac{d}{dt} \Big|_X (\mathbf{d}_{q,p}). \end{aligned}$$

The Derivative Theorem (2.12) can be used to calculate the last term in this expression. Since the vector $\mathbf{d}_{q,p}$ does not change magnitude or direction with respect to an observer fixed in the B frame, the derivative becomes

Fig. 2.22: Points p and q on the Same Rigid Body

$$\mathbf{v}_{\mathbb{X},p} = \mathbf{v}_{\mathbb{X},q} + \underbrace{\frac{d}{dt} \Big|_{\mathbb{B}} (\mathbf{d}_{q,p})}_0 + \boldsymbol{\omega}_{\mathbb{X},\mathbb{B}} \times \mathbf{d}_{q,p}.$$

□

2.6.3 Relative Acceleration

Just as the velocities of two points fixed in one frame can be expressed succinctly in terms of the angular velocity of that frame, their accelerations can be written in terms of angular acceleration.

Theorem 2.17 (Accelerations of Two Points on Single Body). Let p and q be two points fixed in the frame \mathbb{B} which moves in the frame \mathbb{X} . The acceleration of the point p in the frame \mathbb{X} and the acceleration of the point q in the frame \mathbb{X} satisfy

$$\mathbf{a}_{\mathbb{X},p} = \mathbf{a}_{\mathbb{X},q} + \boldsymbol{\alpha}_{\mathbb{X},\mathbb{B}} \times \mathbf{d}_{q,p} + \boldsymbol{\omega}_{\mathbb{X},\mathbb{B}} \times (\boldsymbol{\omega}_{\mathbb{X},\mathbb{B}} \times \mathbf{d}_{q,p})$$

The terms $\boldsymbol{\alpha}_{\mathbb{X},\mathbb{B}} \times \mathbf{d}_{q,p} + \boldsymbol{\omega}_{\mathbb{X},\mathbb{B}} \times (\boldsymbol{\omega}_{\mathbb{X},\mathbb{B}} \times \mathbf{d}_{q,p})$ are referred to as the relative acceleration of the point p with respect to the point q .

Proof. Direct calculation shows that

$$\begin{aligned} \mathbf{a}_{\mathbb{X},p} &= \frac{d}{dt} \Big|_{\mathbb{X}} (\mathbf{v}_{\mathbb{X},p}) = \frac{d}{dt} \Big|_{\mathbb{X}} (\mathbf{v}_{\mathbb{X},q}) + \frac{d}{dt} \Big|_{\mathbb{X}} (\boldsymbol{\omega}_{\mathbb{X},\mathbb{B}} \times \mathbf{d}_{q,p}), \\ &= \mathbf{a}_{\mathbb{X},q} + \frac{d}{dt} \Big|_{\mathbb{X}} (\boldsymbol{\omega}_{\mathbb{X},\mathbb{B}}) \times \mathbf{d}_{q,p} + \boldsymbol{\omega}_{\mathbb{X},\mathbb{B}} \times \frac{d}{dt} \Big|_{\mathbb{X}} (\mathbf{d}_{q,p}). \end{aligned}$$

The required result is obtained when the definition $\alpha_{X,B} = \frac{d}{dt}|_X (\omega_{X,B})$ is introduced and the derivative theorem is employed to calculate $\frac{d}{dt}|_X (\mathbf{d}_{q,p})$. \square

Example 2.6.2. The robotic arm and torso assembly is shown in Figure (2.23).

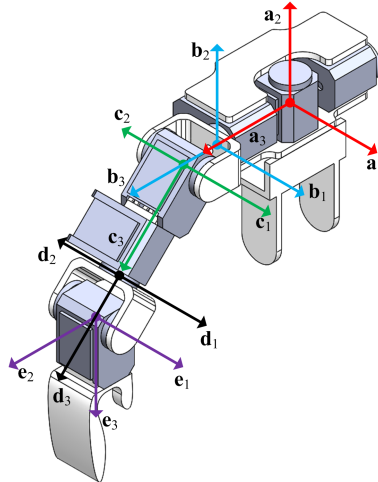


Fig. 2.23: Robotic arm and torso assembly

The frames are fixed in the torso (\mathbb{A}), shoulder (\mathbb{B}), upper arm (\mathbb{C}), lower arm (\mathbb{D}) and hand (\mathbb{E}). The distances between the points a, b, c, d and e are $d_{a,b}, d_{b,c}, d_{c,d}$ and $d_{d,e}$. The angle θ_B measures the rotation of the \mathbb{B} frame relative to the \mathbb{A} frame about the \mathbf{a}_3 axis. The angle θ_C measures the rotation of the \mathbb{C} frame relative to the \mathbb{B} frame about the \mathbf{b}_1 axis. The angle θ_D measures the rotation of the \mathbb{D} frame relative to the \mathbb{C} frame about the \mathbf{c}_3 axis. The angle θ_E measures the rotation of the \mathbb{E} frame relative to the \mathbb{D} frame about the \mathbf{d}_1 axis.

Calculate the velocity of point d (the origin of frame \mathbb{D}) in the \mathbb{A} frame. Calculate the acceleration of point d in the \mathbb{A} frame. Express these answers in terms of the basis for the \mathbb{A} frame.

Solution: First, the angular velocities of frames $\mathbb{B}, \mathbb{C}, \mathbb{D}$ and \mathbb{E} with respect to frame \mathbb{A} are calculated using the Addition Theorem

$$\begin{aligned}\boldsymbol{\omega}_{\mathbb{A},\mathbb{B}} &= \dot{\theta}_B \mathbf{b}_3, \\ \boldsymbol{\omega}_{\mathbb{A},\mathbb{C}} &= \boldsymbol{\omega}_{\mathbb{A},\mathbb{B}} + \dot{\theta}_C \mathbf{c}_1, \\ \boldsymbol{\omega}_{\mathbb{A},\mathbb{D}} &= \boldsymbol{\omega}_{\mathbb{A},\mathbb{C}} + \dot{\theta}_D \mathbf{d}_3.\end{aligned}$$

The position of point b in the \mathbb{A} frame is observed to not change as a function of time, due to the alignment of the \mathbf{a}_3 and \mathbf{b}_3 axes, such that

$$\begin{aligned}\mathbf{r}_{\mathbb{A},b} &= d_{a,b}\mathbf{a}_3, \\ \mathbf{v}_{\mathbb{A},b} &= \mathbf{0}, \\ \mathbf{a}_{\mathbb{A},b} &= \mathbf{0}.\end{aligned}$$

In the shoulder (with respect to frame \mathbb{B}), points b and c are fixed in relation to one another. Therefore, their velocities satisfy the equation

$$\mathbf{v}_{\mathbb{A},c} = \underbrace{\mathbf{v}_{\mathbb{A},b}}_{\mathbf{0}} + \underbrace{\boldsymbol{\omega}_{\mathbb{A},\mathbb{B}}}_{\dot{\theta}_{\mathbb{B}}\mathbf{b}_3} \times \underbrace{\mathbf{d}_{b,c}}_{d_{b,c}\mathbf{b}_3} = \mathbf{0}.$$

This is due to the fact that point c , like point b , lies on the vector \mathbf{a}_3 . Taking the derivative of this expression results in the relative acceleration of point c as $\mathbf{a}_{\mathbb{A},c} = 0$. The points c and d are fixed on the upper arm \mathbb{C} . The relative velocity equation for this pair of points is

$$\begin{aligned}\mathbf{v}_{\mathbb{A},d} &= \underbrace{\mathbf{v}_{\mathbb{A},c}}_{\mathbf{0}} + \underbrace{\boldsymbol{\omega}_{\mathbb{A},\mathbb{C}}}_{(\dot{\theta}_{\mathbb{B}}\mathbf{b}_3 + \dot{\theta}_{\mathbb{C}}\mathbf{c}_1)} \times \underbrace{\mathbf{d}_{c,d}}_{(d_{c,d}\mathbf{c}_3)}, \\ &= d_{c,d}\dot{\theta}_{\mathbb{B}}\mathbf{b}_3 \times \mathbf{c}_3 - d_{c,d}\dot{\theta}_{\mathbb{C}}\mathbf{c}_2.\end{aligned}$$

Since $\mathbf{c}_3 = -\sin\theta_{\mathbb{C}}\mathbf{b}_2 + \cos\theta_{\mathbb{C}}\mathbf{b}_3$, this equation can be rewritten as

$$\mathbf{v}_{\mathbb{A},d} = d_{c,d}\dot{\theta}_{\mathbb{B}}\sin\theta_{\mathbb{C}}\mathbf{b}_1 - d_{c,d}\dot{\theta}_{\mathbb{C}}\mathbf{c}_2.$$

The expression for the velocity in terms of the basis for the \mathbb{A} frame is

$$\mathbf{v}_{\mathbb{A},d}^{\mathbb{A}} = \mathbf{R}_{\mathbb{B}}^{\mathbb{A}} \begin{Bmatrix} d_{c,d}\dot{\theta}_{\mathbb{B}}\sin\theta_{\mathbb{C}} \\ 0 \\ 0 \end{Bmatrix} - \mathbf{R}_{\mathbb{B}}^{\mathbb{A}} \mathbf{R}_{\mathbb{C}}^{\mathbb{B}} \begin{Bmatrix} 0 \\ d_{c,d}\dot{\theta}_{\mathbb{C}} \\ 0 \end{Bmatrix}$$

where

$$\mathbf{R}_{\mathbb{A}}^{\mathbb{B}} = \begin{bmatrix} \cos\theta_{\mathbb{B}} & \sin\theta_{\mathbb{B}} & 0 \\ -\sin\theta_{\mathbb{B}} & \cos\theta_{\mathbb{B}} & 0 \\ 0 & 0 & 1 \end{bmatrix}, \quad \mathbf{R}_{\mathbb{B}}^{\mathbb{C}} = \begin{bmatrix} 1 & 0 & 0 \\ 0 & \cos\theta_{\mathbb{C}} & \sin\theta_{\mathbb{C}} \\ 0 & -\sin\theta_{\mathbb{C}} & \cos\theta_{\mathbb{C}} \end{bmatrix}.$$

The accelerations of the points c and d satisfy the equation

$$\mathbf{a}_{\mathbb{A},d} = \mathbf{a}_{\mathbb{A},c} + \boldsymbol{\omega}_{\mathbb{A},\mathbb{C}} \times (\boldsymbol{\omega}_{\mathbb{A},\mathbb{C}} \times \mathbf{d}_{c,d}) + \boldsymbol{\alpha}_{\mathbb{A},\mathbb{C}} \times \mathbf{d}_{c,d}.$$

This expression will be built term-by-term. The angular acceleration is defined to be

$$\begin{aligned}\boldsymbol{\alpha}_{\mathbb{A},\mathbb{C}} &= \frac{d}{dt} \Big|_{\mathbb{A}} (\boldsymbol{\omega}_{\mathbb{A},\mathbb{C}}), \\ &= \frac{d}{dt} \Big|_{\mathbb{B}} (\dot{\theta}_{\mathbb{B}}\mathbf{b}_3 + \dot{\theta}_{\mathbb{C}}\mathbf{c}_1) + \boldsymbol{\omega}_{\mathbb{A},\mathbb{B}} \times (\dot{\theta}_{\mathbb{C}}\mathbf{b}_1 + \dot{\theta}_{\mathbb{B}}\mathbf{b}_3), \\ &= \ddot{\theta}_{\mathbb{B}}\mathbf{b}_3 + \ddot{\theta}_{\mathbb{C}}\mathbf{b}_1 + \dot{\theta}_{\mathbb{B}}\dot{\theta}_{\mathbb{C}}\mathbf{b}_2.\end{aligned}$$

Next, expanding the terms that involve cross products

$$\begin{aligned}\boldsymbol{\alpha}_{\mathbb{A},\mathbb{C}} \times \mathbf{d}_{c,d} &= \begin{vmatrix} \mathbf{b}_1 & \mathbf{b}_2 & \mathbf{b}_3 \\ \ddot{\theta}_{\mathbb{C}} & \dot{\theta}_{\mathbb{B}}\theta_{\mathbb{C}} & \ddot{\theta}_{\mathbb{B}} \\ 0 & -d_{c,d}\sin\theta_{\mathbb{C}} & d_{c,d}\cos\theta_{\mathbb{C}} \end{vmatrix}, \\ &= d_{c,d}((\dot{\theta}_{\mathbb{B}}\theta_{\mathbb{C}}\cos\theta_{\mathbb{C}} + \ddot{\theta}_{\mathbb{B}}\sin\theta_{\mathbb{C}})\mathbf{b}_1 - \ddot{\theta}_{\mathbb{C}}\cos\theta_{\mathbb{C}}\mathbf{b}_2 - \ddot{\theta}_{\mathbb{C}}\sin\theta_{\mathbb{C}}\mathbf{b}_3).\end{aligned}$$

$$\begin{aligned}\boldsymbol{\omega}_{\mathbb{A},\mathbb{C}} \times (\boldsymbol{\omega}_{\mathbb{A},\mathbb{C}} \times \mathbf{d}_{c,d}) &= \boldsymbol{\omega}_{\mathbb{A},\mathbb{C}} \times \begin{vmatrix} \mathbf{b}_1 & \mathbf{b}_2 & \mathbf{b}_3 \\ \dot{\theta}_{\mathbb{C}} & 0 & \dot{\theta}_{\mathbb{B}} \\ 0 & -d_{c,d}\sin\theta_{\mathbb{C}} & d_{c,d}\cos\theta_{\mathbb{C}} \end{vmatrix}, \\ &= \begin{vmatrix} \mathbf{b}_1 & \mathbf{b}_2 & \mathbf{b}_3 \\ \dot{\theta}_{\mathbb{C}} & 0 & \dot{\theta}_{\mathbb{B}} \\ (d_{c,d}\dot{\theta}_{\mathbb{B}}\sin\theta_{\mathbb{C}}) (-d_{c,d}\dot{\theta}_{\mathbb{C}}\cos\theta_{\mathbb{C}}) & (-d_{c,d}\dot{\theta}_{\mathbb{C}}\cos\theta_{\mathbb{C}}) & \end{vmatrix}, \\ &= d_{c,d}(\dot{\theta}_{\mathbb{B}}\dot{\theta}_{\mathbb{C}}\cos\theta_{\mathbb{C}}\mathbf{b}_1 + (\dot{\theta}_{\mathbb{B}}^2\sin\theta_{\mathbb{C}} + \dot{\theta}_{\mathbb{C}}^2\cos\theta_{\mathbb{C}})\mathbf{b}_2 - \dot{\theta}_{\mathbb{C}}^2\cos\theta_{\mathbb{C}}\mathbf{b}_3).\end{aligned}$$

The expression for the acceleration of point d relative to frame \mathbb{A} , expressed in terms of the basis for the \mathbb{A} frame, is obtained by collecting these terms

$$\mathbf{a}_{\mathbb{A},d}^{\mathbb{A}} = d_{c,d} \mathbf{R}_{\mathbb{B}}^{\mathbb{A}} \left\{ \begin{array}{l} \ddot{\theta}_{\mathbb{B}}\sin\theta_{\mathbb{C}} + 2\cos\theta_{\mathbb{C}}\dot{\theta}_{\mathbb{C}}\dot{\theta}_{\mathbb{C}} \\ \dot{\theta}_{\mathbb{B}}^2\sin\theta_{\mathbb{C}} + \dot{\theta}_{\mathbb{C}}^2\cos\theta_{\mathbb{C}} - \ddot{\theta}_{\mathbb{C}}\cos\theta_{\mathbb{C}} + 2\rho\dot{\phi}\dot{\theta}\cos\phi \\ -\dot{\theta}_{\mathbb{C}}^2\cos\theta_{\mathbb{C}} - \ddot{\theta}_{\mathbb{C}}\sin\theta_{\mathbb{C}} \end{array} \right\}.$$

The calculations above can also be found in Example ?? of the MATLAB Workbook for DCRS.

2.6.4 Common Coordinate Systems

Before closing this chapter on kinematics, some common coordinate systems that occur frequently in applications are summarized. Each of the rotational coordinate systems may be viewed as defining at least one rotating frame that moves with respect to the background frame. The definition of angular velocity in Section (2.5.1), the Addition Theorem for Angular Velocity in Section (2.6.1), and the relative velocity and relative acceleration theorems in Sections (2.6.2) and (2.6.3) all provide insight into the structure of the velocity and acceleration expressions in terms of these coordinate systems.

2.6.4.1 Cartesian Coordinates

The simplest coordinate system is the Cartesian system. In this construction there is a single frame of reference \mathbb{X} with basis $\mathbf{x}_1, \mathbf{x}_2, \mathbf{x}_3$. The basis for the frame \mathbb{X} is assumed to be stationary. The position, velocity and acceleration of a point p that follows some time-varying trajectory are given by

$$\begin{aligned}\mathbf{r}_{\mathbb{X},p}(t) &= x(t)\mathbf{x}_1 + y(t)\mathbf{x}_2 + z(t)\mathbf{x}_3, \\ \mathbf{v}_{\mathbb{X},p}(t) &= \dot{x}(t)\mathbf{x}_1 + \dot{y}(t)\mathbf{x}_2 + \dot{z}(t)\mathbf{x}_3, \\ \mathbf{a}_{\mathbb{X},p}(t) &= \ddot{x}(t)\mathbf{x}_1 + \ddot{y}(t)\mathbf{x}_2 + \ddot{z}(t)\mathbf{x}_3.\end{aligned}$$

2.6.4.2 Cylindrical Coordinates

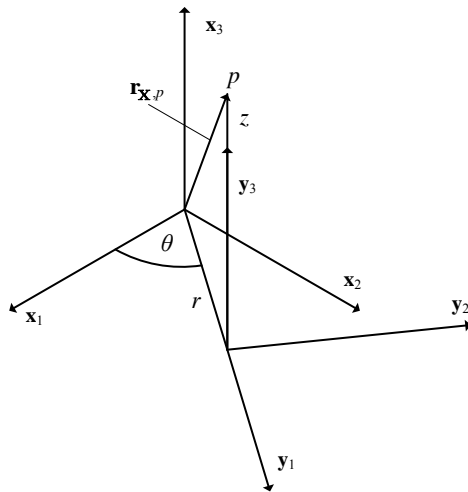


Fig. 2.24: Frame Definitions for Cylindrical Coordinates

Cylindrical coordinates can be constructed by introducing a frame \mathbb{Y} that rotates relative to the stationary frame \mathbb{X} . In this construction the position vector $\mathbf{r}_{\mathbb{X},p}$ is projected onto the $\mathbf{x}_1 - \mathbf{x}_2$ plane, as shown in Figure (2.24), and the vector \mathbf{y}_1 is oriented along this projection. The angle θ measures the angle from the \mathbf{x}_1 basis vector to the \mathbf{y}_1 basis vectors. The unit vector \mathbf{y}_2 lies in the $\mathbf{x}_1 - \mathbf{x}_2$ plane, is perpendicular to \mathbf{y}_1 and is oriented in the direction of increasing θ as shown in Figure (2.24). The unit vector \mathbf{y}_3 is selected so that the \mathbb{Y} defines a dextral, orthonormal frame. The bases for the frames \mathbb{X} and \mathbb{Y} are related by the rotation matrix

$$\mathbf{R}_{\mathbb{Y}}^{\mathbb{X}} = \begin{bmatrix} \cos \theta & -\sin \theta & 0 \\ \sin \theta & \cos \theta & 0 \\ 0 & 0 & 1 \end{bmatrix}. \quad (2.6.2)$$

The position vector $\mathbf{r}_{\mathbb{X},p} = x(t)\mathbf{x}_1 + y(t)\mathbf{x}_2 + z(t)\mathbf{x}_3$ can now be written as

$$\mathbf{r}_{\mathbb{X},p} = r(t)\mathbf{y}_1(t) + z(t)\mathbf{y}_2(t) \quad (2.6.3)$$

where the radius $r(t)$ is always measured along the projection of the position vector onto the $\mathbf{x}_1 - \mathbf{x}_2$ plane ($r \geq 0$). The cylindrical coordinate system uses the parameters (r, θ, z) to characterize position, velocity, and acceleration of the particle p instead of the parameters (x, y, z) used in the Cartesian coordinate system. The purpose of introducing the additional frame \mathbb{Y} is to obtain the position, velocity, and acceleration vectors $\mathbf{r}_{\mathbb{X},p}, \mathbf{v}_{\mathbb{X},p}, \mathbf{a}_{\mathbb{X},p}$ with respect to the background frame \mathbb{X} in terms of (r, θ, z) and the basis for the \mathbb{Y} frame.

Theorem 2.18 (Cylindrical Coordinate Position, Velocity and Acceleration).

The position $\mathbf{r}_{\mathbb{X},p}$, velocity $\mathbf{v}_{\mathbb{X},p}$ and acceleration $\mathbf{a}_{\mathbb{X},p}$ of the point p with respect to the \mathbb{X} frame is given in terms of the cylindrical coordinates (r, θ, z) and cylindrical basis \mathbb{Y} by the expressions

$$\mathbf{r}_{\mathbb{X},p} = r\mathbf{y}_1 + z\mathbf{y}_2, \quad (2.6.4)$$

$$\mathbf{v}_{\mathbb{X},p} = r\dot{\theta}\mathbf{y}_1 + r\dot{\theta}\mathbf{y}_2 + \dot{z}\mathbf{y}_3, \quad (2.6.5)$$

$$\mathbf{a}_{\mathbb{X},p} = (r\ddot{\theta}^2)\mathbf{y}_1 + (2r\dot{\theta}\ddot{\theta} + r\ddot{\theta})\mathbf{y}_2 + \ddot{z}\mathbf{y}_3. \quad (2.6.6)$$

Proof. There are several ways to derive the above equations. It is possible to change coordinates between the Cartesian coordinates (x, y, z) and cylindrical coordinates (r, θ, z) by using the change of variables that are given by the functional relationships

$$x = r\cos \theta, \quad (2.6.7)$$

$$y = r\sin \theta,$$

$$z = z,$$

or the inverse of these relationships,

$$r = \sqrt{x^2 + y^2 + z^2},$$

$$\theta = \arctan(y/x),$$

$$z = z.$$

For example, since the velocity $\mathbf{v}_{\mathbb{X},p}$ in Cartesian coordinates is given by

$$\mathbf{v}_{\mathbb{X},p} = \dot{x}\mathbf{x}_1 + \dot{y}\mathbf{x}_2 + \dot{z}\mathbf{x}_3 \quad (2.6.8)$$

\dot{x} , \dot{y} , \dot{z} can be calculated from above, substituted into Equation (2.6.8), and substitute the rotation matrix in Equation (2.6.2) to obtain a velocity expression in terms of (r, θ, z) and $\mathbf{y}_1, \mathbf{y}_2, \mathbf{y}_3$. This approach is tedious and is left as an exercise in favor of illustrating the effectiveness of the theorems introduced in Section (2.5.1).

These theorems greatly simplify this calculation. By construction, the angular velocity of the cylindrical coordinate frame \mathbb{Y} with respect to the \mathbb{X} frame is just

$$\boldsymbol{\omega}_{\mathbb{X},\mathbb{Y}} = \dot{\theta} \mathbf{x}_3 = \dot{\theta} \mathbf{y}_3 \quad (2.6.9)$$

according to Theorem (2.13). The derivative of the position vector $\mathbf{r}_{\mathbb{X},P}$ can be obtained with the \mathbb{X} basis held fixed as

$$\begin{aligned} \mathbf{v}_{\mathbb{X},P} &= \frac{d}{dt} \Big|_{\mathbb{X}} (\mathbf{r}_{\mathbb{X},P}) = \frac{d}{dt} \Big|_{\mathbb{Y}} (\mathbf{r}_{\mathbb{X},P}) + \boldsymbol{\omega}_{\mathbb{X},\mathbb{Y}} \times \mathbf{r}_{\mathbb{X},P}, \\ &= \dot{r} \mathbf{y}_1 + \dot{z} \mathbf{y}_3 + \dot{\theta} \mathbf{y}_3 \times (r \mathbf{y}_1 + z \mathbf{y}_3), \\ &= \dot{r} \mathbf{y}_1 + r \dot{\theta} \mathbf{y}_2 + \dot{z} \mathbf{y}_3. \end{aligned}$$

The derivative can be calculated a second time to obtain the acceleration

$$\begin{aligned} \mathbf{a}_{\mathbb{X},P} &= \frac{d}{dt} \Big|_{\mathbb{X}} (\mathbf{v}_{\mathbb{X},P}) = \frac{d}{dt} \Big|_{\mathbb{Y}} (\mathbf{v}_{\mathbb{X},P}) + \boldsymbol{\omega}_{\mathbb{X},\mathbb{Y}} \times \mathbf{v}_{\mathbb{X},P}, \\ &= \ddot{r} \mathbf{y}_1 + (\dot{r} \dot{\theta} + r \ddot{\theta}) \mathbf{y}_2 + \ddot{z} \mathbf{y}_3 \\ &\quad + \dot{\theta} \mathbf{y}_3 \times (\dot{r} \mathbf{y}_1 + r \dot{\theta} \mathbf{y}_2 + \dot{z} \mathbf{y}_3), \\ &= (\ddot{r} - r \dot{\theta}^2) \mathbf{y}_1 + (2r \dot{\theta} + r \ddot{\theta}) \mathbf{y}_2 + \ddot{z} \mathbf{y}_3. \end{aligned}$$

□

2.6.4.3 Spherical Coordinates

The definition of spherical coordinates is achieved with the introduction of two rotating frames of reference, in contrast to the single rotating frame introduced for cylindrical coordinate systems. The definition of these two rotating frames is discussed in Problem (2.26), and this construction is briefly reviewed here. First, the position vector $\mathbf{r}_{\mathbb{X},P}$ is projected onto the $\mathbf{x}_1 - \mathbf{x}_2$ plane, and this projected vector defines the direction of the \mathbf{z}_1 unit vector. The angle θ measures the rotation of the vector \mathbf{z}_1 from the \mathbf{x}_1 axis. The \mathbf{z}_2 unit vector is defined so that it lies in the $\mathbf{x}_1 - \mathbf{x}_2$ plane, is perpendicular to the vector \mathbf{y}_1 and points in the direction of increasing angle θ . The unit vector \mathbf{z}_3 is defined such that the frame \mathbb{Z} is a dextral, orthonormal basis.

Next, the second rotating frame \mathbb{Y} is introduced defined by a right-handed, orthonormal set of unit vectors denoted by $\mathbf{y}_\phi, \mathbf{y}_\theta, \mathbf{y}_\rho$ so that they are initially coincident with the basis for the \mathbb{Z} frame. Then, the vectors $\mathbf{y}_\phi, \mathbf{y}_\theta, \mathbf{y}_\rho$ are rotated about the $\mathbf{y}_\theta = \mathbf{x}_2$ axis until the \mathbf{y}_ρ unit vector aligns with the position vector $\mathbf{r}_{\mathbb{X},P}$.

The frame \mathbb{Z} is obtained by rotating the original frame \mathbb{X} through an angle of θ about the $\mathbf{x}_3 = \mathbf{z}_3$ axis, and the frame \mathbb{Y} is constructed by subsequently rotating through an angle of ϕ about the $\mathbf{z}_2 = \mathbf{y}_\theta$ axis. When these two rotations have been performed, the position vector of the point p can be written in terms of the distance ρ from the point p to the origin. The goal of this construction is to write the position $\mathbf{r}_{\mathbb{X},p}$, velocity $\mathbf{v}_{\mathbb{X},p}$, and acceleration $\mathbf{a}_{\mathbb{X},p}$ with respect to the stationary frame \mathbb{X} in terms of the spherical coordinates (ρ, ϕ, θ) and spherical basis $\mathbf{y}_\rho, \mathbf{y}_\phi, \mathbf{y}_\theta$.

Theorem 2.19 (Spherical Coordinate Position, Velocity, and Acceleration).

The position $\mathbf{r}_{\mathbb{X},p}$, velocity $\mathbf{v}_{\mathbb{X},p}$ and acceleration $\mathbf{a}_{\mathbb{X},p}$ of the point p with respect to the \mathbb{X} frame is given in terms of the spherical coordinates (ρ, ϕ, θ) and spherical basis $\mathbf{y}_\rho, \mathbf{y}_\phi, \mathbf{y}_\theta$ by the expressions

$$\begin{aligned}\mathbf{r}_{\mathbb{X},p} &= \rho \mathbf{y}_\rho, \\ \mathbf{v}_{\mathbb{X},p} &= \dot{\rho} \mathbf{y}_\rho + \rho \dot{\theta} \sin \phi \mathbf{y}_\theta + \rho \dot{\phi} \mathbf{y}_\phi, \\ \mathbf{a}_{\mathbb{X},p} &= (\ddot{\rho} - \rho \dot{\theta}^2 \sin^2 \phi - \rho \dot{\phi}^2) \mathbf{y}_\rho \\ &\quad + (2\dot{\rho} \dot{\theta} \sin \phi + \rho \ddot{\theta} \sin \phi) \mathbf{y}_\theta \\ &\quad + (\rho \ddot{\phi} + 2\dot{\phi} \dot{\rho} - \rho \dot{\theta}^2 \sin \phi \cos \phi) \mathbf{y}_\phi.\end{aligned}$$

Proof. As in the discussion of cylindrical coordinates, it is possible to derive the conclusions in this theorem several different ways. The most direct method uses the definition of angular velocity in Section (2.5) and the derived theorems in that section. The angular velocity of the \mathbb{Y} frame in the \mathbb{X} frame follows from Theorem (2.15)

$$\boldsymbol{\omega}_{\mathbb{X},\mathbb{Y}} = \dot{\theta} \mathbf{z}_3 + \dot{\phi} \mathbf{y}_\theta.$$

The time derivative of the position with respect to an observer fixed in the \mathbb{X} frame can be calculated as

$$\begin{aligned}\mathbf{v}_{\mathbb{X},p} &= \frac{d}{dt} \Big|_{\mathbb{X}} (\mathbf{r}_{\mathbb{X},p}) = \frac{d}{dt} \Big|_{\mathbb{Y}} (\mathbf{r}_{\mathbb{X},p}) + \boldsymbol{\omega}_{\mathbb{X},\mathbb{Y}} \times (\mathbf{r}_{\mathbb{X},p}), \\ &= \dot{\rho} \mathbf{y}_\rho + (\dot{\theta} \mathbf{z}_3 + \dot{\phi} \mathbf{y}_\theta) \times \rho \mathbf{y}_\rho, \\ &= \dot{\rho} \mathbf{y}_\rho + \rho \dot{\theta} \underbrace{(\mathbf{z}_3 \times \mathbf{y}_\rho)}_{\sin \phi \mathbf{y}_\theta} + \rho \dot{\phi} \underbrace{(\mathbf{y}_\theta \times \mathbf{y}_\rho)}_{\mathbf{y}_\phi}, \\ &= \dot{\rho} \mathbf{y}_\rho + \rho \dot{\theta} \sin \phi \mathbf{y}_\theta + \rho \dot{\phi} \mathbf{y}_\phi.\end{aligned}$$

The acceleration can evaluated by calculating the derivative of the velocity. The calculation of the cross product $\boldsymbol{\omega}_{\mathbb{X},\mathbb{Y}} \times \mathbf{r}_{\mathbb{X},p}$ is evaluated using the expression $\boldsymbol{\omega}_{\mathbb{X},\mathbb{Y}} = \dot{\theta} \mathbf{z}_3 + \dot{\phi} \mathbf{y}_\theta$ directly. An alternative approach is taken in this case. The *angular velocity* in terms of the \mathbb{Y} basis is expressed as

$$\boldsymbol{\omega}_{\mathbb{X},\mathbb{Y}} = \dot{\theta}\mathbf{z}_3 + \dot{\phi}\mathbf{y}_\theta = \dot{\theta}(\cos\phi\mathbf{y}_\rho - \sin\phi\mathbf{y}_\phi) + \dot{\phi}\mathbf{y}_\theta.$$

With this expression, the acceleration of the point p can be calculated as

$$\begin{aligned}\mathbf{a}_{\mathbb{X},p} &= \frac{d}{dt} \Big|_{\mathbb{Y}} (\mathbf{v}_{\mathbb{X},p}) + \boldsymbol{\omega}_{\mathbb{X},\mathbb{Y}} \times \mathbf{v}_{\mathbb{X},p}, \\ &= \ddot{\rho}\mathbf{y}_\rho + (\dot{\rho}\dot{\phi} + \rho\ddot{\phi})\mathbf{y}_\phi + (\dot{\rho}\dot{\theta}\sin\phi + \rho\dot{\phi}\dot{\theta}\cos\phi + \rho\ddot{\theta}\sin\phi)\mathbf{y}_\theta \\ &\quad + \begin{vmatrix} \mathbf{y}_\phi & \mathbf{y}_\theta & \mathbf{y}_\rho \\ -\dot{\theta}\sin\phi & \dot{\phi} & \dot{\theta}\cos\phi \\ \rho\dot{\phi} & \rho\dot{\theta}\sin\phi & \dot{\rho} \end{vmatrix}.\end{aligned}$$

The cross product is expanded to yield

$$\begin{aligned}\begin{vmatrix} \mathbf{y}_\phi & \mathbf{y}_\theta & \mathbf{y}_\rho \\ -\dot{\theta}\sin\phi & \dot{\phi} & \dot{\theta}\cos\phi \\ \rho\dot{\phi} & \rho\dot{\theta}\sin\phi & \dot{\rho} \end{vmatrix} &= (\dot{\rho}\dot{\phi} - \rho\dot{\theta}^2\sin\phi\cos\phi)\mathbf{y}_\phi \\ &\quad + (\rho\dot{\phi}\dot{\theta}\cos\phi + \dot{\rho}\dot{\theta}\sin\phi)\mathbf{y}_\theta - (\rho\dot{\theta}^2\sin^2\phi + \rho\dot{\phi}^2)\mathbf{y}_\rho.\end{aligned}$$

Terms are collected to get the final expression for the acceleration

$$\begin{aligned}\mathbf{a}_{\mathbb{X},p} &= (\ddot{\rho} - \rho\dot{\theta}^2\sin^2\phi - \rho\dot{\phi}^2)\mathbf{y}_\rho + (2\dot{\rho}\dot{\theta}\sin\phi + 2\rho\dot{\phi}\dot{\theta}\cos\phi + \rho\ddot{\theta}\sin\phi)\mathbf{y}_\theta \\ &\quad + (2\dot{\rho}\dot{\phi} + \rho\ddot{\phi} - \rho\dot{\theta}^2\sin\phi\cos\phi)\mathbf{y}_\phi.\end{aligned}$$

□

The final form of the velocity and acceleration in spherical coordinates are also calculated in Example ?? of the MATLAB Workbook for DCRS.

2.7 Problems for Chapter 2, Kinematics

2.7.1 Problems on N -tuples and $M \times N$ Arrays

Problem 2.1 (Solution 2.1). Consider the matrix product $\mathbf{A}^T \mathbf{B} \mathbf{A}$ where $\mathbf{A} \in \mathbb{R}^{M \times N}$ and $\mathbf{B} \in \mathbb{R}^{M \times M}$. Derive an expression for element in the i^{th} row and j^{th} column of this product in terms of the rows \mathbf{a}_i^T of \mathbf{A}^T , the columns \mathbf{a}_j of \mathbf{A} and the matrix \mathbf{B} .

Problem 2.2 (Solution 2.2). Consider the transpose $(\mathbf{AB})^T$ of the product \mathbf{AB} where $\mathbf{A} \in \mathbb{R}^{I \times J}$ and $\mathbf{B} \in \mathbb{R}^{J \times K}$. Show that the transpose $(\mathbf{AB})^T$ is given by

$$(\mathbf{AB})^T = \mathbf{B}^T \mathbf{A}^T.$$

Problem 2.3 (Solution 2.3). Generalize the results of Problem 2.2. Show that for any finite sequence of consistently dimensioned matrices $\mathbf{A}_1, \mathbf{A}_2 \cdots \mathbf{A}_n$

$$(\mathbf{A}_1 \mathbf{A}_2 \cdots \mathbf{A}_{n-1} \mathbf{A}_n)^T = \mathbf{A}_n^T \mathbf{A}_{n-1}^T \cdots \mathbf{A}_2^T \mathbf{A}_1^T.$$

Problem 2.4 (Solution 2.4). The identity matrix of order N is the unique matrix \mathbb{I} such that

$$\mathbb{I}\mathbf{A} = \mathbf{A}\mathbb{I} = \mathbf{A}$$

holds for all $\mathbf{A} \in \mathbb{R}^{N \times N}$. Show that the identity matrix is equal to a diagonal matrix of ones.

Problem 2.5 (Solution 2.5). The *inverse matrix* \mathbf{A}^{-1} is defined for a matrix \mathbf{A} whenever

$$(\mathbf{A}^{-1})\mathbf{A} = \mathbf{A}(\mathbf{A}^{-1}) = \mathbb{I}.$$

Note that this equation can hold true only for square matrices. Show that not every matrix has an inverse.

Problem 2.6 (Solution 2.6). When a matrix $\mathbf{A} \in \mathbb{R}^{N \times N}$ has an inverse, it is unique. Prove this fact.

Problem 2.7 (Solution 2.7). The definition of the inverse \mathbf{A}^{-1} of a *square* matrix \mathbf{A} was stated in terms of the two conditions

$$\mathbf{A}^{-1}\mathbf{A} = \mathbb{I},$$

and

$$\mathbf{A}\mathbf{A}^{-1} = \mathbb{I}.$$

Each of these conditions can be generalized so that they apply to non-square matrices. A matrix $\mathbf{B}_L \in \mathbb{R}^{N \times M}$ is the left inverse of a matrix $\mathbf{A} \in \mathbb{R}^{M \times N}$ provided

$$\mathbf{B}_L \mathbf{A} = \mathbb{I}_N$$

where \mathbb{I}_N is the identify matrix on \mathbb{R}^N . A matrix $\mathbf{B}_R \in \mathbb{R}^{N \times M}$ is the right inverse of a matrix $\mathbf{A} \in \mathbb{R}^{M \times N}$ provided

$$\mathbf{AB}_R = \mathbb{I}_M$$

where \mathbb{I}_M is the identity matrix on \mathbb{R}^M .

It is clear from these definitions that a square matrix is invertible if and only if it has a left inverse and a right inverse and these two matrices are identical. Find a matrix that has a left inverse, but does not have a right inverse. Find a matrix that has a right inverse, but does not have a left inverse.

Problem 2.8 (Solution 2.8). Suppose that the matrix equation

$$\mathbf{Au} = \mathbf{0}$$

holds for any arbitrary N -tuple $\mathbf{u} \in \mathbb{R}^N$, where $\mathbf{A} \in \mathbb{R}^{M \times N}$. Argue that it must be the case that the matrix \mathbf{A} is identically equal to zero,

$$\mathbf{A} \equiv \mathbf{0} \in \mathbb{R}^{M \times N}.$$

Why must \mathbf{u} be emphasized as any arbitrary N -tuple? Construct a counterexample where

$$\mathbf{Au} = \mathbf{0}$$

for some specific \mathbf{u} , but it holds that $\mathbf{A} \neq \mathbf{0}$.

Problem 2.9 (Solution 2.9). An *orthogonal matrix* is a matrix \mathbf{A} for which the inverse exists and is equal to its transpose.

$$\mathbf{A}^{-1} = \mathbf{A}^T.$$

Show that multiplying a vector $\mathbf{v} \in \mathbb{R}^3$ by an orthogonal matrix $\mathbf{A} \in \mathbb{R}^{3 \times 3}$ does not change its length.

Problem 2.10 (Solution 2.10). A square matrix \mathbf{A} is *diagonalizable* if there is an invertible matrix \mathbf{P} such that

$$\mathbf{P}^{-1}\mathbf{AP} = \mathbf{D}$$

where \mathbf{D} is a diagonal matrix. Show that every diagonalizable matrix is invertible.

2.7.2 Problems on Vectors, Bases, Frames

Problem 2.11. Derive Equation (2.1.5) from Equation (2.1.4).

Problem 2.12 (Solution 2.12). The *scalar triple product* of three vectors $\mathbf{u}, \mathbf{v}, \mathbf{w}$ is given by

$$\mathbf{u} \times \mathbf{v} \cdot \mathbf{w}.$$

Show that the scalar triple product is equal to the volume of the parallelepiped spanned by the vectors $\mathbf{u}, \mathbf{v}, \mathbf{w}$.

Problem 2.13 (Solution 2.13). Prove that the following properties hold for the scalar triple product $\mathbf{u} \times \mathbf{v} \cdot \mathbf{w}$ of three vectors $\mathbf{u}, \mathbf{v}, \mathbf{w}$.

(i) The value of $\mathbf{u} \times \mathbf{v} \cdot \mathbf{w}$ changes sign if any pair of the three vectors $\mathbf{u}, \mathbf{v}, \mathbf{w}$ are interchanged. That is,

$$\begin{aligned}\mathbf{u} \times \mathbf{v} \cdot \mathbf{w} &= -\mathbf{v} \times \mathbf{u} \cdot \mathbf{w}, \\ &= -\mathbf{u} \times \mathbf{w} \cdot \mathbf{v}, \\ &= -\mathbf{w} \times \mathbf{v} \cdot \mathbf{u}.\end{aligned}$$

(ii) The value of $\mathbf{u} \times \mathbf{v} \cdot \mathbf{w}$ does not change if the dot and cross products are interchanged. That is,

$$\mathbf{u} \times \mathbf{v} \cdot \mathbf{w} = \mathbf{u} \cdot \mathbf{v} \times \mathbf{w}.$$

Problem 2.14 (Solution 2.14). Show that the determinant of a 3×3 matrix is equal to the scalar triple product of its columns, that is,

$$\det(\mathbf{A}) = \mathbf{a}_1 \times \mathbf{a}_2 \cdot \mathbf{a}_3$$

where

$$\mathbf{A} = [\mathbf{a}_1 \ \mathbf{a}_2 \ \mathbf{a}_3].$$

Problem 2.15 (Solution 2.15). Show that the cross product $\mathbf{w} = \mathbf{u} \times \mathbf{v}$ can be written as the product of a matrix $\mathbf{S}(\mathbf{u})$ (whose elements depend on \mathbf{u}) and the 3-tuple that represents \mathbf{v} in

$$\mathbf{w} = \begin{Bmatrix} w_1 \\ w_2 \\ w_3 \end{Bmatrix} = \mathbf{S}(\mathbf{u})\mathbf{v}.$$

Problem 2.16 (Solution 2.16). Show that

$$\mathbf{S}^2(\mathbf{w}) = -\|\mathbf{w}\|^2 \mathbb{I} + \mathbf{w} \mathbf{w}^2$$

for any $\mathbf{w} \in \mathbb{R}^3$.

Problem 2.17. Show that

$$\mathbf{S}^3(\mathbf{w}) = -\|\mathbf{w}\|^2 \mathbf{S}(\mathbf{w})$$

for any $\mathbf{w} \in \mathbb{R}^3$.

2.7.3 Problems on Rotation Matrices

Problem 2.18 (Solution 2.18). Show that the product of any finite number of rotation matrices \mathbf{R}_i , for $i = 1 \dots N$,

$$\mathbf{R}_1 \mathbf{R}_2 \cdots \mathbf{R}_N$$

is a rotation matrix. If the product $\mathbf{R}_1 \mathbf{R}_2 \cdots \mathbf{R}_N$ maps representations of a vector \mathbf{v} with respect to the frame \mathbb{Y} into the frame \mathbb{X} via the relationship

$$\mathbf{v}^{\mathbb{X}} = (\mathbf{R}_1 \mathbf{R}_2 \cdots \mathbf{R}_N) \mathbf{v}^{\mathbb{Y}},$$

what is the inverse transformation that maps the representation $\mathbf{v}^{\mathbb{X}}$ into $\mathbf{v}^{\mathbb{Y}}$?

Problem 2.19 (Solution 2.19). The following problem has been submitted by Professor Joseph Vignola of the Catholic University of America. Figures (2.25), (2.26) and (2.27) depict the popular puzzle Rubik's Cube. Devise a system that could be used to describe the steps taken in solving the puzzle using the concepts of frames.

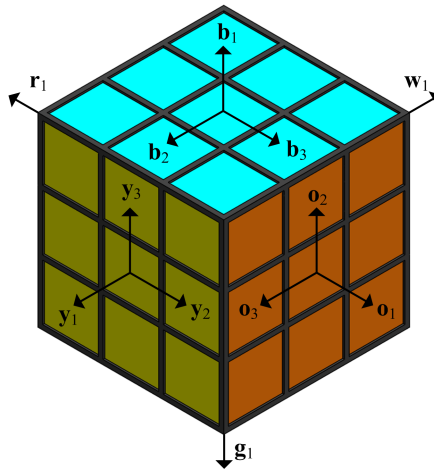


Fig. 2.25: Definition of Frames on Rubik's Cube

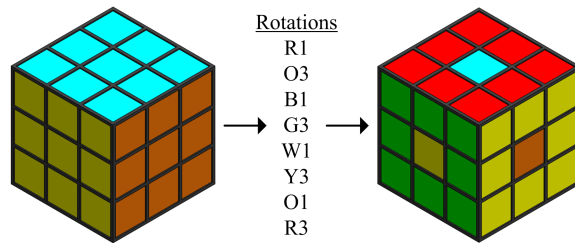


Fig. 2.26: First Sequence of Rotations

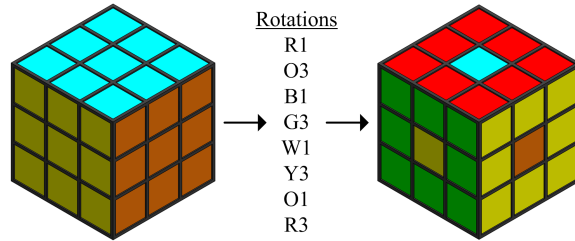


Fig. 2.27: Second Sequence of Rotations

Problem 2.20 (Solution 2.20). Derive the single axis rotation matrix $\mathbf{R}_Y^X(\alpha_1)$ in Theorem (2.6) by carrying out the following two steps: project the y_2, y_3 axes onto the axes x_2, x_3 , and then use Theorem (2.5).

Problem 2.21 (Solution ??). Derive the single axis rotation matrix $\mathbf{R}_Y^X(\alpha_2)$ in Theorem (2.6) by carrying out the following two steps: project the y_1, y_3 axes onto the axes x_1, x_3 , and then use Theorem (2.5).

Problem 2.22 (Solution ??). Derive the single axis rotation matrix $\mathbf{R}_X^Y(\alpha_1)$ in Theorem (2.6) two different ways. In the first approach, project the axes x_2, x_3 onto the axes y_2, y_3 , and then use Theorem (2.5). In the second approach, use the results of Problem (2.20) and Theorem (2.3).

Problem 2.23 (Solution ??). Derive the single axis rotation matrix $\mathbf{R}_X^Y(\alpha_2)$ two different ways. In the first approach, project the axes x_1, x_3 onto the axes y_1, y_3 , and then use Theorem (2.5). In the second approach, use the results of Problem (2.21) and Theorem (2.3).

Problem 2.24 (Solution ??). Derive the single axis rotation matrix $\mathbf{R}_X^Y(\alpha_3)$ two different ways. In the first approach, project the axes x_1, x_2 onto the axes y_1, y_2 , and then use Theorem (2.5). In the second approach, use the results of Theorem (2.6) and Theorem (2.3).

Problem 2.25 (Solution ??). Let \mathbf{R}_Y^X be the rotation matrix that relates the frames \mathbb{Y} and \mathbb{X} . Show that +1 is an eigenvalue of the matrix \mathbf{R}_Y^X . What is the physical interpretation of the eigenvector \mathbf{v} corresponding to the eigenvalue +1?

Problem 2.26 (Solution ??). The classical definition of spherical coordinates from calculus is shown in Figure (2.28). The change of basis from rectangular Cartesian coordinates to spherical coordinates is a simple application of the techniques derived in this section: two single axis rotations are used. The first rotation matrix $\mathbf{R}_Z^X(\theta)$ maps the \mathbb{X} basis $\mathbf{x}_1, \mathbf{x}_2, \mathbf{x}_3$ into the intermediate \mathbb{Z} -frame which has the basis $\mathbf{z}_1, \mathbf{z}_2, \mathbf{z}_3$, and the second rotation matrix $\mathbf{R}_Y^Z(\phi)$ maps the intermediate \mathbb{Z} -frame into the frame \mathbb{Y} with spherical coordinates basis $\mathbf{y}_\phi, \mathbf{y}_\theta, \mathbf{y}_\rho$. First, define the rotation matrix $\mathbf{R}_Z^X(\theta)$ associated with rotation through the angle θ about the common $\mathbf{x}_3 = \mathbf{z}_3$.

Next, define the rotation matrix $\mathbf{R}_Y^Z(\phi)$ generated by rotation through the angle ϕ about the common $\mathbf{z}_2 = \mathbf{y}_\theta$ axis. Finally, any vector \mathbf{v} can be written in rectangular Cartesian coordinates as

$$\mathbf{v}^X = \begin{Bmatrix} x_1 \\ x_2 \\ x_3 \end{Bmatrix}.$$

The representation of the same vector with respect to the \mathbb{Y} -frame is just

$$\mathbf{v}^Y = \begin{Bmatrix} 0 \\ 0 \\ \rho \end{Bmatrix}$$

where $\rho^2 = x_1^2 + x_2^2 + x_3^2$. Use the change of basis relationship

$$\mathbf{v}^X = \mathbf{R}_Z^X(\theta) \mathbf{R}_Y^Z(\phi) \mathbf{v}^Y$$

to obtain the classical spherical coordinate definitions of x_1, x_2, x_3 in terms of ρ, θ, ϕ .

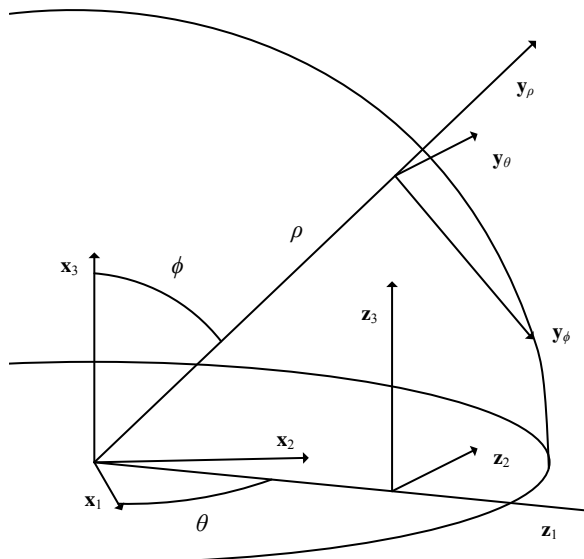


Fig. 2.28: Spherical Coordinates

Problem 2.27 (Solution ??). Azimuth θ and elevation ϕ angles are a common pair of angles used to determine the line-of-sight (LOS) of celestial observations. The definitions of these two angles is depicted in Figure (2.29). The symbol \mathbb{X} denotes the local-vertical-local horizontal (LVLH) frame with basis $\mathbf{x}_1, \mathbf{x}_2, \mathbf{x}_3$. In a flat world

model it is reasonable to take \mathbf{x}_1 aligned with true north, to take \mathbf{x}_2 aligned with true east, and to take \mathbf{x}_3 to point toward the center of gravity of the earth. The angle θ measures the rotation about the \mathbf{x}_3 axis from \mathbf{x}_1 to the projection of the LOS direction \mathbf{y}_{LOS} onto the local horizontal plane. The elevation ϕ is measured from (the projection of the LOS direction onto) the local horizontal plane to the LOS direction \mathbf{y}_{LOS} . Determine the rotation matrix $\mathbf{R}_{\mathbb{X}}^{\mathbb{Y}}$ as the product of two single axis rotations by introducing an intermediate frame.

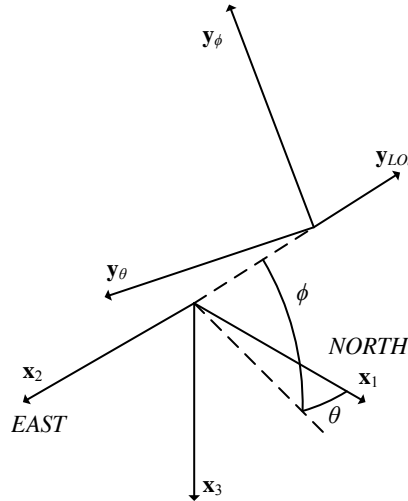


Fig. 2.29: Azimuth (θ) and Elevation (ϕ) Angles Relative to a Local-Vertical-Local-Horizontal (LVLH) frame.

Problem 2.28 (Solution ??). Define a sequence of frames of reference that are attached to the rigid bodies that make up the two-arm subsystem shown in Figures (2.30) through (2.33). The frame \mathbb{Y} rotates through the angle θ_1 about the $\mathbf{x}_1 = -\mathbf{y}_2$ axis. The frame \mathbb{Z} rotates through the angle θ_2 about the $\mathbf{y}_3 = \mathbf{z}_3$ axis. The frame \mathbb{A} rotates through the angle θ_3 about the $\mathbf{a}_3 = -\mathbf{z}_3$ axis. What are the rotation matrices $\mathbf{R}_{\mathbb{Y}}^{\mathbb{X}}$, $\mathbf{R}_{\mathbb{Z}}^{\mathbb{Y}}$, $\mathbf{R}_{\mathbb{A}}^{\mathbb{Z}}$ and $\mathbf{R}_{\mathbb{A}}^{\mathbb{X}}$?

Problem 2.29. Derive the expression in Theorem (2.8) for the axis-angle parameterization of a rotation matrix that maps the \mathbb{A} frame into the \mathbb{B} frame as depicted in Figure (2.17). Use a graphical procedure to carry out the proof.

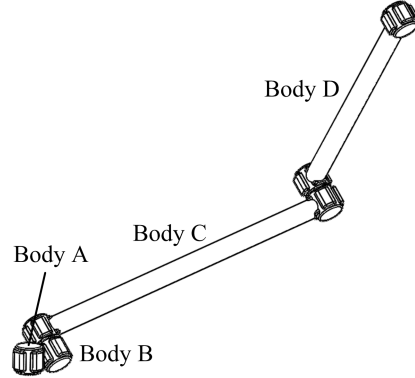


Fig. 2.30: Detail illustration of Two Arm Model

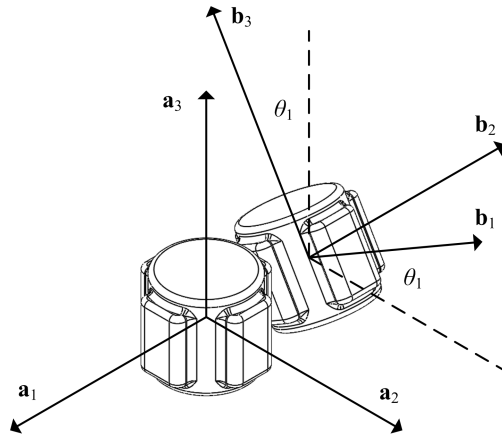


Fig. 2.31: Definition of Frames A, B

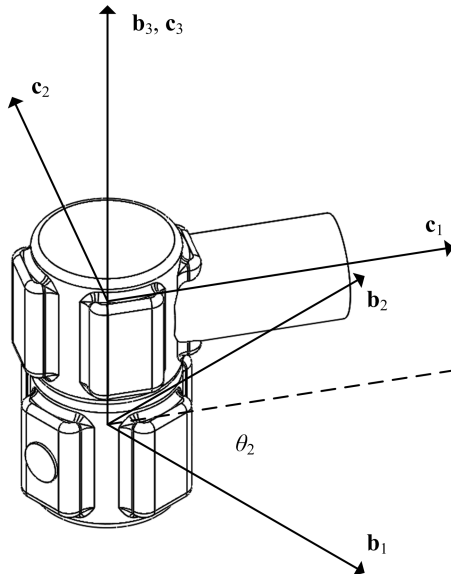
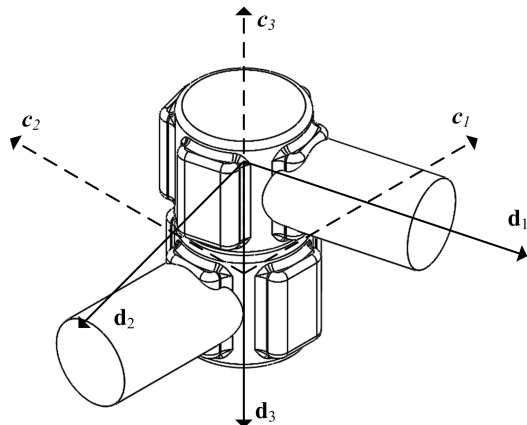
2.7.4 Problems on Position, Velocity, Acceleration

Problem 2.30 (Solution ??). The frame \mathbb{Y} rotates with respect to the frame \mathbb{X} , and the rotation matrix that relates these two frames is given by

$$\mathbf{R}_{\mathbb{Y}}^{\mathbb{X}}(t) = \begin{bmatrix} \cos(2\pi t) & \sin(2\pi t) & 0 \\ -\sin(2\pi t) & \cos(2\pi t) & 0 \\ 0 & 0 & 1 \end{bmatrix}.$$

The vector \mathbf{v} can be expressed in terms of the \mathbb{Y} frame as

$$\mathbf{v} = 8\mathbf{y}_1 - 13\mathbf{y}_2 + 17\mathbf{y}_3.$$

Fig. 2.32: Definition of Frames \mathbb{B}, \mathbb{C} Fig. 2.33: Definition of Frames \mathbb{C}, \mathbb{D}

Find each of the following:

1. Calculate the derivative of the vector \mathbf{v} with the \mathbb{Y} basis held fixed.
2. Calculate the derivative of the vector \mathbf{v} with the \mathbb{X} basis held fixed.
3. Interpret the motion of the \mathbb{Y} -frame relative to the \mathbb{X} -frame.

Problem 2.31 (Solution ??). The frame \mathbb{Y} rotates with respect to the frame \mathbb{X} , and the rotation matrix that relates these two frames is given by

$$\mathbf{R}_{\mathbb{Y}}^{\mathbb{X}}(t) = \begin{bmatrix} \cos(40\pi t) & 0 & -\sin(40\pi t) \\ 0 & 1 & 0 \\ \sin(40\pi t) & 0 & \cos(40\pi t) \end{bmatrix}.$$

The vector \mathbf{v} can be expressed in terms of the \mathbb{X} frame as

$$\mathbf{v} = 3\mathbf{x}_1 + 7\mathbf{x}_2 - 11\mathbf{x}_3.$$

Find each of the following:

1. Calculate the derivative of the vector \mathbf{v} with the \mathbb{Y} basis held fixed.
2. Calculate the derivative of the vector \mathbf{v} with the \mathbb{X} basis held fixed.
3. Interpret the motion of the \mathbb{Y} -frame relative to the \mathbb{X} -frame.

Problem 2.32 (Solution ??). A compact disc with body fixed frame \mathbb{B} rotates relative to the housing which has body fixed frame \mathbb{X} . A bug crawls on the surface of the compact disc. The location of the bug as a function of time relative to the CD is given by $r_{\mathbb{B},p}(t) = 8t^2\mathbf{b}_1 + (9t + e^t)\mathbf{b}_2$.

1. Calculate the velocity of the bug $\mathbf{v}_{\mathbb{B},p}$ with respect to the \mathbb{B} -frame. Express your answer in the \mathbb{B} -basis. Express your answer in the \mathbb{X} -basis.
2. Calculate the velocity of the bug $\mathbf{v}_{\mathbb{X},p}$ with respect to the \mathbb{X} frame. Express your answer in the \mathbb{B} -basis. Express your answer in the \mathbb{X} -basis.
3. Calculate the acceleration of the bug $\mathbf{a}_{\mathbb{B},p}$ with respect to the \mathbb{B} -frame. Express your answer in the \mathbb{B} -basis. Express your answer in the \mathbb{X} -basis.
4. Calculate the acceleration of the bug $\mathbf{a}_{\mathbb{X},p}$ with respect to the \mathbb{X} -frame. Express your answer in the \mathbb{B} -basis. Express your answer in the \mathbb{X} -basis.

2.7.5 Problems on Angular Velocity

Problem 2.33 (Solution ??). Show that

$$\mathbf{S}(\mathbf{R}\boldsymbol{\omega}) = \mathbf{R}\mathbf{S}(\boldsymbol{\omega})(\mathbf{R})^T$$

for any rotation matrix \mathbf{R} and any 3-tuple $\boldsymbol{\omega}$.

Problem 2.34 (Solution ??). Show that the matrix $e^{\mathbf{S}(\boldsymbol{\omega})}$ is a rotation matrix for any 3-tuple $\boldsymbol{\omega}$.

2.7.6 Problems on the Theorems of Kinematics

2.7.6.1 Problems on the Addition of Angular Velocities

Problem 2.35 (Solution ??). Let the orientation of the \mathbb{D} -frame relative to the \mathbb{A} -frame be given by the 3–2–1 Euler angles. Show that

$$\boldsymbol{\omega}_{A,D}^A = \begin{bmatrix} \cos\theta\cos\psi & -\sin\psi & 0 \\ \cos\theta\sin\psi & \cos\psi & 0 \\ -\sin\theta & 0 & 1 \end{bmatrix} \begin{Bmatrix} \dot{\phi} \\ \dot{\theta} \\ \dot{\psi} \end{Bmatrix}.$$

Problem 2.36 (Solution ??). Let the orientation of the D -frame relative to the A -frame be given by the $3-2-1$ Euler angles. Show that

$$\boldsymbol{\omega}_{A,D}^D = \begin{bmatrix} 1 & 0 & -\sin\theta \\ 0 & \cos\phi & \cos\theta\sin\phi \\ 0 & -\sin\phi & \cos\theta\cos\phi \end{bmatrix} \begin{Bmatrix} \dot{\phi} \\ \dot{\theta} \\ \dot{\psi} \end{Bmatrix}.$$

Problem 2.37 (Solution ??). Let the orientation of the D -frame relative to the A -frame be given by the $3-1-3$ Euler angles. Show that

$$\boldsymbol{\omega}_{A,D}^A = \begin{bmatrix} 0 \cos\alpha & \sin\alpha\sin\beta & 0 \\ 0 \sin\alpha & -\cos\alpha\sin\beta & 0 \\ 1 & 0 & \cos\beta \end{bmatrix} \begin{Bmatrix} \dot{\alpha} \\ \dot{\beta} \\ \dot{\gamma} \end{Bmatrix}.$$

Problem 2.38 (Solution ??). Let the orientation of the D -frame relative to the A -frame be given by the $3-1-3$ Euler angles. Show that

$$\boldsymbol{\omega}_{A,D}^D = \begin{bmatrix} \sin\beta\sin\gamma & \cos\gamma & 0 \\ \cos\gamma\sin\beta & -\sin\gamma & 0 \\ \cos\beta & 0 & 1 \end{bmatrix} \begin{Bmatrix} \dot{\alpha} \\ \dot{\beta} \\ \dot{\gamma} \end{Bmatrix}.$$

Problem 2.39 (Solution ??). Consider the construction of spherical coordinates in terms of two successive rotation matrices discussed in Problem (2.26). What are the angular velocities $\omega_{X,Z}, \omega_{Z,Y}, \omega_{X,Y}$? Express your answer in terms of the X basis. Express your answer in terms of the Y basis.

Problem 2.40 (Solution ??). Consider the construction of the frame Y that is used for determining the line-of-sight in Problem (2.27). What is the angular velocity $\omega_{X,Y}$? Express your answer in terms of the X -frame. Express your answer in terms of the Y -frame.

2.7.7 Problems on Relative Velocity and Acceleration

Problem 2.41 (Solution ??). The PUMA robot shown in Figure (2.34) is modeled via frames 1, 2 and 3 that are fixed in links 1, 2 and 3, respectively. The ground frame is denoted the 0 frame in the figure. The angle θ_i measures the rotation of frame i relative to frame $i-1$ for $i = 1, 2, 3$ is measured from \mathbf{x}_{i-1} to \mathbf{x}_i about the \mathbf{z}_{i-1} axis. Find the velocity in the ground frame of the point r using the theorem on the relative velocity of two points on the same rigid body. Express your answer in terms of the basis for 1 frame and the 2 frame.

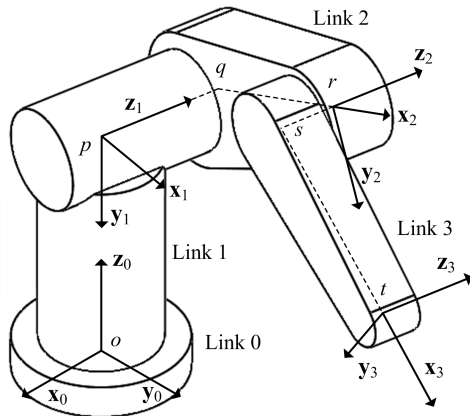


Fig. 2.34: Definition of Frames for PUMA Robot

Problem 2.42 (Solution ??). Calculate the acceleration in the 0 frame of the point r on the PUMA robot studied in Problem (2.41) and shown in Figure (2.34). Use the relative acceleration formula to calculate your solution. Express your answer in terms of the basis for the 1 frame.

Problem 2.43 (Solution ??). The SCARA robot shown in Figure (2.35) is modeled via frames 1, 2 and 3 that are fixed in links 1, 2 and 3, respectively. The ground frame is denoted as frame 0 in the figure. The angle θ_i measures the rotation of frame i relative to the frame $i - 1$ about the z_{i-1} axis for $i = 1, 2, 3$. Each angle θ_i is measured from the x_{i-1} axis to the x_i about the z_{i-1} axis for $i = 1, 2, 3$. Find the velocity in the 0 frame of the point t . Express your answer in terms of the basis for the 0 frame and the 2 frame.

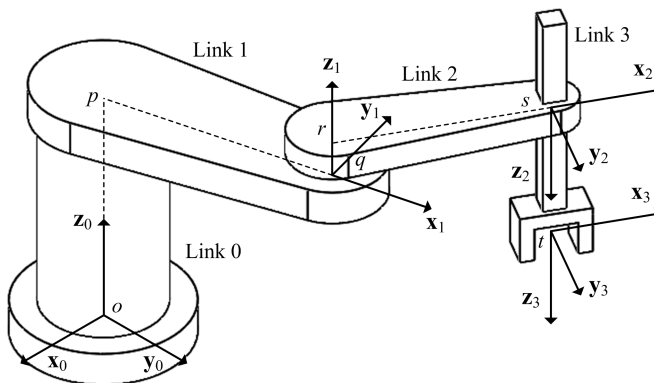


Fig. 2.35: Definition of Frames and Points for SCARA Robot in Problem (2.43)

Problem 2.44 (Solution ??). Calculate the acceleration in the 0 frame of the point t on the SCARA robot studied in Problem (2.43) and depicted in Figure (2.35). Use the relative acceleration formula to calculate your solution. Express your answer in terms of the basis for the 1 frame.

Problem 2.45 (Solution ??). The spherical wrist depicted in Figure (2.36) has four links numbered 0, 1, 2 and 3. Frame i is fixed in link i for $i = 0, 1, 2, 3$. The angle ψ measures the rotation of the 2 frame about the $\mathbf{z}_0 = \mathbf{z}_1$ axis. The angle θ measures the rotation of the 2 frame relative to the 1 frame about the $\mathbf{y}_1 = \mathbf{y}_2$ axis. The angle ϕ measures the rotation of the 3 frame relative to the 2 frame about the $\mathbf{x}_2 = \mathbf{x}_3$ axis. Find the velocity $\mathbf{v}_{0,q}$ using the relative velocity formula by noting that the points p

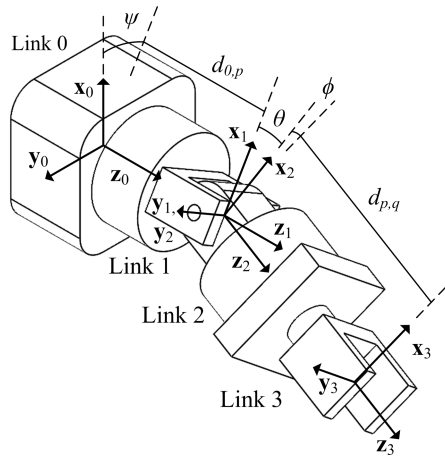


Fig. 2.36: Definition of Frames for Problem (2.45)

and q have fixed positions relative to frame 2. Express your answer in terms of the basis for the 0 and 2 frames.

Problem 2.46 (Solution ??). Using the relative acceleration formula for two points on the same rigid body, calculate the acceleration in the 0 frame of the point q on the spherical wrist studied in Problem (2.45) and depicted in Figure (2.36). Express your answer in terms of the basis for the 1 frame.

Problem 2.47 (Solution ??). What are the velocities in the ground frame of the masses m_1 and m_2 in Figure (5.17)?

Problem 2.48 (Solution ??). What is the velocity in the ground frame of the midpoint of the bar in Figure (5.18)?

Problem 2.49 (Solution ??). What are the velocities in the ground frame of the link mass centers in Figure (5.24)?

Problem 2.50 (Solution ??). What is the velocity in the ground frame of point s of the PUMA robot studied in Problem (2.41)? Write your answer in terms of the basis of the 1 frame.

Problem 2.51 (Solution ??). What are the velocities in the ground frame of the link mass centers of the PUMA robot in Problem (2.41)?

Problem 2.52 (Solution ??). What are the velocities in the ground frame of the link mass centers of the Cartesian robot in Problem (5.24)? Express your answer in terms of the basis for the 0 frame.

Problem 2.53 (Solution ??). What are the velocities in the ground frame of the link mass centers of the spherical wrist studied in Problem (2.45) and depicted in Figure (2.36)? Express your answer in terms of the basis for the 2 frame.

Problem 2.54 (Solution ??). What are the velocities in the ground frame of the link mass centers of the SCARA robot in Problem (5.26) and depicted in Figure (5.31)? Express your answer in terms of the basis for the 1 frame.

Problem 2.55 (Solution ??). What are the velocities in the ground frame of the link mass centers of the cylindrical robot studied in Problem (5.28) and depicted in Figure (5.33)? Express your answer in terms of the basis for the 1 frame.

2.7.8 Problems on Common Coordinate Systems

Problem 2.56 (Solution ??). Consider the construction of position, velocity and acceleration within the cylindrical coordinate system in Theorem (2.18). Derive the expressions in Equations (2.6.4), (2.6.5) and (2.6.6) by following the alternative strategy discussed at the beginning of the proof of Theorem (2.18). That is, directly use the change of variables that are given by the functional relationships

$$x = r\cos\theta, \quad (2.7.1)$$

$$y = r\sin\theta, \quad (2.7.2)$$

$$z = z. \quad (2.7.3)$$

Specifically, carry out the following steps:

1. Calculate \dot{x} , \dot{y} , \dot{z} from Equations (2.7.1) - (2.7.3) in terms of (r, θ, z) and their time derivatives.
2. Substitute these results into Equation (2.6.8).
3. Finally, use the rotation matrix in Equation (2.6.2) to eliminate the basis vectors $\mathbf{x}_1, \mathbf{x}_2, \mathbf{x}_3$ to obtain a final expression in terms on $(r(t), \theta(t), z(t))$, their time derivatives, and $\mathbf{y}_1, \mathbf{y}_2, \mathbf{y}_3$.

Problem 2.57 (Solution ??). Consider the construction of position, velocity and acceleration expressed in terms of the spherical coordinate system in Theorem (2.19).

Use the results of Problem (2.26) and the strategy outlined in Problem (2.56) to verify the expressions in Theorem (2.19). Specifically, carry out the following steps:

1. Calculate $\dot{\rho}$, $\dot{\phi}$, $\dot{\theta}$ from the solution of Problem (2.26) in terms of (ρ, ϕ, θ) and their time derivatives.
2. Substitute these results into Equation (2.6.8).
3. Finally, use the rotation matrix $\mathbf{R}_{\mathbb{Y}}^{\mathbb{X}}$ that relates the basis $\mathbf{y}_\rho, \mathbf{y}_\phi, \mathbf{y}_\theta$ of the spherical coordinates to the basis for the Cartesian coordinates to eliminate the basis vectors $\mathbf{x}_1, \mathbf{x}_2, \mathbf{x}_3$, and thereby obtain a final expression for velocities and accelerations in terms on $(\rho(t), \phi(t), \theta(t))$, their time derivatives, and $\mathbf{y}_\rho, \mathbf{y}_\phi, \mathbf{y}_\theta$.

Chapter 3

Kinematics of Robotic Systems

Abstract In this chapter, the general principles of kinematics in Chapter (2) are applied to robotics to help model their geometry and enable the construction of dynamic models. Applications of these principles are diverse and include the study of industrial robotic manipulators, the design and analysis of ground vehicles, the creation of models of flight vehicles, and the development of models of space vehicles. This chapter introduces the special structure that the principles of kinematics can take in the study of robotic systems that have the form of a *kinematic chain* or are constructed from assemblies of kinematic chains that do not form closed loops. Robotic systems having a *tree topology* are an example of the latter class. Upon the completion of this chapter, the student should be able to

- Define and use *homogeneous transformations* to represent *rigid body motion*.
- Define and use *homogeneous coordinates* to represent position vectors.
- Define the assumptions underlying the *Denavit-Hartenberg convention*.
- Use the *Denavit-Hartenberg convention* to model a *kinematic chain*.
- Derive the Jacobian matrix relating derivatives of the generalized coordinates to the velocity and angular velocity.
- Derive and use *the recursive $O(N)$ formulation* of kinematics.

3.1 Homogeneous Transformations and Rigid Motion

Sections 2.1 and 2.4 in Chapter 2 discuss the fundamental properties of *rotation matrices* and their use in change of basis formulae. In applications to robotics, however, information about both the rotation and the translation of coordinate systems is often required. This section will show that *homogeneous transformations* are a succinct way of describing these *rigid body motions*.

Suppose there are two bodies with body fixed frames \mathbb{X} and \mathbb{Y} , respectively, as shown in Figure (3.1). The location of a generic point p with respect to the two different frames \mathbb{X} and \mathbb{Y} is defined through the vector identity

$$\mathbf{r}_{\mathbb{X},p} = \mathbf{r}_{\mathbb{Y},p} + \mathbf{d}_{\mathbb{X},\mathbb{Y}}, \quad (3.1.1)$$

which is defined in Figure 3.1. In this equation $\mathbf{r}_{\mathbb{X},p}$ is the position of the point p relative to the frame \mathbb{X} , while $\mathbf{r}_{\mathbb{Y},p}$ is the position of the point p with respect to the frame \mathbb{Y} . The vector $\mathbf{d}_{\mathbb{X},\mathbb{Y}}$ is the relative offset between the origin of the \mathbb{X} frame and the \mathbb{Y} frame.

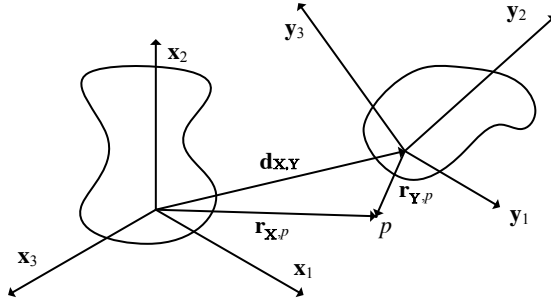


Fig. 3.1: Two Rigid Bodies, Body-Fixed Frames, Position Vectors

No particular basis is implied in Equation (3.1.1): it is an equation in terms of vectors. If the vectors that appear in Equation (3.1.1) are expressed in terms of coordinates relative to their respective body fixed frames,

$$\mathbf{r}_{\mathbb{X},p}^{\mathbb{X}} = \mathbf{R}_{\mathbb{Y}}^{\mathbb{X}} \mathbf{r}_{\mathbb{Y},p}^{\mathbb{Y}} + \mathbf{d}_{\mathbb{X},\mathbb{Y}}^{\mathbb{X}}, \quad (3.1.2)$$

where $\mathbf{R}_{\mathbb{Y}}^{\mathbb{X}}$ is the rotation matrix relating the frames. This identity follows from the fundamental definitions and properties of rotation matrices.

Note that the position $\mathbf{r}_{\mathbb{X},p}$ is expressed in terms of the \mathbb{X} basis, and the position $\mathbf{r}_{\mathbb{Y},p}$ is expressed in terms of the \mathbb{Y} basis. This convention is common in robotics and is the foundation of many of the approaches in this chapter that are tailored to the study of robotics. It is desirable to relate the coordinate representations $\mathbf{r}_{\mathbb{X},p}^{\mathbb{X}}$ and $\mathbf{r}_{\mathbb{Y},p}^{\mathbb{Y}}$, so the 4×4 *homogeneous transformation* matrix $\mathbf{H}_{\mathbb{Y}}^{\mathbb{X}}$ is introduced in Equation (3.1.3) to cast Equation (3.1.2) in the form of a matrix equation.

$$\begin{Bmatrix} \mathbf{r}_{\mathbb{X},p}^{\mathbb{X}} \\ 1 \end{Bmatrix} = \underbrace{\begin{bmatrix} \mathbf{R}_{\mathbb{Y}}^{\mathbb{X}} & \mathbf{d}_{\mathbb{X},\mathbb{Y}}^{\mathbb{X}} \\ \mathbf{0} & 1 \end{bmatrix}}_{\mathbf{H}_{\mathbb{Y}}^{\mathbb{X}}} \begin{Bmatrix} \mathbf{r}_{\mathbb{Y},p}^{\mathbb{Y}} \\ 1 \end{Bmatrix}. \quad (3.1.3)$$

In contrast to the techniques associated with 3×3 rotation matrices and the change of basis formulae introduced in Chapter (2), the *homogeneous transformation* operates on 4 -tuples of *homogeneous coordinates* $\mathbf{p}^{\mathbb{X}}$ and $\mathbf{p}^{\mathbb{Y}}$ of the point p , such that

$$\mathbf{p}^{\mathbb{X}} := \begin{Bmatrix} \mathbf{r}_{\mathbb{X},p}^{\mathbb{X}} \\ 1 \end{Bmatrix} \quad \text{and} \quad \mathbf{p}^{\mathbb{Y}} := \begin{Bmatrix} \mathbf{r}_{\mathbb{Y},p}^{\mathbb{Y}} \\ 1 \end{Bmatrix}.$$

It is a standard convention in robotics literature to suppress all the subscripts in the definition of the *homogeneous coordinates*. However, it is important to keep in mind that the *homogeneous coordinates* are implicitly associated with a specific choice of both the origin of position vectors and basis. In this text, although the notation is cumbersome, the subscripts and superscripts will be retained to make explicit the origins and bases used.

The final form of the transformation that represents a rigid body motion can be expressed as

$$\mathbf{p}^{\mathbb{X}} = \underbrace{\begin{bmatrix} \mathbf{R}_{\mathbb{Y}}^{\mathbb{X}} & \mathbf{d}_{\mathbb{X},\mathbb{Y}}^{\mathbb{X}} \\ \mathbf{0}^T & 1 \end{bmatrix}}_{\mathbf{H}_{\mathbb{Y}}^{\mathbb{X}}} \mathbf{p}^{\mathbb{Y}},$$

or more succinctly as,

$$\mathbf{p}^{\mathbb{X}} = \mathbf{H}_{\mathbb{Y}}^{\mathbb{X}} \mathbf{p}^{\mathbb{Y}}. \quad (3.1.4)$$

The notation in Equation (3.1.4) closely resembles the matrix equation that relates the coordinates $\mathbf{v}^{\mathbb{X}}$ and $\mathbf{v}^{\mathbb{Y}}$ of a vector \mathbf{v} under a rotation of basis,

$$\mathbf{v}^{\mathbb{X}} = \mathbf{R}_{\mathbb{Y}}^{\mathbb{X}} \mathbf{v}^{\mathbb{Y}}. \quad (3.1.5)$$

While notation has been chosen such that Equations (3.1.4) and (3.1.5) have the same appearance, there is a substantial difference between the matrices $\mathbf{H}_{\mathbb{Y}}^{\mathbb{X}}$ and $\mathbf{R}_{\mathbb{Y}}^{\mathbb{X}}$. A homogeneous transformation is *not* an orthogonal transformation. That is, in general, $(\mathbf{H}_{\mathbb{Y}}^{\mathbb{X}})^{-1} \neq (\mathbf{H}_{\mathbb{Y}}^{\mathbb{X}})^T$. Instead, the inverse of a homogeneous transformation is explicitly derived in Theorem (3.1).

Theorem 3.1 (Homogeneous Transformation Inverse). *The inverse $(\mathbf{H}_{\mathbb{Y}}^{\mathbb{X}})^{-1}$ of any homogeneous transformation $\mathbf{H}_{\mathbb{Y}}^{\mathbb{X}}$ defined as*

$$\mathbf{H}_{\mathbb{Y}}^{\mathbb{X}} := \begin{bmatrix} \mathbf{R}_{\mathbb{Y}}^{\mathbb{X}} & \mathbf{d}_{\mathbb{X},\mathbb{Y}}^{\mathbb{X}} \\ \mathbf{0}^T & 1 \end{bmatrix}$$

is given by

$$(\mathbf{H}_{\mathbb{Y}}^{\mathbb{X}})^{-1} = \begin{bmatrix} (\mathbf{R}_{\mathbb{Y}}^{\mathbb{X}})^T & -(\mathbf{R}_{\mathbb{Y}}^{\mathbb{X}})^T \mathbf{d}_{\mathbb{X},\mathbb{Y}}^{\mathbb{X}} \\ \mathbf{0}^T & 1 \end{bmatrix}.$$

Proof. The coordinates of the point p with respect to the \mathbb{X} frame and \mathbb{Y} frame satisfy

$$\mathbf{r}_{\mathbb{X},p}^{\mathbb{X}} = \mathbf{R}_{\mathbb{Y}}^{\mathbb{X}} \mathbf{r}_{\mathbb{Y},p}^{\mathbb{Y}} + \mathbf{d}_{\mathbb{X},\mathbb{Y}}^{\mathbb{X}}.$$

This equation may be solved for the coordinates $\mathbf{r}_{\mathbb{Y},p}^{\mathbb{Y}}$ relative to the frame \mathbb{Y} and obtain

$$\mathbf{r}_{\mathbb{Y},p}^{\mathbb{Y}} = (\mathbf{R}_{\mathbb{Y}}^{\mathbb{X}})^T \mathbf{r}_{\mathbb{X},p}^{\mathbb{X}} - (\mathbf{R}_{\mathbb{Y}}^{\mathbb{X}})^T \mathbf{d}_{\mathbb{X},\mathbb{Y}}^{\mathbb{Y}}.$$

This last expression can be put in matrix form and the theorem is proved. \square

The following example shows how the use of homogeneous transformations and homogeneous coordinates can facilitate the study of typical robotic subsystems.

Example 3.1.1. This example studies a robotic system designed to expand the workspace of a planar laser rangefinder, shown in Figure (3.2a) into a spatial workspace. As shown in Figure (3.2b), this sensor payload mounts the laser scanner from Figure (3.2a) onto a robotic platform capable of yaw-angle motion. Within the scanner, a laser sweeps in a planar motion to make range measurements along the line of sight of the laser. In Figure (3.2b), frame \mathbb{A} is fixed to the base of the sensor payload, frame \mathbb{B} is fixed to the motorized carriage that rotates relative to the fixed base, frame \mathbb{C} is fixed to the casing of the scanner unit, and frame \mathbb{D} is fixed to the laser moving within the scanner unit. The line of sight of the laser is always along the $\mathbf{x}_{\mathbb{D}}$ axis of the frame \mathbb{D} .

The angle θ measures the rotation of the carriage frame \mathbb{C} relative to the base frame \mathbb{D} about the positive $\mathbf{z}_{\mathbb{A}} = \mathbf{z}_{\mathbb{B}}$ axis, from the positive $\mathbf{x}_{\mathbb{A}}$ axis to the positive $\mathbf{x}_{\mathbb{B}}$ axis. The scanner housing is rigidly attached to the carriage; therefore, frames \mathbb{B} and \mathbb{C} do not rotate relative to one another. The angle ϕ measure the rotation of the laser frame \mathbb{D} relative to the housing frame \mathbb{C} about the positive $\mathbf{z}_{\mathbb{D}} = -\mathbf{y}_{\mathbb{C}}$ axis, from the positive $\mathbf{x}_{\mathbb{C}}$ axis to the positive $\mathbf{y}_{\mathbb{D}}$ axis.

The relative positioning of the frames $\mathbb{A}, \mathbb{B}, \mathbb{C}$ and \mathbb{D} is shown in Figure (3.3). Use *homogeneous transformations* to represent the kinematics of this robotic subsystem and show how laser ranging measurements made in frame \mathbb{D} may be represented in frame \mathbb{A} .

Solution: The problem statement aims to represent a point \mathbf{p} defined by a known position vector known in the \mathbb{D} frame $\mathbf{p}^{\mathbb{D}}$ with respect to the \mathbb{A} frame, or $\mathbf{p}^{\mathbb{A}}$. This is done by constructing the homogenous transformation $\mathbf{H}_{\mathbb{D}}^{\mathbb{A}}$, such that

$$\mathbf{p}^{\mathbb{A}} = \mathbf{H}_{\mathbb{D}}^{\mathbb{A}} \mathbf{p}^{\mathbb{D}}.$$

By definition, $\mathbf{H}_{\mathbb{C}}^{\mathbb{B}}$ is given by

$$\mathbf{H}_{\mathbb{C}}^{\mathbb{B}} = \begin{bmatrix} \mathbf{R}_{\mathbb{C}}^{\mathbb{B}} & \mathbf{d}_{\mathbb{B},\mathbb{C}}^{\mathbb{B}} \\ \mathbf{0} & 1 \end{bmatrix}.$$

Since the sensor frame \mathbb{C} does not rotate relative to the carriage frame \mathbb{B} , the rotation matrix $\mathbf{R}_{\mathbb{C}}^{\mathbb{B}}$ is the identity matrix. The vector that connects the origin of the \mathbb{B} frame to the origin of the \mathbb{C} frame is

$$\mathbf{d}_{\mathbb{B},\mathbb{C}} = d_{q,r} \mathbf{x}_{\mathbb{B}} + d_{p,q} \mathbf{z}_{\mathbb{B}}.$$

The homogenous transformation $\mathbf{H}_{\mathbb{C}}^{\mathbb{B}}$ is then

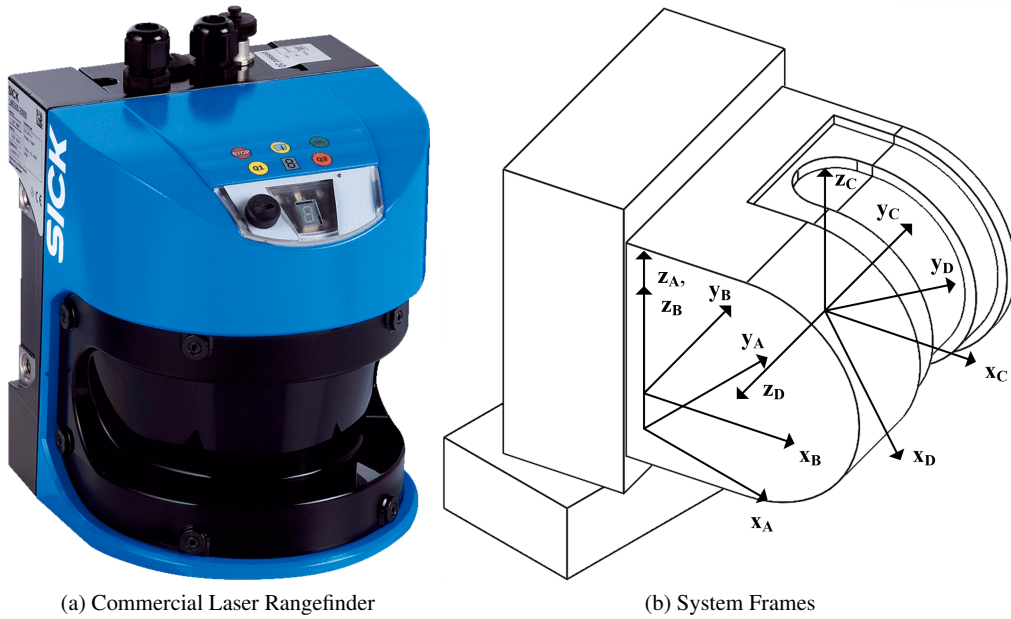


Fig. 3.2: Articulating Laser Ranging Sensor

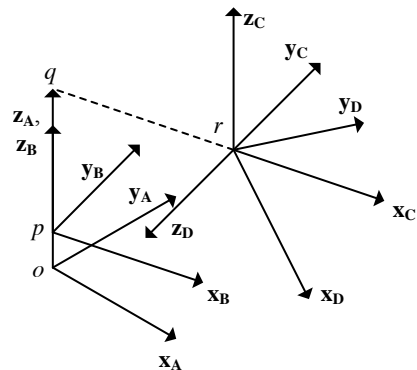


Fig. 3.3: Relative Positioning of frames A, B, C, D.

$$\mathbf{H}_{\mathbb{C}}^{\mathbb{B}} = \left[\begin{bmatrix} 1 & 0 & 0 \\ 0 & 1 & 0 \\ 0 & 0 & 1 \end{bmatrix} \begin{cases} d_{q,r} \\ 0 \\ d_{p,q} \end{cases} \right].$$

The homogeneous transformation \mathbf{H}_B^A is calculated in a similar fashion. As before,

$$\mathbf{H}_B^A = \begin{bmatrix} \mathbf{R}_B^A & \mathbf{d}_{A,B}^A \\ \mathbf{0}^T & 1 \end{bmatrix}.$$

The basis vectors of frames A and B may be related such that

$$\begin{aligned} \mathbf{x}_B &= \cos \theta \mathbf{x}_A + \sin \theta \mathbf{y}_A, \\ \mathbf{y}_B &= -\sin \theta \mathbf{x}_A + \cos \theta \mathbf{y}_A, \\ \mathbf{z}_B &= \mathbf{z}_A. \end{aligned}$$

From these expressions it is seen that the rotation matrix that relates the A and B frames is a single axis rotation about the common $\mathbf{z}_A = \mathbf{z}_B$ axis, such that

$$\mathbf{R}_A^B = \begin{bmatrix} \cos \theta & \sin \theta & 0 \\ -\sin \theta & \cos \theta & 0 \\ 0 & 0 & 1 \end{bmatrix}.$$

The vector that connects the origin of the A frame to the origin of the B frame is

$$\mathbf{d}_{A,B} = d_{o,p} \mathbf{z}_A.$$

When this rotation matrix and vector offset are substituted into the homogeneous transformation, \mathbf{H}_B^A is determined to be

$$\mathbf{H}_B^A = \left[\begin{bmatrix} \cos \theta & -\sin \theta & 0 \\ \sin \theta & \cos \theta & 0 \\ 0 & 0 & 1 \end{bmatrix} \begin{Bmatrix} 0 \\ 0 \\ d_{o,p} \end{Bmatrix} \right].$$

These two homogeneous transformations can be combined to yield The individual transformations satisfy

$$\mathbf{p}^B = \mathbf{H}_C^B \mathbf{p}^C \quad \text{and} \quad \mathbf{p}^A = \mathbf{H}_B^A \mathbf{p}^B.$$

It follows that

$$\begin{aligned} \mathbf{p}^A &= \mathbf{H}_B^A \mathbf{H}_C^B \mathbf{p}^C, \\ &= \left[\begin{bmatrix} \cos \theta & -\sin \theta & 0 \\ \sin \theta & \cos \theta & 0 \\ 0 & 0 & 1 \end{bmatrix} \begin{Bmatrix} 0 \\ 0 \\ d_{o,p} \end{Bmatrix} \right] \left[\begin{bmatrix} 1 & 0 & 0 \\ 0 & 1 & 0 \\ 0 & 0 & 1 \end{bmatrix} \begin{Bmatrix} d_{q,r} \\ 0 \\ d_{p,q} \end{Bmatrix} \right] \mathbf{p}^C. \end{aligned}$$

The measurement made by the sensor returns a range $r(t)$ along the line of sight of the laser at time t ,

$$\mathbf{r}_{D,p} = r(t) \mathbf{x}_R.$$

The line of sight of the laser rotates relative to the frame \mathbb{C} that is fixed in the casing of the scanner unit. Based on the frame representations in Figure (3.2b), the basis vectors of frames \mathbb{C} and \mathbb{D} may be related and used to create a rotation matrix between the two frames, such that

$$\begin{aligned}\mathbf{x}_{\mathbb{D}} &= \sin\phi\mathbf{x}_{\mathbb{C}} - \cos\phi\mathbf{z}_{\mathbb{C}}, \\ \mathbf{y}_{\mathbb{D}} &= \cos\phi\mathbf{x}_{\mathbb{C}} + \sin\phi\mathbf{z}_{\mathbb{C}}, \quad \text{and} \\ \mathbf{z}_{\mathbb{D}} &= -\mathbf{y}_{\mathbb{C}},\end{aligned}\quad \mathbf{R}_{\mathbb{C}}^{\mathbb{D}} = \begin{bmatrix} \sin\phi & 0 & -\cos\phi \\ \cos\phi & 0 & \sin\phi \\ 0 & -1 & 0 \end{bmatrix},$$

The range measurement in the line of sight frame can be related to the ground frame by the expression

$$\mathbf{p}^{\mathbb{A}} = \mathbf{H}_{\mathbb{B}}^{\mathbb{A}} \mathbf{H}_{\mathbb{C}}^{\mathbb{B}} \mathbf{H}_{\mathbb{D}}^{\mathbb{C}} \begin{Bmatrix} r(t) \\ 0 \\ 0 \\ 1 \end{Bmatrix} \quad \text{and} \quad \mathbf{H}_{\mathbb{D}}^{\mathbb{C}} = \left[\begin{bmatrix} \sin\phi & \cos\phi & 0 \\ 0 & 0 & -1 \\ -\cos\phi & \sin\phi & 0 \end{bmatrix} \begin{Bmatrix} 0 \\ 0 \\ 0 \end{Bmatrix} \right] \begin{Bmatrix} 1 \end{Bmatrix}.$$

In summary, the kinematic relation that gives the coordinates of the image point relative to the \mathbb{A} frame, in terms of the range reading $r := r(t)$ and the rotation angles θ and ϕ , is the matrix product

$$\begin{aligned}\mathbf{p}^{\mathbb{A}} &= \left[\begin{bmatrix} \cos\theta & -\sin\theta & 0 \\ \sin\theta & \cos\theta & 0 \\ 0 & 0 & 1 \end{bmatrix} \begin{Bmatrix} 0 \\ 0 \\ d_{o,p} \end{Bmatrix} \right] \left[\begin{bmatrix} 1 & 0 & 0 \\ 0 & 1 & 0 \\ 0 & 0 & 1 \end{bmatrix} \begin{Bmatrix} d_{q,r} \\ 0 \\ d_{p,q} \end{Bmatrix} \right] \left[\begin{bmatrix} \sin\phi & \cos\phi & 0 \\ 0 & 0 & -1 \\ -\cos\phi & \sin\phi & 0 \end{bmatrix} \begin{Bmatrix} 0 \\ 0 \\ 0 \end{Bmatrix} \right] \begin{Bmatrix} r \\ 0 \\ 0 \end{Bmatrix}, \\ &= \begin{bmatrix} \cos\theta\sin\phi & \cos\phi\cos\theta & \sin\theta & d_{q,r}\cos\theta \\ \sin\phi\sin\theta & \cos\phi\sin\theta & -\cos\theta & d_{q,r}\sin\theta \\ -\cos\phi & \sin\phi & 0 & d_{o,p} + d_{p,q} \\ 0 & 0 & 0 & 1 \end{bmatrix} \begin{Bmatrix} r \\ 0 \\ 0 \\ 1 \end{Bmatrix}.\end{aligned}$$

Example ?? of the MATLAB Workbook for DCRS solves this problem using symbolic computation.

3.2 Ideal Joints

Before introducing some specific conventions and algorithms for studying the kinematics of robotic systems, a few preliminaries are required that go beyond the fundamental theorems of kinematics introduced in Chapter (2). The specialized principles of kinematics and dynamics employed for robotic systems fall within the broader study of *multibody dynamics*. Multibody dynamics is the study of the dynamics of mechanical systems that are comprised of several interconnected bodies. The most

common assumption in classical multibody dynamics is that the bodies are *rigid*, but generalizations that consider flexible bodies have also been developed. An account of the fundamentals of multibody dynamics can be found in [45]. In this book, the bodies under consideration are assumed to be rigid.

Just as models for the individual bodies can vary in their complexity, so too can the nature of the mathematical constraints that relate their motion. Later in Chapter (5), a common, general form for constraints on permissible motions will be defined. This chapter will focus on specific constraints induced by *ideal joints* (e.g., Figure (1.6) from Chapter (1)) that connect two rigid bodies.

Suppose there are two rigid bodies denoted \mathbb{A} and \mathbb{B} undergoing independent motions. From prior study of rigid motions, it is known that for the most general motions of the rigid bodies \mathbb{A} and \mathbb{B} , three translation variables and three angles are required to define the location and orientation of each body. 12 variables in total are required to describe the kinematics of the two independent bodies. However, when considering robotic systems, bodies will be interconnected. When the two bodies are interconnected, the number of variables required to describe the location and orientation of both bodies is reduced in number. For example, suppose the bodies are “welded” together. If the position and orientation of one of the bodies is prescribed as a function of time, the location and orientation of the other body is also known as a function of time. In this case, only six variables that depend on time are required to describe the constrained motion of the system that consists of two rigid bodies.

It is possible to expand on this idea and study more complicated notions of the ways the two bodies can interact with one another. The discussion of constraints between bodies will describe how different frames \mathbb{A} and \mathbb{B} that are fixed in each rigid body can move relative to each other. The frames \mathbb{A} and \mathbb{B} will be referred to as *joint coordinate systems* or *joint frames* since they will be used to define precisely the manner in which the two bodies can interact. The *joint coordinate systems* are used to relate how the joint frames \mathbb{A} and \mathbb{B} may rotate relative to one another, or how the origins of the the two frames can translate relative to one another. A schematic figure of the two bodies with their joint coordinate systems *before* enforcing any constraints is given in Figure (3.4).

3.2.1 The Prismatic Joint

A *prismatic joint* is an *ideal joint* that only allows relative translation along a single direction that is fixed in each of the joint frames \mathbb{A} and \mathbb{B} . A schematic of a typical prismatic joint is shown in Figure (3.5a) and (3.5b), with the direction of translation along the z-axis of the two coordinate frames \mathbb{A} and \mathbb{B} . This joint does not allow change in the relative orientation of the two bodies. The direction of relative translation is fixed and constant relative to each of the bodies \mathbb{A} and \mathbb{B} . Since no change in the relative orientation is permitted between the two bodies, the rotation matrix $\mathbf{R}_{\mathbb{A}}^{\mathbb{B}}$ relating the joint coordinate systems is constant.

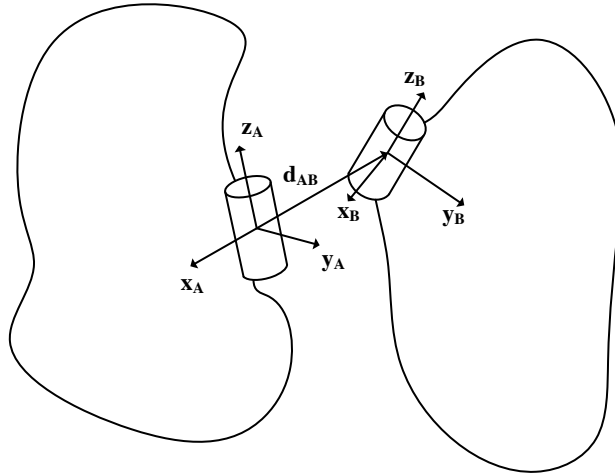
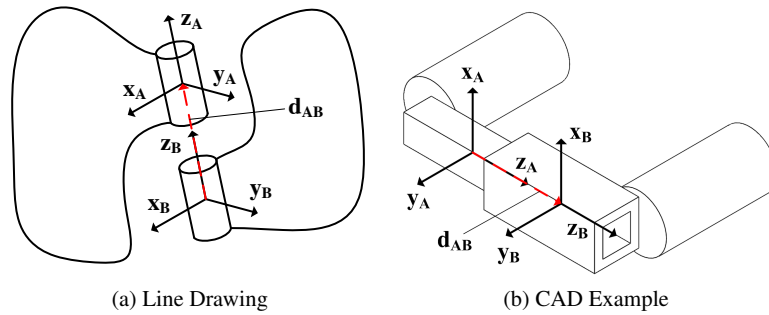
Fig. 3.4: Two Rigid Bodies with Joint Coordinate Systems *Prior* to Constraint

Fig. 3.5: Ideal Prismatic Joint

This constraint is equivalent to requiring that the three relative rotation angles that parameterize the relative rotation matrix are held constant. Frequently, the two *joint coordinate systems* are chosen such that they are aligned, making \mathbf{R}_A^B the identity matrix.

Suppose that \mathbf{z}_A is the direction of relative translation permitted by body A and that \mathbf{z}_B is the direction of relative translation permitted by body B. The relative offset vector relating the origins of the joint frames must satisfy

$$\mathbf{d}_{A,B}(t) = d_{A,B}(t)\mathbf{z}_A = d_{A,B}(t)\mathbf{z}_B. \quad (3.2.1)$$

The definitions above imply that the *homogeneous transform* \mathbf{H}_A^B relating the *joint coordinate systems* A and B is given by

$$\mathbf{H}_A^B(t) = \begin{bmatrix} \begin{bmatrix} 1 & 0 & 0 \\ 0 & 1 & 0 \\ 0 & 0 & 1 \end{bmatrix} & \begin{pmatrix} 0 \\ 0 \\ d_{A,B}(t) \end{pmatrix} \\ \begin{pmatrix} 0 & 0 & 0 \end{pmatrix} & 1 \end{bmatrix}, \quad (3.2.2)$$

for all time $t \in \mathbb{R}^+$. Analogous expressions can be derived if the 1 or 2 axes are used to define the degree of freedom. The task of deriving the homogeneous transforms in these cases as an exercise.

Altogether, there are five independent scalar conditions implied by Equation (3.2.2) and the requirement that \mathbf{R}_A^B is a constant matrix. Three constraints arise from the requirement that the frames do not rotate relative to one another, and two more constraints enforce the condition that no translation perpendicular to the $\mathbf{z}_A = \mathbf{z}_B$ axis occurs. Since there are five constraints imposed on the motion of the two bodies, the *prismatic joint* is a single degree of freedom *ideal joint*. The *homogeneous transformation* that characterizes the relationship between the two *joint coordinate systems* can be written in terms of a single time varying parameter, $d_{A,B}(t)$. The relative translation, or displacement, $d_{A,B}(t)$ is the *joint variable* for the *prismatic joint*.

3.2.2 The Revolute Joint

In the last section, the *prismatic joint* was seen to constrain the motion of two bodies so that only translation along a single direction is possible. The *revolute joint* is an analogous single degree of freedom *ideal joint* that constrains the motion of two bodies so that only *rotation* about a single axis is possible. A schematic of a typical revolute joint is given in Figures (3.6a) and (3.6b) with the axis of rotation fixed along the z-axis of frame A and B.

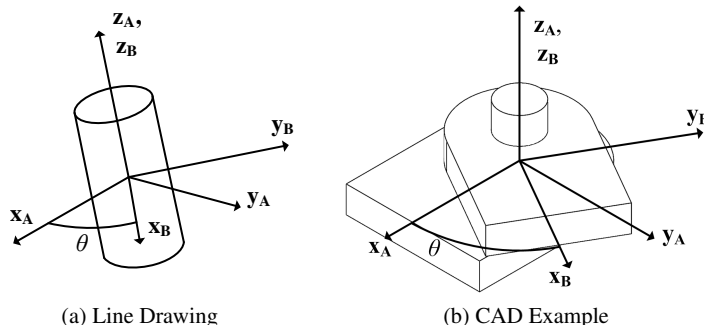


Fig. 3.6: Ideal Revolute Joint

The mathematical relationships that describe this physical constraint can, again, be expressed in terms of the joint coordinate frames \mathbb{A} and \mathbb{B} . The revolute joint restricts the translational motion of the two bodies by requiring that the origin of the joint frames \mathbb{A} and \mathbb{B} differ by a constant vector, which is often selected to be zero. In the case that the origins coincide for all time, $\mathbf{d}_{\mathbb{A},\mathbb{B}}(t) = 0$.

$$\mathbf{d}_{\mathbb{A},\mathbb{B}}(t) = 0. \quad (3.2.3)$$

The bodies are able to rotate relative to one another about a single, common joint axis. Suppose that the common axis of rotation is $\mathbf{z}_{\mathbb{A}} = \mathbf{z}_{\mathbb{B}}$. The rotation matrix $\mathbf{R}_{\mathbb{A}}^{\mathbb{B}}$ that maps the joint frame \mathbb{A} into the joint frame \mathbb{B} must have the form

$$\mathbf{R}_{\mathbb{A}}^{\mathbb{B}}(t) = \begin{bmatrix} \cos \theta(t) & \sin \theta(t) & 0 \\ -\sin \theta(t) & \cos \theta(t) & 0 \\ 0 & 0 & 1 \end{bmatrix}, \quad (3.2.4)$$

for all times $t \in \mathbb{R}^+$. Again, similar expressions can be derived if the axis of rotation is selected to be the 1 or 2 axes. These derivations are left as an exercise.

Equation (3.2.4) and the fact that $\mathbf{d}_{\mathbb{A},\mathbb{B}}(t) = 0$ imply that the *homogeneous transform* that relates the *joint coordinate systems* is given by

$$\mathbf{H}_{\mathbb{A}}^{\mathbb{B}}(t) = \begin{bmatrix} \left[\begin{array}{ccc} \cos \theta(t) & \sin \theta(t) & 0 \\ -\sin \theta(t) & \cos \theta(t) & 0 \\ 0 & 0 & 1 \end{array} \right] & \left\{ \begin{array}{c} 0 \\ 0 \\ 0 \end{array} \right\} \\ \left\{ \begin{array}{c} 0 \\ 0 \\ 0 \end{array} \right\} & 1 \end{bmatrix}.$$

Equation (3.2.4) and the condition $\mathbf{d}_{\mathbb{A},\mathbb{B}}(t) = 0$ induce a total of five scalar constraints on the motion of bodies \mathbb{A} and \mathbb{B} . Three of the scalar constraints result from the condition $\mathbf{d}_{\mathbb{A},\mathbb{B}}(t) = 0$, which prevents relative translation. The rotational restraint in Equation (3.2.4) imposes two additional scalar relationships. The *revolute joint* is a one degree of freedom *ideal joint*. The angle $\theta(t)$ is the *joint variable* for the single degree of freedom *revolute joint*.

3.2.3 Other Ideal Joints

In this book, the robotic systems that are considered are constructed from collections of rigid bodies, or links, that are connected by either *prismatic joints* or *revolute joints*. It is possible to construct other *ideal joints* using these two joint primitives by introducing one or more “zero length links” that are connected by revolute and/or prismatic joints. Any *ideal joint* having between 1 and 6 degrees of freedom can be derived in this way. Alternatively, it is also possible to derive directly the form of the homogeneous transformation that represents an ideal joint. The next example carries this out for the *universal joint*.

Example 3.2.1. A universal joint is a common ideal mechanical joint and is depicted in Figure (3.7). Let frames \mathbb{A} and \mathbb{B} be fixed in the links that are connected by the universal joint in Figure (3.7). The frames are defined such that a rotation about the axis \mathbf{a}_3 induces a rotation about the \mathbf{b}_3 axis.

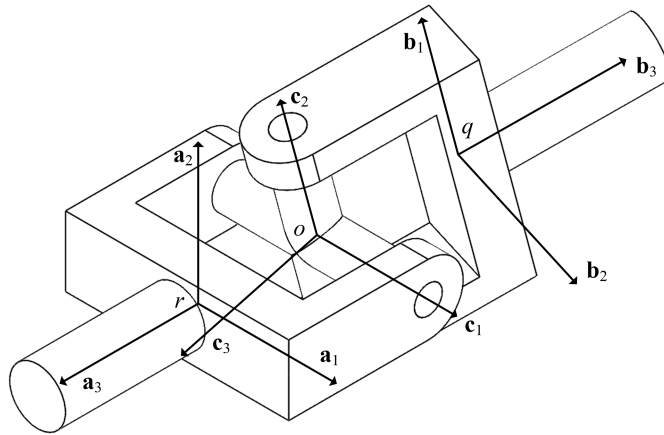


Fig. 3.7: Universal Joint Frames

What are the constraints imposed on the motion of links \mathbb{A} and \mathbb{B} by the universal joint? Find the homogeneous transformation that represents the rigid body motion between frames \mathbb{A} and \mathbb{B} .

Solution: The universal joint restricts the motion so that the position of the point o on body \mathbb{A} coincides with the position of point o on body \mathbb{B} for all time. In other words, it must be true that

$$\mathbf{r}_{0,r} - d_{r,o}\mathbf{a}_3 = \mathbf{r}_{0,q} - d_{q,o}\mathbf{b}_3$$

for any motion of the bodies that is consistent with the constraints imposed by the universal joint. The three entries of this vector equation impose 3 scalar constraints on the motion of the bodies.

Angles $\theta_{\mathbb{A}}$ and $\theta_{\mathbb{B}}$ may be chosen such that the rotation matrices that relate the \mathbb{A} , \mathbb{B} , and \mathbb{C} frames are

$$\mathbf{R}_{\mathbb{A}}^{\mathbb{C}} = \begin{bmatrix} \cos \theta_{\mathbb{A}} & 0 & -\sin \theta_{\mathbb{A}} \\ 0 & 1 & 0 \\ \sin \theta_{\mathbb{A}} & 0 & \cos \theta_{\mathbb{A}} \end{bmatrix} \quad \text{and} \quad \mathbf{R}_{\mathbb{B}}^{\mathbb{C}} = \begin{bmatrix} 0 & 1 & 0 \\ \sin \theta_{\mathbb{B}} & 0 & \cos \theta_{\mathbb{B}} \\ \cos \theta_{\mathbb{B}} & 0 & -\sin \theta_{\mathbb{B}} \end{bmatrix},$$

and the angular velocities of frame \mathbb{C} with respect to frames \mathbb{A} and \mathbb{B} satisfy

$$\boldsymbol{\omega}_{\mathbb{A},\mathbb{C}} = \dot{\theta}_{\mathbb{A}} \mathbf{c}_2 \quad \text{and} \quad \boldsymbol{\omega}_{\mathbb{B},\mathbb{C}} = \dot{\theta}_{\mathbb{B}} \mathbf{c}_1.$$

Combining these two equations into a single condition with respect to \mathbf{c}_3 results in

$$(\boldsymbol{\omega}_{A,C} - \boldsymbol{\omega}_{B,C}) \cdot \mathbf{c}_3 = 0.$$

This equation is a fourth scalar constraint on the motion of the system, and the number of degrees of freedom of the joint is $6 - 4 = 2$.

The homogeneous transform that represents the rigid body motion between frames A and B can be expressed in terms of the two angles θ_A and θ_B . The homogeneous transformation \mathbf{H}_A^B that relates the homogeneous coordinates \mathbf{p}^A and \mathbf{p}^B of some arbitrary point p is, by definition,

$$\mathbf{p}^A = \underbrace{\begin{bmatrix} \mathbf{R}_B^A & \mathbf{d}_{A,B}^A \\ \mathbf{0}^T & 1 \end{bmatrix}}_{\mathbf{H}_A^B} \mathbf{p}^B.$$

From the definitions of \mathbf{R}_A^C and \mathbf{R}_B^C above,

$$\begin{aligned} \mathbf{R}_A^B &= \underbrace{\begin{bmatrix} 0 & \sin \theta_B & \cos \theta_B \\ 1 & 0 & 0 \\ 0 & \cos \theta_B & -\sin \theta_B \end{bmatrix}}_{\mathbf{R}_C^B} \underbrace{\begin{bmatrix} \cos \theta_A & 0 & -\sin \theta_A \\ 0 & 1 & 0 \\ \sin \theta_A & 0 & \cos \theta_A \end{bmatrix}}_{\mathbf{R}_A^C}, \\ &= \begin{bmatrix} \cos \theta_B \sin \theta_A & \sin \theta_B & \cos \theta_B \cos \theta_A \\ \cos \theta_A & 0 & -\sin \theta_A \\ -\sin \theta_A \sin \theta_B & \cos \theta_B & -\cos \theta_A \sin \theta_B \end{bmatrix}. \end{aligned}$$

From inspection of Figure (3.7),

$$\mathbf{d}_{A,B} = -d_{r,o} \mathbf{a}_3 + d_{q,o} \mathbf{b}_3.$$

Defining this with respect to the A basis results in

$$\mathbf{d}_{A,B}^A = \begin{Bmatrix} 0 \\ 0 \\ -d_{r,o} \end{Bmatrix} + d_{q,o} \begin{Bmatrix} -\sin \theta_A \sin \theta_B \\ \cos \theta_B \\ -\cos \theta_A \sin \theta_B \end{Bmatrix} = \begin{Bmatrix} -d_{q,o} \sin \theta_A \sin \theta_B \\ d_{q,o} \cos \theta_B \\ -(d_{r,o} + d_{q,o} \cos \theta_A \sin \theta_B) \end{Bmatrix}.$$

As a result, the homogeneous transformation that relates motion of the A and B frames is given by

$$\begin{aligned} \mathbf{H}_B^A &= \begin{bmatrix} \mathbf{R}_B^A & \mathbf{d}_{A,B}^A \\ \mathbf{0}^T & 1 \end{bmatrix}, \\ &= \begin{bmatrix} \cos \theta_B \sin \theta_A & \cos \theta_A & -\sin \theta_A \sin \theta_B \\ \sin \theta_B & 0 & \cos \theta_B \\ \cos \theta_B \cos \theta_A & -\sin \theta_A & -\cos \theta_A \sin \theta_B \end{bmatrix} \begin{Bmatrix} -d_{q,o} \sin \theta_A \sin \theta_B \\ d_{q,o} \cos \theta_B \\ -(d_{r,o} + d_{q,o} \cos \theta_A \sin \theta_B) \end{Bmatrix} \begin{Bmatrix} 1 \end{Bmatrix}. \end{aligned}$$

It is evident $\mathbf{H}_B^A := \mathbf{H}_B^A(\theta_A, \theta_B)$; that is, the homogeneous transformation \mathbf{H}_B^A that relates the joint frames is a function of two time-varying parameters, θ_A and θ_B . As a result, as noted earlier, the universal joint is a two degree of freedom ideal joint. Example ?? in the MATLAB Workbook solves this problem using MATLAB.

3.3 The Denavit-Hartenberg (DH) Convention

Section (3.1) introduced homogeneous transformations and showed that they can be used to represent rigid body motion. Each homogeneous transformation is specified in terms of a rotation matrix describing the orientation and a vector describing the translation of a rigid body motion. No particular framework was introduced for the selection of the frames of reference that are implicit in the definition of a homogeneous transform. It is always possible to choose the orientation and origin of the frames to fit the problem at hand.

This section describes the *Denavit-Hartenberg (DH) Convention*, one of the most popular conventions for the construction of homogeneous transformations associated with robotic systems. This convention is used to model robots that have the structure of *kinematic chains*. A wide variety of robotic systems are included in this class, including the SCARA robot (Problem (3.1)), cylindrical robots (Problem (3.2)), and modular robots (Problem (3.3)).

Even if the robotic system under consideration does not have the form of a kinematic chain, it is often possible to analyze subsystems of the robotic system using the *Denavit-Hartenberg Convention*. If the system has the connectivity of a *topological tree*, the *Denavit-Hartenberg Convention* can be used without modification to model the kinematics of any of the branches of the tree relative to the core body. The anthropomorphic robot in Figure (2.3) is an example of a robotic system that has the connectivity of a topological tree.

3.3.1 Kinematic Chains, Numbering in the DH Convention

The description of the connectivity of general robotic systems can be complex. Connectivity of robotic systems is often categorized into three classes of systems: those that (1) form kinematic chains, (2) form topological trees, and (3) contain closed loops. It is possible to define connectivity in abstract form via the introduction of the connectivity graph of the system. The interested reader is referred to [46] for a detailed account. In this book, the following definition will suffice.

Definition 3.1 (Kinematic Chains). A mechanical system comprised of $N + 1$ rigid bodies that are interconnected by N ideal joints is a *kinematic chain* provided

- 1) Exactly two of the bodies are connected to only one other body. These are the first and last bodies in the kinematic chain. All of the remaining bodies are connected to two different rigid bodies.
- 2) It is possible to traverse the mechanical system from the first to the last body visiting every body in the system exactly one time.

In the *DH convention* we number the rigid bodies, or links, in the kinematic chain starting with 0 for the first body and ending with N for the last body. We number the ideal joints starting with 1 and ending with N .

In practice, there shouldn't be a problem identifying a *kinematic chain*. However, there are a few other conventions that are followed for describing the kinematics of a chain. In the Denavit-Hartenberg Convention, each body i has a body fixed frame designated simply by i for $i = 0, \dots, N$. Frame 0 is denoted the *root frame*, *core frame* or the *base frame* of the kinematic chain. Often the *root frame* is identified with the ground or inertial frame, as is the case of a robotic manipulator that is located along an assembly line. However, there are some common exceptions to this rule. In the case of a system having connectivity of a topological tree, the frame 0 is often identified with the central body. The anthropomorphic robot is an example of this case. Frame 0 may also not be fixed in an inertial frame. For example, when constructing a model of the space shuttle remote manipulator system (RMS), the shuttle is usually selected as the base frame. For the RMS, the shuttle would be denoted the *root frame*.

Another convention followed in this book is based on the assumption that each joint in the *kinematic chain* shown in Figure (3.8) is either a *revolute joint* or a *prismatic joint*. The generic symbol $q_i(t)$ for $i = 1, \dots, N$ is used to denote the *joint variable*. In other words,

$$q_i(t) = \begin{cases} \theta_i(t) & \text{if joint } i \text{ is a prismatic joint,} \\ d_i(t) & \text{if joint } i \text{ is a revolute joint.} \end{cases}$$

By definition, joint variable $q_i(t)$ describes how frame i is articulated, or actuated, for $i = 1, \dots, N$. For example, if joint i is a revolute joint, the joint variable $q_i(t) = \theta_i(t)$ defines how frame i rotates relative to frame $i - 1$. Joint variable $q_i(t)$ is said to actuate frame i or link i .

Finally, the vectors \mathbf{z}_{i-1} are defined in the basis for frame $i - 1$ as the direction associated with the degree of freedom associated with joint i , for $i = 1, \dots, N$. For example, \mathbf{z}_0 is the direction of the degree of freedom q_1 in joint 1, \mathbf{z}_1 is the direction of the degree of freedom q_2 in joint \mathbf{z}_2 , etc. The numbering of joints, links or bodies, frames and axes of the degrees of freedom for a kinematic chain is depicted in Figure (3.8).

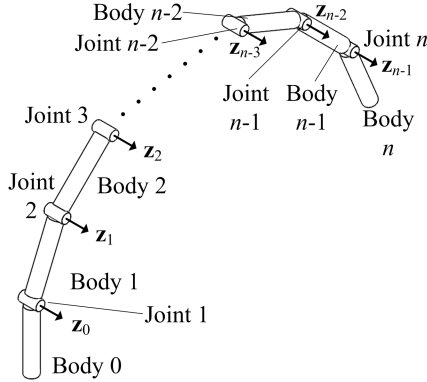


Fig. 3.8: Body and Joint Numbering of a Kinematic Chain for DH Convention

3.3.2 Definition of Frames in the DH Convention

The definition of a *homogeneous transformation* associated with some arbitrary rigid body motion generally requires six parameters. If the frame under consideration is located with an arbitrary origin position with an arbitrary orientation with respect to a base frame, it will require in general three independent translational variables and three independent rotational angles to map the frame onto the base frame, or vice versa. The *DH Convention* defines a specific set of criteria followed when selecting the frames that are used to describe a *kinematic chain*. Between a given pair of bodies, two successive frames in the chain are oriented as depicted in Figure (3.9). With these restrictions on the choice of the relative origin positions and relative orientations of the successive frames, the DH Convention uses four parameters to characterize the *homogeneous transform* between pairs of frames.

Definition 3.2 (Denavit-Hartenberg (DH) Convention). A set of $N + 1$ frames that describe a kinematic chain satisfy the assumptions of the *DH Convention* provided that the basis vector \mathbf{x}_i of frame i intersects and is perpendicular to the basis vector \mathbf{z}_{i-1} for all $i = 1 \dots N$. For such kinematic chains, for the i^{th} link, the *rotation* θ_i , the *twist* α_i , the *displacement* d_i , and the *offset* a_i of the i^{th} link are defined in Figure (3.9). These parameters are described below:

- 1) The *link rotation* θ_i is the angle from the positive \mathbf{x}_{i-1} axis to the positive \mathbf{x}_i axis about the \mathbf{z}_{i-1} axis.
- 2) The *link twist* α_i is the angle from the positive \mathbf{z}_{i-1} axis to the positive \mathbf{z}_i axis about the \mathbf{x}_i axis.
- 3) The *link displacement* d_i is the perpendicular distance from \mathbf{x}_{i-1} to the \mathbf{x}_i axis.
- 4) The *link offset* a_i is the perpendicular distance from \mathbf{z}_{i-1} to the \mathbf{z}_i axis.

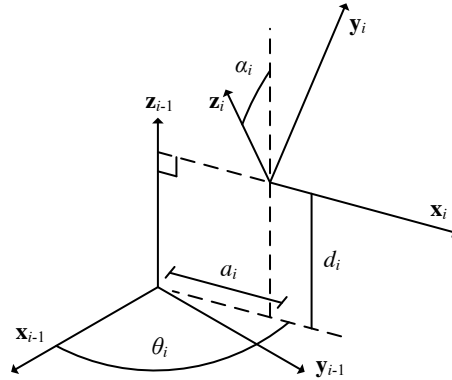


Fig. 3.9: Geometry of the Denavit-Hartenberg Convention

The *DH Convention* relates each pair of body fixed frames $i - 1$ and i in the kinematic chain using a homogeneous transform with a specific structure. The frames in the kinematic chain are selected so that they take the configuration shown in Figure (3.9). The basis vector \mathbf{x}_i is chosen so that it intersects and is perpendicular to the basis vector \mathbf{z}_{i-1} . This is the fundamental assumption underlying the *Denavit-Hartenberg Convention*.

3.3.3 Homogeneous Transforms in the Denavit-Hartenberg Convention

If the frames $i = 0, \dots, N$ satisfy the *DH Convention* in Definition (3.2), it is possible to derive the corresponding transformation that maps homogeneous coordinates in frame i onto the homogeneous coordinates in frame $i - 1$. Consider Figure (3.11) in which the position vectors $\mathbf{r}_{i,p}$ and $\mathbf{r}_{i-1,p}$ are shown, along with the relative offset $\mathbf{d}_{i-1,i}$ between the origin of frames $i - 1$ and i . The homogeneous transformation that relates these two frames follows from the general definitions discussed in Section (3.1). The homogenous transformation \mathbf{H}_i^{i-1} is defined such that

$$\mathbf{H}_i^{i-1} = \begin{bmatrix} \mathbf{R}_i^{i-1} & \mathbf{d}_{i-1,i}^{i-1} \\ \mathbf{0}^T & 1 \end{bmatrix}. \quad (3.3.1)$$

The following theorem gives a succinct expression for the homogeneous transform \mathbf{H}_i^{i-1} between two consecutive frames in a kinematic chain that are constructed according to the *DH Convention*.

Theorem 3.2 (DH-Convention Homogeneous Transformation). Suppose that frames $i - 1$ and i are two consecutive frames in a kinematic chain that satisfies the assumptions of the DH Convention. The homogeneous transformation that relates the homogeneous coordinates in the frames $i - 1$ and i is given by

$$\mathbf{H}_i^{i-1} = \begin{bmatrix} \mathbf{R}_i^{i-1} & \mathbf{d}_{i-1,i}^{i-1} \\ 0 & 1 \end{bmatrix},$$

with the rotation matrix \mathbf{R}_i^{i-1} defined as

$$\mathbf{R}_i^{i-1} = \begin{bmatrix} \cos \theta_i - \sin \theta_i \cos \alpha_i & \sin \theta_i \sin \alpha_i \\ \sin \theta_i & \cos \theta_i \cos \alpha_i & -\cos \theta_i \sin \alpha_i \\ \mathbf{0}^T & \sin \alpha_i & \cos \alpha_i \end{bmatrix},$$

and the relative offset $\mathbf{d}_{i-1,i}^{i-1}$ given by

$$\mathbf{d}_{i-1,i}^{i-1} = \begin{pmatrix} a_i \cos \theta_i \\ a_i \sin \theta_i \\ d_i \end{pmatrix}.$$

The parameters $\theta_i, \alpha_i, d_i, a_i$ are the rotation, twist, displacement and offset of link i , respectively.

Proof. The conclusions of Theorem (3.2) are drawn using the principles of kinematics derived in Chapter (2). Introduce the auxiliary \mathbb{A} frame depicted in Figure (3.10). The matrices that relate the $i - 1, \mathbb{A}$ and i frames are the single axis rotation matrices

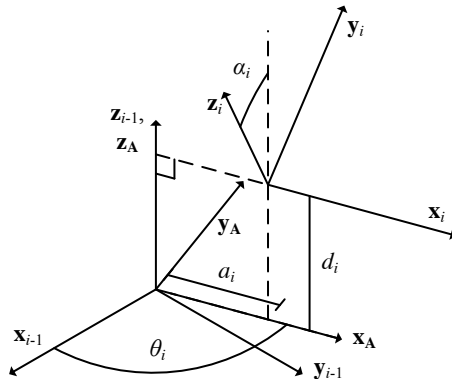


Fig. 3.10: Intermediate Frame \mathbb{A} in the Denavit-Hartenberg Convention

$$\mathbf{R}_{i-1}^{\mathbb{A}} = \begin{bmatrix} \cos \theta_i & \sin \theta_i & 0 \\ -\sin \theta_i \cos \theta_i & 0 & 1 \\ 0 & 0 & 1 \end{bmatrix} \quad \text{and} \quad \mathbf{R}_A^i = \begin{bmatrix} 1 & 0 & 0 \\ 0 & \cos \alpha_i & \sin \alpha_i \\ 0 & -\sin \alpha_i & \cos \alpha_i \end{bmatrix}.$$

The rotation matrix from the $i-1$ to the i frame is constructed from the cascade of single axis rotations, such that

$$\begin{aligned} \mathbf{R}_{i-1}^i &= \mathbf{R}_A^i \mathbf{R}_{i-1}^{\mathbb{A}} = \begin{bmatrix} 1 & 0 & 0 \\ 0 & \cos \alpha_i & \sin \alpha_i \\ 0 & -\sin \alpha_i & \cos \alpha_i \end{bmatrix} \begin{bmatrix} \cos \theta_i & \sin \theta_i & 0 \\ -\sin \theta_i \cos \theta_i & 0 & 1 \\ 0 & 0 & 1 \end{bmatrix}, \\ &= \begin{bmatrix} \cos \theta_i & \sin \theta_i & 0 \\ -\cos \alpha_i \sin \theta_i & \cos \alpha_i \cos \theta_i & \sin \alpha_i \\ \sin \alpha_i \sin \theta_i & -\sin \alpha_i \cos \theta_i & \cos \alpha_i \end{bmatrix}. \end{aligned}$$

The vector from the origin of the $i-1$ frame to the i frame is

$$\mathbf{d}_{i-1,i} = a_i \mathbf{x}_i + d_i \mathbf{z}_{i-1}.$$

This vector can be written in terms components relative to the basis for the $i-1$ frame as

$$\mathbf{d}_{i-1,i}^{i-1} = a_i \begin{Bmatrix} \cos \theta_i \\ \sin \theta_i \\ 0 \end{Bmatrix} + d_i \begin{Bmatrix} 0 \\ 0 \\ 1 \end{Bmatrix} = \begin{Bmatrix} a_i \cos \theta_i \\ a_i \sin \theta_i \\ d_i \end{Bmatrix}.$$

The homogeneous coordinates \mathbf{p}^i and \mathbf{p}^{i-1} of an arbitrary point p are consequently related via the identity

$$\underbrace{\begin{Bmatrix} \mathbf{r}_{0,i-1}^{i-1} \\ 1 \end{Bmatrix}}_{\mathbf{p}^{i-1}} = \underbrace{\begin{bmatrix} \mathbf{R}_i^{i-1} & \mathbf{d}_{i-1,i}^{i-1} \\ \mathbf{0}^T & 1 \end{bmatrix}}_{\mathbf{H}_i^{i-1}} \underbrace{\begin{Bmatrix} \mathbf{r}_{0,i}^i \\ 1 \end{Bmatrix}}_{\mathbf{p}^i}.$$

□

Example ?? in the MATLAB Workbook for DCRS creates a function that calculates homogeneous transformations that map between adjacent frames in a kinematic chain using the DH convention.

3.3.4 The DH Procedure

The DH Convention can form the foundation for a systematic procedure for determining the model of a kinematic chain. Suppose a kinematic chain is under consideration in which the bodies are numbered from 0 to N , and the joints are numbered from 1 to N as described in Definition (3.1). The first step in the procedure assigns the unit vectors \mathbf{z}_0 through \mathbf{z}_{N-1} to the axes of the degrees of freedom for each of the joints. If the i^{th} joint is a revolute joint, \mathbf{z}_{i-1} is assigned to the axis of rotation

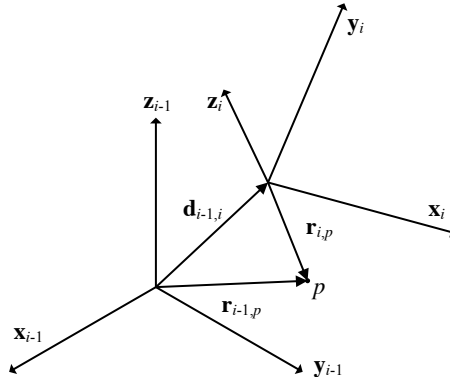


Fig. 3.11: Construction of the Homogeneous Transform in the DH Convention

of the joint. If the i^{th} joint is a prismatic joint, \mathbf{z}_{i-1} is assigned to the direction of translation in the joint.

After axes \mathbf{z}_0 through \mathbf{z}_{N-1} have been assigned to the directions of the degrees of freedom, the origins of the frames are selected. The origin of frame 0 can be chosen to be any convenient point along the \mathbf{z}_0 axis. The origin of each of the remaining frames for $i = 1 \dots N$ must be selected so that successive pairs of frames are configured as illustrated in Figure (3.9).

The remaining origins are selected recursively, starting from \mathbf{z}_1 using the previously defined \mathbf{z}_0 , then \mathbf{z}_2 using \mathbf{z}_1 , and continuing through \mathbf{z}_{N-1} . The origin of the frame i must be selected so that the vector \mathbf{x}_i intersects and is perpendicular to \mathbf{z}_{i-1} . Carefully adhering to this procedure ensures that the kinematic model is consistent with the *DH Convention*. The selection of \mathbf{x}_i and the origin of the i frame depends on the relative orientation of the vectors \mathbf{z}_{i-1} and \mathbf{z}_i .

If \mathbf{z}_{i-1} and \mathbf{z}_i are not coplanar, there is a unique direction normal to both vectors. The origin of frame i must be chosen so that \mathbf{x}_i aligns with this unique normal. Frame i is then completed by defining $\mathbf{y}_i = \mathbf{z}_i \times \mathbf{x}_i$ to ensure the frame is dexterous.

If the vectors \mathbf{z}_{i-1} and \mathbf{z}_i are coplanar, there are two cases to consider, leading to two possibilities for the choice of the origin. The first case is when the coplanar vectors \mathbf{z}_{i-1} and \mathbf{z}_i are parallel. In this case there are an infinite number of vectors that intersect and are perpendicular to both \mathbf{z}_{i-1} and \mathbf{z}_i . In principle, it is possible to choose the origin of frame i in this case so that the \mathbf{x}_i axis aligns with any of the infinite number of common normals. The second case is when the coplanar vectors \mathbf{z}_{i-1} and \mathbf{z}_i intersect at a single point. In this case the vector \mathbf{x}_i is defined to be normal to the plane spanned by \mathbf{z}_{i-1} and \mathbf{z}_i , and the origin of frame i is chosen as point of intersection of \mathbf{z}_{i-1} and \mathbf{z}_i .

The procedure above is summarized in the table below.

The *DH Procedure*, as summarized above, is not a simple process, and the frames generated by the procedure can be counter intuitive. An experienced analyst might choose frames in a completely different manner. However, the advantage of the *DH*

Denavit-Hartenberg Procedure for Kinematic Chains

- 1) Number the links in the kinematic chain from $0, \dots, N$, and number the joints in the kinematic chain from $1, \dots, N$.
- 2) Assign the unit vectors $\mathbf{z}_0, \mathbf{z}_1, \dots, \mathbf{z}_{N-1}$ to the axes of the degrees of freedom for joints $1, \dots, N$.
- 3) Choose the origin of the 0 frame along the \mathbf{z}_0 axis.
- 4) Repeat the following for $i = 1, \dots, N - 1$:
 - 4.1) If the vectors \mathbf{z}_{i-1} and \mathbf{z}_i are not coplanar, select the origin of frame i so that \mathbf{x}_i is aligned with the common normal to \mathbf{z}_{i-1} and \mathbf{z}_i .
 - 4.3) If the vectors \mathbf{z}_{i-1} and \mathbf{z}_i are parallel, choose the origin i at any convenient location along the \mathbf{z}_i axis. Choose \mathbf{x}_i along one of the infinite number of common normals to \mathbf{z}_{i-1} and \mathbf{z}_i .
 - 4.4) If the vectors \mathbf{z}_{i-1} and \mathbf{z}_i intersect, choose the origin i at the point of intersection. Select \mathbf{x}_i to be perpendicular to the plane spanned by \mathbf{z}_{i-1} and \mathbf{z}_i .
 - 4.5) Choose the axis \mathbf{y}_i to satisfy the right hand rule given \mathbf{z}_i and \mathbf{x}_i selected above.
- 5) Choose the last frame so that \mathbf{x}_N intersects and is perpendicular to \mathbf{z}_{N-1} . Otherwise, choose the frame so that it is aligned with the problem at hand.

Procedure is that it facilitates communication: anyone familiar with the procedure can reconstruct how the unknowns have been selected from a simple table of *link parameters*. The following examples show how the procedure can be used in practical problems with a simple model that utilizes two body fixed frames.

Example 3.3.1. Derive a kinematic model for the 3D laser ranging sensor depicted in Figure (3.12) using the Denavit-Hartenberg convention.

Solution:

Figure (3.13) depicts the DH-compliant frames selected to model the three bodies and two joints. First, the two joint axes \mathbf{z}_0 and \mathbf{z}_1 were assigned to the axes of rotation of the two joints. The origin of frame 0 is chosen to lie within the horn of the servo motor used to rotate the first joint. Since \mathbf{z}_0 and \mathbf{z}_1 intersect, the origin of frame 1 is chosen to be the point of intersection.

The vector \mathbf{x}_0 is chosen as an arbitrary perpendicular vector to \mathbf{z}_0 starting from the frame 0 origin. The vector \mathbf{x}_1 is chosen to be normal to the plane spanned by vectors \mathbf{z}_0 and \mathbf{z}_1 and starting from the frame 1 origin. The vectors \mathbf{y}_0 and \mathbf{y}_1 both start at their respective frame origins and are defined by $\mathbf{z}_0 \times \mathbf{x}_0$ and $\mathbf{z}_1 \times \mathbf{x}_1$, respectively. The link rotation θ_1 is measured about the positive \mathbf{z}_0 axis from the \mathbf{x}_0 to the \mathbf{x}_1 axis. The link twist $\alpha_1 = \frac{\pi}{2}$ is measured about the positive \mathbf{x}_1 axis from \mathbf{z}_0 and \mathbf{z}_1 . The link displacement $d_1 = d_{o,p}$ is the distance from the \mathbf{x}_0 axis to the \mathbf{x}_1 axis measured along the \mathbf{z}_0 direction. The link offset $a_1 = 0$ because the \mathbf{z}_0 and \mathbf{z}_1 axis intersect. For frame 2, the \mathbf{z}_2 axis is chosen to align with \mathbf{z}_1 . Since \mathbf{z}_1 and \mathbf{z}_2 are parallel, the origin

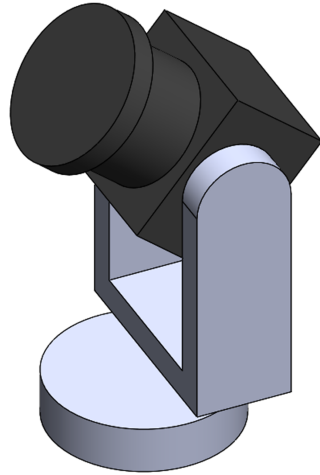


Fig. 3.12: A Laser Ranging Sensor Assembly

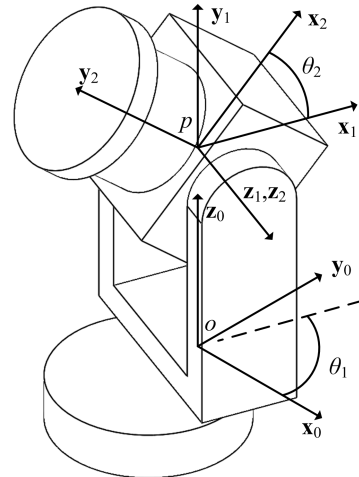


Fig. 3.13: Assignment of Frames to Scanner Assembly

of frame 2 may be arbitrarily chosen along \mathbf{z}_2 ; for convenience, the frame 2 origin is chosen to coincide with the frame 1 origin. The axis \mathbf{x}_2 is chosen to be orthogonal to $\mathbf{z}_2 = \mathbf{z}_1$ and pass through point p . The frame is then completed by setting $\mathbf{y}_2 = \mathbf{z}_2 \times \mathbf{x}_2$. The link rotation is measured about the \mathbf{z}_1 axis from the \mathbf{x}_1 to the \mathbf{x}_2 axis. The link twist $\alpha_2 = 0$ since the \mathbf{z}_1 and \mathbf{z}_2 axes coincide. The link displacement $d_2 = 0$ and link offset $a_2 = 0$ because the origin of the 1 and 2 frames coincide.

In summary, the link parameters for the scanner assembly is shown in the table below.

Joint	Rotation θ	Twist α	Displacement d	Offset a
1	θ_1	$\frac{\pi}{2}$	$d_{o,p}$	0
2	θ_2	0	0	0

Example ?? in the MATLAB Workbook for DCRS solves for homogeneous transforms that map between successive frames in this kinematic chain using MATLAB.

The last example required only two frames, but it is not uncommon that *dozens* of frames are required in models of realistic robotic systems. The next example considers a single leg of a humanoid robot model that utilizes five different frames.

Example 3.3.2. Define a set of frames 0 through 6 for the leg assembly depicted in Figure (3.14) that are consistent with the *DH convention*. Choose frame 0 to be fixed in the link that corresponds to the pelvis.

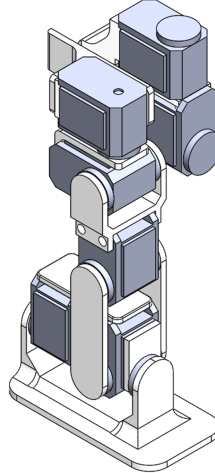


Fig. 3.14: Leg Assembly of the Humanoid Robot

Solution: First, label the links and joints, assign the basis vectors $\mathbf{z}_0, \mathbf{z}_1, \mathbf{z}_2, \mathbf{z}_3, \mathbf{z}_4$ and \mathbf{z}_5 to the revolute joints of the leg assembly and select the origin for frame 0, as shown in Figure (3.15). Choose $\mathbf{z}_6 = \mathbf{z}_5$ for the foot link frame.

Next, the frame i origins and basis vectors \mathbf{x}_i are chosen so that \mathbf{x}_i intersects and is perpendicular to \mathbf{z}_{i-1} for joints 1 through 6. In the following analysis, the variable $d_{i,j}$ represents the unsigned distance from point i to point j .

Joint 1 is shown in Figure (3.16a). Since \mathbf{z}_0 and \mathbf{z}_1 are not coplanar, the direction of the unit vector $\mathbf{x}_1 = \mathbf{z}_1 \times \mathbf{z}_0$ is defined as the normal of the plane spanned by \mathbf{z}_0 and \mathbf{z}_1 and the origin of frame 1 is defined at point q such that \mathbf{x}_1 intersects

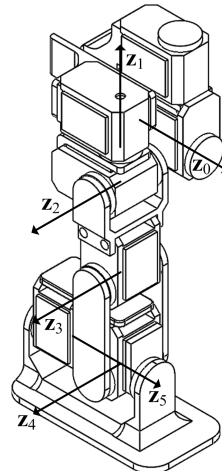


Fig. 3.15: Definitions of Degree of Freedom Axes $\mathbf{z}_0, \mathbf{z}_1, \mathbf{z}_2, \mathbf{z}_3, \mathbf{z}_4, \mathbf{z}_5$

\mathbf{z}_0 at point p . The link displacement $d_1 = d_{o,p}$ is the distance between the \mathbf{x}_0 and \mathbf{x}_1 axes measured along the \mathbf{z}_0 direction. The link rotation θ_1 is measured about the positive \mathbf{z}_0 axis, from \mathbf{x}_0 to \mathbf{x}_1 . The link offset $a_1 = -d_{p,q}$ is the distance between the \mathbf{z}_0 and \mathbf{z}_1 axes measured along the \mathbf{x}_1 direction. The link twist $\alpha_1 = -\frac{\pi}{2}$ is measured about the positive \mathbf{x}_1 axis, from \mathbf{z}_0 to \mathbf{z}_1 .

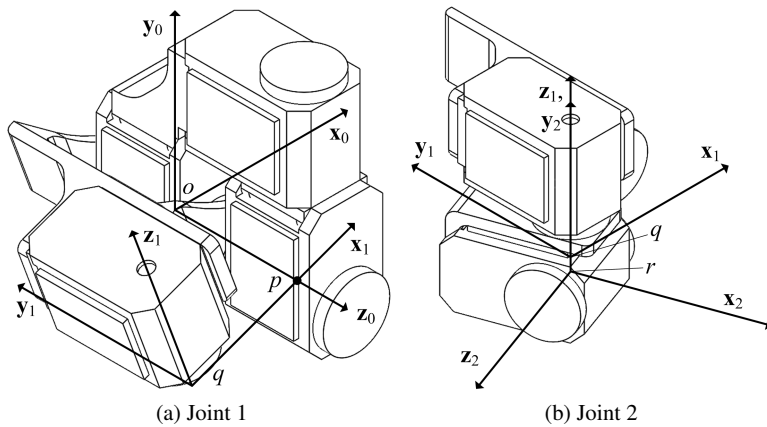


Fig. 3.16: Leg Assembly Joint 1 and 2 Definitions

Joint 2 is shown in Figure (3.16b). The \mathbf{z}_1 and \mathbf{z}_2 axes intersect at point r . Since \mathbf{x}_2 must be perpendicular to and intersect both of these vectors, it passes through point

r and is perpendicular to the plane spanned by \mathbf{z}_1 and \mathbf{z}_2 . The link displacement $d_2 = -d_{q,r}$ is the distance between the \mathbf{x}_1 and \mathbf{x}_2 axes measured along the \mathbf{z}_1 direction. The link rotation θ_2 is measured about the positive \mathbf{z}_1 axis, from \mathbf{x}_1 to \mathbf{x}_2 . The link offset $a_2 = 0$ because axes \mathbf{z}_1 and \mathbf{z}_2 intersect. The link twist $\alpha_2 = \frac{\pi}{2}$ is measured about the positive \mathbf{x}_2 axis, from \mathbf{z}_1 to \mathbf{z}_2 .

Joint 3 is shown in Figure (3.17a). The \mathbf{z}_2 and \mathbf{z}_3 axes are parallel, allowing the origin of frame 3 to be chosen at any point along \mathbf{z}_3 ; the origin of frame 3 is chosen as the intersection of \mathbf{z}_3 and the plane spanned by \mathbf{x}_2 and \mathbf{y}_2 . \mathbf{x}_3 is chosen as the unit vector from the frame 2 origin to the frame 3 origin. The link displacement $d_3 = 0$ because \mathbf{x}_2 and \mathbf{x}_3 intersect. The link rotation θ_3 is measured about the positive \mathbf{z}_2 axis, from \mathbf{x}_2 to \mathbf{x}_3 . The link offset $a_3 = d_{r,s}$ is the distance between the \mathbf{z}_2 and \mathbf{z}_3 axes measured along the \mathbf{x}_3 direction. The link twist $\alpha_3 = 0$ because axes \mathbf{z}_2 and \mathbf{z}_3 are parallel.

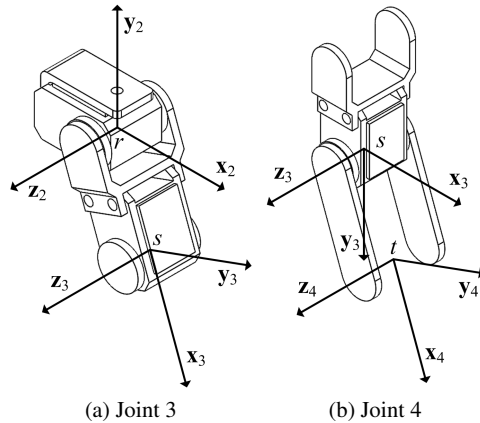


Fig. 3.17: Leg Assembly Joint 3 and 4 Definitions

Joint 4 is shown in Figure (3.17b). The \mathbf{z}_3 and \mathbf{z}_4 axes are parallel, allowing the origin of frame 4 to be chosen at any point along \mathbf{z}_4 ; the origin of frame 4 is chosen as the intersection of \mathbf{z}_4 and the plane spanned by \mathbf{x}_3 and \mathbf{y}_3 . \mathbf{x}_4 is chosen as the unit vector from the frame 3 origin to the frame 4 origin. The link displacement $d_4 = 0$ because \mathbf{x}_3 and \mathbf{x}_4 intersect. The link rotation θ_4 is measured about the positive \mathbf{z}_3 axis, from \mathbf{x}_3 to \mathbf{x}_4 . The link offset $a_4 = d_{s,t}$ is the distance between the \mathbf{z}_3 and \mathbf{z}_4 axes measured along the \mathbf{x}_4 direction. The link twist $\alpha_4 = 0$ because axes \mathbf{z}_3 and \mathbf{z}_4 are parallel.

Joint 5 is shown in Figure (3.18a). The \mathbf{z}_4 and \mathbf{z}_5 axes intersect at point t . Since \mathbf{x}_5 must be perpendicular to and intersect both of these vectors, it passes through point t and is perpendicular to the plane spanned by \mathbf{z}_4 and \mathbf{z}_5 . The link displacement $d_5 = 0$ because axes \mathbf{x}_1 and \mathbf{x}_2 intersect. The link rotation θ_5 is measured about the positive

\mathbf{z}_4 axis, from \mathbf{x}_4 to \mathbf{x}_5 . The link offset $a_5 = 0$ because axes \mathbf{z}_4 and \mathbf{z}_5 intersect. The link twist $\alpha_5 = \frac{\pi}{2}$ is measured about the positive \mathbf{x}_5 axis, from \mathbf{z}_4 to \mathbf{z}_5 .

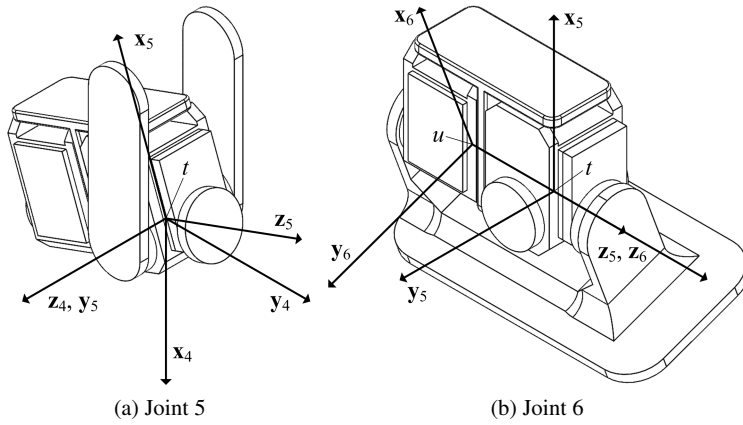


Fig. 3.18: Leg Assembly Joint 5 and 6 Definitions

Joint 6 is shown in Figure (3.18b). Since \mathbf{z}_5 and \mathbf{z}_6 axes are parallel, the origin of frame 6 may be set at any point along \mathbf{z}_6 ; the point u is chosen to position the foot frame origin in the motor actuating the foot. \mathbf{x}_6 is chosen orthogonal to $\mathbf{z}_6 = \mathbf{z}_5$ such that $\mathbf{x}_6 = \mathbf{x}_5$ when $\theta_6 = 0$. The link displacement $d_5 = -d_{t,u}$ is the distance between the \mathbf{x}_5 and \mathbf{x}_6 axes measured along the \mathbf{z}_5 direction. The link rotation θ_6 is measured about the positive \mathbf{z}_5 axis, from \mathbf{x}_5 to \mathbf{x}_6 . The link offset $a_6 = 0$ because axes \mathbf{z}_4 and \mathbf{z}_5 intersect. The link twist $\alpha_5 = 0$ is measured about the positive \mathbf{x}_6 axis, from \mathbf{z}_5 to \mathbf{z}_6 . In summary, the link parameters for leg assembly are given in the table below.

Joint	Displacement d	Rotation θ	Offset a	Twist α
1	$d_{o,p}$	$\theta_1(t)$	$-d_{p,q}$	$-\frac{\pi}{2}$
2	$-d_{q,r}$	$\theta_2(t)$	0	$\frac{\pi}{2}$
3	0	$\theta_3(t)$	$d_{r,s}$	0
4	0	$\theta_4(t)$	$d_{s,t}$	0
5	0	$\theta_5(t)$	0	$\frac{\pi}{2}$
6	$-d_{t,u}$	$\theta_6(t)$	0	0

Example ?? in the MATLAB Workbook solves for the homogeneous transforms that describe the rigid body motion between each pair of frames in this example.

3.3.5 Angular Velocity and Velocity in the DH Convention

So far, in Chapter (3) general principles of kinematics for three dimensional, complex systems have been introduced. This section adapts some of these principles to the analysis of robotic systems that form kinematic chains and for which the DH convention applies. This section introduces the *Jacobian matrices* that relate the velocity of specific points of interest and the angular velocity of the bodies on which they lie to the time derivative of the joint variables.

Theorem 3.3 (DH-Convention Jacobian Matrix). Suppose there is an N link kinematic chain whose bodies, joints and degrees of freedom are numbered consistent with the Denavit-Hartenberg convention. The $6 \times N$ Jacobian matrix \mathbf{J}^0 relates the velocity of point p fixed on body N and angular velocity of body N in the 0 frame to the time derivatives of the joint variables $\dot{q}_1, \dots, \dot{q}_N$

$$\begin{Bmatrix} \mathbf{v}_{0,p}^0 \\ \boldsymbol{\omega}_{0,N}^0 \end{Bmatrix} = \mathbf{J}^0 \dot{\mathbf{q}} = \begin{bmatrix} \mathbf{J}_v^0 \\ \mathbf{J}_\omega^0 \end{bmatrix} \begin{Bmatrix} \dot{q}_1 \\ \vdots \\ \dot{q}_N \end{Bmatrix}.$$

The $3 \times N$ submatrix \mathbf{J}_ω^0 is given by

$$\begin{aligned} \mathbf{J}_\omega^0 &= [\rho_1 \mathbf{z}_0^0 \ \rho_2 \mathbf{z}_1^0 \ \rho_3 \mathbf{z}_2^0 \cdots \ \rho_N \mathbf{z}_{N-1}^0], \\ &= [\rho_1 \mathbf{e}_3 \ \rho_2 \mathbf{R}_1^0 \mathbf{e}_3 \ \rho_3 \mathbf{R}_2^0 \mathbf{e}_3 \cdots \ \rho_N \mathbf{R}_{N-1}^0 \mathbf{e}_3], \end{aligned}$$

where ρ_i is equal to 1 if joint i is a revolute joint and is equal to 0 if joint i is a prismatic joint.

The $3 \times N$ submatrix \mathbf{J}_v^0 is given by

$$\mathbf{J}_v^0 = [\mathbf{j}_1^0 \ \mathbf{j}_2^0 \ \cdots \ \mathbf{j}_N^0].$$

If joint i is a prismatic joint, the i^{th} column \mathbf{j}_i^0 is defined by the equation

$$\mathbf{j}_i^0 = \mathbf{z}_{i-1}^0 = \mathbf{R}_{i-1}^0 \mathbf{e}_3.$$

If joint i is a revolute joint, the i^{th} column \mathbf{j}_i^0 is defined by the equation

$$\mathbf{j}_i^0 = \mathbf{z}_{i-1}^0 \times (\mathbf{r}_{0,p}^0 - \mathbf{r}_{0,i-1}^0).$$

Proof. The derivation of the form of the submatrix \mathbf{J}_ω^0 follows directly from the Addition Theorem for angular velocities. $\boldsymbol{\omega}_{0,N}$ can be written expanded such that

$$\boldsymbol{\omega}_{0,N} = \boldsymbol{\omega}_{0,1} + \boldsymbol{\omega}_{1,2} + \cdots + \boldsymbol{\omega}_{N-1,N}.$$

The angular velocity between a pair of bodies depends on whether the joint between those bodies is prismatic or revolute. If joint i is prismatic, there will be no relative angular velocity and $\omega_{i-1,i} = \mathbf{0}$. If joint i is revolute, the angular velocity between the bodies is solely about the \mathbf{z}_{i-1} axis at an angular speed of $\dot{\theta}_i$. As a result, the angular velocity $\omega_{i-1,i}$ is defined as $\rho_i \dot{\theta}_i \mathbf{z}_{i-1}$, where $\rho_i = 0$ for prismatic joints and $\rho_i = 1$ for revolute joints. Collecting these into the formulation for $\omega_{0,N}$ results in

$$\omega_{0,N} = \rho_1 \dot{\theta}_1 \mathbf{z}_0 + \rho_2 \dot{\theta}_2 \mathbf{z}_1 + \cdots + \rho_N \dot{\theta}_N \mathbf{z}_{N-1}.$$

The form of \mathbf{J}_ω^0 stated in the theorem results when these vectors are expressed with respect to the frame 0 basis.

The form of the matrix \mathbf{J}_v^0 can be determined by first noting that each column \mathbf{j}_i^0 contains the coordinates of the velocity of point p in the 0 frame when all of the derivatives of the *joint variables* are equal to zero except the i^{th} , which is set to one. In this case,

$$\mathbf{v}_{0,p}^0 = \mathbf{j}_i^0 = \left[\mathbf{j}_1^0 \ \mathbf{j}_2^0 \ \cdots \ \mathbf{j}_i^0 \ \cdots \ \mathbf{j}_N^0 \right] \begin{Bmatrix} 0 \\ 0 \\ \vdots \\ 1 \\ \vdots \\ 0 \\ 0 \end{Bmatrix}.$$

If the i^{th} joint is a *prismatic joint*, $\dot{q}_i = \dot{d}_i = 1$, and the other joint variable derivatives are equal to zero, the velocity of the point p is $\dot{d}_i \mathbf{z}_{i-1} = \mathbf{z}_{i-1}$.

If the i^{th} joint is a *revolute joint*, Theorem (2.16) can be applied to determine the velocity in the 0 frame of the point p .

$$\begin{aligned} \mathbf{v}_{0,p} &= \underbrace{\mathbf{v}_{0,i-1}}_0 + \underbrace{\omega_{0,i}}_{\omega_{i-1,i}} \times (\mathbf{r}_{0,p} - \mathbf{r}_{0,i-1}) = \omega_{i-1,i} \times (\mathbf{r}_{0,p} - \mathbf{r}_{0,i-1}), \\ &= \dot{\theta}_i \mathbf{z}_{i-1} \times (\mathbf{r}_{0,p} - \mathbf{r}_{0,i-1}) = \mathbf{z}_{i-1} \times (\mathbf{r}_{0,p} - \mathbf{r}_{0,i-1}). \end{aligned}$$

Recall that the calculation above assumes that all of the derivatives of the *joint variables* \dot{q}_j for $j \neq i$ are set equal to zero, and $\dot{q}_i = \dot{\theta}_i = 1$. The conclusion of the theorem is obtained when these vectors are expressed in terms of coordinates relative to the basis for the 0 frame. \square

The superscript on \mathbf{J}^k is used to denote that the velocity $\mathbf{v}_{0,p}$ and angular velocity $\omega_{0,N}$ are expressed in components relative to the k frame, such that

$$\begin{Bmatrix} \mathbf{v}_{0,p}^k \\ \omega_{0,N}^k \end{Bmatrix} = \mathbf{J}^k \dot{\mathbf{q}}.$$

By extension, the change of basis operation for the Jacobian may be defined as

$$\mathbf{J}^0 = \begin{bmatrix} \mathbf{R}_k^0 & \mathbf{0} \\ \mathbf{0} & \mathbf{R}_k^0 \end{bmatrix} \mathbf{J}^k.$$

Example 3.3.3. Calculate the Jacobian matrix \mathbf{J}^0 that relates the velocity $\mathbf{v}_{0,r}$ of point r and the angular velocity $\boldsymbol{\omega}_{0,2}$ of frame 2 in the 0 frame to the derivatives of the generalized coordinates $\dot{\mathbf{q}}$ of the leg assembly in Example (3.3.2). Since the required velocities only depend on θ_1 and θ_2 and their derivatives, the 6×2 Jacobian matrix \mathbf{J}^0 may be expressed concisely as

$$\begin{Bmatrix} \mathbf{v}_{0,2}^0 \\ \boldsymbol{\omega}_{0,2}^0 \end{Bmatrix} = \mathbf{J}^0 \begin{Bmatrix} \dot{\theta}_1 \\ \dot{\theta}_2 \end{Bmatrix}.$$

Calculate the matrix \mathbf{J}^0 in two ways: (1) find the velocities and angular velocities from first principles and identify the Jacobian matrix from these expressions, and (2) use Theorem (3.3) to calculate the Jacobian matrix directly.

Solution: As a first steps, the rotation matrices \mathbf{R}_0^1 and \mathbf{R}_1^2 are calculated, such that

$$\mathbf{R}_0^1 = \begin{bmatrix} \cos \theta_1 & \sin \theta_1 & 0 \\ 0 & 0 & -1 \\ -\sin \theta_1 & \cos \theta_1 & 0 \end{bmatrix} \quad \text{and} \quad \mathbf{R}_1^2 = \begin{bmatrix} \cos \theta_2 & \sin \theta_2 & 0 \\ 0 & 0 & 1 \\ \sin \theta_2 & -\cos \theta_2 & 0 \end{bmatrix}.$$

Next, the angular velocity $\boldsymbol{\omega}_{0,2}$ is derived using the Addition Theorem (2.15) from Chapter (2), $\boldsymbol{\omega}_{0,2} = \dot{\theta}_1 \mathbf{z}_0 + \dot{\theta}_2 \mathbf{z}_1$. The angular velocity may be expressed with respect to frame 0 using \mathbf{R}_0^1 , such that

$$\boldsymbol{\omega}_{0,2}^0 = \underbrace{\begin{Bmatrix} 0 \\ 0 \\ 1 \end{Bmatrix}}_{\mathbf{e}_3} \dot{\theta}_1 + \underbrace{\begin{bmatrix} \cos \theta_1 & 0 & -\sin \theta_1 \\ \sin \theta_1 & 0 & \cos \theta_1 \\ 0 & -1 & 0 \end{bmatrix}}_{\mathbf{R}_1^0} \underbrace{\begin{Bmatrix} 0 \\ 0 \\ 1 \end{Bmatrix}}_{\mathbf{e}_3} \dot{\theta}_2 = \underbrace{\begin{Bmatrix} 0 \\ 0 \\ 1 \end{Bmatrix}}_{\mathbf{e}_3} \dot{\theta}_1 + \underbrace{\begin{Bmatrix} -\sin \theta_1 \\ \cos \theta_1 \\ 0 \end{Bmatrix}}_{\mathbf{e}_3} \dot{\theta}_2.$$

Collecting these expressions into matrix form results in

$$\boldsymbol{\omega}_{0,2}^2 = \mathbf{J}_{\boldsymbol{\omega}}^0 \begin{Bmatrix} \dot{\theta}_1 \\ \dot{\theta}_2 \end{Bmatrix} = \begin{bmatrix} 0 & -\sin \theta_1 \\ 0 & \cos \theta_1 \\ 1 & 0 \end{bmatrix} \begin{Bmatrix} \dot{\theta}_1 \\ \dot{\theta}_2 \end{Bmatrix}.$$

The velocity of the origin of the 2 frame (point r) is computed from the relative velocity Theorem (2.16) in Chapter (2), due to the fact that points r and p have constant positioning with respect to the upper hip basis (frame 1).

$$\begin{aligned}\mathbf{v}_{0,r} &= \underbrace{\mathbf{v}_{0,p}}_0 + \boldsymbol{\omega}_{0,1} \times (-d_{p,q}\mathbf{x}_1 - d_{q,r}\mathbf{z}_1), \\ &= \begin{vmatrix} \mathbf{x}_1 & \mathbf{y}_1 & \mathbf{z}_1 \\ 0 & -\dot{\theta}_1 & 0 \\ -d_{p,q} & 0 & -d_{q,r} \end{vmatrix}, \\ &= d_{q,r}\dot{\theta}_1\mathbf{x}_1 - d_{p,q}\dot{\theta}_1\mathbf{z}_1\end{aligned}$$

Evaluating the velocity in terms of the basis for the 0 frame results in

$$\begin{aligned}\mathbf{v}_{0,r}^0 &= \begin{bmatrix} \cos\theta_1 & 0 & -\sin\theta_1 \\ \sin\theta_1 & 0 & \cos\theta_1 \\ 0 & -1 & 0 \end{bmatrix} \begin{Bmatrix} d_{q,r}\dot{\theta}_1 \\ 0 \\ -d_{p,q}\dot{\theta}_1 \end{Bmatrix}, \\ &= \begin{Bmatrix} d_{q,r}\cos\theta_1 + d_{p,q}\sin\theta_1 \\ d_{q,r}\sin\theta_1 - d_{p,q}\cos\theta_1 \\ 0 \end{Bmatrix} \dot{\theta}_1 + \begin{Bmatrix} 0 \\ 0 \\ 0 \end{Bmatrix} \dot{\theta}_2. \\ \mathbf{v}_{0,2}^0 &= \mathbf{J}_v^0 \begin{Bmatrix} \dot{\theta}_1 \\ \dot{\theta}_2 \end{Bmatrix} = \begin{bmatrix} (d_{q,r}\cos\theta_1 + d_{p,q}\sin\theta_1) & 0 \\ (d_{q,r}\sin\theta_1 - d_{p,q}\cos\theta_1) & 0 \\ 0 & 0 \end{bmatrix} \begin{Bmatrix} \dot{\theta}_1 \\ \dot{\theta}_2 \end{Bmatrix}.\end{aligned}$$

The full Jacobian matrix with respect to frame 0 can be constructed by concatenating these two submatrices, such that

$$\begin{aligned}\begin{Bmatrix} \mathbf{v}_{0,2}^0 \\ \boldsymbol{\omega}_{0,2}^0 \end{Bmatrix} &= \begin{bmatrix} \mathbf{J}_v \\ \mathbf{J}_\omega \end{bmatrix} \begin{Bmatrix} \dot{\theta}_1 \\ \dot{\theta}_2 \end{Bmatrix}, \\ &= \begin{bmatrix} (d_{q,r}\cos\theta_1 + d_{p,q}\sin\theta_1) & 0 \\ (d_{q,r}\sin\theta_1 - d_{p,q}\cos\theta_1) & 0 \\ 0 & 0 \\ 0 & -\sin\theta_1 \\ 0 & \cos\theta_1 \\ 1 & 0 \end{bmatrix} \begin{Bmatrix} \dot{\theta}_1 \\ \dot{\theta}_2 \end{Bmatrix}. \quad (3.3.2)\end{aligned}$$

For the second part of this solution, the same quantity will be computed using Theorem (3.3). For this system every joint is revolute; thus,

$$\rho_1 = \rho_2 = 1.$$

The unit vectors \mathbf{z}_0^0 and \mathbf{z}_1^0 are obtained from the formulations of the rotation matrices \mathbf{R}_1^0 and $\mathbf{R}_2^0 = \mathbf{R}_1^0\mathbf{R}_2^1$, such that

$$\mathbf{z}_0^0 = \begin{Bmatrix} 0 \\ 0 \\ 1 \end{Bmatrix}, \quad \mathbf{z}_1^0 = \begin{Bmatrix} -\sin\theta_1 \\ \cos\theta_1 \\ 0 \end{Bmatrix}.$$

Combining these into the submatrix \mathbf{J}_ω results in

$$\mathbf{J}_{\omega}^0 = \begin{bmatrix} \rho_1 \mathbf{z}_0^0 & \rho_2 \mathbf{z}_1^0 \end{bmatrix} = \begin{bmatrix} 0 & -\sin \theta_1 \\ 0 & \cos \theta_1 \\ 1 & 0 \end{bmatrix}.$$

For the calculation of \mathbf{J}_v , calculations are required for the two columns vectors

$$\mathbf{j}_i^0 = \mathbf{z}_{i-1}^0 \times (\mathbf{r}_{0,2}^0 - \mathbf{r}_{0,i-1}^0)$$

for $i = 1, 2$. For $i = 1$,

$$\mathbf{j}_1 = \mathbf{z}_0 \times (\mathbf{r}_{0,r} - \mathbf{0}) = \begin{vmatrix} \mathbf{x}_1 & \mathbf{y}_1 & \mathbf{z}_1 \\ 0 & -1 & 0 \\ -d_{p,q} & -d_{o,p} & -d_{q,r} \end{vmatrix} = d_{q,r} \mathbf{x}_1 - d_{p,q} \mathbf{z}_1.$$

Representing this vector with respect to frame 0 results in

$$\mathbf{j}_1^0 = \begin{bmatrix} \cos \theta_1 & 0 & -\sin \theta_1 \\ \sin \theta_1 & 0 & \cos \theta_1 \\ 0 & -1 & 0 \end{bmatrix} \begin{Bmatrix} d_{q,r} \\ 0 \\ -d_{p,q} \end{Bmatrix} = \begin{Bmatrix} d_{q,r} \cos \theta_1 + d_{p,q} \sin \theta_1 \\ d_{q,r} \sin \theta_1 - d_{p,q} \cos \theta_1 \\ 0 \end{Bmatrix}. \quad (3.3.3)$$

For $i = 2$,

$$\mathbf{j}_2 = \mathbf{z}_1 \times (\mathbf{r}_{0,r} - \mathbf{r}_{0,q}) = \begin{vmatrix} \mathbf{x}_1 & \mathbf{y}_1 & \mathbf{z}_1 \\ 0 & 0 & 1 \\ 0 & 0 & -d_{q,r} \end{vmatrix} = \mathbf{0}.$$

This vector remains $\mathbf{0}$ regardless of frame representation. The resulting Jacobian submatrix \mathbf{J}_v^0 is given by

$$\mathbf{J}_v^0 = [\mathbf{j}_1^0 \ \mathbf{j}_2^0] = \begin{bmatrix} d_{q,r} \cos \theta_1 + d_{p,q} \sin \theta_1 & 0 \\ d_{q,r} \sin \theta_1 - d_{p,q} \cos \theta_1 & 0 \\ 0 & 0 \end{bmatrix}.$$

As a result, the full Jacobian matrix calculated as

$$\mathbf{J} = \begin{bmatrix} \mathbf{J}_v^0 \\ \mathbf{J}_{\omega}^0 \end{bmatrix}$$

yields the same Jacobian matrix found in Equation (3.3.2).

3.4 Recursive $O(N)$ Formulation of Forward Kinematics

The Denavit-Hartenberg procedure is one of many strategies that can be used to formulate the kinematics of robotic systems. This section will introduce an alternative approach for modeling the kinematics of robot systems. This technique is an ex-

ample of a *recursive formulation* of the kinematics of a robotic system. Numerous variants of these formulations have appeared in the literature. The text [14] gives a comprehensive account of this approach by one of the early developers of the method. The specific variant presented in this text of this family of methods is based on the family of papers [38], [37], [22], [39], [16], [25], [26] because they provide a unified approach to both kinematics and dynamics.

These papers deduce the recursive algorithms for kinematics and dynamics of robots by employing the similar structure of techniques in estimation and filtering theory. For example, [38] explains that recursive formulations can be interpreted in the framework of Kalman filtering and smoothing. Kalman filtering is a well-known procedure in estimation theory that derives recursive updates of estimates, as well as associated efficient numerical techniques for their computation. One of the major contributions of the family of papers inspired by [38], and its immediate successors in [22], [23], [39], [25] and [26] has been to show how certain factorizations that appear in the context of Kalman filtering can be used directly to solve problems in dynamics and control of multibody systems. This chapter covers the recursive formulations of forward kinematics, while Chapter (4) discusses the extension of these techniques to forward dynamics.

Figure (3.19) depicts a kinematic chain for which the kinematic equations will be derived. This kinematic chain is comprised of $N + 1$ links numbered from $N + 1$ to 1, which are connected with N joints numbered N to 1.

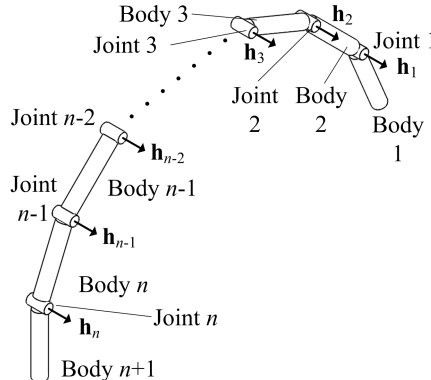


Fig. 3.19: Body and Joint Numbering of a Kinematic Chain for the Recursive Formulation

In contrast to the DH convention, the links and joints are numbered from the tip of the kinematic chain to the root. This section and Chapter (4) will show that this methodology of numbering the bodies and joints yields system matrices that can be factored as products of block lower triangular, diagonal and upper triangular factors. It is the special structure of these matrices that enables fast and recursive solution procedures to be devised. The numbering of consecutive joints in the kinematic

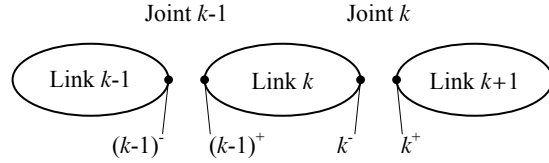


Fig. 3.20: Joint Side Labeling of a Kinematic Chain for the Recursive Formulation

chain is shown in Figure (3.20). The notation $b := N + 1$ will be used to refer to the *base body*, that is, link $N + 1$.

The two sides of joint k are denoted by k^- and k^+ . Specifically, the notation k^- refers to the point at joint k fixed on body k . By definition, point k^- is on the outboard side of joint k , toward the free end of the kinematic chain. The notation k^+ refers to the point at joint k fixed on body $k + 1$. The point k^+ is on the inboard side of joint k , toward the base body of the kinematic chain.

Each joint k is defined by a vector \mathbf{h}_k that describes the direction of the degree of freedom at joint k . For a revolute joint, \mathbf{h}_k is along the rotational axis, while for a prismatic joint, \mathbf{h}_k is along the translational axis. In the following discussion, it will be assumed that all joints under consideration are revolute. Modifications for prismatic joints are discussed in Problem (3.3).

The velocities and angular velocities are collected in 6×1 vectors \mathcal{V}_{k^-} and \mathcal{V}_{k^+} , and the derivatives of the velocities and angular velocities are collected in the vectors \mathcal{A}_{k^-} and \mathcal{A}_{k^+} . This section will address the evaluation of \mathcal{V}_{k^-} and \mathcal{V}_{k^+} , whereas \mathcal{A}_{k^-} and \mathcal{A}_{k^+} will be treated in Section (3.4.3). In this convention the superscript + or - denotes on which side of joint k the quantity is calculated. The subscript is used to specify the joint at which the velocities or their derivatives are calculated. These velocity vectors are defined as

$$\mathcal{V}_{k^-} := \begin{Bmatrix} \mathbf{v}_{b,k^-}^k \\ \boldsymbol{\omega}_{b,k^-}^k \end{Bmatrix} \quad \text{and} \quad \mathcal{V}_{k^+} := \begin{Bmatrix} \mathbf{v}_{b,k^+}^{k+1} \\ \boldsymbol{\omega}_{b,k^+}^{k+1} \end{Bmatrix}.$$

By definition \mathbf{v}_{b,k^-} is the velocity vector of point k^- in the base frame $b = N + 1$, and $\boldsymbol{\omega}_{b,k^-}$ is the angular velocity vector of the body that contains point k^- relative to the base frame $b = N + 1$. The term \mathbf{v}_{b,k^-}^k contains the components relative to the basis for frame k of the velocity vector \mathbf{v}_{b,k^-} . The term $\boldsymbol{\omega}_{b,k^-}^k$ contains the components relative to the basis for frame k of the angular velocity vector $\boldsymbol{\omega}_{b,k^-}$. While this notation may seem unnecessarily complex, the following observations may help make it easier to interpret the entries in \mathcal{V}_{k^-} and \mathcal{V}_{k^+} .

- The velocity and angular velocity vectors that are contained in \mathcal{V}_{k^-} and \mathcal{V}_{k^+} refer to the points k^- and k^+ , respectively.
- The components of the velocity and angular velocity vectors that are contained in \mathcal{V}_{k^-} are given with respect to the frame k in which the point k^- is fixed. The

components of the vectors in \mathcal{V}_{k^+} are given with respect to frame $k + 1$ in which the point k^+ is fixed.

Finally, it should be noted that the notation ω_{b,k^-} and ω_{b,k^+} is somewhat misleading. In general, the vector $\omega_{A,B}$ is defined in Definition (2.9) as the angular velocity vector of the frame B in the frame A . Because the frames A and B are often fixed in some rigid body, $\omega_{A,B}$ is often described as the angular velocity of body B relative to body A . The vectors ω_{b,k^-} and ω_{b,k^+} are the angular velocities of “the frame containing point k^- ” or “the frame containing point k^+ ” relative to the base frame. That is,

$$\omega_{b,k^-} = \omega_{b,(k-1)^+} = \omega_{b,k} \quad \text{and} \quad \omega_{b,(k+1)^-} = \omega_{b,k^+} = \omega_{b,k+1}$$

Since this notation is common in the literature, this convention will be utilized when describing recursive formulations of kinematics and dynamics in Sections (3.4) and (4.8).

3.4.1 Recursive Calculation of Velocity and Angular Velocity

The following theorem summarizes the matrix equation that enables recursive calculation of velocities and angular velocities based on the numbering of bodies from the tip to the base of the chain.

Theorem 3.4 (Recursive Velocity and Angular Velocity). *The velocities and angular velocities $\{\mathcal{V}_{k^-}\}_{k=1,\dots,N}$ of the N -link kinematic chain depicted in Figures (3.19) and (3.20) satisfy the equation*

$$\left\{ \begin{array}{c} \mathcal{V}_{1^-} \\ \mathcal{V}_{2^-} \\ \mathcal{V}_{3^-} \\ \vdots \\ \mathcal{V}_{(N-1)^-} \\ \mathcal{V}_{N^-} \end{array} \right\} = \left[\begin{array}{ccccc} 0 & \mathcal{R}_{2,1}^T \varphi_{2,1}^T & 0 & \cdots & 0 & 0 \\ 0 & 0 & \mathcal{R}_{3,2}^T \varphi_{3,2}^T & \cdots & 0 & 0 \\ 0 & 0 & 0 & \cdots & 0 & 0 \\ \vdots & \vdots & \vdots & \ddots & \vdots & \vdots \\ 0 & 0 & 0 & \cdots & 0 & \mathcal{R}_{N-1,N}^T \varphi_{N-1,N}^T \\ 0 & 0 & 0 & \cdots & 0 & 0 \end{array} \right] \left\{ \begin{array}{c} \mathcal{V}_{1^-} \\ \mathcal{V}_{2^-} \\ \mathcal{V}_{3^-} \\ \vdots \\ \mathcal{V}_{(N-1)^-} \\ \mathcal{V}_{N^-} \end{array} \right\} \quad (3.4.1)$$

$$+ \left[\begin{array}{ccccc} \mathcal{H}_1 & 0 & 0 & \cdots & 0 & 0 \\ 0 & \mathcal{H}_2 & 0 & \cdots & 0 & 0 \\ 0 & 0 & \mathcal{H}_3 & \cdots & 0 & 0 \\ \vdots & \vdots & \vdots & \ddots & \vdots & \vdots \\ 0 & 0 & 0 & \cdots & \mathcal{H}_{N-1} & 0 \\ 0 & 0 & 0 & \cdots & 0 & \mathcal{H}_N \end{array} \right] \left\{ \begin{array}{c} \dot{\theta}_1 \\ \dot{\theta}_2 \\ \dot{\theta}_3 \\ \vdots \\ \dot{\theta}_{N-1} \\ \dot{\theta}_N \end{array} \right\} \quad (3.4.2)$$

where $\varphi_{k-1,k}^T$ is given in Equation (3.4.9), $\mathcal{R}_{k-1,k}$ is given in Equation (3.4.13), and \mathcal{H}_k is given in Equation (3.4.13) for $k = 1, \dots, N$.

Proof. Assuming that every joint is revolute, Theorem (2.17) ensures

$$\mathbf{v}_{b,k^-} = \mathbf{v}_{b,k^+}, \quad (3.4.3)$$

$$\mathbf{v}_{b,(k-1)^-} = \mathbf{v}_{b,k^-} + \boldsymbol{\omega}_{b,k^-} \times \mathbf{d}_{k,(k-1)}. \quad (3.4.4)$$

In addition, the angular velocities of adjacent links be written using the Addition Theorem for angular velocities in Theorem (2.15), resulting in

$$\boldsymbol{\omega}_{b,k^-} = \boldsymbol{\omega}_{b,(k-1)^+}, \quad (3.4.5)$$

$$\boldsymbol{\omega}_{b,k^-} = \boldsymbol{\omega}_{b,k^+} + \mathbf{h}_k \dot{\theta}_k. \quad (3.4.6)$$

Equation (3.4.6) implies that the rotation angle θ_k about joint k defines the rotation of the outboard link k relative to the inboard link $k+1$.

Equations (3.4.3) through (3.4.6) are vector equations, and the most convenient basis for computing solutions may be chosen. Equation (3.4.4) and (3.4.5) may be expressed in terms of the basis for frame k fixed in link k as

$$\begin{Bmatrix} \mathbf{v}_{b,(k-1)^+}^k \\ \boldsymbol{\omega}_{b,(k-1)^+}^k \end{Bmatrix} = \begin{bmatrix} \mathbb{I} & -\mathbf{S}(\mathbf{d}_{k,k-1}^k) \\ \mathbf{0} & \mathbb{I} \end{bmatrix} \begin{Bmatrix} \mathbf{v}_{b,k^-}^k \\ \boldsymbol{\omega}_{b,k^-}^k \end{Bmatrix} = \begin{bmatrix} \mathbb{I} & \mathbf{S}(\mathbf{d}_{k-1,k}^k) \\ \mathbf{0} & \mathbb{I} \end{bmatrix} \begin{Bmatrix} \mathbf{v}_{b,k^-}^k \\ \boldsymbol{\omega}_{b,k^-}^k \end{Bmatrix} \quad (3.4.7)$$

$$= \begin{bmatrix} \mathbb{I} & \mathbf{S}(\mathbf{d}_{k,k-1}^k)^T \\ \mathbf{0} & \mathbb{I} \end{bmatrix} \begin{Bmatrix} \mathbf{v}_{b,k^-}^k \\ \boldsymbol{\omega}_{b,k^-}^k \end{Bmatrix} \quad (3.4.8)$$

where $\mathbf{S}(\cdot)$ is the skew operator defined in Chapter (2). Recall that the 6×1 vectors \mathcal{V}_{k^-} and \mathcal{V}_{k^+} are defined as

$$\mathcal{V}_{k^-} := \begin{Bmatrix} \mathbf{v}_{b,k^-}^k \\ \boldsymbol{\omega}_{b,k^-}^k \end{Bmatrix} \quad \text{and} \quad \mathcal{V}_{(k-1)^+} := \begin{Bmatrix} \mathbf{v}_{b,(k-1)^+}^k \\ \boldsymbol{\omega}_{b,(k-1)^+}^k \end{Bmatrix}.$$

Defining the transposed transition operator $\varphi_{k,k-1}^T$ as

$$\varphi_{k,k-1}^T := \begin{bmatrix} \mathbb{I} & \mathbf{S}(\mathbf{d}_{k,k-1}^k)^T \\ \mathbf{0} & \mathbb{I} \end{bmatrix} = \begin{bmatrix} \mathbb{I} & -\mathbf{S}(\mathbf{d}_{k,k-1}^k) \\ \mathbf{0} & \mathbb{I} \end{bmatrix} = \begin{bmatrix} \mathbb{I} & \mathbf{S}(\mathbf{d}_{k-1,k}^k) \\ \mathbf{0} & \mathbb{I} \end{bmatrix} \quad (3.4.9)$$

allows Equation (3.4.7) to be written as

$$\mathcal{V}_{(k-1)^+} = \varphi_{k,k-1}^T \mathcal{V}_{k^-}. \quad (3.4.10)$$

Next, the vector equations from Equations (3.4.3) and (3.4.6) are cast as a single matrix equation by expressing these equations in terms of their components relative to the basis for either frame k or $k+1$. By convention, it is assumed that \mathcal{V}_{k^-} contains components relative to the basis for the frame in which point k^- is fixed, which is the k frame basis. Similarly, \mathcal{V}_{k^+} contains components relative to the basis for the frame in which point k^+ is fixed, which is the $k+1$ frame basis. It follows that

$$\begin{Bmatrix} \mathbf{v}_{b,k^-}^k \\ \boldsymbol{\omega}_{b,k^-}^k \end{Bmatrix} = \begin{bmatrix} \mathbf{R}_{k+1}^k & \mathbf{0} \\ \mathbf{0} & \mathbf{R}_{k+1}^k \end{bmatrix} \begin{Bmatrix} \mathbf{v}_{b,k^+}^{k+1} \\ \boldsymbol{\omega}_{b,k^+}^{k+1} \end{Bmatrix} + \begin{Bmatrix} \mathbf{0} \\ \mathbf{h}_k^k \end{Bmatrix} \dot{\theta}_k. \quad (3.4.11)$$

This equation can be written in the form

$$\mathcal{V}_{k^-} = \mathcal{R}_{k,k+1} \mathcal{V}_{k^+} + \mathcal{H}_k \dot{\theta}_k \quad (3.4.12)$$

by introducing the notation

$$\mathcal{H}_k := \begin{Bmatrix} \mathbf{0} \\ \mathbf{h}_k^k \end{Bmatrix} \quad \text{and} \quad \mathcal{R}_{k,k+1} := \begin{bmatrix} \mathbf{R}_{k+1}^k & \mathbf{0} \\ \mathbf{0} & \mathbf{R}_{k+1}^k \end{bmatrix}. \quad (3.4.13)$$

The matrix $\mathcal{R}_{k,k+1}$ is a rotation matrix: it satisfies the equation $\mathcal{R}_{k,k+1} = \mathcal{R}_{k+1,k}^T$ since its constituent submatrices $\mathbf{R}_{k,k+1}$ are rotation matrices. Equations (3.4.10) and (3.4.12) may be combined to obtain

$$\mathcal{V}_{k^-} = \mathcal{R}_{k,k+1} \varphi_{k+1,k}^T \mathcal{V}_{(k+1)^-} + \mathcal{H}_k \dot{\theta}_k, \quad (3.4.14)$$

which may also be written as

$$\mathcal{V}_{k^-} = \phi_{k,k-1}^T \mathcal{V}_{(k+1)^-} + \mathcal{H}_k \dot{\theta}_k,$$

if $\phi_{k,k-1}^T$ is defined such that

$$\phi_{k,k-1}^T = \mathcal{R}_{k+1,k}^T \varphi_{k+1,k}^T. \quad (3.4.15)$$

Equation (3.4.1) results when Equation (3.4.14) is expressed for each of the joints $k = 1 \dots N$ and organized in matrix form. It is assumed in the theorem that $\mathcal{V}_{(N+1)^-} = \mathbf{0}$, although the modification for a prescribed base motion is straightforward. \square

The structure of Equation (3.4.1) facilitates a recursive algorithm for the solution of velocities and angular velocities in the kinematic chain. Suppose the joint angular rates $\dot{\theta}_1, \dot{\theta}_2, \dots, \dot{\theta}_N$ are given for each of the joints in the kinematic chain. From Equation (3.4.1), \mathcal{V}_{N^-} can be computed from the last row as

$$\mathcal{V}_{N^-} = \mathcal{H}_N \dot{\theta}_N.$$

Next, from the $(N-1)^{st}$ row, $\mathcal{V}_{(N-1)^-}$ may be calculated as

$$\begin{aligned} \mathcal{V}_{(N-1)^-} &= \phi_{N-1,N}^T \mathcal{V}_{N^-} + \mathcal{H}_{N-1} \dot{\theta}_{N-1}, \\ &= \phi_{N-1,N}^T \mathcal{H}_N \dot{\theta}_N + \mathcal{H}_{N-1} \dot{\theta}_{N-1}. \end{aligned}$$

Continuing this process from the inboard joints to the outboard joints provides a solution for all the velocities and angular velocities in the kinematic chain. These steps are summarized in Figure (3.21).

Recursive Algorithm for Velocities and Angular Velocities
<ol style="list-style-type: none"> 1) Number the joints and links in the kinematic chain from $N, \dots, 1$ starting at the base and moving to the tip. 2) Assign the unit vectors \mathbf{h}_k to the joint degrees of freedom for $k = 1, \dots, N$. 3) Define the relative position vectors $\mathbf{d}_{k,k+1}$ for $k = 1, \dots, N - 1$. 4) Iterate from inboard to outboard joints for $k = N, N - 1, \dots, 2, 1$. <ol style="list-style-type: none"> 4.1) Form the transposed transition operator $\phi_{k,k-1}^T = \mathcal{R}_{k+1,k}^T \varphi_{k+1,k}^T.$ <ol style="list-style-type: none"> 4.2) Calculate the velocity and angular velocity $\mathcal{V}_{k^-} = \phi_{k,k-1}^T \mathcal{V}_{(k+1)^-} + \mathcal{H}_k \dot{\theta}_k.$

Fig. 3.21: Table Recursive Algorithm for Velocities and Angular Velocities

3.4.2 Efficiency and Computational Cost

It is not necessary to form the entire matrix appearing in Equation (3.4.1) in practice. The recursive algorithm can be used in either symbolic or numerical calculations. It is efficient and fast. To help gauge the efficiency of the above algorithm in general terms, a few standard metrics of computational workload for typical tasks in linear algebra will be reviewed. One common unit of computational work is the *floating point operation*, or *flop*, which is defined as the computational work required to perform a multiplication of two real numbers and addition of two real numbers. Suppose that $c(N)$ is the computational cost of a given algorithm measured in flops. An algorithm is said to require on the order of the function $f(N)$, or $O(f(N))$, *flops* whenever

$$\lim_{N \rightarrow \infty} \frac{c(N)}{f(N)} = \text{constant} \quad (3.4.16)$$

For many common numerical tasks the function $f(N)$ is some polynomial of N . For example, it is easy to show that the dot product of two N -tuples requires on the order of N flops. The multiplication of a general, full $N \times N$ matrix times an N -tuple requires of the order of N^2 floating point operations. The solution of a set of N linear matrix equations, in comparison, requires of the order of N^3 floating point operations when the associated coefficient matrix is full. Additional discussion of computational workload can be found in [18], as well as specifications of cost for various common numerical algorithms.

This description gives information about the asymptotic cost of an algorithm as N becomes large. The value of the constant is of interest when making finer

comparisons of the computational workload. The recursive algorithm above requires on the order of N floating point operations. In other words, the computational cost grows like a linear function of the number of unknowns. This algorithm is one of the several variants of *recursive $O(N)$ formulations* of kinematics and dynamics for robotic systems. The reduction in computational workload that is afforded via recursive $O(N)$ formulations, in comparison to alternatives that require either the multiplication or inversion of full matrices, can be critical in applications involving the robotic system control. This topic will be discussed in further detail in Chapter (4).

Example 3.4.1. Use the recursive formulation summarized in Figure (3.22) to calculate the velocities and angular velocities of the two link robot shown in Figure (3.22) with link lengths of L .

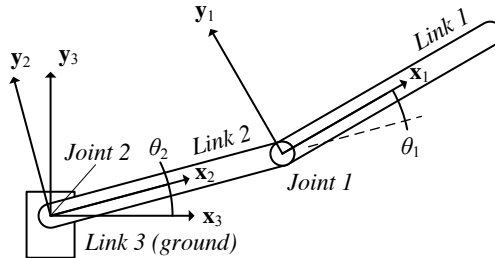


Fig. 3.22: Two Link Robotic Arm

Solution: From Figure (3.22) the rotation matrices that relate the bases for the frames 1,2 and 3 are

$$\begin{Bmatrix} \mathbf{x}_1 \\ \mathbf{y}_1 \\ \mathbf{z}_1 \end{Bmatrix} = \underbrace{\begin{bmatrix} \cos \theta_1 & \sin \theta_1 & 0 \\ -\sin \theta_1 & \cos \theta_1 & 0 \\ 0 & 0 & 1 \end{bmatrix}}_{\mathbf{R}_2^1} \begin{Bmatrix} \mathbf{x}_2 \\ \mathbf{y}_2 \\ \mathbf{z}_2 \end{Bmatrix} \quad \text{and} \quad \begin{Bmatrix} \mathbf{x}_2 \\ \mathbf{y}_2 \\ \mathbf{z}_2 \end{Bmatrix} = \underbrace{\begin{bmatrix} \cos \theta_2 & \sin \theta_2 & 0 \\ -\sin \theta_2 & \cos \theta_2 & 0 \\ 0 & 0 & 1 \end{bmatrix}}_{\mathbf{R}_3^2} \begin{Bmatrix} \mathbf{x}_3 \\ \mathbf{y}_3 \\ \mathbf{z}_3 \end{Bmatrix}.$$

Since all of the revolute joints are along the common $\mathbf{z}_1 = \mathbf{z}_2 = \mathbf{z}_3$ axis,

$$\mathbf{h}_1^1 = \begin{Bmatrix} 0 \\ 0 \\ 1 \end{Bmatrix} \quad \text{and} \quad \mathcal{H}_1 := \left\{ \mathbf{h}_1^1 \right\} = \left\{ \begin{Bmatrix} 0 \\ 0 \\ 0 \end{Bmatrix}, \begin{Bmatrix} 0 \\ 0 \\ 1 \end{Bmatrix} \right\},$$

$$\mathbf{h}_2^2 = \begin{Bmatrix} 0 \\ 0 \\ 1 \end{Bmatrix} \quad \text{and} \quad \mathcal{H}_2 := \begin{Bmatrix} \mathbf{0} \\ \mathbf{h}_2^2 \end{Bmatrix} = \begin{Bmatrix} \begin{Bmatrix} 0 \\ 0 \\ 0 \\ 0 \\ 0 \\ 1 \end{Bmatrix} \end{Bmatrix}.$$

The offset vectors that describe the relative position of the joints are obtained by inspection as

$$\mathbf{d}_{2,1}^2 = \begin{Bmatrix} L \\ 0 \\ 0 \end{Bmatrix} \quad \text{and} \quad \mathbf{d}_{3,2}^3 = \begin{Bmatrix} 0 \\ 0 \\ 0 \end{Bmatrix}.$$

These definitions aid in the construction of the constituent matrices that form the recursive equations. The transposed transition operator $\varphi_{2,1}^T$ and rotation matrix $\mathcal{R}_{2,1}^T$ are given by

$$\begin{aligned} \varphi_{2,1}^T &= \begin{bmatrix} \mathbb{I} & \mathbf{S}(\mathbf{d}_{1,2}^2) \\ \mathbf{0} & \mathbb{I} \end{bmatrix} = \begin{bmatrix} \begin{bmatrix} 1 & 0 & 0 \\ 0 & 1 & 0 \\ 0 & 0 & 1 \end{bmatrix} & \begin{bmatrix} 0 & 0 & 0 \\ 0 & 0 & L \\ 0 & -L & 0 \end{bmatrix} \\ \begin{bmatrix} 0 & 0 & 0 \\ 0 & 0 & 0 \\ 0 & 0 & 0 \end{bmatrix} & \begin{bmatrix} 1 & 0 & 0 \\ 0 & 1 & 0 \\ 0 & 0 & 1 \end{bmatrix} \end{bmatrix}, \\ \mathcal{R}_{2,1}^T &= \begin{bmatrix} (\mathbf{R}_1^2)^T & 0 \\ 0 & (\mathbf{R}_1^2)^T \end{bmatrix} = \begin{bmatrix} \mathbf{R}_2^1 & 0 \\ 0 & \mathbf{R}_2^1 \end{bmatrix}, \\ &= \begin{bmatrix} \begin{bmatrix} \cos\theta_1 & \sin\theta_1 & 0 \\ -\sin\theta_1 & \cos\theta_1 & 0 \\ 0 & 0 & 1 \end{bmatrix} & \begin{bmatrix} 0 & 0 & 0 \\ 0 & 0 & 0 \\ 0 & 0 & 0 \end{bmatrix} \\ \begin{bmatrix} 0 & 0 & 0 \\ 0 & 0 & 0 \\ 0 & 0 & 0 \end{bmatrix} & \begin{bmatrix} \cos\theta_1 & \sin\theta_1 & 0 \\ -\sin\theta_1 & \cos\theta_1 & 0 \\ 0 & 0 & 1 \end{bmatrix} \end{bmatrix}. \end{aligned}$$

For the two link system shown, $N = 2$. The resulting recursive equations for the velocities are

$$\begin{Bmatrix} \mathcal{V}_{1^-} \\ \mathcal{V}_{2^-} \end{Bmatrix} = \begin{bmatrix} \mathbf{0} & \mathcal{R}_{2,1}^T \varphi_{2,1}^T \\ \mathbf{0} & \mathbf{0} \end{bmatrix} \begin{Bmatrix} \mathcal{V}_{1^-} \\ \mathcal{V}_{2^-} \end{Bmatrix} + \begin{bmatrix} \mathcal{H}_1 & 0 \\ 0 & \mathcal{H}_2 \end{bmatrix} \begin{Bmatrix} \dot{\theta}_1 \\ \dot{\theta}_2 \end{Bmatrix}. \quad (3.4.17)$$

From the last block of this set of equations, it can be seen that

$$\mathcal{V}_{2^-} = \begin{Bmatrix} 0 \\ 0 \\ 0 \\ 0 \\ 0 \\ 1 \end{Bmatrix} \dot{\theta}_2.$$

Likewise, expressions for $\varphi_{2,1}^T \mathcal{V}_{2^-}$ and $\mathcal{R}_{2,1}^T \varphi_{2,1}^T \mathcal{V}_{2^-}$ may be calculated as

$$\varphi_{2,1}^T \mathcal{V}_{2^-} = \begin{Bmatrix} 0 \\ L \\ 0 \\ 0 \\ 0 \\ 1 \end{Bmatrix} \dot{\theta}_2 \quad \text{and} \quad \mathcal{R}_{2,1}^T \varphi_{2,1}^T \mathcal{V}_{2^-} = \begin{Bmatrix} L \sin \theta_1 \\ L \cos \theta_1 \\ 0 \\ 0 \\ 0 \\ 1 \end{Bmatrix} \dot{\theta}_2.$$

Using these expression, the velocities and angular velocities in \mathcal{V}_{1^-} may be calculated as

$$\mathcal{V}_{1^-} = \begin{Bmatrix} L \dot{\theta}_2 \sin \theta_1 \\ L \dot{\theta}_2 \cos \theta_1 \\ 0 \\ 0 \\ 0 \\ \dot{\theta}_2 \end{Bmatrix} + \begin{Bmatrix} 0 \\ 0 \\ 0 \\ 0 \\ 0 \\ 1 \end{Bmatrix} \dot{\theta}_1 = \begin{Bmatrix} L \dot{\theta}_2 \sin \theta_1 \\ L \dot{\theta}_2 \cos \theta_1 \\ 0 \\ 0 \\ 0 \\ \dot{\theta}_1 + \dot{\theta}_2 \end{Bmatrix}.$$

For this example, these calculations may be easily verified geometrically. Joint 2 does not move in the ground frame, therefore $\mathbf{v}_{3,2^-} = 0$ and $\boldsymbol{\omega}_{3,2^-} = \dot{\theta}_2 \mathbf{z}_2$, leading to

$$\mathcal{V}_{2^-} = \begin{Bmatrix} \mathbf{v}_{3,2^-}^2 \\ \boldsymbol{\omega}_{3,2^-} \end{Bmatrix} = \begin{Bmatrix} \begin{Bmatrix} 0 \\ 0 \\ 0 \\ 0 \\ 0 \\ \dot{\theta}_2 \end{Bmatrix} \\ \begin{Bmatrix} 0 \\ 0 \\ 0 \\ 0 \\ 0 \\ 1 \end{Bmatrix} \end{Bmatrix},$$

which matches the solution of the Equation (3.4.17) derived from the last row of the matrix equation.

From Theorem (2.16), the velocity of joint 1 is given by

$$\mathbf{v}_{3,1^-} = \underbrace{\mathbf{v}_{3,2^-}}_0 + \boldsymbol{\omega}_{3,2^-} \times L \mathbf{x}_2 = L \dot{\theta}_2 \mathbf{y}_2.$$

Using the rotation matrix \mathbf{R}_2^1 to calculate the components of this velocity in terms of the basis for the 1 frame results in

$$\mathbf{v}_{3,1^-}^1 = L \dot{\theta}_2 \begin{Bmatrix} \sin \theta_1 \\ \cos \theta_1 \\ 0 \end{Bmatrix}.$$

From the Addition Theorem (2.15), the angular velocity of link 1 is given by

$$\begin{aligned} \boldsymbol{\omega}_{3,1^-} &= \dot{\theta}_2 \mathbf{z}_2 + \dot{\theta}_1 \mathbf{z}_1 \\ &= (\dot{\theta}_1 + \dot{\theta}_2) \mathbf{z}_1, \end{aligned}$$

and it has components relative to the basis for the 1 frame given by

$$\boldsymbol{\omega}_{3,1^-}^1 = \begin{Bmatrix} 0 \\ 0 \\ \dot{\theta}_1 + \dot{\theta}_2 \end{Bmatrix}.$$

Assembling these two expressions into \mathcal{V}_{1^-} results in

$$\mathcal{V}_{1^-} = \begin{Bmatrix} \mathbf{v}_{3,1^-}^1 \\ \boldsymbol{\omega}_{3,1^-}^1 \end{Bmatrix} = \begin{Bmatrix} \begin{Bmatrix} L\dot{\theta}_2 \sin \theta_1 \\ L\dot{\theta}_2 \cos \theta_1 \\ 0 \\ 0 \\ 0 \\ \dot{\theta}_1 + \dot{\theta}_2 \end{Bmatrix} \\ \begin{Bmatrix} 0 \\ 0 \\ 0 \\ 0 \\ 0 \\ \dot{\theta}_1 + \dot{\theta}_2 \end{Bmatrix} \end{Bmatrix},$$

which matches the solution to Equation (3.4.17) for the vector \mathcal{V}_{1^-} associated with the first link.

3.4.3 Recursive Calculation of Acceleration and Angular Acceleration

This section derives recursive algorithms for calculating of the acceleration and angular acceleration of the bodies in a robot that form a kinematic chain. In Section (3.4.1) the velocities and angular velocities have been collected in the 6×1 arrays

$$\mathcal{V}_{k^-} := \begin{Bmatrix} \mathbf{v}_{b,k^-}^k \\ \boldsymbol{\omega}_{b,k^-}^k \end{Bmatrix} \quad \text{and} \quad \mathcal{V}_{k^+} := \begin{Bmatrix} \mathbf{v}_{b,k^+}^{k+1} \\ \boldsymbol{\omega}_{b,k^+}^{k+1} \end{Bmatrix}.$$

In this section the following derivatives of the velocities *with respect to the link frame k* will be considered as the unknowns in the recursive formulation

$$\mathcal{A}_{k^-} := \left\{ \frac{d}{dt} \Big|_k (\mathbf{v}_{b,k^-}) \right\} \quad \text{and} \quad \mathcal{A}_{k^+} := \left\{ \frac{d}{dt} \Big|_{k+1} (\mathbf{v}_{b,k^+}) \right\}.$$

It is assumed that the vectors \mathcal{A}_{k^-} and \mathcal{A}_{k^+} have been written in terms of components relative to the frame k and $k+1$, respectively. The $(\cdot)^k$ and $(\cdot)^{k+1}$ notation that describes the basis used to define the components is suppressed in these definitions.

The entries in the vectors \mathcal{A}_{k^-} and \mathcal{A}_{k^+} do not contain the linear accelerations \mathbf{a}_{b,k^-} and \mathbf{a}_{b,k^+} of the points k^- and k^+ in the base frame. In most applications these accelerations $\mathbf{a}_{b,k^-}, \mathbf{a}_{b,k^+}$ in the base frame are the primary focus of the analysis, not the accelerations in the body fixed frames. However, the linear accelerations in the base frame can be calculated from the entries in \mathcal{A}_{k^-} and \mathcal{A}_{k^+} . The Derivative

Theorem (2.12) results in

$$\begin{aligned}\mathbf{a}_{b,k^-} &= \frac{d}{dt} \Big|_b (\mathbf{v}_{b,k^-}) = \frac{d}{dt} \Big|_k (\mathbf{v}_{b,k^-}) + \boldsymbol{\omega}_{b,k^-} \times \mathbf{v}_{b,k^-}, \\ \mathbf{a}_{b,k^+} &= \frac{d}{dt} \Big|_b (\mathbf{v}_{b,k^+}) = \frac{d}{dt} \Big|_{k+1} (\mathbf{v}_{b,k^+}) + \boldsymbol{\omega}_{b,k^+} \times \mathbf{v}_{b,k^+}.\end{aligned}$$

However, the vectors \mathcal{A}_{k^-} and \mathcal{A}_{k^+} do contain the angular accelerations in the base frame of the links k and $k+1$, since by definition

$$\begin{aligned}\boldsymbol{\alpha}_{b,k^-} &= \frac{d}{dt} \Big|_b (\boldsymbol{\omega}_{b,k^-}) = \frac{d}{dt} \Big|_k (\boldsymbol{\omega}_{b,k^-}) + \underbrace{\boldsymbol{\omega}_{b,k^-} \times \boldsymbol{\omega}_{b,k^-}}_0, \\ \boldsymbol{\alpha}_{b,k^+} &= \frac{d}{dt} \Big|_b (\boldsymbol{\omega}_{b,k^+}) = \frac{d}{dt} \Big|_{k+1} (\boldsymbol{\omega}_{b,k^+}) + \underbrace{\boldsymbol{\omega}_{b,k^+} \times \boldsymbol{\omega}_{b,k^+}}_0.\end{aligned}$$

These calculations can be organized into a pair of 6×1 vectors as follows once the derivatives of velocities \mathcal{A}_{k^-} and \mathcal{A}_{k^+} are known

$$\begin{aligned}\left\{ \begin{array}{l} \mathbf{a}_{b,k^-}^k \\ \boldsymbol{\alpha}_{b,k^-}^k \end{array} \right\} &= \mathcal{A}_{k^-} + \left\{ \begin{array}{l} \boldsymbol{\omega}_{b,k^-}^k \times \mathbf{v}_{b,k^-}^k \\ \mathbf{0} \end{array} \right\}, \\ \left\{ \begin{array}{l} \mathbf{a}_{b,k^+}^{k+1} \\ \boldsymbol{\alpha}_{b,k^+}^{k+1} \end{array} \right\} &= \mathcal{A}_{k^+} + \left\{ \begin{array}{l} \boldsymbol{\omega}_{b,k^+}^{k+1} \times \mathbf{v}_{b,k^+}^{k+1} \\ \mathbf{0} \end{array} \right\}.\end{aligned}$$

A set of matrix equations analogous to those presented in Theorem (3.4) can be obtained for the derivatives of the velocities and angular velocities of a kinematic chain. These algorithms can be derived using the matrix equation given in the following theorem.

Theorem 3.5 (Recursive Velocity and Angular Velocity Derivatives). *The derivatives of the velocities $\{\mathcal{A}_{k^-}\}_{k=1,\dots,N}$ of the N -link kinematic chain depicted in Figures (3.19) and (3.20) satisfy the equation*

$$\left\{ \begin{array}{c} \mathcal{A}_{1^-} \\ \mathcal{A}_{2^-} \\ \mathcal{A}_{3^-} \\ \vdots \\ \mathcal{A}_{N-1^-} \\ \mathcal{A}_{N^-} \end{array} \right\} = \left[\begin{array}{cccccc} 0 & \mathcal{R}_{2,1}^T \varphi_{2,1}^T & 0 & \cdots & 0 & 0 \\ 0 & 0 & \mathcal{R}_{3,2}^T \varphi_{3,2}^T & \cdots & 0 & 0 \\ \vdots & \vdots & \vdots & \ddots & \vdots & \vdots \\ 0 & 0 & 0 & \cdots & 0 & \mathcal{R}_{N,N-1}^T \varphi_{N,N-1}^T \\ 0 & 0 & 0 & \cdots & 0 & 0 \end{array} \right] \left\{ \begin{array}{c} \mathcal{A}_{1^-} \\ \mathcal{A}_{2^-} \\ \mathcal{A}_{3^-} \\ \vdots \\ \mathcal{A}_{N-1^-} \\ \mathcal{A}_{N^-} \end{array} \right\} \quad (3.4.18)$$

$$+ \left[\begin{array}{ccccc} \mathcal{H}_1 & 0 & 0 & \cdots & 0 & 0 \\ 0 & \mathcal{H}_2 & 0 & \cdots & 0 & 0 \\ 0 & 0 & \mathcal{H}_3 & \cdots & 0 & 0 \\ \vdots & \vdots & \vdots & \ddots & \vdots & \vdots \\ 0 & 0 & 0 & \cdots & \mathcal{H}_{N-1} & 0 \\ 0 & 0 & 0 & \cdots & 0 & \mathcal{H}_N \end{array} \right] \left\{ \begin{array}{c} \dot{\theta}_1 \\ \dot{\theta}_2 \\ \dot{\theta}_3 \\ \vdots \\ \dot{\theta}_{N-1} \\ \dot{\theta}_N \end{array} \right\} + \left\{ \begin{array}{c} \mathcal{N}_1 \\ \mathcal{N}_2 \\ \mathcal{N}_3 \\ \vdots \\ \mathcal{N}_{N-1} \\ \mathcal{N}_N \end{array} \right\} \quad (3.4.19)$$

where $\varphi_{k,k-1}^T$ is given in Equation (3.4.9), $\mathcal{R}_{k-1,k}$ is given in Equation (3.4.13), \mathcal{H}_k is given in Equation (3.4.13) and \mathcal{N}_k is given in Equation (3.4.29) for $k = 1 \dots N$.

Proof. The derivative while holding the basis for frame k constant of the velocity

$$\mathbf{v}_{b,(k-1)^+} = \mathbf{v}_{b,k^-} + \boldsymbol{\omega}_{b,k^-} \times \mathbf{d}_{k,k-1} \quad (3.4.20)$$

is equal to

$$\begin{aligned} \frac{d}{dt} \Big|_k (\mathbf{v}_{b,(k-1)^+}) &= \frac{d}{dt} \Big|_k (\mathbf{v}_{b,k^-}) + \frac{d}{dt} \Big|_k (\boldsymbol{\omega}_{b,k^-} \times \mathbf{d}_{k,k-1}), \\ &= \frac{d}{dt} \Big|_k (\mathbf{v}_{b,k^-}) - \mathbf{d}_{k,k-1} \times \frac{d}{dt} \Big|_k (\boldsymbol{\omega}_{b,k^-}) + \boldsymbol{\omega}_{b,k^-} \times \underbrace{\frac{d}{dt} \Big|_k ((\mathbf{d}_{k,k-1}))}_0. \end{aligned} \quad (3.4.21)$$

A similar calculation starting with the angular velocity

$$\boldsymbol{\omega}_{b,k^-} = \boldsymbol{\omega}_{b,k^+} + \boldsymbol{\omega}_{k^+,k^-} = \boldsymbol{\omega}_{b,k^+} + \boldsymbol{\omega}_{k+1,k} = \boldsymbol{\omega}_{b,k^+} + \mathbf{h}_k \dot{\theta}_k \quad (3.4.22)$$

yields

$$\frac{d}{dt} \Big|_k (\boldsymbol{\omega}_{b,k^-}) = \frac{d}{dt} \Big|_k (\boldsymbol{\omega}_{b,k^+}) + \frac{d}{dt} \Big|_k (\mathbf{h}_k \dot{\theta}_k). \quad (3.4.23)$$

This last equation is needed in recursive form. The derivative $\frac{d}{dt} \Big|_k (\boldsymbol{\omega}_{b,k^+})$ on the right hand side of Equation (3.4.23) needs to be replaced with $\frac{d}{dt} \Big|_{k+1} (\boldsymbol{\omega}_{b,k^+})$.

These two derivatives may be related by the expression

$$\frac{d}{dt}\Big|_k (\boldsymbol{\omega}_{b,k^+}) = \frac{d}{dt}\Big|_{k+1} (\boldsymbol{\omega}_{b,k^+}) + \boldsymbol{\omega}_{k,k+1} \times \boldsymbol{\omega}_{b,k^+} = \frac{d}{dt}\Big|_{k+1} (\boldsymbol{\omega}_{b,k^+}) + (-\mathbf{h}_k \dot{\theta}_k) \times \boldsymbol{\omega}_{b,k^+}. \quad (3.4.24)$$

Combining Equations (3.4.22) and (3.4.24) yields

$$\begin{aligned} \frac{d}{dt}\Big|_k (\boldsymbol{\omega}_{b,k^-}) &= \frac{d}{dt}\Big|_{k+1} (\boldsymbol{\omega}_{b,k^+}) + \mathbf{h}_k \ddot{\theta}_k + (-\mathbf{h}_k \dot{\theta}_k) \times (\boldsymbol{\omega}_{b,k^-} - \mathbf{h}_k \dot{\theta}_k), \\ &= \frac{d}{dt}\Big|_{k+1} (\boldsymbol{\omega}_{b,k^+}) + \mathbf{h}_k \ddot{\theta}_k + (-\mathbf{h}_k \dot{\theta}_k) \times \boldsymbol{\omega}_{b,k^+}. \end{aligned} \quad (3.4.25)$$

All of the Equations (3.4.20) through (3.4.25) are vector equations; any convenient basis to represent the vectors in these equations may be used. By convention in the recursive formulation, the basis for the frame k is used for terms labeled $(k-1)^+$ or k^- . This implies that the basis for the frame $k+1$ is used for terms labeled k^+ . When Equations (3.4.21) and (3.4.25) are assembled, the result is

$$\left\{ \begin{array}{l} \frac{d}{dt}\Big|_k (\mathbf{v}_{b,(k-1)^+}) \\ \frac{d}{dt}\Big|_k (\boldsymbol{\omega}_{b,(k-1)^+}) \end{array} \right\} = \begin{bmatrix} \mathbb{I} & -\mathbf{S}(\mathbf{d}_{k,k-1}^k) \\ 0 & \mathbb{I} \end{bmatrix} \left\{ \begin{array}{l} \frac{d}{dt}\Big|_k (\mathbf{v}_{b,k^-}) \\ \frac{d}{dt}\Big|_k (\boldsymbol{\omega}_{b,k^-}) \end{array} \right\}. \quad (3.4.26)$$

Introducing the vectors $\mathcal{A}_{(k-1)^+}$ and \mathcal{A}_{k^-} results in

$$\mathcal{A}_{(k-1)^+} = \left\{ \begin{array}{l} \frac{d}{dt}\Big|_k (\mathbf{v}_{b,(k-1)^+}) \\ \frac{d}{dt}\Big|_k (\boldsymbol{\omega}_{b,(k-1)^+}) \end{array} \right\} \quad \text{and} \quad \mathcal{A}_{k^-} = \left\{ \begin{array}{l} \frac{d}{dt}\Big|_k (\mathbf{v}_{b,k^-}) \\ \frac{d}{dt}\Big|_k (\boldsymbol{\omega}_{b,k^-}) \end{array} \right\},$$

and this equation becomes

$$\mathcal{A}_{(k-1)^+} = \varphi_{k,k-1}^T \mathcal{A}_{k^-}. \quad (3.4.27)$$

An equation that relates $\mathcal{A}_{(k-1)^+}$ and \mathcal{A}_{k^-} requires the additional derivatives

$$\begin{aligned} \frac{d}{dt}\Big|_k (\mathbf{v}_{b,k^-}) &= \frac{d}{dt}\Big|_k (\mathbf{v}_{b,k^+}) = \frac{d}{dt}\Big|_{k+1} (\mathbf{v}_{b,k^+}) + \boldsymbol{\omega}_{k,k+1} \times \mathbf{v}_{b,k^+} \\ &= \frac{d}{dt}\Big|_{k+1} (\mathbf{v}_{b,k^+}) + (-\mathbf{h}_k \dot{\theta}_k) \times \mathbf{v}_{b,k^+} \end{aligned} \quad (3.4.28)$$

Equations (3.4.25) and (3.4.28) may be combined to obtain

$$\begin{aligned} \left\{ \begin{array}{l} \frac{d}{dt}\Big|_k (\mathbf{v}_{b,k^-}) \\ \frac{d}{dt}\Big|_k (\boldsymbol{\omega}_{b,k^-}) \end{array} \right\} &= \begin{bmatrix} \mathbf{R}_{k+1}^k & \mathbf{0} \\ \mathbf{0} & \mathbf{R}_{k+1}^k \end{bmatrix} \left\{ \begin{array}{l} \frac{d}{dt}\Big|_{k+1} (\mathbf{v}_{b,k^+}) \\ \frac{d}{dt}\Big|_{k+1} (\boldsymbol{\omega}_{b,k^+}) \end{array} \right\} \\ &+ \left\{ \begin{array}{l} \mathbf{0} \\ \mathbf{h}_k^k \end{array} \right\} \ddot{\theta}_k + \left\{ \begin{array}{l} -\mathbf{h}_k^k \dot{\theta}_k \times \mathbf{v}_{b,k^+} \\ -\mathbf{h}_k^k \dot{\theta}_k \times \boldsymbol{\omega}_{b,k^-} \end{array} \right\}, \end{aligned}$$

which may be written in compact matrix form as

$$\mathcal{A}_{k^-} = \mathcal{R}_{k,k+1} \mathcal{A}_{k^+} + \mathcal{H}_k \ddot{\theta}_k + \mathcal{N}_k,$$

where

$$\mathcal{N}_k = \begin{Bmatrix} -\mathbf{h}_k^k \dot{\theta}_k \times \mathbf{v}_{b,k^+}^k \\ -\mathbf{h}_k^k \dot{\theta}_k \times \boldsymbol{\omega}_{b,k^+}^k \end{Bmatrix} = \begin{Bmatrix} -\mathbf{h}_k^k \dot{\theta}_k \times \mathbf{v}_{b,k^-}^k \\ -\mathbf{h}_k^k \dot{\theta}_k \times \boldsymbol{\omega}_{b,k^-}^k \end{Bmatrix} = \begin{bmatrix} -\mathbf{S}(\mathbf{h}_k^k \dot{\theta}_k) & \mathbf{0} \\ \mathbf{0} & -\mathbf{S}(\mathbf{h}_k^k \dot{\theta}_k) \end{bmatrix} \mathcal{V}_{k^-}. \quad (3.4.29)$$

Equations (3.4.27) and (3.4.29) may be combined to obtain

$$\mathcal{A}_{k^-} = \mathcal{R}_{k+1,k}^T \varphi_{k+1,k}^T \mathcal{A}_{(k+1)^-} + \mathcal{H}_k \ddot{\theta}_k + \mathcal{N}_k$$

or equivalently

$$\mathcal{A}_{k^-} = \phi_{k+1,k}^T \mathcal{A}_{(k+1)^-} + \mathcal{H}_k \ddot{\theta}_k + \mathcal{N}_k \quad (3.4.30)$$

Equation (3.4.18) results when Equation (3.4.30) is expressed for each joint $k = 1, \dots, N$ and the equations are collected in matrix form. Finally, once the derivatives of the velocity and angular velocity have been calculated, the accelerations and angular accelerations of the links in the base frame may be determined from the following identities,

$$\begin{aligned} \mathbf{a}_{b,k^-} &= \frac{d}{dt} \Big|_b (\mathbf{v}_{b,k^-}), \\ &= \frac{d}{dt} \Big|_k (\mathbf{v}_{b,k^-}) + \boldsymbol{\omega}_{b,k^-} \times \mathbf{v}_{b,k^-}, \end{aligned}$$

$$\begin{aligned} \boldsymbol{\alpha}_{b,k^-} &= \frac{d}{dt} \Big|_b (\boldsymbol{\omega}_{b,k^-}), \\ &= \frac{d}{dt} \Big|_k (\boldsymbol{\omega}_{b,k^-}) + \boldsymbol{\omega}_{b,k^-} \times \boldsymbol{\omega}_{b,k^-}, \\ &= \frac{d}{dt} \Big|_k (\boldsymbol{\omega}_{b,k^-}). \end{aligned}$$

□

It is important to note that the coefficient matrix

$$\left[\begin{array}{ccccc} 0 & \mathcal{R}_{2,1}^T \varphi_{2,1}^T & 0 & \cdots & 0 \\ 0 & 0 & \mathcal{R}_{3,2}^T \varphi_{3,2}^T & \cdots & 0 \\ 0 & 0 & 0 & \cdots & 0 \\ \vdots & \vdots & \vdots & \ddots & \vdots \\ 0 & 0 & 0 & \cdots & 0 \\ 0 & 0 & 0 & \cdots & 0 \end{array} \right] \quad (3.4.31)$$

on the right side of the Equation (3.4.31) is identical to that in Equation (3.4.1). It is the structure of this matrix that enables a recursive calculation of the derivatives of the velocities. Suppose the joint rates $\dot{\theta}_1, \dot{\theta}_2, \dots, \dot{\theta}_N$ and the joint accelerations

$\dot{\theta}_1, \dot{\theta}_2, \dots, \dot{\theta}_N$ are given; the associated velocities and angular velocities for the kinematic chain may be calculated using the recursive algorithm from Figure (3.20). Then, using these results, the derivatives of the velocity may be calculated. The last row in Equation (3.4.18) does not depend on the other rows, enabling the solution of the equation $\mathcal{A}_{N^-} = \mathcal{H}_N \ddot{\theta}_N + \mathcal{N}_N$ for \mathcal{A}_{N^-} .

All of the terms on the right hand side of this equation are known. For example, the equation

$$\mathcal{N}_N = \begin{Bmatrix} -\mathbf{h}_N^N \dot{\theta}_N \times \mathbf{v}_{b,N^+} \\ -\mathbf{h}_N^N \dot{\theta}_N \times \boldsymbol{\omega}_{b,N^+} \end{Bmatrix} = \begin{bmatrix} -\mathbf{S}(\mathbf{h}_N^N \dot{\theta}_N) & 0 \\ 0 & -\mathbf{S}(\mathbf{h}_N^N \dot{\theta}_N) \end{bmatrix} \begin{Bmatrix} \mathbf{v}_{b,N^+}^N \\ \boldsymbol{\omega}_{b,N^+}^N \end{Bmatrix}$$

may be evaluated immediately since the velocity of the base body is assumed to be given; it is equal to zero when the base $b = N + 1$ is stationary.

Next, $\mathcal{A}_{(N-1)^-}$ is calculated from the equation $\mathcal{A}_{(N-1)^-} = \phi_{N,N-1}^T \mathcal{A}_{N^-} + \mathcal{H}_{N-1} \ddot{\theta}_{N-1} + \mathcal{N}_{N-1}$, so that

$$\mathcal{A}_{(N-1)^-} = \phi_{N,N-1}^T \mathcal{A}_{N^-} + \mathcal{H}_{N-1} \ddot{\theta}_{N-1} + \begin{Bmatrix} -\mathbf{h}_{N-1}^{N-1} \dot{\theta}_{N-1} \times \mathbf{v}_{b,(N-1)^+}^{N-1} \\ \mathbf{h}_{N-1}^{N-1} \dot{\theta}_{N-1} \times \boldsymbol{\omega}_{b,(N-1)^+}^{N-1} \end{Bmatrix}.$$

As before, the right hand side of this equation is known since the velocities and angular velocities have already been solved for, along with \mathcal{A}_{N^-} . The algorithm continues recursively from the inboard to the outboard joints, until all the derivatives of velocity $\mathcal{A}_{N^-}, \mathcal{A}_{(N-1)^-}, \dots, \mathcal{A}_{1^-}$ are known. These steps are summarized in Figure (3.23).

Recursive Algorithm for Derivatives of Velocity and Angular Velocity

- 1) Find the velocities and angular velocities using the algorithm in Section (3.4.1).
- 2) Iterate from inboard to outboard joints for $k = N, N-1 \dots 2, 1$, do the following:

- 2.1) Form the transposed position operator

$$\phi_{k,k-1}^T = \mathcal{R}_{k,k-1}^T \varphi_{k,k-1}^T$$

- 2.2) Calculate the bias acceleration

$$\mathcal{N}_k = \begin{Bmatrix} -\mathbf{h}_k^k \dot{\theta}_k \times \mathbf{v}_{b,k^+} \\ -\mathbf{h}_k^k \dot{\theta}_k \times \boldsymbol{\omega}_{b,k^+} \end{Bmatrix} = \begin{bmatrix} -\mathbf{S}(\mathbf{h}_k^k \dot{\theta}_k) & \mathbf{0} \\ \mathbf{0} & -\mathbf{S}(\mathbf{h}_k^k \dot{\theta}_k) \end{bmatrix} \mathcal{V}_{k^-}$$

- 2.3) Calculate the derivative of the velocity

$$\mathcal{A}_{k^-} = \phi_{k+1,k}^T \mathcal{A}_{(k+1)^-} + \mathcal{H}_k \ddot{\theta}_k + \mathcal{N}_k$$

- 2.4) Calculate the accelerations and angular accelerations in the base frame.

$$\begin{Bmatrix} \mathbf{a}_{b,k^-}^k \\ \boldsymbol{\alpha}_{b,k^-}^k \end{Bmatrix} = \mathcal{A}_{k^-} + \begin{Bmatrix} \boldsymbol{\omega}_{b,k^-}^k \times \mathbf{v}_{b,k^-}^k \\ \mathbf{0} \end{Bmatrix}$$

Fig. 3.23: Recursive Algorithm for Calculation of Accelerations and Angular Accelerations

Example 3.4.2. Use the recursive algorithm to solve for the derivative of the velocities for the two link robotic arm depicted in Figure (3.22) with a link length of L . Check the solutions by direct calculation from first principles.

Solution: Example (3.4.1) already derives $\varphi_{2,1}^T$ and $\mathcal{R}_{2,1}^T$. The general form of the equations of recursion for the derivatives of the velocities can be written as

$$\begin{Bmatrix} \mathcal{A}_{1^-} \\ \mathcal{A}_{2^-} \end{Bmatrix} = \begin{bmatrix} \mathbf{0} & \mathcal{R}_{2,1}^T \varphi_{2,1}^T \\ \mathbf{0} & \mathbf{0} \end{bmatrix} \begin{Bmatrix} \mathcal{A}_{1^-} \\ \mathcal{A}_{2^-} \end{Bmatrix} + \begin{bmatrix} \mathcal{H}_1 & \mathbf{0} \\ \mathbf{0} & \mathcal{H}_2 \end{bmatrix} \begin{Bmatrix} \ddot{\theta}_1 \\ \ddot{\theta}_2 \end{Bmatrix} + \begin{Bmatrix} \mathcal{N}_1 \\ \mathcal{N}_2 \end{Bmatrix}. \quad (3.4.32)$$

Each of the vectors \mathcal{N}_k for $k = 1, 2$ is defined to be

$$\mathcal{N}_k = \begin{Bmatrix} (-\mathbf{h}_k^k \dot{\theta}_k) \times \mathbf{v}_{3,k^+} \\ (-\mathbf{h}_k^k \dot{\theta}_k) \times \boldsymbol{\omega}_{3,k^+} \end{Bmatrix} = \begin{Bmatrix} (-\mathbf{h}_k^k \dot{\theta}_k) \times \mathbf{v}_{3,k^-} \\ (-\mathbf{h}_k^k \dot{\theta}_k) \times \boldsymbol{\omega}_{3,k^-} \end{Bmatrix} = \begin{bmatrix} -\mathbf{S}(\mathbf{h}_k^k \dot{\theta}_k) & \mathbf{0} \\ \mathbf{0} & -\mathbf{S}(\mathbf{h}_k^k \dot{\theta}_k) \end{bmatrix} \mathcal{V}_{k^-}.$$

The validity of these equations may be verified by deriving the derivative of the velocities directly. Starting at the joint nearest the root, for which $k = 2$, by definition

$$\mathcal{A}_{2^-} := \left\{ \frac{d}{dt} \Big|_2 ((\mathbf{v}_{3,2^-})) \right\} = \left\{ \frac{d}{dt} \Big|_3 ((\mathbf{v}_{3,2^-})) + \underbrace{\omega_{2,3} \times \mathbf{v}_{3,2^-}}_0 \right\} = \left\{ \mathbf{a}_{3,2^-}^2 \right\} + \left\{ \omega_{2,3}^2 \times \mathbf{v}_{3,2^-}^2 \right\}.$$

However, $\mathbf{a}_{3,2^-} = \mathbf{v}_{3,2^-} = \mathbf{0}$ for all time since joint 2 is fixed in the base frame. Also, it is known that $\omega_{3,2^-} = \dot{\theta}_2 \mathbf{z}_2 = \dot{\theta}_2 \mathbf{z}_3$ from which it follows that $\alpha_{3,2^-} = \frac{d}{dt} \Big|_3 ((\omega_{3,2^-})) = \ddot{\theta}_2 \mathbf{z}_3$. Collecting these into \mathcal{A}_{2^-} results in

$$\mathcal{A}_{2^-} := \begin{Bmatrix} 0 \\ 0 \\ 0 \\ 0 \\ 0 \\ \ddot{\theta}_2 \end{Bmatrix}. \quad (3.4.33)$$

This is precisely the solution of the last row of the matrix Equation (3.4.32). To illustrate this, for $k = 2$ the vector \mathcal{N}_2 is given by

$$\mathcal{N}_2 = \mathbf{0} = \begin{Bmatrix} (-\mathbf{h}_2^2 \dot{\theta}_2) \times \mathbf{v}_{3,2^-} \\ \underbrace{0}_0 \\ (-\mathbf{h}_2^2 \dot{\theta}_2) \times (\mathbf{h}_2^2 \ddot{\theta}_2) \end{Bmatrix}, \quad (3.4.34)$$

and the following solution is obtained for \mathcal{A}_{2^-} when $\mathcal{N}_2 = \mathbf{0}$ is substituted from above, such that

$$\mathcal{A}_{2^-} := \mathcal{H}_2 \ddot{\theta}_2 + \mathcal{N}_2 = \begin{Bmatrix} 0 \\ 0 \\ 0 \\ 0 \\ 0 \\ 1 \end{Bmatrix} \ddot{\theta}_2 + \begin{Bmatrix} 0 \\ 0 \\ 0 \\ 0 \\ 0 \\ 0 \end{Bmatrix}$$

which is the Equation (3.4.33).

Next, the derivatives of the velocity and angular velocity for $k = 1$ will be calculated. By definition,

$$\mathcal{A}_{1^-} := \left\{ \frac{d}{dt} \Big|_1 ((\mathbf{v}_{3,1^-})) \right\}.$$

The velocity of joint 1 has been calculated in Example (3.4.1) as

$$\mathbf{v}_{3,1^-} = L \dot{\theta}_2 \mathbf{y}_2.$$

The derivative Theorem in (2.12) can be used to obtain

$$\begin{aligned}\frac{d}{dt} \Big|_1 (L\dot{\theta}_2 \mathbf{y}_2) &= \frac{d}{dt} \Big|_2 (L\dot{\theta}_2 \mathbf{y}_2) + \underbrace{\boldsymbol{\omega}_{1,2} \times (L\dot{\theta}_2 \mathbf{y}_2)}_{(-\dot{\theta}_1 \mathbf{z}_1)}, \\ &= L\ddot{\theta}_2 \mathbf{y}_2 + L\dot{\theta}_1 \dot{\theta}_2 \mathbf{x}_2.\end{aligned}$$

The rotation matrix \mathbf{R}_2^1 can be used to calculate the components of this vector relative to the basis for the 1 frame,

$$\left(\frac{d}{dt} \Big|_1 (\mathbf{v}_{3,1^-}) \right)^1 = L\dot{\theta}_1 \dot{\theta}_2 \begin{Bmatrix} \cos \theta_1 \\ -\sin \theta_1 \\ 0 \end{Bmatrix} + L\ddot{\theta}_2 \begin{Bmatrix} \sin \theta_1 \\ \cos \theta_1 \\ 0 \end{Bmatrix}.$$

The angular velocity $\boldsymbol{\omega}_{3,1^-}$ can be differentiated directly to get

$$\frac{d}{dt} \Big|_1 ((\mathbf{v}_{3,1^-})) = \frac{d}{dt} \Big|_1 ((\dot{\theta}_1 + \dot{\theta}_2) \mathbf{z}_1) = (\ddot{\theta}_1 + \ddot{\theta}_2) \mathbf{z}_1,$$

or

$$\left(\frac{d}{dt} \Big|_1 (\boldsymbol{\omega}_{3,1^-}) \right)^1 = \begin{Bmatrix} 0 \\ 0 \\ \ddot{\theta}_1 + \ddot{\theta}_2 \end{Bmatrix}.$$

Collecting these results into the formulation for \mathcal{A}_{1^-} results in

$$\mathcal{A}_{1^-} = \begin{Bmatrix} L\dot{\theta}_1 \dot{\theta}_2 \begin{Bmatrix} \cos \theta_1 \\ -\sin \theta_1 \\ 0 \end{Bmatrix} + L\ddot{\theta}_2 \begin{Bmatrix} \sin \theta_1 \\ \cos \theta_1 \\ 0 \end{Bmatrix} \\ \begin{Bmatrix} 0 \\ 0 \\ \ddot{\theta}_1 + \ddot{\theta}_2 \end{Bmatrix} \end{Bmatrix}.$$

It will be shown that this expression for \mathcal{A}_{1^-} follows from the general form in Equation (3.4.32). In Equation (3.4.32), the top row can be extracted to yield

$$\mathcal{A}_{1^-} = \mathcal{R}_{2,1}^T \boldsymbol{\varphi}_{2,1}^T \mathcal{V}_{2^-} + \mathcal{H}_1 \ddot{\theta}_1 + \mathcal{N}_1.$$

The nonlinear term \mathcal{N}_1 is evaluated to be

$$\mathcal{N}_1 = \begin{Bmatrix} -\mathbf{h}_1^1 \dot{\theta}_1 \times \mathbf{v}_{3,1^-} \\ -\mathbf{h}_1^1 \dot{\theta}_1 \times \boldsymbol{\omega}_{3,1^-} \end{Bmatrix} = \begin{Bmatrix} -\begin{Bmatrix} 0 \\ 0 \\ 1 \end{Bmatrix} \dot{\theta}_1 \times \begin{Bmatrix} \sin \theta_1 \\ \cos \theta_1 \\ 0 \end{Bmatrix} L\dot{\theta}_2 \\ -\begin{Bmatrix} 0 \\ 0 \\ 1 \end{Bmatrix} \dot{\theta}_1 \times \begin{Bmatrix} 0 \\ 0 \\ \dot{\theta}_1 + \dot{\theta}_2 \end{Bmatrix} L\dot{\theta}_2 \end{Bmatrix} = \begin{Bmatrix} L\dot{\theta}_1 \dot{\theta}_2 \begin{Bmatrix} \cos \theta_1 \\ -\sin \theta_1 \\ 0 \end{Bmatrix} \\ \begin{Bmatrix} 0 \\ 0 \\ 0 \end{Bmatrix} \end{Bmatrix}.$$

Substituting the expression for \mathcal{N}_1 into \mathcal{A}_{1^-} results in

$$\begin{aligned}\mathcal{A}_{1^-} &= \left[\begin{bmatrix} \cos\theta_1 & \sin\theta_1 & 0 \\ -\sin\theta_1 & \cos\theta_1 & 0 \\ 0 & 0 & 1 \end{bmatrix} \quad \begin{bmatrix} 0 & 0 & 0 \\ 0 & 0 & 0 \\ 0 & 0 & 0 \end{bmatrix} \right] \left[\begin{bmatrix} 1 & 0 & 0 \\ 0 & 1 & 0 \\ 0 & 0 & 1 \end{bmatrix} \quad \begin{bmatrix} 0 & 0 & 0 \\ 0 & 0 & L \\ 0 & -L & 0 \end{bmatrix} \right] \left[\begin{bmatrix} 0 \\ 0 \\ 0 \end{bmatrix} \quad \begin{bmatrix} 0 \\ 0 \\ 0 \end{bmatrix} \right] + \begin{bmatrix} 0 \\ 0 \\ 0 \end{bmatrix} + \mathcal{N}_1, \\ &= \left\{ \begin{bmatrix} L\ddot{\theta}_2 \sin\theta_1 \\ L\ddot{\theta}_2 \cos\theta_1 \\ 0 \\ 0 \\ 0 \\ \ddot{\theta}_2 \end{bmatrix} + \begin{bmatrix} 0 \\ 0 \\ 0 \\ 0 \\ 0 \\ \ddot{\theta}_1 \end{bmatrix} + \begin{bmatrix} L\dot{\theta}_1\dot{\theta}_2 \cos\theta_1 \\ -L\dot{\theta}_1\dot{\theta}_2 \sin\theta_1 \\ 0 \\ 0 \\ 0 \\ 0 \end{bmatrix} \right\} = \left\{ \begin{bmatrix} L\ddot{\theta}_2 \sin\theta_1 + L\dot{\theta}_1\dot{\theta}_2 \cos\theta_1 \\ L\ddot{\theta}_2 \cos\theta_1 - L\dot{\theta}_1\dot{\theta}_2 \sin\theta_1 \\ 0 \\ 0 \\ 0 \\ \ddot{\theta}_1 + \ddot{\theta}_2 \end{bmatrix} \right\}.\end{aligned}$$

The same result was obtained when \mathcal{A}_1^- was calculated from first principles.

As noted in the discussion of recursive accelerations, the entries in \mathcal{A}_k^- are not usually of interest in applications themselves, but can be used in the calculation of quantities of practical interest. Next, the accelerations and angular accelerations of interest will be calculated. First, the accelerations of the points 1⁻ and 2⁻ can be calculated from first principles. Since the point 2⁻ does not move with respect to the base frame, $\mathbf{a}_{3,2^-} = \mathbf{0}$. Alternatively, the angular acceleration in the base frame of the 2 frame is

$$\boldsymbol{\alpha}_{3,2^-} = \frac{d}{dt} \Big|_3 (\dot{\theta}_2 \mathbf{z}_3) = \ddot{\theta}_2 \mathbf{z}_3 = \ddot{\theta}_2 \mathbf{z}_2.$$

The acceleration and angular accelerations for link 2 are consequently

$$\left\{ \begin{array}{l} \mathbf{a}_{3,2^-}^2 \\ \boldsymbol{\alpha}_{3,2^-}^2 \end{array} \right\} = \left\{ \begin{array}{l} \begin{pmatrix} 0 \\ 0 \\ 0 \\ 0 \\ 0 \\ \ddot{\theta}_2 \end{pmatrix} \\ \begin{pmatrix} 0 \\ 0 \\ 0 \\ 0 \\ 0 \\ \ddot{\theta}_1 \end{pmatrix} \end{array} \right\}, \quad (3.4.35)$$

The acceleration of point 1⁻ is

$$\mathbf{a}_{3,1^-} = -L\dot{\theta}_2^2 \mathbf{x}_2 + L\ddot{\theta}_2 \mathbf{y}_2,$$

and the angular acceleration of link 1 is

$$\boldsymbol{\alpha}_{3,1^-} = (\ddot{\theta}_1 + \ddot{\theta}_2) \mathbf{z}_1$$

The following expressions are obtained when these equations are cast in terms of components relative to the basis for frame 1:

$$\left\{ \begin{array}{l} \mathbf{a}_{3,1^-} \\ \boldsymbol{\alpha}_{3,1^-} \end{array} \right\} = \left\{ \begin{array}{l} -L\dot{\theta}_2^2 \begin{Bmatrix} \cos\theta_1 \\ -\sin\theta_1 \\ 0 \end{Bmatrix} + L\ddot{\theta}_2 \begin{Bmatrix} \sin\theta_1 \\ \cos\theta_1 \\ 0 \end{Bmatrix} \\ \begin{Bmatrix} 0 \\ 0 \\ \dot{\theta}_1 + \dot{\theta}_2 \end{Bmatrix} \end{array} \right\}. \quad (3.4.36)$$

Next, the accelerations and angular accelerations in Equations (3.4.35) and (3.4.36) are calculated using the recursive formulation and the quantities \mathcal{A}_{k^-} computed earlier. The entries in \mathcal{A}_{k^-} are used to calculate the accelerations in the base frame from the identity

$$\left\{ \begin{array}{l} \mathbf{a}_{3,k^-}^k \\ \boldsymbol{\alpha}_{3,k^-}^k \end{array} \right\} = \mathcal{A}_{k^-} + \left\{ \begin{array}{l} \boldsymbol{\omega}_{3,k^-}^k \times \mathbf{v}_{3,k^-}^k \\ \mathbf{0} \end{array} \right\}.$$

For the inboard link $k = 2$, the last term on the right is

$$\left\{ \begin{array}{l} \boldsymbol{\omega}_{3,2^-}^2 \times \mathbf{v}_{3,2^-}^2 \\ \mathbf{0} \end{array} \right\} = \left\{ \begin{array}{l} \begin{Bmatrix} 0 \\ 0 \\ \dot{\theta}_2 \end{Bmatrix} \times \begin{Bmatrix} 0 \\ 0 \\ 0 \end{Bmatrix} \\ \begin{Bmatrix} 0 \\ 0 \\ 0 \end{Bmatrix} \end{array} \right\} = \mathbf{0},$$

while for the outboard link $k = 1$

$$\begin{aligned} \left\{ \begin{array}{l} \boldsymbol{\omega}_{3,1^-}^1 \times \mathbf{v}_{3,1}^1 \\ \mathbf{0} \end{array} \right\} &= \left\{ \begin{array}{l} \begin{Bmatrix} 0 \\ 0 \\ \dot{\theta}_1 + \dot{\theta}_2 \end{Bmatrix} \times \begin{Bmatrix} L\dot{\theta}_2 \sin\theta_1 \\ L\dot{\theta}_2 \cos\theta_1 \\ 0 \end{Bmatrix} \\ \begin{Bmatrix} 0 \\ 0 \\ 0 \end{Bmatrix} \end{array} \right\} = \left\{ \begin{array}{l} \begin{Bmatrix} -L\dot{\theta}_2(\dot{\theta}_1 + \dot{\theta}_2)\cos\theta_1 \\ L\dot{\theta}_2(\dot{\theta}_1 + \dot{\theta}_2)\sin\theta_1 \\ 0 \end{Bmatrix} \\ \begin{Bmatrix} 0 \\ 0 \\ 0 \end{Bmatrix} \end{array} \right\}, \\ &= \left\{ \begin{array}{l} (-L\dot{\theta}_2^2 - L\dot{\theta}_1\dot{\theta}_2) \begin{Bmatrix} \cos\theta_1 \\ \sin\theta_1 \\ 0 \end{Bmatrix} \\ \begin{Bmatrix} 0 \\ 0 \\ 0 \end{Bmatrix} \end{array} \right\}. \end{aligned}$$

The acceleration in the ground frame of link $k = 2$ is

$$\begin{Bmatrix} \mathbf{a}_{3,2^-}^2 \\ \boldsymbol{\alpha}_{3,2^-}^2 \end{Bmatrix} = \begin{Bmatrix} \begin{Bmatrix} 0 \\ 0 \\ 0 \\ 0 \\ 0 \end{Bmatrix} \\ \begin{Bmatrix} \ddot{\theta}_2 \end{Bmatrix} \end{Bmatrix} = \mathcal{A}_{2^-} + \mathbf{0},$$

and the acceleration in the ground frame of the first link is

$$\begin{Bmatrix} \mathbf{a}_{3,1^-}^1 \\ \boldsymbol{\alpha}_{3,1^-}^1 \end{Bmatrix} = \begin{Bmatrix} \begin{Bmatrix} -L\dot{\theta}_2^2 \cos \theta_1 + L\ddot{\theta}_2 \sin \theta_1 \\ L\dot{\theta}_2^2 \sin \theta_1 + L\ddot{\theta}_2 \cos \theta_1 \\ 0 \\ 0 \\ 0 \end{Bmatrix} \\ \begin{Bmatrix} \ddot{\theta}_1 + \ddot{\theta}_2 \end{Bmatrix} \end{Bmatrix} = \mathcal{A}_{1^-} + \begin{Bmatrix} \boldsymbol{\omega}_{3,1^-}^1 \times \mathbf{v}_{3,1}^1 \\ \mathbf{0} \end{Bmatrix}.$$

The *recursive O(N) formulation* does not impose restrictions on the selection of the degrees of freedom as does the Denavit-Hartenberg convention. For example, while it is always the case that the axes $\mathbf{z}_0, \mathbf{z}_1, \mathbf{z}_2, \dots, \mathbf{z}_{N-1}$ define the directions of the degrees of freedom in the Denavit-Hartenberg convention, the directions of the degrees of freedom $\mathbf{h}_1, \mathbf{h}_2, \mathbf{h}_3, \dots, \mathbf{h}_N$ in the recursive *O(N)* formulation can be any axes. In fact, it is an easy matter to solve for the velocities, accelerations or forces using the recursive *O(N)* formulation for a system whose kinematic variables have been selected in accordance with the Denavit-Hartenberg convention; the only modification required is to reorder the degrees of freedom and the frames used in the recursive order *N* formulation. This is shown in the next example.

Example 3.4.3. Use the Denavit-Hartenberg procedure to define the degrees of freedom for the arm assembly shown in Figure (3.24). Solve for the velocities of the joints and angular velocities of the links using the recursive *O(N)* formulation.

Solution: Figure (3.25) illustrates a set of frames 0, 1, 2, 3 and 4 shown in the solution of Problem (3.10) to satisfy the requirements of the Denavit-Hartenberg convention.

The rotation matrices that relate the 0, 1, 2, 3 and 4 frames of the Denavit-Hartenberg convention are shown in Problem (3.10) to be

$$\begin{aligned} \mathbf{R}_0^1 &= \begin{bmatrix} \cos \theta_1 & \sin \theta_1 & 0 \\ 0 & 0 & 1 \\ \sin \theta_1 & -\cos \theta_1 & 0 \end{bmatrix}, & \mathbf{R}_1^2 &= \begin{bmatrix} \cos \theta_2 & \sin \theta_2 & 0 \\ 0 & 0 & -1 \\ -\sin \theta_2 & \cos \theta_2 & 0 \end{bmatrix}, \\ \mathbf{R}_2^3 &= \begin{bmatrix} \cos \theta_3 & \sin \theta_3 & 0 \\ 0 & 0 & 1 \\ \sin \theta_3 & -\cos \theta_3 & 0 \end{bmatrix}, & \mathbf{R}_3^4 &= \begin{bmatrix} \cos \theta_4 & \sin \theta_4 & 0 \\ -\sin \theta_4 & \cos \theta_4 & 0 \\ 0 & 0 & 1 \end{bmatrix}. \end{aligned}$$

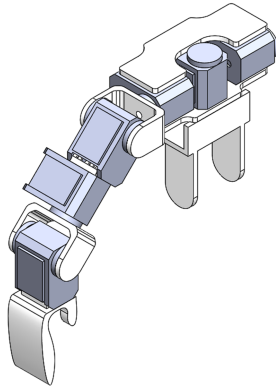


Fig. 3.24: Humanoid Arm

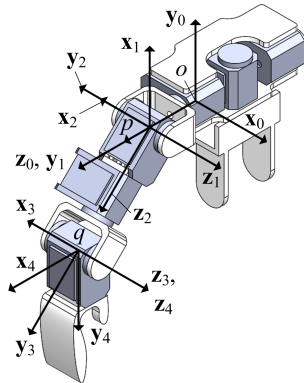


Fig. 3.25: Definition of Frames Consistent with the Denavit-Hartenberg Convention

with the link rotations $\theta_1, \theta_2, \theta_3$ and θ_4 defined about the $\mathbf{z}_0, \mathbf{z}_1, \mathbf{z}_2$ and \mathbf{z}_3 axes.

Using these frames, the joint velocities and link angular velocities will be formulated in terms of the DH convention variables $\theta_1, \theta_2, \theta_3$ by employing the *recursive $O(N)$ formulation*. The ordering of the joints and links in the recursive $O(N)$ formulation starts at the outer most bodies and increases towards the base. The joint angles ($q_1(t), q_2(t), q_3(t)$) for the recursive $O(N)$ formulation are just the angles defined in the Denavit-Hartenberg convention in reverse order; that is,

$$\mathbf{q}(t) = \begin{Bmatrix} q_1(t) \\ q_2(t) \\ q_3(t) \end{Bmatrix} = \begin{Bmatrix} \theta_3(t) \\ \theta_2(t) \\ \theta_1(t) \end{Bmatrix}$$

Similarly, the frames used in the recursive $O(N)$ formulation are also numbered in reverse order. The frames 1, 2, 3, 4, 5 used in the recursive $O(N)$ formulation, moving

from the outer to the inner bodies, are the frames 4, 3, 2, 1, 0 of the Denavit Hartenberg formulation. This fact implies that the rotation matrices that relate the frames 1, 2, 3, 4 and 5 of the recursive $O(N)$ formulation are

$$\begin{aligned}\mathbf{R}_5^4 &= \begin{bmatrix} \cos\theta_1 & \sin\theta_1 & 0 \\ 0 & 0 & 1 \\ \sin\theta_1 & -\cos\theta_1 & 0 \end{bmatrix}, & \mathbf{R}_4^3 &= \begin{bmatrix} \cos\theta_2 & \sin\theta_2 & 0 \\ 0 & 0 & -1 \\ -\sin\theta_2 & \cos\theta_2 & 0 \end{bmatrix}, \\ \mathbf{R}_3^2 &= \begin{bmatrix} \cos\theta_3 & \sin\theta_3 & 0 \\ 0 & 0 & 1 \\ \sin\theta_3 & -\cos\theta_3 & 0 \end{bmatrix}, & \mathbf{R}_2^1 &= \begin{bmatrix} \cos\theta_4 & \sin\theta_4 & 0 \\ -\sin\theta_4 & \cos\theta_4 & 0 \\ 0 & 0 & 1 \end{bmatrix}.\end{aligned}$$

This ordering of the degrees of freedom and the frames in the recursive $O(N)$ formulation are depicted in Figure (3.26).

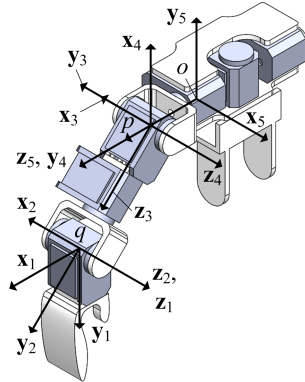


Fig. 3.26: Definition of Frames in Recursive $O(N)$ Formulation of Arm Assembly

It only remains to define the offsets $\mathbf{d}_{i+1,i}$ between joint $i+1$ and joint i and the directions of the degrees of freedom \mathbf{h}_i for $i = 1, 2, 3, 4$. The directions of the degrees of freedom can be obtained directly from the figures, such that

$$\mathbf{h}_1^1 = \begin{Bmatrix} 0 \\ 0 \\ 1 \end{Bmatrix}, \quad \mathbf{h}_2^2 = \begin{Bmatrix} 0 \\ 1 \\ 0 \end{Bmatrix}, \quad \mathbf{h}_3^3 = \begin{Bmatrix} 0 \\ -1 \\ 0 \end{Bmatrix}, \quad \mathbf{h}_4^4 = \begin{Bmatrix} 0 \\ 1 \\ 0 \end{Bmatrix}.$$

The offset vectors that connect joints $i+1$ and i may also be determined from the figures

$$\mathbf{d}_{1,2}^2 = \begin{Bmatrix} 0 \\ 0 \\ 0 \end{Bmatrix}, \quad \mathbf{d}_{2,3}^3 = \begin{Bmatrix} 0 \\ 0 \\ -d_{pq} \end{Bmatrix}, \quad \mathbf{d}_{3,4}^4 = \begin{Bmatrix} 0 \\ 0 \\ 0 \end{Bmatrix}, \quad \mathbf{d}_{4,5}^5 = \begin{Bmatrix} 0 \\ 0 \\ -d_{op} \end{Bmatrix}.$$

When a symbolic mathematics computer program is used to carry out the recursive $O(N)$ formulation of this system, \mathcal{V}_{1^-} , \mathcal{V}_{2^-} , and \mathcal{V}_{3^-} are determined to be

$$\begin{aligned}\mathcal{V}_{4^-} &= \begin{Bmatrix} 0 \\ 0 \\ 0 \\ 0 \\ \dot{\theta}_1 \\ 0 \end{Bmatrix} & \mathcal{V}_{3^-} &= \begin{Bmatrix} 0 \\ 0 \\ 0 \\ 0 \\ -\dot{\theta}_2 \\ -\dot{\theta}_1 \end{Bmatrix} & \mathcal{V}_{2^-} &= \begin{Bmatrix} -d_{pq}\dot{\theta}_2 \cos \theta_3 \\ -d_{pq}\dot{\theta}_2 \sin \theta_3 \\ 0 \\ -\dot{\theta}_1 \sin \theta_3 \\ \dot{\theta}_3 + \dot{\theta}_1 \cos \theta_3 \\ -\dot{\theta}_2 \end{Bmatrix}, \\ \mathcal{V}_{1^-} &= \begin{Bmatrix} d_{pq}\dot{\theta}_2 \sin \theta_3 \sin \theta_4 - d_{pq}\dot{\theta}_2 \cos \theta_3 \cos \theta_4 \\ -d_{pq}\dot{\theta}_2 \cos \theta_3 \sin \theta_4 - d_{pq}\dot{\theta}_2 \cos \theta_4 \sin \theta_3 \\ 0 \\ -\sin \theta_4(\dot{\theta}_3 + \dot{\theta}_1 \cos \theta_3) - \dot{\theta}_1 \cos \theta_4 \sin \theta_3 \\ \cos \theta_4(\dot{\theta}_3 + \dot{\theta}_1 \cos \theta_3) - \dot{\theta}_1 \sin \theta_3 \sin \theta_4 \\ \dot{\theta}_4 - \dot{\theta}_2 \end{Bmatrix}.\end{aligned}$$

3.5 Inverse Kinematics

The general tools in Chapter (2) and the early sections of this chapter can be employed to derive fast and systematic methods for the analysis of problems of *forward kinematics*. As discussed in Chapter (1), however, applications abound in which problems of *inverse kinematics* must also be solved. The synthesis of flapping motion based on camera measurement of the wings of a bird is an example of a problem of *inverse kinematics*. There are several reasons why problems of *inverse kinematics* can be significantly more difficult to solve than those of *forward kinematics* for a kinematic chain. First, it can be difficult to determine if there exists any solution at all to some *inverse kinematics* problems. Second, even if there is a solution, the solution may not be unique. Third, it is not uncommon that the solution of an *inverse kinematics* problem is determined by the roots of a transcendental, nonlinear set of algebraic equations for which the determination of the roots of these equations is far from trivial. Fourth, many inverse kinematics problems arise as part of a more complex task. If a controller must be designed to drive a robotic arm so that the tool follows some prescribed trajectory, corresponding perhaps to a weld on an automotive frame, it may be necessary to solve the inverse kinematics problem every few milliseconds. The solution of the tracking control problem uses the solution of the inverse kinematics problem. In fact, the solution of the inverse kinematics problem is also often used during the robotic design process. These *optimization* based techniques can be used effectively in design studies, where the solution of the *inverse kinematics* problem need not be solved in real time.

Because of these considerations, two general approaches, analytical and numerical, to the solution of inverse kinematics problems will be studied in this section. Advantages of analytical methods are faster to execute and are therefore amenable to applications wherein the *inverse kinematics* problem has to be solved in *real-time*. These applications include problems of tracking control in which the inner loop defines a set of joint variables that must be tracked, and the outer loop induces feedback that depends on the tracking error. This control architecture is quite common in robotic applications and is discussed in some detail in Chapter (5). However, an analytical solution cannot be guaranteed in the general case for a kinematic chain. In contrast, numerical techniques are significantly more general than analytical techniques, but can be much more time consuming than the analytical methods owing to the use of an iterative approach to estimating the solution, as opposed to a deterministic approach to calculate the solution.

3.5.1 Solvability

In the study of inverse kinematics, the goal is to determine the values of the joint variables defining a manipulator configuration that will place the end effector at a desired position and orientation. If the manipulator arm is a kinematic chain, the solution is usually given relative to the base. In particular, if the DH parameterization is used, the solution is specified in terms of the link displacements, offsets, twist, and rotation angles, and by the location of the base frame in the world coordinate system.

In considering a general inverse kinematics problem, it may *always* be the case that *no solution* exists for a specified target end effector location and orientation. For example, suppose the kinematic chain is constructed solely of revolute joints and has a maximum total length while “stretched out” of 1 meter. Now imagine that the target location and orientation of the end effector is sought at a distance 2 meters from the base of the robotic arm. There is no choice of joint variables that can attain the desired end effector location and pose due to the geometric limitations of the robotic arm. In this case the desired, or target, position and orientation of the end effector is not feasible or consistent for the robot arm under consideration. Clearly, the desired pose of the end effector must lie in the workspace of the robotic arm, or the inverse kinematics problem is inconsistent or infeasible. The general study of which end effector poses yield well-posed inverse kinematics problems can be quite subtle and falls under the topic of accessibility, attainability, or controllability in nonlinear control theory [33], [41], [10].

Suppose an N degree of freedom kinematic chain is under consideration that consists of revolute and prismatic joints. The inverse kinematics problem seeks to determine the values of joint rotations or displacements for $i = 1, \dots, N$, given the numerical value of the homogeneous transformation matrix \mathbf{H}_0^N . If the dimension of the task space is M , then there are M independent equations with N unknown joint variables in this formulation. Any of the following three situations may arise:

- $M = N$: There are enough equations to solve for the unknowns, if they are consistent. However, these equations are nonlinear. Hence, there may be one or more solutions to the inverse kinematics problem. The number of solutions is finite.
- $M > N$: The number of robot degrees of freedom is not sufficient to account for all possibilities of end effector position and orientation. Hence, the inverse kinematics problem may or may not have a solution.
- $M < N$: There are more degrees of freedom than required to provide the desired end effector position and orientation. Hence, there may be an infinite collection of solutions to the inverse kinematics problem. In this case the robotic arm is said to be *redundant*.

The cases discussed above are illustrated in the following example, which clarifies the qualitative differences between the three cases.

Example 3.5.1. Consider the planar manipulators shown in Figures (3.27a), (3.27b), and (3.27c).

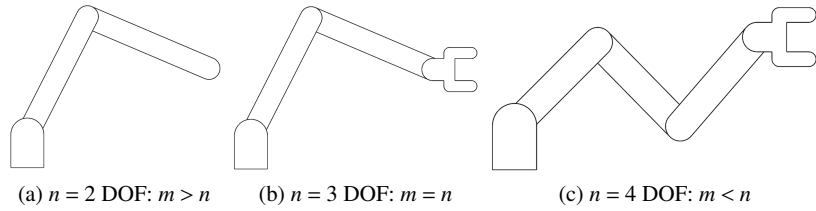


Fig. 3.27: Solvability for a Planar Workspace End Effector ($m = 3$)

Suppose that the lengths of the intermediate links are equal to 1 meter, and that the end effector frame n has its origin at (i) the end of link 2 for (3.27a), (ii) the joint between links 2 and 3 for (3.27b), and (iii) the joint between links 3 and 4 for (3.27c).

While many choices of joint variables are possible, the DH convention is employed for the arms. The ground frame is therefore frame 0 and the end effector is frame N , where $N = 2$ in (a), $N = 3$ in (b), and $N = 4$ in (c). The link rotation θ_i for $i = 1, \dots, N$ is measured from the frame fixed in link $i - 1$ to the frame fixed in link i . Since the manipulators are constrained to lie in the plane, the pose of the end effector is determined by the location of the origin of the end effector frame and the rotation of the end effector frame relative to its inboard neighboring link. Hence, the workspace has dimension $M = 3$ for the manipulators shown in (a), (b), and (c).

For the manipulator in (a), the end effector is missing, and the number of degrees of freedom is $N = 2 < M = 3$. The first two links are sufficient to position what would be the base of the end effector frame, but the robot lacks the end effector to rotate into the desired orientation. An alternative structure could have been to have a single

link and the end effector; the end effector could rotate to any desired orientation, but could only be positioned along a circle of radius matching the distance between the two joints.

For the manipulator in (b), there are three degrees of freedom $N = M = 3$. According to the above discussion, there may be one or more solutions to the inverse kinematics problem; however, there will be a finite number of solutions.

For the manipulator in (c), there are $N = 4 > 3 = M$ degrees of freedom. Because the manipulator has more degrees of freedom than end effector constraints, it is possible that there are an infinite number of solutions in this case. This can be visualized by fixing the end effector to the desired position and orientation and observing the four bar mechanism that results in the three intermediate links. This mechanism may be adjusted into an infinite number of different configurations for the fixed end effector configuration (assuming the end effector is not fixed at its outer workspace boundary).

The inverse kinematics problem studied in this chapter can be developed in terms of homogeneous transforms. It is assumed that a robotic manipulator that has the form of an N degree of freedom kinematic chain is given. The goal is to position the terminal (or tool) frame of the arm at a prescribed position and orientation in the workspace. The position and orientation of the tool frame in the ground frame is represented by the usual product of homogeneous transforms

$$\mathbf{H}_N^0 = \mathbf{H}_N^0(q_1, \dots, q_N) := \mathbf{H}_1^0(q_1)\mathbf{H}_2^1(q_2)\dots\mathbf{H}_N^{N-1}(q_N).$$

Each homogeneous transform \mathbf{H}_i^{i-1} is a function of one of the joint variables (q_1, q_2, \dots, q_N) , and the composite transform \mathbf{H}_N^0 that maps the tool frame N to the ground frame 0 is a function of all N joint variables. Each joint variable q_i is either a rotation angle or displacement, depending on whether it corresponds to a revolute or prismatic joint.

The *inverse kinematics* problem assumes that a desired location and orientation of the tool frame is given that is represented by a homogeneous transformation \mathbf{H} . A solution (q_1, q_2, \dots, q_n) of the *inverse kinematics* problem therefore must satisfy the matrix equation

$$\mathbf{H}_N^0(q_1, \dots, q_N) = \mathbf{H}_1^0(q_1)\mathbf{H}_2^1(q_2)\dots\mathbf{H}_N^{N-1}(q_N) = \mathbf{H}.$$

Since the last row of this matrix is identically equal to 0 or 1, there are 12 scalar equations in this matrix equation. There are N unknowns. Nine of these scalar equations arise from the rotation matrix that appears as a submatrix of the homogeneous transformation, and three of these scalar equations that arise from the offset vector contained in the homogeneous transform. As discussed in Chapter (2), a general rotation matrix is characterized by three independent angles; therefore, six of the nine scalar equations arising from the rotation matrix six are redundant. This matrix

equation can generates at most six independent scalar equations that relate the joint variables to the pose of the end effector.

Two general strategies will be studied to solve this inverse kinematics problem: analytical and computational methods. Analytical methods are investigated in Section 3.5.2, while the computational approaches are presented in Section 3.5.3.

3.5.2 Analytical Methods

Analytical methods for solving inverse kinematics problems often are tailored to a particular problem at hand, and a specific strategy adopted for one robot may not be applicable to a different robot. However, general templates have been developed to guide the construction of analytical solutions based on algebraic or geometric strategies. These approaches are discussed in Section 3.5.2.1 and 3.5.3, respectively.

3.5.2.1 Algebraic Methods

This section presents an algebraic method for generating a solution of an inverse kinematics problem based on a guideline that loosely applies to all robots. Although it does not prescribe a specific answer for a given problem, it guides the process by which an analytical solution is developed.

For an N degree of freedom manipulator, the steps for constructing an analytic solution of an inverse kinematics problem are as follows:

1. Solve the forward kinematics problem: (i) assign the Denavit-Hartenberg parameters and link coordinate frames, (ii) derive the homogenous transformation matrices $\mathbf{H}_1^0, \mathbf{H}_2^1, \dots, \mathbf{H}_N^{N-1}$, and (iii) obtain \mathbf{H}_N^0 as a function of joint variables.
2. Symbolically compute the following matrix equation:

$$\left(\mathbf{H}_1^0\right)^{-1} \mathbf{H}_N^0 = \mathbf{H}_2^1 \mathbf{H}_3^2 \cdots \mathbf{H}_N^{N-1},$$

and equate corresponding elements of the matrices on both sides of the above equation to search for “simpler” trigonometric equations for solving joint variables.

3. If required, continue repeating this process (multiplying each side by the next joint’s inverse homogenous transform), until the joint variables are solved:

$$\begin{aligned} & \left(\mathbf{H}_2^1\right)^{-1} \left(\mathbf{H}_1^0\right)^{-1} \mathbf{H}_N^0 = \mathbf{H}_3^2 \mathbf{H}_4^3 \cdots \mathbf{H}_N^{N-1}, \\ & \left(\mathbf{H}_3^2\right)^{-1} \left(\mathbf{H}_2^1\right)^{-1} \left(\mathbf{H}_1^0\right)^{-1} \mathbf{H}_N^0 = \mathbf{H}_4^3 \mathbf{H}_5^4 \cdots \mathbf{H}_N^{N-1}, \\ & \quad \vdots \end{aligned}$$

As discussed, the algebraic approach summarized above does not prescribe a specific set of equations that must be solved at each step of the procedure. The structure and sparsity of the homogeneous matrix equations in each step must be studied carefully to determine specific relationships between joint variables and end effector pose. This process is illustrated in the next two examples that illustrate the use of the methodology for simple robotic manipulators.

In addition, given the large number of trigonometric functions present in many of these examples, a shorthand is used. The functions $\sin \theta_1$ and $\cos \theta_1$ will instead be represented as $s\theta_1$ and $c\theta_1$, respectively.

Example 3.5.2. For the three degree of freedom, planar manipulator shown in Figure (3.28a) with DH Parameters defined in the table below, the location (p_x, p_y) and the orientation γ of the end effector is given.

Joint	Displacement d	Rotation θ	Offset a	Twist α
1	0	θ_1	L_1	0
2	0	θ_2	L_2	0
3	0	θ_3	0	0

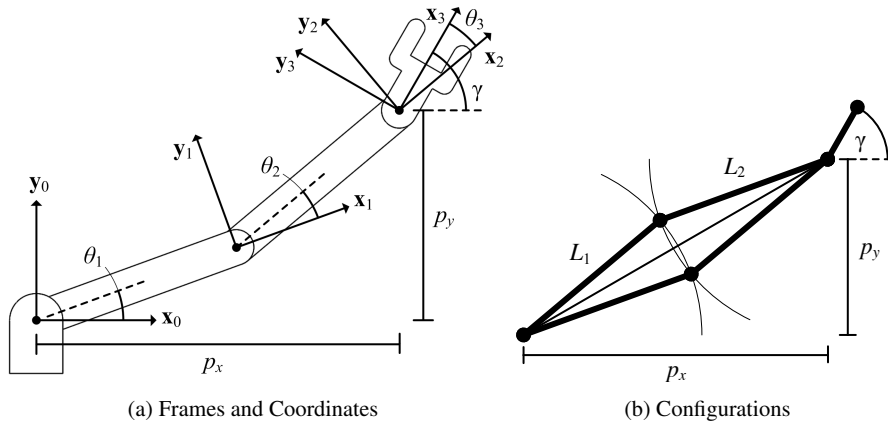


Fig. 3.28: Three Degree of Freedom Robotic Arm

Calculate the joint angles θ_1 , θ_2 and θ_3 associated with this configuration.
Solution: By inspection of the geometry, the kinematics equations are obtained as

$$\begin{aligned} p_x &= L_1 \cos \theta_1 + L_2 \cos(\theta_1 + \theta_2), \\ p_y &= L_1 \sin \theta_1 + L_2 \sin(\theta_1 + \theta_2), \\ \gamma &= \theta_1 + \theta_2 + \theta_3. \end{aligned}$$

Given that the first two equations are only a function of θ_1 and θ_2 , they may be solved for these two angles. The third equation may then be used to calculate θ_3 . As shown in Figure (3.28b), two solutions exist for the inverse kinematics problem.

Example 3.5.3. Consider the three degree of freedom robotic arm shown schematically in Figure (3.29) with the DH parameters given in the table below.

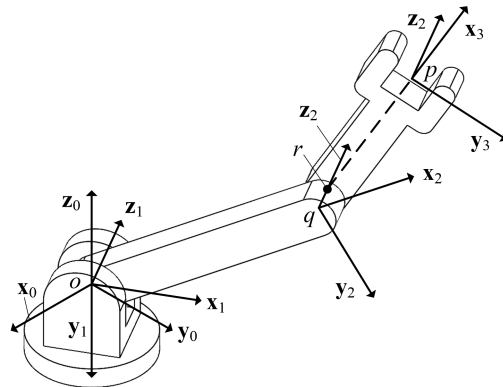


Fig. 3.29: Schematic of a Three Degree of Freedom Robotic Arm

Joint	Displacement d	Rotation θ	Offset a	Twist α
1	0	θ_1	0	-90°
2	0	θ_2	$d_{o,q}$	0
3	$d_{q,r}$	θ_3	$d_{r,p}$	0

Let the point p be the origin of the 3 frame, and \mathbf{p}^i the homogeneous coordinates of p in the i frame for $i = 1, 2, 3$. The forward kinematics can be solved for this choice of DH parameters to obtain the homogeneous transformations

$$\mathbf{H}_1^0 = \begin{bmatrix} c\theta_1 & 0 & -s\theta_1 & 0 \\ s\theta_1 & 0 & c\theta_1 & 0 \\ 0 & -1 & 0 & 0 \\ 0 & 0 & 0 & 1 \end{bmatrix}, \quad \mathbf{H}_2^1 = \begin{bmatrix} c\theta_2 & -s\theta_2 & 0 & d_{o,q}c\theta_2 \\ s\theta_2 & c\theta_2 & 0 & d_{o,q}s\theta_2 \\ 0 & 0 & 1 & 0 \\ 0 & 0 & 0 & 1 \end{bmatrix}, \quad \mathbf{H}_3^2 = \begin{bmatrix} c\theta_3 & -s\theta_3 & 0 & d_{r,p}c\theta_3 \\ s\theta_3 & c\theta_3 & 0 & d_{r,p}s\theta_3 \\ 0 & 0 & 1 & d_{q,r} \\ 0 & 0 & 0 & 1 \end{bmatrix},$$

and

$$\mathbf{H}_3^0 = \begin{bmatrix} c\theta_1c\theta_2c\theta_3 - c\theta_1s\theta_2s\theta_3 & -c\theta_1c\theta_2s\theta_3 - c\theta_1s\theta_2c\theta_3 & -s\theta_1 & p_1^0 \\ s\theta_1c\theta_2c\theta_3 - s\theta_1s\theta_2s\theta_3 & -s\theta_1c\theta_2s\theta_3 - s\theta_1s\theta_2c\theta_3 & c\theta_1 & p_2^0 \\ -s\theta_2c\theta_3 - c\theta_2s\theta_3 & s\theta_2s\theta_3 - c\theta_2c\theta_3 & 0 & p_3^0 \\ 0 & 0 & 0 & 1 \end{bmatrix},$$

with

$$\begin{aligned} p_1^0 &= d_{r,p} (c\theta_1 c\theta_2 c\theta_3 - c\theta_1 s\theta_2 s\theta_3) - d_{q,r} s\theta_1 + d_{o,q} c\theta_1 c\theta_2, \\ p_2^0 &= d_{r,p} (s\theta_1 c\theta_2 c\theta_3 - s\theta_1 s\theta_2 s\theta_3) + d_{q,r} c\theta_1 + d_{o,q} s\theta_1 c\theta_2, \\ p_3^0 &= d_{r,p} (-s\theta_2 c\theta_3 - c\theta_2 s\theta_3) - d_{o,q} s\theta_2. \end{aligned}$$

The solution of the inverse kinematics problem begins by solving the equation

$$\mathbf{p}^0 = \mathbf{H}_2^0 \mathbf{H}_3^2 \mathbf{p}^3 \longrightarrow (\mathbf{H}_2^0)^{-1} \mathbf{p}^0 = \mathbf{H}_3^2 \mathbf{p}^3$$

given

$$\mathbf{p}^3 = \begin{bmatrix} 0 \\ 0 \\ 0 \\ 1 \end{bmatrix}, \quad \text{and} \quad \mathbf{p}^0 = \begin{bmatrix} p_1^0 \\ p_2^0 \\ p_3^0 \\ 1 \end{bmatrix}.$$

The inverse transformation $(\mathbf{H}_2^0)^{-1}$ is given by

$$(\mathbf{H}_2^0)^{-1} = (\mathbf{H}_1^0 \mathbf{H}_2^1)^{-1} = \begin{bmatrix} c\theta_1 c\theta_2 & s\theta_1 c\theta_2 & -s\theta_2 & -d_{o,q} \\ -c\theta_1 s\theta_2 & -s\theta_1 s\theta_2 & -c\theta_2 & 0 \\ -s\theta_1 & c\theta_1 & 0 & 0 \\ 0 & 0 & 0 & 1 \end{bmatrix},$$

which results in

$$\begin{bmatrix} c\theta_1 c\theta_2 & s\theta_1 c\theta_2 & -s\theta_2 & -d_{o,q} \\ -c\theta_1 s\theta_2 & -s\theta_1 s\theta_2 & -c\theta_2 & 0 \\ -s\theta_1 & c\theta_1 & 0 & 0 \\ 0 & 0 & 0 & 1 \end{bmatrix} \mathbf{p}^0 = \begin{bmatrix} c\theta_3 & -s\theta_3 & 0 & d_{r,p} c\theta_3 \\ s\theta_3 & c\theta_3 & 0 & d_{r,p} s\theta_3 \\ 0 & 0 & 1 & d_{q,r} \\ 0 & 0 & 0 & 1 \end{bmatrix} \mathbf{p}^3.$$

When terms on both sides are equated, three scalar equations are obtained

$$c\theta_1 c\theta_2 p_1^0 + s\theta_1 c\theta_2 p_2^0 - s\theta_2 p_3^0 - d_{o,q} = d_{r,p} c\theta_3, \quad (3.5.1)$$

$$-c\theta_1 s\theta_2 p_1^0 - s\theta_1 s\theta_2 p_2^0 - c\theta_2 p_3^0 = d_{r,p} s\theta_3, \quad (3.5.2)$$

$$s\theta_1 p_1^0 + c\theta_1 p_2^0 - d_{q,r} = 0. \quad (3.5.3)$$

Iterating again leads to the equation

$$(\mathbf{H}_1^0)^{-1} \mathbf{p}^0 = \mathbf{H}_3^1 \mathbf{p}^3.$$

Repeating this procedure results in three additional equations

$$\begin{aligned} c\theta_1 p_1^0 + s\theta_1 p_2^0 &= d_{r,p} c_{23} + d_{o,q} c\theta_2, \\ -s\theta_1 p_1^0 + c\theta_1 p_2^0 &= d_{q,r}, \\ p_3^0 &= -d_{r,p} s_{23} - d_{o,q} s\theta_2, \end{aligned}$$

where

$$c_{23} = \cos(\theta_2 + \theta_3) \quad \text{and} \quad s_{23} = \sin(\theta_2 + \theta_3).$$

From Equation 3.5.3, θ_1 may be calculated as

$$\theta_1 = \tan^{-1}\left(\frac{p_2^0}{p_1^0}\right) \pm \tan^{-1}\left(\frac{d_{q,r}}{\sqrt{(p_1^0)^2 + (p_2^0)^2 - d_{q,r}^2}}\right).$$

Next, summing the squares of Equations 3.5.1 through 3.5.3 results in

$$(p_1^0)^2 + (p_2^0)^2 + (p_3^0)^2 = d_{o,q}^2 + d_{q,r}^2 + d_{r,p}^2 + 2d_{o,q}d_{r,p}c\theta_3.$$

It follows that

$$c\theta_3 = \frac{(p_1^0)^2 + (p_2^0)^2 + (p_3^0)^2 - d_{o,q}^2 - d_{q,r}^2 - d_{r,p}^2}{2d_{o,q}d_{r,p}}$$

with $s\theta_3 = \sqrt{1 - (c\theta_3)^2}$ and $\tan\theta_3 = \left(\frac{s\theta_3}{c\theta_3}\right)$. If d is defined such that

$$d^2 = (p_1^0)^2 + (p_2^0)^2 + (p_3^0)^2 - d_{q,r}^2,$$

then

$$c\theta_3^2 = \frac{(d^2 - d_{o,q}^2 - d_{r,p}^2)^2}{(2d_{o,q}d_{r,p})^2}, \quad s\theta_3 = \frac{\sqrt{(2d_{o,q}d_{r,p})^2 - (d^2 - d_{o,q}^2 - d_{r,p}^2)^2}}{2d_{o,q}d_{r,p}},$$

and

$$\begin{aligned} \tan\theta_3 &= \frac{\sqrt{(2d_{o,q}d_{r,p})^2 - (d^2 - d_{o,q}^2 - d_{r,p}^2)^2}}{d^2 - d_{o,q}^2 - d_{r,p}^2}, \\ &= \frac{\sqrt{(2d_{o,q}d_{r,p} + d^2 - d_{o,q}^2 - d_{r,p}^2)(2d_{o,q}d_{r,p} - d^2 + d_{o,q}^2 + d_{r,p}^2)}}{d^2 - d_{o,q}^2 - d_{r,p}^2}, \\ &= \frac{\sqrt{(d^2 - [d_{o,q} - d_{r,p}]^2)(-d^2 + [d_{o,q} + d_{r,p}]^2)}}{d^2 - d_{o,q}^2 - d_{r,p}^2}. \end{aligned}$$

Finally, from Equations 3.5.1 and 3.5.2, P and Q can be defined via the identities as

$$\begin{aligned}
P &= \underbrace{\left(c\theta_1 c\theta_2 p_1^0 + s\theta_1 c\theta_2 p_2^0 - s\theta_2 p_3^0 \right) p_3^0 + }_{1(a)} \\
&\quad \underbrace{\left(-c\theta_1 s\theta_2 p_1^0 - s\theta_1 s\theta_2 p_2^0 - c\theta_2 p_3^0 \right) \left(c\theta_1 p_1^0 + s\theta_1 p_2^0 \right),}_{1(b)} \\
&= \left((p_3^0)^2 + (c\theta_1 p_1^0 + s\theta_1 p_2^0)^2 \right) s\theta_2, \\
&= -p_3^0 (d_{r,p} c\theta_3 + d_{o,q}) - d_{r,p} s\theta_3 (c\theta_1 p_1^0 + s\theta_1 p_2^0),
\end{aligned}$$

and

$$\begin{aligned}
Q &= \underbrace{\left(c\theta_1 c\theta_2 p_1^0 + s\theta_1 c\theta_2 p_2^0 - s\theta_2 p_3^0 \right) \left(c\theta_1 p_1^0 + s\theta_1 p_2^0 \right)}_{1(a)} \\
&\quad + \underbrace{\left(-c\theta_1 s\theta_2 p_1^0 - s\theta_1 s\theta_2 p_2^0 - c\theta_2 p_3^0 \right) (-p_3^0)}_{1(b)} \\
&= \left((p_3^0)^2 + (c\theta_1 p_1^0 + s\theta_1 p_2^0)^2 \right) c\theta_2 \\
&= -p_3^0 (d_{r,p} s\theta_3) + (d_{r,p} c\theta_3 + d_{o,q}) (c\theta_1 p_1^0 + s\theta_1 p_2^0).
\end{aligned}$$

As a result, $\theta_2 = \tan^{-1} \left(\frac{P}{Q} \right)$.

The analytical techniques employed in this book are based on the fact that many commercially available robotic manipulators terminate in a spherical wrist that carries a payload or tool. This general topology allows the *inverse kinematics* problem to be decomposed into two sub-problems: (i) positioning the wrist center, and (ii) orienting the end effector through the wrist. The decomposition of the general *inverse kinematics* problem into the independent problems of locating the wrist center and orienting the tool frame is known as *kinematic decoupling*.

The following two examples illustrates this process for six degree of freedom robotic manipulators.

Example 3.5.4. This example shows how kinematic decoupling can substantially simplify the solution of an inverse kinematics problem. While the analytical solution for a general six degree of freedom robot is difficult to construct, the decomposition into two independent three degree of freedom problems makes the problem tractable. The position of the wrist point w in Figure (3.30), which has homogeneous coordinates \mathbf{w}^i in the frame i , does not depend on the rotation angles of the last three joints. Therefore,

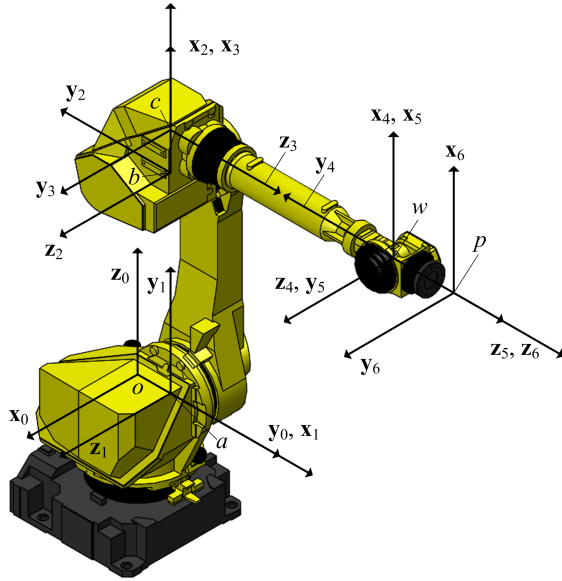


Fig. 3.30: FANUC Robot

$$\mathbf{w}^0 = \mathbf{H}_3^0 \mathbf{w}^3 = \mathbf{H}_3^0 \begin{bmatrix} 0 \\ 0 \\ d_4 \\ 1 \end{bmatrix},$$

with

$$\mathbf{w}^0 = \mathbf{p}^0 - \mathbf{d}_{w,p} \quad \Rightarrow \quad \mathbf{w}^0 = \begin{bmatrix} p_1^0 \\ p_2^0 \\ p_3^0 \\ 1 \end{bmatrix} - \left[\mathbf{R}_6^0 \begin{bmatrix} 0 \\ 0 \\ d_6 \\ 1 \end{bmatrix} \right] = \begin{bmatrix} p_1^0 - d_6 a_x \\ p_2^0 - d_6 a_y \\ p_3^0 - d_6 a_z \\ 1 \end{bmatrix} = \begin{bmatrix} w_1^0 \\ w_2^0 \\ w_3^0 \\ 1 \end{bmatrix}.$$

By equating the above two equations, three scalar equations will be obtained that can be solved for three unknowns θ_1 , θ_2 , and θ_3 . However, by pre-multiplying by the inverse of \mathbf{H}_1^0 , simpler equations can be obtained. Starting from

$$(\mathbf{H}_1^0)^{-1} \mathbf{w}^0 = \mathbf{H}_3^1 \mathbf{w}^3,$$

yields

$$\begin{aligned} w_1^0 c_1 + w_2^0 s_1 - a_1 &= a_2 c_2 + a_3 c_2 s_3 + d_4 s_2 s_3, \\ w_3^0 &= a_2 s_2 + a_3 s_2 s_3 - d_4 c_2 s_3, \\ w_1^0 s_1 - w_2^0 c_1 &= 0. \end{aligned}$$

First, by solving the third equation, θ_1 is obtained as

$$\theta_1^1 = \text{Atan2}\left(\frac{w_2^0}{w_1^0}\right), \quad \text{and} \quad \theta_1^2 = \theta_1^1 + 180^\circ.$$

The angle θ_1^1 is the front reach solution and θ_1^2 is the back reach solution. Due to mechanical constraints the second solution is not feasible for this manipulator.

Next, by solving the first two equations, θ_2 and θ_3 will be obtained from the expression

$$\theta_3 = 2\text{Atan2}\left(\frac{d_4 \pm \sqrt{d_4^2 + a_3^2 - \left(\frac{(w_1^0 c_1 + w_2^0 s_1 - a_1)^2 + (w_3^0)^2 - a_2^2 - a_3^2 - d_4^2}{2a_2}\right)^2}}{a_3 + \frac{(w_1^0 c_1 + w_2^0 s_1 - a_1)^2 + (w_3^0)^2 - a_2^2 - a_3^2 - d_4^2}{2a_2}}\right).$$

The two solutions of θ_3 arise from the fully stretched and folded back configurations. In case of no real root, the assigned wrist point position is not reachable. Then,

$$\theta_2 = \text{Atan2}\left(\frac{\sin \theta_2}{\cos \theta_2}\right),$$

with

$$\begin{aligned} \cos \theta_2 &= \frac{(w_1^0 c_1 + w_2^0 s_1 - a_1)(a_2 + a_3 c_3 + d_4 s_3) + w_3^0 (a_3 s_3 - d_4 c_3)}{(a_2 + a_3 c_3 + d_4 s_3)^2 + (a_3 s_3 - d_4 c_3)^2}, \\ \sin \theta_2 &= \frac{w_3^0 - (a_3 s_3 - d_4 c_3) \cos \theta_2}{(a_2 + a_3 c_3 + d_4 s_3)}. \end{aligned}$$

Given the wrist point location, mathematically there are at most 4 possible arm configurations. Due to the mechanical constraints, only 2 of them are feasible.

Next, when solving for the final three joints, \mathbf{H}_6^3 is known and the forward kinematics equation can be transformed to the equation

$$\mathbf{H}_6^3 = (\mathbf{H}_3^0)^{-1} \mathbf{H}_6^0.$$

Equating the (3,3) elements of the matrices on each side of the equality above, it follows that

$$\begin{aligned} \cos \theta_5 &= (a_x c_1 s_{23} + a_y s_1 s_{23} - a_z c_{23}), \\ \sin \theta_5 &= \pm \sqrt{1 - (a_x c_1 s_{23} + a_y s_1 s_{23} - a_z c_{23})^2}. \end{aligned}$$

Therefore, in general for each set of θ_1 , θ_2 , θ_3 , two solutions exist for θ_5 via the expression

$$\theta_5 = \pm \text{Atan2}\left(\frac{s5}{c5}\right).$$

Next, equating the (1,3) and (2,3) elements of the homogeneous transforms on either side of the equality gives

$$\cos \theta_4 = \frac{a_x c1 c23 + a_y s1 c23 + a_z s23}{s5},$$

$$\sin \theta_4 = \frac{a_x s1 - a_y c1}{s5}.$$

Hence, corresponding to each set of solutions for θ_1 , θ_2 , θ_3 , and θ_5 , a unique solution of θ_2 can be obtained from

$$\theta_4 = \text{Atan2}\left(\frac{s4}{c4}\right).$$

Similarly, equating the elements (3,1) and elements (3,2) yields

$$\cos \theta_6 = -\frac{n_x c1 s23 + n_y s1 s23 - n_z c23}{s5},$$

$$\sin \theta_6 = \frac{o_x c1 s23 + o_y s1 s23 - o_z c23}{s5},$$

and for each set of θ_1 , θ_2 , θ_3 , and θ_5 , a unique solution of θ_6 is obtained from

$$\theta_6 = \text{Atan2}\left(\frac{s6}{c6}\right).$$

When $\theta_5 = 0$ or π , the sixth joint axis \mathbf{z}_5 aligns with the fourth joint axis \mathbf{z}_3 , making θ_4 and θ_6 not independent (this is an example of kinematic degeneracy). In this case, one of them can be arbitrarily set to zero. For example, set $\theta_4 = 0$ and θ_6 can be uniquely obtained from elements (1,1) and (2,1) in the equations

$$(c1 c23) \cos \theta_6 + s1 \sin \theta_6 = n_x,$$

$$(s1 c23) \cos \theta_6 - c1 \sin \theta_6 = n_y.$$

In conclusion, for each solution set of the first three joints, there are two possible wrist configurations. Hence, mathematically a total of eight configurations are possible. However, due to physical limitations, only four of them are feasible. When $\theta_5 = 0$ or π , the wrist is in a singular configuration and only sum or difference of θ_4 and θ_6 can be computed.

Example 3.5.5. This example solves the inverse kinematics problem for the spherical robotic manipulator shown in Figure (3.45) with a spherical wrist added to the

initial three links. Assume the desired position and orientation of the tool frame is defined in terms of the prescribed homogeneous transform \mathbf{H} given by

$$\mathbf{H}_n^0(q_1 \dots q_N) = \mathbf{H} = \begin{bmatrix} \mathbf{R} & \mathbf{d} \\ \mathbf{0}^T & 1 \end{bmatrix} = \begin{bmatrix} r_{11} & r_{12} & r_{13} \\ r_{21} & r_{22} & r_{23} \\ r_{31} & r_{32} & r_{33} \\ 0 & 0 & 0 \end{bmatrix} \begin{Bmatrix} d_1 \\ d_2 \\ d_3 \\ 1 \end{Bmatrix}.$$

When the Denavit-Hartenberg convention is used to represent the kinematics of the robot, the homogeneous transform from the 3 frame to the 0 frame is given by

$$\mathbf{H}_3^0 = \begin{bmatrix} \mathbf{R}_3^0 & \mathbf{d}_{0,3}^0 \\ \mathbf{0}^T & 1 \end{bmatrix}, \quad (3.5.4)$$

while that from the tool frame to the 3-frame

$$\mathbf{H}_6^3 = \begin{bmatrix} \mathbf{R}_6^3 & \mathbf{d}_{3,6}^3 \\ \mathbf{0}^T & 1 \end{bmatrix}.$$

The composite transform \mathbf{H}_6^0 from the tool frame to the 0 frame is given by the product

$$\begin{aligned} \mathbf{H}_6^0 &= \mathbf{H}_3^0 \mathbf{H}_6^3 = \begin{bmatrix} \mathbf{R}_3^0 & \mathbf{d}_{0,3}^0 \\ \mathbf{0}^T & 1 \end{bmatrix} \begin{bmatrix} \mathbf{R}_6^3 & \mathbf{d}_{3,6}^3 \\ \mathbf{0}^T & 1 \end{bmatrix} \\ &= \begin{bmatrix} \mathbf{R}_3^0 \mathbf{R}_6^3 (\mathbf{R}_3^0 \mathbf{d}_{3,6}^3 + \mathbf{d}_{0,3}^0) \\ \mathbf{0}^T & 1 \end{bmatrix} = \begin{bmatrix} \mathbf{R}_6^0 & \mathbf{d}_{0,6}^0 \\ \mathbf{0}^T & 1 \end{bmatrix}. \end{aligned}$$

By inspection of the robotic manipulator, it can be seen that $\mathbf{d}_{3,6}^3 = \mathbf{0}$. It follows that

$$\mathbf{d}_{0,6}^0 = \mathbf{d}_{0,3}^0 = \begin{Bmatrix} d_{p,q} \cos \theta_1 \sin \theta_2 \\ d_{p,q} \sin \theta_1 \sin \theta_2 \\ d_{o,p} - d_{p,q} \cos \theta_2 \end{Bmatrix} = \begin{Bmatrix} d_1 \\ d_2 \\ d_3 \end{Bmatrix}$$

when $p = q$. The magnitude of the vector $\mathbf{d}_{0,6}^0$ can be used to calculate to find

$$d_{p,q}^2 \cos^2 \theta_1 \sin^2 \theta_2 + d_{p,q}^2 \sin^2 \theta_1 \sin^2 \theta_2 + d_{p,q}^2 \cos^2 \theta_2 = d_1^2 + d_2^2 + (d_3 - d_{o,p})^2.$$

Thus, the axial extension $d_{p,q}$ is calculated in terms of the given parameters as

$$d_{p,q} = \sqrt{d_1^2 + d_2^2 + (d_3 - d_{o,p})^2}.$$

The angle θ_2 can consequently be calculated from the third entry as

$$\theta_2 = \cos^{-1}((d_{o,p} - d_3)/d_{p,q}).$$

Then, the θ_1 is computed from the first component of the vector $\mathbf{d}_{0,6}^0$ using the expression

$$\theta_1 = \cos^{-1}(d_1/(d_{p,q} \sin \theta_2)).$$

This completes the solution of the subproblem that locates the wrist center, which coincides with origin of frame 3. Next is the task of determining the joint angles that orient the tool frame in the desired pose. It is required that

$$\mathbf{R}_3^0 \mathbf{R}_6^3 = \mathbf{R}. \quad (3.5.5)$$

But since this problem is *kinematically decoupled*, the rotation matrix \mathbf{R}_3^0 is a function of only θ_1 and θ_2

$$\mathbf{R}_3^0 = \mathbf{R}_3^0(\theta_1, \theta_2),$$

and the matrix \mathbf{R}_6^3 is function of $\theta_4, \theta_5, \theta_6$

$$\mathbf{R}_6^3 := \mathbf{R}_6^3(\theta_4, \theta_5, \theta_6).$$

Since θ_1 and θ_2 have already been determined, Equation (3.5.5) can be premultiplied by the matrix $(\mathbf{R}_3^0)^T$ to obtain

$$\mathbf{R}_6^3 = (\mathbf{R}_3^0)^T \mathbf{R} := \bar{\mathbf{R}} := \begin{bmatrix} \bar{r}_{11} & \bar{r}_{12} & \bar{r}_{13} \\ \bar{r}_{21} & \bar{r}_{22} & \bar{r}_{23} \\ \bar{r}_{31} & \bar{r}_{32} & \bar{r}_{33} \end{bmatrix}.$$

A new rotation matrix $\bar{\mathbf{R}} := (\mathbf{R}_3^0)^T \mathbf{R}$ has been defined in this equation, and all the entries in the matrix $\bar{\mathbf{R}}$ are known. By definition the matrix equation can be factored as

$$\mathbf{R}_6^3 = \mathbf{R}_4^3(\theta_4) \mathbf{R}_5^4(\theta_5) \mathbf{R}_6^5(\theta_6) = \bar{\mathbf{R}},$$

with

$$\mathbf{R}_4^3 = \begin{bmatrix} \cos \theta_4 & 0 & -\sin \theta_4 \\ \sin \theta_4 & 0 & \cos \theta_4 \\ 0 & -1 & 0 \end{bmatrix}, \quad \mathbf{R}_5^4 = \begin{bmatrix} \cos \theta_5 & 0 & \sin \theta_5 \\ \sin \theta_5 & 0 & -\cos \theta_5 \\ 0 & 1 & 0 \end{bmatrix}, \quad \mathbf{R}_6^5 = \begin{bmatrix} \cos \theta_6 & -\sin \theta_6 & 0 \\ \sin \theta_6 & \cos \theta_6 & 0 \\ 0 & 0 & 1 \end{bmatrix}.$$

Premultiplying each side of this equation by $(\mathbf{R}_4^3)^T$ results in

$$\begin{bmatrix} \cos \theta_5 \cos \theta_6 & -\cos \theta_5 \sin \theta_6 & \sin \theta_5 \\ \sin \theta_5 \cos \theta_6 & -\sin \theta_5 \sin \theta_6 & -\cos \theta_5 \\ \sin \theta_6 & \cos \theta_6 & 0 \end{bmatrix} = \begin{bmatrix} \cos \theta_4 & \sin \theta_4 & 0 \\ 0 & 0 & -1 \\ -\sin \theta_4 & \cos \theta_4 & 0 \end{bmatrix} \begin{bmatrix} \bar{r}_{11} & \bar{r}_{12} & \bar{r}_{13} \\ \bar{r}_{21} & \bar{r}_{22} & \bar{r}_{23} \\ \bar{r}_{31} & \bar{r}_{32} & \bar{r}_{33} \end{bmatrix} \quad (3.5.6)$$

$$= \begin{bmatrix} (\bar{r}_{11} \cos \theta_4 + \bar{r}_{21} \sin \theta_4) & (\bar{r}_{12} \cos \theta_4 + \bar{r}_{22} \sin \theta_4) & (\bar{r}_{13} \cos \theta_4 + \bar{r}_{23} \sin \theta_4) \\ -\bar{r}_{31} & -\bar{r}_{32} & -\bar{r}_{33} \\ (-\bar{r}_{11} \sin \theta_4 + \bar{r}_{21} \cos \theta_4) & (-\bar{r}_{12} \sin \theta_4 + \bar{r}_{22} \cos \theta_4) & (-\bar{r}_{13} \sin \theta_4 + \bar{r}_{23} \cos \theta_4) \end{bmatrix}. \quad (3.5.7)$$

The angle θ_5 may be solved for from the (2,3) entry of the matrix Equation (3.5.6)

$$\theta_5 = \cos^{-1}(\bar{r}_{33}),$$

and then used to determine the angle θ_6 from the (2, 1) entry

$$\theta_6 = \cos^{-1}(-\bar{r}_{31}/\sin\theta_5).$$

The angle θ_4 may be found by postmultiplying Equation (3.5.6) by $\bar{\mathbf{R}}^T$, which gives

$$\begin{bmatrix} \cos\theta_5 \cos\theta_6 & -\cos\theta_5 \sin\theta_6 & \sin\theta_5 \\ \sin\theta_5 \cos\theta_6 & -\sin\theta_5 \sin\theta_6 & -\cos\theta_5 \\ \sin\theta_6 & \cos\theta_6 & 0 \end{bmatrix} \begin{bmatrix} \bar{r}_{11} & \bar{r}_{21} & \bar{r}_{31} \\ \bar{r}_{12} & \bar{r}_{22} & \bar{r}_{32} \\ \bar{r}_{13} & \bar{r}_{23} & \bar{r}_{33} \end{bmatrix} = \begin{bmatrix} \cos\theta_4 & \sin\theta_4 & 0 \\ 0 & 0 & -1 \\ -\sin\theta_4 \cos\theta_4 & 0 & 0 \end{bmatrix}.$$

When the product of the matrices on the left is calculated, the (1,1) entry of the resulting matrix product yields

$$\begin{aligned} \theta_4 &= \cos^{-1}\left(\left[\cos\theta_5 \cos\theta_6 \quad -\cos\theta_5 \sin\theta_6 \quad \sin\theta_5\right] \begin{bmatrix} \bar{r}_{11} \\ \bar{r}_{12} \\ \bar{r}_{13} \end{bmatrix}\right), \\ &= \cos^{-1}(\bar{r}_{11} \cos\theta_5 \cos\theta_6 - \bar{r}_{12} \cos\theta_5 \sin\theta_6 + \bar{r}_{13} \sin\theta_5 \sin\theta_6). \end{aligned}$$

This step completes the subproblem of finding the joint angles that orient the tool frame at a specified pose. The above procedure shows that the solution procedure is not unique. It is possible to derive other, equally valid expressions for the kinematic variables. For example, the angle θ_6 could have instead been calculated from the (2,2) entry of the matrix Equation (3.5.6)

$$\theta_6 = \sin^{-1}(\bar{r}_{32}/\sin\theta_5).$$

This is a common feature of analytical solution procedures for inverse kinematics problems.

3.5.2.2 Geometric Methods

An alternative approach for generating the analytical model for a kinematic chain's inverse kinematics is the geometric approach. In many kinematic chains, equations for one or more of the kinematic variables may be found using geometric and/or trigonometric identities based on the structure of the robot. Common identities used in this process include the laws of sines and cosines and the Pythagorean theorem. However, this approach depends entirely on the geometry of a given kinematic chain and cannot be generalized into a systematic algorithm for automated analysis. The following provides an example of geometric analysis on a three degree of freedom kinematic chain.

Example 3.5.6. Use a geometric approach to determine the inverse kinematics of the three degree of freedom robotic manipulator shown in Figure (3.31). Assume the end effector coordinates (x_e, y_e, z_e) are given.

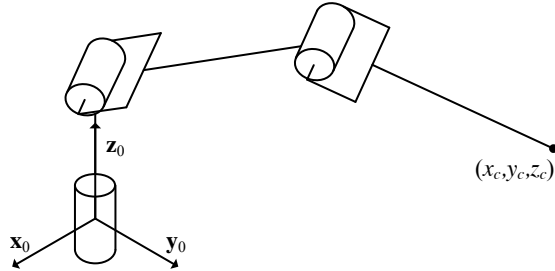


Fig. 3.31: Elbow Manipulator

Solution: First, θ_1 may be calculated by the projection of the end effector point onto the x, y -plane, as shown in Figure (3.32). The x - and y -coordinates of the end-effector position may be represented by the parametric equations

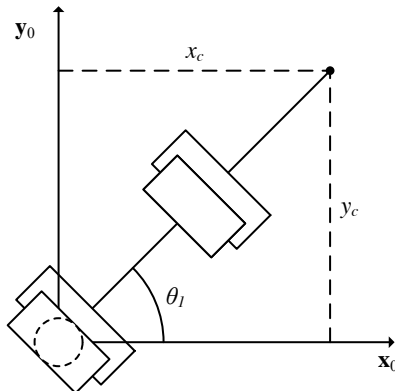


Fig. 3.32: x, y -Plane Projection for Calculating θ_1

$$x_e = r_{xy} \cos \theta_1, \quad (3.5.8)$$

$$y_e = r_{xy} \sin \theta_1, \quad (3.5.9)$$

where $r_{xy} = (x_e^2 + y_e^2)^{0.5}$ is the magnitude of the x, y -plane projection. The four-quadrant solution of these parametric equations is represented by

$$\theta_1 = \text{atan2}(y_e, x_e) \quad (3.5.10)$$

where atan2 is the four-quadrant arctangent function. This function utilizes the signs of y_e and x_e to determine the appropriate quadrant for the angle satisfying the arctangent of the quotient. A second solution for θ_1 may also be found as

$$\theta_1 = 180^\circ + \text{atan2}(y_e, x_e). \quad (3.5.11)$$

As seen in Figure (3.32), doing this requires an appropriately large θ_2 to revolve the arm past 90° to point in the proper direction. This observation also indicates that the further solutions of θ_2 and θ_3 depend on the value of θ_1 . As a result, for the remainder of the solution, the two cases must be considered separately. To determine the values of θ_2 and θ_3 associated with a given value of θ_1 .

A special case is observed if $x_e = y_e = 0$. Neither solution above is valid in this case, meaning that the inverse kinematics cannot be solved. This is a case of a singularity, discussed in Section (3.5.4.1).

Assuming two valid values of θ_1 are calculated, the solution continues by considering the planar kinematic chain created by joints 2 and 3, as shown in Figure (3.33). In this plane, the end effector must reach point (r_e, z_e) . As shown in Figure (3.33), there are two possible configurations that place the end effector at the desired point. Figure (3.34) shows the trigonometric analysis used to calculate the two sets

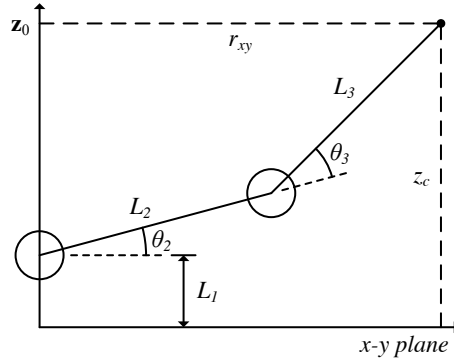
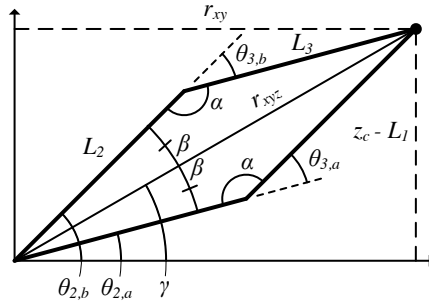


Fig. 3.33: Planar Kinematic Chain for Calculating θ_2 and θ_3

of angles $(\theta_{2,a}, \theta_{3,a})$ and $(\theta_{2,b}, \theta_{3,b})$ for a given θ_1 that reach the desired end effector position. First, the distance r_{xyz} and angle γ are calculated using the expressions

Fig. 3.34: Trigonometric Analysis for θ_2 and θ_3

$$r_{xyz} = (r_{xy}^2 + z_e^2)^{0.5}, \quad (3.5.12)$$

$$\gamma = \text{atan2}(z_e, r_{xy}). \quad (3.5.13)$$

Then, the angle β is found using the law of cosines, such that

$$L_3^2 = r_{xyz}^2 + L_2^2 - 2r_{xyz}L_2 \cos\beta,$$

$$\cos\beta = \frac{r_{xyz}^2 + L_2^2 - L_3^2}{2r_{xyz}L_2}.$$

Using the cosine, an appropriate value for β given the geometry of the system may be determined. Using γ and β , the two θ_2 values may be calculated such that

$$\theta_2 = \gamma \pm \beta. \quad (3.5.14)$$

To calculate θ_3 , the angle α may be calculated using the law of sines, such that

$$\frac{\sin\alpha}{r_{xyz}} = \frac{\sin\beta}{L_3}. \quad (3.5.15)$$

Using the sine, an appropriate value for β given the geometry of the system may be determined. Then, depending on the specific θ_2 chosen, θ_3 may be calculated such that

$$\theta_3 = \pm(180^\circ - \alpha). \quad (3.5.16)$$

3.5.3 Optimization Methods

The last example showed that *kinematic decoupling* can be used to derive the solution of *inverse kinematics* problems via analytical methods. Still there exist many other robotic system and inverse kinematics problems that are not amenable to analytic solution. Such problems can often be tackled by using numerical techniques for the approximate solution of optimization problems. There is an extensive literature that studies these techniques, and most introductory numerical methods courses taught in an undergraduate curriculum include some discussion of the fundamentals. The details of the underlying numerical algorithms will not be covered in this book, but rather concentrate on casting the inverse kinematics problem in a canonical form. Any of a variety of standard approaches can then be used to approximate the solution of the inverse kinematics problem.

The classical problem of *optimization theory* that concerns this book seeks to find the extremum of a real-valued function $J : \mathbb{R}^N \rightarrow \mathbb{R}$ over some admissible subset $Q \subseteq \mathbb{R}^N$. The extrema of the function J are the set of points at which the function has a local minima or local maxima, or at which it has an inflection point. The vector $\mathbf{q}^* \in Q$ is said to be a *local minimizer* of J if there is a neighborhood \mathcal{N} containing \mathbf{q}^* such that

$$J(\mathbf{q}^*) \leq J(\mathbf{q}) \quad (3.5.17)$$

for all $\mathbf{q} \in \mathcal{N} \subseteq Q$. If the neighborhood \mathcal{N} can be taken to be all of Q , \mathbf{q}^* is a *global minimizer* of J over Q . The form

$$\mathbf{q}^* = \underset{\mathbf{q} \in \mathcal{N}}{\operatorname{argmin}} J(\mathbf{q}) \quad (3.5.18)$$

can be used to designate the minimizer of J over the neighborhood \mathcal{N} . Equations (3.5.17) or (3.5.18) state a problem of *constrained optimization*. It is required that the optimal \mathbf{q}^* exists in the admissible set $Q \subseteq \mathbb{R}^N$. If the admissible set $Q \equiv \mathbb{R}^N$, the problem is an *unconstrained optimization problem*. The general conditions that dictate when the extrema of a given function J exist and when they are unique can be very complex. The derivation of equations that characterize the solutions of such *optimization* problems can also be found in the literature. The interested student is referred to the large number of good references on this subject, typical ones being [35] or [47]. This book aims to cast the problems of *inverse kinematics* into the form of the problem in Equations (3.5.17) or (3.5.18).

The first step in posing the inverse kinematics problems as an optimization problem consists of defining an appropriate error or cost functional that must be optimized. For example, to solve an inverse kinematics problem and find the joint variables q_1, \dots, q_N that locate a point p fixed on the robot at some desired point p_d in the inertial frame, the cost functional J could be defined to be

$$\begin{aligned} J(\mathbf{q}) &:= \frac{1}{2} \|\mathbf{r}_{o,p}^o(\mathbf{q}) - \mathbf{r}_{o,p_d}^o\|^2, \\ &= \frac{1}{2} (\mathbf{r}_{o,p}^o(\mathbf{q}) - \mathbf{r}_{o,p_d}^o)^T (\mathbf{r}_{o,p}^o(\mathbf{q}) - \mathbf{r}_{o,p_d}^o). \end{aligned}$$

In this expression the position $\mathbf{r}_{0,p}^0 := \mathbf{r}_{0,p}^o(\mathbf{q})$ of the point p on the robot depends on the value of the joint variables \mathbf{q} , but the position of the desired point \mathbf{r}_{0,p_d}^0 does not. This quadratic function is common in applications, but many alternative functions could also be used. In general, a good cost functional is constructed so that

- (1) it is a differentiable function of the unknowns \mathbf{q} ,
- (2) it is non-negative, and
- (3) it has a minimum value at the desired configuration.

Ideally, that the minimum value is unique, but many problems of *inverse kinematics* are structured such that there are many possible solutions. Example (3.5.7) discussed below is of this type. Differentiable cost functions are chosen, if possible, because many algorithms have been developed that can exploit derivatives in approximating the solution of the extremization problem. Generally speaking, smooth cost functions lead to more efficient solution techniques. Both the theory and collection of numerical methods for optimization of smooth functionals are more mature and well-developed than that for non-smooth functions. In addition, the cost functional can often be expressed efficiently in terms of the specialized kinematics formulations already developed for robotic systems. If \mathbf{p}^N are the homogeneous coordinates of point p in the tool frame N and \mathbf{p}_d^0 are the given homogeneous coordinates of the desired point p_d in the ground frame, the cost functional J can be written as

$$J(\mathbf{q}) := \frac{1}{2} (\mathbf{H}_N^0(\mathbf{q}) \mathbf{p}^N - \mathbf{p}_d^0)^T (\mathbf{H}_N^0(\mathbf{q}) \mathbf{p}^N - \mathbf{p}_d^0).$$

For this choice of the cost functional, the problem of inverse kinematics is that of finding $\mathbf{q}^* \in Q$ where

$$\mathbf{q}^* = \underset{\mathbf{q} \in N}{\operatorname{argmin}} J(\mathbf{q})$$

for some neighborhood $N \subseteq Q$ where Q is the set of admissible joint variables.

Example 3.5.7. This example examines some of the inherent difficulties associated with solving the inverse kinematic problem using standard numerical techniques for optimization problems for complex robotic systems. Consider again the flapping wing robotic system in Figure (1.25). Suppose that the trajectories of photoreflective markers fixed to the wings of birds in flight have been experimentally collected using high speed cameras. Derive an optimization problem whose solution could yield the joint angles that induce the measured motion of the wings. Discuss any potential difficulties that might be encountered in the numerical solution of this inverse kinematics problem.

Solution: When the Denavit-Hartenberg convention is used to represent the kine-

matics of the flapping wing robot, the following four homogenous transformations relate the body fixed frames 0, 1, 2, 3, 4:

$$\begin{aligned}\mathbf{H}_1^0(\theta_1) &= \left[\begin{bmatrix} \cos \theta_1 & 0 & \sin \theta_1 \\ \sin \theta_1 & 0 & -\cos \theta_1 \\ 0 & 1 & 0 \\ 0 & 0 & 0 \end{bmatrix} \begin{Bmatrix} 0 \\ 0 \\ d_{o,p} \\ 1 \end{Bmatrix} \right], \\ \mathbf{H}_2^1(\theta_2) &= \left[\begin{bmatrix} \cos \theta_2 & -\sin \theta_2 & 0 \\ \sin \theta_2 & \cos \theta_2 & 0 \\ 0 & 0 & 1 \end{bmatrix} \begin{Bmatrix} \cos \theta_2 d_{p,q} \\ \sin \theta_2 d_{p,q} \\ 0 \\ 1 \end{Bmatrix} \right], \\ \mathbf{H}_3^2(\theta_3) &= \left[\begin{bmatrix} \cos \theta_3 & -\sin \theta_3 & 0 \\ \sin \theta_3 & \cos \theta_3 & 0 \\ 0 & 0 & 1 \end{bmatrix} \begin{Bmatrix} \cos \theta_3 d_{q,r} \\ \sin \theta_3 d_{q,r} \\ 0 \\ 1 \end{Bmatrix} \right], \\ \mathbf{H}_4^3(\theta_4) &= \left[\begin{bmatrix} \cos \theta_4 & -\sin \theta_4 & 0 \\ \sin \theta_4 & \cos \theta_4 & 0 \\ 0 & 0 & 1 \end{bmatrix} \begin{Bmatrix} \cos \theta_4 d_{r,s} \\ \sin \theta_4 d_{r,s} \\ 0 \\ 1 \end{Bmatrix} \right].\end{aligned}$$

An error function may be defined to measure how close the positions fixed on the wings are to the desired, experimentally measured positions. Suppose that these points observed in the experiment are the origins of the 2, 3, and 4 frames, or points q, r , and s . It is known that

$$\begin{aligned}\mathbf{q}^0 &= \mathbf{H}_1^0(\theta_1)\mathbf{H}_2^1(\theta_2)\mathbf{q}^2 = \mathbf{H}_1^0(\theta_1)\mathbf{H}_2^1(\theta_2)\begin{Bmatrix} 0 \\ 0 \\ 0 \\ 1 \end{Bmatrix}, \\ \mathbf{r}^0 &= \mathbf{H}_1^0(\theta_1)\mathbf{H}_2^1(\theta_2)\mathbf{H}_3^2(\theta_3)\mathbf{r}^3 = \mathbf{H}_1^0(\theta_1)\mathbf{H}_2^1(\theta_2)\mathbf{H}_3^2(\theta_3)\begin{Bmatrix} 0 \\ 0 \\ 0 \\ 1 \end{Bmatrix}, \\ \mathbf{s}^0 &= \mathbf{H}_1^0(\theta_1)\mathbf{H}_2^1(\theta_2)\mathbf{H}_3^2(\theta_3)\mathbf{H}_4^3(\theta_4)\mathbf{s}^4 = \mathbf{H}_1^0(\theta_1)\mathbf{H}_2^1(\theta_2)\mathbf{H}_3^2(\theta_3)\mathbf{H}_4^3(\theta_4)\begin{Bmatrix} 0 \\ 0 \\ 0 \\ 1 \end{Bmatrix},\end{aligned}$$

where $\mathbf{q}^0, \mathbf{r}^0, \mathbf{s}^0$ are the homogeneous coordinates of the points q, r, s in the 0 frame and $\mathbf{q}^2, \mathbf{r}^3, \mathbf{s}^4$ are the homogeneous coordinates of q, r, s in the 2, 3, 4 frames, respectively. By inspection, points q, r, s have straightforward representations in the frames 2, 3, 4,

$$\mathbf{q}^2 = \mathbf{r}^3 = \mathbf{s}^4 = \begin{Bmatrix} 0 \\ 0 \\ 0 \\ 1 \end{Bmatrix}.$$

Suppose that the locations of the points q, r, s in the 0 frame that have been collected in the experiments are denoted by $\mathbf{q}_e^0, \mathbf{r}_e^0, \mathbf{s}_e^0$. The tracking error can be written as

$$\begin{aligned}\mathbf{e}_q &:= \mathbf{q}^0 - \mathbf{q}_e^0, \\ \mathbf{e}_r &:= \mathbf{r}^0 - \mathbf{r}_e^0, \\ \mathbf{e}_s &:= \mathbf{s}^0 - \mathbf{s}_e^0.\end{aligned}$$

One possible and commonly used measure of error is the weighted quadratic cost

$$e := \frac{1}{2} \sum_{i=q,r,s} w_i \mathbf{e}_i^T \mathbf{e}_i$$

where the summation is carried out over the points $i = q, r, s$ and w_i is a positive weighting for each point $i = q, r, s$. Because the error measure is a sum of real quadratic terms, the error measure is always nonnegative and is equal to zero only when the positions of points q, r, s exactly match the experimentally measured positions. The weights w_i for $i = q, r, s$ enable the analyst to emphasize the contributions to the total error of the error in matching the positions of q, r or s . When the definitions of the homogeneous transformations is substituted in the total error equation,

$$\begin{aligned}e &:= e \begin{pmatrix} \theta_1 \\ \theta_2 \\ \theta_3 \\ \theta_4 \end{pmatrix}, \\ &= \frac{1}{2} w_q \left(\mathbf{H}_1^0(\theta_1) \mathbf{H}_2^1(\theta_2) \begin{Bmatrix} 0 \\ 0 \\ 0 \\ 1 \end{Bmatrix} - \mathbf{q}_e^0 \right) \cdot \left(\mathbf{H}_1^0(\theta_1) \mathbf{H}_2^1(\theta_2) \begin{Bmatrix} 0 \\ 0 \\ 0 \\ 1 \end{Bmatrix} - \mathbf{q}_e^0 \right) \\ &\quad + \frac{1}{2} w_T \left(\mathbf{H}_1^0(\theta_1) \mathbf{H}_2^1(\theta_2) \mathbf{H}_3^2(\theta_3) \begin{Bmatrix} 0 \\ 0 \\ 0 \\ 1 \end{Bmatrix} - \mathbf{r}_e^0 \right) \cdot \left(\mathbf{H}_1^0(\theta_1) \mathbf{H}_2^1(\theta_2) \mathbf{H}_3^2(\theta_3) \begin{Bmatrix} 0 \\ 0 \\ 0 \\ 1 \end{Bmatrix} - \mathbf{r}_e^0 \right) \\ &\quad + \frac{1}{2} w_s \left(\mathbf{H}_1^0(\theta_1) \mathbf{H}_2^1(\theta_2) \mathbf{H}_3^2(\theta_3) \mathbf{H}_4^3(\theta_4) \begin{Bmatrix} 0 \\ 0 \\ 0 \\ 1 \end{Bmatrix} - \mathbf{s}_e^0 \right) \cdot \left(\mathbf{H}_1^0(\theta_1) \mathbf{H}_2^1(\theta_2) \mathbf{H}_3^2(\theta_3) \mathbf{H}_4^3(\theta_4) \begin{Bmatrix} 0 \\ 0 \\ 0 \\ 1 \end{Bmatrix} - \mathbf{s}_e^0 \right).\end{aligned}$$

Some insight into the qualitative features of the solution of the minimization problem can be gained by considering a few simple examples. First, suppose that

$$d_{o,p} = d_{p,q} = d_{q,r} = d_{r,s} = .05 \text{ meters},$$

$$w_q = w_r = 0,$$

$$\mathbf{s}_e^0 = \begin{Bmatrix} .1512 \\ 0 \\ .0512 \\ 1 \end{Bmatrix}.$$

The choice of $w_q = w_r = 0$ means that the total error does not depend on the relative error between the points s, r and the experimentally observed values of these points. Solving the optimization problem with this set of parameters will find a set of joint angles that position the terminal point s close to the experimentally observed value. As is typical for redundant manipulators, this problem does not have a unique set of joints angles that minimize the error measure. Two such minimizers, designated as configurations A and B , are

$$\begin{aligned} (\theta_1^A, \theta_2^A, \theta_3^A, \theta_4^A) &= (-3.14, -1.99, -2.45, 8.18) \quad \text{rad}, \\ (\theta_1^B, \theta_2^B, \theta_3^B, \theta_4^B) &= (0, .819, -2.54, 1.48) \quad \text{rad}. \end{aligned}$$

These two minimizers both yield a measure of error e that is equal to zero to machine precision. Both choices of joint angles induce a tip position of point s that coincides, within machine accuracy, with the experimentally observed position as shown in Figure (3.35). It is difficult to visualize the complexity of even this simple case

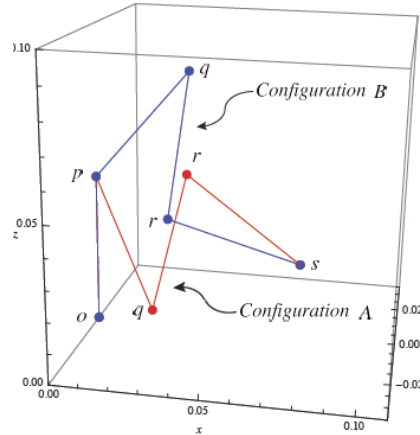


Fig. 3.35: Two minimizers of the error functional, configurations A and B

because the joint angles vary in a four dimensional set. Figure (3.36) and (3.37)

depict the contours of the error function that is “sliced” along a plane that passes through the optimum value

$$\begin{aligned} e^A(\theta_2, \theta_4) &= e(\theta_1^A, \theta_2, \theta_3^A, \theta_4), \\ e^B(\theta_2, \theta_4) &= e(\theta_1^B, \theta_2, \theta_3^B, \theta_4). \end{aligned}$$

In other words $e^A(\theta_2, \theta_4)$ depicts the error contours as θ_2 and θ_4 are varied, but θ_1

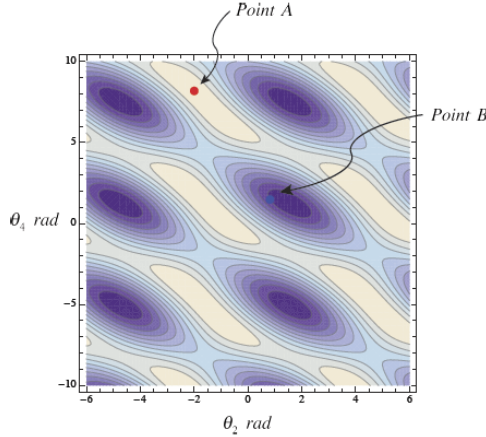


Fig. 3.36: Error contours of $e^A(\theta_2, \theta_4)$

and θ_3 are fixed at the optimum values for configuration A. The function $e^B(\theta_2, \theta_4)$ is similar, but θ_1 and θ_3 are fixed at their optimal values in configuration B. Clearly the optimal values are located at different relative minima of the error functions. Even more importantly, as shown in Figure (3.38) these local optima are not unique. There are an infinite number of relative minima. Figure (3.38) depicts a plot of the function $e^B(\theta_2, \theta_4)$ to convey the complexity of the error function being extremized. The first study simplified the form of the error function so that $w_q = w_r = 0$, and the value of error in the first example case does not depend on the location of the points q, r . Now consider a more interesting example. Suppose that the experimentally observed trajectories of q, r, s obey the following laws as a function of time t ,

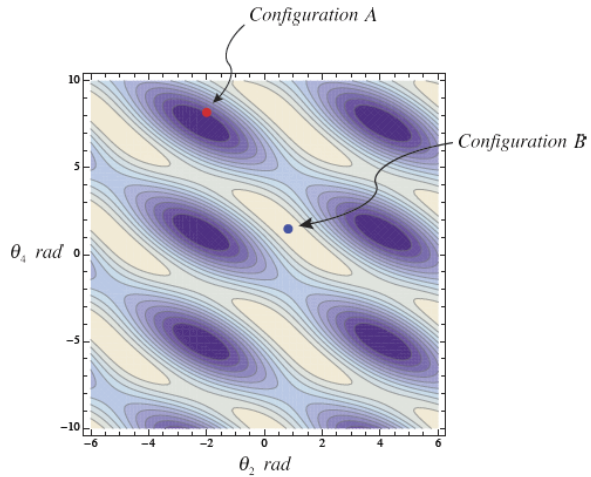


Fig. 3.37: Error contours of $e^B(\theta_2, \theta_4)$

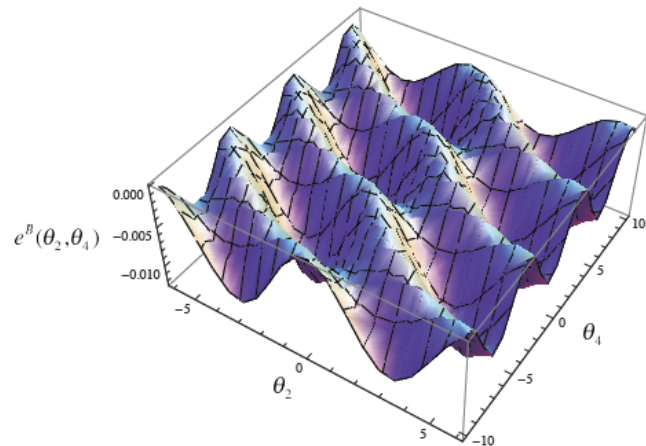


Fig. 3.38: Plot of $e^B(\theta_2, \theta_4)$

$$\mathbf{q}_e^0(t) = \begin{pmatrix} .05 \\ 0 \\ .05 \\ 1 \end{pmatrix} \text{ meters,} \quad \mathbf{r}_e^0(t) = \begin{pmatrix} .075 \\ 0 \\ .05 \\ 1 \end{pmatrix} \text{ meters,}$$

$$\mathbf{s}_e^0(t) = \begin{pmatrix} .1 \\ 0 \\ .05 \\ 1 \end{pmatrix} + \frac{.05}{2} \begin{pmatrix} \cos \alpha(t) \\ 0 \\ \sin \alpha(t) \\ 0 \end{pmatrix} \text{ meters,}$$

where $\alpha(t_i) = \frac{(i-1)\pi}{n_i}$, i is the index of time step t_i , and there are N_s samples. The experimentally observed trajectory of point r in this case is a fixed point located at $(.075, 0, .05)$. The experimentally observed trajectory of point s lies on the arc of the circle in the $\mathbf{x}_0 - \mathbf{z}_0$ plane with a center at $(.1, 0, .05)$. It is observed that point q is fixed at point $(.05, 0, .05)$ during the experiment. Figure (3.39) depicts the sequence of configurations of the robot as a function of time that solves the inverse kinematics problem at each time step when $w_r = w_q = w_5 = 1$ are selected. Note that the solution of the inverse kinematics problem yields a set of joint angles that minimizes the error between the points q, r, s on the robot and their experimentally observed values. Also note that, in general, this does not guarantee that the points q, r, s match exactly the experimentally observed values.

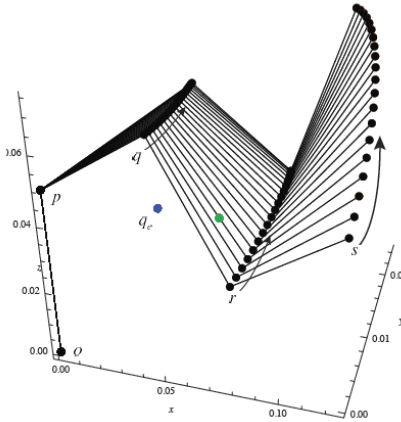


Fig. 3.39: Configurations of the Flapping Wing Robot for Time-Varying Observed Trajectory

3.5.4 Inverse Velocity Kinematics

Just as inverse kinematics allows the calculation of joint angles given an end effector position and orientation, inverse velocity kinematics allows for the calculation of joint angle velocities based on a given end effector velocity and angular velocity. The solvability of the inverse velocity kinematics problem depends on the number of specified task space velocity parameters m and the number of n joint velocities to be calculated. As with the inverse kinematics problem, there are three cases to consider:

- $m > n$, where the robot does not have a sufficient number of independent joint variables to provide all possible end-effector movements. As a result, the inverse velocity kinematics problem may not have a solution.
- $m < n$, where the robot possess more degrees of freedom than are required to generate the desired end effector solutions. As a result, there are infinite solutions to the inverse differential kinematics problem. As before, this case is called redundancy.
- $m = n$, where the robot possesses equal numbers of degrees of freedom and end effector workspace.

Unlike inverse kinematics, the mapping from the joint angle velocities into the end effector velocity and angular velocity is known to be linear. As discussed in Section (3.3.5), this mapping is called the *Jacobian matrix*. When $m = n$, the Jacobian matrix is square. If the determinant of this matrix is non-zero, the matrix is invertible, providing a straightforward solution for the joint angle velocities, such that

$$\begin{Bmatrix} \dot{q}_1 \\ \vdots \\ \dot{q}_N \end{Bmatrix} = (\mathbf{J}^0)^{-1} \begin{Bmatrix} \mathbf{v}_{0,p}^0 \\ \boldsymbol{\omega}_{0,N}^0 \end{Bmatrix}.$$

The Jacobian matrix represents the geometry of the robotic arm at a given configuration. At some configurations, the determinant of the Jacobian may become zero. By definition, the inverse of a matrix does not exist if that matrix's determinant is zero. The geometric cause of a Jacobian's determinant becoming zero is singularity.

3.5.4.1 Singularity

At a singular configuration, there is at least one velocity or angular velocity coordinate along or about which it s impossible to translate or rotate the end effector, regardless of the joint velocities selected. Mathematically, the Jacobian matrix determinant becomes zero at a singular configuration because the matrix is no longer full rank and one or more of its columns becomes linearly dependent on the other columns. Singularities can be categorized into two groups: workspace boundary singularities and workspace interior singularities.

Workspace boundary singularities occur when the robot is fully stretched out or folded back onto itself such that the end effector is at the boundary of its workspace. Since the end effector's motion is restricted to the subset of direction pointing tangential to the workspace boundary or within it, it has lost its full mobility and the Jacobian reflects that.

Workspace interior singularities occur within the workspace and are typically due to one or more joint axes lining up along the kinematic chain. When two joint axes align, their impact on the motion of the end effector is identical. This creates a linear dependence between the two columns corresponding to these joints in the Jacobian, reducing the rank of the matrix.

Singular configurations should usually be avoided since most manipulators are designed for tasks in which all degrees of freedom are required. Furthermore, near singular configurations, the joint velocities required to maintain the desired end effector velocity in certain directions may become extremely large.

For common six degree of freedom manipulators, the most common singular configurations are listed below.

1. *Two collinear revolute joint axes:* this type is most common in spherical wrist assemblies that have three mutually perpendicular axes intersecting at a single point. As the second joint rotates, the first and third joints may align, creating two linearly independent columns in the Jacobian. Mechanical restrictions are usually imposed on the wrist design to prevent the wrist axes from generating a wrist singularity.
2. *Three parallel coplanar revolute joint axes:* this type occurs in an elbow manipulator with a spherical wrist when it is fully extended or fully retracted.
3. *Four revolute joint axes intersecting at one point.*
4. *Four coplanar revolute joints.*
5. *Six revolute joints intersecting along a line.*
6. *A prismatic joint axis perpendicular to two parallel coplanar revolute joints.*

In addition to the Jacobian singularities, the motion of a manipulator is restricted if the joint variables are constrained with upper and lower bounds. When a joint reaches its boundary, this effectively removes a degree of freedom.

3.6 Problems for Chapter 3, Kinematics of Robotic Systems

3.6.1 Problems on Homogeneous Transformations

Problem 3.1 (Solution ??). Consider the SCARA robot shown in Figure (3.40).

- (i) Derive the homogeneous transform H_B^A .
- (ii) Derive the homogeneous transform H_C^B .
- (iii) Derive the homogeneous transform H_D^C .

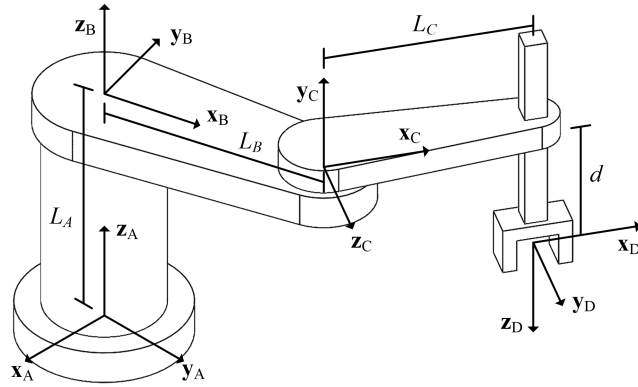


Fig. 3.40: SCARA Robot and Frame Definitions

- (iv) What are the homogeneous coordinates \mathbf{p}^A of the origin of the \mathbb{D} frame in the frame \mathbb{A} ?
- (v) Write a program that calculates \mathbf{H}_D^A and \mathbf{p}^A using the results (i)-(iv) above.

Problem 3.2 (Solution ??). Consider the cylindrical robot shown in Figure (3.41).

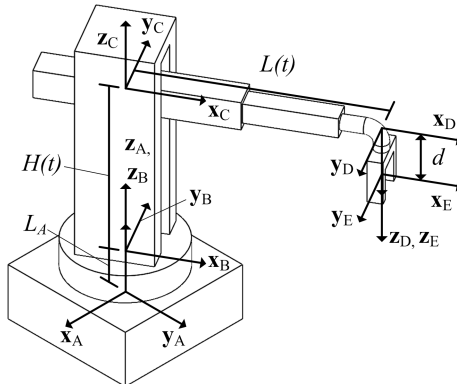


Fig. 3.41: Cylindrical Robot and Frame Definitions

- (i) Derive the homogeneous transform \mathbf{H}_B^A .
- (ii) Derive the homogeneous transform \mathbf{H}_C^B .
- (iii) Derive the homogeneous transform \mathbf{H}_D^C .
- (iv) What are the homogeneous coordinates \mathbf{p}^A of the origin of the \mathbb{E} frame in the frame \mathbb{A} ?
- (v) Write a program that calculates \mathbf{H}_D^A and \mathbf{p}^A using the results in (i)-(iv) above.

Problem 3.3 (Solution ??). Consider the modular robot shown in Figure 3.42. The frames $\mathbb{B}, \mathbb{C}, \mathbb{D}, \mathbb{E}$ are body fixed frames of reference. Each cube has dimensions $2A \times 2A \times 2A$. The short links having body fixed frames \mathbb{C} and \mathbb{D} , which are constructed from two such blue cubes, have a length that is D as measured to the center of each end cube. The link to which the body fixed \mathbb{B} frame is attached has a length L measured from the faces of the cubes at each end.

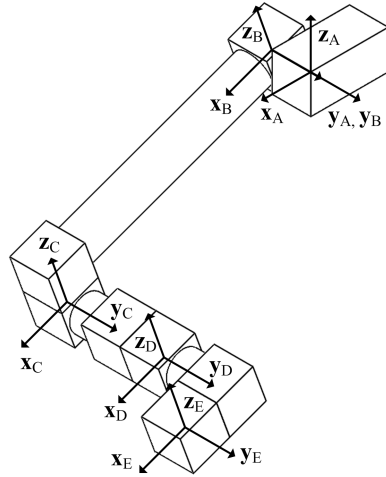


Fig. 3.42: Modular Robot and Frame Definitions

- (i) Suppose that the angle $\theta_{\mathbb{B}}$ measures rotation about the positive $y_{\mathbb{A}} = y_{\mathbb{B}}$ axis, as measured from the positive $z_{\mathbb{A}}$ axis to the positive $z_{\mathbb{B}}$ axis. Derive the homogeneous transform $H_{\mathbb{B}}^{\mathbb{A}}$.
- (ii) Suppose that the angle $\theta_{\mathbb{C}}$ measures the angle about the positive $z_{\mathbb{B}} = z_{\mathbb{C}}$ axis, as measured from the positive $x_{\mathbb{B}}$ axis to the positive $x_{\mathbb{C}}$ axis. Derive the homogeneous transform $H_{\mathbb{C}}^{\mathbb{B}}$.
- (iii) Suppose that the angle $\theta_{\mathbb{D}}$ measures the angle about the positive $y_{\mathbb{C}} = y_{\mathbb{D}}$ axis, as measured from the positive $z_{\mathbb{C}}$ axis to the positive $z_{\mathbb{D}}$ axis. Derive the homogeneous transform $H_{\mathbb{D}}^{\mathbb{C}}$.
- (iv) Suppose that the angle $\theta_{\mathbb{E}}$ measures the angle about the positive $x_{\mathbb{D}} = x_{\mathbb{E}}$ axis, as measured from the positive $y_{\mathbb{D}}$ axis to the positive $y_{\mathbb{E}}$ axis. Derive the homogeneous transform $H_{\mathbb{E}}^{\mathbb{D}}$.
- (v) What are the homogeneous coordinates $p^{\mathbb{A}}$ of the origin of the \mathbb{E} frame in the frame \mathbb{A} ?
- (vi) Find the homogeneous transformation $H_{\mathbb{E}}^{\mathbb{A}}$ and $p^{\mathbb{A}}$ using the results in (i) through (v) above.

3.6.2 Problems on Ideal Joints and Constraints

Problem 3.4 (Solution ??). Consider the spherical joint depicted in Figure (3.43). Derive the homogeneous transform that relates the joint coordinates systems of the spherical joint when the 3-2-1 Euler angles are used to parameterize the rotation matrix $\mathbf{R}_{\mathbb{A}}^{\mathbb{B}}$ for the system shown.

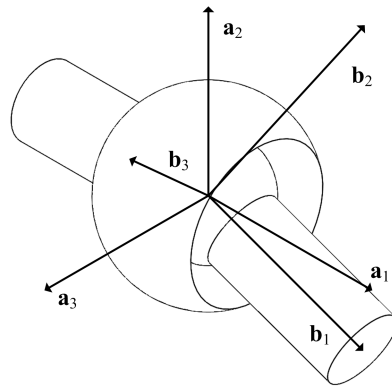


Fig. 3.43: Spherical joint

Problem 3.5 (Solution ??). Derive another definition of the universal joint, different from that given in Example (3.2.1), by selecting different angles of rotation that map the \mathbb{A} frame into the \mathbb{B} frame. Derive the corresponding homogeneous transformation.

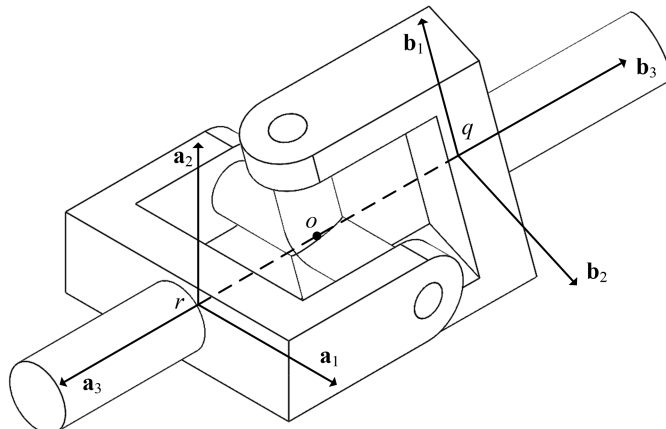


Fig. 3.44: Universal Joint

3.6.3 Problems on Denavit-Hartenberg Convention

Problem 3.6 (Solution ??). Derive a kinematic model for the SCARA robotic manipulator in Problem (3.1) using the Denavit-Hartenberg convention.

Problem 3.7 (Solution ??). Derive a kinematic model for the cylindrical robotic manipulator in Problem (3.2) using the Denavit-Hartenberg convention.

Problem 3.8 (Solution ??). Derive a kinematic model for the modular robotic arm in Problem (3.3) using the Denavit-Hartenberg convention.

Problem 3.9 (Solution ??). Derive a kinematic model for the spherical robotic manipulator depicted in Figure (3.45) using the Denavit-Hartenberg Convention.

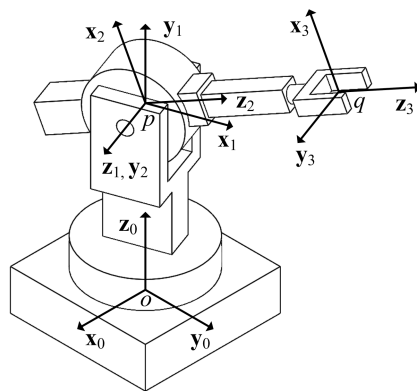


Fig. 3.45: Spherical Robot

Problem 3.10 (Solution ??). Derive a kinematic model for the arm assembly depicted in Figure (3.46) using the Denavit-Hartenberg convention.

Problem 3.11 (Solution ??). The Space Shuttle Remote Manipulator System (SS-RMS) is shown in (3.47). Use the Denavit-Hartenberg Convention to derive a kinematic model of the end effector frame position. What are the *homogeneous* transformations that characterize the *rigid body motion* of each adjacent pair of frames?

Problem 3.12 (Solution ??). A six degree of freedom industrial robot is depicted in Figure (3.48). A set of body fixed frames is introduced as shown in Figure (3.49). Verify that this collection of frames satisfies the underlying assumptions of the Denavit-Hartenberg Convention. Define the link rotation, twist, offset and displacement associated with this definition of frames. Determine the homogeneous transformations that relate each pair of consecutive frames.

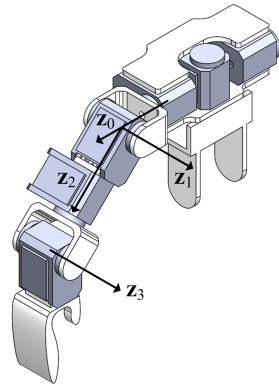


Fig. 3.46: Humanoid Arm Assembly with Revolute Axes Defined

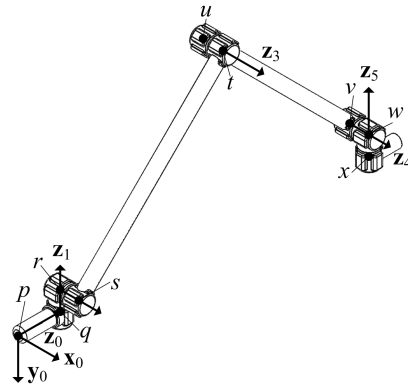


Fig. 3.47: Space Shuttle Remote Manipulator System (SSRMS)

3.6.4 Problems on Angular Velocity and Velocity for Kinematic Chains

Problem 3.13 (Solution ??). Consider the schematic of the PUMA robot in Figure (3.50). Define the link parameters of the *Denavit-Hartenberg Convention* for this robot. Derive *homogeneous transformation* that maps the end frame 3 into the inertial frame 0 using the *Denavit-Hartenberg Convention*. Derive the *Jacobian matrix*

$$\begin{Bmatrix} \mathbf{v}_{0,t}^0 \\ \boldsymbol{\omega}_{0,3}^0 \end{Bmatrix} = \begin{bmatrix} \mathbf{J}_v \\ \mathbf{J}_\omega \end{bmatrix} \begin{Bmatrix} \dot{q}_1 \\ \dot{q}_2 \\ \dot{q}_3 \end{Bmatrix}$$

Problem 3.14 (Solution ??). Consider the *spherical wrist* which is shown in Figure (3.51).

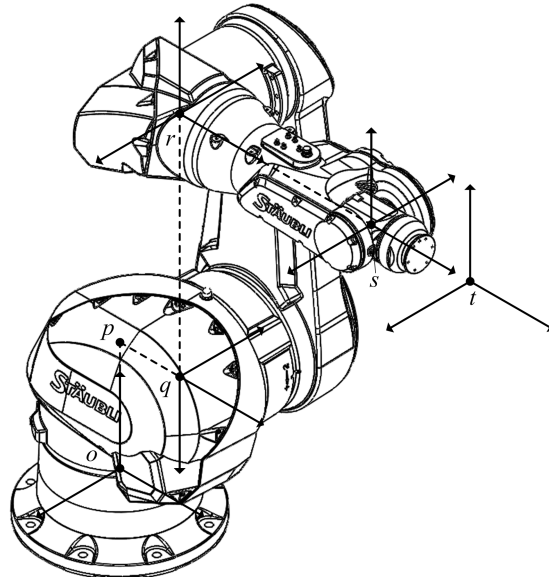


Fig. 3.48: Industrial Robot with Frames Illustrated

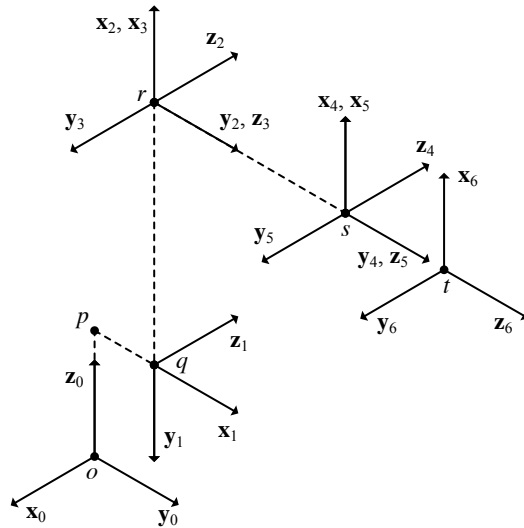


Fig. 3.49: Industrial Robot Frames Labeled

Find the Jacobian matrix that relates the velocities and angular velocities to the joint variables in the equation

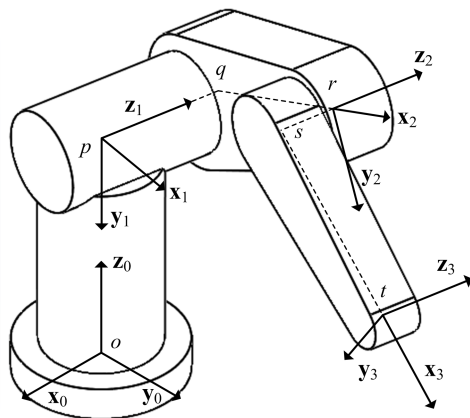


Fig. 3.50: PUMA Robot

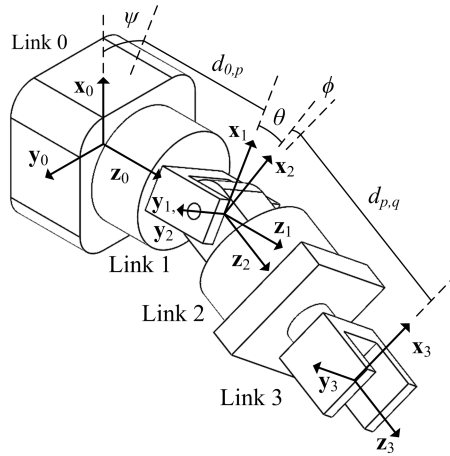


Fig. 3.51: The Spherical Wrist

$$\begin{Bmatrix} \mathbf{v}_{0,3}^0 \\ \boldsymbol{\omega}_{0,3}^0 \end{Bmatrix} = \begin{bmatrix} \mathbf{J}_v \\ \mathbf{J}_\omega \end{bmatrix} \begin{Bmatrix} \dot{\psi} \\ \dot{\theta} \\ \dot{\phi} \end{Bmatrix}.$$

Problem 3.15 (Solution ??). Repeat Problem (3.14) using the *Denavit-Hartenberg Convention*. Find the Jacobian matrix.

$$\begin{Bmatrix} \mathbf{v}_{0,3}^0 \\ \boldsymbol{\omega}_{0,3}^0 \end{Bmatrix} = \begin{bmatrix} \mathbf{J}_v \\ \mathbf{J}_\omega \end{bmatrix} \begin{Bmatrix} \dot{\theta}_1 \\ \dot{\theta}_2 \\ \dot{\theta}_3 \end{Bmatrix}$$

Compare the results with those from Problem (3.14).

Problem 3.16 (Solution ??). Calculate the Jacobian matrix \mathbf{J}^0 that relates the velocity of the point p and the angular velocity $\boldsymbol{\omega}_{0,2}$ to the derivatives of the joint angles in the laser scanner in Example (3.3.1). In other words, find the Jacobian matrix \mathbf{J}^0 in the equation

$$\begin{Bmatrix} \mathbf{v}_{0,r}^0 \\ \boldsymbol{\omega}_{0,2}^0 \end{Bmatrix} = \mathbf{J}^0 \begin{Bmatrix} \dot{\theta}_1 \\ \dot{\theta}_2 \end{Bmatrix}$$

Calculate the Jacobian matrix \mathbf{J}^0 two ways. First, find the velocities and angular velocities from first principles and identify the Jacobian matrix from these expressions. Second, use Theorem (3.3) to calculate the Jacobian directly.

Problem 3.17 (Solution ??). Calculate the Jacobian matrix \mathbf{J}^0 that relates the velocity of the origin of frame 4 and the angular velocity $\boldsymbol{\omega}_{0,4}$ to the derivatives of the joint angles in the arm assembly in Problem (3.10). In other words, find the Jacobian \mathbf{J}^0 in the matrix equation

$$\begin{Bmatrix} \mathbf{v}_{0,4}^0 \\ \boldsymbol{\omega}_{0,4}^0 \end{Bmatrix} = \begin{bmatrix} \mathbf{J}_v^0 \\ \mathbf{J}_\omega^0 \end{bmatrix} \begin{Bmatrix} \dot{\theta}_1 \\ \dot{\theta}_2 \\ \dot{\theta}_3 \\ \dot{\theta}_4 \end{Bmatrix}$$

Problem 3.18 (Solution ??). Derive the homogenous transform that maps the 4 frame to the 0 frame for the robotic flapping wing shown in Figure (3.52).

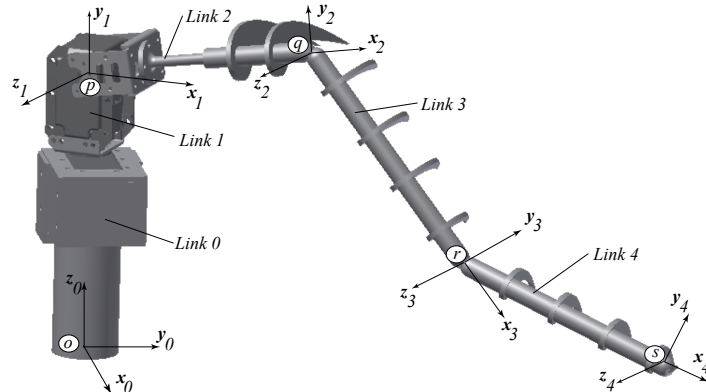


Fig. 3.52: Flapping Wing Robot

Problem 3.19 (Solution ??). Use the Denavit Hartenberg Procedure to define the joint angles θ_1, θ_2 and θ_3 for the PUMA robot discussed in Problem (3.13). Use the recursive Order (N) formulation to solve for the velocities of the joints and the angular velocities of the links in the PUMA robot.

Problem 3.20 (Solution ??). Use the Denavit Hartenberg Procedure to define the joint angles θ_1, θ_2 and θ_3 for the spherical wrist studied in Problem (3.15). Renumber the frames and joints consistent with the recursive Order (N) formulation, but keep the definition of the joint angles. Use the recursive Order (N) formulation to solve for the velocities of the joints and the angular velocities of the links.

Problem 3.21. A three degree of freedom Cartesian robot is shown in Figure (3.53). The system is comprised of a frame that moves along the \mathbf{z}_0 direction, a crossbar that moves relative to the frame in the \mathbf{z}_1 direction, and a tool assembly that moves relative to the the crossbar in the \mathbf{z}_2 direction. The motion of the frame relative to the ground is measured by the coordinate $z(t)$, the motion of the crossbar relative to the frame is measured by $x(t)$, and the motion of the tool assembly relative to the crossbar is measured by $y(t)$. Suppose that the *spherical wrist* studied in Problems (3.15) is rigidly attached to the end of the tool assembly on the Cartesian robot. Find the *Jacobian matrix* for this robotic system.

$$\left\{ \begin{array}{c} \mathbf{v}_{0,3}^0 \\ \boldsymbol{\omega}_{0,6}^0 \end{array} \right\} = \left[\begin{array}{c} \mathbf{J}_v \\ \mathbf{J}_\omega \end{array} \right] \dot{\mathbf{q}} = \left[\begin{array}{c} \mathbf{J}_v \\ \mathbf{J}_\omega \end{array} \right] \left\{ \begin{array}{c} \dot{x} \\ \dot{y} \\ \dot{z} \\ \dot{\theta}_1 \\ \dot{\theta}_2 \\ \dot{\theta}_3 \end{array} \right\}$$

3.6.5 Problems on Inverse Kinematics

Problem 3.22. Suppose that a spherical wrist subassembly is attached at frame D of the SCARA robot in Problem (3.1). Find an analytical solution using kinematic decoupling for the inverse kinematics problem of locating and orienting the terminal frame using kinematic decoupling.

Problem 3.23. Suppose that a spherical wrist subassembly is attached to the cylindrical robot in Problem (3.2). Find an analytical solution for the inverse kinematics problem of locating and orienting the terminal frame.

Problem 3.24. Suppose that a spherical wrist subassembly is attached to point t of the PUMA robot in Problem (3.13). Find an analytical solution using kinematic decoupling for the inverse kinematics problem of locating and orienting the terminal frame.

Problem 3.25. Suppose that a spherical wrist subassembly is attached at the origin of the 3 frame of the Cartesian robot, as discussed in Problem (3.21). Find an analytical solution using kinematic decoupling for the inverse kinematics problem of locating and orienting the terminal frame.

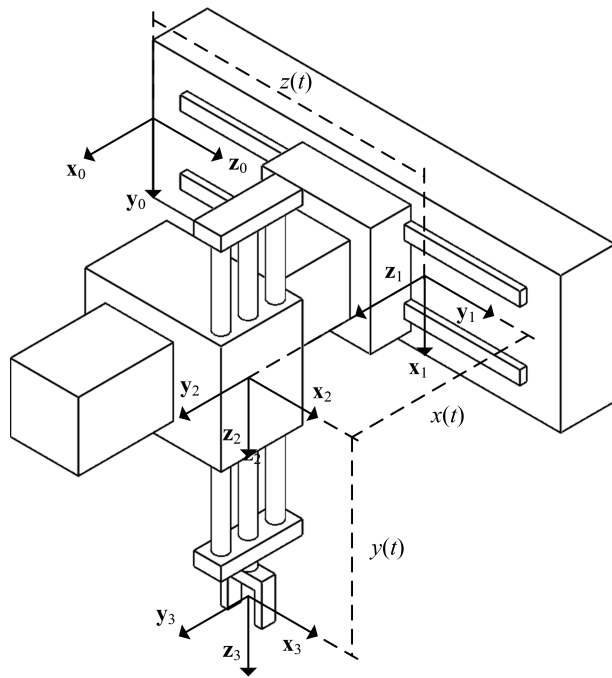


Fig. 3.53: Cartesian Robot Frames and Coordinates

Chapter 4

Newton-Euler Formulations

Abstract The field of dynamics consists of the study of *kinematics* and *kinetics*. Chapter (2) discusses the foundations of kinematics, and Chapter (3) presents specific formulations for kinematics of spatial robotic systems. The study of *kinematics* provides the language used to describe the *geometry of motion*. The field of *kinetics* studies the connection between the forces and moments that act on a mechanical system and its resulting motion. Two general approaches to the study of *kinetics* are covered in this chapter and the next. This chapter discusses the collection of methods known as *Newton-Euler formulations* of the dynamics of robotic systems. Chapter (5) presents an alternative approach, those methods based on techniques of *analytical mechanics*. Upon the completion of this chapter, the student should be able to

- Define and calculate the *linear momentum* of a rigid body.
- Define and calculate the *angular momentum* of a rigid body.
- Define and calculate the *center of mass* and inertia matrix of a rigid body.
- State and employ *Euler's Laws* for the motion of rigid bodies in a robotic system.
- Employ *recursive Order N Formulations* to study robotic system dynamics.

4.1 Linear Momentum of Rigid Bodies

Elementary principles that describe the dynamics of a point mass or particle define the *linear momentum* as the product of the mass of the particle and its velocity. The *linear momentum* of a system of particles is the sum of the *linear momenta* of the individual particles in the system. As highlighted in the following definition, the *linear momentum* of a rigid body can be viewed as a limiting case of the definition for a system of particles. The *linear momentum* of a rigid body is the integral of the velocity over all the differential mass elements that make up the rigid body.

Definition 4.1. The linear momentum $\mathbf{p}_{\mathbb{X}}$ of a rigid body in the frame \mathbb{X} is defined to be

$$\mathbf{p}_{\mathbb{X}} := \int \mathbf{v} dm,$$

where $\mathbf{v} := \mathbf{v}_{\mathbb{X},dm}$ is the velocity of the differential mass element dm in the frame \mathbb{X} as shown in Figure (4.1).

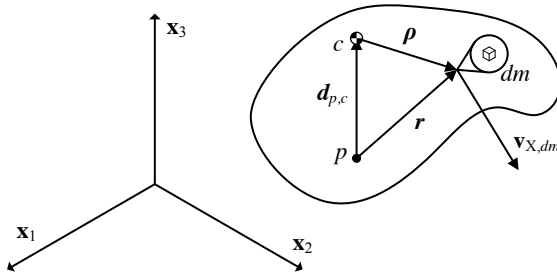


Fig. 4.1: Rigid Body with Differential Mass Element

Definition (4.1) is given in terms of the velocity of each of the infinite collection of points that make up the rigid body under consideration. The *center of mass* is introduced to obtain an expression for *linear momentum* that depends on the velocity of a single point. As a result, the *center of mass* is used to describe the motion of a mechanical system in terms of a finite set of variables.

Definition 4.2. The position $\mathbf{r}_c := \mathbf{r}_{\mathbb{X},c}$ in the frame \mathbb{X} of the *center of mass* of a rigid body is defined by the equation

$$\mathbf{r}_c = \frac{1}{M} \int \mathbf{r} dm$$

where $M = \int dm$ is the total mass of the rigid body and $\mathbf{r} := \mathbf{r}_{\mathbb{X},dm}$ is the position vector of the differential mass dm in the frame \mathbb{X} .

The above definition of the *center of mass* can be used to derive an expression for the *linear momentum* of a rigid body in terms of the center of mass velocity. The *linear momentum* of a rigid body is the product of the rigid body center of mass velocity and the total rigid body mass.

Theorem 4.1. *The linear momentum of a rigid body in the frame \mathbb{X} is given by*

$$\mathbf{p}_{\mathbb{X}} = M \mathbf{v}_{\mathbb{X},c}$$

where M is the mass of the rigid body and $\mathbf{v}_{\mathbb{X},c}$ is the velocity of the center of mass in the \mathbb{X} frame.

Proof. By definition the linear momentum is given by

$$\mathbf{p}_{\mathbb{X}} = \int \mathbf{v} dm.$$

The center of mass velocity may be calculated by taking the time derivative of $\mathbf{r}_{\mathbb{X},dm}$ and utilizing Definition (4.2), such that

$$\mathbf{v}_{\mathbb{X},c} = \frac{d}{dt} \Big|_{\mathbb{X}} (\mathbf{r}_{\mathbb{X},c}) = \frac{1}{M} \frac{d}{dt} \Big|_{\mathbb{X}} \left(\int \mathbf{r} dm \right) = \frac{1}{M} \int \frac{d}{dt} \Big|_{\mathbb{X}} (\mathbf{r}) dm = \frac{1}{M} \int \mathbf{v} dm = \frac{1}{M} \mathbf{p}_{\mathbb{X}}.$$

The equation above relies on the fact that in this case “the derivative of the integral” is equal to the “integral of the derivative,” which can be written as

$$\frac{d}{dt} \Big|_{\mathbb{X}} \left(\int \cdot \right) = \int \frac{d}{dt} \Big|_{\mathbb{X}} (\cdot).$$

This is a special case of the Leibnitz integral rule that assumes there is no flux of linear momentum across the domain of integration. \square

Applications to robotic systems often introduce numerous frames of reference to formulate the equations of motion. The next example uses the definition of the *center of mass* to calculate its location for a link in a typical robotic system.

Example 4.1.1. For the SCARA robot shown in Figure (4.2), calculate the location of the center of mass $\mathbf{r}_c := \mathbf{r}_{\mathbb{B},c}$ of the outer arm (link 2), shown in Figure (4.3a), relative to the \mathbb{B} frame. Construct this approximation by using the geometric primitive shown in Figure (4.3a) constructed of two rectangular prisms with dimensions labeled. Also assume that the mass distribution within the link is uniform.

Solution: By definition, the location of the center of mass in the \mathbb{B} frame satisfies

$$\mathbf{r}_c := \mathbf{r}_{\mathbb{B},c} = \frac{1}{M} \int \mathbf{r} dm,$$

where the vector $\mathbf{r} := \mathbf{r}_{\mathbb{B},dm}$ connects the origin of the \mathbb{B} frame to the differential mass element dm . From introductory dynamics, it is known that when the body is comprised of N discrete subcomponents this equation can be written as

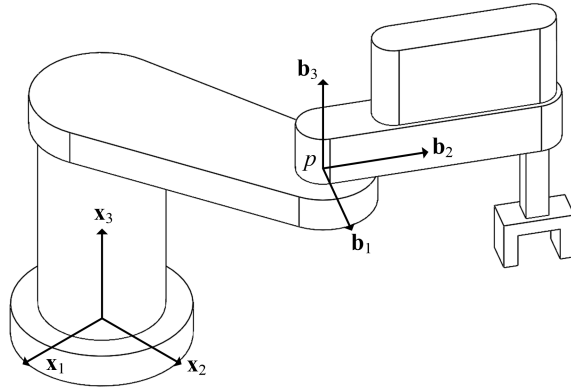


Fig. 4.2: SCARA Robot

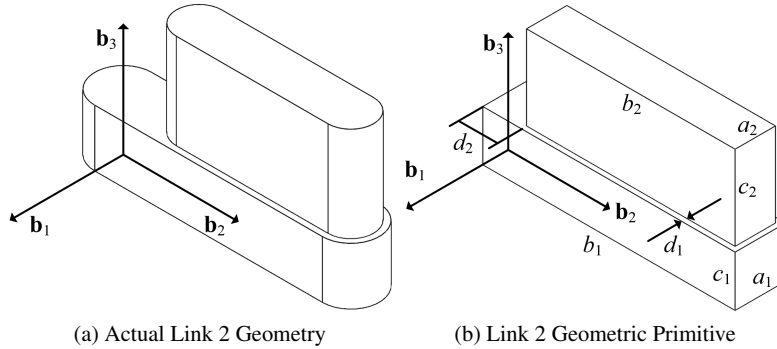


Fig. 4.3: SCARA Robot Link 2 Inertia Estimation

$$\mathbf{r}_c = \frac{\sum_{i=1}^N M_i \mathbf{r}_{c_i}}{\sum_{i=1}^N M_i},$$

where M_i is the mass of subcomponent i and $\mathbf{r}_{c_i} := \mathbf{r}_{\mathbb{B},c_i}$ is the location of the center of mass of body i in the \mathbb{B} frame. The locations of the center of mass of each subcomponent are defined as

$$\mathbf{r}_{c_1} = \frac{1}{2} b_1 \mathbf{b}_2 + \frac{1}{2} c_1 \mathbf{b}_3, \quad \mathbf{r}_{c_2} = \left(d_2 + \frac{1}{2} b_2 \right) \mathbf{b}_2 + \left(c_1 + \frac{1}{2} c_2 \right) \mathbf{b}_3.$$

The final expression for the location of the center of mass of the composite rigid body is consequently

$$\mathbf{r}_c := \mathbf{r}_{\mathbb{B},c} = \frac{\frac{1}{2}M_1b_1 + M_2(d_2 + \frac{1}{2}b_2)}{M_1 + M_2}\mathbf{b}_2 + \frac{\frac{1}{2}M_1c_1 + M_2(c_1 + \frac{1}{2}c_2)}{M_1 + M_2}\mathbf{b}_3.$$

It will be shown later in this chapter that the initial step in deriving the equations of motion for a robot often requires the evaluation of the *linear momentum* of its links. The next examples illustrate how the calculation of the linear momentum for realistic three dimensional solids, such as the links of robotic systems, is simplified when the location and velocity of the *mass center* are known.

Example 4.1.2. Calculate the linear momentum for the outer arm show in Figure (4.3a) of the SCARA robot depicted in Figure (4.2) using Theorem (4.1) and the results of Example (4.1.1). Assume that the velocity of the point p $\mathbf{v}_{\mathbb{X},p}$ and angular velocity $\boldsymbol{\omega}_{\mathbb{X},\mathbb{B}}$ of the body are given as

$$\begin{aligned}\mathbf{v}_{\mathbb{X},p} &= v_1\mathbf{b}_1 + v_2\mathbf{b}_2 + v_3\mathbf{b}_3, \\ \boldsymbol{\omega}_{\mathbb{X},\mathbb{B}} &= \omega_1\mathbf{b}_1 + \omega_2\mathbf{b}_2 + \omega_3\mathbf{b}_3.\end{aligned}$$

Assume that at the moment under consideration, the \mathbb{B} frame and \mathbb{X} frames are aligned (i.e., $\mathbf{R}_{\mathbb{B}}^{\mathbb{X}}$ is the identity matrix). Express the answer in terms of the basis for the \mathbb{B} frame.

Solution: From Theorem (4.1) the linear momentum is given by $\mathbf{p}_{\mathbb{X}} = M\mathbf{v}_{\mathbb{X},c}$. The velocity of the center of mass can be calculated using the Relative Velocity Theorem (2.16) in Chapter (2) as

$$\begin{aligned}\mathbf{v}_{\mathbb{X},c} &= \mathbf{v}_{\mathbb{X},p} + \boldsymbol{\omega}_{\mathbb{X},\mathbb{B}} \times \mathbf{d}_{p,c}, \\ &= \mathbf{v}_{\mathbb{X},p} + \boldsymbol{\omega}_{\mathbb{X},\mathbb{B}} \times \mathbf{r}_c,\end{aligned}$$

where $\mathbf{r}_c := \mathbf{r}_{\mathbb{B},c}$ in the instant shown. From Example (4.1.1), the components relative to the basis for \mathbb{B} of the vector \mathbf{r}_c are given by

$$\mathbf{r}_c^{\mathbb{B}} = \begin{Bmatrix} x_c \\ y_c \\ z_c \end{Bmatrix} = \begin{Bmatrix} 0 \\ \frac{\frac{1}{2}M_1b_1 + M_2(d_2 + \frac{1}{2}b_2)}{M_1 + M_2} \\ \frac{\frac{1}{2}M_1c_1 + M_2(c_1 + \frac{1}{2}c_2)}{M_1 + M_2} \end{Bmatrix}.$$

The linear momentum in the \mathbb{X} frame expressed in terms of the basis for the \mathbb{B} frame is therefore given by

$$\mathbf{p}_{\mathbb{X}}^{\mathbb{B}} = (M_1 + M_2) \begin{Bmatrix} v_1 \\ v_2 \\ v_3 \end{Bmatrix} + (M_1 + M_2) \begin{bmatrix} 0 & -\omega_3 & \omega_2 \\ \omega_3 & 0 & -\omega_1 \\ -\omega_2 & \omega_1 & 0 \end{bmatrix} \begin{Bmatrix} 0 \\ \frac{\frac{1}{2}M_1b_1 + M_2(d_2 + \frac{1}{2}b_2)}{M_1 + M_2} \\ \frac{\frac{1}{2}M_1c_1 + M_2(c_1 + \frac{1}{2}c_2)}{M_1 + M_2} \end{Bmatrix}.$$

Example 4.1.3. A rectangular prism with uniform density and a body fixed frame \mathbb{B} moves relative to the frame \mathbb{X} as shown in Figure (4.4). Calculate the linear momentum of the body in the frame \mathbb{X} at the instant shown. At this instant assume that the velocity $\mathbf{v}_{\mathbb{X},p}$ of point p and the angular velocity $\boldsymbol{\omega}_{\mathbb{X},\mathbb{B}}$ are given by

$$\begin{aligned}\mathbf{v}_{\mathbb{X},p} &= v_1 \mathbf{b}_1 + v_2 \mathbf{b}_2 + v_3 \mathbf{b}_3, \\ \boldsymbol{\omega}_{\mathbb{X},\mathbb{B}} &= \omega_1 \mathbf{b}_1 + \omega_2 \mathbf{b}_2 + \omega_3 \mathbf{b}_3.\end{aligned}$$

Use Definition (4.1) to calculate the answer, and then check the result using Theo-

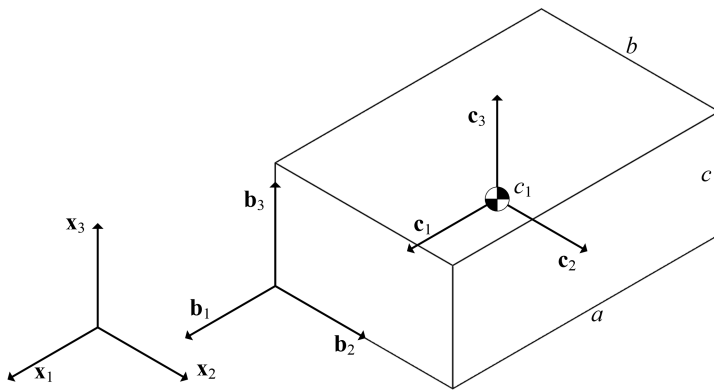


Fig. 4.4: Rectangular Prism

rem (4.1).

Solution: As specified, the solution for this problem will first be generated by integrating over the domain of the rigid body. Then, the same solution will be calculated by considering the velocity of the *center of mass* and invoking Theorem (4.1). In addition the \mathbb{B} frame defined at point p in the problem statement, an additional frame \mathbb{C} is defined parallel to \mathbb{B} with its origin at the center of mass c_1 . The velocity of a differential mass element can be written using Theorem (2.16) in Chapter (2) as

$$\mathbf{v} := \mathbf{v}_{\mathbb{X},dm} = \mathbf{v}_{\mathbb{X},p} + \boldsymbol{\omega}_{\mathbb{X},\mathbb{B}} \times \mathbf{r},$$

where the vector $\mathbf{r} := \mathbf{r}_{\mathbb{B},dm}$ is given by

$$\mathbf{r} = x \mathbf{b}_1 + y \mathbf{b}_2 + z \mathbf{b}_3.$$

The linear momentum, by Definition (4.1), can be written as

$$\mathbf{p}_{\mathbb{X}} = \int \mathbf{v} dm = \int (\mathbf{v}_{\mathbb{X},p} + \boldsymbol{\omega}_{\mathbb{X},B} \times \mathbf{r}) dm.$$

The only term in the integrand that varies over the body is the vector \mathbf{r} . Thus, the terms $\mathbf{v}_{\mathbb{X},p}$ and $\boldsymbol{\omega}_{\mathbb{X},B}$ may be factored out of the integrand to obtain

$$\mathbf{p}_{\mathbb{X}} = \mathbf{v}_{\mathbb{X},p} \int dm + \boldsymbol{\omega}_{\mathbb{X},B} \times \int \mathbf{r} dm.$$

From the definitions of the rigid body and the center of mass position, it is known that

$$M = \int dm \quad \text{and} \quad \mathbf{r}_c := \mathbf{r}_{\mathbb{B},c} = \frac{1}{M} \int \mathbf{r} dm.$$

Substituting these expressions into the formulation for $\mathbf{p}_{\mathbb{X}}$ results in

$$\begin{aligned} \mathbf{p}_{\mathbb{X}} &= M\mathbf{v}_{\mathbb{X},p} + \boldsymbol{\omega}_{\mathbb{X},B} \times (M\mathbf{r}_c), \\ &= M(\mathbf{v}_{\mathbb{X},p} + \boldsymbol{\omega}_{\mathbb{X},B} \times \mathbf{r}_c). \end{aligned} \quad (4.1.1)$$

The location of the center of mass is $\mathbf{r}_c = -\frac{a}{2}\mathbf{b}_1 + \frac{b}{2}\mathbf{b}_2 + \frac{c}{2}\mathbf{b}_3$. When \mathbf{r}_c , $\mathbf{v}_{\mathbb{X},p}$, and $\boldsymbol{\omega}_{\mathbb{X},B}$ are substituted into Equation (4.1.1), the final expression is obtained as

$$\mathbf{p}_{\mathbb{X}}^{\mathbb{B}} = M \begin{Bmatrix} v_1 + \frac{1}{2}(c\omega_2 - b\omega_3) \\ v_2 + \frac{1}{2}(-a\omega_3 - c\omega_1) \\ v_3 + \frac{1}{2}(b\omega_1 + a\omega_2) \end{Bmatrix}.$$

Alternatively, Theorem (4.1) specifies that

$$\mathbf{p}_{\mathbb{X}} = M\mathbf{v}_{\mathbb{X},c}. \quad (4.1.2)$$

The velocity of the center of mass may be derived using Theorem (2.16) as

$$\mathbf{v}_{\mathbb{X},c} = \mathbf{v}_{\mathbb{X},p} + \boldsymbol{\omega}_{\mathbb{X},B} \times \mathbf{r}_c$$

where \mathbf{r}_c is the vector that connects the point p to the center of mass. Substituting this into Equation (4.1.2) results in

$$\mathbf{p}_{\mathbb{X}} = M(\mathbf{v}_{\mathbb{X},p} + \boldsymbol{\omega}_{\mathbb{X},B} \times \mathbf{r}_c), \quad (4.1.3)$$

which is identical to Equation (4.1.1), showing that both approaches yield the same answer.



4.2 Angular Momentum of Rigid Bodies

4.2.1 First Principles

The *angular momentum* about a point p of a single particle in motion is equal to the “moment of momentum.” That is, the *angular momentum* is the cross product of the position vector that connects the point p to the particle and the *linear momentum* of the particle. The *angular momentum* of a system of particles is the sum of the *angular momenta* of the individual particles. As with the *linear momentum* of a rigid body, the definition of the *angular momentum* of a rigid body can be interpreted as a limiting case as the number of particles increases. The summation over all the particles in the system is replaced by an integral over all the differential mass elements that make up the rigid body.

Definition 4.3. The angular momentum $\mathbf{h}_{\mathbb{X},p}$ of a rigid body in the frame \mathbb{X} about point p is given by

$$\mathbf{h}_{\mathbb{X},p} = \int \mathbf{r} \times \mathbf{v} dm$$

where $\mathbf{r} := \mathbf{r}_{p,dm}$ is the vector connecting the point p to the differential mass dm and $\mathbf{v} := \mathbf{v}_{\mathbb{X},dm}$ is the velocity of the differential mass dm in the frame \mathbb{X} .

There is no restriction on the point p about which the *angular momentum* may be calculated in Definition (4.3). In practice, it is often convenient to calculate the *angular momentum* about an arbitrary point p by relating it to the *angular momentum* about the *center of mass*. Theorem (4.2) describes this relationship.

Theorem 4.2. The angular momentum in the frame \mathbb{X} of a rigid body about the arbitrary point p is given by

$$\mathbf{h}_{\mathbb{X},p} = \mathbf{h}_{\mathbb{X},c} + \mathbf{d}_{p,c} \times (M \mathbf{v}_{\mathbb{X},c})$$

where $\mathbf{h}_{\mathbb{X},c}$ is the angular momentum in the frame \mathbb{X} of the rigid body about its center of mass c , M is mass of the rigid body, $\mathbf{d}_{p,c}$ is the vector connecting the point p to the center of mass c , and $\mathbf{v}_{\mathbb{X},c}$ is the velocity of the center of mass c in the frame \mathbb{X} .

Proof. The proof of Theorem 4.2 relies on a decomposition of the vector $\mathbf{r} := \mathbf{r}_{p,dm}$ that locates the differential mass element dm into the sum of a vector $\mathbf{d}_{p,c}$ from the point p to the center of mass c and the vector $\boldsymbol{\rho}$ from the *center of mass* to the differential mass element dm . This decomposition is illustrated in Figure (4.1). Applying this decomposition to the definition of $\mathbf{h}_{\mathbb{X},p}$ results in

$$\mathbf{h}_{\mathbb{X},p} = \int \mathbf{r} \times \mathbf{v} dm = \int (\mathbf{d}_{p,c} + \boldsymbol{\rho}) \times \mathbf{v} dm.$$

Since the vector $\mathbf{d}_{p,c}$ does not vary over the mass integral, it may be removed from the integral and

$$\mathbf{h}_{\mathbb{X},p} = \mathbf{d}_{p,c} \times \int \mathbf{v} dm + \int \boldsymbol{\rho} \times \mathbf{v} dm.$$

Based on prior analysis, the two integrals in this expression may be represented as

$$\mathbf{h}_{\mathbb{X},c} = \int \boldsymbol{\rho} \times \mathbf{v} dm \quad \text{and} \quad \int \mathbf{v} dm = M \mathbf{v}_{\mathbb{X},c},$$

resulting in the desired final formulation of $\mathbf{h}_{\mathbb{X},p}$, such that

$$\mathbf{h}_{\mathbb{X},p} = \mathbf{d}_{p,c} \times (M \mathbf{v}_{\mathbb{X},c}) + \mathbf{h}_{\mathbb{X},c}.$$

□

The next two examples show that the *angular momentum* of realistic three dimensional bodies, such as the rigid links of a robotic system, can be calculated directly from their definition. As when calculating *linear momentum*, the task of calculating the *angular momentum* can be facilitated by utilizing the knowledge of the position and velocity of the *center of mass*.

An important qualitative observation will also be made in these examples: the calculation of *angular momentum* for rigid bodies often introduces some common integrals over the body, namely the *cross products of inertia* and the *moments of inertia*. These integrals appear so frequently that they are discussed in detail in Sections (4.2.2) and (4.2.3) of this chapter. The *cross products of inertia* and *moments of inertia* also appear frequently in calculations of the kinetic energy of a robotic system; hence their important role in the *analytical mechanics* formulations that are presented in Chapter (5).

Example 4.2.1. A rectangular prism with body fixed frame \mathbb{B} is shown in Figure (4.5). It rotates about the $\mathbf{x}_3 = \mathbf{b}_3$ axis at the angular rate $\dot{\theta}_1$. Calculate the angular momentum $\mathbf{h}_{\mathbb{X},o}$ in the \mathbb{X} frame about the point o using Definition (4.3).

Solution: The velocity in \mathbb{X} of the differential mass element dm is given by

$$\mathbf{v} := \mathbf{v}_{\mathbb{X},dm} = \boldsymbol{\omega}_{\mathbb{X},\mathbb{B}} \times \mathbf{r}$$

where $\mathbf{r} := \mathbf{r}_{\mathbb{X},dm}$ is the position vector of the differential mass element. The vector \mathbf{r} is represented in terms of the basis for the \mathbf{b} frame as

$$\mathbf{r} = x \mathbf{b}_1 + y \mathbf{b}_2 + z \mathbf{b}_3$$

where (x, y, z) are the coordinates along the $\mathbf{b}_1, \mathbf{b}_2, \mathbf{b}_3$ directions. The velocity \mathbf{v} of the differential mass of (x, y, z) is consequently

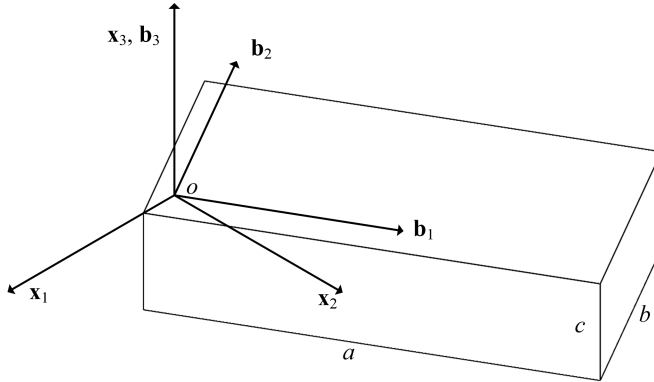


Fig. 4.5: Rectangular Prism

$$\mathbf{v} = \begin{bmatrix} \mathbf{b}_1 & \mathbf{b}_2 & \mathbf{b}_3 \\ 0 & 0 & \dot{\theta} \\ x & y & z \end{bmatrix} = -y\dot{\theta}\mathbf{b}_1 + x\dot{\theta}\mathbf{b}_2.$$

The definition of angular momentum results in

$$\begin{aligned} \mathbf{h}_{\mathbb{X},p} &= \int \mathbf{r} \times \mathbf{v} dm = \int \begin{vmatrix} \mathbf{b}_1 & \mathbf{b}_2 & \mathbf{b}_3, \\ x & y & z \\ -y\dot{\theta} & x\dot{\theta} & 0 \end{vmatrix} dm \\ &= \left(- \int xz dm \right) \dot{\theta} \mathbf{b}_1 + \left(- \int yz dm \right) \dot{\theta} \mathbf{b}_2 + \left(\int (x^2 + y^2) dm \right) \dot{\theta} \mathbf{b}_3 \end{aligned} \quad (4.2.1)$$

where the fact that $\dot{\theta}, \mathbf{b}_1, \mathbf{b}_2$ and \mathbf{b}_3 do not vary with the integration over the body allowed those variables to be removed from the integrals. To evaluate the integrals, the single integration over the mass of the body can be re-cast as a volumetric integral. Assuming ρ is the uniform density of the solid, the differential mass dm may be defined as $dm = \rho dx dy dz$, along the three basis vectors $\mathbf{b}_1, \mathbf{b}_2$ and \mathbf{b}_3 . Using this expansion, it can be seen that the integrals $(-\int xz dm)$ and $(-\int yz dm)$ are equal to zero. For the first,

$$\int xz dm = \rho \int_{-\frac{c}{2}}^{\frac{c}{2}} \int_{-\frac{b}{2}}^{\frac{b}{2}} \int_0^a xz dx dy dz = \underbrace{\int_{-\frac{c}{2}}^{\frac{c}{2}} zdz \int_{-\frac{b}{2}}^{\frac{b}{2}} dy}_{0} \int_0^a xdx.$$

A similar result holds for $\int yz dm$. The third integral may be evaluated as

$$\begin{aligned}
\int (x^2 + y^2) dm &= \rho \int_{-\frac{c}{2}}^{\frac{c}{2}} \int_{-\frac{b}{2}}^{\frac{b}{2}} \int_0^a (x^2 + y^2) dx dy dz, \\
&= \rho \int_{-\frac{c}{2}}^{\frac{c}{2}} dz \left(\int_{-\frac{b}{2}}^{\frac{b}{2}} dy \int_0^a x^2 dx + \int_{-\frac{b}{2}}^{\frac{b}{2}} y^2 dy \int_0^a dx \right), \\
&= \left(\rho c b \frac{1}{3} a^3 + a \frac{2}{3} \left(\frac{b}{2} \right)^3 \right) = \rho abc \left(\frac{1}{3} a^2 + \frac{1}{12} b^2 \right) = m \left(\frac{1}{3} a^2 + \frac{1}{12} b^2 \right),
\end{aligned} \tag{4.2.2}$$

where $m = \rho abc$, based on the definitions of the prism density and the geometry in Figure (4.5). It is concluded that the angular momentum can be written in the form

$$\begin{aligned}
\mathbf{h}_{\mathbb{X},p} &= M \left(\frac{1}{3} a^2 + \frac{1}{12} b^2 \right) \dot{\theta} \mathbf{b}_3 = \left(\frac{1}{12} M (a^2 + b^2) + \frac{1}{4} Ma^2 \right) \dot{\theta} \mathbf{b}_3, \\
&= \left(I_{33,c} + M \left(\frac{a}{2} \right)^2 \right) \dot{\theta} \mathbf{b}_3 = I_{33,o} \dot{\theta} \mathbf{b}_3,
\end{aligned}$$

where $I_{33,c}$ is the \mathbf{b}_3 -axis moment of inertia of the body with respect to the center of mass and $I_{33,o}$ is the \mathbf{b}_3 -axis moment of inertia of the body with respect to point o .

It will be shown in the sections that follow that the quantities $(-\int xz dm)$ and $(-\int yz dm)$ are examples of the *cross products of inertia* of a rigid body that measure of the symmetry of a rigid body. The integral $\int (y^2 + z^2) dm$ is an example of a *moment of inertia* of a rigid body. It measures the resistance of a rigid body to rotation.

Example 4.2.2. Calculate the angular momentum in \mathbb{X} of the rectangular prism studied in Example (4.2.1) using Theorem (4.2).

Solution: First, the angular momentum $\mathbf{h}_{\mathbb{X},c}$ of the body is evaluated about its center of mass. For this example, the origin of the body fixed frame \mathbb{B} is fixed at the center of mass, as shown in Figure (4.6). The position of a differential mass dm with respect to this frame is defined as

$$\mathbf{r} = \alpha \mathbf{b}_1 + \beta \mathbf{b}_2 + \gamma \mathbf{b}_3,$$

where (α, β, γ) are the coordinates along the $\mathbf{b}_1, \mathbf{b}_2, \mathbf{b}_3$ directions. By following the same essential steps as in Example (4.2.1), it can be shown that

$$\mathbf{h}_{\mathbb{X},c} = \left(- \int \alpha \gamma dm \right) \dot{\theta} \mathbf{b}_1 + \left(- \int \beta \gamma dm \right) \dot{\theta} \mathbf{b}_2 + \int (\alpha^2 + \beta^2) dm \dot{\theta} \mathbf{b}_3.$$

A critical observation here is that the limits of integration in these three integrals differ from the corresponding expression in Equation (4.2.2). As a result,

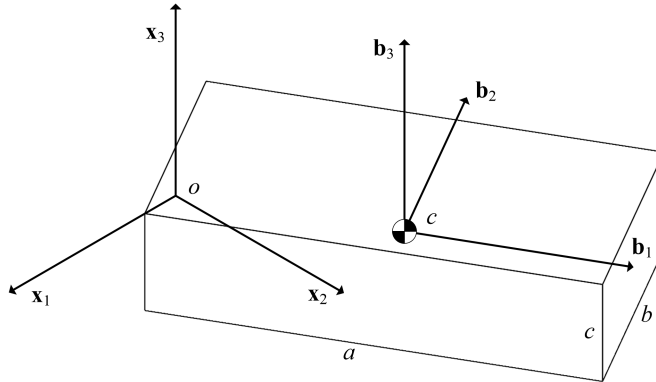


Fig. 4.6: Rectangular Prisms with Body Fixed Frame at Center of Mass

$$\begin{aligned}\int \alpha\gamma dm &= \rho \int_{-\frac{c}{2}}^{\frac{c}{2}} \int_{-\frac{b}{2}}^{\frac{b}{2}} \int_{-\frac{a}{2}}^{\frac{a}{2}} \alpha\gamma d\alpha d\beta d\gamma = 0, \\ \int \beta\gamma dm &= \rho \int_{-\frac{c}{2}}^{\frac{c}{2}} \int_{-\frac{b}{2}}^{\frac{b}{2}} \int_{-\frac{a}{2}}^{\frac{a}{2}} \beta\gamma d\alpha d\beta d\gamma = 0, \\ \int (\alpha^2 + \beta^2) dm &= \rho \int_{-\frac{c}{2}}^{\frac{c}{2}} \int_{-\frac{b}{2}}^{\frac{b}{2}} \int_{-\frac{a}{2}}^{\frac{a}{2}} (\alpha^2 + \beta^2) d\alpha d\beta d\gamma = \frac{1}{12}m(a^2 + b^2).\end{aligned}$$

The first two integrals, $\int \alpha\gamma dm$ and $\int \beta\gamma dm$, can be shown to be zero simply by virtue of the fact that

$$\int_{-\frac{c}{2}}^{\frac{c}{2}} \gamma d\gamma = \frac{1}{2}\gamma^2 \Big|_{-\frac{c}{2}}^{\frac{c}{2}} = 0$$

appears as a factor in both expressions. The last integral to be expanded is

$$\begin{aligned}\int (\alpha^2 + \beta^2) dm &= \rho \int_{-\frac{c}{2}}^{\frac{c}{2}} d\gamma \left(\int_{-\frac{b}{2}}^{\frac{b}{2}} d\beta \int_{-\frac{a}{2}}^{\frac{a}{2}} \alpha^2 d\alpha + \int_{-\frac{b}{2}}^{\frac{b}{2}} d\beta \int_{-\frac{a}{2}}^{\frac{a}{2}} \beta^2 d\alpha \right) \\ &= \rho c \left(b \frac{2}{3} \left(\frac{a}{2}\right)^3 + a \frac{2}{3} \left(\frac{b}{2}\right)^3 \right) = \rho abc \left(\frac{1}{12}a^2 + \frac{1}{12}b^2 \right) = \frac{1}{12}M(a^2 + b^2).\end{aligned}$$

The final expression for $\mathbf{h}_{\mathbb{X},c}$ is therefore

$$\mathbf{h}_{\mathbb{X},c} = \frac{1}{12}M(a^2 + b^2)\dot{\theta}\mathbf{b}_3$$

Theorem (4.2) gives the following expression for the angular momentum about the point o

$$\mathbf{h}_{\mathbb{X},o} = \mathbf{h}_{\mathbb{X},c} + \mathbf{d}_{o,c} \times (M\mathbf{v}_{\mathbb{X},c}).$$

For this example, $\mathbf{d}_{o,c} = (a/2)\mathbf{b}_1$ and $\mathbf{v}_{\mathbb{X},c} = (a/2)\dot{\theta}\mathbf{b}_2$, resulting in

$$\begin{aligned}\mathbf{h}_{\mathbb{X},o} &= \frac{1}{12}m(a^2 + b^2)\dot{\theta}\mathbf{b}_3 + \left(\frac{a}{2}\mathbf{b}_1\right) \times \left(M\frac{a}{2}\dot{\theta}\mathbf{b}_2\right) \\ &= \left(\frac{1}{12}m(a^2 + b^2) + \frac{1}{4}Ma^2\right)\dot{\theta}\mathbf{b}_3 := \underbrace{\left(I_{33,c} + M\left(\frac{a}{2}\right)^2\right)}_{:=I_{33,o}}\dot{\theta}\mathbf{b}_3.\end{aligned}$$

This is the same result as in Example (4.2.1). It will also be shown that the coefficient $I_{33,o}$ defined in the equation as

$$I_{33,o} := I_{33,c} + M\left(\frac{a}{2}\right)^2$$

can also be obtained via the application of the Parallel Axis Theorem for inertia discussed in Section (4.2.3.3).

Theorem (4.2) states a general relationship between the angular momentum about an arbitrary point p and about the center of mass c of a rigid body. The theorem was derived by decomposing the position vector into the sum $\mathbf{r} = \mathbf{d}_{p,c} + \boldsymbol{\rho}$. Another useful form for the angular momentum can be achieved by decomposing the velocity vector instead of the position vector. The next theorem makes use of this strategy. The resulting form for the angular momentum will be critical in the discussions of the inertia matrix in the following sections.

Theorem 4.3. *The angular momentum $\mathbf{h}_{\mathbb{X},p}$ of a rigid body in the frame \mathbb{X} about the point p is given by*

$$\mathbf{h}_{\mathbb{X},p} = \mathbf{d}_{p,c} \times (M\mathbf{v}_{\mathbb{X},p}) + \int \mathbf{r} \times (\boldsymbol{\omega}_{\mathbb{X},\mathbb{B}} \times \mathbf{r}) dm$$

where M is the total mass of the body, the vector $\mathbf{d}_{p,c}$ connects the point p to the center of mass c , $\mathbf{v}_{\mathbb{X},p}$ is the velocity of the point p in the frame \mathbb{X} , $\boldsymbol{\omega}_{\mathbb{X},\mathbb{B}}$ is the angular velocity of the body frame \mathbb{B} in the frame \mathbb{X} , and $\mathbf{r} := \mathbf{r}_{p,dm}$ is the vector from the point p to the differential mass dm .

Proof. From the definition of the *angular momentum* for a rigid body,

$$\mathbf{h}_{\mathbb{X},p} = \int \mathbf{r} \times \mathbf{v} dm.$$

Because the point p and the differential mass are on the same body, the velocity \mathbf{v} may be defined with respect to the velocity of point p using Theorem (2.16) in Chapter (2),

$$\mathbf{h}_{\mathbb{X},p} = \int \mathbf{r} \times (\mathbf{v}_{\mathbb{X},p} + \boldsymbol{\omega}_{\mathbb{X},\mathbb{B}} \times \mathbf{r}) dm.$$

The velocity of the point p does not vary over the integral, and the first term may be simplified by noting that

$$\int \mathbf{r} \times \mathbf{v}_{\mathbb{X},p} dm = \left(\int \mathbf{r} dm \right) \times \mathbf{v}_{\mathbb{X},p} = \mathbf{d}_{p,c} \times (M \mathbf{v}_{\mathbb{X},p}).$$

Combining these expressions results in

$$\mathbf{h}_{\mathbb{X},p} = \mathbf{d}_{p,c} \times (M \mathbf{v}_{\mathbb{X},p}) + \int \mathbf{r} \times (\boldsymbol{\omega}_{\mathbb{X},\mathbb{B}} \times \mathbf{r}) dm.$$

□

4.2.2 Angular Momentum and Inertia

The last section introduced the definition of angular momentum for rigid bodies and derived theorems that can be used for its calculation. As shown in Examples (4.2.1) and (4.2.2), the calculation of angular momentum can require the evaluation of integrals over the body that have the form $(-\int xz dm)$, $(-\int yz dm)$ and $\int(x^2 + y^2) dm$. The integrals $(-\int xz dm)$ and $(-\int yz dm)$ are examples of the *cross products of inertia*, and the integral $\int(x^2 + y^2) dm$ is an example of a *moment of inertia* of a rigid body. The cross products and moments of inertia are used to construct the *inertia matrix* for a rigid body. These definitions are important because most commonly encountered expressions for *angular momentum* in applications are cast in terms of the *inertia matrix*.

Definition 4.4. Let \mathbb{Y} be a frame whose origin is located at the point p . Suppose the position vector $\mathbf{r} := \mathbf{r}_{\mathbb{Y},dm}$ of a differential mass element dm in the rigid body is expressed in terms of the \mathbb{Y} basis as

$$\mathbf{r} = x\mathbf{y}_1 + y\mathbf{y}_2 + z\mathbf{y}_3.$$

The *inertial matrix* $\mathbf{I}_p^{\mathbb{Y}}$ of the rigid body about the point p relative to the frame \mathbb{Y} is given by

$$\mathbf{I}_p^{\mathbb{Y}} = \begin{bmatrix} I_{11} & I_{12} & I_{13} \\ I_{12} & I_{22} & I_{23} \\ I_{13} & I_{23} & I_{33} \end{bmatrix} = \begin{bmatrix} \int(y^2 + z^2) dm & -\int xy dm & -\int xz dm \\ -\int xy dm & \int(x^2 + z^2) dm & -\int yz dm \\ -\int xz dm & -\int yz dm & \int(x^2 + y^2) dm \end{bmatrix}.$$

The diagonal terms I_{11}, I_{22}, I_{33} are the moments of inertia, and the off-diagonal entries I_{12}, I_{13}, I_{23} are the products of inertia, about the point p with respect to the \mathbb{Y} basis.

The *inertia matrix* \mathbf{I}_p^Y about the point p relative to the frame Y utilizes the Y superscript to denote the basis vectors for which the matrix is defined. As in earlier chapters, the convention that a superscript denotes the coordinates of a vector relative to a specific choice of frame is used. For example, if \mathbf{a} is an arbitrary vector, \mathbf{a}^Y denotes the components of the vector \mathbf{a} as expressed in terms of the Y basis. The *inertia matrix* about a point p relative to a frame Y contains the components of the *inertia tensor* expressed in terms of the *tensor basis* $Y \otimes Y$. A vector is a first order tensor, and the *inertia tensor* is a second order tensor. The Appendix contains a detailed discussion of tensors for the interested reader.

The point p used to define the *angular momentum* $\mathbf{h}_{X,p}$ in Definition (4.3) can be any point in the mechanical system. The most general form for the *angular momentum* in terms of the *inertia matrix* that will be used is derived in the following theorem.

Theorem 4.4. Suppose that a body with fixed frame B moves relative to the frame X . The components $\mathbf{h}_{X,p}^Y$ of the angular momentum in X relative to the basis of the frame Y are given by

$$\mathbf{h}_{X,p}^Y = \mathbf{I}_p^Y \boldsymbol{\omega}_{X,B}^Y + (\mathbf{d}_{p,c} \times (M\mathbf{v}_{X,p}))^Y \quad (4.2.3)$$

where $\boldsymbol{\omega}_{X,B}$ is the angular velocity of the B frame in the X frame, \mathbf{I}_p^Y is the inertia matrix about the point p relative to the frame Y , $\mathbf{d}_{p,c}$ is the vector connecting the point p to the center of mass c , and $\mathbf{v}_{X,p}$ is the velocity of the point p in the frame X .

This theorem will be proven while carrying out the proof of Theorem (4.5). Equation (4.2.3) is useful in many applications because of its generality. For example, this theorem will constitute the technical foundation for the most general variant of *Euler's Second Law* of motion for rigid bodies presented in Section (4.3) of this chapter. This form of *Euler's Second Law* serves as the foundation for the numerically efficient *Recursive Order (N) formulations* of kinematics and dynamics of robotic systems.

Still, despite its generality, Theorem (4.4) is frequently modified so that it is easier to use in direct application to individual problems. It is most common to select the point p in applications so that the term $(\mathbf{d}_{p,c} \times M\mathbf{v}_{X,p})^Y$ is identically equal to zero. This is most easily accomplished by choosing the point p to be either fixed in the frame X , or by selecting the point p to be the *center of mass* of the rigid body.

Theorem 4.5. Suppose that a body with fixed frame \mathbb{B} moves relative to the frame \mathbb{X} , and that the point p is either the center of mass of the rigid body or is a point of the rigid body that is fixed in the frame \mathbb{X} . Then the components $\mathbf{h}_{\mathbb{X},p}^{\mathbb{Y}}$ of the angular momentum in \mathbb{X} relative to the basis for a frame \mathbb{Y} are given by the matrix product

$$\mathbf{h}_{\mathbb{X},p}^{\mathbb{Y}} = \mathbf{I}_p^{\mathbb{Y}} \boldsymbol{\omega}_{\mathbb{X},\mathbb{B}}^{\mathbb{Y}}$$

where $\boldsymbol{\omega}_{\mathbb{X},\mathbb{B}}$ is the angular velocity of the \mathbb{B} frame in the \mathbb{X} frame and $\mathbf{I}_p^{\mathbb{Y}}$ is the inertia matrix about the point p relative to the frame \mathbb{Y} .

Proof. First, the conclusion reached in Theorem (4.5) will be expanded upon. Suppose that the *angular velocity* vector $\boldsymbol{\omega}_{\mathbb{X},\mathbb{Y}}$, position vector $\mathbf{r} := \mathbf{r}_{p,dm}$, and *angular momentum* vector $\mathbf{h}_{\mathbb{X},p}$ are expressed in terms of the basis for the \mathbb{Y} frame as

$$\begin{aligned}\boldsymbol{\omega}_{\mathbb{X},\mathbb{B}} &:= \omega_1 \mathbf{y}_1 + \omega_2 \mathbf{y}_2 + \omega_3 \mathbf{y}_3, \\ \mathbf{r} &:= x \mathbf{y}_1 + y \mathbf{y}_2 + z \mathbf{y}_3, \\ \mathbf{h}_{\mathbb{X},p} &:= h_1 \mathbf{y}_1 + h_2 \mathbf{y}_2 + h_3 \mathbf{y}_3.\end{aligned}$$

The matrix equation $\mathbf{h}_{\mathbb{X},p}^{\mathbb{Y}} = \mathbf{I}_p^{\mathbb{Y}} \boldsymbol{\omega}_{\mathbb{X},\mathbb{B}}^{\mathbb{Y}}$ becomes

$$\begin{Bmatrix} h_1 \\ h_2 \\ h_3 \end{Bmatrix} = \begin{bmatrix} I_{11} & I_{12} & I_{13} \\ I_{21} & I_{22} & I_{23} \\ I_{31} & I_{32} & I_{33} \end{bmatrix} \begin{Bmatrix} \omega_1 \\ \omega_2 \\ \omega_3 \end{Bmatrix}.$$

The proof of this theorem follows from Theorem (4.3) when it is noted that the point p is by hypothesis either the *center of mass* or a point that is fixed in the ground frame. In the former case $\mathbf{d}_{p,c} = \mathbf{0}$, and in the latter case $\mathbf{v}_{\mathbb{X},p} = \mathbf{0}$. Theorem (4.3) implies that

$$\mathbf{h}_{\mathbb{X},p} = \underbrace{\mathbf{d}_{p,c} \times M \mathbf{v}_{\mathbb{X},p}}_{=0} + \int \mathbf{r} \times (\boldsymbol{\omega}_{\mathbb{X},\mathbb{B}} \times \mathbf{r}) dm.$$

Since each of the vectors is assumed to be given in terms of their components relative to the same basis \mathbb{Y} , it can be directly computed that

$$\begin{aligned}\mathbf{h}_{\mathbb{X},p} &= \int \begin{vmatrix} \mathbf{y}_1 & \mathbf{y}_2 & \mathbf{y}_3 \\ x & y & z \\ (z\omega_2 - y\omega_3) & (x\omega_3 - z\omega_1) & (y\omega_1 - x\omega_2) \end{vmatrix} dm, \\ &= \int \left\{ \begin{aligned} &\left((y^2 + z^2)\omega_1 - xy\omega_2 - xz\omega_3 \right) \mathbf{y}_1 \\ &+ \left(-xy\omega_1 + (x^2 + z^2)\omega_2 - yz\omega_3 \right) \mathbf{y}_2 \\ &+ \left(-xz\omega_1 - yz\omega_2 + (x^2 + y^2)\omega_3 \right) \mathbf{y}_3 \end{aligned} \right\} dm.\end{aligned}$$

This equation can be rewritten as

$$\mathbf{h}_{\mathbb{X},p}^{\mathbb{Y}} = \begin{Bmatrix} h_1 \\ h_2 \\ h_3 \end{Bmatrix} = \underbrace{\begin{bmatrix} \int(y^2+z^2)dm - \int xydm & -\int xzdm \\ -\int xydm & \int(x^2+z^2)dm - \int yzdm \\ -\int xzdm & -\int yzdm & \int(x^2+y^2)dm \end{bmatrix}}_{\mathbf{I}_p^{\mathbb{Y}}} \underbrace{\begin{Bmatrix} \omega_1 \\ \omega_2 \\ \omega_3 \end{Bmatrix}}_{\boldsymbol{\omega}_{\mathbb{X},\mathbb{B}}^{\mathbb{Y}}}.$$

The steps above also prove Theorem (4.5), where the term $\mathbf{d}_{pc} \times (M\mathbf{v}_{\mathbb{X},p})$ is not equal to zero in general. In that case, it has been shown that $\mathbf{h}_{\mathbb{X},p}^{\mathbb{Y}} = \mathbf{I}_p^{\mathbb{Y}} \boldsymbol{\omega}_{\mathbb{X},\mathbb{B}}^{\mathbb{Y}} + (\mathbf{d}_{pc} \times (M\mathbf{v}_{x,p}))^{\mathbb{Y}}$. \square

Theorem (4.5) will be used in numerous applications, and it is vital to note the different roles of the frames \mathbb{X} , \mathbb{B} and \mathbb{Y} in the theorem. The body fixed frame is \mathbb{B} , which is assumed to move relative to the frame \mathbb{X} . In the next section *Euler's Laws* will be stated which hold in an *inertial frame*. The inertial frame will be chosen to be \mathbb{X} . In other words, the frames \mathbb{X} and \mathbb{B} are connected to the physics of the problem at hand. The frame \mathbb{Y} can be any frame whatsoever, and is used to provide a basis to conveniently express the components of the physical vectors $\boldsymbol{\omega}_{\mathbb{X},\mathbb{B}}$ and $\mathbf{h}_{\mathbb{X},p}$.

Example 4.2.3. The inertia matrix $\mathbf{I}_c^{\mathbb{D}}$ of a satellite depicted in the configuration shown in Figure (4.7) about its own center of mass is given by

$$\mathbf{I}_c^{\mathbb{D}} = \begin{bmatrix} I_{11} & 0 & 0 \\ 0 & I_{22} & 0 \\ 0 & 0 & I_{33} \end{bmatrix}. \quad (4.2.4)$$

Suppose that the satellite is traveling in an orbit as described in Example (2.3.4) in Chapter (2). The inclination of the orbital plane is ψ and the right ascension is ϕ . Assume that at the instant shown the distance from the center of the earth to the center of mass of the satellite is R and that the velocity of the center of mass of the satellite is

$$\mathbf{v}_{\mathbb{E},c} = V \underbrace{(\cos\xi \mathbf{b}_1 + \sin\xi \mathbf{b}_2)}_{\text{unit vector tangent to path}} = V\mathbf{d}_1, \quad (4.2.5)$$

where V is the speed and ξ measures the angle of rotation of the velocity vector with respect to the \mathbf{b}_1 axis. The unit vector \mathbf{d}_1 is along the direction of flight of the satellite and is depicted in Figure (4.9). Calculate the angular momentum in the \mathbb{E} frame of the satellite about the center of the earth. Express the answer in terms of the basis for the \mathbb{E} frame.

Solution: Theorem (4.2) can be used to relate the angular momentum of the satellite about the center of the earth and about its own center of mass

$$\mathbf{h}_{\mathbb{E},o} = \mathbf{h}_{\mathbb{E},c} + \mathbf{d}_{o,c} \times (M\mathbf{v}_{\mathbb{E},c}). \quad (4.2.6)$$

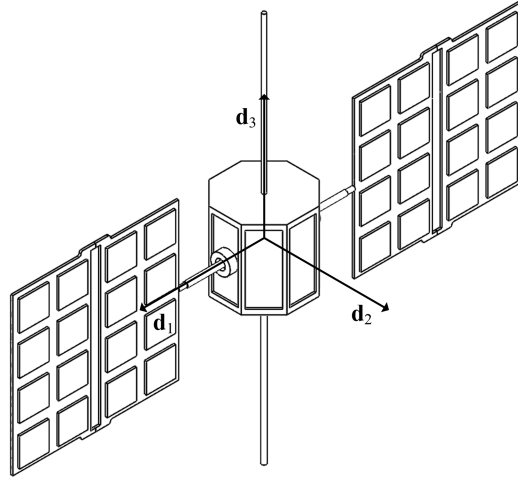


Fig. 4.7: Satellite with Body Fixed Frame

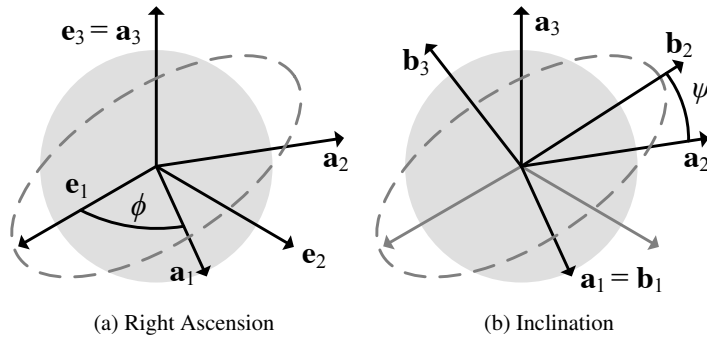


Fig. 4.8: Orbital Plane Definition

The angular momentum of the vehicle about its own center of mass is calculated using Theorem (4.5) to be

$$\mathbf{h}_{E,c}^D = \mathbf{I}_c^D \boldsymbol{\omega}_{E,D}^D.$$

The angular velocity of the satellite in the earth frame is

$$\begin{aligned} \boldsymbol{\omega}_{E,D} &= \underbrace{\boldsymbol{\omega}_{E,B}}_0 + \underbrace{\boldsymbol{\omega}_{B,D}}_{\dot{\xi} \mathbf{d}_3}, \\ &= \dot{\xi} \mathbf{b}_3 = \dot{\xi} \mathbf{d}_3, \end{aligned}$$

so that

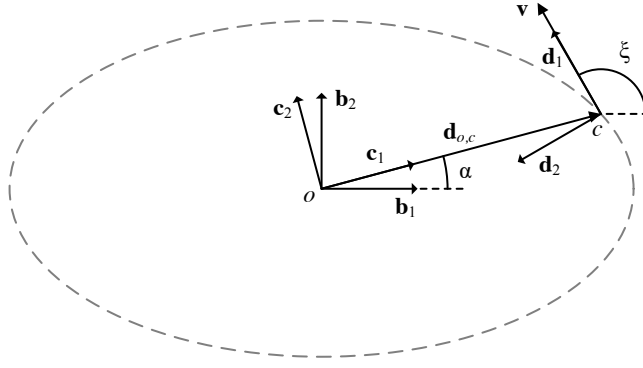


Fig. 4.9: Frame Definitions in the Orbital Plane

$$\mathbf{h}_{\mathbb{B},c}^{\mathbb{D}} = \begin{bmatrix} I_{11} & 0 & 0 \\ 0 & I_{22} & 0 \\ 0 & 0 & I_{33} \end{bmatrix} \begin{Bmatrix} 0 \\ 0 \\ \xi \end{Bmatrix} = \begin{Bmatrix} 0 \\ 0 \\ I_{33}\xi \end{Bmatrix}. \quad (4.2.7)$$

The vector that connects the center of the earth to the mass center of the satellite is $\mathbf{r}_c := \mathbf{r}_{\mathbb{X},c}$ where

$$\mathbf{r}_c = R\mathbf{c}_1 = R(\cos\alpha\mathbf{b}_1 + \sin\alpha\mathbf{b}_2).$$

The second term in Equation (4.2.6) can be expanded as

$$\begin{aligned} \mathbf{d}_{o,c} \times M\mathbf{v}_{\mathbb{B},c} &= MVR \begin{vmatrix} \mathbf{b}_1 & \mathbf{b}_2 & \mathbf{b}_3 \\ \cos\alpha & \sin\alpha & 0 \\ \cos\xi & \sin\xi & 0 \end{vmatrix}, \\ &= MVR(\cos\alpha\sin\xi - \cos\xi\sin\alpha)\mathbf{b}_3, \\ &= MVR\sin(\xi - \alpha)\mathbf{b}_3. \end{aligned} \quad (4.2.8)$$

The sum of terms in Equation (4.2.7) and (4.2.8) gives the desired result if these two terms are represented in a common basis. The relationship between the frame \mathbb{D} and \mathbb{B} is given by the rotation matrix

$$\mathbf{R}_{\mathbb{B}}^{\mathbb{D}} = \begin{bmatrix} \cos\xi & \sin\xi & 0 \\ -\sin\xi & \cos\xi & 0 \\ 0 & 0 & 1 \end{bmatrix}.$$

The angular momentum is

$$\begin{aligned}\mathbf{h}_{\mathbb{E},o}^{\mathbb{D}} &= \begin{Bmatrix} 0 \\ 0 \\ I_{33}\dot{\xi} \end{Bmatrix} + \begin{bmatrix} \cos\xi & \sin\xi & 0 \\ -\sin\xi & \cos\xi & 0 \\ 0 & 0 & 1 \end{bmatrix} \begin{Bmatrix} 0 \\ 0 \\ mVR\sin(\xi-\alpha) \end{Bmatrix}, \\ &= \begin{Bmatrix} 0 \\ 0 \\ I_{33}\dot{\xi} + mVR\sin(\xi-\alpha) \end{Bmatrix}.\end{aligned}$$

The expression for the components relative to the basis for the \mathbb{E} frame can be obtained by premultiplying this equation by the rotation matrix $\mathbf{R}_{\mathbb{B}}^{\mathbb{E}}$ from Example (2.3.4) in Chapter (2),

$$\mathbf{h}_{\mathbb{E},o}^{\mathbb{E}} = \mathbf{R}_{\mathbb{A}}^{\mathbb{E}} \mathbf{R}_{\mathbb{B}}^{\mathbb{A}} \mathbf{R}_{\mathbb{D}}^{\mathbb{B}} \mathbf{h}_{\mathbb{E},o}^{\mathbb{D}}$$

As a result, the angular momentum of the satellite about the center of the earth is given by

$$\mathbf{h}_{\mathbb{E},0}^{\mathbb{E}} = \underbrace{\begin{bmatrix} \cos\phi & -\sin\phi & 0 \\ \sin\phi & \cos\phi & 0 \\ 0 & 0 & 1 \end{bmatrix}}_{\mathbf{R}_{\mathbb{A}}^{\mathbb{E}}} \underbrace{\begin{bmatrix} 1 & 0 & 0 \\ 0 & \cos\psi & -\sin\psi \\ 0 & \sin\psi & \cos\psi \end{bmatrix}}_{\mathbf{R}_{\mathbb{B}}^{\mathbb{A}}} \underbrace{\begin{bmatrix} \cos\xi & -\sin\xi & 0 \\ \sin\xi & \cos\xi & 0 \\ 0 & 0 & 1 \end{bmatrix}}_{\mathbf{R}_{\mathbb{D}}^{\mathbb{B}}} \begin{Bmatrix} 0 \\ 0 \\ h_3 \end{Bmatrix}$$

where $h_3 = I_{33}\dot{\xi} + mVR\sin(\xi-\alpha)$.

4.2.3 Calculation of the Inertia Matrix

The integrals that appear in the Definition (4.4) depend on the choice of the frame \mathbb{Y} . With all the possible choices available for the frame \mathbb{Y} in Theorem (4.5), it is important that efficient techniques are available for calculating inertia matrices relative to different coordinate frames. This section describes several theorems and techniques that facilitate the calculation of the *inertia matrix* in typical applications.

Sections (4.2.3.1) and (4.2.3.3) discuss the *inertia rotation transformation law* and the *Parallel Axis Theorem*. The *inertial rotation transformation law* describes how to relate inertia matrices calculated with respect to two frames with the same origin but different orientations. The *Parallel Axis Theorem* describes how to relate inertia matrices calculated with respect to two frames having parallel orientations, but with origins at the *center of mass* and an arbitrary point p . By combining these two results, the *inertia matrix* relative to any arbitrary frame can be calculated if the *inertia matrix* relative to a given frame is known.

Section (4.2.3.2) summarizes the construction of *principal axes* with respect to which the *inertia matrix* assumes a diagonal form. When possible, it is convenient to cast problems in terms of the *principal axes*, as it reduces the number of parameters in the equations of motion.

Section (4.2.3.4) details the role of symmetry in the calculation of the *inertia matrix*. It will be shown that by identifying coordinate planes of symmetry it is often possible to conclude that certain *products of inertia* in the *inertia matrix* are zero, without having to calculate them explicitly.

4.2.3.1 The Inertia Rotation Transformation Law

This section derives the equation used to relate rotation matrices that are defined from frames that have a common origin, but are rotated relative to one another. The equations derived in Theorem (4.6) are a special case of the *tensor transformation* laws familiar in *tensor analysis*. A comprehensive treatment can be found in [7]. The theorem below summarizes the transformation laws that relate the inertia matrices associated with frames that are rotated relative to one another.

Theorem 4.6. Let \mathbf{I}_p^Y and \mathbf{I}_p^Z be the inertia matrices of a rigid body relative to the frames \mathbb{Y} and \mathbb{Z} , respectively, which have a common origin at p . These inertia matrices satisfy

$$\begin{aligned}\mathbf{I}_p^Z &= \mathbf{R}_Y^Z \mathbf{I}_p^Y (\mathbf{R}_Y^Z)^T = \mathbf{R}_Y^Z \mathbf{I}_p^Y \mathbf{R}_Z^Y, \\ \mathbf{I}_p^Y &= \mathbf{R}_Z^Y \mathbf{I}_p^Z (\mathbf{R}_Z^Y)^T = \mathbf{R}_Z^Y \mathbf{I}_p^Z \mathbf{R}_Y^Z.\end{aligned}$$

These expressions should be compared and contrasted to the transformation laws for the components of a vector \mathbf{u} ,

$$\mathbf{u}^Z = \mathbf{R}_Y^Z \mathbf{u}^Y.$$

The coordinate change for a vector, which is a first order tensor, premultiplies the components by a rotation matrix. The coordinate transformation for the inertia matrix, which is a second order tensor, premultiplies and postmultiplies the components by a rotation matrix and its transpose, respectively. See the Appendix for a detailed discussion.

Proof. The inertia matrices satisfies the equation that relates the *angular momentum* and the *angular velocity* vectors in Theorem (4.5),

$$\mathbf{h}_{X,p}^Y = \mathbf{I}_p^Y \boldsymbol{\omega}_{X,B}^Y \quad \text{and} \quad \mathbf{h}_{X,p}^Z = \mathbf{I}_p^Z \boldsymbol{\omega}_{X,B}^Z.$$

But the *angular momentum* $\mathbf{h}_{X,p}$ and *angular velocity* $\boldsymbol{\omega}_{X,B}$ are themselves vectors whose components transform via the application of the rotation matrices \mathbf{R}_Y^Z or \mathbf{R}_Z^Y , such that

$$\mathbf{h}_{X,p}^Y = \mathbf{R}_Z^Y \mathbf{h}_{X,p}^Z \quad \text{and} \quad \boldsymbol{\omega}_{X,B}^Y = \mathbf{R}_Z^Y \boldsymbol{\omega}_{X,B}^Z.$$

If these are substituted into the equations above, the formulation results in

$$\begin{aligned}\mathbf{R}_Z^Y \mathbf{h}_{X,p}^Z &= \mathbf{I}_p^Y \mathbf{R}_Z^Y \boldsymbol{\omega}_{X,B}^Z, \\ \mathbf{h}_{X,p}^Z &= \underbrace{\mathbf{R}_Y^Z \mathbf{I}_p^Y (\mathbf{R}_Y^Z)^T}_{\mathbf{I}_p^Z} \boldsymbol{\omega}_{X,B}^Z.\end{aligned}$$

The second equation in the theorem follows from the first when the first is premultiplied by \mathbf{R}_Z^Y and postmultiplied by $(\mathbf{R}_Z^Y)^T$. \square

Example 4.2.4. The inertia matrix of the rigid body shown in Figure (4.10) relative to the body fixed frame B that has its origin at the point p is given by

$$\mathbf{I}_p^B = \begin{bmatrix} I_{11} & 0 & 0 \\ 0 & I_{22} & 0 \\ 0 & 0 & I_{33} \end{bmatrix}.$$

The link is fixed with respect to the ground frame Y that shares an origin with frame B at point p . Frame Y is mapped into frame B by a 30° rotation about y_3 . Calculate the inertia matrix about the point p relative to the Y frame shown in Figure (4.10).

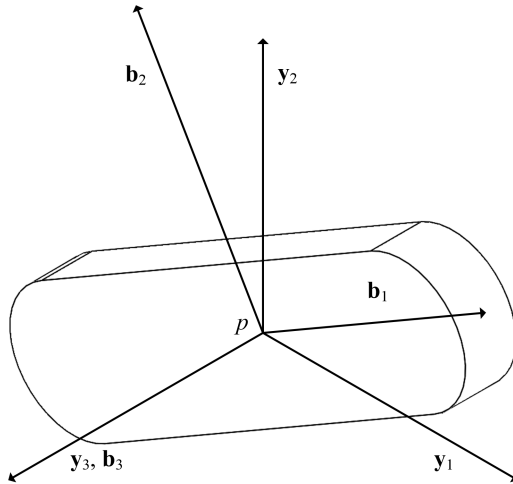


Fig. 4.10: Single Link Rotated with Respect to Ground Frame

Solution: The transformation law for the inertia matrix yields the following theorem that relates the inertia matrices \mathbf{I}_p^Y and \mathbf{I}_p^B

$$\mathbf{I}_p^Y = \mathbf{R}_B^Y \mathbf{I}_p^B (\mathbf{R}_B^Y)^T.$$

The change of basis between the frames \mathbb{B} and \mathbb{Y} can be derived by inspection of the geometry and is determined by the rotation matrices

$$\mathbf{R}_{\mathbb{B}}^{\mathbb{Y}} = \begin{bmatrix} \frac{\sqrt{3}}{2} & -\frac{1}{2} & 0 \\ \frac{1}{2} & \frac{\sqrt{3}}{2} & 0 \\ 0 & 0 & 1 \end{bmatrix} \quad \text{and} \quad \mathbf{R}_{\mathbb{Y}}^{\mathbb{B}} = \begin{bmatrix} \frac{\sqrt{3}}{2} & \frac{1}{2} & 0 \\ -\frac{1}{2} & \frac{\sqrt{3}}{2} & 0 \\ 0 & 0 & 1 \end{bmatrix}.$$

Putting these results together yields the desired inertia matrix

$$\begin{aligned} \mathbf{I}_p^{\mathbb{Y}} &= \begin{bmatrix} \frac{\sqrt{3}}{2} & -\frac{1}{2} & 0 \\ \frac{1}{2} & \frac{\sqrt{3}}{2} & 0 \\ 0 & 0 & 1 \end{bmatrix} \begin{bmatrix} I_{11} & 0 & 0 \\ 0 & I_{22} & 0 \\ 0 & 0 & I_{33} \end{bmatrix} \begin{bmatrix} \frac{\sqrt{3}}{2} & \frac{1}{2} & 0 \\ -\frac{1}{2} & \frac{\sqrt{3}}{2} & 0 \\ 0 & 0 & 1 \end{bmatrix}, \\ &= \begin{bmatrix} \frac{3}{4}I_{11} + \frac{1}{4}I_{22} & \frac{\sqrt{3}}{4}I_{11} - \frac{\sqrt{3}}{4}I_{22} & 0 \\ \frac{\sqrt{3}}{4}I_{11} - \frac{\sqrt{3}}{4}I_{22} & \frac{1}{4}I_{11} + \frac{3}{4}I_{22} & 0 \\ 0 & 0 & I_{33} \end{bmatrix}. \end{aligned}$$

Example 4.2.5. The *inertia matrix* of the satellite shown in Figure (4.11a) about its center of mass relative to the \mathbb{D} frame is given by the sum

$$\mathbf{I}_c^{\mathbb{D}} = \begin{bmatrix} I_{11} & 0 & 0 \\ 0 & I_{22} & 0 \\ 0 & 0 & I_{33} \end{bmatrix} + \begin{bmatrix} K_{11} & 0 & 0 \\ 0 & K_{22} & 0 \\ 0 & 0 & K_{33} \end{bmatrix}$$

where I_{11}, I_{22}, I_{33} are the *moments of inertia* of the central body about the system *center of mass* and K_{11}, K_{22}, K_{33} are the *moments of inertia* of the solar arrays about the system *center of mass*. Use the *inertia rotation transformation law* to derive the system *inertia matrix* when the solar arrays are rotated by 90° about the \mathbf{d}_1 axis as depicted in Figure (4.11b).

Solution: Let the \mathbb{C} frame be a set of axes fixed relative to the solar arrays. The origin of the \mathbb{C} frame is located at the system *center of mass*, and the \mathbb{C} frame is parallel to the \mathbb{D} frame as shown in Figure (4.11a). In Figure (4.11b) the solar arrays have been rotated by 90° . The rotation matrix that relates the \mathbb{C} frame and the \mathbb{D} frame depicted in Figure (4.11b) is given by

$$\mathbf{R}_{\mathbb{C}}^{\mathbb{D}} = \begin{bmatrix} 1 & 0 & 0 \\ 0 & 0 & -1 \\ 0 & 1 & 0 \end{bmatrix}.$$

By the *inertia rotation transformation law*, the *inertia matrix* of the solar arrays about the system *center of mass* relative to the \mathbb{D} frame depicted in Figure (4.11a) is given by

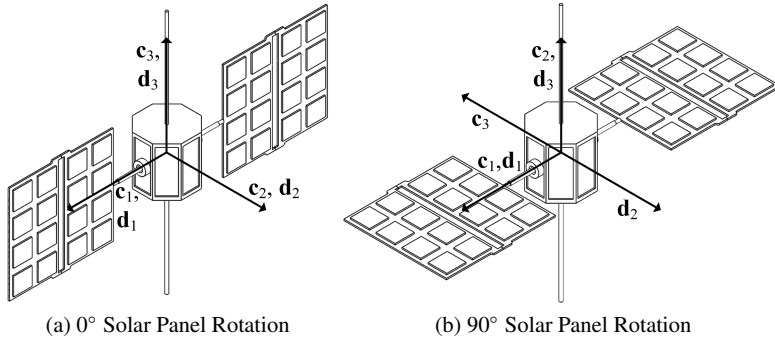


Fig. 4.11: Satellite with Central Body and Solar Panel Fixed Frames

$$\begin{aligned} \mathbf{I}_c^D &= \mathbf{R}_C^D \mathbf{I}_c^C \mathbf{R}_D^C, \\ &= \begin{bmatrix} 1 & 0 & 0 \\ 0 & 0 & -1 \\ 0 & 1 & 0 \end{bmatrix} \begin{bmatrix} K_{11} & 0 & 0 \\ 0 & K_{22} & 0 \\ 0 & 0 & K_{33} \end{bmatrix} \begin{bmatrix} 1 & 0 & 0 \\ 0 & 0 & 1 \\ 0 & -1 & 0 \end{bmatrix} = \begin{bmatrix} K_{11} & 0 & 0 \\ 0 & K_{33} & 0 \\ 0 & 0 & K_{22} \end{bmatrix}. \end{aligned}$$

The *inertia matrix* for the satellite about its *center of mass* is consequently given by the sum

$$\begin{bmatrix} I_{11} + K_{11} & 0 & 0 \\ 0 & I_{22} + K_{33} & 0 \\ 0 & 0 & I_{33} + K_{22} \end{bmatrix}$$

Note that the rotation transformation in this case agrees with intuition: the new inertia matrix is just obtained by permuting the entries of the original inertia matrix of the solar arrays.

4.2.3.2 Principal Axes of Inertia

Theorem (4.6) provides a direct way to calculate the *inertia matrix* relative to some rotated frame from the *inertia matrix* associated with a given frame, provided the two frames have a common origin. In general, the *inertia matrix* is a full 3×3 matrix. There are certain choices of the frame that simplify the form of the inertia matrix. The definition of the *principal axes*, given below, describes a choice of coordinates that yields a diagonal *inertia matrix*.

Definition 4.5. The frame \mathbb{Y} having origin at p defines a set of *principal axes* at the point p for a rigid body whenever the *inertia matrix* $\mathbf{I}_p^{\mathbb{Y}}$ is diagonal,

$$\mathbf{I}_p^{\mathbb{Y}} = \begin{bmatrix} I_{11} & 0 & 0 \\ 0 & I_{22} & 0 \\ 0 & 0 & I_{33} \end{bmatrix}$$

The diagonal terms I_{11}, I_{22}, I_{33} are the *principal moments of inertia* associated with the basis \mathbb{Y} .

For rigid bodies with complex geometry, it may not be evident that there is any special structure of the *inertia matrix*. However, for any point in a rigid body there is *always* a set of axes at the point relative to which the *inertia matrix* is diagonal. That is, there exists a set of *principal axes* at every point in the rigid body. The following theorem summarizes this fact.

Theorem 4.7. Let p be a point in a rigid body. There is a set of principal axes fixed in the body that have their origin at point p .

Proof. This theorem will be proven in detail because the procedure is constructive and provides a way of directly solving practical problems. Background material for this section can be found in Appendix. Suppose an *inertia matrix* $\mathbf{I}_p^{\mathbb{Z}}$ relative to the basis of the frame \mathbb{Z} is given. First, the *eigenvectors* $\boldsymbol{\phi}_1, \boldsymbol{\phi}_2, \boldsymbol{\phi}_3$ and eigenvalues $\lambda_1, \lambda_2, \lambda_3$ are calculated from the solution of the *algebraic eigenvalue problem*

$$\mathbf{I}_p^{\mathbb{Z}} \boldsymbol{\phi}_i = \lambda_i \boldsymbol{\phi}_i.$$

From Theorem (8.11) in the Appendix, since $\mathbf{I}_p^{\mathbb{B}}$ is real and symmetric, it is always possible to scale the *eigenvectors* so that the *modal matrix* $\Phi = [\boldsymbol{\phi}_1 \ \boldsymbol{\phi}_2 \ \boldsymbol{\phi}_3]$ has the properties that

$$\Phi^T \Phi = \begin{bmatrix} 1 & 0 & 0 \\ 0 & 1 & 0 \\ 0 & 0 & 1 \end{bmatrix} \quad \text{and} \quad \Phi^T \mathbf{I}_p^{\mathbb{Z}} \Phi = \begin{bmatrix} \lambda_1 & 0 & 0 \\ 0 & \lambda_2 & 0 \\ 0 & 0 & \lambda_3 \end{bmatrix}.$$

From this, it is concluded that it is possible to choose the eigenvectors so that the matrix Φ is orthogonal. In fact, the *eigenvectors* in the columns of Φ may always be ordered and scaled so that they correspond to a right hand basis. Define the frame \mathbb{Y} via the introduction of the rotation matrix $\mathbf{R}_{\mathbb{Y}}^{\mathbb{Z}} := \Phi$. As a result,

$$\mathbf{I}_p^{\mathbb{Y}} = \mathbf{R}_{\mathbb{Z}}^{\mathbb{Y}} \mathbf{I}_p^{\mathbb{Z}} (\mathbf{R}_{\mathbb{Z}}^{\mathbb{Y}})^T = \Phi^T \mathbf{I}_p^{\mathbb{Z}} \Phi = \begin{bmatrix} \lambda_1 & 0 & 0 \\ 0 & \lambda_2 & 0 \\ 0 & 0 & \lambda_3 \end{bmatrix}.$$

The frame \mathbb{Y} defines a set of *principal axes* at p for the rigid body. The *principal moments of inertia* are the eigenvalues $\lambda_1, \lambda_2, \lambda_3$. \square

Example 4.2.6. Find a set of *principal axes* the inertia matrix

$$\mathbf{I}_p^{\mathbb{Y}} = \begin{bmatrix} 3 & -1 & 0 \\ -1 & 3 & 0 \\ 0 & 0 & 5 \end{bmatrix}.$$

Solution: The characteristic polynomial is

$$p(\lambda) = \det[\mathbf{I}_p^{\mathbb{Y}} - \lambda\mathbb{I}] = \det \begin{vmatrix} (3-\lambda) & -1 & 0 \\ -1 & (3-\lambda) & 0 \\ 0 & 0 & 5-\lambda \end{vmatrix} = (5-\lambda)(\lambda-4)(\lambda-2).$$

The eigenvalues, or principal moments of inertia, are the roots of the characteristic polynomial $\lambda_1 = 2$, $\lambda_2 = 4$, and $\lambda_3 = 5$. The principal axes are determined from the eigenvectors associated with each of these roots. For $\lambda_3 = 5$, the eigenvector must satisfy

$$\begin{aligned} [\mathbf{I}_p^{\mathbb{Y}} - \lambda\mathbb{I}]\boldsymbol{\phi} &= \mathbf{0}, \\ &= \begin{bmatrix} -2 & -1 & 0 \\ -1 & -2 & 0 \\ 0 & 0 & 0 \end{bmatrix} \begin{Bmatrix} \phi_1 \\ \phi_2 \\ \phi_3 \end{Bmatrix} = \begin{Bmatrix} 0 \\ 0 \\ 0 \end{Bmatrix}. \end{aligned}$$

From the first two equations, it must be the case that $\phi_1 = \phi_2 = 0$, while the third equation allows for ϕ_3 to be arbitrary. A unit eigenvector associated with $\lambda_3 = 5$ may then be defined as

$$\boldsymbol{\phi}_3 = \begin{Bmatrix} 0 \\ 0 \\ 1 \end{Bmatrix}.$$

Repeating this procedure for $\lambda_1 = 2$ results in

$$\begin{bmatrix} 1 & -1 & 0 \\ -1 & 1 & 0 \\ 0 & 0 & 4 \end{bmatrix} \begin{Bmatrix} \phi_1 \\ \phi_2 \\ \phi_3 \end{Bmatrix} = \begin{Bmatrix} 0 \\ 0 \\ 0 \end{Bmatrix}.$$

The last equation yields $\phi_3 = 0$, while the first two equations require that $\phi_1 = \phi_2$. As a result, a unit eigenvector $\boldsymbol{\phi}_1$ associated with $\lambda_1 = 2$ is

$$\boldsymbol{\phi}_1 = \begin{Bmatrix} \frac{1}{\sqrt{2}} \\ \frac{1}{\sqrt{2}} \\ 0 \end{Bmatrix}.$$

Repeating this procedure for $\lambda_2 = 4$ results in

$$\begin{bmatrix} -1 & -1 & 0 \\ -1 & -1 & 0 \\ 0 & 0 & 1 \end{bmatrix} \begin{Bmatrix} \phi_1 \\ \phi_2 \\ \phi_3 \end{Bmatrix} = \begin{Bmatrix} 0 \\ 0 \\ 0 \end{Bmatrix}.$$

As before, the third equation specifies that $\phi_3 = 0$ and the first two equations require that $\phi_1 = -\phi_2$. A unit eigenvector $\boldsymbol{\phi}_2$ corresponding to $\lambda = 4$ is defined as

$$\boldsymbol{\phi}_2 = \begin{Bmatrix} \frac{1}{\sqrt{2}} \\ \frac{-1}{\sqrt{2}} \\ 0 \end{Bmatrix}.$$

To obtain the desired rotation matrix, the unit eigenvectors must be assembled into a rotation matrix \mathbf{R} , taking care to make sure that $\det(\mathbf{R}) = +1$. This may be facilitated by multiplying the unit vector by -1 .

$$\mathbf{R} = [\boldsymbol{\phi}_1 \ -\boldsymbol{\phi}_2 \ \boldsymbol{\phi}_3] = \begin{bmatrix} \frac{1}{\sqrt{2}} & -\frac{1}{\sqrt{2}} & 0 \\ \frac{1}{\sqrt{2}} & \frac{1}{\sqrt{2}} & 0 \\ 0 & 0 & 1 \end{bmatrix}.$$

It may be verified that this matrix satisfies the relationships

$$\mathbf{R}^T \mathbf{R} = \mathbf{R} \mathbf{R}^T = \mathbb{I} \quad \text{and} \quad \mathbf{R}^T \mathbf{I}_p^{\mathbb{Y}} \mathbf{R} = \begin{bmatrix} 2 & 0 & 0 \\ 0 & 4 & 0 \\ 0 & 0 & 5 \end{bmatrix}.$$

4.2.3.3 The Parallel Axis Theorem

Theorem (4.6) summarizes how the inertia relative to one set of axes may be used to calculate the inertia relative to a rotated basis. The two frames must have the same origin when applying Theorem (4.6). The *Parallel Axis Theorem*, in contrast, relates the inertia matrix about a point p in terms of the inertia matrix about the *center of mass*. In this case the frames are not rotated relative to each other; they are parallel.

Theorem 4.8. Let the position of a differential mass element in a rigid body be given by the coordinates (x, y, z) relative to a basis whose origin is at p , and by the coordinates (α, β, γ) relative to a parallel frame whose origin is at the center of mass. Suppose the two coordinate systems are related by the equations

$$x = \alpha + \bar{x}, \quad y = \beta + \bar{y}, \quad z = \gamma + \bar{z}.$$

The moments of inertia relative to these two frames satisfy

$$I_{11,p} = I_{11,c} + M(\bar{y}^2 + \bar{z}^2), \quad I_{22,p} = I_{22,c} + M(\bar{x}^2 + \bar{z}^2), \quad I_{33,p} = I_{33,c} + M(\bar{x}^2 + \bar{y}^2).$$

In these equations $I_{11,p}$, $I_{22,p}$, $I_{33,p}$ and $I_{11,c}$, $I_{22,c}$, $I_{33,c}$ are the moments of inertia relative to the frame that has its origin at point p and point c , respectively. The cross products of inertia relative to the two frames satisfy

$$I_{12,p} = I_{12,c} - M\bar{x}\bar{y}, \quad I_{13,p} = I_{13,c} - M\bar{x}\bar{z}, \quad I_{23,p} = I_{23,c} - M\bar{y}\bar{z}.$$

In these equations $I_{12,p}$, $I_{13,p}$, $I_{23,p}$ and $I_{12,c}$, $I_{13,c}$, $I_{23,c}$ are the cross products of inertia relative to the frame that has its origin at points p and point c , respectively.

Proof. As all of the equations for the *moments of inertia* are similar, the equation is only derived for $I_{11,p}$. By definition,

$$\begin{aligned} I_{11,p} &= \int (y^2 + z^2) dm = \int ((\beta + \bar{y})^2 + (\gamma + \bar{z})^2) dm, \\ &= \underbrace{\int (\beta^2 + \gamma^2) dm}_{I_{11,c}} + \underbrace{(\bar{y}^2 + \bar{z}^2)}_{=0} \int dm + 2\bar{y} \underbrace{\int \beta dm}_{=0} + 2\bar{z} \underbrace{\int \gamma dm}_{=0}. \end{aligned}$$

The first term on the right is equal by definition to the *moment of inertia* about the *center of mass*. The last two terms on the right are equal to zero by the definition of the *center of mass*, which is located at the origin of the (α, β, γ) coordinate system.

The analysis of the *cross products of inertia* is similar; only the equation for $I_{12,p}$ is derived. By definition,

$$\begin{aligned} I_{12,p} &= - \int xy dm = - \int (\alpha + \bar{x})(\beta + \bar{y}) dm, \\ &= - \underbrace{\int \alpha \beta dm}_{I_{12,c}} - \bar{x} \bar{y} \int dm - \bar{x} \underbrace{\int \beta dm}_{=0} - \bar{y} \underbrace{\int \alpha dm}_{=0}. \end{aligned}$$

The first term on the right is by definition the *cross product of inertia* $I_{12,c}$. The last two terms are zero by the definition of the *center of mass*, which is located at the origin of the (α, β, γ) coordinate system. \square

The Parallel Axis Theorem is lengthy as written in Theorem (4.8). The following theorem expresses the Parallel Axis Theorem in matrix form and can be useful in programming implementations.

Theorem 4.9. *The Parallel Axis Theorem in theorem (4.8) can be written in matrix form as*

$$\mathbf{I}_p^{\mathbb{B}} = \mathbf{I}_c^{\mathbb{B}} - M\mathbf{S}^2(\bar{\mathbf{r}}) \quad (4.2.9)$$

where M is the mass of the rigid body, $\mathbf{I}_p^{\mathbb{B}}$ is the inertia matrix about the point p relative to the frame \mathbb{B} , $\mathbf{I}_c^{\mathbb{B}}$ is the inertia matrix relative to a frame that is parallel to \mathbb{B} and that has its origin at the center of mass, $\mathbf{S}(\cdot)$ is the skew operator and $\bar{\mathbf{r}} := (\bar{x}, \bar{y}, \bar{z})$.

Proof. The proof stems directly from the expansion of the term $\mathbf{S}^2(\bar{\mathbf{r}})$, which is

$$\begin{aligned} \mathbf{S}^2(\bar{\mathbf{r}}) &= \mathbf{S}(\bar{\mathbf{r}})\mathbf{S}(\bar{\mathbf{r}}), \\ &= \begin{bmatrix} 0 & -\bar{z} & \bar{y} \\ \bar{z} & 0 & -\bar{x} \\ -\bar{y} & \bar{x} & 0 \end{bmatrix} \begin{bmatrix} 0 & -\bar{z} & \bar{y} \\ \bar{z} & 0 & -\bar{x} \\ -\bar{y} & \bar{x} & 0 \end{bmatrix}, \\ &= \begin{bmatrix} -(\bar{y}^2 + \bar{z}^2) & \bar{xy} & \bar{xz} \\ \bar{xy} & -(\bar{x}^2 + \bar{z}^2) & \bar{yz} \\ \bar{xz} & \bar{yz} & -(\bar{x}^2 + \bar{y}^2) \end{bmatrix}. \end{aligned}$$

By inspection, Equation (4.2.9) is identical to the collection of scalar equations in the conclusion of Theorem (4.8). \square

Example 4.2.7. This problem calculates the *inertia matrix* for the horizontal arm of the cylindrical robot shown in Figure (4.12). Use the *inertia rotation transformation law* and the *Parallel Axis Theorem* to calculate the inertia matrix $\mathbf{I}_o^{\mathbb{X}}$ for the horizontal arm with respect to the frame \mathbb{X} with origin at point o from the inertia matrix

$$\mathbf{I}_c^{\mathbb{B}} = \begin{bmatrix} I_{11} & 0 & 0 \\ 0 & I_{22} & 0 \\ 0 & 0 & I_{33} \end{bmatrix}$$

of the horizontal arm about its own *center of mass* at point c . Note that \mathbf{b}_i is not parallel to \mathbf{x}_i for $i = 1, 2, 3$.

Solution:

First, a virtual frame \mathbb{C} will be defined at the horizontal link center of mass that is parallel with frame \mathbb{X} . The rotation matrix

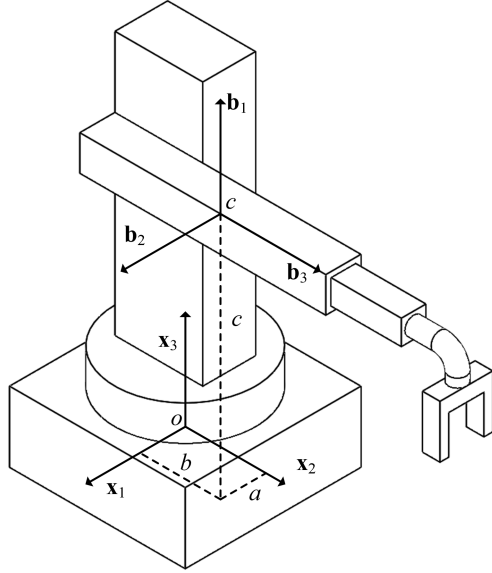


Fig. 4.12: Cylindrical Robot

$$\mathbf{R}_{\mathbb{B}}^{\mathbb{C}} = \begin{bmatrix} 0 & 1 & 0 \\ 0 & 0 & 1 \\ 1 & 0 & 0 \end{bmatrix}$$

maps the basis for the \mathbb{B} frame into the \mathbb{C} frame. The inertia matrix with respect to the \mathbb{C} frame is then

$$\mathbf{I}_c^{\mathbb{C}} = \mathbf{R}_{\mathbb{B}}^{\mathbb{C}} \mathbf{I}_c^{\mathbb{B}} (\mathbf{R}_{\mathbb{B}}^{\mathbb{C}})^T = \begin{bmatrix} 0 & 1 & 0 \\ 0 & 0 & 1 \\ 1 & 0 & 0 \end{bmatrix} \begin{bmatrix} I_{11} & 0 & 0 \\ 0 & I_{22} & 0 \\ 0 & 0 & I_{33} \end{bmatrix} \begin{bmatrix} 0 & 0 & 1 \\ 1 & 0 & 0 \\ 0 & 1 & 0 \end{bmatrix} = \begin{bmatrix} I_{22} & 0 & 0 \\ 0 & I_{33} & 0 \\ 0 & 0 & I_{11} \end{bmatrix}.$$

The *inertia rotation transformation law* yields the inertia $\mathbf{I}_c^{\mathbb{C}}$ that corresponds to the reordering of the *principal moments of inertia* I_{11}, I_{22}, I_{33} . Let α, β, γ be the coordinates located at the center of mass along the $\mathbf{c}_1, \mathbf{c}_2, \mathbf{c}_3$ directions, respectively. The coordinates x, y, z are along the $\mathbf{x}_1, \mathbf{x}_2, \mathbf{x}_3$ directions. In general,

$$x = \alpha + \bar{x}, \quad y = \beta + \bar{y}, \quad z = \gamma + \bar{z} \quad (4.2.10)$$

The constants $\bar{x}, \bar{y}, \bar{z}$ may be calculated by evaluating these equations at a particular point. For example, the origin of the \mathbb{C} frame has coordinates $(\alpha, \beta, \gamma) = (0, 0, 0)$ with respect to the \mathbb{C} frame, and it has coordinates $(x, y, z) = (a, b, c)$ with respect to the \mathbb{X} frame. When these values are substituted into Equation (4.2.10),

$$a = 0 + \bar{x}, \quad b = 0 + \bar{y}, \quad c = 0 + \bar{z}$$

By the *Parallel Axis Theorem*, the *moments of inertia* are

$$\begin{aligned} I_{11,o} &= I_{11,c} + M(\bar{y}^2 + \bar{z}^2) = I_{22} + M(b^2 + c^2), \\ I_{22,o} &= I_{22,c} + M(\bar{x}^2 + \bar{z}^2) = I_{33} + M(a^2 + c^2), \\ I_{33,o} &= I_{33,c} + M(\bar{x}^2 + \bar{y}^2) = I_{11} + M(a^2 + b^2), \end{aligned}$$

and the *cross products of inertia* are

$$\begin{aligned} I_{12,o} &= I_{12,c} - M\bar{x}\bar{y} = -M(a)(b) = -Mab, \\ I_{13,o} &= I_{13,c} - M\bar{x}\bar{z} = -M(a)(c) = -Mac, \\ I_{23,o} &= I_{23,c} - M\bar{y}\bar{z} = -Mbc. \end{aligned}$$

Collecting these into $\mathbf{I}_o^{\mathbb{X}}$ results in

$$\mathbf{I}_o^{\mathbb{X}} = \begin{bmatrix} M(b^2 + c^2) & -Mab & -Mac \\ -Mab & M(a^2 + c^2) & -Mbc \\ -Mac & -Mbc & M(a^2 + b^2) \end{bmatrix}.$$

4.2.3.4 Symmetry and Inertia

The explicit calculation of the integrals that appear in the inertia matrix can be difficult to calculate analytically. In cases of complex geometry, the calculation of closed form expressions can be intractable. Numerical techniques to estimate the inertia matrix are now a standard feature of solid modeling and computer aided design software. The algorithms involved in such calculations are not complex, and require implementation of numerical quadrature formulae to estimate the integrals as a weighted sum of functional evaluations. The most difficult task in implementing this approximation procedure is the characterization of the geometry of the rigid body, but this is precisely the job at which solid modeling and computer aide design programs excel.

Still, even for the most complex geometric models, it is often possible to reduce the work required to evaluate the inertia matrix by utilizing the body's symmetry. The identification of a specific coordinate plane of symmetry implies that *cross products of inertia* involving the coordinate perpendicular to the plane of symmetry are equal to zero. Before stating this theorem, the mathematical definition of a *coordinate plane of symmetry* will be presented.

Definition 4.6. Suppose that x_1, x_2, x_3 are coordinates along the basis vectors $\mathbf{x}_1, \mathbf{x}_2, \mathbf{x}_3$ of the frame \mathbb{X} . The $x_1 - x_2$ plane of the frame \mathbb{X} is a *plane of symmetry* of a rigid body if for each differential mass element in the body located at (x_1, x_2, x_3) there is a differential mass element located at $(x_1, x_2, -x_3)$. In other words,

$$\rho(x_1, x_2, x_3)dx_1dx_2dx_3 = \rho(x_1, x_2, -x_3)dx_1dx_2dx_3$$

for all x_1, x_2, x_3 in the body where the density of the rigid body is ρ . Similar definitions of the $1 - 3$ and $2 - 3$ planes of symmetry hold.

This definition specifies that a *plane of symmetry* splits the body into two pieces that are reflections of each other across the *plane of symmetry*. The importance of identifying a *plane of symmetry* in applications is demonstrated in the following theorem.

Theorem 4.10. Suppose that the $x_i - x_j$ plane of the \mathbb{X} frame is a plane of symmetry of the rigid body. Then the cross products of inertia

$$\begin{aligned} I_{ik}^{\mathbb{X}} &= 0, \\ I_{jk}^{\mathbb{X}} &= 0, \end{aligned}$$

for $k \neq i$ and $k \neq j$. If there exist at least two planes of symmetry relative to the frame \mathbb{X} , the frame \mathbb{X} defines a set of principal axes for the rigid body.

Proof. The proof of this theorem is built on a few fundamental facts from calculus.

Definition 4.7. A function $f : \mathbb{R} \rightarrow \mathbb{R}$ is an *odd function* if and only if

$$-f(x) = f(-x)$$

for all $x \in \mathbb{R}$.

Building on this definition for a single variable function, a multivariable function $f : \mathbb{R}^N \rightarrow \mathbb{R}$ is an *odd function* in the i^{th} argument if the function $x_i \rightarrow f(x_1, \dots, x_i, \dots, x_N)$ is an *odd function* when the other variables are held fixed. In addition, there is a special property of odd functions related to integration.

Proposition 4.2.1. The integral of an *odd function* over a symmetric domain is equal to zero.

Proof. The proof of this proposition will be presented in enough detail that the same sequence of arguments can be used to prove Theorem (4.8). Suppose that f is an odd function. The integration over the symmetric domain will be performed by extending f to be equal to zero for all x that are not in the domain. The integral of f over the domain is then

$$\begin{aligned}
\int_{-\infty}^{\infty} f(x)dx &= \int_{-\infty}^0 f(x)dx + \int_0^{\infty} f(x)dx, \\
&= - \int_0^{-\infty} f(x)dx + \int_0^{\infty} f(x)dx, \\
&= - \int_0^{\infty} f(-\xi)(-d\xi) + \int_0^{\infty} f(x)dx, \\
&= - \int_0^{\infty} -f(\xi)(-d\xi) + \int_0^{\infty} f(x)dx, \\
&= - \int_0^{\infty} f(\xi)d\xi + \int_0^{\infty} f(x)dx, \\
&= 0,
\end{aligned}$$

which proves the proposition. \square

The proof of Theorem (4.10) has the same structure. Suppose that the $x_1 - x_2$ plane of the frame \mathbb{X} is a *plane of symmetry* of the rigid body. By definition,

$$I_{13} = - \int x_1 x_3 dm$$

By using the fact that the density $\rho(x_1, x_2, x_3) \equiv 0$ outside of the body, this integral can be written as

$$\begin{aligned}
I_{13} &= - \int x_1 x_3 dm, \\
&= - \int \int \left(\int_{-\infty}^{\infty} x_3 \rho(x_1, x_2, x_3) dx_3 \right) x_1 dx_1 dx_2, \\
&= - \int \int \left(\int_{-\infty}^0 \rho(x_1, x_2, x_3) dx_3 + \int_0^{\infty} \rho(x_1, x_2, x_3) dx_3 \right) x_1 dx_1 dx_2, \\
&= - \int \int \left(- \int_0^{-\infty} x_3 \rho(x_1, x_2, x_3) dx_3 + \int_0^{\infty} x_3 \rho(x_1, x_2, x_3) dx_3 \right) x_1 dx_1 dx_2, \\
&= - \int \int \left(- \int_0^{\infty} (-\xi) \rho(x_1, x_2, -\xi) (-d\xi) + \int_0^{\infty} x_3 \rho(x_1, x_2, x_3) dx_3 \right) x_1 dx_1 dx_2, \\
&= - \int \int \left(- \int_0^{\infty} \xi \rho(x_1, x_2, \xi) d\xi + \int_0^{\infty} x_3 \rho(x_1, x_2, x_3) dx_3 \right) x_1 dx_1 dx_2, \\
&= 0.
\end{aligned}$$

The integrand in I_{13} is an *odd function* of x_3 that is integrated over a symmetric domain, and is equal to zero. \square

Example 4.2.8. Suppose that link 1 of a PUMA robot is oriented relative to the \mathbb{X} frame as shown in Figure (4.13). Use symmetry arguments to deduce the form of

its inertia matrix. Calculate the inertia matrix assuming that the base is the union of two cylindrical bodies having a common uniform density. Use symmetry arguments to confirm that the individual inertia matrices calculated as intermediate results have the correct form.

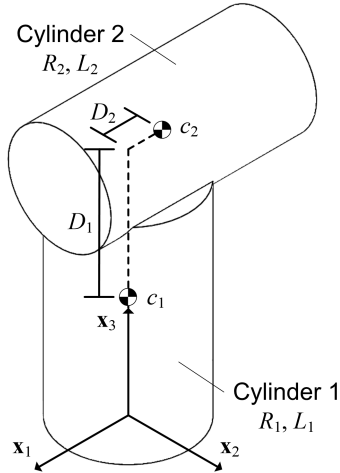


Fig. 4.13: PUMA Link 1 with Single Plane of Symmetry

Solution: From the figure it is apparent that the $\mathbf{x}_1 - \mathbf{x}_3$ coordinate plane of the $\bar{\mathbf{X}}$ frame is a plane of symmetry. Theorem (4.10) implies that all of the *cross products of inertia* are zero that involve the coordinate along the \mathbf{x}_2 direction that is perpendicular to the plane of symmetry. Therefore,

$$I_{12} = 0 \quad \text{and} \quad I_{23} = 0,$$

which results in an *inertia matrix* $\mathbf{I}_0^{\bar{\mathbf{X}}}$ of the form

$$\mathbf{I}_0^{\bar{\mathbf{X}}} = \begin{bmatrix} I_{11} & 0 & I_{13} \\ 0 & I_{22} & 0 \\ I_{13} & 0 & I_{33} \end{bmatrix}.$$

The inertia for the composite body will be calculated with respect to the $\bar{\mathbf{X}}$ frame about the point o by calculating the inertia of each cylinder and summing the result. First, the vertical cylinder will be considered. Fix a frame \mathbb{C} at the center of mass c_1 of the vertical cylinder, with each of its axes $\mathbf{c}_1, \mathbf{c}_2, \mathbf{c}_3$ parallel to the corresponding axes $\mathbf{x}_1, \mathbf{x}_2, \mathbf{x}_3$. The inertia matrix of the vertical cylinder with respect to the \mathbb{C} frame located at its center of mass is given by

$$\mathbf{I}_{c_1}^{\mathbb{C}} = \begin{bmatrix} \frac{1}{12}M_1(3R_1^2 + L_1^2) & 0 & 0 \\ 0 & \frac{1}{12}M_1(3R_1^2 + L_1^2) & 0 \\ 0 & 0 & \frac{1}{2}M_1R_1^2 \end{bmatrix}.$$

This inertia matrix must be diagonal since the $x_1 - x_3$ and $x_2 - x_3$ coordinate planes of the \mathbb{C} frame are planes of symmetry of the vertical cylinder. All the cross products of inertia with respect to coordinates perpendicular to these planes must vanish, which implies that all the cross products are zero.

Next, the *Parallel Axis Theorem* is used to calculate the inertia $\mathbf{I}_o^{\mathbb{X}}$ of the vertical cylinder about the point o with respect to the \mathbb{X} frame. Let α, β, γ be the coordinates along the $\mathbf{c}_1, \mathbf{c}_2, \mathbf{c}_3$ axes, respectively, and let x, y, z be the coordinates along the $\mathbf{x}_1, \mathbf{x}_2, \mathbf{x}_3$ axes. The coordinates are related by the equations

$$x = \alpha + \bar{x}, \quad y = \beta + \bar{y}, \quad z = \gamma + \bar{z}.$$

The offsets $(\bar{x}, \bar{y}, \bar{z})$ may be calculated by evaluating the coordinates of some fixed point in the \mathbb{C} and \mathbb{X} frames. The origin of the \mathbb{C} frame has coordinates $(0, 0, 0)$ with respect to the \mathbb{C} frame, while its coordinates are $(0, 0, \frac{L_1}{2})$ relative to the \mathbb{X} frame. We substitute these values and obtain

$$0 = 0 + \bar{x}, \quad 0 = 0 + \bar{y}, \quad \frac{L_1}{2} = 0 + \bar{z}.$$

The *Parallel Axis Theorem* then yields the inertia $\mathbf{I}_o^{\mathbb{X}}$ of the vertical cylinder about the point o relative to the \mathbb{X} frame as

$$\mathbf{I}_o^{\mathbb{X}} = \begin{bmatrix} \frac{1}{12}M_1(4L_1^2 + 3R_1^2) & 0 & 0 \\ 0 & \frac{1}{12}M_1(4L_1^2 + 3R_1^2) & 0 \\ 0 & 0 & \frac{1}{2}M_1R_1^2 \end{bmatrix}. \quad (4.2.11)$$

Again, this *inertia matrix* has the anticipated form. The $x_1 - x_3$ and $x_2 - x_3$ coordinate planes of the \mathbb{X} frame are planes of symmetry of the vertical cylinder, and it follows that all the cross products of inertia are zero by Theorem (4.10).

Next, the inertia matrix of the horizontal cylinder will be calculated about the point o with respect to the \mathbb{X} frame. Let the \mathbb{B} frame define a set of axes parallel to the \mathbb{X} frame, but whose origin c_2 is located at the *center of mass* of the horizontal cylinder. The *inertia matrix* $\mathbf{I}_{c_2}^{\mathbb{B}}$ of the horizontal cylinder about its *center of mass* c_2 with respect to the \mathbb{B} frame is given by

$$\mathbf{I}_{c_2}^{\mathbb{B}} = \begin{bmatrix} \frac{1}{2}M_2R_2^2 & 0 & 0 \\ 0 & \frac{1}{12}M_2(3R_2^2 + L_2^2) & 0 \\ 0 & 0 & \frac{1}{12}M_2(3R_2^2 + L_2^2) \end{bmatrix}.$$

The \mathbb{B} axes are known to be principal axes of the cylinder since each of the coordinate planes of the \mathbb{B} frame are a plane of symmetry for the horizontal cylinder. As before, the *Parallel Axis Theorem* is used to derive the inertia matrix $\mathbf{I}_o^{\mathbb{X}}$ of the horizontal cylinder about the point o with respect to the \mathbb{X} axes. Let α, β, γ now be

the coordinates of a chosen point along the $\mathbf{b}_1, \mathbf{b}_2, \mathbf{b}_3$ basis vectors, and let x, y, z be the coordinates along the $\mathbf{x}_1, \mathbf{x}_2, \mathbf{x}_3$ basis vectors. The location of point c_2 is $(0, 0, 0)$ relative to the \mathbb{B} frame and $(-D_2, 0, \frac{L_1}{2} + D_1)$ relative to the \mathbb{X} frame. combining these results in

$$\begin{aligned}\frac{1}{2}W_1 - W_2 &= 0 + \bar{x} \\ 0 &= 0 + \bar{y} \\ H_1 &= 0 + \bar{z}\end{aligned}$$

The *Parallel Axis Theorem* guarantees that we have for the horizontal cylinder that

$$\mathbf{I}_o^{\mathbb{X}} = \begin{bmatrix} M_2(D_1 + \frac{L_1}{2})^2 + \frac{1}{2}M_2R_2^2 & 0 & M_2D_2(D_1 + \frac{L_1}{2}) \\ 0 & K & 0 \\ M_2D_2(D_1 + \frac{L_1}{2}) & 0 & M_2D_2^2 + \frac{1}{12}M_2(L_2^2 + 3R_2^2) \end{bmatrix} \quad (4.2.12)$$

where $K = M_2D_2^2 + M_2(D_1 + \frac{L_1}{2})^2 + \frac{1}{12}M_2(L_2^2 + 3R_2^2)$. Only the $\mathbf{x}_1 - \mathbf{x}_3$ plane of the \mathbb{X} frame is a plane of symmetry for the the composite body. Theorem (4.10) asserts that the cross products I_{12} and I_{23} are equal to zero for the inertia matrix of this body about the point o relative to the \mathbb{X} frame. The final solution for the inertia matrix of the composite body is obtained by summing the inertia matrices in Equations (4.2.11) and (4.2.12).

4.3 The Newton-Euler Equations

A first course in dynamics introduces Newton's laws of motion, which are applicable to bodies that are idealized as point masses. *Newton's First Law* holds that in the absence of applied external forces, a mass at rest remains at rest, or if it is in motion it travels along a straight line with constant velocity. *Newton's Second Law* maintains that the sum of forces acting on a point mass is equal to the time rate of change of the *linear momentum* of the point mass. A critical feature of the Newton's laws of motion is that they are stated with respect to observations made in an *inertial reference frame*.

Robotic systems are most often comprised of collections of rigid bodies whose mass is distributed spatially. While it is sometimes possible to create reasonable approximations of robotic systems using lumped mass or point mass approximations, this is frequently not the case. The required generalization of Newton's laws of motion for rigid bodies having distributed mass are given by *Euler's Laws* of motion.

Theorem 4.11 (Euler's First Law). *The resultant force \mathbf{f} acting on a rigid body is equal to the time rate of change in an inertial frame \mathbb{X} of the linear momentum*

$\mathbf{p}_{\mathbb{X}}$

$$\frac{d}{dt} \Big|_{\mathbb{X}} (\mathbf{p}_{\mathbb{X}}) = \mathbf{f}.$$

Theorem 4.12 (Euler's Second Law). *Let p be a point that is fixed in the inertial frame \mathbb{X} . The resultant moment \mathbf{m}_p about point p acting on a rigid body is equal to the time rate of change in an inertial frame \mathbb{X} of the angular momentum $\mathbf{h}_{\mathbb{X},p}$ about the point p .*

$$\frac{d}{dt} \Big|_{\mathbb{X}} (\mathbf{h}_{\mathbb{X},p}) = \mathbf{m}_p.$$

Theorems (4.11) and (4.12) can be used in applications, but it is often the case that alternative forms are sought. *Euler's First Law* can also be stated as the fact that the resultant force acting on a rigid body is equal to the mass of the rigid body multiplied by the acceleration of the *center of mass* of the body in an *inertial frame*.

Theorem 4.13. *The resultant force \mathbf{f} acting on a rigid body is equal to the mass multiplied by the acceleration in an inertial frame \mathbb{X} of the center of mass of the rigid body.*

$$M\mathbf{a}_{\mathbb{X},c} = \mathbf{f}.$$

Proof. The time rate of change in the *inertial frame* \mathbb{X} of the linear momentum is

$$\frac{d}{dt} \Big|_{\mathbb{X}} (\mathbf{p}_{\mathbb{X}}) = \frac{d}{dt} \Big|_{\mathbb{X}} \left(\int \mathbf{v} dm \right) = \frac{d}{dt} \Big|_{\mathbb{X}} (M\mathbf{v}_{\mathbb{X},c}) = M\mathbf{a}_{\mathbb{X},c}.$$

□

The form of *Euler's Second Law* stated in Theorem (4.12) requires that the point p is fixed in the *inertial frame* \mathbb{X} . This restriction can be a serious drawback in many applications. For example, in space robotics it is not convenient to impose this condition. However, a suitable alternative form may be derived. *Euler's Second Law* can also be stated for the case when the point p is selected to be the *center of mass* of the rigid body.

Theorem 4.14. *The resultant moment \mathbf{m}_c acting on a rigid body about the center of mass c is equal to the time rate of change in the inertial frame \mathbb{X} of the angular momentum $\mathbf{h}_{\mathbb{X},c}$ about the center of mass.*

$$\frac{d}{dt} \Big|_{\mathbb{X}} (\mathbf{h}_{\mathbb{X},c}) = \mathbf{m}_c.$$

Proof. Theorem (4.2) defines the relationship between the *angular momentum* about a point p and the *center of mass* to be

$$\mathbf{h}_{\mathbb{X},p} = \mathbf{h}_{\mathbb{X},c} + \mathbf{d}_{p,c} \times (M\mathbf{v}_{\mathbb{X},c}).$$

Suppose that p is some point fixed in the inertial frame \mathbb{X} . Substituting this expression into *Euler's Second Law* results in

$$\begin{aligned} \frac{d}{dt} \Big|_{\mathbb{X}} (\mathbf{h}_{\mathbb{X},p}) &= \frac{d}{dt} \Big|_{\mathbb{X}} (\mathbf{h}_{\mathbb{X},c}) + \frac{d}{dt} \Big|_{\mathbb{X}} (\mathbf{d}_{p,c} \times (M\mathbf{v}_{\mathbb{X},c})), \\ &= \frac{d}{dt} \Big|_{\mathbb{X}} (\mathbf{h}_{\mathbb{X},c}) + \underbrace{\frac{d}{dt} \Big|_{\mathbb{X}} (\mathbf{d}_{p,c}) \times M\mathbf{v}_{\mathbb{X},c}}_{\mathbf{v}_{\mathbb{X},c}} + \mathbf{d}_{p,c} \times M \underbrace{\frac{d}{dt} \Big|_{\mathbb{X}} (\mathbf{v}_{\mathbb{X},c})}_{\mathbf{a}_{\mathbb{X},c}}. \end{aligned}$$

The second term on the right is equal to zero, and *Euler's First Law* used to substitute in the third term on the right to obtain

$$\mathbf{m}_p = \frac{d}{dt} \Big|_{\mathbb{X}} (\mathbf{h}_{\mathbb{X},p}) = \frac{d}{dt} \Big|_{\mathbb{X}} (\mathbf{h}_{\mathbb{X},c}) + \mathbf{d}_{p,c} \times \mathbf{f}.$$

This equation can be rearranged as

$$\frac{d}{dt} \Big|_{\mathbb{X}} (\mathbf{h}_{\mathbb{X},c}) = \underbrace{\mathbf{m}_p - \mathbf{d}_{p,c} \times \mathbf{f}}_{\mathbf{m}_c}.$$

□

The above proof illustrates that Theorems (4.12) and (4.14) are equivalent; either form could be selected as Euler's Second Law. As a final topic in this section, alternative laws are presented that are derived from *Euler's Second Law* that relate *angular momentum* and moments about an *arbitrary point* p that is fixed on a rigid body.

Theorem 4.15. Let point p be fixed on a rigid body, but otherwise arbitrary. The resultant moment \mathbf{m}_p about p of the external forces and moments acting on a rigid body and the angular momentum about p of the rigid body satisfy the three following equivalent equations:

$$\mathbf{m}_p = \frac{d}{dt} \Big|_{\mathbb{X}} (\mathbf{h}_{\mathbb{X},c}) + \mathbf{d}_{p,c} \times (M\mathbf{a}_{\mathbb{X},c}), \quad (4.3.1)$$

$$\mathbf{m}_p = \frac{d}{dt} \Big|_{\mathbb{X}} (\mathbf{h}_{\mathbb{X},p}) + (\mathbf{d}_{p,c} \times \boldsymbol{\omega}_{\mathbb{X},\mathbb{B}}) \times M\mathbf{v}_{\mathbb{X},c} \quad (4.3.2)$$

$$\mathbf{m}_p = \frac{d}{dt} \Big|_{\mathbb{X}} (\mathbf{I}_p \boldsymbol{\omega}_{\mathbb{X},\mathbb{B}}) + \mathbf{d}_{p,c} \times (M\mathbf{a}_{\mathbb{X},p}). \quad (4.3.3)$$

In these equations $\mathbf{h}_{\mathbb{X},c}$ and $\mathbf{h}_{\mathbb{X},p}$ are the angular momentum in the \mathbb{X} frame about the center of mass c and point p , respectively, $\mathbf{d}_{p,c}$ is the vector connecting the point p to the center of mass c of the rigid body, \mathbf{I}_p is the inertia tensor relative to the point p , $\boldsymbol{\omega}_{\mathbb{X},\mathbb{B}}$ is the angular velocity of the \mathbb{B} frame in the \mathbb{X} frame, $\mathbf{a}_{\mathbb{X},c}$ is the acceleration of the center of mass in the \mathbb{X} frame, and $\mathbf{v}_{\mathbb{X},c}$ is the velocity of the center of mass in the \mathbb{X} frame.

Proof. Euler's Second Law for the center of mass of the body states

$$\mathbf{m}_c = \frac{d}{dt} \Big|_{\mathbb{X}} (\mathbf{h}_{\mathbb{X},c}). \quad (4.3.4)$$

The resultant moment about the point p can be written in terms of the resultant moment about the center of mass c as

$$\mathbf{m}_p = \mathbf{m}_c + \mathbf{d}_{p,c} \times \mathbf{f} \quad (4.3.5)$$

where \mathbf{f} is the resultant force acting on the rigid body. The proof of Equation (4.3.1) utilizes Equations (4.3.4) and (4.3.5) to show that

$$\begin{aligned} \mathbf{m}_p - \mathbf{d}_{p,c} \times \mathbf{f} &= \frac{d}{dt} \Big|_{\mathbb{X}} (\mathbf{h}_{\mathbb{X},c}), \\ \mathbf{m}_p &= \frac{d}{dt} \Big|_{\mathbb{X}} (\mathbf{h}_{\mathbb{X},c}) + \mathbf{d}_{p,c} \times \mathbf{f}, \\ &= \frac{d}{dt} \Big|_{\mathbb{X}} (\mathbf{h}_{\mathbb{X},c}) + \mathbf{d}_{p,c} \times (M\mathbf{a}_{\mathbb{X},c}). \end{aligned}$$

For the proof of Equation (4.3.2), Theorem (4.2) states that

$$\mathbf{h}_{\mathbb{X},p} = \mathbf{h}_{\mathbb{X},c} + \mathbf{d}_{p,c} \times (M\mathbf{v}_{\mathbb{X},c}). \quad (4.3.6)$$

Substituting Equation (4.3.6) into Equation (4.3.4) yields

$$\begin{aligned}\mathbf{m}_p - \mathbf{d}_{p,c} \times \mathbf{f} &= \frac{d}{dt} \Big|_{\mathbb{X}} (\mathbf{h}_{\mathbb{X},p} - \mathbf{d}_{p,c} \times M\mathbf{v}_{\mathbb{X},c}), \\ &= \frac{d}{dt} \Big|_{\mathbb{X}} (\mathbf{h}_{\mathbb{X},p}) - \frac{d}{dt} \Big|_{\mathbb{X}} (\mathbf{d}_{p,c} \times M\mathbf{v}_{\mathbb{X},c}).\end{aligned}$$

This equation can be rewritten using the identity

$$\frac{d}{dt} \Big|_{\mathbb{X}} (\mathbf{d}_{p,c} \times M\mathbf{v}_{\mathbb{X},c}) = \left(\frac{d}{dt} \Big|_{\mathbb{B}} (\mathbf{d}_{p,c}) + \boldsymbol{\omega}_{\mathbb{X},\mathbb{B}} \times \mathbf{d}_{p,c} \right) \times M\mathbf{v}_{\mathbb{X},c} + \mathbf{d}_{p,c} \times M\mathbf{a}_{\mathbb{X},c}, \quad (4.3.7)$$

$$= -(\mathbf{d}_{p,c} \times \boldsymbol{\omega}_{\mathbb{X},\mathbb{B}}) \times M\mathbf{v}_{\mathbb{X},c} + \mathbf{d}_{p,c} \times M\mathbf{a}_{\mathbb{X},c}, \quad (4.3.8)$$

to show that

$$\mathbf{m}_p - \mathbf{d}_{p,c} \times \mathbf{f} = \frac{d}{dt} \Big|_{\mathbb{X}} (\mathbf{h}_{\mathbb{X},p}) + (\mathbf{d}_{p,c} \times \boldsymbol{\omega}_{\mathbb{X},\mathbb{B}}) \times M\mathbf{v}_{\mathbb{X},c} - \mathbf{d}_{p,c} \times M\mathbf{a}_{\mathbb{X},c}.$$

The mass multiplied by the acceleration $\mathbf{a}_{\mathbb{X},c}$ of the *center of mass* is equal to the resultant applied force from *Euler's First Law*, which shows that Equation (4.3.2) holds

$$\mathbf{m}_p = \frac{d}{dt} \Big|_{\mathbb{X}} (\mathbf{h}_{\mathbb{X},p}) + (\mathbf{d}_{p,c} \times \boldsymbol{\omega}_{\mathbb{X},\mathbb{B}}) \times M\mathbf{v}_{\mathbb{X},c}. \quad (4.3.9)$$

The *angular momentum* about the point p and the *inertia matrix* \mathbf{I}_p have been related in Theorem (4.4) via the identity

$$\mathbf{h}_{\mathbb{X},p} = \mathbf{I}_p \boldsymbol{\omega}_{\mathbb{X},\mathbb{B}} + \mathbf{d}_{p,c} \times M\mathbf{v}_{\mathbb{X},p}$$

The proof of Equation (4.3.3) begins by substituting in the above expression for angular momentum into Equation (4.3.9), and expanding the velocity $\mathbf{v}_{\mathbb{X},p}$ using the Relative Velocity Theorem (2.16) in terms of point c , such that

$$\begin{aligned}\mathbf{m}_p &= \frac{d}{dt} \Big|_{\mathbb{X}} (\mathbf{I}_p \boldsymbol{\omega}_{\mathbb{X},\mathbb{B}} + \mathbf{d}_{p,c} \times M\mathbf{v}_{\mathbb{X},p}) + (\mathbf{d}_{p,c} \times \boldsymbol{\omega}_{\mathbb{X},\mathbb{B}}) \times M\mathbf{v}_{\mathbb{X},c}, \\ &= \frac{d}{dt} \Big|_{\mathbb{X}} (\mathbf{I}_p \boldsymbol{\omega}_{\mathbb{X},\mathbb{B}}) + \frac{d}{dt} \Big|_{\mathbb{X}} (\mathbf{d}_{p,c} \times M\mathbf{v}_{\mathbb{X},c}) \\ &\quad + \frac{d}{dt} \Big|_{\mathbb{X}} (\mathbf{d}_{p,c} \times M(\mathbf{d}_{p,c} \times \boldsymbol{\omega}_{\mathbb{X},\mathbb{B}})) + (\mathbf{d}_{p,c} \times \boldsymbol{\omega}_{\mathbb{X},\mathbb{B}}) \times M\mathbf{v}_{\mathbb{X},c}.\end{aligned}$$

Equation (4.3.8) may be used to replace the second term in the above equation and cancel out the final term, resulting in

$$\mathbf{m}_p = \frac{d}{dt} \Big|_{\mathbb{X}} (\mathbf{I}_p \boldsymbol{\omega}_{\mathbb{X},\mathbb{B}}) + \frac{d}{dt} \Big|_{\mathbb{X}} (\mathbf{d}_{p,c} \times M(\mathbf{d}_{p,c} \times \boldsymbol{\omega}_{\mathbb{X},\mathbb{B}})) + \mathbf{d}_{p,c} \times M\mathbf{a}_{\mathbb{X},c}.$$

The derivative in the second term of the above equation may be expanded and the third term expressed in terms of the velocity $\mathbf{v}_{\mathbb{X},c}$, such that

$$\begin{aligned}
\mathbf{m}_p &= \frac{d}{dt} \Big|_{\mathbb{X}} (\mathbf{I}_p \boldsymbol{\omega}_{\mathbb{X},\mathbb{B}}) + \frac{d}{dt} \Big|_{\mathbb{X}} (\mathbf{d}_{p,c} \times M(\mathbf{d}_{p,c} \times \boldsymbol{\omega}_{\mathbb{X},\mathbb{B}})) + \mathbf{d}_{p,c} \times M \mathbf{a}_{\mathbb{X},c}, \\
&= \frac{d}{dt} \Big|_{\mathbb{X}} (\mathbf{I}_p \boldsymbol{\omega}_{\mathbb{X},\mathbb{B}}) + \underbrace{(\mathbf{v}_{\mathbb{X},c} - \mathbf{v}_{\mathbb{X},p}) \times M(\mathbf{d}_{p,c} \times \boldsymbol{\omega}_{\mathbb{X},\mathbb{B}})}_{=0} \\
&\quad + \mathbf{d}_{p,c} \times M \frac{d}{dt} \Big|_{\mathbb{X}} (\mathbf{d}_{p,c} \times \boldsymbol{\omega}_{\mathbb{X},\mathbb{B}}) + \mathbf{d}_{p,c} \times M \frac{d}{dt} \Big|_{\mathbb{X}} (\mathbf{v}_{\mathbb{X},c}).
\end{aligned}$$

Combining the final two equations and applying the derivative results in the desired equation from Equation (4.3.3)

$$\begin{aligned}
\mathbf{m}_p &= \frac{d}{dt} \Big|_{\mathbb{X}} (\mathbf{I}_p \boldsymbol{\omega}_{\mathbb{X},\mathbb{B}}) + \mathbf{d}_{p,c} \times M \frac{d}{dt} \Big|_{\mathbb{X}} (\mathbf{v}_{\mathbb{X},c} + \mathbf{d}_{p,c} \times \boldsymbol{\omega}_{\mathbb{X},\mathbb{B}}), \\
&= \frac{d}{dt} \Big|_{\mathbb{X}} (\mathbf{I}_p \boldsymbol{\omega}_{\mathbb{X},\mathbb{B}}) + \mathbf{d}_{p,c} \times M \frac{d}{dt} \Big|_{\mathbb{X}} (\mathbf{v}_{\mathbb{X},c} + \boldsymbol{\omega}_{\mathbb{X},\mathbb{B}} \times \mathbf{d}_{c,p}), \\
&= \frac{d}{dt} \Big|_{\mathbb{X}} (\mathbf{I}_p \boldsymbol{\omega}_{\mathbb{X},\mathbb{B}}) + \mathbf{d}_{p,c} \times M \frac{d}{dt} \Big|_{\mathbb{X}} (\mathbf{v}_{\mathbb{X},p}), \\
&= \frac{d}{dt} \Big|_{\mathbb{X}} (\mathbf{I}_p \boldsymbol{\omega}_{\mathbb{X},\mathbb{B}}) + \mathbf{d}_{p,c} \times M \mathbf{a}_{\mathbb{X},p}.
\end{aligned}$$

□

4.4 Euler's Equation for a Rigid Body

Euler's First and Second Laws as stated in Theorems (4.11) and (4.12) can be used to derive the equations of motion for mechanical systems comprised of rigid bodies. When treating complex mechanical systems that consist of rigid bodies connected by ideal joints, the choice of kinematic variables and frames of reference can be quite complicated. The choice of kinematic variables is often tailored to the problem at hand to simplify calculations. The following theorem discusses one of the most common such applications of Euler's First and Second laws, *Euler's Equations* of rotational motion for a single rigid body. It is assumed in these equations that the body fixed frame defines a set of principal axes that have their origin at the center of mass.

Theorem 4.16. Suppose that a rigid body with body fixed frame \mathbb{B} moves in the inertial frame \mathbb{X} . Let the origin of the \mathbb{B} frame be located in the center of mass, and let the \mathbb{B} frame define a set of principal axes for the rigid body. Euler's Equations for the rotational motion of the rigid body are given by

$$\begin{Bmatrix} m_1 \\ m_2 \\ m_3 \end{Bmatrix} = \begin{Bmatrix} I_1\dot{\omega}_1 + \omega_2\omega_3(I_3 - I_2) \\ I_2\dot{\omega}_2 + \omega_1\omega_3(I_1 - I_3) \\ I_3\dot{\omega}_3 + \omega_1\omega_2(I_2 - I_1) \end{Bmatrix}$$

where the applied moment about the center of mass and the angular velocity are given by, respectively,

$$\begin{aligned} \mathbf{m}_c &= m_1\mathbf{b}_1 + m_2\mathbf{b}_2 + m_3\mathbf{b}_3, \\ \boldsymbol{\omega}_{\mathbb{X},\mathbb{B}} &= \omega_1\mathbf{b}_1 + \omega_2\mathbf{b}_2 + \omega_3\mathbf{b}_3, \end{aligned}$$

$\mathbf{b}_1, \mathbf{b}_2, \mathbf{b}_3$ are a basis for the \mathbb{B} frame, and I_1, I_2, I_3 are the principal moments of inertia relative to the \mathbb{B} frame.

Proof. Let the principal moments of inertia with respect to the \mathbb{B} frame be I_1, I_2 and I_3 . The components in \mathbb{B} of the angular momentum in \mathbb{X} about the center of mass of the body is given by Theorem (4.5) as

$$\begin{aligned} \mathbf{h}_{\mathbb{X},c}^{\mathbb{B}} &= \mathbf{I}_c^{\mathbb{B}} \boldsymbol{\omega}_{\mathbb{X},\mathbb{B}}^{\mathbb{B}}, & (4.4.1) \\ &= \begin{bmatrix} I_1 & 0 & 0 \\ 0 & I_2 & 0 \\ 0 & 0 & I_3 \end{bmatrix} \begin{Bmatrix} \omega_1 \\ \omega_2 \\ \omega_3 \end{Bmatrix} = \begin{Bmatrix} I_1\omega_1 \\ I_2\omega_2 \\ I_3\omega_3 \end{Bmatrix}, \end{aligned}$$

where ω_1, ω_2 and ω_3 are the components of the angular velocity vector with respect to the body frame. Euler's Second Law in Theorem (4.14) can be written

$$\mathbf{m}_c = \frac{d}{dt} \Big|_{\mathbb{X}} (\mathbf{h}_{\mathbb{X},c}) = \frac{d}{dt} \Big|_{\mathbb{B}} (\mathbf{h}_{\mathbb{X},c}) + \boldsymbol{\omega}_{\mathbb{X},\mathbb{B}} \times \mathbf{h}_{\mathbb{X},c} \quad (4.4.2)$$

using the Derivative Theorem (2.12) in Chapter (2) above to obtain the expression in terms of the derivative $\frac{d}{dt}|_{\mathbb{B}}(\cdot)$. It is straightforward to expand Equation (4.4.2) using Equation (4.4.1), which is given in terms of the basis for the \mathbb{B} frame. The cross product term is

$$\begin{aligned} \boldsymbol{\omega}_{\mathbb{X},\mathbb{B}} \times \mathbf{h}_{\mathbb{X},c} &= \begin{vmatrix} \mathbf{b}_1 & \mathbf{b}_2 & \mathbf{b}_3 \\ \omega_1 & \omega_2 & \omega_3 \\ I_1\omega_1 & I_2\omega_2 & I_3\omega_3 \end{vmatrix}, \\ &= \omega_2\omega_3(I_3 - I_2)\mathbf{b}_1 + \omega_1\omega_3(I_1 - I_3)\mathbf{b}_2 + \omega_1\omega_2(I_2 - I_1)\mathbf{b}_3. \end{aligned}$$

The final equations of motion are consequently

$$\mathbf{m}_c^{\mathbb{B}} = \begin{Bmatrix} m_1 \\ m_2 \\ m_3 \end{Bmatrix} = \begin{Bmatrix} I_1\dot{\omega}_1 + \omega_2\omega_3(I_3 - I_2) \\ I_2\dot{\omega}_2 + \omega_1\omega_3(I_1 - I_3) \\ I_3\dot{\omega}_3 + \omega_1\omega_2(I_2 - I_1) \end{Bmatrix}.$$

□

4.5 Equations of Motion for Mechanical Systems

Euler's First Law in Theorem (4.11) and *Euler's Second Law* in Theorem (4.12) give a complete description of the dynamics of mechanical systems that consist of rigid bodies. This section discusses the use of these principles in realistic problems that arise when studying robotic systems.

4.5.1 The General Strategy

A general outline of the steps used to derive the equations of motion from *Euler's Laws* for mechanical systems is given in Figure (4.14). The set of steps that appear

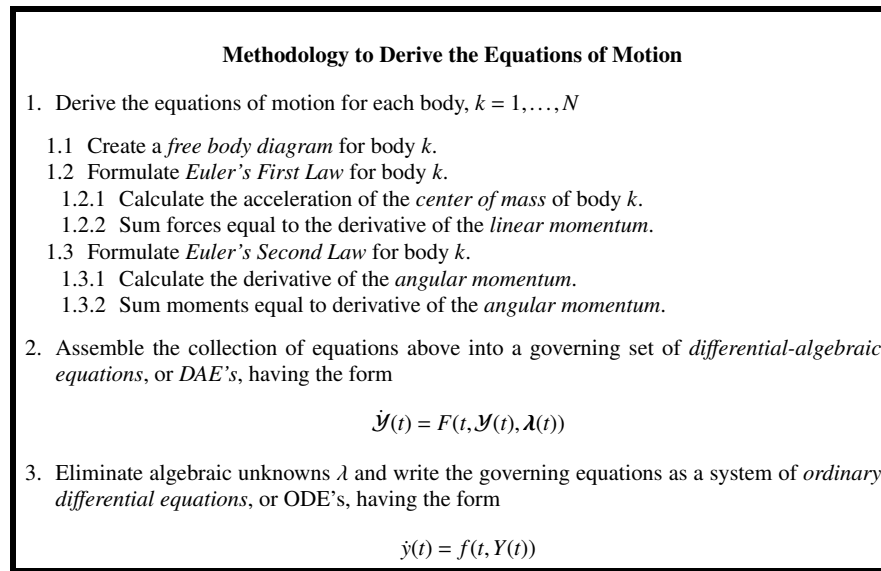


Fig. 4.14: Methodology to Derive the Equations of Motion

in Figure (4.14) can be difficult to apply in practice, and experience is required to become adept at deriving the equations of motion for complex systems. The complexity of the resulting equations can vary dramatically based on the selection of the kinematic variables, or depending on the choice of frames, in a particular problem.

The successful application of the steps in Figure (4.14) requires numerous theorems and principles that have been introduced in Chapters (2), (3), and (4). The calculation of the acceleration of the *center of mass* builds on the foundations developed in Chapter (2) and on the specific formulations of kinematics for robotics summarized in Chapter (3). The determination of the derivative of the *angular momentum* in Steps 2.2.1 or 2.3.1 of Figure (4.14) requires a working knowledge of the use of *angular velocities* introduced in Chapter (2) in Section (2.5.1) and the Derivative Theorem in Theorem (2.12). Even with a strong understanding of these definitions and underlying principles, practice will guide the careful selection of the kinematic variables and frames in a particular problem.

4.5.2 Free Body Diagrams

The creation of an accurate *free body diagram* is essential in the sequence of steps in Figure (4.14). The *free body diagram* releases a rigid body from all external constraints on the body and represents the effect of these constraints by unknown reaction forces and moments that act between the bodies. The representation of constraint forces and moments that act between bodies in a mechanical system connected by *ideal joints* can be treated systematically. The sum of the *number of degrees of freedom* of an *ideal joint* and the number of constraint reaction forces and moments that act between the bodies connected by that joint is always equal to six. In fact, much more can be said about the *complementary nature* of the kinematic constraints introduced by an ideal joint and the associated reaction forces and moments. This complementarity is the subject of the next theorem.

Theorem 4.17. *The number of degrees of freedom N_{DOF} of an ideal joint that connects two rigid bodies and the number of reaction forces and moments N_R that act between these bodies at the joint satisfies the equation*

$$N_{DOF} + N_R = 6.$$

If the ideal joint prevents relative translation along k mutually orthogonal directions, there are in general k reaction forces that act on the adjacent bodies along these directions. The reaction forces serve to constrain the relative translation. If the ideal joint prevents relative rotation between the two bodies about k mutually orthogonal directions there are in general k constraint reaction moments. The reaction moments that act along these directions serve to constrain the relative rotation. The internal reaction forces and moments acting on each body have the same magnitude, but opposite directions.

Before applying this theorem in a number of examples, it must be emphasized that the statement of the theorem concludes that there are *in general* k reaction forces or moments. It can occur that the value of some of the components of these reaction forces or moments are equal to zero. Strictly speaking, it is perhaps more accurate to say that the joint in question can support k reaction forces or moments, but that some of these reactions may be equal to zero. The next few examples will show how to create *free body diagrams* for some typical mechanical systems. Each example has been selected to emphasize the practical implications of Theorem (4.17) and the methodology outlined in Figure (4.14)

Example 4.5.1. The base, vertical column and inner arm of a PUMA robot are depicted in Figure (4.15). In this example the ground frame is denoted as \mathbb{X} , the frame \mathbb{A} is fixed in the revolving vertical column, and the inner arm has body fixed frame \mathbb{B} . The revolute joint 1 defines a single axis rotation of the vertical column through the angle θ_1 about the $\mathbf{x}_3 = \mathbf{a}_3$ axis at point o . The revolute joint 2 defines a single axis rotation of the inner arm through the angle θ_2 about the $\mathbf{a}_2 = \mathbf{b}_2$ axis at point q . Create *free body diagrams* for bodies 1 and 2 in this robotic system.

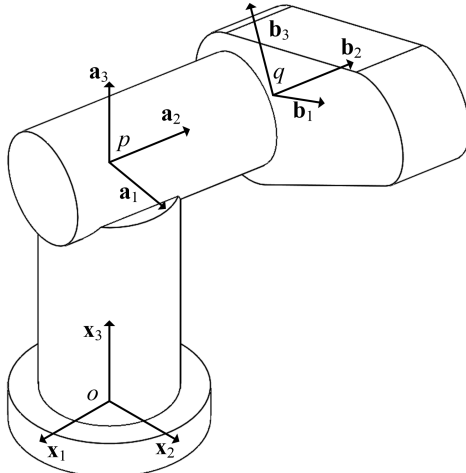


Fig. 4.15: Base Body and Inner Arm of PUMA Robot

Solution: There is a revolute joint at point o , and its joint variable is θ_1 . There must be three orthogonal reaction forces that constrain the relative displacement between the base link 0 and link 1 at point o . There must also be two orthogonal reaction moments that prevent rotation of link 1 relative to the $x_1 - x_2$ plane of the \mathbb{X} frame. These forces and moments that act on link 1 are represented in terms of the basis for the \mathbb{X} frame, so they have the form

$$\mathbf{g} = g_1 \mathbf{x}_1 + g_2 \mathbf{x}_2 + g_3 \mathbf{x}_3,$$

$$\mathbf{n} = n_1 \mathbf{x}_1 + n_2 \mathbf{x}_2.$$

In addition to the forces and moments due to the joint constraints, an actuator is included in the robotic system to move the joint through its degree of freedom. In a revolute joint, the actuator will supply a torque along the joint axis. For joint 1, this torque \mathbf{t} is applied about the $\mathbf{x}_3 = \mathbf{a}_3$ axis, such that

$$\mathbf{t} = t_3 \mathbf{x}_3 = t_3 \mathbf{a}_3.$$

The revolute joint at point q allows only relative rotation between link 1 and link 2 about the $\mathbf{a}_2 = \mathbf{b}_2$ axis. There must be three orthogonal reaction forces that prevent relative displacement between these two bodies, and there must be two orthogonal reaction moments that constrain rotation relative to the plane perpendicular to the $\mathbf{a}_2 = \mathbf{b}_2$ axis. The constraint reaction forces \mathbf{f} and moments \mathbf{m} that act on link 1 at point q in terms of the basis for the \mathbb{A} frame are

$$\mathbf{f} = f_1 \mathbf{a}_1 + f_2 \mathbf{a}_2 + f_3 \mathbf{a}_3,$$

$$\mathbf{m} = m_1 \mathbf{a}_1 + m_3 \mathbf{a}_3.$$

A second actuator also controls the relative rotation between the inner arm and vertical column by supplying a second torque along the revolute joint 2 axis. For joint 2, this torque $\boldsymbol{\tau}$ is applied about the $\mathbf{a}_2 = \mathbf{b}_2$ axis and is given by

$$\boldsymbol{\tau} = \tau_2 \mathbf{a}_2 = \tau_2 \mathbf{b}_2.$$

By convention, free body diagrams are constructed from the terminal link to the base. Therefore, as shown in Figure (4.16b), the forces and moments for joint 2 are applied without modification to point q on link 2. However, the loading acting on link 1 due to joint 2 must have equal magnitude but opposite direction in relation to the loading acting on link 2 due to joint 2, as shown in Figure (4.16b). Figure (4.16b) also includes the loading on link 1 due to joint 1.

Example 4.5.2. Two solar arrays are to the base body of a satellite by two revolute joints, as shown in Figure (4.17). The frame \mathbb{C} is fixed in the base body of the satellite, and frames \mathbb{A} and \mathbb{B} are fixed in the solar arrays. Create *free body diagrams* of each body in this mechanical system.

Solution: For this example, all of the reaction forces and moments are represented in terms of the basis for the frame \mathbb{C} that is fixed in the core body. The revolute joint between bodies \mathbb{A} and \mathbb{C} prevents all relative motion except rotation about the $\mathbf{c}_1 = \mathbf{a}_1$ axis. The constraint forces and moments at this joint that act on the satellite body are shown in Figure (4.18b) and are given by

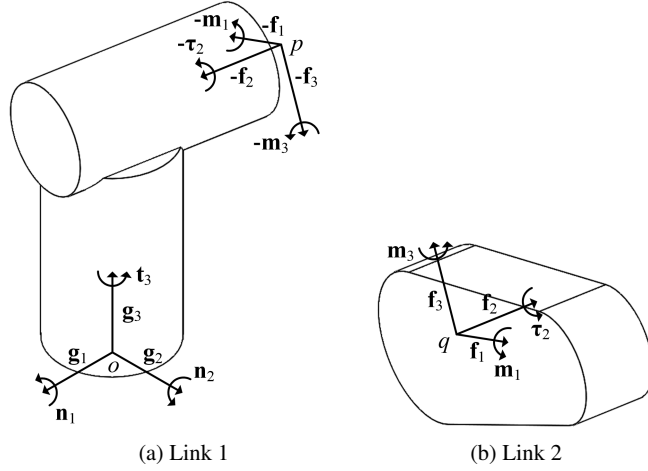


Fig. 4.16: Link Free Body Diagrams

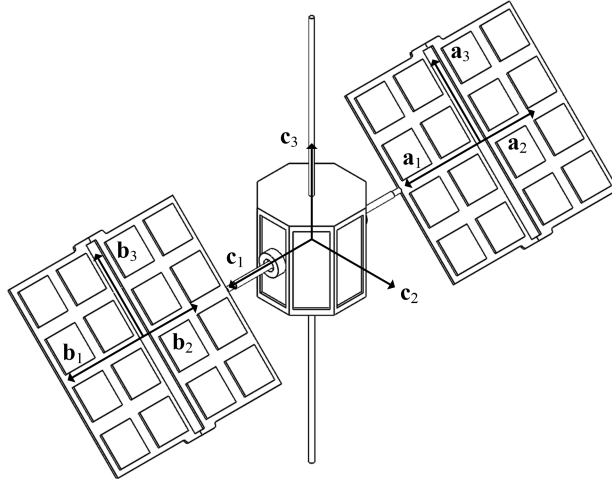


Fig. 4.17: Satellite with Two Solar Arrays

$$\mathbf{f} = f_1 \mathbf{c}_1 + f_2 \mathbf{c}_2 + f_3 \mathbf{c}_3,$$

$$\mathbf{m} = m_2 \mathbf{c}_2 + m_3 \mathbf{c}_3.$$

The actuation torque \mathbf{t} acts on the satellite body and drives the relative motion about the degree of freedom axis $\mathbf{c}_1 = \mathbf{a}_1$. It is written

$$\mathbf{t} = t_1 \mathbf{c}_1 = t_1 \mathbf{a}_1.$$

Similarly, the constraint forces and torques that act on the satellite body due to the solar array \mathbb{B} are expressed as

$$\begin{aligned}\mathbf{g} &= g_1\mathbf{c}_1 + g_2\mathbf{c}_2 + g_3\mathbf{c}_3, \\ \mathbf{n} &= n_2\mathbf{c}_2 + n_3\mathbf{c}_3.\end{aligned}$$

and the actuation moment that drives relative motion is

$$\boldsymbol{\tau} = \tau_1\mathbf{c}_1 = \tau_1\mathbf{b}_1.$$

These reaction forces and moments, as well as the actuation torque, are also depicted in Figure (4.18b).

For the free body diagram of the satellite body shown in Figure (4.18a), the loading equal and opposite to the loading applied on each solar panel array is applied on the satellite body at the shared point between each pairs of bodies.

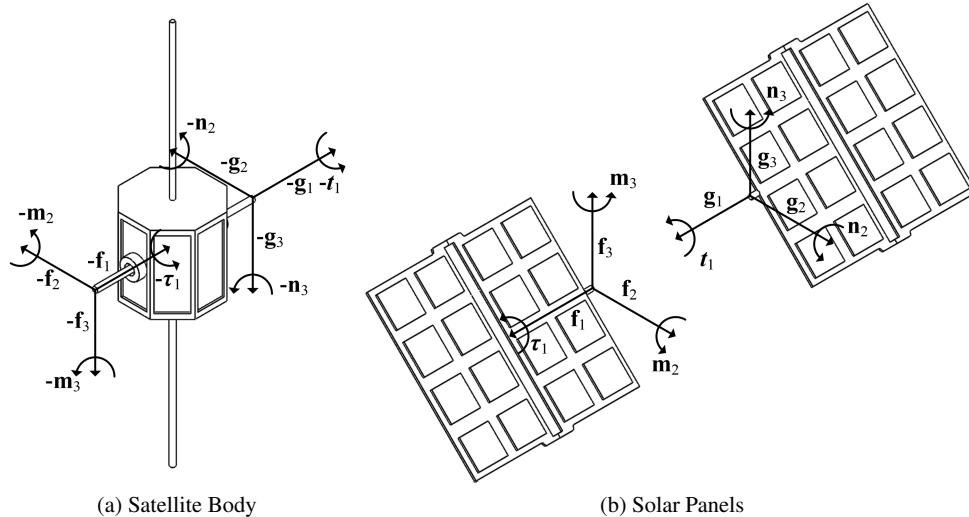


Fig. 4.18: Satellite Free Body Diagrams

The free body diagrams developed in Examples (4.5.1) and (4.5.2) are prototypical of those derived in a host of mechanical systems encountered in applications. Additional examples are considered in the problems at the end of this chapter. The goal in creating free body diagrams is to enable the determination of the equations of motion from Euler's First and Second Laws. The following examples use the free

body diagram to cast the equations of motion in simple case studies. In Example (4.5.3), the mass and inertia matrix that appear in Euler's Laws are assumed to be negligible, and the force and moment summations take a particularly simple form. We use this analysis to confirm that the composite joint satisfies Theorem (4.17).

Example 4.5.3. The composite joint shown in Figure (4.19) is constructed from a rectangular bar, collar and yoke which have body fixed frames A, B, and C, respectively. Relative displacement is allowed between the rectangular bar and the collar along the $\mathbf{a}_3 = \mathbf{b}_3$ axis, and relative rotation is allowed between the collar and yoke about the $\mathbf{c}_1 = \mathbf{b}_1$ axis. Create free body diagrams for the rectangular bar, collar and

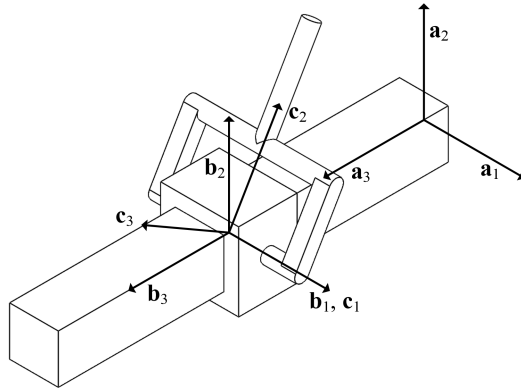


Fig. 4.19: Composite Joint, Prismatic and Revolute

yoke. If the collar shown in Figure (4.20b) has negligible mass and inertia, determine equivalent free body diagrams for the loading transmission directly between the rectangular bar and the yoke.

Solution: The revolute joint between the collar and yoke permits only relative rotation about the $\mathbf{c}_1 = \mathbf{b}_1$ axis, so there must be three perpendicular forces that restrain relative translation between these two bodies. There must also be two perpendicular moments acting between the two bodies that prevent relative rotation. The reaction forces \mathbf{f} and moments \mathbf{m} acting on the yoke are represented in terms of the basis for the C frame as

$$\begin{aligned}\mathbf{f} &= f_1\mathbf{c}_1 + f_2\mathbf{c}_2 + f_3\mathbf{c}_3, \\ \mathbf{m} &= m_2\mathbf{c}_2 + m_3\mathbf{c}_3.\end{aligned}$$

Equal and opposite reaction forces $-\mathbf{f}$ and moments $-\mathbf{m}$ act on the collar due to this joint.

The prismatic joint between the collar and the rectangular bar permits relative displacement along the $\mathbf{a}_3 = \mathbf{b}_3$ axis. There are two perpendicular forces that prevent

relative displacement orthogonal to the $\mathbf{a}_3 = \mathbf{b}_3$ axis, and there are three moments that act between the bodies to constrain relative rotation. The reaction forces and moments that act on the collar are denoted \mathbf{g} and \mathbf{n} , respectively, and are represented in terms of the basis for the \mathbb{B} frame as

$$\begin{aligned}\mathbf{g} &= g_1\mathbf{b}_1 + g_2\mathbf{b}_2, \\ \mathbf{n} &= n_1\mathbf{b}_1 + n_2\mathbf{b}_2 + n_3\mathbf{b}_3.\end{aligned}$$

Equal and opposite reaction forces $-\mathbf{g}$ and moments $-\mathbf{n}$ act on the rectangular bar due to this joint.

Figures (4.20a), (4.20b), and (4.21) illustrate the three free body diagrams for the yoke, collar and rectangular bar, respectively, that include the reaction forces and moments due to these two joints.

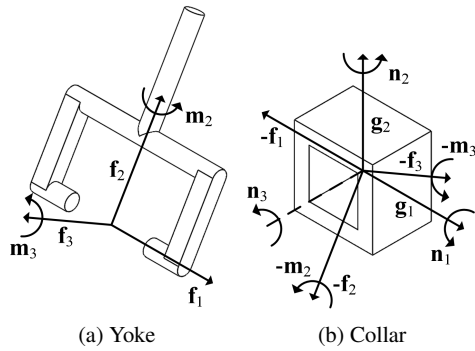


Fig. 4.20: Composite Joint Free Body Diagrams

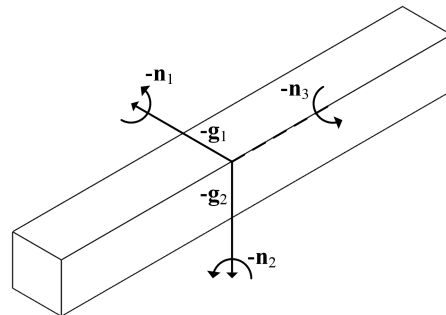


Fig. 4.21: Composite Joint Rectangular Bar Free Body Diagram

Next, the composite joint is analyzed assuming that the collar has negligible mass and inertia. Given that the collar has neither mass nor inertia, it is unnecessary to create a free body diagram for that component and to consider it as a purely geometric entity (instead of mechanical) that enforces the pair of joint constraints. The simplest approach for deriving the loading between these two bodies connected by a pair of ideal joints is to utilize a set of basis vectors that align with the two axes of the ideal joints. In this case, frame \mathbb{B} aligns with both the prismatic and revolute joints.

The prismatic joint does not permit a force along \mathbf{b}_3 , and the revolute joint does not permit a moment about \mathbf{b}_1 . The remaining four components of force and moment may be non-zero. As a result, the internal forces \mathbf{g} and moments \mathbf{n} acting on the yoke may be defined as

$$\begin{aligned}\mathbf{g} &= g_1 \mathbf{b}_1 + g_2 \mathbf{b}_2, \\ \mathbf{n} &= n_2 \mathbf{b}_2 + n_3 \mathbf{b}_3.\end{aligned}$$

As before, an equal and opposite reactive force $-\mathbf{g}$ and moment $-\mathbf{n}$ act on the rectangular bar.

Figures (4.22a) and (4.22b) illustrate the free body diagrams for the yoke and rectangular bar acting under the assumption that the dynamics of the collar may be ignored.

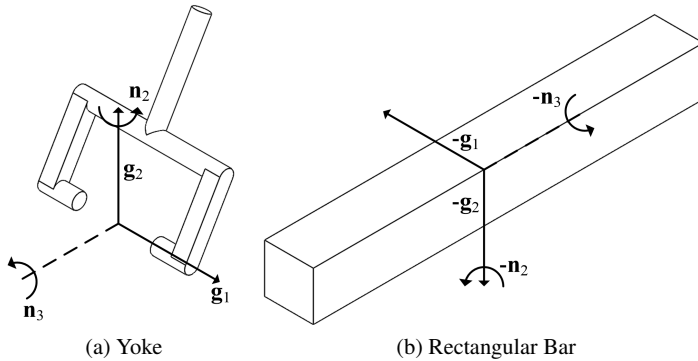


Fig. 4.22: Composite Joint Free Body Diagrams assuming Massless Collar

Example 4.5.4. The composite joint shown in Figure (4.23) is constructed from a cylindrical shaft, collar and yoke which have body fixed frames \mathbb{A} , \mathbb{B} , and \mathbb{C} , respectively. Relative displacement and rotation is allowed between the rectangular

bar and the collar along/about the $\mathbf{a}_3 = \mathbf{b}_3$ axis, and relative rotation is allowed between the collar and yoke about the $\mathbf{b}_1 = \mathbf{c}_1$ axis. Create free body diagrams for the

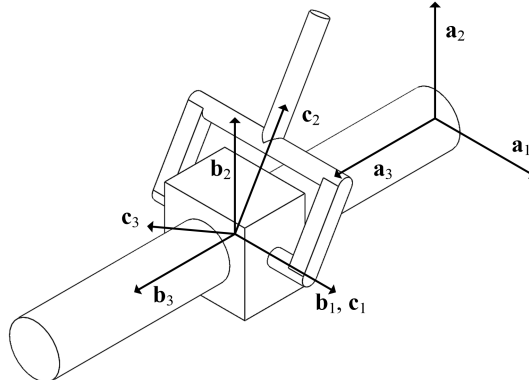


Fig. 4.23: Composite Joint, Cylindrical and Revolute

cylindrical rod, collar and yoke. If the collar shown in Figure (4.24b) has negligible mass and inertia, determine equivalent free body diagrams for the loading transmission directly between the cylindrical rod and the yoke.

Solution: As in Example (4.5.3), the revolute joint between the collar and yoke allows only relative rotation. There are consequently three perpendicular forces and two perpendicular moments acting between these two bodies. The reaction forces \mathbf{f} and moments \mathbf{m} acting on the yoke can be expressed in terms of the \mathbb{C} basis as

$$\begin{aligned}\mathbf{f} &= f_1 \mathbf{c}_1 + f_2 \mathbf{c}_2 + f_3 \mathbf{c}_3, \\ \mathbf{m} &= m_2 \mathbf{c}_2 + m_3 \mathbf{c}_3.\end{aligned}$$

The cylindrical joint between the cylindrical shaft and collar permits rotation about and translation along the $\mathbf{a}_3 = \mathbf{b}_3$ axis. It follows that there are two perpendicular reaction forces and two perpendicular reaction moments that act between these two bodies. The reaction forces \mathbf{g} and moments \mathbf{n} that act on the collar defined in terms of the basis for the \mathbb{B} frame are

$$\begin{aligned}\mathbf{g} &= g_1 \mathbf{b}_1 + g_2 \mathbf{b}_2, \\ \mathbf{n} &= n_1 \mathbf{b}_1 + n_2 \mathbf{b}_2.\end{aligned}$$

Figures (4.24a), (4.24b), and (4.25) illustrate the three free body diagrams for the yoke, collar and cylindrical rod, respectively, that include the reaction forces and moments due to these two joints. As before, the revolute joint loading is applied directly to the yoke, and the equal and opposite loading is applied to the collar. Likewise, the cylindrical joint loading is applied directly to the collar, and the equal and opposite loading is applied to the cylindrical rod.

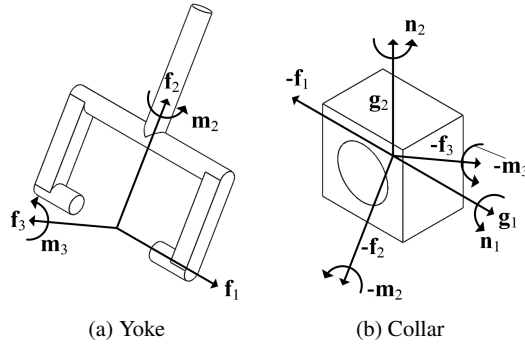


Fig. 4.24: Composite Joint Free Body Diagrams

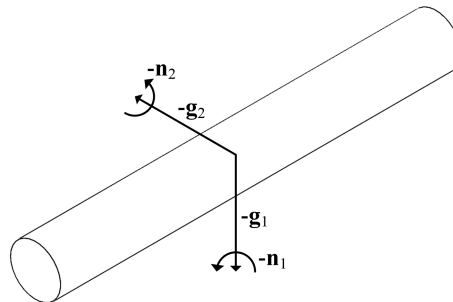


Fig. 4.25: Composite Joint Cylindrical Rod Free Body Diagram

Next, the composite joint is analyzed assuming that the collar has negligible mass and inertia. As before, a set of basis vectors aligning with the two joint axes will be utilized; in this case, \mathbb{B} aligns with both the cylindrical and revolute joints. The cylindrical joint does not permit a force along \mathbf{b}_3 or a moment about \mathbf{b}_3 , and the revolute joint does not permit a moment about \mathbf{b}_1 . The remaining three components of force and moment may be non-zero. As a result, the internal forces \mathbf{g} and moments \mathbf{n} acting on the yoke may be defined as

$$\begin{aligned}\mathbf{g} &= g_1 \mathbf{b}_1 + g_2 \mathbf{b}_2, \\ \mathbf{n} &= n_2 \mathbf{b}_2.\end{aligned}$$

Figures (4.26a) and (4.26b) illustrate the free body diagrams for the yoke and cylindrical rod acting under the assumption that the dynamics of the collar may be ignored. As before, the composite joint loading is applied directly to the yoke, and the equal and opposite loading is applied to the cylindrical rod.

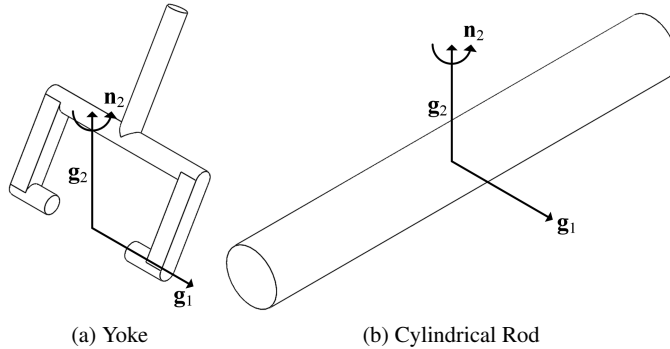


Fig. 4.26: Composite Joint Free Body Diagrams assuming Massless Collar

The last few examples have derived the appropriate free body diagrams that are associated with rigid bodies connected by ideal joints. Euler's First and Second Laws have been applied in the case where the mass and inertia matrix of one of the bodies are negligible; the resulting equations of motion resemble those obtained in elementary statics problems of engineering. The next two examples study robotic systems in three spatial dimensions. First, a single degree of freedom of motion is considered, followed by the generalization to the two degree of freedom case. The resulting equations of motion significantly increase in complexity as the number of degrees of freedom increase.

Example 4.5.5. This example studies the two link robot described in Example (4.5.1). In this example, revolute joint 1 between the base and vertical cylinder is fixed ($\theta_1 = \text{constant}$), and revolute joint 2 between the vertical cylinder and inner arm is allowed to rotate through angle θ_2 . Derive the equations of motion of the arm using Euler's First and Second Laws. The location of the mass centers in this system are depicted in Figure (4.27).

Solution: The free body diagram for the arm has already been constructed in Figure (4.16b). The acceleration of the center of mass of the arm is given by

$$\mathbf{a}_{X,c_2} = \mathbf{a}_{X,q} + \boldsymbol{\omega}_{X,B} \times (\boldsymbol{\omega}_{X,B} \times \mathbf{d}_{q,c_2}) + \boldsymbol{\alpha}_{X,B} \times \mathbf{d}_{q,c_2},$$

where in this problem $\mathbf{a}_{X,q} = 0$, $\boldsymbol{\omega}_{X,B} = \dot{\theta}_2 \mathbf{a}_2 = \dot{\theta}_2 \mathbf{b}_2$, $\boldsymbol{\alpha}_{X,B} = \ddot{\theta}_2 \mathbf{a}_2 = \ddot{\theta}_2 \mathbf{b}_2$, and $\mathbf{d}_{q,c_2} = x_{q,c_2} \mathbf{b}_1$ since θ_1 is a constant and the vertical column is held fixed. Note that one does not simply differentiate $\dot{\theta}_2$ in $\boldsymbol{\omega}_{X,B} = \dot{\theta}_1 \mathbf{a}_2$ to conclude that the angular acceleration $\boldsymbol{\alpha}_{X,B} = \ddot{\theta}_2 \mathbf{a}_2$. The definition of the angular acceleration and the Derivative Theorem in (2.12) in Chapter (2) should always be used to obtain the correct expression. For example, in this problem,

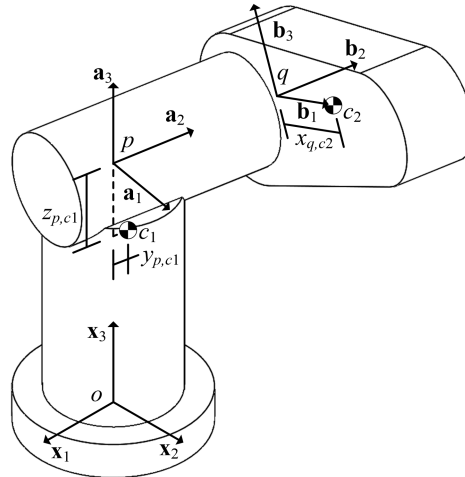


Fig. 4.27: Links 0 – 2 of PUMA Robotic Arm

$$\alpha_{\mathbb{X},\mathbb{B}} = \frac{d}{dt} \Big|_{\mathbb{X}} (\omega_{\mathbb{X},\mathbb{B}}) = \frac{d}{dt} \Big|_{\mathbb{B}} (\omega_{\mathbb{X},\mathbb{B}}) + \underbrace{\omega_{\mathbb{X},\mathbb{B}} \times \omega_{\mathbb{X},\mathbb{B}}}_{0} = \ddot{\theta}_2 \mathbf{b}_2.$$

However, in the next Example (4.5.6), it will be shown that it is not always the case that $\alpha_{\mathbb{X},\mathbb{B}}$ is “merely” a vector having magnitude equal to $\ddot{\theta}_{\mathbb{B}}$. Upon substitution, it can be seen that

$$\mathbf{a}_{\mathbb{X},c_2} = x_{q,c_2} \dot{\theta}_2^2 \mathbf{b}_1 - x_{q,c_2} \ddot{\theta}_2 \mathbf{b}_3.$$

Euler's First Law yields

$$M_2(x_{q,c_2} \dot{\theta}_2^2 \mathbf{b}_1 - x_{q,c_2} \ddot{\theta}_2 \mathbf{b}_3) = f_1 \mathbf{b}_1 + f_2 \mathbf{b}_2 + f_3 \mathbf{b}_3,$$

which can be rewritten as in terms of the components as

$$M_2 \begin{Bmatrix} x_{q,c_2} \dot{\theta}_2^2 \\ 0 \\ -x_{q,c_2} \ddot{\theta}_2 \end{Bmatrix} = \begin{Bmatrix} f_1 \\ f_2 \\ f_3 \end{Bmatrix}. \quad (4.5.1)$$

The $x_1 - x_3$ and $x_1 - x_2$ planes of the \mathbb{B} frame are planes of symmetry of the arm, so that the angular momentum in \mathbb{X} of the arm about its own center of mass is

$$\mathbf{h}_{\mathbb{X},c_2}^{\mathbb{B}} = \begin{bmatrix} I_{11} & 0 & 0 \\ 0 & I_{22} & 0 \\ 0 & 0 & I_{33} \end{bmatrix} \begin{Bmatrix} 0 \\ \dot{\theta}_2 \\ 0 \end{Bmatrix} = \begin{Bmatrix} 0 \\ I_{22} \dot{\theta}_2 \\ 0 \end{Bmatrix}.$$

Euler's Second Law can be written as

$$\frac{d}{dt} \Big|_{\mathbb{X}} (\mathbf{h}_{\mathbb{X},c_2}) = m_1 \mathbf{b}_1 + \tau_2 \mathbf{b}_2 + m_3 \mathbf{b}_3 + \mathbf{d}_{c_2,q} \times \mathbf{f}.$$

Since the cross product can be expanded as

$$\begin{aligned} \mathbf{d}_{c_2,q} \times \mathbf{f} &= \begin{vmatrix} \mathbf{b}_1 & \mathbf{b}_2 & \mathbf{b}_3 \\ -x_{q,c_2} & 0 & 0 \\ f_1 & f_2 & f_3 \end{vmatrix}, \\ &= x_{q,c_2} f_3 \mathbf{b}_2 - x_{q,c_2} f_2 \mathbf{b}_3, \end{aligned}$$

it is possible to use the Derivative Theorem in (2.12) in Chapter (2) to obtain

$$\left\{ \begin{array}{l} m_1 \\ \tau_2 + x_{q,c_2} f_3 \\ m_3 - x_{q,c_2} f_2 \end{array} \right\} = \underbrace{\left\{ \begin{array}{l} 0 \\ I_{22} \ddot{\theta}_2 \\ 0 \end{array} \right\}}_{\text{from } \frac{d}{dt} \Big|_{\mathbb{B}} (\mathbf{h}_{\mathbb{X},c_2})} + \underbrace{\left\{ \begin{array}{l} 0 \\ 0 \\ 0 \end{array} \right\}}_{\text{from } \boldsymbol{\omega}_{\mathbb{X},\mathbb{B}} \times \mathbf{h}_{\mathbb{X},c_2}} \quad (4.5.2)$$

The final system of governing equations for this problem include Equation (4.5.1) and (4.5.2). There is one set of three equations governing translation and one set of three equations governing rotation. The unknowns in these equations include θ_2 and its derivatives, as well as the reaction forces and torques f_1, f_2, f_3, m_1, m_3 . Note that there are exactly six equations and six unknowns in the final form of the governing equations. The variable θ_2 is known as a *differential unknown* since derivatives of this variable appear in the governing equations. The variables g_1, g_2, g_3, n_1, n_3 are known as *algebraic unknowns* because their derivatives do not appear in the governing equations.

Example 4.5.6. Derive the equations of motion for the two link robotic system shown in Figures (4.27), (4.16a) and (4.16b) and studied in Examples (4.5.1) and (4.5.5). In contrast to Example (4.5.5), both of the joint variables θ_1 and θ_2 are unknown in the discussion that follows.

Solution: First, the kinematics of the two links will be defined to facilitate calculation of the dynamic model during the link-by-link analysis. The rotation matrices between the three bodies are defined as

$$\mathbf{R}_{\mathbb{A}}^{\mathbb{X}} = \begin{bmatrix} \cos \theta_1 & -\sin \theta_1 & 0 \\ \sin \theta_1 & \cos \theta_1 & 0 \\ 0 & 0 & 1 \end{bmatrix} \quad \text{and} \quad \mathbf{R}_{\mathbb{B}}^{\mathbb{A}} = \begin{bmatrix} \cos \theta_2 & 0 & \sin \theta_2 \\ 0 & 1 & 0 \\ -\sin \theta_2 & 0 & \cos \theta_2 \end{bmatrix}.$$

Next, the angular velocities and accelerations between the links will be defined. The angular velocity of link 1 may be defined with respect to frame \mathbb{X} as

$$\boldsymbol{\omega}_{\mathbb{X},\mathbb{A}} = \dot{\theta}_1 \mathbf{x}_3 = \dot{\theta}_1 \mathbf{a}_3.$$

The angular velocity of link 2 is determined by the Addition Theorem in (2.15) in Chapter (3), so that

$$\begin{aligned}\boldsymbol{\omega}_{X,B} &= \boldsymbol{\omega}_{X,A} + \boldsymbol{\omega}_{A,B}, \\ &= \dot{\theta}_2 \mathbf{a}_2 + \dot{\theta}_1 \mathbf{a}_3.\end{aligned}$$

The angular acceleration of these bodies may be found by taking the derivative of these angular velocities with respect to the \mathbb{X} frame. For link 1, this results in

$$\boldsymbol{\alpha}_{X,A} = \frac{d}{dt} \Big|_{\mathbb{X}} (\boldsymbol{\omega}_{X,A}) = \ddot{\theta}_1 \mathbf{x}_3 = \ddot{\theta}_1 \mathbf{a}_3.$$

However, for the angular acceleration of link 2, the Derivative Theorem (2.12) of Chapter (2) must be used to reformulate the \mathbb{X} frame derivative in terms of frame \mathbb{A} ,

$$\begin{aligned}\boldsymbol{\alpha}_{X,B} &= \frac{d}{dt} \Big|_{\mathbb{X}} (\boldsymbol{\omega}_{X,B}) = \frac{d}{dt} \Big|_{\mathbb{A}} (\boldsymbol{\omega}_{X,B}) + \boldsymbol{\omega}_{X,A} \times \boldsymbol{\omega}_{X,B}, \\ &= -\dot{\theta}_1 \dot{\theta}_2 \mathbf{a}_1 + \ddot{\theta}_2 \mathbf{a}_2 + \ddot{\theta}_1 \mathbf{a}_3.\end{aligned}$$

As noted in the previous example, the angular acceleration is not generally the time derivative of the joint angle coefficients (as was the case in link 1); the Derivative Theorem also accounts for the time rate of change of the basis vectors as well.

Next, the velocities points c_1 and c_2 will be calculated. Within link 1, the Relative Velocity Theorem (2.16) will be used to calculate the velocities of points c_1 and q . (In the next step, the velocity of point q will be used to calculate the velocity of point c_2 .) For point c_1 ,

$$\begin{aligned}\mathbf{v}_{X,c_1} &= \underbrace{\mathbf{v}_{X,o}}_{=0} + \boldsymbol{\omega}_{X,A} \times \mathbf{d}_{o,c_1} = \dot{\theta}_1 \mathbf{a}_3 \times (y_{p,c_1} \mathbf{a}_2 + (d_{o,p} - z_{p,c_1}) \mathbf{a}_3), \\ &= -y_{p,c_1} \dot{\theta}_1 \mathbf{a}_1.\end{aligned}$$

Likewise, the velocity of point q is

$$\begin{aligned}\mathbf{v}_{X,q} &= \underbrace{\mathbf{v}_{X,o}}_{=0} + \boldsymbol{\omega}_{X,A} \times \mathbf{d}_{o,q} = \dot{\theta}_1 \mathbf{a}_3 \times (d_{p,q} \mathbf{a}_2 + d_{o,p} \mathbf{a}_3), \\ &= -d_{p,q} \dot{\theta}_1 \mathbf{a}_1.\end{aligned}$$

As points q and c_2 are both fixed on body 2, the relative velocity theorem may also be used to determine the velocity of point c_2 from the velocity of point q , such that

$$\begin{aligned}
\mathbf{v}_{\mathbb{X},c_2} &= \mathbf{v}_{\mathbb{X},q} + \boldsymbol{\omega}_{\mathbb{X},\mathbb{B}} \times \mathbf{d}_{q,c_2} = -d_{p,q}\dot{\theta}_1\mathbf{a}_1 + (\dot{\theta}_2\mathbf{a}_2 + \dot{\theta}_1\mathbf{a}_3) \times x_{q,c_2}\mathbf{b}_1, \\
&= -d_{p,q}\dot{\theta}_1\mathbf{a}_1 + (\dot{\theta}_2\mathbf{a}_2 + \dot{\theta}_1\mathbf{a}_3) \times (x_{q,c_2} \cos \theta_2 \mathbf{a}_1 - x_{q,c_2} \sin \theta_2 \mathbf{a}_3), \\
&= -d_{p,q}\dot{\theta}_1\mathbf{a}_1 + \begin{vmatrix} \mathbf{a}_1 & \mathbf{a}_2 & \mathbf{a}_3 \\ 0 & \dot{\theta}_2 & \dot{\theta}_1 \\ x_{q,c_2} \cos \theta_2 & 0 & -x_{q,c_2} \sin \theta_2 \end{vmatrix}, \\
&= (-d_{p,q}\dot{\theta}_1 - x_{q,c_2}\dot{\theta}_2 \sin \theta_2)\mathbf{a}_1 + x_{q,c_2}\dot{\theta}_1 \cos \theta_2 \mathbf{a}_2 - x_{q,c_2}\dot{\theta}_2 \cos \theta_2 \mathbf{a}_3.
\end{aligned}$$

Next, this kinematic analysis will be used to construct the equations of motion for links 1 and 2, starting with link 2. Based on the free body diagram of link 2 in Figure (4.16b), Euler's First Law for link 2 can be written as

$$f_1\mathbf{b}_1 + f_2\mathbf{b}_2 + f_3\mathbf{b}_3 = \frac{d}{dt} \Big|_{\mathbb{A}} (\mathbf{p}_{\mathbb{X}}) = M_2 \left(\frac{d}{dt} \Big|_{\mathbb{A}} (\mathbf{v}_{\mathbb{X},c_2}) + \boldsymbol{\omega}_{\mathbb{X},\mathbb{A}} \times \mathbf{v}_{\mathbb{X},c_2} \right),$$

where

$$\begin{aligned}
\frac{d}{dt} \Big|_{\mathbb{A}} (\mathbf{v}_{\mathbb{X},c_2}) &= (-d_{p,q}\ddot{\theta}_1 - x_{q,c_2}\ddot{\theta}_2 \sin \theta_2 - x_{q,c_2}\dot{\theta}_2^2 \cos \theta_2)\mathbf{a}_1 \\
&\quad + (x_{q,c_2}\ddot{\theta}_1 \cos \theta_2 - x_{q,c_2}\dot{\theta}_1\dot{\theta}_2 \sin \theta_2)\mathbf{a}_2 \\
&\quad - (x_{q,c_2}\ddot{\theta}_2 \cos \theta_2 - x_{q,c_2}\dot{\theta}_2^2 \sin \theta_2)\mathbf{a}_3
\end{aligned}$$

and

$$\begin{aligned}
\boldsymbol{\omega}_{\mathbb{X},\mathbb{A}} \times \mathbf{v}_{\mathbb{X},c_2} &= \begin{vmatrix} \mathbf{a}_1 & \mathbf{a}_2 & \mathbf{a}_3 \\ 0 & 0 & \dot{\theta}_1 \\ (-d_{p,q}\dot{\theta}_1 - x_{q,c_2}\dot{\theta}_2 \sin \theta_2) & x_{q,c_2}\dot{\theta}_1 \cos \theta_2 - x_{q,c_2}\dot{\theta}_2 \cos \theta_2 \\ & \end{vmatrix}, \\
&= -x_{q,c_2}\dot{\theta}_1^2 \cos \theta_2 \mathbf{a}_1 + (-d_{p,q}\dot{\theta}_1^2 - x_{q,c_2}\dot{\theta}_1\dot{\theta}_2 \sin \theta_2)\mathbf{a}_2.
\end{aligned}$$

Combining these expressions into a single equation results in

$$\begin{bmatrix} \cos \theta_2 & 0 & -\sin \theta_2 \\ 0 & 1 & 0 \\ \sin \theta_2 & 0 & \cos \theta_2 \end{bmatrix} \begin{Bmatrix} f_1 \\ f_2 \\ f_3 \end{Bmatrix} = \begin{Bmatrix} -M_2 d_{p,q}\ddot{\theta}_1 - M_2 x_{q,c_2}\ddot{\theta}_2 \sin \theta_2 - M_2 x_{q,c_2}(\dot{\theta}_1^2 + \dot{\theta}_2^2) \cos \theta_2 \\ -M_2 d_{p,q}\dot{\theta}_1^2 + M_2 x_{q,c_2}\dot{\theta}_1 \cos \theta_2 - 2M_2 x_{q,c_2}\dot{\theta}_1\dot{\theta}_2 \sin \theta_2 \\ -M_2 x_{q,c_2}\dot{\theta}_2 \cos \theta_2 + x_{q,c_2}\dot{\theta}_2^2 \sin \theta_2 \end{Bmatrix}. \quad (4.5.3)$$

Despite it being link 2 being under consideration, because the simplest representation of $\mathbf{v}_{\mathbb{X},c_2}$ is with respect to the \mathbb{A} frame, the equation of motion is analyzed with respect to this frame. When evaluating this vector equation, either these components will need to be mapped into the \mathbb{B} frame to match the force components, or the force components will need to be mapped into the \mathbb{A} frame.

Euler's Second Law applied to link 2 results in

$$\frac{d}{dt} \Big|_{\mathbb{A}} (\mathbf{h}_{\mathbb{X},c_2}) = m_1\mathbf{b}_1 + \tau_2\mathbf{b}_2 + m_3\mathbf{b}_3 + \mathbf{d}_{c_2,q} \times (f_1\mathbf{b}_1 + f_2\mathbf{b}_2 + f_3\mathbf{b}_3).$$

The left hand side may be solved by utilizing the Derivative Theorem to formulate the derivative in terms of the \mathbb{B} frame, and utilizing the angular momentum repre-

sentation $\mathbf{h}_{\mathbb{X},c_2}^{\mathbb{B}}$,

$$\begin{aligned}\frac{d}{dt}\Big|_{\mathbb{X}}(\mathbf{h}_{\mathbb{X},c_2}) &= \frac{d}{dt}\Big|_{\mathbb{B}}(\mathbf{h}_{\mathbb{X},c_2}) + \boldsymbol{\omega}_{\mathbb{X},\mathbb{B}} \times \mathbf{h}_{\mathbb{X},c_2}, \\ \frac{d}{dt}\Big|_{\mathbb{X}}(\mathbf{h}_{\mathbb{X},c_2}^{\mathbb{B}}) &= \frac{d}{dt}\Big|_{\mathbb{B}}(\mathbf{I}_{c_2}^{\mathbb{B}} \boldsymbol{\omega}_{\mathbb{X},\mathbb{B}}^{\mathbb{B}}) + \boldsymbol{\omega}_{\mathbb{X},\mathbb{B}}^{\mathbb{B}} \times \mathbf{I}_{c_2}^{\mathbb{B}} \boldsymbol{\omega}_{\mathbb{X},\mathbb{B}}^{\mathbb{B}}, \\ &= \mathbf{I}_{c_2}^{\mathbb{B}} \boldsymbol{\alpha}_{\mathbb{X},\mathbb{B}}^{\mathbb{B}} + \boldsymbol{\omega}_{\mathbb{X},\mathbb{B}}^{\mathbb{B}} \times \mathbf{I}_{c_2}^{\mathbb{B}} \boldsymbol{\omega}_{\mathbb{X},\mathbb{B}}^{\mathbb{B}}.\end{aligned}$$

The angular velocity $\boldsymbol{\omega}_{\mathbb{X},\mathbb{B}}^{\mathbb{B}}$ may be determined from the formulation of $\boldsymbol{\omega}_{\mathbb{X},\mathbb{B}}$ above using a change of basis,

$$\boldsymbol{\omega}_{\mathbb{X},\mathbb{B}}^{\mathbb{B}} = \mathbf{R}_{\mathbb{A}}^{\mathbb{B}} \boldsymbol{\omega}_{\mathbb{X},\mathbb{B}}^{\mathbb{A}} = \begin{bmatrix} \cos \theta_2 & 0 & -\sin \theta_2 \\ 0 & 1 & 0 \\ \sin \theta_2 & 0 & \cos \theta_2 \end{bmatrix} \begin{Bmatrix} 0 \\ \dot{\theta}_2 \\ \dot{\theta}_1 \end{Bmatrix} = \begin{Bmatrix} -\dot{\theta}_1 \sin \theta_2 \\ \dot{\theta}_2 \\ \dot{\theta}_1 \cos \theta_2 \end{Bmatrix}.$$

By a similar transformation, $\boldsymbol{\alpha}_{\mathbb{X},\mathbb{B}}^{\mathbb{B}}$ may be determined to be

$$\boldsymbol{\alpha}_{\mathbb{X},\mathbb{B}}^{\mathbb{B}} = \begin{Bmatrix} -\dot{\theta}_1 \dot{\theta}_2 \cos \theta_2 - \ddot{\theta}_1 \sin \theta_2 \\ \ddot{\theta}_2 \\ -\dot{\theta}_1 \dot{\theta}_2 \sin \theta_2 + \ddot{\theta}_1 \cos \theta_2 \end{Bmatrix}.$$

The load acting on link 2 may be evaluated by noting that $\mathbf{d}_{c_2,q} = -x_{q,c_2} \mathbf{b}_1$, resulting in

$$\begin{aligned}m_1 \mathbf{b}_1 + \tau_2 \mathbf{b}_2 + m_3 \mathbf{b}_3 + \mathbf{d}_{c_2,q} \times (f_1 \mathbf{b}_1 + f_2 \mathbf{b}_2 + f_3 \mathbf{b}_3), \\ = m_1 \mathbf{b}_1 + \tau_2 \mathbf{b}_2 + m_3 \mathbf{b}_3 - x_{q,c_2} \mathbf{b}_1 \times (f_1 \mathbf{b}_1 + f_2 \mathbf{b}_2 + f_3 \mathbf{b}_3), \\ = m_1 \mathbf{b}_1 + (\tau_2 + x_{q,c_2} f_3) \mathbf{b}_2 + (m_3 - x_{q,c_2} f_2) \mathbf{b}_3.\end{aligned}$$

Representing Euler's Second Law for link 2 with respect to the \mathbb{B} frame results in

$$\begin{aligned}\begin{bmatrix} I_{11} & 0 & 0 \\ 0 & I_{22} & 0 \\ 0 & 0 & I_{33} \end{bmatrix} \begin{Bmatrix} -\dot{\theta}_1 \dot{\theta}_2 \cos \theta_2 - \ddot{\theta}_1 \sin \theta_2 \\ \ddot{\theta}_2 \\ -\dot{\theta}_1 \dot{\theta}_2 \sin \theta_2 + \ddot{\theta}_1 \cos \theta_2 \end{Bmatrix} \\ + \begin{bmatrix} 0 & -\dot{\theta}_1 \cos \theta_2 & \dot{\theta}_2 \\ \dot{\theta}_1 \cos \theta_2 & 0 & \dot{\theta}_1 \sin \theta_2 \\ -\dot{\theta}_2 & -\dot{\theta}_1 \sin \theta_2 & 0 \end{bmatrix} \begin{Bmatrix} -I_{11} \dot{\theta}_1 \sin \theta_2 \\ I_{22} \dot{\theta}_2 \\ I_{33} \dot{\theta}_1 \cos \theta_2 \end{Bmatrix} = \begin{Bmatrix} m_1 \\ \tau_2 + x_{q,c_2} f_3 \\ m_3 - x_{q,c_2} f_2 \end{Bmatrix},\end{aligned}$$

or

$$\begin{Bmatrix} I_{11}(-\dot{\theta}_1 \dot{\theta}_2 \cos \theta_2 - \ddot{\theta}_1 \sin \theta_2) + (I_{33} - I_{22}) \dot{\theta}_1 \dot{\theta}_2 \cos \theta_2 \\ I_{22} \dot{\theta}_2 + (I_{33} - I_{11}) \dot{\theta}_1^2 \sin \theta_2 \cos \theta_2 \\ I_{33}(-\dot{\theta}_1 \dot{\theta}_2 \sin \theta_2 + \ddot{\theta}_1 \cos \theta_2) + (I_{11} - I_{22}) \dot{\theta}_1 \dot{\theta}_2 \sin \theta_2 \end{Bmatrix} = \begin{Bmatrix} m_1 \\ \tau_2 + x_{q,c_2} f_3 \\ m_3 - x_{q,c_2} f_2 \end{Bmatrix}. \quad (4.5.4)$$

Next, the equations of motion for link 1 will be calculated. Based on the free body diagram of link 1 in Figure (4.16a), Euler's First Law for link 1 can be written as

$$\begin{aligned} g_1\mathbf{a}_1 + g_2\mathbf{a}_2 + g_3\mathbf{a}_3 - f_1\mathbf{b}_1 - f_2\mathbf{b}_2 - f_3\mathbf{b}_3 &= \frac{d}{dt}\Big|_{\mathbb{X}}(\mathbf{p}_{\mathbb{X}}), \\ &= M_1\left(\frac{d}{dt}\Big|_{\mathbb{A}}(\mathbf{v}_{\mathbb{X},c_1}) + \boldsymbol{\omega}_{\mathbb{X},\mathbb{A}} \times \mathbf{v}_{\mathbb{X},c_1}\right), \end{aligned}$$

where

$$\frac{d}{dt}\Big|_{\mathbb{A}}(\mathbf{v}_{\mathbb{X},c_1}) = -y_{p,c_1}\ddot{\theta}_1\mathbf{a}_1$$

and

$$\boldsymbol{\omega}_{\mathbb{X},\mathbb{A}} \times \mathbf{v}_{\mathbb{X},c_1} = \begin{vmatrix} \mathbf{a}_1 & \mathbf{a}_2 & \mathbf{a}_3 \\ 0 & 0 & \dot{\theta}_1 \\ -y_{p,c_1}\dot{\theta}_1 & 0 & 0 \end{vmatrix} = -y_{p,c_1}\dot{\theta}_1^2\mathbf{a}_2.$$

Representing Euler's First Law for link 1 with respect to the \mathbb{A} frame results in

$$\begin{Bmatrix} g_1 \\ g_2 \\ t_3 \end{Bmatrix} - \begin{Bmatrix} \cos\theta_2 & 0 & \sin\theta_2 \\ 0 & 1 & 0 \\ -\sin\theta_2 & 0 & \cos\theta_2 \end{Bmatrix} \begin{Bmatrix} f_1 \\ f_2 \\ f_3 \end{Bmatrix} = M_1 \begin{Bmatrix} -y_{p,c_1}\ddot{\theta}_1 \\ -y_{p,c_1}\dot{\theta}_1^2 \\ 0 \end{Bmatrix}. \quad (4.5.5)$$

Euler's Second Law applied to link 2 results in

$$\frac{d}{dt}\Big|_{\mathbb{X}}(\mathbf{h}_{\mathbb{X},c_1}) = \left(-m_1\mathbf{b}_1 - \tau_2\mathbf{b}_2 - m_3\mathbf{b}_3 - \mathbf{d}_{c_1,q} \times (f_1\mathbf{b}_1 + f_2\mathbf{b}_2 + f_3\mathbf{b}_3) \right. \\ \left. + n_1\mathbf{a}_1 + n_2\mathbf{a}_2 + t_3\mathbf{a}_3 + \mathbf{d}_{c_1,o} \times (g_1\mathbf{b}_1 + g_2\mathbf{b}_2 + g_3\mathbf{b}_3) \right).$$

As before, the left hand side may be solved by utilizing the Derivative Theorem to formulate the derivative in terms of the \mathbb{A} frame and utilizing the angular momentum representation $\mathbf{h}_{\mathbb{X},c_1}^{\mathbb{A}}$ in

$$\begin{aligned} \frac{d}{dt}\Big|_{\mathbb{X}}(\mathbf{h}_{\mathbb{X},c_1}) &= \frac{d}{dt}\Big|_{\mathbb{A}}(\mathbf{h}_{\mathbb{X},c_1}) + \boldsymbol{\omega}_{\mathbb{X},\mathbb{A}} \times \mathbf{h}_{\mathbb{X},c_1}, \\ \frac{d}{dt}\Big|_{\mathbb{X}}(\mathbf{h}_{\mathbb{X},c_1}^{\mathbb{A}}) &= \frac{d}{dt}\Big|_{\mathbb{A}}(\mathbf{I}_{c_1}^{\mathbb{A}} \boldsymbol{\omega}_{\mathbb{X},\mathbb{A}}^{\mathbb{A}}) + \boldsymbol{\omega}_{\mathbb{X},\mathbb{A}}^{\mathbb{A}} \times \mathbf{I}_{c_1}^{\mathbb{A}} \boldsymbol{\omega}_{\mathbb{X},\mathbb{A}}^{\mathbb{A}}, \\ &= \mathbf{I}_{c_1}^{\mathbb{A}} \boldsymbol{\alpha}_{\mathbb{X},\mathbb{A}}^{\mathbb{A}} + \boldsymbol{\omega}_{\mathbb{X},\mathbb{A}}^{\mathbb{A}} \times \mathbf{I}_{c_1}^{\mathbb{A}} \boldsymbol{\omega}_{\mathbb{X},\mathbb{A}}^{\mathbb{A}}. \end{aligned}$$

The angular velocity $\boldsymbol{\omega}_{\mathbb{X},\mathbb{A}}^{\mathbb{A}}$ and acceleration $\boldsymbol{\alpha}_{\mathbb{X},\mathbb{A}}^{\mathbb{A}}$ may be determined from the formulations of $\boldsymbol{\omega}_{\mathbb{X},\mathbb{A}}$ and $\boldsymbol{\alpha}_{\mathbb{X},\mathbb{A}}$ above, with

$$\boldsymbol{\omega}_{\mathbb{X},\mathbb{A}}^{\mathbb{A}} = \begin{Bmatrix} 0 \\ 0 \\ \dot{\theta}_1 \end{Bmatrix} \quad \text{and} \quad \boldsymbol{\alpha}_{\mathbb{X},\mathbb{A}}^{\mathbb{A}} = \begin{Bmatrix} 0 \\ 0 \\ \ddot{\theta}_1 \end{Bmatrix}.$$

In addition, for the inertia matrix, because there is only a single plane of symmetry, the (2,3) and (3,2) entries of the inertia matrix will be non-zero. It follows that

$$\begin{aligned} \mathbf{I}_{c_1}^{\mathbb{A}} \boldsymbol{\alpha}_{\mathbb{X}, \mathbb{A}}^{\mathbb{A}} + \boldsymbol{\omega}_{\mathbb{X}, \mathbb{A}}^{\mathbb{A}} \times \mathbf{I}_{c_1}^{\mathbb{A}} \boldsymbol{\omega}_{\mathbb{X}, \mathbb{A}}^{\mathbb{A}} &= \begin{bmatrix} K_{11} & 0 & 0 \\ 0 & K_{22} & K_{23} \\ 0 & K_{32} & K_{33} \end{bmatrix} \begin{Bmatrix} 0 \\ 0 \\ \ddot{\theta}_1 \end{Bmatrix} + \begin{Bmatrix} 0 \\ 0 \\ \dot{\theta}_1 \end{Bmatrix} \times \begin{bmatrix} K_{11} & 0 & 0 \\ 0 & K_{22} & K_{23} \\ 0 & K_{32} & K_{33} \end{bmatrix} \begin{Bmatrix} 0 \\ 0 \\ \ddot{\theta}_1 \end{Bmatrix}, \\ &= \begin{Bmatrix} 0 \\ K_{23}\ddot{\theta}_1 \\ K_{33}\ddot{\theta}_1 \end{Bmatrix} + \begin{Bmatrix} 0 \\ 0 \\ \dot{\theta}_1 \end{Bmatrix} \times \begin{Bmatrix} 0 \\ K_{23}\dot{\theta}_1 \\ K_{33}\dot{\theta}_1 \end{Bmatrix} = \begin{Bmatrix} 0 \\ K_{23}\ddot{\theta}_1 \\ K_{33}\ddot{\theta}_1 - K_{23}\dot{\theta}_1^2 \end{Bmatrix}. \end{aligned}$$

The load acting on link 2 may be evaluated by representing it in terms of frame \mathbb{A} . Noting that $\mathbf{d}_{c_1, q} = (d_{p,q} - y_{p,c_1})\mathbf{a}_2 + z_{p,c_1}\mathbf{a}_3$ and $\mathbf{d}_{c_1, o} = -y_{p,c_1}\mathbf{a}_2 - (d_{o,p} - z_{p,c_1})\mathbf{a}_3$, it is written as

$$\begin{aligned} &- \begin{bmatrix} \cos\theta_2 & 0 & \sin\theta_2 \\ 0 & 1 & 0 \\ -\sin\theta_2 & 0 & \cos\theta_2 \end{bmatrix} \begin{Bmatrix} m_1 \\ \tau_2 \\ m_3 \end{Bmatrix} - \begin{Bmatrix} 0 \\ d_{p,q} - y_{p,c_1} \\ z_{p,c_1} \end{Bmatrix} \times \begin{bmatrix} \cos\theta_2 & 0 & \sin\theta_2 \\ 0 & 1 & 0 \\ -\sin\theta_2 & 0 & \cos\theta_2 \end{bmatrix} \begin{Bmatrix} f_1 \\ f_2 \\ f_3 \end{Bmatrix} \\ &+ \begin{Bmatrix} n_1 \\ n_2 \\ t_3 \end{Bmatrix} + \begin{Bmatrix} 0 \\ -y_{p,c_1} \\ -(d_{o,p} - z_{p,c_1}) \end{Bmatrix} \times \begin{Bmatrix} g_1 \\ g_2 \\ g_3 \end{Bmatrix}, \\ &= - \begin{Bmatrix} m_1 \cos\theta_2 + m_3 \sin\theta_2 \\ \tau_2 \\ -m_1 \sin\theta_2 + m_3 \cos\theta_2 \end{Bmatrix} - \begin{Bmatrix} 0 \\ d_{p,q} - y_{p,c_1} \\ z_{p,c_1} \end{Bmatrix} \times \begin{Bmatrix} f_1 \cos\theta_2 - f_3 \sin\theta_2 \\ f_2 \\ f_1 \sin\theta_2 + f_3 \cos\theta_2 \end{Bmatrix} \\ &+ \begin{Bmatrix} n_1 \\ n_2 \\ t_3 \end{Bmatrix} + \begin{Bmatrix} 0 \\ -y_{p,c_1} \\ -(d_{o,p} - z_{p,c_1}) \end{Bmatrix} \times \begin{Bmatrix} g_1 \\ g_2 \\ g_3 \end{Bmatrix}, \\ &= - \begin{Bmatrix} m_1 \cos\theta_2 + m_3 \sin\theta_2 + (d_{p,q} - y_{p,c_1})(f_1 \sin\theta_2 + f_3 \cos\theta_2) - z_{p,c_1}f_2 \\ \tau_2 + z_{p,c_1}(f_1 \cos\theta_2 - f_3 \sin\theta_2) \\ -m_1 \sin\theta_2 + m_3 \cos\theta_2 - (d_{p,q} - y_{p,c_1})(f_1 \cos\theta_2 - f_3 \sin\theta_2) \end{Bmatrix} \\ &+ \begin{Bmatrix} n_1 - y_{p,c_1}g_3 + (d_{o,p} - z_{p,c_1})g_2 \\ n_2 - (d_{o,p} - z_{p,c_1})g_1 \\ t_3 + y_{p,c_1}g_1 \end{Bmatrix}. \end{aligned}$$

Combining the angular momentum derivative and loading into Euler's Second Law for link 1 results in

$$\begin{Bmatrix} 0 \\ K_{23}\ddot{\theta}_1 \\ K_{33}\ddot{\theta}_1 - K_{23}\dot{\theta}_1^2 \end{Bmatrix} = - \begin{Bmatrix} m_1 \cos\theta_2 + m_3 \sin\theta_2 + (d_{p,q} - y_{p,c_1})(f_1 \sin\theta_2 + f_3 \cos\theta_2) - z_{p,c_1}f_2 \\ \tau_2 + z_{p,c_1}(f_1 \cos\theta_2 - f_3 \sin\theta_2) \\ -m_1 \sin\theta_2 + m_3 \cos\theta_2 - (d_{p,q} - y_{p,c_1})(f_1 \cos\theta_2 - f_3 \sin\theta_2) \end{Bmatrix} \\ + \begin{Bmatrix} n_1 - y_{p,c_1}g_3 + (d_{o,p} - z_{p,c_1})g_2 \\ n_2 - (d_{o,p} - z_{p,c_1})g_1 \\ t_3 + y_{p,c_1}g_1 \end{Bmatrix}. \quad (4.5.6)$$

In summary, the complete set of governing equations for this example includes Equations (4.5.3), (4.5.4), (4.5.5) and (4.5.6). There is one set of three equations governing translation and one set of three equations governing rotation for each body. The unknowns in these equations include the geometric variables θ_1, θ_2 and their derivatives, and the forces and moments $f_1, f_2, f_3, g_1, g_2, g_3, m_1, m_2, n_1, n_3$. Thus

there are twelve unknowns and twelve equations in this problem. As in the last example, θ_1 and θ_2 are *differential unknowns* and the constraint forces and torques are *algebraic unknowns*.

The equations of motion for mechanical systems in realistic problems with three dimensional kinematics can be quite complicated in form. The next example studies another two link robotic system. Because of the symmetry of the bodies with respect to the selected frames of reference, and the restriction of motion so that only θ_2 varies, the equations of motion take a familiar form in Example (4.5.7).

Example 4.5.7. The inner arm (link 1) of the SCARA robot shown in Figure (4.28) is locked in place relative to the base, and the outer arm (link 2) is articulated through the angle θ_2 . Derive the equations of motion for the outer arm using Euler's First and Second Laws.

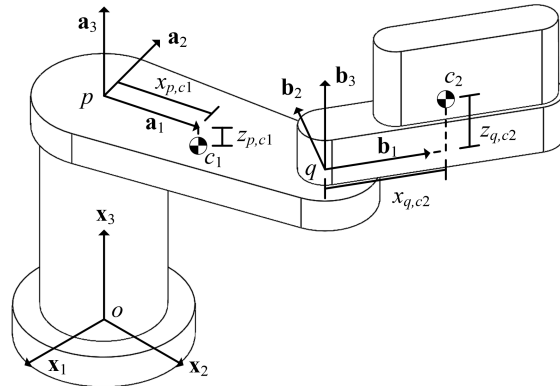


Fig. 4.28: Links 0 – 2 of a SCARA Robotic Arm

Solution: First, three frames \mathbb{X} , \mathbb{A} , and \mathbb{B} are defined at points o , p , and q , respectively, as shown in Figure (4.28). Frame \mathbb{X} is the inertial frame, frame \mathbb{A} is fixed in the inner arm, and frame \mathbb{B} is fixed in the outer arm. The vertical column is denoted link 0, the inner arm is link 1 and the outer arm is link 2 in this example. The location of the center of mass of the outer arm is defined as

$$\mathbf{r}_{\mathbb{B},c} = x_{q,c2} \mathbf{b}_1 + z_{q,c2} \mathbf{b}_3$$

in terms of the body fixed basis. The inertia matrix $\mathbf{I}_c^{\mathbb{B}}$ with respect to a frame that has its origin at the center of mass and that is parallel to the \mathbb{B} frame is

$$\mathbf{I}_c^{\mathbb{B}} = \begin{bmatrix} I_{11} & 0 & I_{13} \\ 0 & I_{22} & 0 \\ I_{13} & 0 & I_{33} \end{bmatrix}.$$

Since the $1 - 3$ plane of the \mathbb{B} frame is a plane of symmetry for the outer arm, it is known that $I_{12} = I_{23} = 0$. The acceleration of the center of mass of the outer arm in the inertial frame is given by

$$\begin{aligned} \mathbf{a}_{\mathbb{X},c} &= \mathbf{a}_{\mathbb{X},q} + \boldsymbol{\omega}_{\mathbb{X},\mathbb{B}} \times (\boldsymbol{\omega}_{\mathbb{X},\mathbb{B}} \times \mathbf{d}_{q,c_2}) + \boldsymbol{\alpha}_{\mathbb{X},\mathbb{B}} \times \mathbf{d}_{q,c_2}, \\ &= \mathbf{0} - x_{q,c_2} \dot{\theta}_2^2 \mathbf{b}_1 + x_{q,c_2} \ddot{\theta}_2 \mathbf{b}_2, \end{aligned}$$

when θ_1 is constant. A free body diagram of the outer arm is depicted in Figure (4.29). Euler's First Law yields the components relative to the \mathbb{B} frame

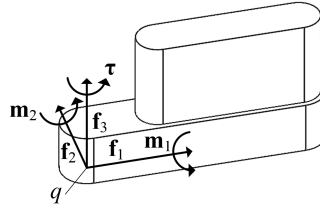


Fig. 4.29: Free Body Diagram of the Outer Arm

$$\begin{Bmatrix} f_1 \\ f_2 \\ f_3 \end{Bmatrix} = M_2 \begin{Bmatrix} -x_{q,c_2} \dot{\theta}_2^2 \\ x_{q,c_2} \ddot{\theta}_2 \\ 0 \end{Bmatrix}. \quad (4.5.7)$$

Euler's Second Law is written $\mathbf{m}_c = \frac{d}{dt}|_{\mathbb{X}}(\mathbf{h}_{\mathbb{X},c})$, and the applied moment about the center of mass is given by

$$\mathbf{m}_c = m_1 \mathbf{b}_1 + m_2 \mathbf{b}_2 + \tau \mathbf{b}_3 + \begin{vmatrix} \mathbf{b}_1 & \mathbf{b}_2 & \mathbf{b}_3 \\ -x_{q,c_2} & 0 & -z_{q,c_2} \\ f_1 & f_2 & f_3 \end{vmatrix}.$$

The angular momentum about the center of mass is

$$\mathbf{h}_{\mathbb{X},c}^{\mathbb{B}} = \begin{bmatrix} I_{11} & 0 & I_{13} \\ 0 & I_{22} & 0 \\ I_{13} & 0 & I_{33} \end{bmatrix} \begin{Bmatrix} 0 \\ 0 \\ \dot{\theta}_2 \end{Bmatrix} = \begin{Bmatrix} I_{13}\dot{\theta}_2 \\ 0 \\ I_{33}\dot{\theta}_2 \end{Bmatrix}$$

since $\boldsymbol{\omega}_{\mathbb{X},\mathbb{B}} = \dot{\theta}_2 \mathbf{b}_3$ when the inner arm is stationary. The Derivative Theorem from Chapter (2) is used to simplify the calculation in Euler's Second Law. The moment \mathbf{m}_c is

$$\mathbf{m}_c = \frac{d}{dt} \Big|_{\mathbb{X}} (\mathbf{h}_{\mathbb{X},c}) = \frac{d}{dt} \Big|_{\mathbb{B}} (\mathbf{h}_{\mathbb{X},c}) + \boldsymbol{\omega}_{\mathbb{X},\mathbb{B}} \times \mathbf{h}_{\mathbb{X},c}.$$

Combination of the moment equations above yields

$$\begin{Bmatrix} m_1 + z_{q,c_3} f_2 \\ m_2 - z_{q,c_3} f_1 + x_{q,c_3} f_3 \\ \tau - x_{q,c_3} f_2 \end{Bmatrix} = \begin{Bmatrix} I_{13}\ddot{\theta}_2 \\ 0 \\ I_{33}\ddot{\theta}_2 \end{Bmatrix} + \begin{Bmatrix} 0 \\ I_{13}\dot{\theta}_2^2 \\ 0 \end{Bmatrix}. \quad (4.5.8)$$

In summary, a complete set of governing equations is obtained by collecting the six Equations (4.5.7) and (4.5.8) to solve for the six unknowns. These unknowns include the angle θ_2 and its derivatives, and the reaction forces and moments f_1, f_2, f_3, m_1 and m_2 .

The equations of motion derived in Example (4.5.7) assumed a particularly simple form due to symmetry and the fact that there is but a single degree of freedom. In general, however, the equations of motion can be quite complex. In this next example it is shown that by allowing the joint variable θ_1 in Example (4.5.7) to vary in time as an unknown, the resulting equations of motion for the system again become increasingly more complicated.

Example 4.5.8. Consider again the SCARA robot studied in Example (4.5.7). In this example, derive the equations of motion for the two degrees of freedom system, where θ_1 and θ_2 vary in time.

Solution: First, the outer arm, link 2, will be considered. Note the changes to the governing equations from Example (4.5.7) when both θ_1 and θ_2 vary with time. The angular velocity of the \mathbb{B} frame in the \mathbb{X} frame is now given by

$$\boldsymbol{\omega}_{\mathbb{X},\mathbb{B}} = \boldsymbol{\omega}_{\mathbb{X},\mathbb{A}} + \boldsymbol{\omega}_{\mathbb{A},\mathbb{B}} = (\dot{\theta}_1 + \dot{\theta}_2)\mathbf{b}_3.$$

The form of the angular acceleration follows from this definition and the application of the Derivative Theorem

$$\boldsymbol{\alpha}_{\mathbb{X},\mathbb{B}} = \frac{d}{dt} \Big|_{\mathbb{X}} (\boldsymbol{\omega}_{\mathbb{X},\mathbb{B}}) = \frac{d}{dt} \Big|_{\mathbb{B}} (\boldsymbol{\omega}_{\mathbb{X},\mathbb{B}}) + \underbrace{\boldsymbol{\omega}_{\mathbb{X},\mathbb{B}} \times \boldsymbol{\omega}_{\mathbb{X},\mathbb{B}}}_{0} = (\ddot{\theta}_1 + \ddot{\theta}_2)\mathbf{b}_3 n$$

The acceleration of the center of mass of the outer arm is now given by

$$\begin{aligned} \mathbf{a}_{\mathbb{X},c_2} &= \mathbf{a}_{\mathbb{X},q} + \boldsymbol{\omega}_{\mathbb{X},\mathbb{B}} \times (\boldsymbol{\omega}_{\mathbb{X},\mathbb{B}} \times \mathbf{d}_{q,c_2}) + \boldsymbol{\alpha}_{\mathbb{X},\mathbb{B}} \times \mathbf{d}_{q,c_2}, \\ &= \underbrace{-d_{p,q}\dot{\theta}_1^2 \mathbf{a}_1 + d_{p,q}\dot{\theta}_1 \mathbf{a}_2 - x_{q,c_2}(\dot{\theta}_1 + \dot{\theta}_2)^2 \mathbf{b}_1}_{\mathbf{a}_{\mathbb{X},q}} + x_{q,c_2}(\dot{\theta}_1 + \dot{\theta}_2)\mathbf{b}_2. \end{aligned}$$

The force summation for the free body diagram depicted in Figure (4.29) yields the equations

$$\begin{aligned} \begin{Bmatrix} f_1 \\ f_2 \\ f_3 \end{Bmatrix} &= M_2 \left(\begin{Bmatrix} -x_{q,c_2}(\dot{\theta}_1 + \dot{\theta}_2)^2 \\ x_{q,c_2}(\dot{\theta}_1 + \dot{\theta}_2) \\ 0 \end{Bmatrix} + \mathbf{R}_{\mathbb{A}}^{\mathbb{B}} \begin{Bmatrix} -d_{p,q}\dot{\theta}_1^2 \\ d_{p,q}\dot{\theta}_1 \\ 0 \end{Bmatrix} \right), \quad (4.5.9) \\ &= M_2 \left(\begin{Bmatrix} -x_{q,c_2}(\dot{\theta}_1 + \dot{\theta}_2)^2 \\ x_{q,c_2}(\dot{\theta}_1 + \dot{\theta}_2) \\ 0 \end{Bmatrix} + \begin{bmatrix} \cos\theta_2 & \sin\theta_2 & 0 \\ -\sin\theta_2 & \cos\theta_2 & 0 \\ 0 & 0 & 1 \end{bmatrix} \begin{Bmatrix} -d_{p,q}\dot{\theta}_1^2 \\ d_{p,q}\dot{\theta}_1 \\ 0 \end{Bmatrix} \right). \end{aligned}$$

The angular momentum of the outer arm about its own center of mass becomes

$$\mathbf{h}_{\mathbb{X},c_2}^{\mathbb{B}} = \begin{bmatrix} I_{11} & 0 & I_{13} \\ 0 & I_{22} & 0 \\ I_{13} & 0 & I_{33} \end{bmatrix} \begin{Bmatrix} 0 \\ 0 \\ \dot{\theta}_1 + \dot{\theta}_2 \end{Bmatrix} = \begin{Bmatrix} I_{13}(\dot{\theta}_1 + \dot{\theta}_2) \\ 0 \\ I_{33}(\dot{\theta}_1 + \dot{\theta}_2) \end{Bmatrix}.$$

The moment summation is now given by

$$\begin{Bmatrix} m_1 + z_{q,c_2}f_2 \\ m_2 - z_{q,c_2}f_1 + x_{q,c_2} \\ \tau - x_{q,c_2}f_2 \end{Bmatrix} = \begin{Bmatrix} I_{13}(\ddot{\theta}_1 + \ddot{\theta}_2) \\ 0 \\ I_{33}(\ddot{\theta}_1 + \ddot{\theta}_2) \end{Bmatrix} + \begin{Bmatrix} 0 \\ I_{13}(\dot{\theta}_1 + \dot{\theta}_2)^2 \\ 0 \end{Bmatrix}. \quad (4.5.10)$$

The free body diagram of the inner arm is shown in Figure (4.30). The accelera-

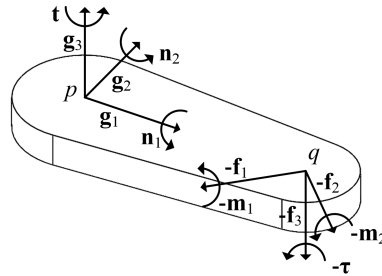


Fig. 4.30: Free Body Diagram of Inner Arm

tion of the center of mass of the inner arm is given by

$$\mathbf{a}_{\mathbb{X},c_1} = \underbrace{\mathbf{a}_{\mathbb{X},p}}_0 - x_{p,c_1}\dot{\theta}_1^2 \mathbf{a}_1 + x_{p,c_1}\dot{\theta}_1 \mathbf{a}_2,$$

and the angular momentum about the center of mass is given by

$$\mathbf{h}_{\mathbb{X},c_1}^{\mathbb{A}} = \begin{bmatrix} K_{11} & 0 & K_{13} \\ 0 & K_{22} & 0 \\ K_{13} & 0 & K_{33} \end{bmatrix} \begin{Bmatrix} 0 \\ 0 \\ \dot{\theta}_1 \end{Bmatrix} = \begin{Bmatrix} K_{13}\dot{\theta}_1 \\ 0 \\ K_{33}\dot{\theta}_1 \end{Bmatrix}.$$

The force summation for the free body diagram shown in Figure (4.30) yields

$$\begin{Bmatrix} g_1 \\ g_2 \\ g_3 \end{Bmatrix} + \mathbf{R}_{\mathbb{B}}^{\mathbb{A}} \begin{Bmatrix} -f_1 \\ -f_2 \\ -f_3 \end{Bmatrix} = M_1 \begin{Bmatrix} -x_{p,c_1} \dot{\theta}_1^2 \\ x_{p,c_1} \ddot{\theta}_1 \\ 0 \end{Bmatrix},$$

or

$$\begin{Bmatrix} g_1 \\ g_2 \\ g_3 \end{Bmatrix} + \begin{bmatrix} \cos \theta_2 & -\sin \theta_2 & 0 \\ \sin \theta_2 & \cos \theta_2 & 0 \\ 0 & 0 & 1 \end{bmatrix} \begin{Bmatrix} -f_1 \\ -f_2 \\ -f_3 \end{Bmatrix} = M_1 \begin{Bmatrix} -x_{p,c_1} \dot{\theta}_1^2 \\ x_{p,c_1} \ddot{\theta}_1 \\ 0 \end{Bmatrix}. \quad (4.5.11)$$

The applied moments about the center of mass can be computed from the expression

$$\begin{aligned} \mathbf{m}_{c_1} &= n_1 \mathbf{a}_1 + n_2 \mathbf{a}_2 + t \mathbf{a}_3 - m_1 \mathbf{b}_1 - m_2 \mathbf{b}_2 - \tau \mathbf{b}_3 \\ &+ \begin{vmatrix} \mathbf{a}_1 & \mathbf{a}_2 & \mathbf{a}_3 \\ -x_{p,c_1} & 0 & z_{p,c_1} \\ g_1 & g_2 & g_3 \end{vmatrix} + ((d_{p,q} - x_{p,c_1}) \mathbf{a}_1 + z_{p,c_1} \mathbf{a}_3) \times (-f_1 \mathbf{b}_1 - f_2 \mathbf{b}_2 - f_3 \mathbf{b}_3). \end{aligned}$$

This expression may be simplified and written in terms of frame \mathbb{A} as

$$\begin{aligned} \mathbf{m}_{c_1}^{\mathbb{A}} &= \begin{Bmatrix} n_1 - z_{p,c_1} g_2 \\ n_2 + z_{p,c_1} g_1 + x_{p,c_1} g_3 \\ t - x_{p,c_1} g_2 \end{Bmatrix} + \mathbf{R}_{\mathbb{B}}^{\mathbb{A}} \begin{Bmatrix} -m_1 + z_{p,c_1} f_2 + (d_{p,q} - x_{p,c_1}) f_3 \sin \theta_2 \\ -m_2 - z_{p,c_1} f_1 + (d_{p,q} - x_{p,c_1}) f_3 \cos \theta_2 \\ -\tau - (d_{p,q} - x_{p,c_1}) f_1 \sin \theta_2 - (d_{p,q} - x_{p,c_1}) f_2 \cos \theta_2 \end{Bmatrix}, \\ &= \begin{Bmatrix} n_1 - z_{p,c_1} g_2 \\ n_2 + z_{p,c_1} g_1 + x_{p,c_1} g_3 \\ t - x_{p,c_1} g_2 \end{Bmatrix} \quad (4.5.12) \end{aligned}$$

$$+ \begin{bmatrix} \cos \theta_2 & -\sin \theta_2 & 0 \\ \sin \theta_2 & \cos \theta_2 & 0 \\ 0 & 0 & 1 \end{bmatrix} \begin{Bmatrix} -m_1 + z_{p,c_1} f_2 + (d_{p,q} - x_{p,c_1}) f_3 \sin \theta_2 \\ -m_2 - z_{p,c_1} f_1 + (d_{p,q} - x_{p,c_1}) f_3 \cos \theta_2 \\ -\tau - (d_{p,q} - x_{p,c_1}) f_1 \sin \theta_2 - (d_{p,q} - x_{p,c_1}) f_2 \cos \theta_2 \end{Bmatrix}. \quad (4.5.13)$$

The moment summation for the free body diagram in Figure (4.30) is consequently

$$\mathbf{m}_{c_1}^{\mathbb{A}} = \begin{Bmatrix} K_{13} \ddot{\theta}_1 \\ 0 \\ K_{33} \ddot{\theta}_1 \end{Bmatrix} + \begin{Bmatrix} 0 \\ K_{13} \dot{\theta}_1^2 \\ 0 \end{Bmatrix} \quad (4.5.14)$$

where $\mathbf{m}_{c_1}^{\mathbb{A}}$ is given in Equation (4.5.12).

The final system of governing equations for this example includes Equations (4.5.9), (4.5.10), (4.5.11) and (4.5.14). There is one set of three equations governing translation for each body, and there is one set of three equation governing rotation for each body. The *differential unknowns* in the governing equations include θ_1, θ_2 and their derivatives. The *algebraic unknowns* are the reaction forces and torques $f_1, f_2, f_3, g_1, g_2, g_3, n_1, n_2, m_1, m_2$. There are a total of 12 unknowns and 12 equations.



4.6 Structure of Governing Equations: Newton-Euler Formulations

Examples (4.5.5), (4.5.6), (4.5.7) and (4.5.8) demonstrate that the system of equations obtained via the application of Euler's First and Second Law to robotics applications is unavoidably complicated. An essential step in the study of Newton-Euler formulations casts the derived equations into one of a few possible canonical mathematical forms. This step is important from a theoretical standpoint since in many cases analysts have developed a theory that can be consulted to study existence, uniqueness, or stability of solutions for general classes of problems. From a practical viewpoint, once the equations are written in a standard form, it is possible to employ common and well-understood numerical techniques for their study. While there are many possible structural forms in which the governing equations can be cast, two standard forms will be considered in this book. The equations of motion will be written as a system of *differential-algebraic equations* or *DAEs*, or as a set of *ordinary differential equations* or *ODEs*.

4.6.1 Differential-Algebraic Equations (DAEs)

There are two types of variables that appear in the governing equations in Newton-Euler formulations of dynamics, as shown in Examples (4.5.5), (4.5.6), (4.5.7) and (4.5.8). One set of variables are explicitly differentiated with respect to time, while others are not. The subset of variables that are differentiated with respect to time are referred to as *differential unknowns*, while those that are not differentiated are known as *algebraic unknowns*. A collection of equations that couples both types of variables constitutes a system of *differential-algebraic equations*, or *DAEs*. The form of DAEs that will be used in this text have the structure

$$\begin{aligned}\dot{\mathbf{x}}(t) &= \mathbf{f}(t, \mathbf{x}(t), \mathbf{y}(t)), \\ \mathbf{0} &= \mathbf{g}(t, \mathbf{x}(t), \mathbf{y}(t)),\end{aligned}\tag{4.6.1}$$

where $\mathbf{x}(t) \in \mathbb{R}^N$ is the collections of differential variables, $\mathbf{y}(t) \in \mathbb{R}^M$ is the collection of algebraic variables, the function $\mathbf{f} : \mathbb{R}^+ \times \mathbb{R}^N \times \mathbb{R}^M \rightarrow \mathbb{R}^N$ and $\mathbf{g} : \mathbb{R}^+ \times \mathbb{R}^N \times \mathbb{R}^M \rightarrow \mathbb{R}^M$. There are a total of $N \times M$ variables in the above $N \times M$ equations. It is straightforward to express the equations derived via Newton-Euler methods in this form, as shown in the next examples.

Example 4.6.1. Write the governing equations in Example (4.5.5) as a set of DAEs that have the structure shown in Equation (4.6.1).

Solution: The unknown variables that appear in Equations (4.5.1) and (4.6.1) are θ_2 , f_1 , f_2 , f_3 , m_1 , and m_3 . Define the differential variables and algebraic variables

as, respectively,

$$\mathbf{x} = \begin{Bmatrix} x_1 & x_2 \end{Bmatrix}^T = \begin{Bmatrix} \theta_2 & \dot{\theta}_2 \end{Bmatrix}^T, \\ \mathbf{y} = \begin{Bmatrix} y_1 & y_2 & y_3 & y_4 & y_5 \end{Bmatrix}^T = \begin{Bmatrix} f_1 & f_2 & f_3 & m_1 & m_3 \end{Bmatrix}^T.$$

The differential subset of equations becomes

$$\dot{\mathbf{x}} = \begin{Bmatrix} \dot{x}_1 \\ \dot{x}_2 \end{Bmatrix} = \mathbf{f}(t, \mathbf{x}, \mathbf{y}) = \begin{Bmatrix} x_2 \\ \frac{1}{I_{22}}(\tau_2 + x_{q,c_2}y_3) \end{Bmatrix} \quad (4.6.2)$$

The algebraic subset of equations is

$$\begin{Bmatrix} 0 \\ 0 \\ 0 \\ 0 \\ 0 \end{Bmatrix} = \mathbf{g}(t, \mathbf{x}, \mathbf{y}) = \begin{Bmatrix} y_1 - M_2 x_{q,c_2} x_2^2 \\ y_2 \\ y_3 + M_2 x_{q,c_2} \frac{1}{I_{22}} (\tau_2 + x_{q,c_2} y_3) \\ y_4 \\ y_5 - x_{q,c_2} y_2 \end{Bmatrix} \quad (4.6.3)$$

With the functions $\mathbf{f} : \mathbb{R}^+ \times \mathbb{R}^2 \times \mathbb{R}^5 \rightarrow \mathbb{R}^2$ and $\mathbf{g} : \mathbb{R}^+ \times \mathbb{R}^2 \times \mathbb{R}^5 \rightarrow \mathbb{R}^5$ defined in Equations (4.6.2) and (4.6.3), the governing equations have the form of the DAEs in Equation (4.6.1).

Example 4.6.2. Write the governing equations in Example (4.5.7) as a set of DAEs that have the structure shown in Equation (4.5.8).

Solution: The unknown variables that appear in Equations (4.5.7) and (4.5.8) are θ_2 , f_1 , f_2 , f_3 , m_1 , and m_2 . Define the differential and algebraic variables as, respectively,

$$\mathbf{x} = \begin{Bmatrix} x_1 & x_2 \end{Bmatrix}^T = \begin{Bmatrix} \theta_2 & \dot{\theta}_2 \end{Bmatrix}^T, \\ \mathbf{y} = \begin{Bmatrix} y_1 & y_2 & y_3 & y_4 & y_5 \end{Bmatrix}^T = \begin{Bmatrix} f_1 & f_2 & f_3 & m_1 & m_2 \end{Bmatrix}^T.$$

The subset of differential equations becomes

$$\dot{\mathbf{x}} = \begin{Bmatrix} \dot{x}_1 \\ \dot{x}_2 \end{Bmatrix} = \mathbf{f}(t, \mathbf{x}(t), \mathbf{y}(t)) = \begin{Bmatrix} x_2 \\ \frac{1}{M_2 x_{q,c_2}} y_2 \end{Bmatrix}.$$

The subset of algebraic equations is

$$\begin{pmatrix} 0 \\ 0 \\ 0 \\ 0 \\ 0 \end{pmatrix} = \mathbf{g}(t, \mathbf{x}(t), \mathbf{y}(t)) = \begin{pmatrix} y_1 + M_2 x_{q,c_2} x_2^2 \\ y_3 \\ y_4 + z_{q,c_2} y_2 - I_{13} \frac{1}{M_2 x_{q,c_2}} y_2 \\ y_5 - z_{q,c_2} y_1 + x_{q,c_2} y_3 - I_{13} x_2^2 \\ \tau - x_{q,c_2} y_2 - I_{33} \frac{1}{M_2 x_{q,c_2}} y_2 \end{pmatrix}.$$

With the functions $\mathbf{f} : \mathbb{R}^+ \times \mathbb{R}^2 \times \mathbb{R}^5 \rightarrow \mathbb{R}^2$ and $\mathbf{g} : \mathbb{R}^+ \times \mathbb{R}^2 \times \mathbb{R}^5 \rightarrow \mathbb{R}^5$ defined in Equations (4.6.2) and (4.6.3), the governing equations have the form of the DAEs in Equation (4.6.1).

4.6.2 Ordinary Differential Equations (ODEs)

In most applications of Newton-Euler formulations to realistic robotic systems, the resulting equations contain both differential and algebraic variables. As discussed in the last section, it is natural to study these systems as a collection of DAEs. Still, it is most common in the literature to eliminate the algebraic unknowns via algebraic manipulation. There are technical conditions, expressed in terms of the Jacobian of the algebraic constraint equations in Equation (4.6.1), that guarantee that it is possible to solve the last M equations in (4.6.1) for the algebraic unknowns \mathbf{y} in terms of (t, \mathbf{x}) . The expressions for \mathbf{y} in terms of (t, \mathbf{x}) can then be substituted into the first line of Equation (4.6.1), thereby eliminating the algebraic unknowns. The interested reader should consult [27] or [2] for the complete description. When this procedure is feasible, the resulting form of the governing equations is a collection *ordinary differential equations* or *ODEs* of the form

$$\dot{\mathbf{x}}(t) = \mathbf{f}(t, \mathbf{x}(t)) \quad (4.6.4)$$

where $\mathbf{x}(t) \in \mathbb{R}^N$ and $\mathbf{f} : \mathbb{R}^+ \times \mathbb{R}^N \rightarrow \mathbb{R}^N$. It must be emphasized that although the procedure discussed above to reformulate a set of DAEs in the form of Equation (4.6.1) into Equation (4.6.4) is easy to describe in principle, it can be difficult to achieve in practice. This is certainly the case for complex robotic systems. Despite the difficulty of the task, there are several reasons that motivate the attempt:

(1) Order Reduction: For any system, the number of $N + M$ DAEs is always larger than the reduced number of N ODEs. The difference in complexity can be substantial for robotic systems. In fact, most of the unknowns in a kinematic chain are associated with the algebraic variables. If it is desired to construct a feedback law that must be updated in real-time, the cost in estimation of the solution of a set of DAEs can be prohibitive. For example, for an L link kinematic chain having one degree of freedom at each joint, $N \approx 2L$ and $M \approx 5L$.

(2) Theoretical Foundations: The study of ODEs and their numerical approximation is much more mature than the corresponding state of affairs for DAEs. The

study of DAEs is continuously evolving. Furthermore, the current theoretical framework for DAEs is more difficult to state and has more restrictions on its applicability. Broad statements about the existence, stability, convergence and stability of DAEs are less common. Again, references [2], [27] can be consulted for advanced presentations.

(3) Control Theoretic Issues: It has already been noted in (1) above that the computational cost associated with the numerical solution of DAEs can be prohibitive in control applications. Just as importantly, nearly all of the supporting theory and algorithms for the control of robotic systems has been derived for systems of ordinary differential or discrete difference equations. This body of research is impressive and represents decades of research and development. The study of the control of DAEs does not have as mature a theoretical and computational infrastructure.

The next two examples illustrate how the algebraic unknowns can be eliminated for relatively simple problems.

Example 4.6.3. Obtain a governing ordinary differential equation from the differential-algebraic equations in Example (4.5.5) by eliminating the algebraic unknowns.

Solution: The formulation of the differential-algebraic equations for Example (4.5.5) presented in Example (4.6.1) will be used to obtain the desired ordinary differential equation form. The second differential equation in this example states

$$I_{22}\ddot{\theta}_2 = \tau_2 + x_{q,c_2}y_3. \quad (4.6.5)$$

The desired ordinary differential equation is obtained by eliminating the algebraic variable y_3 from this equation. This can be done by considering the sole algebraic equation with y_3 as a factor,

$$0 = y_3 + M_2x_{q,c_2}\ddot{\theta}_2,$$

Combining these two equations results in

$$(I_{22} + M_2x_{q,c_2}^2)\ddot{\theta}_2 = \tau_2.$$

This equation is the familiar equation in terms of the moment of inertia about the 2 axis through point q . The moment of inertia about the 2 axis through point q is given by the Parallel Axis Theorem

$$I_{22,q} = I_{22} + M_2x_{q,c_2}^2,$$

and the final form of the governing equation is

$$I_{22,q}\ddot{\theta}_2 = \tau_2.$$

Example 4.6.4. Obtain a governing ordinary differential equation from the differential-algebraic equations in Example (4.5.7) by eliminating the algebraic unknowns.

Solution: Combining the equations from the second row in the Equation (4.5.7) and the third row of Equation (4.5.8) results in

$$(I_{33} + M_2 x_{q,c_2}^2) \ddot{\theta}_2 = \tau$$

for the rotational equation of motion about the vertical axis. This equation can be written in a simpler form by observing that the Parallel Axis Theorem states that

$$I_{33,p} = I_{33} + M_2 x_{q,c_2}^2,$$

where $I_{33,p}$ is the moment of inertia about the 3 axis passing through point p . As a result,

$$I_{33,p} \ddot{\theta}_2 = \tau$$

is the moment equation about this axis.

4.7 Recursive Newton-Euler Formulations

4.7.1 Recursive Calculation of Forces and Moments

In Chapter (3) recursive algorithms for determining velocities and derivatives of velocities have been derived for the kinematic chain depicted in Figure (3.19) or Figure (3.20). The joints are numbered from N to 1 starting at the joint nearest the base body and decreasing toward the tip. The recursive algorithms developed in Sections (3.4.1) and (3.4.3) start with the joint connected to the base body, and then solve for velocities or derivatives of velocities as we move from inboard to outboard joints.

This section will show that the calculation of joint forces and torques can be carried out starting at joint 1 toward the tip of the kinematic chain and proceeding inward toward the base. As in the study of velocities and accelerations, a recursive method is possible because of the special structures of the matrices that relates joint forces and torques, acceleration, and angular acceleration. The reason that the recursion in this section progresses from tip to base is because the coefficient matrix in Theorem (4.18) is exactly equal to the transpose of the coefficient matrix that appears in either Theorem (3.4) or Theorem (3.5). The following theorem summarizes this matrix equation.

Theorem 4.18. The forces and moments in \mathcal{F}_k^- for the kinematics chain depicted in Figure (3.19) and Figure (3.20) satisfy the equation

$$\begin{Bmatrix} \mathcal{F}_1^- \\ \mathcal{F}_2^- \\ \mathcal{F}_3^- \\ \vdots \\ \mathcal{F}_{N-1}^- \\ \mathcal{F}_N^- \end{Bmatrix} = \begin{bmatrix} 0 & 0 & 0 \dots & 0 & 0 \\ \varphi_{2,1}\mathcal{R}_{2,1} & 0 & 0 \dots & 0 & 0 \\ 0 & \varphi_{3,2}\mathcal{R}_{3,2} & 0 \dots & 0 & 0 \\ \vdots & \vdots & \vdots \ddots & \vdots & \vdots \\ 0 & 0 & 0 \dots & 0 & 0 \\ 0 & 0 & 0 \dots & \varphi_{N,N-1}\mathcal{R}_{N,N-1} & 0 \end{bmatrix} \begin{Bmatrix} \mathcal{F}_1^- \\ \mathcal{F}_2^- \\ \mathcal{F}_3^- \\ \vdots \\ \mathcal{F}_{N-1}^- \\ \mathcal{F}_N^- \end{Bmatrix} \quad (4.7.1)$$

$$+ \begin{bmatrix} M_1 & 0 & 0 \dots & 0 & 0 \\ 0 & M_2 & 0 \dots & 0 & 0 \\ 0 & 0 & M_3 \dots & 0 & 0 \\ \vdots & \vdots & \vdots \ddots & \vdots & \vdots \\ 0 & 0 & 0 \dots & M_{N-1} & 0 \\ 0 & 0 & 0 \dots & 0 & M_N \end{bmatrix} \begin{Bmatrix} \mathcal{A}_1^- \\ \mathcal{A}_2^- \\ \mathcal{A}_3^- \\ \vdots \\ \mathcal{A}_{N-1}^- \\ \mathcal{A}_N^- \end{Bmatrix} + \begin{Bmatrix} \mathcal{P}_1 \\ \mathcal{P}_2 \\ \mathcal{P}_3 \\ \vdots \\ \mathcal{P}_{N-1} \\ \mathcal{P}_N \end{Bmatrix} \quad (4.7.2)$$

where $\varphi_{k,k-1}$ is given in Equation (4.7.5), \mathcal{F}_k^- is defined in Equation (4.7.5), \mathcal{A}_k^- is defined in Equation (4.7.6), M_k is given in Equation (4.7.11), and \mathcal{P}_k is given in Equation (4.7.12) for $k = 1, \dots, N$.

Proof. Recall that in this convention the links of the kinematic chain are numbered from the outer most body to the root or base body b . The acceleration in the base frame of the center of mass c_k of body k is given by

$$\mathbf{a}_{b,c_k} = \mathbf{a}_{b,k} + \boldsymbol{\alpha}_{b,k} \times \mathbf{d}_{k,c_k} + \boldsymbol{\omega}_{b,k} \times (\boldsymbol{\omega}_{b,k} \times \mathbf{d}_{k,c_k}),$$

where $\mathbf{a}_{b,k}$ is the acceleration in the base frame of the origin of frame k , $\boldsymbol{\alpha}_{b,k}$ is the angular acceleration in the base frame of frame k , $\boldsymbol{\omega}_{b,k}$ is the angular velocity in the base frame of frame k , and \mathbf{d}_{k,c_k} is the vector from the origin of frame k to the center of mass c_k of link k . Applying Euler's First Law to body k as shown in Figure (4.31)

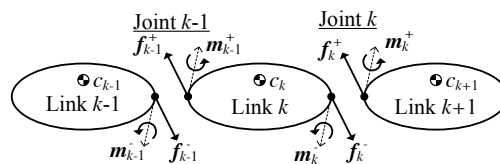


Fig. 4.31: Joint Loading Convention

results in

$$\mathbf{f}_k^- + \mathbf{f}_{k-1}^+ = M_k(\mathbf{a}_{b,k} + \boldsymbol{\alpha}_{b,k} \times \mathbf{d}_{k,c_k} \times \boldsymbol{\omega}_{b,k} \times (\boldsymbol{\omega}_{b,k} \times \mathbf{d}_{k,c_k})). \quad (4.7.3)$$

For Euler's Second Law, the form given in Theorem (4.15) in which moments acting on body k are summed about point k^- ,

$$\sum \mathbf{m} = \frac{d}{dt} \Big|_b (\mathbf{I}_k \boldsymbol{\omega}_{b,k^-}) + \mathbf{d}_{k,c} \times M_k \mathbf{a}_{b,k^-},$$

is used to obtain the equation

$$\mathbf{m}_{k-1}^+ + \mathbf{m}_k^- + \mathbf{d}_{k,k-1} \times \mathbf{f}_{k-1}^+ = \frac{d}{dt} \Big|_k (\mathbf{I}_k \boldsymbol{\omega}_{b,k^-}) + \boldsymbol{\omega}_{b,k^-} \times (\mathbf{I}_k \boldsymbol{\omega}_{b,k^-}) + \mathbf{d}_{p,c} \times M_k \mathbf{a}_{b,k^-}.$$

The Derivative Theorem (2.12) is applied to obtain the familiar form

$$\mathbf{m}_{k-1}^+ + \mathbf{m}_k^- + \mathbf{d}_{k,k-1} \times \mathbf{f}_{k-1}^+ = \mathbf{I}_k \boldsymbol{\alpha}_{b,k^-} + \boldsymbol{\omega}_{b,k^-} \times (\mathbf{I}_k \boldsymbol{\omega}_{b,k^-}) + \mathbf{d}_{k,c_k} \times M_k \mathbf{a}_{b,k^-}. \quad (4.7.4)$$

Equation (4.7.3) and Equation (4.7.4) give a complete description of the dynamics of body k ; however, they must be expressed in terms of the vectors

$$\mathcal{F}_k^- := \left\{ \begin{array}{l} \mathbf{f}_k^- \\ \mathbf{m}_k^- \end{array} \right\} \quad (4.7.5)$$

and

$$\mathcal{A}_k^- := \left\{ \begin{array}{l} \frac{d}{dt} \Big|_k (\mathbf{v}_{b,k^-}) \\ \frac{d}{dt} \Big|_k (\boldsymbol{\omega}_{b,k^-}) \end{array} \right\}. \quad (4.7.6)$$

The desired form can be achieved by recalling that the acceleration \mathbf{a}_{b,k^-} is defined as

$$\mathbf{a}_{b,k^-} = \frac{d}{dt} \Big|_b (\mathbf{v}_{b,k^-}) = \frac{d}{dt} \Big|_k (\mathbf{v}_{b,k^-}) + \boldsymbol{\omega}_{b,k^-} \times \mathbf{v}_{b,k^-}, \quad (4.7.7)$$

and the angular acceleration $\boldsymbol{\alpha}_{b,k^-}$ is defined as

$$\boldsymbol{\alpha}_{b,k^-} = \frac{d}{dt} \Big|_b (\boldsymbol{\omega}_{b,k^-}) = \frac{d}{dt} \Big|_k (\boldsymbol{\omega}_{b,k^-}) + \boldsymbol{\omega}_{b,k^-} \times \boldsymbol{\omega}_{b,k^-} = \frac{d}{dt} \Big|_k (\boldsymbol{\omega}_{b,k^-}). \quad (4.7.8)$$

Substituting Equations (4.7.7) and (4.7.8) into (4.7.3) and (4.7.4) results in

$$\mathbf{f}_k^- = -\mathbf{f}_{k-1}^+ + M_k \left(\frac{d}{dt} \Big|_k (\mathbf{v}_{b,k^-}) + \boldsymbol{\omega}_{b,k} \times \mathbf{v}_{b,k^-} + \frac{d}{dt} \Big|_k (\boldsymbol{\omega}_{b,k^-}) \times \mathbf{d}_{k,c_k} + \boldsymbol{\omega}_{b,k^-} \times (\boldsymbol{\omega}_{b,k^-} \times \mathbf{d}_{k,c_k}) \right)$$

and

$$\begin{aligned} \mathbf{m}_k^- = & -\mathbf{m}_{k-1}^+ - \mathbf{d}_{k,k-1} \times \mathbf{f}_{k-1}^+ + \mathbf{I}_k \frac{d}{dt} \Big|_k (\boldsymbol{\omega}_{b,k^-}) + \boldsymbol{\omega}_{b,k^-} \times (\mathbf{I}_k \boldsymbol{\omega}_{b,k^-}) \\ & + \mathbf{d}_{k,c_k} \times M_k \left(\frac{d}{dt} \Big|_k (\mathbf{v}_{b,k^-}) + \boldsymbol{\omega}_{b,k^-}^- \times \mathbf{v}_{b,k^-} \right). \end{aligned}$$

This pair of equations can be written as a single matrix equation

$$\begin{aligned}\mathcal{F}_k^- := & \left\{ \begin{array}{c} \mathbf{f}_k^- \\ \mathbf{m}_k^- \end{array} \right\} = \left[\begin{array}{cc} \mathbb{I} & 0 \\ \mathbf{S}(\mathbf{d}_{k,k-1}^k) \mathbb{I} & \mathbb{I} \end{array} \right] \left\{ \begin{array}{c} -\mathbf{f}_{k-1}^+ \\ -\mathbf{m}_{k-1}^+ \end{array} \right\} \\ & + \left[\begin{array}{cc} M_k \mathbb{I} & -M_k \mathbf{S}(\mathbf{d}_{k,c_k}^k) \\ M_k \mathbf{S}(\mathbf{d}_{k,c_k}^k) & \mathbf{I}_k \end{array} \right] \left\{ \begin{array}{c} \frac{d}{dt}|_k (\mathbf{v}_{b,k-}) \\ \frac{d}{dt}|_k (\boldsymbol{\omega}_{b,k-}) \end{array} \right\} \\ & + \left\{ \begin{array}{c} M_k \boldsymbol{\omega}_{b,k-} \times (\boldsymbol{\omega}_{b,k-} \times \mathbf{d}_{k,c_k}) + M_k (\boldsymbol{\omega}_{b,k-} \times \mathbf{v}_{b,k-}) \\ \boldsymbol{\omega}_{b,k-} \times (\mathbf{I}_k \boldsymbol{\omega}_{b,k-}) + M_k \mathbf{d}_{k,c_k} \times (\boldsymbol{\omega}_{b,k-} \times \mathbf{v}_{b,k-}) \end{array} \right\}.\end{aligned}\quad (4.7.9)$$

This equation may be written in the compact form

$$\mathcal{F}_k^- = \varphi_{k,k-1} \mathcal{F}_{k-1}^+ + \mathcal{M}_k \mathcal{A}_k^- + \mathcal{P}_k \quad (4.7.10)$$

where the generalized mass or inertia matrix \mathcal{M}_k is defined as

$$\mathcal{M}_k = \left[\begin{array}{cc} M_k \mathbb{I} & -M_k \mathbf{S}(\mathbf{d}_{k,c_k}^k) \\ M_k \mathbf{S}(\mathbf{d}_{k,c_k}^k) & \mathbf{I}_k \end{array} \right] \quad (4.7.11)$$

and the inertial force vector is given as

$$\mathcal{P}_k = \left\{ \begin{array}{c} M_k \boldsymbol{\omega}_{b,k-} \times (\boldsymbol{\omega}_{b,k-} \times \mathbf{d}_{k,c_k}) + M_k (\boldsymbol{\omega}_{b,k-} \times \mathbf{v}_{b,k-}) \\ \boldsymbol{\omega}_{b,k-} \times (\mathbf{I}_k \boldsymbol{\omega}_{b,k-}) + M_k \mathbf{d}_{k,c_k} \times (\boldsymbol{\omega}_{b,k-} \times \mathbf{v}_{b,k-}) \end{array} \right\}. \quad (4.7.12)$$

Internal forces have equal magnitude and opposite direction, which implies that

$$\left\{ \begin{array}{c} \mathbf{f}_{k-} \\ \mathbf{m}_{k-} \end{array} \right\} = \left\{ \begin{array}{c} -\mathbf{f}_{k+} \\ -\mathbf{m}_{k+} \end{array} \right\}.$$

It follows that \mathcal{F}_k^- and \mathcal{F}_k^+ satisfy the equation $\mathcal{F}_k^- = \mathcal{R}_{k,k+1} \mathcal{F}_k^+$. The rotation matrix $\mathcal{R}_{k,k+1}$ appears since, by definition, the entries in \mathcal{F}_k^+ are the components of the forces \mathbf{f}_{k+} and moments \mathbf{m}_{k+} in terms of the basis for the $k+1$ frame. The final form of the recursive equation for the forces is obtained by substituting this equation in Equation (4.7.10), which results in

$$\mathcal{F}_k^- = \varphi_{k,k-1} \mathcal{R}_{k,k-1} \mathcal{F}_{k-1}^- + \mathcal{M}_k \mathcal{A}_k^- + \mathcal{P}_k. \quad (4.7.13)$$

Equation (4.7.1) is obtained when Equation (4.7.13) is expressed for each joint $k = 1, \dots, N$. \square

The coefficient matrix that appears in Equation (4.7.1)

$$\left[\begin{array}{ccccc} 0 & 0 & 0 & \cdots & 0 & 0 \\ \varphi_{2,1} \mathcal{R}_{2,1} & 0 & 0 & \cdots & 0 & 0 \\ 0 & \varphi_{3,2} \mathcal{R}_{3,2} & 0 & \cdots & 0 & 0 \\ \vdots & \vdots & \vdots & \ddots & \vdots & \vdots \\ 0 & 0 & 0 & \cdots & 0 & 0 \\ 0 & 0 & 0 & \cdots & \varphi_{N,N-1} \mathcal{R}_{N,N-1} & 0 \end{array} \right]$$

is the transpose of the coefficient matrix that appears in the recursive calculation of the velocity and acceleration in Equations (3.4.1) in Theorem (3.4) and (3.4.18) in Theorem (3.5). In both of those cases, the structure of the coefficient matrix enables a recursive procedure that starts with the last row, which corresponds to the root of the kinematic chain. In the current case, for solving the forces and moments, the structure of the lead coefficient matrix makes it possible to solve the *first equation* for the forces and moments in \mathcal{F}_1^-

$$\mathcal{F}_1^- = \mathcal{M}_1 \mathcal{A}_1^- + \mathcal{P}_1.$$

Suppose that all of the velocities and angular velocities have been solved for using the recursive algorithm described in Section (3.4.1), and that all of the derivatives of velocities and angular velocities have been solved for using the recursive algorithm summarized in Section (3.4.3). When this is the case, it is possible to evaluate all of the terms on the right side of the above equation immediately and obtain \mathcal{F}_1^- . With this, the solution can proceed to the second row in Equation (4.7.1) and solve for \mathcal{F}_2^- as

$$\mathcal{F}_2^- = \varphi_{2,1} \mathcal{R}_{2,1} \mathcal{F}_1^- + \mathcal{M}_2 \mathcal{A}_2^- + \mathcal{P}_2.$$

Since all the terms required to evaluate the right side of this equation are known, \mathcal{F}_2^- may be calculated. This process is continued until all the joints $k = 1, \dots, N$ have been processed. The following table summarizes this recursive algorithm for the calculation of the reaction forces and moments.

Example 4.7.1. Use the Recursive Order (N) algorithm to solve for the joint forces and torques for link 1 of the two link robotic arm presented in Example (3.4.1) and shown in Figure (4.33).

Solution: First, the joint forces and moments will be computed directly from first principles for body 1, and it will be shown that the same results are computed using the recursive algorithm. The free body diagrams for the two bodies that comprise the kinematic chain are shown in Figures (4.34a) and (4.34b). Euler's First Law for body 1 yields

$$\begin{aligned} \mathbf{f}_{1^-} &= M_1 \mathbf{a}_{b,c_1}, \\ &= M_1 (\mathbf{a}_{b,1^-} + \boldsymbol{\alpha}_{b,1^-} \times \mathbf{d}_{1,c_1} + \boldsymbol{\omega}_{b,1^-} \times (\boldsymbol{\omega}_{b,1^-} \times \mathbf{d}_{1,c_1})) \end{aligned}$$

The following quantities have been derived in Examples (3.4.1) and (3.4.2):

$$\boldsymbol{\omega}_{b,1^-} = (\dot{\theta}_1 + \dot{\theta}_2) \mathbf{z}_1, \quad (4.7.15)$$

$$\boldsymbol{\alpha}_{b,1^-} = (\ddot{\theta}_1 + \ddot{\theta}_2) \mathbf{z}_1, \quad (4.7.16)$$

$$\mathbf{d}_{1,c_1} = \frac{1}{2} L_1 \mathbf{x}_1, \quad (4.7.17)$$

$$\mathbf{a}_{b,1^-} = -L_2 \dot{\theta}_2^2 \mathbf{x}_2 + L_2 \ddot{\theta}_2 \mathbf{y}_2. \quad (4.7.18)$$

Recursive Algorithm for Forces and Moments

1. Solve for the velocities and angular velocities using the recursive algorithm in Section (3.4.1).
2. Solve for the derivatives of the velocities and angular velocities using the recursive algorithm in Section (3.4.3).
3. Iterate from outboard joints to inboard joints.
For $k = 1, 2, \dots, N$

- 3.1 Form the bias inertial force \mathcal{P}_k .

$$\mathcal{P}_k = \left\{ M_k \boldsymbol{\omega}_{b,k}^k \times (\boldsymbol{\omega}_{b,k}^k \times \mathbf{d}_{k,c_k}^k) + M_k (\boldsymbol{\omega}_{b,k}^k \times \mathbf{v}_{b,k}^k) \right. \\ \left. \boldsymbol{\omega}_{b,k}^k \times (\mathbf{I}_k \boldsymbol{\omega}_{b,k}^k) + M_k \mathbf{d}_{k,c_k}^k \times (\boldsymbol{\omega}_{b,k}^k \times \mathbf{v}_{b,k}^k) \right\}.$$

- 3.2 Form the transition operator

$$\phi_{k,k-1} = \varphi_{k,k-1} \mathcal{R}_{k,k-1}.$$

- 3.3 Form the generalized inertia and mass matrix

$$\mathcal{M}_k = \begin{bmatrix} M_k \mathbb{I} & -M_k \mathbf{S}(\mathbf{d}_{k,c_k}^k) \\ M_k \mathbf{S}(\mathbf{d}_{k,c_k}^k) & \mathbf{I}_k \end{bmatrix}.$$

- 3.4 Calculate the forces and moments

$$\mathcal{F}_k^- = \phi_{k,k-1} \mathcal{R}_{k,k-1} \mathcal{F}_{k-1}^- + \mathcal{M}_k \mathcal{A}_k^- + \mathcal{P}_k. \quad (4.7.14)$$

Fig. 4.32: Recursive Algorithm for Calculating Forces and Moments

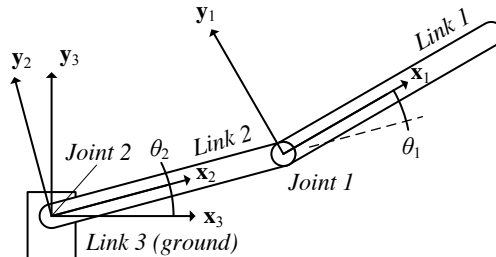


Fig. 4.33: Two Link Robotic Arm

We transform the equations to obtain the force components relative to the frame that is fixed in body 1 using the rotation matrix \mathbf{R}_2^1 in Example (3.4.1),

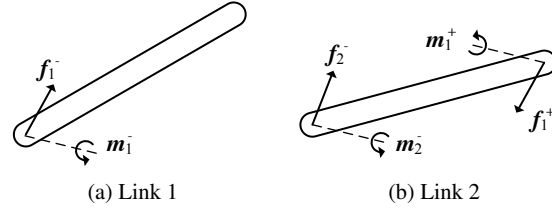


Fig. 4.34: Free Body Diagrams for Two Link Robotic Arm

$$\mathbf{f}_1^- = M_1 \begin{pmatrix} \cos \theta_1 \\ -\sin \theta_1 \\ 0 \end{pmatrix} + L_2 \ddot{\theta}_2 \begin{pmatrix} \sin \theta_1 \\ \cos \theta_1 \\ 0 \end{pmatrix} + \frac{1}{2} L_1 (\dot{\theta}_1 + \dot{\theta}_2) \begin{pmatrix} 0 \\ 1 \\ 0 \end{pmatrix} - \frac{1}{2} L_1 (\dot{\theta}_1 + \dot{\theta}_2)^2 \begin{pmatrix} 1 \\ 0 \\ 0 \end{pmatrix}, \quad (4.7.19)$$

$$= M_1 \begin{pmatrix} -L_2 \dot{\theta}_2^2 \cos \theta_1 + L_2 \ddot{\theta}_2 \sin \theta_1 - \frac{1}{2} L_1 (\dot{\theta}_1 + \dot{\theta}_2)^2 \\ L_2 \dot{\theta}_2^2 \sin \theta_1 + L_2 \ddot{\theta}_2 \cos \theta_1 + \frac{1}{2} L_1 (\dot{\theta}_1 + \dot{\theta}_2)^2 \\ 0 \end{pmatrix}. \quad (4.7.20)$$

The summation of moments acting on body 1 about the point 1^- is given by

$$\begin{aligned} \mathbf{m}_{1^-} &= \frac{d}{dt} \Big|_b \left((\mathbf{I}_{1^-}^1 \boldsymbol{\omega}_{b,1^-}) + \mathbf{d}_{1,c_1} \times M_1 \mathbf{a}_{b,1^-} \right) \\ &= \frac{d}{dt} \Big|_1 \left((\mathbf{I}_{1^-}^1 \boldsymbol{\omega}_{b,1^-}) + \boldsymbol{\omega}_{b,1^-} \times (\mathbf{I}_{1^-}^1 \boldsymbol{\omega}_{b,1^-}) + M_1 \mathbf{d}_{1,c_1} \times \mathbf{a}_{b,1^-} \right) \end{aligned}$$

A change of basis for the point 1^- acceleration yields $\mathbf{a}_{b,1^-}^1$ as

$$\mathbf{a}_{b,1^-}^1 = -L_2 \dot{\theta}_2^2 \begin{pmatrix} \cos \theta_1 \\ -\sin \theta_1 \\ 0 \end{pmatrix} + L_2 \ddot{\theta}_2 \begin{pmatrix} \sin \theta_1 \\ \cos \theta_1 \\ 0 \end{pmatrix},$$

which in turn is used to compute the cross product

$$\begin{aligned} (\mathbf{d}_{1,c_1} \times \mathbf{a}_{b,1^-}) &= \begin{vmatrix} \mathbf{x}_1 & \mathbf{y}_1 & \mathbf{z}_1 \\ \frac{1}{2} L_1 & 0 & 0 \\ (-L_2 \dot{\theta}_2^2 \cos \theta_1 + L_2 \ddot{\theta}_2 \sin \theta_1) & (L_2 \dot{\theta}_2^2 \sin \theta_1 + L_2 \ddot{\theta}_2 \cos \theta_1) & 0 \end{vmatrix}, \\ &= \frac{1}{2} L_1 (L_2 \dot{\theta}_2^2 \sin \theta_1 + L_2 \ddot{\theta}_2 \cos \theta_1) \mathbf{z}_1. \end{aligned}$$

The final expression for moment acting on body 1 is

$$\mathbf{m}_{1^-} = I_{33} (\ddot{\theta}_1 + \ddot{\theta}_2) \mathbf{z}_1 + \frac{1}{2} M_1 L_1 L_2 (\dot{\theta}_2^2 \sin \theta_1 + \ddot{\theta}_2 \cos \theta_1) \mathbf{z}_1. \quad (4.7.21)$$

Equations (4.7.19) and (4.7.21) may be assembled to reach the final expression for the 6×1 vector of joint forces and torques acting at point 1^- on body 1.

$$\mathcal{F}_1^- = \begin{Bmatrix} \mathbf{f}_{1^-} \\ \mathbf{m}_{1^-} \end{Bmatrix} = \begin{Bmatrix} \left\{ \begin{array}{l} -M_1 L_2 \dot{\theta}_2^2 \cos \theta_1 + M_1 L_2 \ddot{\theta}_2 \sin \theta_1 - \frac{1}{2} M_1 L_1 (\dot{\theta}_1 + \dot{\theta}_2)^2 \\ M_1 L_2 \dot{\theta}_2^2 \sin \theta_1 + M_1 L_2 \ddot{\theta}_2 \cos \theta_1 + \frac{1}{2} M_1 L_1 (\ddot{\theta}_1 + \ddot{\theta}_2) \\ 0 \\ 0 \\ 0 \\ I_{33}(\ddot{\theta}_1 + \ddot{\theta}_2) + \frac{1}{2} M_1 L_1 L_2 \dot{\theta}_2^2 \sin \theta_1 + \frac{1}{2} M_1 L_1 L_2 \ddot{\theta}_2 \cos \theta_1 \end{array} \right\} \end{Bmatrix}. \quad (4.7.22)$$

As previously stated, the goal is to verify that the recursive algorithm yields the same result as in (4.7.22), via an efficient, systematic, programmable procedure. The first row of the system equations for the forces and moments yields

$$\begin{Bmatrix} \mathbf{f}_{1^-} \\ \mathbf{m}_{1^-} \end{Bmatrix} = \mathcal{F}_1^- = \mathcal{M}_1 \mathcal{A}_1^- + \mathcal{P}_1.$$

For $k = 1$, the generalized mass matrix is found to be

$$\mathcal{M}_1 = \left[\begin{array}{ccc|ccc} M_1 & 0 & 0 & 0 & 0 & 0 \\ 0 & M_1 & 0 & 0 & 0 & \frac{1}{2} M_1 L_1 \\ 0 & 0 & M_1 & 0 & -\frac{1}{2} M_1 L_1 & 0 \\ \hline 0 & 0 & 0 & I_{11} & 0 & 0 \\ 0 & 0 & -\frac{1}{2} M_1 L_1 & 0 & I_{22} & 0 \\ 0 & \frac{1}{2} M_1 L_1 & 0 & 0 & 0 & I_{33} \end{array} \right],$$

since $\mathbf{d}_{1,c_1}^1 = \left\{ \frac{1}{2} L_1 \ 0 \ 0 \right\}^T$. The product $\mathcal{M}_1 \mathcal{A}_1^-$ is expanded directly as

$$\begin{aligned} \mathcal{M}_1 \mathcal{A}_1^- &= \mathcal{M}_1 \left\{ \begin{array}{c} \left\{ \begin{array}{l} L_2 \dot{\theta}_1 \dot{\theta}_2 \cos \theta_1 + L_2 \ddot{\theta}_2 \sin \theta_1 \\ -L_2 \dot{\theta}_1 \dot{\theta}_2 \sin \theta_1 + L_2 \ddot{\theta}_2 \cos \theta_1 \\ 0 \\ \left\{ \begin{array}{l} 0 \\ 0 \\ \ddot{\theta}_1 + \ddot{\theta}_2 \end{array} \right\} \end{array} \right\} \end{array} \right\}, \\ &= \left\{ \begin{array}{c} \left\{ \begin{array}{l} M_1 (L_2 \dot{\theta}_1 \dot{\theta}_2 \cos \theta_1 + L_2 \ddot{\theta}_2 \sin \theta_1) \\ M_1 (-L_2 \dot{\theta}_1 \dot{\theta}_2 \sin \theta_1 + L_2 \ddot{\theta}_2 \cos \theta_1) + \frac{1}{2} M_1 L_1 (\ddot{\theta}_1 + \ddot{\theta}_2) \\ 0 \\ 0 \\ 0 \\ \frac{1}{2} M_1 L_1 (-L_2 \dot{\theta}_1 \dot{\theta}_2 \sin \theta_1 + L_2 \ddot{\theta}_2 \cos \theta_1) + I_{33}(\ddot{\theta}_1 + \ddot{\theta}_2) \end{array} \right\} \end{array} \right\}. \quad (4.7.23) \end{aligned}$$

The inertial force \mathcal{P}_1 is defined to be

$$\mathcal{P}_1 = \left\{ \begin{array}{l} M_1 \boldsymbol{\omega}_{b,1^-}^1 \times (\boldsymbol{\omega}_{b,1^-}^1 \times \mathbf{d}_{1,c_1}^1) + M_1 (\boldsymbol{\omega}_{b,1^-}^1 \times \mathbf{v}_{b,1^-}^1) \\ \boldsymbol{\omega}_{b,1^-}^1 \times \mathbf{I} \boldsymbol{\omega}_{b,1^-}^1 + M_1 \mathbf{d}_{1,c_1}^1 \times (\boldsymbol{\omega}_{b,1^-}^1 \times \mathbf{v}_{b,1^-}^1) \end{array} \right\}.$$

This complex expression can be evaluated quickly if the termwise expressions are computed and substituted, such that

$$\begin{aligned}
\boldsymbol{\omega}_{b,1^-} \times \mathbf{d}_{1,c_1} &= \frac{1}{2} L_1 (\dot{\theta}_1 + \dot{\theta}_2) \mathbf{y}_1, \\
\boldsymbol{\omega}_{b,1^-} \times (\boldsymbol{\omega}_{b,1^-} \times \mathbf{d}_{1,c_1}) &= -\frac{1}{2} L_1 (\dot{\theta}_1 + \dot{\theta}_2)^2 \mathbf{x}_1, \\
\boldsymbol{\omega}_{b,1^-} \times \mathbf{v}_{b,1^-} &= -L_2 \dot{\theta}_2 (\dot{\theta}_1 + \dot{\theta}_2) \mathbf{x}_2, \\
\mathbf{d}_{1,c_1} \times (\boldsymbol{\omega}_{b,1^-} \times \mathbf{v}_{b,1^-}) &= (-L_2 \dot{\theta}_2 (\dot{\theta}_1 + \dot{\theta}_2)) \begin{vmatrix} \mathbf{x}_1 & \mathbf{y}_1 & \mathbf{z}_1 \\ \frac{1}{2} L_1 & 0 & 0 \\ \cos \theta_1 & -\sin \theta_1 & 0 \end{vmatrix}, \\
&= \frac{1}{2} L_1 L_2 \dot{\theta}_2 (\dot{\theta}_1 + \dot{\theta}_2) \sin \theta_1 \mathbf{z}_1.
\end{aligned}$$

This calculation employs the fact that $\boldsymbol{\omega}_{b,1^-} = (\dot{\theta}_1 + \dot{\theta}_2) \mathbf{z}_1 = (\dot{\theta}_1 + \dot{\theta}_2) \mathbf{z}_2$, $\mathbf{v}_{b,1^-} = L_2 \dot{\theta}_2 \mathbf{y}_2$, and $\mathbf{d}_{1,c_1} = \frac{1}{2} L_1 \mathbf{x}_1$. The inertial force P takes its final form upon substitution of these immediate results,

$$\mathcal{P}_1 = \left\{ \begin{array}{c} \left\{ \begin{array}{c} -\frac{1}{2} M_1 L_1 (\dot{\theta}_1 + \dot{\theta}_2)^2 - M_1 L_2 \dot{\theta}_2 (\dot{\theta}_1 + \dot{\theta}_2) \cos \theta_1 \\ M_1 L_2 \dot{\theta}_2 (\dot{\theta}_1 + \dot{\theta}_2) \sin \theta_1 \\ 0 \\ 0 \\ 0 \\ \frac{1}{2} M_1 L_1 L_2 \dot{\theta}_2 (\dot{\theta}_1 + \dot{\theta}_2) \sin \theta_1 \end{array} \right\} \\ \left\{ \begin{array}{c} 0 \\ 0 \\ 0 \\ I_{33}(\ddot{\theta}_1 + \ddot{\theta}_2) + \frac{1}{2} M_1 L_1 L_2 \dot{\theta}_2^2 \sin \theta_1 + \frac{1}{2} M_1 L_1 L_2 \ddot{\theta}_2 \cos \theta_1 \end{array} \right\} \end{array} \right\}. \quad (4.7.24)$$

Finally, Equations (4.7.23) and Equation (4.7.24) are added. After cancelling like terms, the result

$$\mathcal{M}\mathcal{H}_1^- + \mathcal{P}_1 = \left\{ \begin{array}{c} \left\{ \begin{array}{c} -M_1 L_2 \dot{\theta}_2^2 \cos \theta_1 + M_1 L_2 \ddot{\theta}_2 \sin \theta_1 - \frac{1}{2} M_1 L_1 (\dot{\theta}_1 + \dot{\theta}_2)^2 \\ M_1 L_2 \dot{\theta}_2^2 \sin \theta_1 + M_1 L_2 \ddot{\theta}_2 \cos \theta_1 + \frac{1}{2} M_1 L_1 (\ddot{\theta}_1 + \ddot{\theta}_2) \\ 0 \\ 0 \\ 0 \\ I_{33}(\ddot{\theta}_1 + \ddot{\theta}_2) + \frac{1}{2} M_1 L_1 L_2 \dot{\theta}_2^2 \sin \theta_1 + \frac{1}{2} M_1 L_1 L_2 \ddot{\theta}_2 \cos \theta_1 \end{array} \right\} \\ \left\{ \begin{array}{c} 0 \\ 0 \\ 0 \\ 0 \\ 0 \\ 0 \end{array} \right\} \end{array} \right\} \quad (4.7.25)$$

is the same expression as the one derived via direct application of first principles in Equation (4.7.22). ■

4.8 Recursive Derivation of the Equations of Motion

Sections (3.3.5), (3.4.3), and (4.7.1) have shown that the forward kinematics problem for either velocities or accelerations, as well as the calculation of joint forces or torques, can be solved efficiently via *recursive order (N) algorithms*. This section will show that the equations of motion for robotic systems that form a kinematic

chain as depicted in Figure (3.19) and (3.20) can be written in terms of constituent matrices that have already been introduced in Sections (3.4.1), (3.4.3), and (4.7.1). Reference [24] gives a comprehensive account of this formulation, or see [14] for a similar discussion. The velocities and angular velocities for the kinematic chain are collected in the 6×1 vector

$$\mathcal{V}_k^- = \left\{ \begin{array}{l} \mathbf{v}_{b,k^-} \\ \boldsymbol{\omega}_{b,k^-}^k \end{array} \right\}$$

where point k^- is attached to body k on the outward side of joint k . The terms \mathbf{v}_{b,k^-}^k are the components relative to the basis for the frame k of the velocity vector \mathbf{v}_{b,k^-} . The terms $\boldsymbol{\omega}_{b,k^-}^k$ are the components relative to the basis for the frame k of the angular velocity vector $\boldsymbol{\omega}_{b,k^-}$. Equation (3.4.1) can be written in terms of *system vectors* of unknowns as

$$\mathcal{V}^- = \Gamma^T \mathcal{V}^- + \mathcal{H} \dot{\theta}, \quad (4.8.1)$$

where the assembled system vectors \mathcal{V}^- and $\dot{\theta}$ are defined as

$$\mathcal{V}^- := \left\{ \begin{array}{l} \mathcal{V}_1^- \\ \mathcal{V}_2^- \\ \vdots \\ \mathcal{V}_N^- \end{array} \right\}, \quad \dot{\theta} := \left\{ \begin{array}{l} \dot{\theta}_1 \\ \dot{\theta}_2 \\ \vdots \\ \dot{\theta}_N \end{array} \right\},$$

and the system matrices Γ^T and \mathcal{H} are defined as

$$\Gamma^T = \begin{bmatrix} 0 & \mathcal{R}_{2,1}^T \varphi_{2,1}^T & 0 & \cdots & 0 & 0 \\ 0 & 0 & \mathcal{R}_{3,2}^T \varphi_{3,2}^T & \cdots & 0 & 0 \\ 0 & 0 & 0 & \cdots & 0 & 0 \\ \vdots & \vdots & \vdots & \ddots & \vdots & \vdots \\ 0 & 0 & 0 & \cdots & 0 & \mathcal{R}_{n-1,n}^T \varphi_{N-1,N}^T \\ 0 & 0 & 0 & \cdots & 0 & 0 \end{bmatrix}, \quad \mathcal{H} := \begin{bmatrix} \mathcal{H}_1 & 0 & \cdots & 0 \\ 0 & \mathcal{H}_2 & \cdots & 0 \\ \vdots & \vdots & \ddots & \vdots \\ 0 & 0 & \cdots & \mathcal{H}_N \end{bmatrix},$$

The matrix Γ^T and its transpose Γ will appear repeatedly in the derivatives that follow. A similar equation can be obtained from Theorem (3.5) for the derivatives of the velocities and angular velocities. The vectors \mathcal{A}_k^- that are used to formulate the kinematic problem for the accelerations are defined to be

$$\mathcal{A}_k^- = \left\{ \begin{array}{l} \frac{d}{dt} \Big|_k (\mathbf{v}_{b,k}) \\ \frac{d}{dt} \Big|_k (\boldsymbol{\omega}_{b,k}) \end{array} \right\}.$$

The primary result in Section (3.4.3) as made explicit in Theorem (3.5) is that the derivatives of the velocity and angular velocities satisfy the system equation

$$\mathcal{A}^- = \Gamma^T \mathcal{A}^- + \mathcal{H} \ddot{\theta} + \mathcal{N}, \quad (4.8.2)$$

where the system vectors \mathcal{A}^- and \mathcal{N} are defined as

$$\mathcal{A}^- := \begin{Bmatrix} \mathcal{A}_1^- \\ \mathcal{A}_2^- \\ \vdots \\ \mathcal{A}_N^- \end{Bmatrix} \quad \text{and} \quad \mathcal{N} := \begin{Bmatrix} \mathcal{N}_1 \\ \mathcal{N}_2 \\ \vdots \\ \mathcal{N}_N \end{Bmatrix}.$$

Finally, recall the definition of the 6×1 vector

$$\mathcal{F}_k^- = \begin{Bmatrix} \mathbf{f}_{k^-}^k \\ \mathbf{m}_{k^-}^k \end{Bmatrix}$$

which contains the components relative to frame k of the force vectors \mathbf{f}_{k^-} and moments \mathbf{m}_{k^-} that are applied at point k^- on body k at the joint k . Equation (4.7.3) in Theorem (4.18) holds that the joint forces and moments satisfy the system equation

$$\mathcal{F}^- = \Gamma \mathcal{F}^- + \mathcal{M} \mathcal{A}^- + \mathcal{P}, \quad (4.8.3)$$

where the system vectors \mathcal{F}^- and \mathcal{P} , and system matrix \mathcal{M} , are defined to be

$$\mathcal{F}^- = \begin{Bmatrix} \mathcal{F}_1^- \\ \mathcal{F}_2^- \\ \vdots \\ \mathcal{F}_N^- \end{Bmatrix}, \quad \mathcal{P} = \begin{Bmatrix} \mathcal{P}_1 \\ \mathcal{P}_2 \\ \vdots \\ \mathcal{P}_N \end{Bmatrix}, \quad \text{and} \quad \mathcal{M} = \begin{bmatrix} \mathcal{M}_1 & 0 & \cdots & 0 \\ 0 & \mathcal{M}_2 & \cdots & 0 \\ \vdots & \vdots & \ddots & \vdots \\ 0 & 0 & \cdots & \mathcal{M}_N \end{bmatrix}.$$

The determination of the equations of motion for the kinematic chain depicted in Figures (3.19) and (3.20) is straightforward once Equations (4.8.1), (4.8.2), and (4.8.3) are derived. Equations (4.8.2) and (4.8.3) may be solved for \mathcal{A}^- and \mathcal{F}^- , respectively, to obtain

$$\mathcal{A}^- = (\mathbb{I} - \Gamma^T)^{-1}(\mathcal{H}\ddot{\theta} + \mathcal{N}), \quad (4.8.4)$$

$$\mathcal{F}^- = (\mathbb{I} - \Gamma)^{-1}(\mathcal{M} \mathcal{A}^- + \mathcal{P}). \quad (4.8.5)$$

Equation (4.8.4) is then substituted into (4.8.5) to obtain an expression for the joint forces and torques

$$\mathcal{F}^- = (\mathbb{I} - \Gamma)^{-1} \mathcal{M} (\mathbb{I} - \Gamma^T)^{-1} \mathcal{H} \ddot{\theta} + (\mathbb{I} - \Gamma)^{-1} (\mathcal{M} (\mathbb{I} - \Gamma^T)^{-1} \mathcal{N} + \mathcal{P}). \quad (4.8.6)$$

In this equation, the vector \mathcal{F}^- contains the joint forces and moments acting on each body in the kinematic chain.

The final equations of motion for the kinematic chain are obtained by noting that all of the forces and moments that act on the individual joints of the body can be decomposed into constraint forces and moments \mathcal{F}_c^- and actuation torques as

$$\begin{aligned}\mathcal{F}^- &= \left[\begin{array}{cccc} \mathcal{H}_1 & 0 & \cdots & 0 \\ 0 & \mathcal{H}_2 & \cdots & 0 \\ \vdots & \vdots & \ddots & \vdots \\ 0 & 0 & \cdots & \mathcal{H}_N \end{array} \right] \left\{ \begin{array}{c} T_1 \\ T_2 \\ \vdots \\ T_3 \end{array} \right\} + \mathcal{F}_c^-,\quad (4.8.7) \\ &= \mathcal{H}\mathcal{T} + \mathcal{F}_c^-, \end{aligned}$$

where T_k is the actuation torque generated about the axis \mathbf{h}_k for $k = 1, \dots, M$. The system vector of actuation torques has been introduced into this equation as

$$\mathcal{T} := \left\{ \begin{array}{c} T_1 \\ T_2 \\ \vdots \\ T_N \end{array} \right\}.$$

By definition, the constraint forces and moments \mathcal{F}_c^- are orthogonal to the actuation torques. Since the direction of the k^{th} actuation torque is given by \mathbf{h}_k , the condition that the constraint forces are perpendicular to the actuation forces and moments can be written as

$$\mathcal{H}^T \mathcal{F}_c^- = 0.$$

Equation (4.8.7) can be premultiplied by \mathcal{H}^T to utilize this orthogonality condition and obtain the equation

$$\mathcal{T} = \underbrace{\mathcal{H}^T \mathcal{H} \mathcal{T}}_{\mathbb{I}} + \underbrace{\mathcal{H}^T \mathcal{F}_c^-}_{0} = \mathcal{H}^T \mathcal{F}^-.\quad (4.8.8)$$

This equation calculates the projection of all of the joint forces and moments along the direction of the actuation torques. Recall that each \mathbf{h}_k is a unit vector by definition, which guarantees that

$$\mathcal{H}^T \mathcal{H} = \mathbb{I},$$

with \mathbb{I} an appropriately dimensioned identity matrix. The final equations of motion for the robotic system can be obtained by combining Equations (4.8.6) and (4.8.8) to attain

$$\mathcal{H}^T (\mathbb{I} - \Gamma)^{-1} \mathcal{M} (\mathbb{I} - \Gamma)^{-T} \mathcal{H} \ddot{\theta} + \mathcal{H}^T (\mathbb{I} - \Gamma)^{-1} (\mathcal{M} (\mathbb{I} - \Gamma)^{-T} \mathcal{N}^+ \mathcal{P}) = \mathcal{T}.$$

4.9 Problems for Chapter 4, Newton-Euler Equations

4.9.1 Problems on Linear Momentum

Problems (4.1), (4.2) and (4.3) refer to the robotic manipulator shown in Figures (4.35) and (4.36). This robot has revolute joints about the \mathbf{z}_0 , \mathbf{z}_1 and \mathbf{z}_2 axes. The

joint variables θ_1, θ_2 and θ_3 are measured about the $\mathbf{z}_0, \mathbf{z}_1, \mathbf{z}_2$ axes, respectively. In each case the angle θ_i is measured from the positive \mathbf{x}_{i-1} axis to the positive \mathbf{x}_i axis, for $i = 1, 2, 3$.

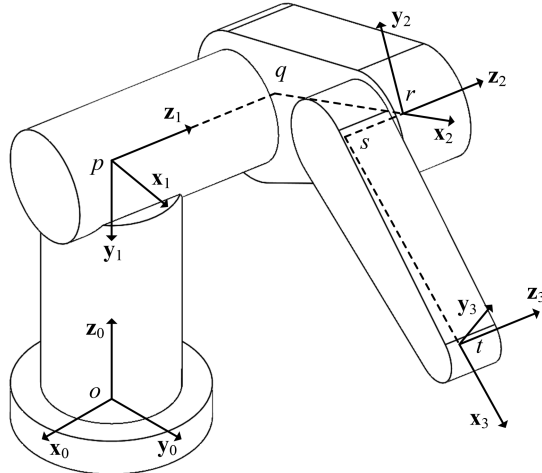


Fig. 4.35: PUMA Robot Frame Definitions

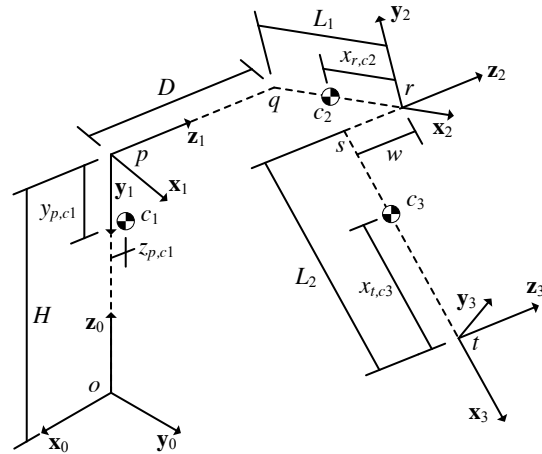


Fig. 4.36: PUMA Robot Joint and Mass Center Offsets

Problem 4.1. Compute the *linear momentum* in the 0 frame of link 1, the shoulder, for the robot shown in Figures (4.35) and (4.36). Express your answer in terms of the basis for the 1 frame and 0 frame.

Problem 4.2. Compute the *linear momentum* in the 0 frame of link 2, the inner arm, for the robot shown in Figures (4.35) and (4.36). Express your answer in terms of the basis for the 2, 1 and 0 frames.

Problem 4.3. Compute the *linear momentum* in the 0 frame of link 3, the outer arm, for the robot shown in Figures (4.35) and (4.36). Express your answer in terms of the basis for the 3, 2, 1 and the 0 frames.

Problems (4.4), (4.5) and (4.6) refer to the SCARA robot shown in Figures (4.37) and (4.38). This robotic manipulator has two revolute joints about the \mathbf{z}_0 and \mathbf{z}_1 directions and a prismatic joint along the \mathbf{z}_2 direction. The joint variables θ_1 and θ_2 are measured about the \mathbf{z}_0 and \mathbf{z}_1 axes, respectively. In each case the angle θ_i is measured from the positive \mathbf{x}_{i-1} axis to the positive \mathbf{x}_i axis, for $i = 1, 2$.

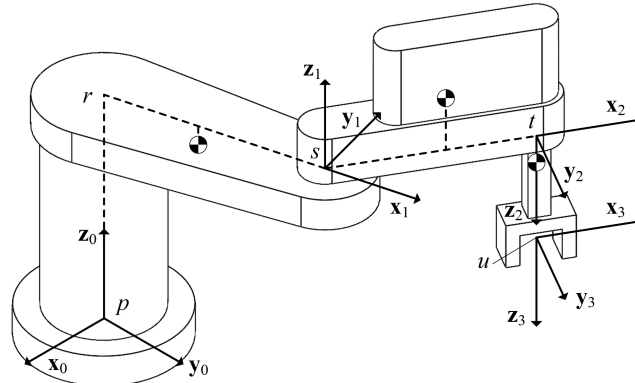


Fig. 4.37: SCARA Robot Frame Definitions

Problem 4.4. Compute the *linear momentum* in the 0 frame of link 1, the inner arm, for the robot shown in Figures (4.37) and (4.38). Express your answer in terms of the basis for the 1 frame and 0 frame.

Problem 4.5. Compute the *linear momentum* in the 0 frame of link 2, the outer arm, for the robot shown in Figures (4.37) and (4.38). Express your answer in terms of the basis for the 2, 1 and 0 frames.

Problem 4.6. Compute the *linear momentum* in the 0 frame of link 3, the tool carriage, for the robot shown in Figures (4.37) and (4.38). Express your answer in terms of the basis for the 3, 2, 1 and 0 frames.

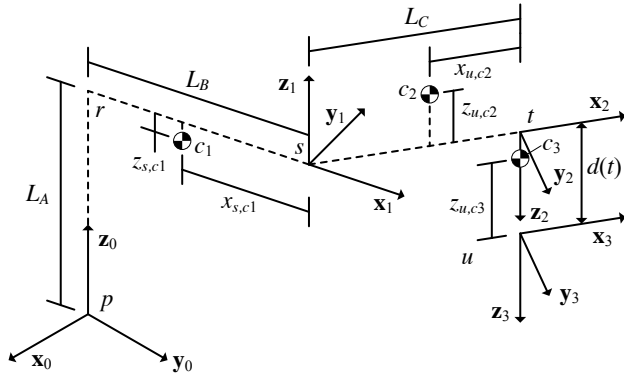


Fig. 4.38: SCARA Robot Joint and Mass Center Offsets

Problems (4.7), (4.8) and (4.9) refer to the robotic manipulator shown in Figures (4.39) and (4.40). This robotic manipulator has a revolute joint along the z_0 direction, and it has a prismatic joints along the z_1 , z_2 and z_3 directions. The tool carriage, which is not shown, has its center of mass located at point t . The joint variable θ_1 is measured about the z_0 axis. The angle θ_1 is measured from the positive x_0 axis to the positive x_1 axis. The height $H(t)$ from the point q to the point r is the joint variable measuring displacement along the z_1 axis, the length $L(t)$ from the point r to the point s is the joint variable measuring displacement along the z_2 direction, and the distance $d(t)$ from the point s to the point t is the joint variable along the z_3 axis.

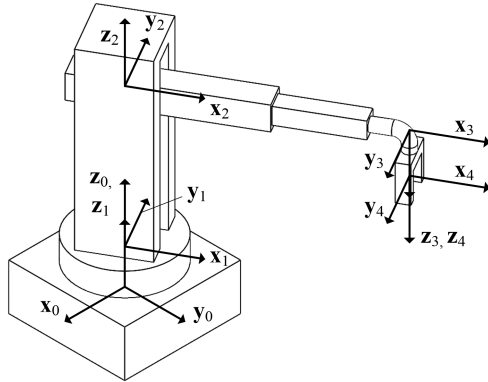


Fig. 4.39: Cylindrical Robot Frame Definitions

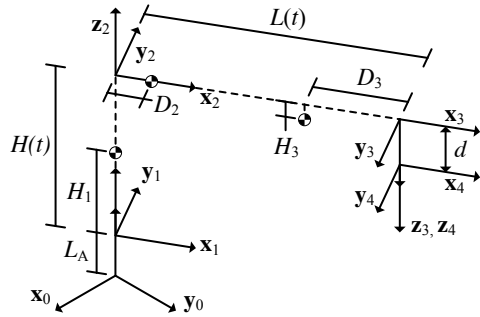


Fig. 4.40: Cylindrical Robot Joint and Mass Center Offsets

Problem 4.7. Compute the *linear momentum* in the 0 frame of link 1, the vertical arm, for the robot shown in Figures (4.39) and (4.40). Express your answer in terms of the basis for the 1 and 0 frames.

Problem 4.8. Compute the *linear momentum* in the 0 frame of link 2, the horizontal arm, for the robot shown in Figures (4.39) and (4.40). Express your answer in terms of the basis for the 2, 1 and 0 frames.

Problem 4.9. Compute the *linear momentum* in the 0 frame of link 3, the tool carriage, for the robot shown in Figures (4.39) and (4.40). Express your answer in terms of the basis for the 4, 3, 2, 1 and 0 frames.

4.9.2 Problems on the Center of Mass

Problem 4.10. Figure (4.41a) depicts the terminal component in an industrial robot. Assume that the mass density is uniform and that the body can be approximated as the union of two cylinders having radii and lengths (R_1, L_1) and (R_2, L_2) . The location of the center of mass of each cylinder is shown in the figure. Find the *mass center* of this composite rigid body.

Problem 4.11. Figure (4.42a) depicts the fixed base of a robotic assembly. Assume that the mass density is uniform and can be approximated as the union of a cylinder with radius and length (R_1, L_1) and a rectangular prism of dimensions (L_2, W_2, H_2) , as shown in (4.42b). The location of the center of mass of each cylinder is also shown in Figure (4.42b). Find the *mass center* of this composite rigid body relative to the X frame.

Problem 4.12. Figure (4.43a) depicts the mounting bracket for an industrial robot. Assume that the mass density is uniform and can be approximated as the union of

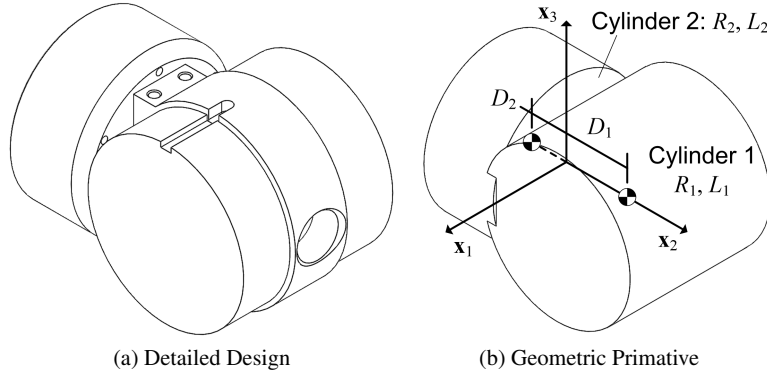


Fig. 4.41: Industrial Robot End Effector Component

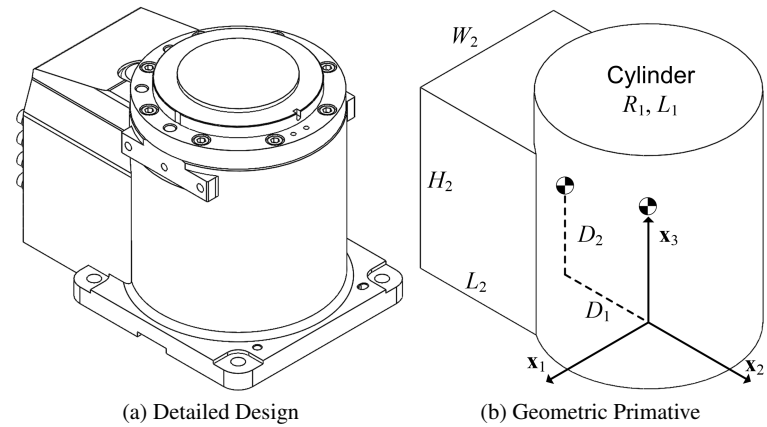


Fig. 4.42: Industrial Robot Fixed Base Component

three rectangular prisms. The location of the center of mass of each is shown in Figures (4.43a) and (4.43b). Find the *mass center* of this composite rigid body.

Problems (4.13) and (4.14) study a two link robot that consists of link 1 and 2, as shown in Figures (4.44a) and (4.44b). The center of mass coordinates of link 1 with respect to frame 1 are $(-x_{c_1}, y_{c_1}, 0)$, and the center of mass coordinates of link 2 with respect to frame 2 are $(-x_{c_2}, 0, z_{c_2})$.

Problem 4.13. The two link robot in Figure (4.44a) is locked in the horizontal configuration shown. At the instant shown, assume that $\theta_1 = 0^\circ$, or $\mathbf{x}_2 = \mathbf{x}_1$. Calculate the location of the center of mass of the robot in this configuration in terms of the frame 1.

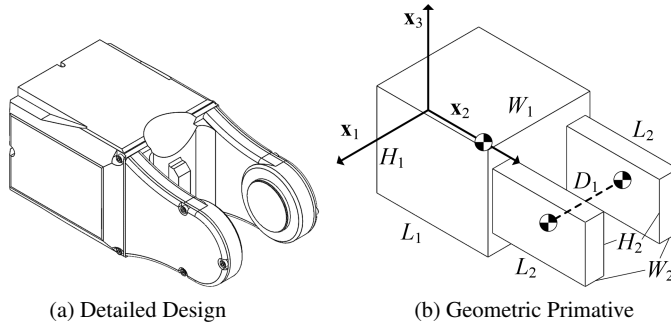


Fig. 4.43: Industrial Robot Mounting Bracket Component

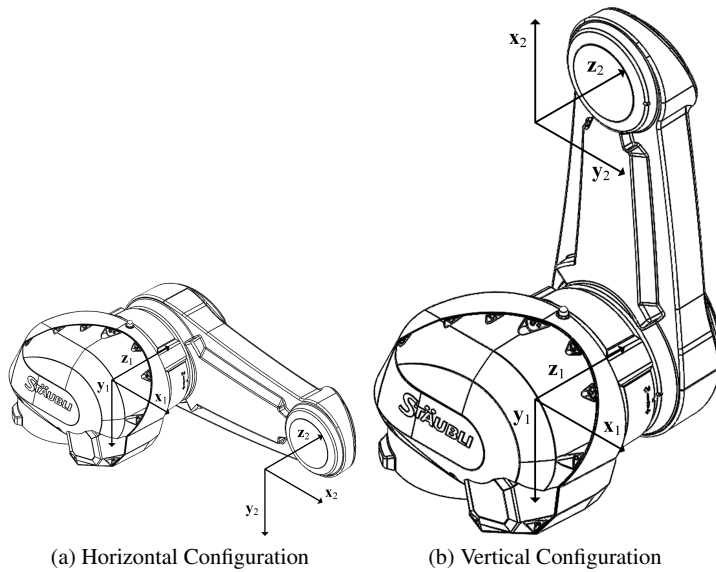


Fig. 4.44: Links 1 and 2 of an Industrial Robot

Problem 4.14. The two link robot in Figure (4.44b) is locked in the vertical configuration shown. As the instant shown, assume that $\theta_1 = 90^\circ$, or $\mathbf{x}_2 = -\mathbf{y}_1$ at the instant shown. Calculate the location of the center of mass of the robot in this configuration in terms of frame 1.

4.9.3 Problems on the Inertia matrix

Problem 4.15. Consider the rigid body studied in Problem (4.10). Assume the origin of frame \mathbb{X} (point x) is located along the axis of cylinder 2 and \mathbf{x}_1 is parallel to the axis of cylinder 1. Use symmetry arguments to show that the form of the *inertia matrix* about the point x relative to the \mathbb{X} frame is given by

$$\mathbf{I}_x^{\mathbb{X}} = \begin{bmatrix} I_{11} & 0 & 0 \\ 0 & I_{22} & 0 \\ 0 & 0 & I_{33} \end{bmatrix}$$

In other words, use symmetry arguments to show that the \mathbb{X} frame defines a set of *principal axes* for the composite body. Derive the entries of this matrix by using the *Parallel Axis Theorem* for each of the components of this composite body.

Problem 4.16. Consider the rigid body studied in Problems (4.10) and (4.15). Calculate the *inertia matrix* relative to axes parallel to the \mathbb{X} frame but whose origin is at the *center of mass* of the composite body.

Problem 4.17. Consider the rigid body studied in Problem (4.12). Use symmetry arguments to show that the form of the *inertia matrix* about the point x (the origin of frame \mathbb{X}) relative to frame \mathbb{X} is given by

$$\mathbf{I}_x^{\mathbb{X}} = \begin{bmatrix} I_{11} & 0 & 0 \\ 0 & I_{22} & 0 \\ 0 & 0 & I_{33} \end{bmatrix}$$

In other words, use symmetry arguments to show that the \mathbb{X} frame defines a set of *principal axes* for the composite body. Derive the entries of this matrix by using the *Parallel Axis Theorem* for each of the components of this composite body.

Problem 4.18. Consider the rigid body studied in Problems (4.12) and (4.17). Calculate the *inertia matrix* relative to axes parallel to the \mathbb{X} frame but whose origin is at the *center of mass* of the composite body.

Problem 4.19. Consider the rigid body studied in Problem (4.11). Use the *Parallel Axis Theorem* to calculate the *inertia matrix* relative to frame \mathbb{X} at its origin.

Problem 4.20. Consider the rigid body studied in Problems (4.10), (4.15) and (4.16). Calculate the *inertia matrix* about the point x relative to the frame that is obtained by rotating the \mathbb{X} frame by 30° about the \mathbf{x}_3 axis.

Problem 4.21. Consider the yoke studied in Problems (4.12), (4.17) and (4.18). Calculate the *inertia matrix* about the point x relative to the frame that is obtained by rotating the \mathbb{X} frame by 45° about the \mathbf{x}_2 axis.

Problem 4.22. Consider the two link robot shown in Figure (4.44a) and studied in Problem (4.13). Calculate the inertia matrix with respect to frame 1 at its origin for the system in this configuration.

Problem 4.23. Consider the two link robot shown in Figure (4.44b) and studied in Problem (4.14). Calculate the inertia matrix with respect to frame 1 at its origin for the system in this configuration.

Problem 4.24. Consider the satellite studied in Example (4.5.2) and shown in Figure (4.17). Let θ_A and θ_B be the joint variables that measure the rotation of solar arrays \mathbb{A} and \mathbb{B} about the $\mathbf{c}_1 = \mathbf{a}_1 = \mathbf{b}_1$ axis. Suppose the principal moments of inertia of the satellite body about its own center of mass relative to the \mathbb{C} frame are given in the form

$$\mathbf{I}_{c_C}^{\mathbb{C}} = \begin{bmatrix} I_{11} & 0 & 0 \\ 0 & I_{22} & 0 \\ 0 & 0 & I_{33} \end{bmatrix}$$

and the principal moments of inertia of each solar array about their own centers of mass (c_A and c_B , respectively) relative to their own body fixed frame are given in the form

$$\mathbf{I}_{c_A}^{\mathbb{A}} = \mathbf{I}_{c_B}^{\mathbb{B}} = \begin{bmatrix} K_{11} & 0 & 0 \\ 0 & K_{22} & 0 \\ 0 & 0 & K_{33} \end{bmatrix}$$

Find an expression for the inertia matrix of the satellite relative to the \mathbb{C} frame for any joint angle θ_A and θ_B .

4.9.4 Problems on Angular Momentum

Problems (4.25), (4.26) and (4.27) refer to the PUMA robot shown in Figures (4.35) and (4.36).

Problem 4.25. Compute the angular momentum in the 0 frame of link 1 (the shoulder) shown in Figures (4.35) and (4.36) about its own center of mass. Express your answer in terms of a frame whose origin is at the center of mass and that is parallel to the 1 frame.

Problem 4.26. Compute the angular momentum in the 0 frame of link 2 (the inner arm) depicted in Figures (4.35) and (4.36) about its own center of mass. Express your answer in terms of a frame whose origin is at the center of mass and that is parallel to the 2 frame.

Problem 4.27. Compute the angular momentum in the 0 frame of link 3 (the outer arm) depicted in Figures (4.35) and (4.36) about its own center of mass. Express your answer in terms of a frame whose origin is at the center of mass and that is parallel to the 3 frame.

Problems (4.28) and (4.29) refer to the robotic manipulator depicted in Figures (4.37) and (4.38).

Problem 4.28. Calculate the angular momentum of the 0 frame of link 1 (the inner arm) shown in Figures (4.37) and (4.38) about its own center of mass. Express your answer in terms of a frame that has its origin at the center of mass and that is parallel to the 1 frame.

Problem 4.29. Calculate the angular momentum in the 0 frame of link 2 (the outer arm) shown in Figures (4.37) and (4.38) about its own center of mass. Express your answer in terms of a frame that has its origin at the center of mass and that is parallel to the 2 frame.

Problems (4.30), (4.31) and (4.32) refer to the robotic manipulator depicted in Figures (4.39) and (4.40).

Problem 4.30. Compute the *angular momentum* in the 0 frame of link 1 (the vertical arm) shown in Figures (4.39) and (4.40) about its own center of mass. Express your answer in terms of the basis for frames 1 and 0.

Problem 4.31. Compute the *angular momentum* in the 0 frame of link 2 (the horizontal arm) shown in Figures (4.39) and (4.40) about its own center of mass. Express your answer in terms of the basis for frames 2, 1 and 0.

Problem 4.32. Compute the *angular momentum* in the 0 frame of link 3 (the tool carriage) shown in Figures (4.39) and (4.40) about its own center of mass. Express your answer in terms of the basis for frames 4, 3, 2, 1 and 0.

4.9.5 Problems on the Newton-Euler Equations

Problem 4.33. Frame \mathbb{A} is fixed in the outer link and frame \mathbb{B} is fixed in the inner link of the *spherical joint* shown in Figure (4.45). What are the constraints on the displacement and rotation imposed by the *spherical joint* on the bodies having fixed frames \mathbb{A} and \mathbb{B} ? How many *degrees of freedom* does the spherical joint have? Draw consistent free body diagrams for the *spherical joint*.

Problem 4.34. The *universal joint* shown in Figure (4.46) is comprised of a yoke with body fixed frame \mathbb{A} , a yoke with body fixed frame \mathbb{B} , and the crossbar with body fixed frame \mathbb{C} . Draw a set of complete free body diagrams for three components that make up the *universal joint*. Then, assume the mass and inertia matrix of the cross bar are negligible and derive an equivalent set of free body diagrams that eliminate the crossbar. How many degrees of freedom does the *universal joint* have?

Problem 4.35. Use the results of Problem (4.3) to write Euler's First Law for link 3 (the outer arm) of the PUMA robot in Figure (4.35).

Problem 4.36. Use the results of Problem (4.6) to write Euler's First Law for link 3 (the tool carriage) for the SCARA robot in Figure (4.37).

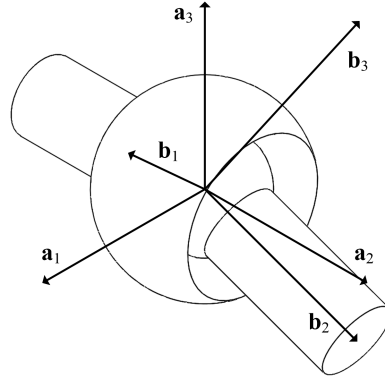


Fig. 4.45: Spherical Joint Frames

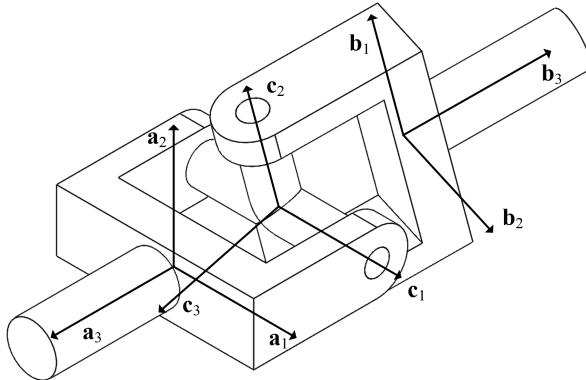


Fig. 4.46: Universal Joint Frames

Problem 4.37. Use the results of Problem (4.7) to write Euler's First Law for link 1 (the vertical arm) of the cylindrical robot in Figure (4.39).

Problem 4.38. Use the results of Problem (4.8) to write Euler's First Law for link 2 (the horizontal arm) of the cylindrical robot in Figure (4.39).

Problem 4.39. Use the results of Problem (4.9) to write Euler's First Law for link 3 (the tool carriage) of the cylindrical robot in Figure (4.39).

Problem 4.40. Use the results of Problem (4.27) to write Euler's Second Law for link 3 (the outer arm) of the PUMA robot shown in Figure (4.35).

Problem 4.41. Use the results of Problem (4.30) to write Euler's Second Law for link 1 (the vertical arm) of the cylindrical robot in Figure (4.39).

Problem 4.42. Use the results of Problem (4.31) to write Euler's Second Law for link 2 (the horizontal arm) of the cylindrical robot in Figure (4.39).

Problem 4.43. Use the results of Problem (4.32) to write Euler's Second Law for link 3 (the tool carriage) of the cylindrical robot in Figure (4.39).

Problem 4.44. Write Euler's Second Law for link 2 (the inner arm) of the robot in Example (4.5.6), taking moments about point q instead of the mass center of the arm. Note that the point q is not fixed in the inertial frame in this problem.

Problem 4.45. Write Euler's Second Law for link 1 (the shoulder) of the robot in Example (4.5.6), taking moments about the point o . Note that the point o is fixed in the inertial frame.

Chapter 5

Analytical Mechanics

Abstract The previous chapter summarized how the equations of motion for robotic systems can be derived from the Newton-Euler equations for individual rigid bodies. This chapter introduces the principles of *analytical mechanics*, an alternative approach for deriving the governing equations of robotic systems. Upon completion of this chapter, the student should be able to

- Define what is meant by a system of *generalized coordinates*.
- Define what is meant by a *virtual variation* of the generalized coordinates.
- Define what is meant by the *virtual work* performed by forces or moments.
- Define what is meant by the set of *generalized forces*.
- State *Hamilton's Principle* and employ it to derive the equations of motion.
- State *Lagrange's Equations* and employ them to derive the equations of motion.
- Apply the principles of analytical mechanics to study robotic systems.

5.1 Hamilton's Principle

5.1.1 Generalized Coordinates

This section introduces a technique that will play an important role in the consideration of analytical mechanics, Hamilton's Principle for conservative mechanical systems. A few definitions from analytical mechanics are required to formulate this principle.

Definition 5.1. A collection of N time-dependent parameters $\mathbf{q}(t) = \{q_1(t), q_2(t), \dots, q_N(t)\}^T$ is a set of *generalized coordinates* for a mechanical system if for any point p in the mechanical system the position $\mathbf{r}_{\mathbb{X},p}(t)$ at any time $t \in \mathbb{R}^+$ with respect to the inertial frame \mathbb{X} can be written uniquely in terms of $\mathbf{q}(t) = \{q_1(t), q_2(t), \dots, q_N(t)\}^T$ and possibly time t . That is, it must be possible to express the position vector $\mathbf{r}_{X,p}(t)$ in the form

$$\mathbf{r}_{\mathbb{X},p}(t) := \mathbf{r}_{\mathbb{X},p}(q_1(t), q_2(t), \dots, q_N(t), t) \quad (5.1.1)$$

uniquely in terms of $\mathbf{q}(t) = \{q_1(t), q_2(t), \dots, q_N(t)\}^T$ for all points p in the mechanical system, and this unique expression holds for all configurations of the mechanical system and for all time $t \in \mathbb{R}^+$. The number N is said to be the *number of degrees of freedom* of the mechanical system.

A few comments are in order regarding this definition. Definition (5.1) requires that the set of generalized coordinates is *minimal* or *independent*. There can be many different choices of generalized coordinates for a specific mechanical system, but any two sets of generalized coordinates must have the same number of time-dependent functions. This means that the number of degrees of freedom is a property of the system and does not depend on the specific choice of generalized coordinates. It is not possible to express any of the individual generalized coordinates in terms of a subset of the remaining coordinates. If this were possible, then it would follow that there are multiple ways to express the identity in Equation (5.1.1), which must be a unique function of the generalized coordinates. Some authors do not insist that a set of generalized coordinates must be minimal, or independent. In fact, Section (5.5) of this chapter will extend the presented definition and introduce *redundant generalized coordinates*. In this text, the phrase generalized coordinates will always refer to a minimal, or independent, set. The phrase *redundant generalized coordinates* will always be used in the event the coordinates are not minimal, nor independent.

Finally, the notation used when discussing collections of generalized coordinates can vary slightly depending on the context. When discussing the *value* that a collection of generalized coordinates take at a particular time $t \in \mathbb{R}^+$, the expression

$$\mathbf{q}(t) = \{q_1(t), q_2(t), \dots, q_N(t)\}$$

is used. Alternatively, when referring to generalized coordinates as a set of *functions* of time, the notation

$$\mathbf{q} = \{q_1, q_2, \dots, q_N\}^T$$

is used.

Example 5.1.1. A point mass is constrained so that it moves on the plane as depicted in Figure (5.1). Show that the coordinates x and y of the point mass along the

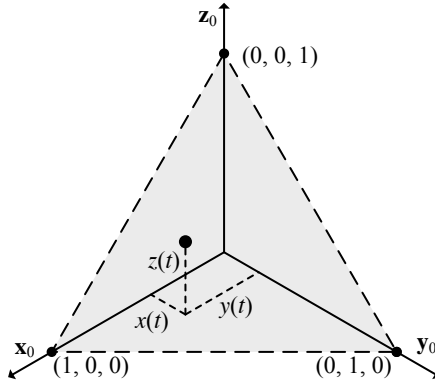


Fig. 5.1: Point Mass Constrained to Move on an Inclined Plane

\mathbf{x}_0 and \mathbf{y}_0 directions are a set of *generalized coordinates* for this mechanical system, $q_1(t) := x(t)$ and $q_2(t) := y(t)$.

Solution: The mechanical system contains a single mass, so it only needs to be shown that the position of the mass has the form

$$\mathbf{r}_{0,m}(t) = \mathbf{r}_{0,m}(q_1(t), q_2(t), t),$$

and that this expression is unique in terms of the time-varying parameters $q_1(t), q_2(t)$.

Let $\{x_p, y_p, z_p\}^T$ be some fixed point that lies on the plane shown in Figure (5.1). The Cartesian coordinates of the mass are given by $\mathbf{r}_{0,m}(t) = \{x(t), y(t), z(t)\}^T$. The condition that the location $\mathbf{r}_{0,m}(t) = \{x(t), y(t), z(t)\}^T$ of the point mass is constrained to lie on the plane requires that the vector

$$\begin{Bmatrix} x(t) \\ y(t) \\ z(t) \end{Bmatrix} - \begin{Bmatrix} x_p \\ y_p \\ z_p \end{Bmatrix}$$

is perpendicular to the normal \mathbf{n} to the plane. Stating this mathematically,

$$\left(\begin{Bmatrix} x(t) \\ y(t) \\ z(t) \end{Bmatrix} - \begin{Bmatrix} x_p \\ y_p \\ z_p \end{Bmatrix} \right) \cdot \mathbf{n} = 0.$$

The unit normal to the plane shown in Figure (5.1) is equal to $\mathbf{n}^T = \frac{1}{\sqrt{3}} \{1, 1, 1\}$. As a result, the constraint that ensures the mass point lies on the plane may be calculated as

$$(x(t) - x_p) + (y(t) - y_p) + (z(t) - z_p) = 0.$$

If the fixed point on the plane is chosen as $\{x_p, y_p, z_p\}^T = \{1, 0, 0\}^T$, the final form of the constraint is

$$x(t) + y(t) + z(t) - 1 = 0.$$

The fixed point on the plane could also have been chosen to be $(0, 1, 0)$ or $(0, 0, 1)$: the constraint equation remains the same for any valid choice of the point $\{x_p, y_p, z_p\}$. Solving this equation for $z(t)$ and substituting the result into $\mathbf{r}_{0,m}(t)$ results in

$$\mathbf{r}_{0,m}(t) = x(t)\mathbf{x}_0 + y(t)\mathbf{y}_0 + (1 - x(t) - y(t))\mathbf{z}_0.$$

Since $x(t)$ and $y(t)$ are independent, this expression is unique in terms of $x(t)$ and $y(t)$. Therefore, the time-varying parameters $x(t)$ and $y(t)$ are indeed a set of generalized coordinates for this system. In this problem, the Cartesian coordinates $\{x(t), y(t), z(t)\}^T$ are not a set of generalized coordinates for the system since they are dependent.

5.1.2 Functionals and the Calculus of Variations

In contrast to the determination of equations of motion from the Newton-Euler equations introduced in Chapter (4), the techniques of analytical mechanics are defined via *extremization problems*. The extremization studied here is posed in terms of the generalized coordinates for a mechanical system. The solution of an extremization problem seeks to find the *extrema* of some quantity. The extrema are the minima, maxima or inflection points of the quantity under consideration. For the solution of an extremization problem for some differentiable real-valued function, there is a standard and well-known procedure from elementary calculus: taking the derivative and setting the derivative equal to zero.

The extremization problems in analytical mechanics are not couched in terms of classical real-valued functions. They are expressed in terms of certain functionals of the generalized coordinates. The solution of extremization problems associated with functionals is the topic of the *calculus of variations*.

Definition 5.2. A *functional* is an operator or mapping whose input is an N -tuple of functions and whose output is a real number. In other words, a functional J is a mapping from a set of functions

$$\mathbf{q} = \{q_1, q_2, \dots, q_N\}^T$$

to a real number,

$$\left\{ \begin{array}{c} q_1 \\ \vdots \\ q_N \end{array} \right\} \mapsto J(q_1, \dots, q_N) \in \mathbb{R}.$$

Some references define a functional as a “function that acts on functions.” If

$$\mathbf{q} = \{q_1, q_2, \dots, q_N\}^T$$

is a set of generalized coordinates, then the integral in time from t_0 to t_f of the kinetic energy or the potential energy are two examples of functionals that act on \mathbf{q} . Note that the input to the functional is a set of functions of time. For example, to evaluate the integral of either the potential energy or the kinetic energy, it is necessary to know the generalized coordinates over the entire time interval of interest.

It was noted that the solution of an extremization problem for a classically differentiable real-valued function is achieved by differentiation of the function and setting the derivative equal to zero. However, the classical definition of a derivative does not apply to a functional. Instead, the *Gateaux derivative*, or *G-derivative*, of a functional is defined. The Gateaux derivative will be used to solve the extremization problems for functionals.

Definition 5.3. Let J be a functional that acts on the collection of functions $\mathbf{q} = \{q_1, q_2, \dots, q_N\}^T$. The *Gateaux derivative*, or *G-derivative*, $DJ(\mathbf{q}, \mathbf{p})$ of the functional J at \mathbf{q} in the \mathbf{p} direction is defined to be

$$DJ(\mathbf{q}, \mathbf{p}) := \lim_{\epsilon \rightarrow 0} \frac{J(\mathbf{q} + \epsilon \mathbf{p}) - J(\mathbf{q})}{\epsilon}.$$

In this equation the direction \mathbf{p} is a vector function of N time-varying scalar functions

$$\mathbf{p}(t) = \{p_1(t), p_2(t), \dots, p_N(t)\}^T.$$

The vector of functions $\mathbf{p} = \{p_1(t), p_2(t), \dots, p_N(t)\}^T$ in Definition (5.3) may also be referred to as the directions of variation or vector of variations. Usually, Definition (5.3) is not used to solve practical problems in analytical mechanics. There are alternative formulations that are often simpler to calculate the G-derivative in specific problems. One such method is summarized in the following theorem.

Theorem 5.1. If the functional J is G-differentiable, the G-derivative $DJ(\mathbf{q}, \mathbf{p})$ of J at \mathbf{q} in the \mathbf{p} direction can be calculated via the identity

$$DJ(\mathbf{q}, \mathbf{p}) = \left. \frac{d}{d\epsilon} J(\mathbf{q} + \epsilon \mathbf{p}) \right|_{\epsilon=0}.$$

Proof. Choose some fixed set of functions of time for the generalized coordinates \mathbf{q} and directions \mathbf{p} , and define the scalar function $g(\epsilon)$ from the equation

$$g(\epsilon) := J(\mathbf{q} + \epsilon \mathbf{p}).$$

Observe that, for a fixed choice of \mathbf{q} and \mathbf{p} , $g(\epsilon)$ is a conventional real-valued function: it maps a real number ϵ into the real number $g(\epsilon)$. An esoteric means to define

the derivative of $g(\epsilon)$ with respect to ϵ is not needed; the classical definition works just fine. Taking the derivative results in

$$\frac{dg}{d\epsilon} = \lim_{\Delta \rightarrow 0} \left(\frac{g(\epsilon + \Delta) - g(\epsilon)}{\Delta} \right)$$

whenever the limit on the right hand side exists. Expanding the quotient on the right hand side in terms of the functional J results in

$$\lim_{\Delta \rightarrow 0} \left(\frac{g(\epsilon + \Delta) - g(\epsilon)}{\Delta} \right) = \lim_{\Delta \rightarrow 0} \left(\frac{J(\mathbf{q} + (\epsilon + \Delta)\mathbf{p}) - J(\mathbf{q} + \epsilon\mathbf{p})}{\Delta} \right).$$

Evaluating $\frac{dg}{d\epsilon}$ at $\epsilon = 0$ finishes the proof of the theorem, showing that

$$\begin{aligned} \frac{dg}{d\epsilon} \Big|_{\epsilon=0} &= \left\{ \lim_{\Delta \rightarrow 0} \left(\frac{J(\mathbf{q} + (\epsilon + \Delta)\mathbf{p}) - J(\mathbf{q} + \epsilon\mathbf{p})}{\Delta} \right) \right\} \Big|_{\epsilon=0}, \\ &= \lim_{\Delta \rightarrow 0} \frac{J(\mathbf{q} + \Delta\mathbf{p}) - J(\mathbf{q})}{\Delta}, \\ &= DJ(\mathbf{q}, \mathbf{p}). \end{aligned}$$

This is the desired result. \square

This section is closed with a definition of *stationarity* of a functional. The definition of stationarity closely resembles the condition used to find the extrema of classically differentiable functions.

Definition 5.4. The functional J is *stationary* at \mathbf{q} over the set of directions \mathcal{P} provided that

$$DJ(\mathbf{q}, \mathbf{p}) = 0$$

for all directions $\mathbf{p} \in \mathcal{P}$.

The definition of the Gateaux derivative $DJ(\mathbf{q}, \mathbf{p})$ of the functional J at \mathbf{q} in the direction \mathbf{p} might initially seem abstract. The following example illustrates the similarity of the Gateaux derivative to the *directional derivative* of vector calculus. This similarity can help visualize the meaning of the Gateaux derivative. In fact, the directional derivative can be viewed rigorously as a special case of the Gateaux derivative.

Example 5.1.2. Consider the hemispherical surface shown in Figure (5.2). The equation that defines this surface is given by

$$x^2 + y^2 + z^2 = R^2$$

where (x, y, z) are the Cartesian coordinates of a point on the surface having radius R . Evaluate the rate of change of z when moving along the two dimensional slice

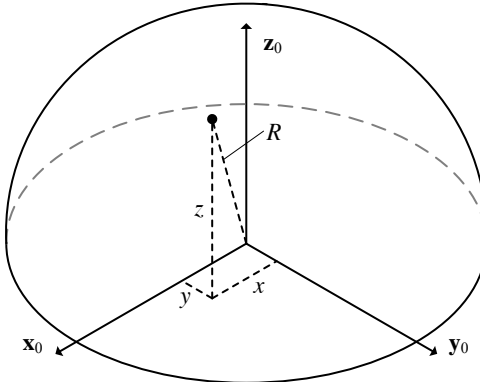


Fig. 5.2: Point on Hemispherical Surface

of the surface where $x = 0$. Evaluate the rate of change of z when moving along the two dimensional slice of the surface when $y = 0$.

Solution: Solving for z as a function of y when $x = 0$ results in

$$z(y) = \sqrt{R^2 - y^2}.$$

The slope of the curve dz/dy gives the rate of change of z as y varies on the plane defined by $x = 0$,

$$\frac{dz}{dy} = -\frac{y}{\sqrt{R^2 - y^2}}.$$

A similar analysis can be used to define the rate of change of z while x varies and $y = 0$,

$$\frac{dz}{dx} = -\frac{x}{\sqrt{R^2 - x^2}}.$$

Each of these examples is a special case of a general analysis that can be described using the *directional derivative*. The directional derivative of a function $f : \mathbb{R}^2 \rightarrow \mathbb{R}$ at $\mathbf{x} \in \mathbb{R}^2$ in the \mathbf{n} direction is given by

$$Df(\mathbf{x}, \mathbf{n}) = \nabla f(\mathbf{x}) \cdot \mathbf{n}$$

where

$$\nabla f(\mathbf{x}) = \left(\frac{\partial f}{\partial x} \mathbf{x}_0 + \frac{\partial f}{\partial y} \mathbf{y}_0 \right) \Big|_{\mathbf{x}}.$$

For the problem at hand,

$$\nabla f(\mathbf{x}) = \frac{-x}{\sqrt{R^2 - x^2 - y^2}} \mathbf{x}_0 + \frac{-y}{\sqrt{R^2 - x^2 - y^2}} \mathbf{y}_0,$$

where the function $f(\mathbf{x}) := z = \sqrt{(R^2 - x^2 - y^2)}$.

The directional derivative at a point on the plane $y = 0$ along the \mathbf{x}_0 direction is given by

$$Df\left(\begin{Bmatrix} x \\ 0 \end{Bmatrix}, \begin{Bmatrix} 1 \\ 0 \end{Bmatrix}\right) = \left. \begin{Bmatrix} -\frac{x}{\sqrt{R^2 - x^2 - y^2}} \\ -\frac{y}{\sqrt{R^2 - x^2 - y^2}} \end{Bmatrix} \right|_{y=0} \cdot \begin{Bmatrix} 1 \\ 0 \end{Bmatrix} = -\frac{x}{\sqrt{R^2 - x^2}}.$$

This is identical to the derivative calculated earlier. Similarly, the directional derivative at a point on the plane $x = 0$ along the \mathbf{y}_0 direction is given by

$$Df\left(\begin{Bmatrix} 0 \\ y \end{Bmatrix}, \begin{Bmatrix} 0 \\ 1 \end{Bmatrix}\right) = \left. \begin{Bmatrix} -\frac{x}{\sqrt{R^2 - x^2 - y^2}} \\ -\frac{y}{\sqrt{R^2 - x^2 - y^2}} \end{Bmatrix} \right|_{x=0} \cdot \begin{Bmatrix} 0 \\ 1 \end{Bmatrix} = -\frac{y}{\sqrt{R^2 - y^2}},$$

which also matches the derivative calculated earlier.

The solution above can also be found in Example ?? of the MATLAB Workbook for DCRS.

5.1.3 Hamilton's Principle for Conservative Systems

The previous section defined the generalized coordinates that can be used to specify the position in physical space of any point in the mechanical system as

$$\mathbf{r}_{\mathbb{X},p}(t) = \mathbf{r}_{\mathbb{X},p}(q_1(t), q_2(t), \dots, q_N(t), t).$$

The introduction of generalized coordinates suggests another way to visualize the motion of a mechanical system. The generalized coordinates are used to define a *trajectory* in *configuration space*.

Definition 5.5. Suppose that $\{q_1, q_2, \dots, q_N\}$ is a set of generalized coordinates for a mechanical system. The *configuration space* is the set of all possible values in \mathbb{R}^N that the generalized coordinates can assume. The mapping

$$t \mapsto \begin{Bmatrix} q_1(t) \\ q_2(t) \\ \dots \\ q_N(t) \end{Bmatrix}$$

defines a *trajectory* or *motion* in *configuration space*.

Figure (5.3) provides a geometric interpretation of trajectories in configuration space. In this figure two trajectories $\mathbf{q}(t)$ and $\hat{\mathbf{q}}(t)$ are depicted and each coordinate axis measures one generalized coordinate q_i for $i = 1, 2, \dots, N$. It must be emphasized that the trajectory shown is an abstract trajectory in configuration space and not a trajectory in physical, three-dimensional space. The trajectory in configuration space will have N components for an N degree of freedom mechanical system, and it is not possible to plot this trajectory in a single spatial representation in general when $N > 3$. Every possible motion of the mechanical system in physical space

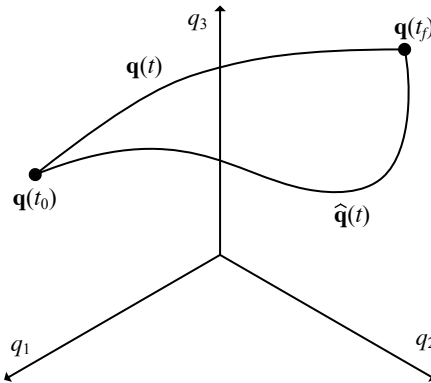


Fig. 5.3: Two Trajectories in Configuration Space

can be seen as corresponding to or *generated by* a trajectory in configuration space. Of all these trajectories that describe possible motions in configuration space, the *actual motion* or *actual trajectory* is denoted by $\mathbf{q}(t) = \{q_1(t), q_2(t), \dots, q_N(t)\}^T$. Any possible motion can be expressed $\hat{\mathbf{q}}(t)$ in configuration space as

$$\hat{\mathbf{q}}(t) = \mathbf{q}(t) + \epsilon \mathbf{p}(t) \quad (5.1.2)$$

where ϵ is a constant and $\mathbf{p}(t_0) = \mathbf{p}(t_f) = 0$. It is common to describe this equation in terms of vector expressions. The *possible motion* $\dot{\mathbf{q}}(t)$ is said to be obtained from the *true motion* $\mathbf{q}(t)$ by a perturbation in the *direction* $\mathbf{p}(t)$.

With these definitions, the first, and in some sense prototypical, governing relationship for analytical mechanics may be given. The following theorem summarizes *Hamilton's Principle for conservative mechanical systems*.

Theorem 5.2. Let $\mathbf{q}(t) := \{q_1(t), q_2(t), \dots, q_N(t)\}^T$ be a collection of generalized coordinates for a conservative mechanical system. Of all the possible motions of the mechanical system that are consistent with the kinematic constraints, the actual motion of the system renders stationary the action functional $A(\mathbf{q})$

$$A(\mathbf{q}) := \int_{t_0}^{t_f} (T - V) dt \quad (5.1.3)$$

where T is the kinetic energy and V is the potential energy of the mechanical system.

One of the impressive features of Hamilton's Principle is its succinct form. It serves as the foundation for other approaches in analytical mechanics including Lagrange's equations discussed in Section (5.2). As shown in the next few examples and the problems at the end of this chapter, Hamilton's Theorem can be used directly to solve problems of interest.

Example 5.1.3. Derive the equations of motion of mechanical system shown in Figure (5.1) and discussed in Example (5.1.1). Choose as the set of generalized coordinates $q_1(t) := x(t)$ and $q_2(t) := y(t)$.

Solution: For the mechanical system shown in Example (5.1.1), the Cartesian coordinates $x(t), y(t), z(t)$ satisfy the equation

$$x(t) + y(t) + z(t) - 1 = 0.$$

The kinetic energy of the system is given by

$$T = \frac{1}{2} m \mathbf{v}_{0,m} \cdot \mathbf{v}_{0,m} = \frac{1}{2} m (\dot{x}^2 + \dot{y}^2 + \dot{z}^2) = \frac{1}{2} m (2\dot{x}^2 + 2\dot{y}^2 + 2\dot{x}\dot{y}).$$

It is standard to write the kinetic energy in quadratic form in terms of a *mass matrix* \mathbf{M} , such that

$$T = \frac{1}{2} \begin{Bmatrix} \dot{x} & \dot{y} \end{Bmatrix} \begin{bmatrix} 2m & m \\ m & 2m \end{bmatrix} \begin{Bmatrix} \dot{x} \\ \dot{y} \end{Bmatrix} = \frac{1}{2} \dot{\mathbf{q}}^T \mathbf{M} \dot{\mathbf{q}}.$$

The potential energy can be expressed as

$$V = mgz = mg(1 - x - y)$$

if the $\mathbf{x}_0, \mathbf{y}_0$ plane is taken as the datum with zero potential energy. The stationarity condition for the action functional will be calculated by requiring

$$DA(\mathbf{q}, \mathbf{p}) = \frac{d}{d\epsilon} A(\mathbf{q} + \epsilon\mathbf{p}) \Big|_{\epsilon=0} = 0$$

for all $\mathbf{p} \in \mathcal{P}$. The possible motions are represented in Equation (5.1.2) as

$$\begin{aligned} \left\{ \begin{array}{l} \hat{q}_1(t) \\ \hat{q}_2(t) \end{array} \right\} &= \left\{ \begin{array}{l} q_1(t) \\ q_2(t) \end{array} \right\} + \epsilon \left\{ \begin{array}{l} p_1(t) \\ p_2(t) \end{array} \right\}, \\ \hat{\mathbf{q}}(t) &= \mathbf{q}(t) + \epsilon\mathbf{p}(t), \end{aligned}$$

where p_1 and p_2 are the directions in \mathbf{p} . The stationarity condition becomes

$$\begin{aligned} DA(\mathbf{q}, \mathbf{p}) &= \frac{d}{d\epsilon} (A(\mathbf{q} + \epsilon\mathbf{p})) \Big|_{\epsilon=0}, \\ &= \frac{d}{d\epsilon} \left\{ \int_{t_0}^{t_f} \left(\frac{1}{2} (\dot{\mathbf{q}} + \epsilon\dot{\mathbf{p}})^T \mathbf{M} (\dot{\mathbf{q}} + \epsilon\dot{\mathbf{p}}) - V(\mathbf{q} + \epsilon\mathbf{p}) \right) d\tau \right\} \Big|_{\epsilon=0}, \\ &= \int_{t_0}^{t_f} \left(\frac{d}{d\epsilon} \left\{ \frac{1}{2} (\dot{\mathbf{q}} + \epsilon\dot{\mathbf{p}})^T \mathbf{M} (\dot{\mathbf{q}} + \epsilon\dot{\mathbf{p}}) - V(\mathbf{q} + \epsilon\mathbf{p}) \right\} \Big|_{\epsilon=0} \right) d\tau, \\ &= \int_{t_0}^{t_f} \left(\left\{ \frac{1}{2} \dot{\mathbf{p}}^T \mathbf{M} (\dot{\mathbf{q}} + \epsilon\dot{\mathbf{p}}) + \frac{1}{2} (\dot{\mathbf{q}} + \epsilon\dot{\mathbf{p}})^T \mathbf{M} \dot{\mathbf{p}} - \left[\frac{\partial V}{\partial x} \quad \frac{\partial V}{\partial y} \right] \mathbf{p} \right\} \Big|_{\epsilon=0} \right) d\tau, \\ &= \int_{t_0}^{t_f} \left\{ \dot{\mathbf{q}}^T \mathbf{M} \dot{\mathbf{p}} - \left[-mg \quad -mg \right] \mathbf{p} \right\} d\tau. \end{aligned} \tag{5.1.4}$$

Integration by parts is used to move the derivative appearing in $\dot{\mathbf{p}}$ onto the derivative of the generalized coordinates $\dot{\mathbf{q}}$, and the value of the variations $\mathbf{p}(t_0) = \mathbf{p}(t_f) = \mathbf{0}$ (based on the discussion following Equation (5.1.2)) are used to formulate $DA(\mathbf{q}, \mathbf{p})$ as

$$\begin{aligned} DA(\mathbf{q}, \mathbf{p}) &= \dot{\mathbf{q}}^T \mathbf{M} \mathbf{p} \Big|_{t_0}^{t_f} - \int_{t_0}^{t_f} \left\{ -\ddot{\mathbf{q}}^T \mathbf{M} + mg \begin{bmatrix} 1 & 1 \end{bmatrix} \right\} \mathbf{p} d\tau, \\ &= \int_{t_0}^{t_f} \left\{ -\mathbf{M} \ddot{\mathbf{q}} + mg \begin{bmatrix} 1 \\ 1 \end{bmatrix} \right\} \cdot \mathbf{p} d\tau = 0. \end{aligned}$$

For this equation to be equal to zero for all choices of the directions $\mathbf{p} \in \mathcal{P}$ as stationarity requires, the integrand must be identically equal to zero. The governing equations thus become

$$\begin{bmatrix} 2 & 1 \\ 1 & 2 \end{bmatrix} \begin{Bmatrix} \ddot{x} \\ \ddot{y} \end{Bmatrix} = g \begin{Bmatrix} 1 \\ 1 \end{Bmatrix}.$$

The derivation of the variational expression in Equation 5.1.4 can also be found in Example ?? of the MATLAB Workbook for DCRS.

Example 5.1.4. This example considers the two mass system shown in Figure (5.4). The two masses are connected to springs with stiffness k , and in the static equilibrium configuration all the springs are unstretched. Derive the equations of motion for this system using Hamilton's Principle.

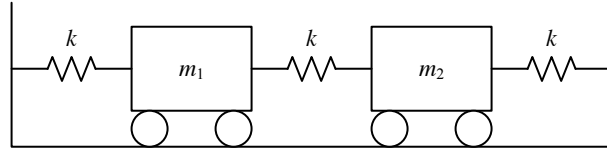


Fig. 5.4: Two Mass System

Solution: The set of generalized coordinates for this system are defined as $q_1(t) := x_1(t)$ and $q_2(t) := x_2(t)$, where $x_1(t)$ and $x_2(t)$ measure the displacement of the masses relative to the inertial frame. Assume that the springs are unstretched when $x_1 = x_2 = 0$. The definitions of the vector of generalized coordinates and directions of variation are $\mathbf{q} = \{q_1 \ q_2\}^T$ and $\mathbf{p} = \{p_1 \ p_2\}^T$, respectively. It can be checked that every admissible configuration of this system can be expressed in terms of these two time-varying parameters, and the position of each mass is given by a unique expression in terms of q_1 and q_2 .

The kinetic energy T and potential energy V of the system are

$$T = \frac{1}{2}m_1\dot{q}_1^2 + \frac{1}{2}m_2\dot{q}_2^2,$$

$$V = \frac{1}{2}Kq_1^2 + \frac{1}{2}K(q_1 - q_2)^2 + \frac{1}{2}Kq_2^2.$$

The expression

$$DA(\mathbf{q}, \mathbf{p}) := \frac{d}{d\epsilon} A(\mathbf{q} + \epsilon\mathbf{p}) \Big|_{\epsilon=0} = 0$$

will be used to calculate the equations of motion from Hamilton's Principle. Recall that the possible motions in Equation (5.1.2) are given by

$$\begin{cases} \hat{q}_1(t) \\ \hat{q}_2(t) \end{cases} = \begin{cases} q_1(t) \\ q_2(t) \end{cases} + \epsilon \begin{cases} p_1(t) \\ p_2(t) \end{cases},$$

$$\hat{\mathbf{q}}(t) = \mathbf{q}(t) + \epsilon\mathbf{p}(t),$$

where p_1, p_2 are the directions of variation in \mathbf{p} . Therefore,

$$\begin{aligned}
& \frac{d}{d\epsilon} A(\mathbf{q} + \epsilon \mathbf{p}) \Big|_{\epsilon=0}, \\
&= \frac{d}{d\epsilon} \left(\int_{t_0}^{t_f} \left(\frac{1}{2} m_1 (\dot{q}_1 + \epsilon \dot{p}_1)^2 + \frac{1}{2} m_2 (\dot{q}_2 + \epsilon \dot{p}_2)^2 - V(\mathbf{q} + \epsilon \mathbf{p}) \right) d\tau \right) \Big|_{\epsilon=0}, \\
&= \int_{t_0}^{t_f} \frac{d}{d\epsilon} \left(\frac{1}{2} m_1 (\dot{q}_1 + \epsilon \dot{p}_1)^2 + \frac{1}{2} m_2 (\dot{q}_2 + \epsilon \dot{p}_2)^2 - V(\mathbf{q} + \epsilon \mathbf{p}) \right) \Big|_{\epsilon=0} d\tau, \\
&= \int_{t_0}^{t_f} \left(m_1 (\dot{q}_1 + \epsilon \dot{p}_1) \dot{p}_1 + m_2 (\dot{q}_2 + \epsilon \dot{p}_2) \dot{p}_2 - \left(\frac{\partial V}{\partial q_1} p_1 + \frac{\partial V}{\partial q_2} p_2 \right) \right) \Big|_{\epsilon=0} d\tau, \\
&= \int_{t_0}^{t_f} (m_1 \dot{q}_1 \dot{p}_1 + m_2 \dot{q}_2 \dot{p}_2 - k(2q_1 + q_2)p_1 - k(q_1 + 2q_2)p_2) d\tau.
\end{aligned}$$

Integration by parts can be used to move the derivatives from \dot{p}_1 and \dot{p}_2 to \dot{q}_1 and \dot{q}_2 in the first two terms, thereby resulting in

$$\begin{aligned}
DA(\mathbf{q}, \mathbf{p}) &= (m_1 \dot{q}_1 p_1 + m_2 \dot{q}_2 p_2) \Big|_{t_0}^{t_f} - \int_{t_0}^{t_f} (m_1 \ddot{q}_1 p_1 + m_2 \ddot{q}_2 p_2) d\tau \quad (5.1.5) \\
&\quad - \int_{t_0}^{t_f} ((2kq_1 - kq_2)p_1 + (-kq_1 + 2kq_2)p_2) d\tau.
\end{aligned}$$

Again, since the values of the variations of the initial and final times satisfy

$$\mathbf{p}(t_0) = \mathbf{p}(t_f) = \mathbf{0}$$

by definition, and stationarity requires $DA(\mathbf{q}, \mathbf{p}) = 0$, the last equation can be written as a matrix

$$\int_{t_0}^{t_f} \left\{ \begin{bmatrix} m_1 & 0 \\ 0 & m_2 \end{bmatrix} \begin{Bmatrix} \ddot{q}_1 \\ \ddot{q}_2 \end{Bmatrix} + \begin{bmatrix} 2k & -k \\ -k & 2k \end{bmatrix} \begin{Bmatrix} q_1 \\ q_2 \end{Bmatrix} \right\} \cdot \begin{Bmatrix} p_1 \\ p_2 \end{Bmatrix} d\tau = 0.$$

This equation must hold for all choices of the directions $p_1, p_2 \in \mathcal{P}$. Therefore, the integrand must be equal to zero, and the equations of motion are

$$\begin{bmatrix} m_1 & 0 \\ 0 & m_2 \end{bmatrix} \begin{Bmatrix} \ddot{q}_1 \\ \ddot{q}_2 \end{Bmatrix} + \begin{bmatrix} 2k & -k \\ -k & 2k \end{bmatrix} \begin{Bmatrix} q_1 \\ q_2 \end{Bmatrix} = \begin{Bmatrix} 0 \\ 0 \end{Bmatrix}.$$

This solution for the variations in Equation 5.1.5 is carried out in Example ?? in the MATLAB Workbook for DCRS.

Example 5.1.5. This example analyzes the two link robotic arm depicted in Figure (5.5). It is assumed that the bars having length L_1 and L_2 have negligible mass in this example. All of the mass is concentrated in the two point masses m_1 and m_2 . Frame 0 is fixed to the ground, and frames \mathbb{B} and \mathbb{C} are fixed to masses m_1 and

m_2 , respectively. Derive the equations of motion for this mechanical system using

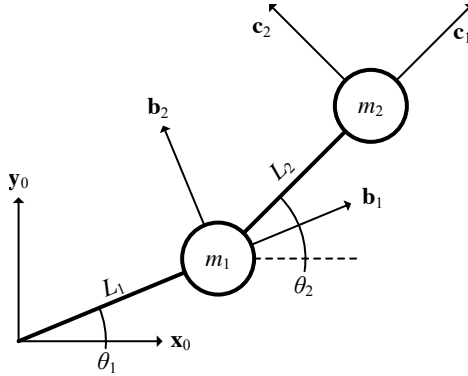


Fig. 5.5: Two Link Robotic Arm with Point Masses, Absolute Joint Angles

Hamilton's Principle for conservative mechanical systems. Note that the angles θ_1 and θ_2 are absolute, not relative angles. Both angles are measured from the inertial x_0 axis.

Solution: The two joint angles θ_1 and θ_2 are selected as generalized coordinates for this mechanical systems. Therefore, $q_1 = \theta_1$ and $q_2 = \theta_2$ for this problem. As required, the position of every point in the system can be written in terms of these time-dependent parameters. The locations of the masses with respect to the frame 0 origin are, respectively,

$$\begin{aligned}\mathbf{r}_{0,1}(t) &= L_1 \cos \theta_1 \mathbf{x}_0 + L_1 \sin \theta_1 \mathbf{y}_0, \\ \mathbf{r}_{0,2}(t) &= (L_1 \cos \theta_1 + L_2 \cos \theta_2) \mathbf{x}_0 + (L_1 \sin \theta_1 + L_2 \sin \theta_2) \mathbf{y}_0.\end{aligned}$$

These expressions are uniquely determined in terms of the angles θ_1 and θ_2 when θ_1 and θ_2 are restricted to $[0, 2\pi)$. The potential energy of the system is defined

$$V = m_1 g L_1 \sin \theta_1 + m_2 g (L_1 \sin \theta_1 + L_2 \sin \theta_2)$$

by assuming gravity acts in the $-\mathbf{y}_0$ direction and the \mathbf{x}_0 axis is the datum for zero potential energy. The kinetic energy of the system is defined as

$$T = \frac{1}{2} m_1 \mathbf{v}_{0,1} \cdot \mathbf{v}_{0,1} + \frac{1}{2} m_2 \mathbf{v}_{0,2} \cdot \mathbf{v}_{0,2}$$

The two velocities required in the kinetic energy can be derived using Theorem (2.16), resulting in $\mathbf{v}_{0,1} = L_1 \dot{\theta}_1 \mathbf{b}_2$ and $\mathbf{v}_{0,2} = L_1 \dot{\theta}_1 \mathbf{b}_2 + L_2 \dot{\theta}_2 \mathbf{c}_2$. Therefore, the kinetic energy is calculated as

$$\begin{aligned} T &= \frac{1}{2}m_1L_1^2\dot{\theta}_1^2 + \frac{1}{2}m_2(L_2^2\dot{\theta}_1^2 + L_2^2\dot{\theta}_2^2 + 2L_1L_2\dot{\theta}_1\dot{\theta}_2(\mathbf{b}_2 \cdot \mathbf{c}_2)), \\ &= \frac{1}{2}(m_1+m_2)L_1^2\dot{\theta}_1^2 + \frac{1}{2}m_2L_2^2\dot{\theta}_2^2 + m_2L_1L_2\dot{\theta}_1\dot{\theta}_2\cos(\theta_2 - \theta_1). \end{aligned}$$

where the dot product $\mathbf{b}_2 \cdot \mathbf{c}_2 = \|\mathbf{b}_2\| \|\mathbf{c}_2\| \cos(\theta_2 - \theta_1)$ from the definition of the dot product. This kinetic energy expression can be written in quadratic form in terms of the derivatives of the generalized coordinates

$$T = \frac{1}{2}\dot{\mathbf{q}}^T \mathbf{M} \dot{\mathbf{q}} = \frac{1}{2} \sum_{i,j} \dot{q}_i m_{ij} \dot{q}_j$$

with $\mathbf{q} = \begin{Bmatrix} q_1 & q_2 \end{Bmatrix}^T$ and

$$\mathbf{M} = \begin{bmatrix} m_{11} & m_{12} \\ m_{21} & m_{22} \end{bmatrix} = \begin{bmatrix} (m_1+m_2)L_1^2 & m_2L_1L_2\cos(q_2-q_1) \\ m_2L_1L_2\cos(q_2-q_1) & m_2L_2^2 \end{bmatrix}.$$

Now, the stationarity condition is enforced for the action functional $A(\hat{q})$ when

$$\begin{aligned} 0 &= DA(\mathbf{q}, \mathbf{p}) = \frac{d}{d\epsilon} A(\mathbf{q} + \epsilon\mathbf{p}) \Big|_{\epsilon=0}, \\ &= \frac{d}{d\epsilon} \left\{ \int_{t_0}^{t_f} \frac{1}{2}(\dot{\mathbf{q}} + \epsilon\dot{\mathbf{p}})^T [\mathbf{M}(\mathbf{q} + \epsilon\mathbf{p})](\dot{\mathbf{q}} + \epsilon\dot{\mathbf{p}}) dt \right\}_{\epsilon=0} - \frac{d}{d\epsilon} \left\{ \int_{t_0}^{t_f} V(\mathbf{q} + \epsilon\mathbf{p}) dt \right\}_{\epsilon=0}, \\ &= \int_{t_0}^{t_f} \frac{1}{2} \left(\dot{\mathbf{p}}^T \mathbf{M} \dot{\mathbf{q}} + \dot{\mathbf{q}}^T \left(\frac{\partial \mathbf{M}}{\partial \mathbf{q}} \cdot \mathbf{p} \right) \dot{\mathbf{q}} + \dot{\mathbf{q}}^T \mathbf{M} \dot{\mathbf{p}} \right) dt - \int_{t_0}^{t_f} \left(\frac{\partial V}{\partial \mathbf{q}} \cdot \mathbf{p} \right) dt, \\ &= \int_{t_0}^{t_f} \left(\dot{\mathbf{q}}^T \mathbf{M} \dot{\mathbf{p}} + \frac{1}{2} \dot{\mathbf{q}}^T \left(\frac{\partial \mathbf{M}}{\partial \mathbf{q}} \cdot \mathbf{p} \right) \dot{\mathbf{q}} \right) dt - \int_{t_0}^{t_f} \left(\frac{\partial V}{\partial \mathbf{q}} \cdot \mathbf{p} \right) dt. \end{aligned}$$

The final step in the above equation is true because \mathbf{M} is symmetric, $\mathbf{M}^T = \mathbf{M}$. Due to the $\frac{\partial \mathbf{M}}{\partial \mathbf{q}} \cdot \mathbf{p}$ term, this expression can be defined more clearly in terms of the explicit summation

$$DA(\mathbf{q}, \mathbf{p}) = \sum_{i,k} \left\{ \int_{t_0}^{t_f} m_{ik} \dot{q}_i \dot{p}_k dt \right\} + \frac{1}{2} \sum_{i,j,k} \left\{ \int_{t_0}^{t_f} \frac{\partial m_{ij}}{\partial q_k} \dot{q}_i \dot{q}_j p_k dt \right\} - \sum_k \int_{t_0}^{t_f} \frac{\partial V}{\partial q_k} p_k dt.$$

Integration by parts is used to remove the derivative on \dot{p} in

$$\int_{t_0}^{t_f} m_{ik} \dot{q}_i \dot{p}_k dt = - \int_{t_0}^{t_f} \left(m_{ik} \ddot{q}_i p_k + \frac{\partial m_{ik}}{\partial q_j} \dot{q}_i \dot{q}_j p_k \right) dt.$$

Replacing the relevant term in $DA(\mathbf{q}, \mathbf{p}) = 0$, the equation

$$0 = \sum_k \int_{t_0}^{t_f} \left\{ -\sum_j m_{kj} \ddot{q}_j - \sum_{i,j} \left(\frac{\partial m_{ik}}{\partial q_j} - \frac{1}{2} \frac{\partial m_{ij}}{\partial q_k} \right) \dot{q}_i \dot{q}_j - \frac{\partial V}{\partial q_k} \right\} p_k dt$$

holds for each admissible direction p_j where $j = 1, 2$. Therefore, the integrand must be identically equal to zero. When each of these terms is calculated and the results are combined, the equations of motion can be written as

$$\begin{aligned} & \begin{bmatrix} (m_1 + m_2)L_1^2 & m_2 L_1 L_2 \cos(\theta_2 - \theta_1) \\ m_2 L_1 L_2 \cos(\theta_2 - \theta_1) & m_2 L_2^2 \end{bmatrix} \begin{Bmatrix} \ddot{\theta}_1 \\ \ddot{\theta}_2 \end{Bmatrix} \\ &= \begin{Bmatrix} m_2 L_1 L_2 \dot{\theta}_2^2 \sin(\theta_2 - \theta_1) - (m_1 + m_2)g L_1 \cos \theta_1 \\ -m_2 L_1 L_2 \dot{\theta}_1^2 \sin(\theta_2 - \theta_1) - m_2 g L_2 \cos \theta_2 \end{Bmatrix}. \end{aligned}$$

The explicit calculation of the entries in the equations of motion is carried out in Example ?? in the MATLAB Workbook for DCRS.

5.1.4 Kinetic Energy for Rigid Bodies

Hamilton's Principle as stated in Theorem (5.2) is general in nature: it holds for any mechanical system. While its application was illustrated in the previous section on simple systems comprised of point masses, it also applies to systems that include collections of rigid or even deformable continua. The references [31] or [12] provide more advanced applications. This book will focus on the application of Hamilton's Principle to robotic systems, and the most general cases to be studied consist of systems comprised of rigid bodies connected by ideal constraints. The following theorem provides a general form of the kinetic energy for the cases studied in this text.

Theorem 5.3. Let \mathbb{B} be a body fixed frame whose origin is located at the mass center of a rigid body that moves in the frame \mathbb{X} . The kinetic energy of the body is given by

$$T = \frac{1}{2} M \mathbf{v}_{\mathbb{X},c} \cdot \mathbf{v}_{\mathbb{X},c} + \frac{1}{2} \boldsymbol{\omega}_{\mathbb{X},\mathbb{B}} \cdot \mathbf{I}_c \boldsymbol{\omega}_{\mathbb{X},\mathbb{B}}$$

where $\mathbf{v}_{\mathbb{X},c}$ is the velocity of the center of mass in the frame \mathbb{X} , $\boldsymbol{\omega}_{\mathbb{X},\mathbb{B}}$ is the angular velocity of the \mathbb{B} frame in the \mathbb{X} frame, and \mathbf{I}_c is the inertia tensor about the center of mass.

This equation writes the kinetic energy associated with rotation in the coordinate free form $\frac{1}{2} \boldsymbol{\omega}_{\mathbb{X},\mathbb{B}} \cdot \mathbf{I}_c \boldsymbol{\omega}_{\mathbb{X},\mathbb{B}}$ with $\boldsymbol{\omega}_{\mathbb{X},\mathbb{B}}$ the angular velocity vector and \mathbf{I}_c the inertia tensor. If a specific basis of some frame \mathbb{Y} is chosen, an explicit form of the kinetic

energy may be formulated as $\frac{1}{2} \omega_{X,B}^Y \cdot I_c^Y \omega_{X,B}^Y$ with $\omega_{X,B}^Y$ the components of $\omega_{X,B}$ in the Y frame basis, and I_c^Y the components of the inertia matrix at point c relative to Y .

Proof. Figure (5.6) depicts a differential mass element that is part of the rigid body having body fixed frame B that moves with respect to the frame X . The kinetic energy of the rigid body is given by definition as

$$T = \frac{1}{2} \int \mathbf{v} \cdot \mathbf{v} dm$$

where $\mathbf{v} := \mathbf{v}_{X,dm}$ is the velocity of the differential mass element in the frame X . Theorem (2.16) allows for this velocity to be rewritten in the form

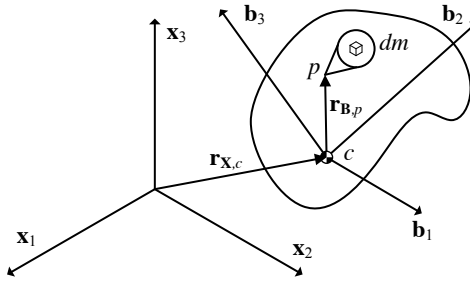


Fig. 5.6: Rigid Body and Differential Mass Element dm

$$\mathbf{v} = \mathbf{v}_{X,c} + \boldsymbol{\omega}_{X,B} \times \mathbf{r}$$

where $\mathbf{r} := \mathbf{r}_{B,p}$ is the vector that connects the origin of the B frame to the point p and $\mathbf{v}_{X,c}$ is the velocity in frame X of the center of mass of the body. The following expression is found by observing that $\mathbf{v}_{X,c}$ and $\boldsymbol{\omega}_{X,B}$ do not vary in the integration over the body

$$\begin{aligned} T &= \frac{1}{2} \int (\mathbf{v}_{X,c} + \boldsymbol{\omega}_{X,B} \times \mathbf{r}) \cdot (\mathbf{v}_{X,c} + \boldsymbol{\omega}_{X,B} \times \mathbf{r}) dm, \\ &= \frac{1}{2} M \mathbf{v}_{X,c} \cdot \mathbf{v}_{X,c} + \boldsymbol{\omega}_{X,B} \times \left(\int \mathbf{r} dm \right) \cdot \mathbf{v}_{X,c} + \frac{1}{2} \boldsymbol{\omega}_{X,B} \times \int \mathbf{r} \cdot (\boldsymbol{\omega}_{X,B} \times \mathbf{r}) dm. \end{aligned}$$

The second term on the right hand side of the equation above is identically zero since the origin of the B frame is selected to be the *center of mass* of the body,

$$\mathbf{0} = \mathbf{r}_{B,c} = \frac{1}{M} \int \mathbf{r} dm.$$

The third term on the right hand side of this equation is evaluated using a property of the *scalar triple product* that states $\mathbf{a} \times \mathbf{b} \cdot \mathbf{c} = \mathbf{a} \cdot \mathbf{b} \times \mathbf{c}$ for any three vectors $\mathbf{a}, \mathbf{b}, \mathbf{c}$. As a result,

$$T = \frac{1}{2} M \mathbf{v}_{\mathbb{X},c} \cdot \mathbf{v}_{\mathbb{X},c} + \frac{1}{2} \boldsymbol{\omega}_{\mathbb{X},\mathbb{B}} \cdot \int \mathbf{r} \times (\boldsymbol{\omega}_{\mathbb{X},c} \times \mathbf{r}) dm.$$

Theorem (4.5) defines the body's moment of inertia based on the evaluation of this integral, resulting in

$$T = \frac{1}{2} M \mathbf{v}_{\mathbb{X},c} \cdot \mathbf{v}_{\mathbb{X},c} + \frac{1}{2} \boldsymbol{\omega}_{\mathbb{X},\mathbb{B}} \cdot \mathbf{I}_c \boldsymbol{\omega}_{\mathbb{X},\mathbb{B}}.$$

□

Theorem (5.3) is appropriate for the calculation of a rigid body as it undergoes general motion relative to the frame \mathbb{X} . Sometimes it is possible to simplify calculations considerably if the motion is constrained in some way. Specialized formulae can be deduced from Theorem (5.3) if the motion of the rigid body is planar. The following theorem discusses another example of constrained motion, the case when a point o of the rigid body is fixed in frame \mathbb{X} .

Theorem 5.4. Suppose that point o on a rigid body having body fixed frame \mathbb{B} is fixed in frame \mathbb{X} . The kinetic energy of the rigid body is given by

$$T = \frac{1}{2} \boldsymbol{\omega}_{\mathbb{X},\mathbb{B}} \cdot \mathbf{I}_o \boldsymbol{\omega}_{\mathbb{X},\mathbb{B}}$$

where $\boldsymbol{\omega}_{\mathbb{X},\mathbb{B}}$ is the angular velocity of the body fixed frame \mathbb{B} in the \mathbb{X} frame and \mathbf{I}_o is the inertia tensor of the rigid body about the point o .

Proof. Since point o is fixed in frame \mathbb{X} , the velocity $\mathbf{v} := \mathbf{v}_{\mathbb{X},dm}$ of the differential mass element can be written as $\mathbf{v} = \boldsymbol{\omega}_{\mathbb{X},\mathbb{B}} \times \mathbf{r}$, where $\mathbf{r} := \mathbf{r}_{0,dm}$ is the vector that connects point o to the differential mass element. We substitute this expression into the definition of the kinetic energy

$$T = \frac{1}{2} \int \mathbf{v} \cdot \mathbf{v} dm = \frac{1}{2} \int (\boldsymbol{\omega}_{\mathbb{X},\mathbb{B}} \times \mathbf{r}) \cdot (\boldsymbol{\omega}_{\mathbb{X},\mathbb{B}} \times \mathbf{r}) dm = \frac{1}{2} \boldsymbol{\omega}_{\mathbb{X},\mathbb{B}} \cdot \int \mathbf{r} \times (\boldsymbol{\omega}_{\mathbb{X},\mathbb{B}} \times \mathbf{r}).$$

Theorem (5.3) can be used to express this integral in terms of the body's moment of inertia at point o , yielding

$$T = \frac{1}{2} \boldsymbol{\omega}_{\mathbb{X},\mathbb{B}} \cdot \int \mathbf{r} \times (\boldsymbol{\omega}_{\mathbb{X},\mathbb{B}} \times \mathbf{r}) dm = \frac{1}{2} \boldsymbol{\omega}_{\mathbb{X},\mathbb{B}} \cdot \mathbf{I}_o \boldsymbol{\omega}_{\mathbb{X},\mathbb{B}}.$$

□

Example 5.1.6. Calculate the kinetic energy of links 1, 2 and 3 of the spherical wrist depicted in Figures (5.7) and (5.8).

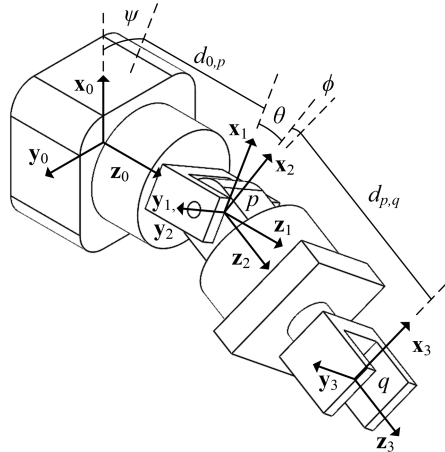


Fig. 5.7: Spherical Wrist Frames and Coordinates

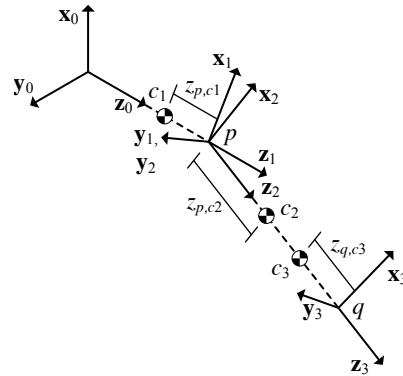


Fig. 5.8: Spherical Wrist Mass Centers

Solution: Define inertia matrix $\mathbf{I}_{c_i}^i$ relative to a frame that is parallel to frame i but has its origin at the center of mass of link i for $i = 1, 2, 3$. Since the $\mathbf{x}_1 - \mathbf{z}_1$ and $\mathbf{y}_1 - \mathbf{z}_1$ planes are planes of symmetry of link 1, the inertia matrix \mathbf{I}_1^1 has the form

$$\mathbf{I}_1^1 = \begin{bmatrix} I_{11,1} & 0 & 0 \\ 0 & I_{22,1} & 0 \\ 0 & 0 & I_{33,1} \end{bmatrix}.$$

The angular velocity of the link 1 is

$$\boldsymbol{\omega}_{0,1}^1 = \begin{Bmatrix} 0 \\ 0 \\ \dot{\psi} \end{Bmatrix}.$$

Therefore, the kinetic energy of link 1 is

$$T_1 = \frac{1}{2} m_1 \underbrace{\mathbf{v}_{0,1} \cdot \mathbf{v}_{0,1}}_0 + \frac{1}{2} \boldsymbol{\omega}_{0,1} \cdot \mathbf{I}_1 \boldsymbol{\omega}_{0,1} = \frac{1}{2} \{ 0 \ 0 \ \dot{\psi} \} \begin{bmatrix} I_{11,1} & 0 & 0 \\ 0 & I_{22,1} & 0 \\ 0 & 0 & I_{33,1} \end{bmatrix} \begin{Bmatrix} 0 \\ 0 \\ \dot{\psi} \end{Bmatrix} = \frac{1}{2} I_{33,1} \dot{\psi}^2.$$

The $\mathbf{x}_2 - \mathbf{y}_2$ and $\mathbf{x}_2 - \mathbf{z}_2$ planes are planes of symmetry of the link 2. Therefore, the inertia matrix \mathbf{I}_2^2 has the structure

$$\mathbf{I}_2^2 = \begin{bmatrix} I_{11,2} & 0 & 0 \\ 0 & I_{22,2} & 0 \\ 0 & 0 & I_{33,2} \end{bmatrix}.$$

The angular velocity of link 2 in the inertial frame is

$$\boldsymbol{\omega}_{0,2} = \dot{\psi} \mathbf{z}_0 + \dot{\theta} \mathbf{y}_1 = \dot{\psi} \mathbf{z}_1 + \dot{\theta} \mathbf{y}_2 = -\dot{\psi} \sin \theta \mathbf{x}_2 + \dot{\theta} \mathbf{y}_2 + \dot{\psi} \cos \theta \mathbf{z}_2,$$

and the velocity of the center of mass of link 2 is

$$\mathbf{v}_{0,2} = \boldsymbol{\omega}_{0,2} \times z_{p,c_2} \mathbf{z}_2 = \begin{vmatrix} \mathbf{x}_2 & \mathbf{y}_2 & \mathbf{z}_2 \\ -\dot{\psi} \sin \theta & \dot{\theta} & \dot{\psi} \cos \theta \\ 0 & 0 & z_{p,c_2} \end{vmatrix} = z_{p,c_2} \dot{\theta} \mathbf{x}_2 + z_{p,c_2} \dot{\psi} \sin \theta \mathbf{y}_2.$$

The kinetic energy of link 2 is computed using these expressions as

$$\begin{aligned} T_2 &= \frac{1}{2} m_2 \mathbf{v}_{0,2} \cdot \mathbf{v}_{0,2} + \frac{1}{2} \boldsymbol{\omega}_{0,2} \cdot \mathbf{I}_2 \boldsymbol{\omega}_{0,2} \\ &= \frac{1}{2} m_2 z_{p,c_2}^2 (\dot{\theta}^2 + \dot{\psi}^2 \sin^2 \theta) \\ &\quad + \frac{1}{2} \{ -\dot{\psi} \sin \theta \dot{\theta} \dot{\psi} \cos \theta \} \begin{bmatrix} I_{11,2} & 0 & 0 \\ 0 & I_{22,2} & 0 \\ 0 & 0 & I_{33,2} \end{bmatrix} \begin{Bmatrix} -\dot{\psi} \sin \theta \\ \dot{\theta} \\ \dot{\psi} \cos \theta \end{Bmatrix}. \end{aligned}$$

The angular velocity of link 3 is

$$\boldsymbol{\omega}_{0,3} = \boldsymbol{\omega}_{0,2} + \dot{\phi} \mathbf{z}_3,$$

$$\boldsymbol{\omega}_{0,3}^2 = \begin{Bmatrix} -\dot{\psi} \sin \theta \\ \dot{\theta} \\ \dot{\psi} \cos \theta \end{Bmatrix} + \begin{Bmatrix} 0 \\ 0 \\ \dot{\phi} \end{Bmatrix} = \begin{Bmatrix} -\dot{\psi} \sin \theta \\ \dot{\theta} \\ \dot{\psi} \cos \theta + \dot{\phi} \end{Bmatrix},$$

$$\boldsymbol{\omega}_{0,3}^3 = \begin{bmatrix} \cos \phi & \sin \phi & 0 \\ -\sin \phi & \cos \phi & 0 \\ 0 & 0 & 1 \end{bmatrix} \begin{Bmatrix} -\dot{\psi} \sin \theta \\ \dot{\theta} \\ \dot{\psi} \cos \theta \end{Bmatrix} + \begin{Bmatrix} 0 \\ 0 \\ \dot{\phi} \end{Bmatrix} = \begin{Bmatrix} -\dot{\psi} \sin \theta \cos \phi + \dot{\theta} \sin \phi \\ \dot{\psi} \sin \theta \sin \phi + \dot{\theta} \cos \phi \\ \dot{\psi} \cos \theta + \dot{\phi} \end{Bmatrix}.$$

The velocity of the center of mass of link 3 can be calculated as

$$\mathbf{v}_{0,3} = \boldsymbol{\omega}_{0,3} \times (d_{p,q} - z_{q,c_3}) \mathbf{z}_2 = \begin{vmatrix} \mathbf{x}_2 & \mathbf{y}_2 & \mathbf{z}_2 \\ -\dot{\psi} \sin \theta & \dot{\theta} & \dot{\psi} \cos \theta + \dot{\phi} \\ 0 & 0 & (d_{p,q} - z_{q,c_3}) \end{vmatrix}$$

$$= (d_{p,q} - z_{q,c_3})(\dot{\theta} \mathbf{x}_2 + \dot{\psi} \sin \theta \mathbf{y}_2).$$

The kinetic energy for link 3 is

$$T_3 = \frac{1}{2} m_3 \mathbf{v}_{0,3} \cdot \mathbf{v}_{0,3} + \frac{1}{2} \boldsymbol{\omega}_{0,3} \cdot \mathbf{I}_3 \boldsymbol{\omega}_{0,3},$$

$$= \frac{1}{2} m_3 (d_{p,q} - z_{q,c_3})^2 (\dot{\theta}^2 + \dot{\psi}^2 \sin^2 \theta)$$

$$+ \frac{1}{2} \begin{Bmatrix} -\dot{\psi} \sin \theta \cos \phi + \dot{\theta} \sin \phi \\ \dot{\psi} \sin \theta \sin \phi + \dot{\theta} \cos \phi \\ \dot{\psi} \cos \theta + \dot{\phi} \end{Bmatrix}^T \begin{bmatrix} I_{11,3} & 0 & 0 \\ 0 & I_{22,3} & 0 \\ 0 & 0 & I_{33,3} \end{bmatrix} \begin{Bmatrix} -\dot{\psi} \sin \theta \cos \phi + \dot{\theta} \sin \phi \\ \dot{\psi} \sin \theta \sin \phi + \dot{\theta} \cos \phi \\ \dot{\psi} \cos \theta + \dot{\phi} \end{Bmatrix},$$

$$= \frac{1}{2} \left\{ m_3 (d_{p,q} - z_{q,c_3})^2 (\dot{\theta}^2 + \dot{\psi}^2 \sin^2 \theta) + I_{11,3} (-\dot{\psi} \sin \theta \cos \phi + \dot{\theta} \sin \phi)^2 \right. \\ \left. + I_{22,3} (\dot{\psi} \sin \theta \sin \phi + \dot{\theta} \cos \phi)^2 + I_{33,3} (\dot{\psi} \cos \theta + \dot{\phi})^2 \right\}.$$

The explicit form of the velocities, angular velocities, and kinetic energies in this example can be found in Example ?? of the MATLAB Workbook for DCRS.

5.2 Lagrange's Equations for Conservative Systems

Hamilton's Principle introduced in Section (5.1.3) is a powerful theorem. It is concise and easy to state. It is possible to appeal to it directly to derive the equations of motion for conservative mechanical systems, as done in Section (5.1.3). It is often the case that the form of the action functional in Hamilton's Principle has the same structural form in many applications under consideration. It is most often the case in applications to mechanical systems that the kinetic energy is a function of the generalized coordinates, their derivatives and possibly time t . In this case this

functional form can be expressed as $T = T(\dot{\mathbf{q}}, \mathbf{q}, t)$. In addition, the potential energy is usually a function of the generalized coordinates and time t , $V = V(\mathbf{q}, t)$. When the kinetic energy and potential energy have this structure, it is possible to calculate the stationarity conditions for the action functional in a general form. The result is the collection of Lagrange's Equations of motion for conservative mechanical systems, which are summarized in the following theorem.

Theorem 5.5. Let $\mathbf{q}(t) := \{q_1(t), q_2(t), \dots, q_n(t)\}^T$ be a collection of generalized coordinates for a conservative mechanical system. Suppose that $T = T(\dot{\mathbf{q}}, \mathbf{q}, t)$ and $V = V(\mathbf{q}, t)$. If the action functional $A(\mathbf{q})$ is stationary, then

$$\frac{d}{dt} \left(\frac{\partial T}{\partial \dot{\mathbf{q}}} \right) - \frac{\partial T}{\partial \mathbf{q}} + \frac{\partial V}{\partial \mathbf{q}} = \mathbf{0}.$$

These equations are known as Lagrange's equations for a conservative mechanical system.

Before proceeding to the proof of Theorem (5.5), it should be noted that this equation should be interpreted as a vector equation where the partial derivatives of the kinetic and potential energies are collected as

$$\frac{\partial T}{\partial \mathbf{q}} := \begin{Bmatrix} \frac{\partial T}{\partial q_1} \\ \vdots \\ \frac{\partial T}{\partial q_N} \end{Bmatrix}, \quad \frac{\partial V}{\partial \mathbf{q}} := \begin{Bmatrix} \frac{\partial V}{\partial q_1} \\ \vdots \\ \frac{\partial V}{\partial q_N} \end{Bmatrix}, \quad \frac{\partial T}{\partial \dot{\mathbf{q}}} := \begin{Bmatrix} \frac{\partial T}{\partial \dot{q}_1} \\ \vdots \\ \frac{\partial T}{\partial \dot{q}_N} \end{Bmatrix}.$$

The k^{th} entry in the vector equation is written explicitly as

$$\frac{d}{dt} \left(\frac{\partial T}{\partial \dot{q}_k} \right) - \frac{\partial T}{\partial q_k} + \frac{\partial V}{\partial q_k} = 0$$

for $k = 1 \dots N$.

Proof. By definition, if the action functional is to be stationary, then

$$DA(\mathbf{q}, \mathbf{p}) = 0$$

for all admissible directions \mathbf{p} . While the definition of the Gateaux derivative could be utilized directly to enforce the condition that the Gateaux derivative vanish for all admissible directions, it is simpler to use Theorem (5.1) and start from the expression that

$$DJ(\mathbf{q}, \mathbf{p}) = \frac{d}{d\epsilon} (A(\mathbf{q} + \epsilon\mathbf{p})) \Big|_{\epsilon=0} = \mathbf{0}.$$

Evaluating the action functional at $\mathbf{q} + \epsilon\mathbf{p}$ results in

$$A(\mathbf{q} + \epsilon\mathbf{p}) = \int_{t_0}^{t_f} (T(\dot{\mathbf{q}}(t) + \epsilon\dot{\mathbf{p}}(t), \mathbf{q}(t) + \epsilon\mathbf{p}(t), t) - V(\mathbf{q}(t) + \epsilon\mathbf{p}(t), t)) dt,$$

and the derivative with respect to ϵ is calculated to be

$$\frac{d}{d\epsilon} (A(\mathbf{q} + \epsilon\mathbf{p})) = \int_{t_0}^{t_f} \left(\frac{\partial T}{\partial(\dot{\mathbf{q}} + \epsilon\dot{\mathbf{p}})} \cdot \dot{\mathbf{p}}(t) + \frac{\partial T}{\partial(\mathbf{q} + \epsilon\mathbf{p})} \cdot \mathbf{p}(t) - \frac{\partial V}{\partial(\mathbf{q} + \epsilon\mathbf{p})} \cdot \mathbf{p}(t) \right) dt.$$

Evaluating this expression when $\epsilon = 0$ results in

$$\frac{d}{d\epsilon} (A(\mathbf{q} + \epsilon\mathbf{p})) \Big|_{\epsilon=0} = \int_{t_0}^{t_f} \left(\frac{\partial T}{\partial \dot{\mathbf{q}}} \cdot \dot{\mathbf{p}}(t) + \frac{\partial T}{\partial \mathbf{q}} \cdot \mathbf{p}(t) - \frac{\partial V}{\partial \mathbf{q}} \cdot \mathbf{p}(t) \right) dt$$

At this point, it is useful to recall the strategy of nearly all problems in elementary calculus of variations. It is desirable to obtain an expression that has the form

$$DA(\mathbf{q}, \mathbf{p}) = \int_{t_0}^{t_f} \{\mathbf{e}(t) \cdot \mathbf{p}(t)\} dt = \mathbf{0}$$

that holds for all choices of the admissible directions $\mathbf{p}(t) \in \mathcal{P}$. If the governing equations can be written in this form, it follows that the only way that the equality holds for all possible, arbitrary admissible directions $\mathbf{p}(t)$ is when the expression $\mathbf{e}(t) \equiv \mathbf{0}$. This observation follows from the *Fundamental Theorem of Variational Calculus* [43] [34]. In many cases when Hamilton's Principle is invoked, the equations may be readily transformed into this form.

In the present case, as well as many other problems of interest discussed later, the critical step is to employ integration by parts to eliminate the derivative that is applied to the admissible variations in $\dot{\mathbf{p}}$. When this term is integrated by parts, the following expression is obtained

$$\int_{t_0}^{t_f} \frac{\partial T}{\partial \dot{\mathbf{q}}} \cdot \dot{\mathbf{p}}(t) dt = \frac{\partial T}{\partial \dot{\mathbf{q}}} \cdot \mathbf{p}(t) \Big|_{t_0}^{t_f} - \int_{t_0}^{t_f} \frac{d}{dt} \left(\frac{\partial T}{\partial \dot{\mathbf{q}}} \right) \cdot \mathbf{p}(t) dt.$$

Substituting this expression into the original set of equations results in

$$DA(\mathbf{q}, \mathbf{p}) = \frac{\partial T}{\partial \dot{\mathbf{q}}} \cdot \mathbf{p}(t) \Big|_{t_0}^{t_f} + \int_{t_0}^{t_f} \left\{ -\frac{d}{dt} \left(\frac{\partial T}{\partial \dot{\mathbf{q}}} \right) + \frac{\partial T}{\partial \mathbf{q}} - \frac{\partial V}{\partial \mathbf{q}} \right\} \cdot \mathbf{p}(t) dt = 0.$$

The admissible variations \mathbf{p} are required to satisfy $\mathbf{p}(t_0) = \mathbf{p}(t_f) = \mathbf{0}$. The Fundamental Theorem of Variational Calculus implies that the terms that multiply the independent and arbitrary admissible directions must be equal to zero,

$$-\frac{d}{dt} \left(\frac{\partial T}{\partial \dot{\mathbf{q}}} \right) + \frac{\partial T}{\partial \mathbf{q}} - \frac{\partial V}{\partial \mathbf{q}} = \mathbf{0}.$$

These are the desired Lagrange's Equations for the conservative mechanical system, completing the proof. \square



Example 5.2.1. Find the equations of motion for the two link robotic arm investigated in Example (5.1.5) using Lagrange's equations for conservative systems.

Solution: Example (5.1.5) calculates the kinetic energy of the robotic arm as

$$T = \frac{1}{2}(m_1 + m_2)L_1^2\dot{\theta}_1^2 + \frac{1}{2}m_2L_2^2\dot{\theta}_2^2 + m_2L_1L_2\cos(\theta_2 - \theta_1)\dot{\theta}_1\dot{\theta}_2,$$

and the potential energy of the robotic arm as

$$V = m_1gL_1\sin\theta_1 + m_2g(L_1\sin\theta_1 + L_2\sin\theta_2).$$

Using these formulations, the required terms associated with the first generalized coordinate may be calculated,

$$\begin{aligned}\frac{\partial T}{\partial \dot{\theta}_1} &= (m_1 + m_2)L_1^2\dot{\theta}_1 + m_2L_1L_2\dot{\theta}_2\cos(\theta_2 - \theta_1), \\ \frac{\partial T}{\partial \theta_1} &= m_2L_1L_2\dot{\theta}_1\dot{\theta}_2\sin(\theta_2 - \theta_1), \\ \frac{\partial V}{\partial \theta_1} &= (m_1 + m_2)gL_1\cos\theta_1,\end{aligned}$$

along with the corresponding terms for the second generalized coordinate,

$$\begin{aligned}\frac{\partial T}{\partial \dot{\theta}_2} &= m_2L_2^2\dot{\theta}_2 + m_2L_1L_2\dot{\theta}_1\cos(\theta_2 - \theta_1), \\ \frac{\partial T}{\partial \theta_2} &= -m_2L_1L_2\dot{\theta}_1\dot{\theta}_2\sin(\theta_2 - \theta_1), \\ \frac{\partial V}{\partial \theta_2} &= m_2gL_2\cos\theta_2.\end{aligned}$$

The total time derivatives are determined as

$$\begin{aligned}\frac{d}{dt}\left(\frac{\partial T}{\partial \dot{\theta}_1}\right) &= (m_1 + m_2)L_1^2\ddot{\theta}_1 + m_2L_1L_2\ddot{\theta}_2\cos(\theta_2 - \theta_1) - m_2L_1L_2\dot{\theta}_2(\dot{\theta}_2 - \dot{\theta}_1)\sin(\theta_2 - \theta_1), \\ \frac{d}{dt}\left(\frac{\partial T}{\partial \dot{\theta}_2}\right) &= m_2L_2^2\ddot{\theta}_2 + m_2L_1L_2\ddot{\theta}_1\cos(\theta_2 - \theta_1) - m_2L_1L_2\dot{\theta}_1(\dot{\theta}_2 - \dot{\theta}_1)\sin(\theta_2 - \theta_1).\end{aligned}$$

When the terms that make up Lagrange's equations are collected together, the governing equations are

$$\begin{aligned}&\begin{bmatrix} (m_1 + m_2)L_1^2 & m_2L_1L_2\cos(\theta_2 - \theta_1) \\ m_2L_1L_2\cos(\theta_2 - \theta_1) & m_2L_2^2 \end{bmatrix} \begin{Bmatrix} \ddot{\theta}_1 \\ \ddot{\theta}_2 \end{Bmatrix} \\ &= \begin{Bmatrix} m_2L_1L_2\dot{\theta}_2^2\sin(\theta_2 - \theta_1) - (m_1 + m_2)gL_1\cos\theta_1 \\ -m_2L_1L_2\dot{\theta}_1^2\sin(\theta_2 - \theta_1) - m_2gL_2\cos\theta_2 \end{Bmatrix}.\end{aligned}$$

These equations are one example of the general form of the equations of motion for robotic systems. In general, the equations of motion often have the form

$$\mathbf{M}(\mathbf{q}(t))\ddot{\mathbf{q}}(t) = \mathbf{n}(\mathbf{q}(t), \dot{\mathbf{q}}(t)) + \boldsymbol{\tau}(t)$$

where $\mathbf{M}(\mathbf{q}(t))$ is the *generalized mass or inertia matrix* that can be a nonlinear function of the generalized coordinates $\mathbf{q}(t)$, $\mathbf{n}(\mathbf{q}(t), \dot{\mathbf{q}}(t))$ is a nonlinear function of the generalized coordinates $\mathbf{q}(t)$ and their derivatives $\dot{\mathbf{q}}(t)$, and $\boldsymbol{\tau}$ is a vector of torques delivered via actuators. Lagrange's equations for the two link robot are also found in Example ?? of the MATLAB Workbook for DCRS.

5.3 Hamilton's Extended Principle

Hamilton's Principle for conservative mechanical systems is sufficient to treat many systems of interest in this book, and a number of generalizations of the basic law exist that extend its applicability. In this section the basic approach discussed in Section (5.1.3) is extended to nonconservative systems. It is possible to cast the formulation in the language of the calculus of variations, as done in Section (5.1.3) and Section (5.2). Instead, this section adopts the language of *virtual displacements*, *virtual work* and *virtual variations* that are popular in many engineering texts.

5.3.1 Virtual Work Formulations

Section (5.2) showed that Lagrange's Equations can be derived as a consequence of Hamilton's Principle using standard techniques from the calculus of variations. More detailed studies of these principles can be found in the books [43], [29]. Many engineering texts, in contrast, study Hamilton's Principle and Lagrange's Equations in terms of virtual displacements, virtual work and the virtual variation operator. See [17], [20] or [12] for more comprehensive discussions. The two approaches have much in common, and results that are derived using one framework or viewpoint could equally well be derived using tools from the alternative approach. The dynamic behavior of a given system under the same assumptions should not differ based on the methodology used to derive those dynamics.

Recall that a possible motion in the language of the calculus of variations, as depicted in Figure 5.3, is understood as a perturbation $\mathbf{q}(t) + \epsilon \mathbf{p}(t)$ of the actual motion $\mathbf{q}(t)$ of the mechanical system at time t . The term $\mathbf{p}(t)$ is known as an admissible direction or admissible variation. Methods of virtual work define a possible motion as the sum $\mathbf{q}(t) + \delta \mathbf{q}(t)$ where $\mathbf{q}(t)$ is the actual motion of the system at time t and $\delta \mathbf{q}(t)$ is the virtual variation, or simply the variation, of the true motion. It is understood in virtual work formulations of analytical mechanics that the virtual variation $\delta \mathbf{q}$ is a perturbation of the true motion $\mathbf{q}(t)$ that is contemporaneous and consistent with the kinematic constraints on the system. That is, the virtual variation $\delta \mathbf{q}(t)$ is viewed as a

possible perturbation of the generalized coordinates that could occur at a fixed time t that does not violate any of the kinematic constraints on the mechanical system.

By the definition of the generalized coordinates for the mechanical system,

$$\mathbf{r}_{\mathbb{X},p}(t) = \mathbf{r}_{\mathbb{X},p}(q_1(t), q_2(t), \dots, q_N(t), t).$$

The virtual displacement $\delta\mathbf{r}_{\mathbb{X},p}$ of the point p due the variation $\delta\mathbf{q}$ of the generalized coordinates is defined via the identity

$$\delta\mathbf{r}_{\mathbb{X},p} := \sum_{k=1}^N \frac{\partial\mathbf{r}_{\mathbb{X},p}}{\partial q_k} \delta q_k.$$

If there are a number of forces \mathbf{f}_p acting on the mechanical system at the set of points $p \in P$, the virtual work that these forces do on the system is the work done by the forces acting through the virtual displacements of the points p . The virtual work is then written as

$$\begin{aligned} \delta W &= \sum_{p \in P} \mathbf{f}_p \cdot \delta\mathbf{r}_{\mathbb{X},p}, \\ &= \sum_{p \in P} \mathbf{f}_p \cdot \sum_{k=1}^N \frac{\partial\mathbf{r}_{\mathbb{X},p}}{\partial q_k} \delta q_k = \sum_{k=1}^N \left(\sum_{p \in P} \mathbf{f}_p \cdot \frac{\partial\mathbf{r}_{\mathbb{X},p}}{\partial q_k} \right) \delta q_k, \\ &= \sum_{k=1}^N Q_k \delta q_k. \end{aligned}$$

The summation in the last line introduces the generalized forces Q_i for $i = 1 \dots N$ that are associated with the generalized coordinates q_i or $i = 1, \dots, N$,

$$Q_k := \sum_{p \in P} \mathbf{f}_p \cdot \frac{\partial\mathbf{r}_{\mathbb{X},p}}{\partial q_k}.$$

The virtual variations $\delta\mathbf{q}$, virtual displacements $\delta\mathbf{r}_{\mathbb{X},p}$, virtual work δW , generalized forces \mathbf{Q} , and the generalized displacements \mathbf{q} are all fundamental quantities in the virtual work formulation of analytical mechanics. The final step in expressing Hamilton's Principle in the language of virtual work introduces the *virtual variation operator*, or simply the *variation operator*, $\delta(\bullet)$. The virtual variation operator can be introduced in a number of equivalent ways, and the interested reader is referred to the discussions in [31], [20], or [17]. The following formal or operational definition that suffices for the applications this text will employ.

Definition 5.6. The virtual variation operator $\delta(\bullet)$ has the following properties:

1. The operator $\delta(\bullet)$ obeys the same rules as the differential operator $d(\bullet)$.
2. The operator $\delta(\bullet)$ acting on time t is identically zero, $\delta t \equiv 0$.
3. The operator $\delta(\bullet)$ commutes with integration or differentiation in the sense that

$$\delta\left(\frac{d}{dt}(\bullet)\right) = \frac{d}{dt}(\delta(\bullet)), \quad (5.3.1)$$

$$\delta\left(\int_{t_0}^{t_f} (\bullet) dt\right) = \int_{t_0}^{t_f} \delta(\bullet) dt. \quad (5.3.2)$$

4. The operator $\delta(\bullet)$ is defined such that

$$\delta q(t_0) = \delta q(t_f) = 0. \quad (5.3.3)$$

Before applying these principles in examples and problems, it can be useful to study more closely the relationship between virtual displacements $\delta \mathbf{r}_{\mathbb{X},p}$ and the velocity $\mathbf{v}_{\mathbb{X},p}$ of the point p in the frame \mathbb{X} . The virtual displacements have been defined as

$$\delta \mathbf{r}_{\mathbb{X},p} := \sum_{k=1}^N \frac{\partial \mathbf{r}_{\mathbb{X},p}}{\partial q_k} \delta q_k,$$

and the velocity $\mathbf{v}_{\mathbb{X},p}$ of the point p in the frame \mathbb{X} can be calculated explicitly as

$$\mathbf{v}_{\mathbb{X},p} = \sum_{k=1}^N \frac{\partial \mathbf{r}_{\mathbb{X},p}}{\partial q_k} \dot{q}_k + \frac{\partial \mathbf{r}_{\mathbb{X},p}}{\partial t}.$$

The similarity in these two expressions can be used to define a pragmatic way to compute the virtual displacement of point p in frame \mathbb{X} . First, the velocity $\mathbf{v}_{\mathbb{X},p}$ of the point p is calculated using the tools in Chapters (2) and (3). Then, δq_k is substituted for each \dot{q}_k , where $k = 1, \dots, N$. Finally, the term $\partial \mathbf{r}_{\mathbb{X},p}/\partial t$ is discarded. The resulting expression is equal to $\delta \mathbf{r}_{\mathbb{X},p}$.

One of the most important properties of virtual variations and the virtual variation operator δ in applications is the fact that constraint forces and torques perform no virtual work. The following examples illustrate this point.

Example 5.3.1. Consider again the point mass constrained to lie on a plane analyzed in Example (5.1.1) and shown in Figure (5.1). Show that the constraint force that acts on the point mass m to ensure that the point remains on the plane does no virtual work.

Solution: The constraint force that keeps the point mass on the plane acts normal to the plane, so it can be written in the form

$$\mathbf{f}(t) = \frac{1}{\sqrt{3}} |\mathbf{f}(t)| \begin{Bmatrix} 1 \\ 1 \\ 1 \end{Bmatrix}.$$

The virtual displacement $\delta \mathbf{r}_{0,m}(t)$ is calculated by taking the virtual variation of the position vector $\mathbf{r}_{0,m}$,

$$\delta \mathbf{r}_{0,m} = \delta x \mathbf{x}_0 + \delta y \mathbf{y}_0 + (-\delta x - \delta y) \mathbf{z}_0.$$

By definition, the virtual work due to the constraint force is calculated to be the dot product

$$\delta W = \mathbf{f} \cdot \delta \mathbf{r}_{0,m} = \frac{1}{\sqrt{3}} |\mathbf{f}| \begin{Bmatrix} 1 \\ 1 \\ 1 \end{Bmatrix} \cdot \begin{Bmatrix} \delta x \\ \delta y \\ -(\delta x + \delta y) \end{Bmatrix} = 0.$$

The virtual work is zero since the constraint force and the virtual displacement are orthogonal. This simple observation generalizes to higher dimensions, as discussed in Section (5.5).

Example 5.3.2. A two link robotic manipulator is illustrated in Figure (5.9). Show that the reaction forces at the revolute joints do not contribute to the virtual work. If m_1 and m_2 are actuation moments applied to bodies 1 and 2 at the revolute joints, show that the virtual work generated by these moments is given by

$$\delta W = m_1 \delta \theta_1 + m_2 \delta \theta_2,$$

where $\delta \theta_1$ and $\delta \theta_2$ are the virtual variations of the generalized coordinates $q_1 := \theta_1$ and $q_2 := \theta_2$.

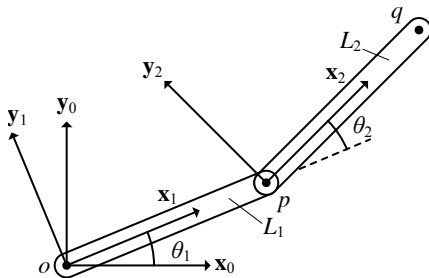


Fig. 5.9: Two Link Robotic Arm

Solution: First, free body diagrams of links 1 and 2 are constructed in terms of

constraint forces and actuation moments acting at the joints. The joint 1 moment $-\mathbf{m}_1$ is not considered as it acts on the ground, which is not a free body. Using these

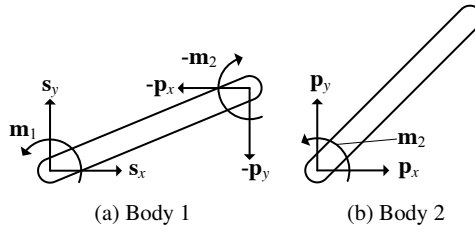


Fig. 5.10: Reaction Forces and Moments

free body diagrams, the constraint forces will be shown to produce no virtual work. Based on Figures (5.10a) and (5.10b), the virtual work needs to be calculated for the force \mathbf{s} acting at point o on body 1, the force $-\mathbf{p}$ acting at point p on body 1, and the force \mathbf{p} acting at the point p on the body 2. The virtual work of these three forces are then computed via the definition

$$\delta W = \sum_i \mathbf{f}_i \cdot \delta \mathbf{r}_{0,i}.$$

There are many different ways to calculate the virtual displacement of the points 0 and 1 in this mechanical system. One approach is to define the position vectors of these points as

$$\begin{aligned}\mathbf{r}_{0,o} &= \mathbf{0}, \\ \mathbf{r}_{0,p} &= L_1 \cos \theta_1 \mathbf{x}_0 + L_1 \sin \theta_1 \mathbf{y}_0,\end{aligned}$$

and compute the virtual displacements by applying the virtual variation operator $\delta(\cdot)$. The resulting virtual displacements are

$$\begin{aligned}\delta \mathbf{r}_{0,o} &= \mathbf{0}, \\ \delta \mathbf{r}_{0,p} &= -L_1 \sin \theta_1 \delta \theta_1 \mathbf{x}_0 + L_1 \cos \theta_1 \delta \theta_1 \mathbf{y}_0.\end{aligned}$$

An alternative approach to compute the virtual displacement is based on computing the velocity. By the definition of the generalized coordinates, position vectors can be expressed in the form

$$\mathbf{r}_{0,i}(t) = \mathbf{r}_{0,i}(q_1(t), q_2(t), \dots, q_N(t), t)$$

where N is the number of degrees of freedom of the mechanical system. Differentiating this vector results in

$$\mathbf{v}_{0,i}(t) = \sum_{j=1}^N \frac{\partial \mathbf{r}_{0,i}}{\partial q_j} \dot{q}_j(t) + \frac{\partial \mathbf{r}_{0,i}}{\partial t},$$

whereas taking the virtual variation $\delta(\cdot)$ of this equation results in

$$\delta \mathbf{r}_{0,i}(t) = \sum_{j=1}^N \frac{\partial \mathbf{r}_{0,i}}{\partial q_j} \delta q_j(t),$$

since $\delta t = 0$. By comparing these two equations, the virtual displacements may be identified from the velocity: simply replace \dot{q}_j with δq_j for $j = 1, \dots, N$ and discard the term $\partial \mathbf{r}_{0,i}/\partial t$. For example, in the problem at hand, the velocity of the point p is $\mathbf{v}_{0,p} = L_1 \dot{\theta}_1 \mathbf{y}_1$ and the virtual displacement is $\delta \mathbf{r}_{0,p} = L_1 \delta \theta_1 \mathbf{y}_1$. The virtual work performed by the constraint forces can now be calculated as

$$\begin{aligned} \delta W &= \sum_i \mathbf{f}_i \cdot \delta \mathbf{r}_{0,i} = \underbrace{\mathbf{s} \cdot \delta \mathbf{r}_{0,o} + (-\mathbf{p} \cdot \delta \mathbf{r}_{0,p})}_{\text{acting on body 1}} + \underbrace{\mathbf{p} \cdot \delta \mathbf{r}_{0,p}}_{\text{acting on body 2}}, \\ &= \mathbf{s} \cdot \mathbf{0} + (\mathbf{p} - \mathbf{p}) \cdot \delta \mathbf{r}_{0,p}, \\ &= 0. \end{aligned}$$

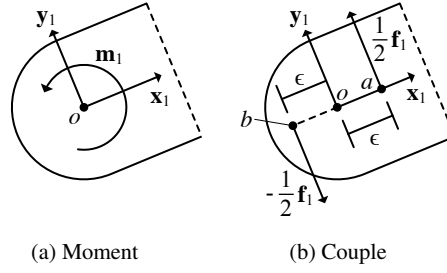
This equation shows that the constraint force between the ground and link 1 contributes zero virtual work because the point of application is fixed with respect to ground, and the constraint force between links 2 and 3 contribute zero virtual work because the force acting on the two bodies is equal and opposite.

Next, the virtual work performed by the actuators will be calculated. The problem statement introduces m_1 and m_2 as the actuation torques that are applied to the robotic system by motors. The definition of the virtual work is stated only in terms of applied forces and not moments or torques. However, from introductory statics, recall that any moment can be represented by a pair of forces with opposite directions and equal magnitudes that are separated by an offset. Such a pair of forces is referred to as a couple. Figure (5.11) illustrates how the moment m_1 acting on body 1 at point o may be represented by a couple consisting of forces with magnitude $\frac{1}{2}f_1$ acting at points a and b equally offset from point o by ϵ along $+\mathbf{x}_1$ (point a) and $-\mathbf{x}_1$ (point b). The virtual displacements may be calculated from the position vectors of points a and b

$$\begin{aligned} \mathbf{r}_{0,a} &= \epsilon \mathbf{x}_1 = \epsilon(\cos \theta_1 \mathbf{x}_0 + \sin \theta_1 \mathbf{y}_0), \\ \mathbf{r}_{0,b} &= -\epsilon \mathbf{x}_1 = -\epsilon(\cos \theta_1 \mathbf{x}_0 + \sin \theta_1 \mathbf{y}_0), \end{aligned}$$

by applying the virtual variation operator, or by calculating the velocities of the points a and b that are fixed to the body 1, and replace $\dot{\theta}_1$ with $\delta \theta_1$. In either case,

$$\begin{aligned} \delta \mathbf{r}_{0,a} &= \epsilon \delta \theta_1 \mathbf{y}_1 = \epsilon \delta \theta_1 (-\sin \theta_1 \mathbf{x}_0 + \cos \theta_1 \mathbf{y}_0), \\ \delta \mathbf{r}_{0,b} &= -\epsilon \delta \theta_1 \mathbf{y}_1 = -\epsilon \delta \theta_1 (-\sin \theta_1 \mathbf{x}_0 + \cos \theta_1 \mathbf{y}_0). \end{aligned}$$

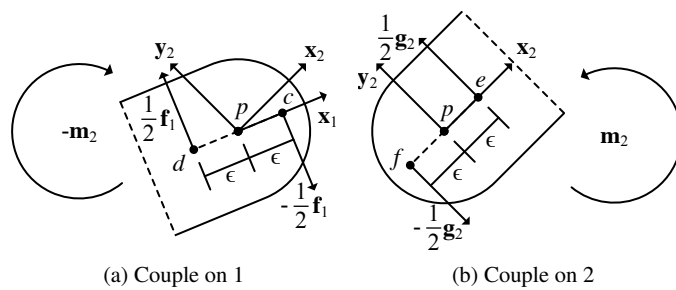
Fig. 5.11: Actuation Moment m_1 and Equivalent Couple

The virtual work that is performed by the pair of forces that make up the couple on body 1 is given by

$$\begin{aligned}\delta W &= \left(\frac{1}{2}f_1\mathbf{y}_1\right) \cdot \delta\mathbf{r}_{0,a} + \left(-\frac{1}{2}f_1\mathbf{y}_1\right) \cdot \delta\mathbf{r}_{0,b} = \frac{1}{2}f_1\epsilon\delta\theta_1 + \left(-\frac{1}{2}f_1\right)(-\epsilon\delta\theta_1), \\ &= f_1\epsilon\delta\theta_1 = m_1\delta\theta_1.\end{aligned}$$

It is important to note that there are a pair of reaction forces that act on the body 0 that are equivalent to the moment $-m_1$ that is applied to the body 0 by the actuator. However, the virtual displacements of all points in body 0 are equal to zero, since body 0 is stationary. The moment acting on body 0 does not contribute to the virtual work.

Next, the virtual work of the actuation moment m_2 that acts on body 2 and the actuation moment $-m_2$ that acts on body 1 are calculated. Figure (5.12a) illustrates the couple acting on body 1 at points c and d fixed on body 1, and Figure (5.12b) illustrates the couple acting on body 2 at points e and f fixed on body 2. The positions of points c, d, e and f are given by the expressions

Fig. 5.12: Couples for Actuation Moment m_2 Acting on Bodies 1 and 2

$$\begin{aligned}\mathbf{r}_{0,c} &= (L_1 + \epsilon)\mathbf{x}_1, \\ \mathbf{r}_{0,d} &= (L_1 - \epsilon)\mathbf{x}_1, \\ \mathbf{r}_{0,e} &= L_1\mathbf{x}_1 + \epsilon\mathbf{x}_2, \\ \mathbf{r}_{0,f} &= L_1\mathbf{x}_1 - \epsilon\mathbf{x}_2,\end{aligned}$$

and are evaluated to calculate the virtual displacements associated with these points as

$$\begin{aligned}\delta\mathbf{r}_{0,c} &= (L + \epsilon)\delta\theta_1\mathbf{y}_1, \\ \delta\mathbf{r}_{0,d} &= (L - \epsilon)\delta\theta_1\mathbf{y}_1, \\ \delta\mathbf{r}_{0,e} &= L_1\delta\theta_1\mathbf{y}_1 + \epsilon(\delta\theta_1 + \delta\theta_2)\mathbf{y}_2, \\ \delta\mathbf{r}_{0,f} &= L_1\delta\theta_1\mathbf{y}_1 - \epsilon(\delta\theta_1 + \delta\theta_2)\mathbf{y}_2.\end{aligned}$$

Note that the couple acting as shown in Figure (5.12a) on link 1 is $-\epsilon f_1 = -m_2$, and the couple acting as in Figure (5.12b) on link 2 is $\epsilon g_2 = m_2$. The virtual work that is performed by the forces that make up the couples that are equivalent to $-m_2$ acting on body 1 and m_2 acting on body 2 can then be summed to yield

$$\begin{aligned}\delta W &= \underbrace{\left(-\frac{1}{2}f_1\mathbf{y}_1\right) \cdot ((L_1 + \epsilon)\delta\theta_1\mathbf{y}_1) + \left(\frac{1}{2}f_1\mathbf{y}_1\right) \cdot ((L_1 - \epsilon)\delta\theta_1\mathbf{y}_1)}_{\text{due to reactions on body 1}} \\ &\quad + \underbrace{\left(\frac{1}{2}g_2\mathbf{y}_2\right) \cdot (L_1\delta\theta_1\mathbf{y}_1 + \epsilon(\delta\theta_1 + \delta\theta_2)\mathbf{y}_2) + \left(-\frac{1}{2}g_2\mathbf{y}_2\right) \cdot (L_1\delta\theta_1\mathbf{y}_1 - \epsilon(\delta\theta_1 + \delta\theta_2)\mathbf{y}_2)}_{\text{due to reactions on body 2}} \\ &= -f_1\epsilon\delta\theta_1 + g_2\epsilon\delta\theta_1 + g_2\epsilon\delta\theta_2 = -m_2\delta\theta_1 + m_2\delta\theta_1 + m_2\delta\theta_2 = m_2\delta\theta_2\end{aligned}$$

since $m_2 = f_2\epsilon = g_2\epsilon$. The total virtual work due to both m_1 acting on link 1 and m_2 acting on links 1 and 2 is therefore

$$\delta W = m_1\delta\theta_1 + m_2\delta\theta_2.$$

The computations in this example are actually quite general upon close inspection. Suppose that there is a kinematic chain in which the generalized coordinates $\mathbf{q} = \{\theta_1, \theta_2, \dots, \theta_N\}$ are the relative angles about a common axis between each adjacent pair of links. If the joint actuation torques are given by \mathbf{m}_i for $i = 1, \dots, N$, then $\delta W = \sum_i \mathbf{m}_i \delta\theta_i$.

It should be carefully noted that the calculation above depends on the fact that the generalized coordinates are relative angles between links. The general result does not hold, for example, if the joint coordinates are all measured from a common datum.

Example 5.3.3. Suppose that the two link robot in Example 5.3.2 is not actuated by motors at the joints, but rather by an artificial muscle that applies a force between points o and q . That is, suppose that the muscle applies a force T at point o directed toward the point q , and a force T at point q directed toward point o . What is the virtual work performed by the artificial muscle? What are the generalized forces?
Solution: Since the velocity of point o is equal to zero, $\delta\mathbf{r}_{0,0} = \mathbf{0}$. The velocities of points p and q are

$$\begin{aligned}\mathbf{v}_{0,p} &= L_1\dot{\theta}_1\mathbf{y}_1, \\ \mathbf{v}_{0,q} &= L_1\dot{\theta}_1\mathbf{y}_1 + L_2\dot{\theta}_2\mathbf{y}_2.\end{aligned}$$

From this, the virtual displacements of points p and q are found to be

$$\begin{aligned}\delta\mathbf{r}_{0,p} &= L_1\delta\theta_1\mathbf{y}_2, \\ \delta\mathbf{r}_{0,q} &= L_1\delta\theta_1\mathbf{y}_2 + L_2\delta\theta_2\mathbf{y}_3.\end{aligned}$$

A unit vector $\mathbf{u}_{o,q}$ can be constructed in the direction of the vector that connects point o to point q as

$$\mathbf{u}_{o,q} = \frac{L_1\mathbf{x}_2 + L_2\mathbf{x}_3}{\|L_1\mathbf{x}_2 + L_2\mathbf{x}_3\|} = \frac{1}{\sqrt{L_1^2 + L_2^2 + 2L_1L_2\cos(\theta_2 - \theta_1)}}(L_1\mathbf{x}_2 + L_2\mathbf{x}_3).$$

Finally, the virtual work performed by the follower forces is written as

$$\begin{aligned}\delta W &= (T\mathbf{u}_{o,q}) \cdot \delta\mathbf{r}_{0,o} + (-T\mathbf{u}_{o,q}) \cdot \delta\mathbf{r}_{0,q} \\ &= -\frac{TL_1L_2\sin(\theta_2 - \theta_1)}{\sqrt{L_1^2 + L_2^2 + 2L_1L_2\cos(\theta_2 - \theta_1)}}(\delta\theta_1 - \delta\theta_2).\end{aligned}$$

The generalized forces are calculated by finding the coefficients in the virtual work δW of the variations $\delta\theta_1$ and $\delta\theta_2$,

$$\mathbf{Q} = \begin{Bmatrix} Q_1 \\ Q_2 \end{Bmatrix} = \begin{Bmatrix} -\frac{TL_1L_2\sin(\theta_2 - \theta_1)}{\sqrt{L_1^2 + L_2^2 + 2L_1L_2\cos(\theta_2 - \theta_1)}} \\ \frac{TL_1L_2\sin(\theta_2 - \theta_1)}{\sqrt{L_1^2 + L_2^2 + 2L_1L_2\cos(\theta_2 - \theta_1)}} \end{Bmatrix}.$$

The solution above can also be found in Example ?? in the MATLAB Workbook for DCRS.

Example 5.3.4. This example considers a rigid body with body fixed frame \mathbb{B} that moves relative to the ground frame \mathbb{X} . The generalized coordinates chosen for this

system are the coordinates $\{x_c, y_c, z_c\}$ of the center of mass of the rigid body relative to the ground frame

$$\mathbf{r}_{\mathbb{X},c} = x_c \mathbf{x}_1 + y_c \mathbf{x}_2 + z_c \mathbf{x}_3,$$

and the $3 - 2 - 1$ Euler angles $\{\psi, \theta, \phi\}$ that relate the orientation of the body frame \mathbb{B} to the ground frame \mathbb{X} via the rotation matrix

$$\mathbf{R}_{\mathbb{X}}^{\mathbb{B}} = \begin{bmatrix} 1 & 0 & 0 \\ 0 & \cos\phi & \sin\phi \\ 0 & -\sin\phi & \cos\phi \end{bmatrix} \begin{bmatrix} \cos\theta & 0 & -\sin\theta \\ 0 & 1 & 0 \\ \sin\theta & 0 & \cos\theta \end{bmatrix} \begin{bmatrix} \cos\psi & \sin\psi & 0 \\ -\sin\psi & \cos\psi & 0 \\ 0 & 0 & 1 \end{bmatrix}.$$

The vector of generalized coordinates \mathbf{q} used to represent the motion of the rigid body is defined as

$$\mathbf{q}^T = \{q_1 \ q_2 \ \dots \ q_6\}^T = \{x_c \ y_c \ z_c \ \phi \ \theta \ \psi\}^T$$

Calculate the virtual work performed by an external force \mathbf{f}

$$\mathbf{f} = f_1 \mathbf{b}_1 + f_2 \mathbf{b}_2 + f_3 \mathbf{b}_3$$

that is applied at a point p that is fixed on the body. The point p is located by the vector $\mathbf{d}_{c,p}$ that connects the center of mass to the point p . This vector is given by

$$\mathbf{d}_{c,p} = d_1 \mathbf{b}_1 + d_2 \mathbf{b}_2 + d_3 \mathbf{b}_3.$$

Find the generalized force $\mathbf{Q} := \{Q_1 \dots Q_6\}^T$ generated by the point force.

Solution: The virtual displacement of the point p will be calculated by calculating its velocity and substituting δq_k for \dot{q}_k for $k = 1, 2, \dots, 6$ as discussed in Section 5.3.1. The velocity of the point of application of the force is related to the velocity of the center of mass as

$$\mathbf{v}_{\mathbb{X},p} = \mathbf{v}_{\mathbb{X},c} + \boldsymbol{\omega}_{\mathbb{X},\mathbb{B}} \times \mathbf{d}_{c,p}.$$

This equation can be rewritten in the form

$$\mathbf{v}_{\mathbb{X},p} = \dot{x}_c \mathbf{x}_1 + \dot{y}_c \mathbf{x}_2 + \dot{z}_c \mathbf{x}_3 - \mathbf{d}_{c,p} \times \boldsymbol{\omega}_{\mathbb{X},\mathbb{B}}.$$

Recall that the angular velocity can be written in terms of the time derivatives of the roll, pitch and yaw angles in the body fixed frame as

$$\boldsymbol{\omega}_{\mathbb{X},\mathbb{B}}^{\mathbb{B}} = \begin{bmatrix} 1 & 0 & -\sin\theta \\ 0 & \cos\phi & \cos\theta \sin\phi \\ 0 & -\sin\phi & \cos\theta \cos\phi \end{bmatrix} \begin{Bmatrix} \dot{\phi} \\ \dot{\theta} \\ \dot{\psi} \end{Bmatrix} = \mathbf{W}(\phi, \theta, \psi) \begin{Bmatrix} \dot{\phi} \\ \dot{\theta} \\ \dot{\psi} \end{Bmatrix}. \quad (5.3.4)$$

These expressions can be combined to obtain a representation of the velocity of point p in terms of the basis for the \mathbb{B} frame as

$$\begin{aligned}\mathbf{v}_{\mathbb{X},p}^{\mathbb{B}} &= \mathbf{R}_{\mathbb{X}}^{\mathbb{B}} \begin{Bmatrix} \dot{x}_c \\ \dot{y}_c \\ \dot{z}_c \end{Bmatrix} - \begin{bmatrix} 0 & -d_3 & d_2 \\ d_3 & 0 & -d_1 \\ -d_2 & d_1 & 0 \end{bmatrix} \begin{bmatrix} 1 & 0 & -\sin\theta \\ 0 & \cos\phi & \cos\theta\sin\phi \\ 0 & -\sin\phi & \cos\theta\cos\phi \end{bmatrix} \begin{Bmatrix} \dot{\phi} \\ \dot{\theta} \\ \dot{\psi} \end{Bmatrix}, \\ &= \left[\mathbf{R}_{\mathbb{X}}^{\mathbb{B}} - \mathbf{S}(\mathbf{d}_{c,p}^{\mathbb{B}}) \mathbf{W}(\phi, \theta, \psi) \right] \begin{Bmatrix} \dot{x}_c \\ \dot{y}_c \\ \dot{z}_c \\ \dot{\phi} \\ \dot{\theta} \\ \dot{\psi} \end{Bmatrix}.\end{aligned}$$

This last equation provides form for the velocity conducive for calculating the components of the virtual displacement of the point p relative to the \mathbb{B} frame. The virtual displacements are

$$\delta \mathbf{r}_{\mathbb{X},p}^{\mathbb{B}} = \left[\mathbf{R}_{\mathbb{X}}^{\mathbb{B}} - \mathbf{S}(\mathbf{d}_{c,p}^{\mathbb{B}}) \mathbf{W}(\phi, \theta, \psi) \right] \begin{Bmatrix} \delta x_c \\ \delta y_c \\ \delta z_c \\ \delta \phi \\ \delta \theta \\ \delta \psi \end{Bmatrix}$$

The virtual work due to the applied force \mathbf{f} is consequently

$$\delta W = \mathbf{f} \cdot \delta \mathbf{r}_{\mathbb{X},p}^{\mathbb{B}} = [f_1 \ f_2 \ f_3] [\mathbf{R}_{\mathbb{X}}^{\mathbb{B}} - \mathbf{S}(\mathbf{d}_{c,p}^{\mathbb{B}}) \mathbf{W}(\phi, \theta, \psi)] \delta \mathbf{q} = \mathbf{Q}^T \delta \mathbf{q}.$$

The generalized forces can be written as

$$\mathbf{Q} = \left[\mathbf{R}_{\mathbb{X}}^{\mathbb{B}} - \mathbf{S}(\mathbf{d}_{c,p}^{\mathbb{B}}) \mathbf{W}(\phi, \theta, \psi) \right]^T \begin{Bmatrix} f_1 \\ f_2 \\ f_3 \end{Bmatrix}.$$

The entries in the vector of generalized forces are computed in Example ?? in the MATLAB Workbook for DCRS.

Example 5.3.5. The rigid bodies shown in Figure (5.13) move relative to the ground frame \mathbb{X} and have body fixed frames \mathbb{B} and \mathbb{C} , respectively. The body \mathbb{C} rotates relative to body \mathbb{B} about a revolute joint along the $\mathbf{b}_3 = \mathbf{c}_3$ axis. Seven generalized coordinates are required for representing this system. One valid choice of coordinates includes the three coordinates of the center of mass of the body \mathbb{B} in terms of the basis for the ground frame \mathbb{X}

$$\mathbf{r}_{\mathbb{X},c_{\mathbb{B}}} = x_{c_{\mathbb{B}}} \mathbf{x}_1 + y_{c_{\mathbb{B}}} \mathbf{x}_2 + z_{c_{\mathbb{B}}} \mathbf{x}_3,$$

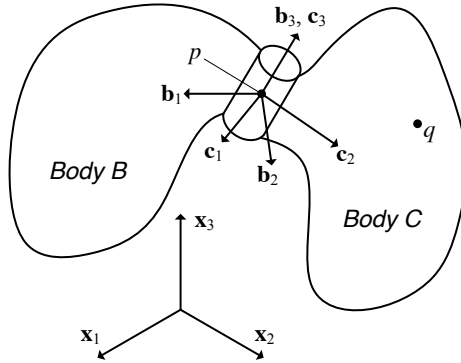


Fig. 5.13: Bodies \mathbb{B} and \mathbb{C} with Shared Revolute Joint Moving in \mathbb{X}

the $3 - 2 - 1$ Euler angles (ψ, θ, ϕ) that relate the \mathbb{B} frame to the \mathbb{X} frame via the rotation matrix

$$\mathbf{R}_{\mathbb{X}}^{\mathbb{B}} = \begin{bmatrix} 1 & 0 & 0 \\ 0 & \cos\phi & \sin\phi \\ 0 & -\sin\phi & \cos\phi \end{bmatrix} \begin{bmatrix} \cos\theta & 0 & -\sin\theta \\ 0 & 1 & 0 \\ \sin\theta & 0 & \cos\theta \end{bmatrix} \begin{bmatrix} \cos\psi & \sin\psi & 0 \\ -\sin\psi & \cos\psi & 0 \\ 0 & 0 & 1 \end{bmatrix},$$

and the angle α that governs the rotation of the \mathbb{C} frame with respect to the \mathbb{B} frame

$$\mathbf{R}_{\mathbb{B}}^{\mathbb{C}} = \begin{bmatrix} \cos\alpha & \sin\alpha & 0 \\ -\sin\alpha & \cos\alpha & 0 \\ 0 & 0 & 1 \end{bmatrix}.$$

The generalized coordinates are ordered in the 7-tuple \mathbf{q} such that

$$\{q_1 \ q_2 \ \dots \ q_7\}^T = \{x_{c_B} \ y_{c_B} \ z_{c_B} \ \phi \ \theta \ \psi \ \alpha\}^T = \{\mathbf{q}_B \ \alpha\}^T.$$

Find the virtual work performed by a force \mathbf{f} acting at a point q fixed on the body \mathbb{C} . Find the virtual work performed by the actuator that applies the moments \mathbf{m} to body \mathbb{C} and $-\mathbf{m}$ to body \mathbb{B} about the $\mathbf{b}_3 = \mathbf{c}_3$ axis. Show that the virtual work performed by the constraint forces and moments at the revolute joint are equal to zero.

Solution: First, the virtual work of a force \mathbf{f} acting at the point q fixed on the body \mathbb{C} is calculated. Since $\mathbf{v}_{\mathbb{X},q} = \mathbf{v}_{\mathbb{X},p} + \boldsymbol{\omega}_{\mathbb{X},\mathbb{C}} \times \mathbf{d}_{p,q}$ and $\boldsymbol{\omega}_{\mathbb{X},\mathbb{C}} = \boldsymbol{\omega}_{\mathbb{X},\mathbb{B}} + \dot{\alpha}\mathbf{b}_3$, the results of Example 5.3.4 enable us to express the velocity into components relative to the basis for the \mathbb{C} frame as follows:

$$\begin{aligned}
\mathbf{v}_{\mathbb{X},q}^{\mathbb{C}} &= \mathbf{R}_{\mathbb{B}}^{\mathbb{C}} \left[\mathbf{R}_{\mathbb{X}}^{\mathbb{B}}, \mathbf{S}(-\mathbf{d}_{c,p}^{\mathbb{B}}) \mathbf{W}(\phi, \theta, \psi) \right] \dot{\mathbf{q}}_{\mathbb{B}} + \mathbf{R}_{\mathbb{B}}^{\mathbb{C}} \mathbf{S}(-\mathbf{d}_{p,q}^{\mathbb{B}}) \mathbf{W}(\phi, \theta, \psi) \begin{Bmatrix} \dot{\phi} \\ \dot{\theta} \\ \dot{\psi} \end{Bmatrix} + \mathbf{S}(-\mathbf{d}_{p,q}^{\mathbb{C}}) \begin{Bmatrix} 0 \\ 0 \\ 1 \end{Bmatrix} \dot{\alpha}, \\
&= \mathbf{R}_{\mathbb{B}}^{\mathbb{C}} \left[\mathbf{R}_{\mathbb{X}}^{\mathbb{B}}, \mathbf{S}(-\mathbf{d}_{c,q}^{\mathbb{B}}) \mathbf{W}(\phi, \theta, \psi) \right] \dot{\mathbf{q}}_{\mathbb{B}} + \mathbf{S}(-\mathbf{d}_{p,q}^{\mathbb{C}}) \begin{Bmatrix} 0 \\ 0 \\ 1 \end{Bmatrix} \dot{\alpha}, \\
&= \mathbf{R}_{\mathbb{B}}^{\mathbb{C}} \left[\mathbf{R}_{\mathbb{X}}^{\mathbb{B}}, \mathbf{S}(-\mathbf{d}_{c,q}^{\mathbb{B}}) \mathbf{W}(\phi, \theta, \psi), \mathbf{S}(-\mathbf{d}_{p,q}^{\mathbb{B}}) \begin{Bmatrix} 0 \\ 0 \\ 1 \end{Bmatrix} \right] \dot{\mathbf{q}}.
\end{aligned}$$

Since the virtual displacement of the point q can be written as

$$\delta \mathbf{r}_{\mathbb{X},q}^{\mathbb{C}} = \mathbf{R}_{\mathbb{B}}^{\mathbb{C}} \left[\mathbf{R}_{\mathbb{X}}^{\mathbb{B}}, \mathbf{S}(-\mathbf{d}_{c,q}^{\mathbb{B}}) \mathbf{W}(\phi, \theta, \psi), \mathbf{S}(-\mathbf{d}_{p,q}^{\mathbb{B}}) \begin{Bmatrix} 0 \\ 0 \\ 1 \end{Bmatrix} \right] \delta \mathbf{q},$$

the virtual work of the force $\mathbf{f} := f_1 \mathbf{b}_1 + f_2 \mathbf{b}_2 + f_3 \mathbf{b}_3$ is

$$\delta W = [f_1 \ f_2 \ f_3] \left[\mathbf{R}_{\mathbb{X}}^{\mathbb{B}}, \mathbf{S}(-\mathbf{d}_{c,q}^{\mathbb{B}}) \mathbf{W}(\phi, \theta, \psi), \mathbf{S}(-\mathbf{d}_{p,q}^{\mathbb{B}}) \begin{Bmatrix} 0 \\ 0 \\ 1 \end{Bmatrix} \right] \delta \mathbf{q}.$$

The equations above have been derived by expressing the vectors in terms of the bases \mathbb{B} or \mathbb{C} . Some authors choose to represent the variational equations as vectors, without choosing some specific basis. For example, given that

$$\delta \boldsymbol{\omega}_{\mathbb{X},\mathbb{B}}^{\mathbb{B}} := \mathbf{W}(\phi, \theta, \psi) \begin{Bmatrix} \delta \phi \\ \delta \theta \\ \delta \psi \end{Bmatrix},$$

then the virtual displacement of the point q can be written as the vector equation

$$\delta \mathbf{r}_{\mathbb{X},q} := \delta \mathbf{r}_{\mathbb{X},p} - \mathbf{d}_{p,q} \times (\delta \boldsymbol{\omega}_{\mathbb{X},\mathbb{B}} + \delta \alpha \mathbf{b}_3) = \delta \mathbf{r}_{\mathbb{X},p} + (\delta \boldsymbol{\omega}_{\mathbb{X},\mathbb{B}} + \delta \alpha \mathbf{b}_3) \times \mathbf{d}_{p,q}$$

where $\delta \mathbf{r}_{\mathbb{X},p}$ is defined as in Example 5.3.4.

Next, the virtual work performed by actuation moments acting on the bodies \mathbb{B} and \mathbb{C} about the revolute joint is computed. The solution proceeds as in the analysis carried out in Example (5.3.2) for the two-dimensional case. It is assumed that the moment generated by the actuator is represented by a pair of equal magnitude forces having opposite directions. It is assumed that a force equal to $\frac{1}{2}\mathbf{f} = \frac{1}{2}f\mathbf{c}_2$ is applied at point a on body \mathbb{C} . The vector $\mathbf{d}_{p,a} = d_{p,a}\mathbf{c}_1$ connects point p to point a on body \mathbb{C} . Similarly, a force of $-\frac{1}{2}\mathbf{f} = -\frac{1}{2}f\mathbf{c}_2$ is applied at point b on body \mathbb{C} . The vector $\mathbf{d}_{p,b} = -\mathbf{d}_{p,a} = -d_{p,a}\mathbf{c}_1$ connects point p to point b on body \mathbb{C} . Therefore, the moment about the $\mathbf{b}_3 = \mathbf{c}_3$ axis applied to body \mathbb{C} is given by

$$m\mathbf{c}_3 = \mathbf{d}_{p,a} \times \left(\frac{1}{2}\mathbf{f} \right) + \mathbf{d}_{p,b} \times \left(-\frac{1}{2}\mathbf{f} \right) = \mathbf{d}_{p,a} \times \mathbf{f} = d_{p,a} f \mathbf{b}_3.$$

A similar analysis is used to determine the form of the moment acting on body \mathbb{B} . A force equal to $-\frac{1}{2}\mathbf{g} = -\frac{1}{2}g\mathbf{b}_2$ is applied at point c on body \mathbb{B} . The vector $\mathbf{d}_{p,c} = d_{p,c}\mathbf{b}_1$ connects point p to point c on body \mathbb{C} . Similarly, a force of $\frac{1}{2}\mathbf{g} = \frac{1}{2}g\mathbf{b}_2$ is applied at point d on body \mathbb{B} . The vector $\mathbf{d}_{p,d} = -\mathbf{d}_{p,c} = -d_{p,c}\mathbf{b}_1$ connects point p to point d on body \mathbb{C} . Therefore, the moment about the $\mathbf{b}_3 = \mathbf{c}_3$ axis applied to body \mathbb{B} is given by

$$-m\mathbf{b}_3 = \mathbf{d}_{p,c} \times \left(-\frac{1}{2}\mathbf{g}\right) + \mathbf{d}_{p,d} \times \left(\frac{1}{2}\mathbf{g}\right) = -\mathbf{d}_{p,c} \times \mathbf{g} = -d_{p,c}g\mathbf{b}_3.$$

The virtual displacements of point $a-d$ are found by calculating the velocity of each point, and converting the velocity to a corresponding virtual displacement. The velocity of the points $a-d$ can be defined as

$$\begin{aligned}\mathbf{v}_{\mathbb{X},a} &= \mathbf{v}_{\mathbb{X},p} + \boldsymbol{\omega}_{\mathbb{X},\mathbb{C}} \times \mathbf{d}_{p,a}, \\ \mathbf{v}_{\mathbb{X},d} &= \mathbf{v}_{\mathbb{X},p} + \boldsymbol{\omega}_{\mathbb{X},\mathbb{C}} \times (-\mathbf{d}_{p,a}), \\ \mathbf{v}_{\mathbb{X},c} &= \mathbf{v}_{\mathbb{X},p} + \boldsymbol{\omega}_{\mathbb{X},\mathbb{B}} \times \mathbf{d}_{p,c}, \\ \mathbf{v}_{\mathbb{X},d} &= \mathbf{v}_{\mathbb{X},p} + \boldsymbol{\omega}_{\mathbb{X},\mathbb{B}} \times (-\mathbf{d}_{p,c}).\end{aligned}$$

The corresponding virtual displacements of point $a-d$ are

$$\begin{aligned}\delta\mathbf{r}_{\mathbb{X},a} &= \delta\mathbf{r}_{\mathbb{X},p} + \delta\boldsymbol{\omega}_{\mathbb{X},\mathbb{C}} \times \mathbf{d}_{p,a}, \\ \delta\mathbf{r}_{\mathbb{X},b} &= \delta\mathbf{r}_{\mathbb{X},p} - \delta\boldsymbol{\omega}_{\mathbb{X},\mathbb{C}} \times \mathbf{d}_{p,a}, \\ \delta\mathbf{r}_{\mathbb{X},c} &= \delta\mathbf{r}_{\mathbb{X},p} + \delta\boldsymbol{\omega}_{\mathbb{X},\mathbb{B}} \times \mathbf{d}_{p,c}, \\ \delta\mathbf{r}_{\mathbb{X},d} &= \delta\mathbf{r}_{\mathbb{X},p} - \delta\boldsymbol{\omega}_{\mathbb{X},\mathbb{B}} \times \mathbf{d}_{p,c}.\end{aligned}$$

The virtual work associated with the actuating moment is then the sum of the virtual work contributions of all of these forces.

$$\begin{aligned}\delta W &= \left(\frac{1}{2}\mathbf{f}\right) \cdot (\delta\mathbf{r}_{\mathbb{X},p} + \delta\boldsymbol{\omega}_{\mathbb{X},\mathbb{C}} \times \mathbf{d}_{p,a}) + \left(-\frac{1}{2}\mathbf{f}\right) \cdot (\delta\mathbf{r}_{\mathbb{X},p} - \delta\boldsymbol{\omega}_{\mathbb{X},\mathbb{C}} \times \mathbf{d}_{p,a}) \\ &\quad + \left(-\frac{1}{2}\mathbf{g}\right) \cdot (\delta\mathbf{r}_{\mathbb{X},p} + \delta\boldsymbol{\omega}_{\mathbb{X},\mathbb{B}} \times \mathbf{d}_{p,c}) + \left(\frac{1}{2}\mathbf{g}\right) \cdot (\delta\mathbf{r}_{\mathbb{X},p} - \delta\boldsymbol{\omega}_{\mathbb{X},\mathbb{B}} \times \mathbf{d}_{p,c}).\end{aligned}$$

Because $m = d_{p,a}f = d_{p,c}g$ based on the formulation of the two couples, the above equation reduces to

$$\delta W = m\delta\alpha$$

for the virtual work performed by an actuation torque about the revolute axis. Note that the actuating moment contributes to the virtual work expression only through the virtual variation $\delta\alpha$. This is an important observation that makes the derivation of the virtual work contributions for many practical robotic systems a simpler task. This result should be compared and contrasted to the analysis for the planar robot in Example (5.3.2).

Hamilton's Principle can now be extended to systems that include nonconservative mechanical forces by employing the definitions of the virtual variation operator, virtual displacements, and the virtual work performed by applied forces. The result is known as Hamilton's Extended Principle.

Theorem 5.6. Let $\mathbf{q}(t) := \{q_1(t), q_2(t), \dots, q_N(t)\}^T$ be a collection of generalized coordinates for a mechanical system that is subject to external nonconservative forces and torques. Of all the possible motions of the mechanical system that are consistent with the kinematic constraints, the actual motion of the system satisfies

$$\delta \int_{t_0}^{t_f} (T - V) dt + \int_{t_0}^{t_f} \delta W_{nc} dt = 0 \quad (5.3.5)$$

where T is the kinetic energy, V is the potential energy and δW_{nc} is the virtual work of the external nonconservative forces acting on the mechanical system.

As in the treatment of conservative systems, Hamilton's Extended Principle can be used directly to solve problems, or it can be used to derive alternative approaches in analytical mechanics. It will first be applied to solve a simple problem.

Example 5.3.6. Consider the point mass that is constrained to lie on the plane shown Example (5.1.3). Suppose that an external force $\mathbf{p}(t)$ acts on the mass where

$$\mathbf{p}(t) = A \cos(\Omega t) \left(\frac{1}{\sqrt{2}} \mathbf{x}_0 - \frac{1}{\sqrt{2}} \mathbf{z}_0 \right) + B \sin(\Omega t) \left(\frac{1}{\sqrt{2}} \mathbf{y}_0 - \frac{1}{\sqrt{2}} \mathbf{z}_0 \right).$$

Find the virtual work performed by this external force and use Hamilton's Extended principle to find the governing equations of this system.

Solution: The force \mathbf{p} is always parallel to the plane, which is evident from the calculation

$$\mathbf{p} \cdot \mathbf{n} = \left(A \cos(\Omega t) \begin{Bmatrix} \frac{1}{\sqrt{2}} \\ 0 \\ -\frac{1}{\sqrt{2}} \end{Bmatrix} + B \sin(\Omega t) \begin{Bmatrix} \frac{1}{\sqrt{2}} \\ \frac{1}{\sqrt{2}} \\ -\frac{1}{\sqrt{2}} \end{Bmatrix} \right) \cdot \frac{1}{\sqrt{3}} \begin{Bmatrix} 1 \\ 1 \\ 1 \end{Bmatrix} = 0.$$

From Example (5.1.3)

$$\begin{aligned} \delta \int_{t_0}^{t_f} (T - V) dt &= \int_{t_0}^{t_f} \{ \dot{\mathbf{q}}^T \mathbf{M} \delta \dot{\mathbf{q}} + mg [1 \ 1] \delta \mathbf{q} \} dt, \\ &= \dot{\mathbf{q}}^T \mathbf{M} \delta \dot{\mathbf{q}} \Big|_{t_0}^{t_f} + \int_{t_0}^{t_f} \left\{ -\mathbf{M} \ddot{\mathbf{q}} + mg \begin{Bmatrix} 1 \\ 1 \end{Bmatrix} \right\} \cdot \delta \mathbf{q} dt. \end{aligned}$$

The virtual work due to the nonconservative, external applied forces is given by

$$\begin{aligned}\delta W &= \mathbf{p} \cdot \delta \mathbf{r}_{0,m} = \left\{ \begin{array}{c} \frac{1}{\sqrt{2}}A \cos(\Omega t) \\ \frac{1}{\sqrt{2}}B \sin(\Omega t) \\ -\frac{1}{\sqrt{2}}A \cos(\Omega t) - \frac{1}{\sqrt{2}}B \sin(\Omega t) \end{array} \right\} \cdot \left\{ \begin{array}{c} \delta q_1 \\ \delta q_2 \\ -\delta q_1 - \delta q_2 \end{array} \right\}, \\ &= \left(\sqrt{2}A \cos(\Omega t) + \frac{1}{\sqrt{2}}B \sin(\Omega t) \right) \delta q_1 + \left(\sqrt{2}B \sin(\Omega t) + \frac{1}{\sqrt{2}}A \cos(\Omega t) \right) \delta q_2.\end{aligned}$$

The final form of *Hamilton's Extended Principle* is obtained when these terms are combined. It must be the case that

$$\begin{aligned}&\delta \int_{t_0}^{t_f} (T - V) dt + \int_{t_0}^{t_f} \delta W dt \\ &= \int_{t_0}^{t_f} \left\{ -\mathbf{M}\ddot{\mathbf{q}} + mg \begin{pmatrix} 1 \\ 1 \end{pmatrix} + \begin{pmatrix} \sqrt{2}A \cos(\Omega t) + \frac{1}{\sqrt{2}}B \sin(\Omega t) \\ \sqrt{2}B \sin(\Omega t) + \frac{1}{\sqrt{2}}A \cos(\Omega t) \end{pmatrix} \right\} \cdot \delta \mathbf{q} dt = 0\end{aligned}$$

for all admissible variations $\delta \mathbf{q}$. This expression must be equal to zero for all choices of the *virtual variation* $\delta \mathbf{q}$, and we conclude that the integrand must be equal to zero. This gives the equations of motion.

It was shown earlier in this chapter that *Lagrange's equations* for conservative systems could be derived from *Hamilton's Principle*. Likewise, *Hamilton's Extended Principle* can be used to derive a form of *Lagrange's equations* for non-conservative systems.

Theorem 5.7. Let $\mathbf{q}(t) := \{q_1(t) q_2(t) \dots q_N(t)\}^T$ be a collection of generalized coordinates for a mechanical system that is subject to nonconservative external forces. Suppose that $T = T(\dot{\mathbf{q}}, \mathbf{q}, t)$ and $V = V(\mathbf{q}, t)$. If the action functional $A(\mathbf{q})$ is stationary, then

$$\frac{d}{dt} \left(\frac{\partial T}{\partial \dot{\mathbf{q}}} \right) - \frac{\partial T}{\partial \mathbf{q}} + \frac{\partial V}{\partial \mathbf{q}} = \mathbf{Q} \quad (5.3.6)$$

with the nonconservative work

$$\delta W_{nc} = \sum Q_k \delta q_k = \mathbf{Q} \cdot \delta \mathbf{q}. \quad (5.3.7)$$

These equations are known as *Lagrange's equations for the nonconservative mechanical system*.

Proof. *Hamilton's Extended Principle* maintains that

$$\delta \int_{t_0}^{t_f} (T - V) dt + \int_{t_0}^{t_f} \delta W_{nc} dt = 0$$

for all *virtual displacements* consistent with the *kinematic constraints* on the mechanical system. Since the *virtual variation operator* $\delta(\bullet)$ commutes with integration and obeys the chain rule just like the differential operator, the variation yields

$$\begin{aligned}\delta \int_{t_0}^{t_f} (T - V) dt &= \int_{t_0}^{t_f} (\delta T - \delta V) dt \\ &= \int_{t_0}^{t_f} \left\{ \frac{\partial T}{\partial \dot{\mathbf{q}}} \delta \dot{\mathbf{q}} + \frac{\partial T}{\partial \mathbf{q}} \delta \mathbf{q} + \frac{\partial T}{\partial t} \delta t - \frac{\partial V}{\partial \mathbf{q}} \delta \mathbf{q} - \frac{\partial V}{\partial t} \delta t \right\} dt.\end{aligned}$$

Since the *variation* δt of time t is equal to zero, and the *variation operator* commutes with differentiation, the above expression can be simplified as

$$\delta \int_{t_0}^{t_f} (T - V) dt = \int_{t_0}^{t_f} \left\{ \frac{\partial T}{\partial \dot{\mathbf{q}}} \frac{d}{dt} (\delta \mathbf{q}) + \frac{\partial T}{\partial \mathbf{q}} \delta \mathbf{q} - \frac{\partial V}{\partial \mathbf{q}} \delta \mathbf{q} \right\} dt.$$

Similar to the analysis of problems arising in the *calculus of variations*, it is desirable to cast this equation in the form

$$\int_{t_0}^{t_f} \mathbf{e}(t) \cdot \delta \mathbf{q}(t) dt = \mathbf{0},$$

and observe that it must hold for all *virtual variations* $\delta \mathbf{q}$ consistent with the constraints. Similar to before, this is achieved when the integrand that multiplies $\delta \mathbf{q}$ is zero, that is

$$\mathbf{e}(t) \equiv \mathbf{0}.$$

As in the proof of Theorem (5.5), this is possible when the derivative that acts on the *variation* $\delta \mathbf{q}(t)$ is eliminated by integration by parts. It follows that

$$\delta \int_{t_0}^{t_f} (T - V) dt + \int_{t_0}^{t_f} \delta W_{nc} dt = \int_{t_0}^{t_f} \left\{ -\frac{d}{dt} \left(\frac{\partial T}{\partial \dot{\mathbf{q}}} \right) + \frac{\partial T}{\partial \mathbf{q}} - \frac{\partial V}{\partial \mathbf{q}} + \mathbf{Q} \right\} \cdot \delta \mathbf{q}(t) dt$$

holds for all $\delta \mathbf{q}(t)$ that are consistent with the constraints. The proof of the theorem is complete with an application of the Fundamental Theorem of Variational Calculus. \square

5.4 Lagrange's Equations for Robotic Systems

Lagrange's equations for nonconservative systems, as summarized in Theorem (5.7), can be used for many mechanical systems. Several typical problems have been studied in the examples, and others that are tutorial in nature can be found in Problems (5.9) through (5.14). This section discusses the form of the governing equations for common *robotic systems*. It will be shown that the equations are not difficult to derive in principle, although the algebraic manipulations can be tedious.

Computer programs that perform *symbolic computations* can be used to great advantage in these problems.

5.4.1 Natural Systems

Let $\mathbf{q} = \{q_1, q_2, \dots, q_N\}^T$ be a set of *generalized coordinates* for a mechanical system. The set of robotic systems studied in this section are assumed to satisfy two fundamental assumptions. First, the kinetic energy of the system has the form

$$T = \frac{1}{2} \dot{\mathbf{q}}^T \mathbf{M}(\mathbf{q}) \dot{\mathbf{q}} = \frac{1}{2} \sum_{i,j}^N \dot{q}_i m_{ij} (q_1, \dots, q_n) \dot{q}_j \quad (5.4.1)$$

where the *generalized inertia or mass matrix* \mathbf{M} is symmetric and is a uniformly positive definite function of the *generalized coordinates*. A system for which the *kinetic energy* has the form in Equation (5.4.1) is known as a *natural system*, or T_2 system, see [31]. It is also assumed that the *potential energy* of the system has the form

$$V = V(q_1, q_2, \dots, q_N). \quad (5.4.2)$$

Under these assumptions, the equations of motion for the robotic system can be derived from Lagrange's equations for nonconservative systems.

Theorem 5.8. Suppose $\mathbf{q} = \{q_1, q_2, \dots, q_N\}^T$ is a set of generalized coordinates for a natural system, where Equation (5.4.1) holds. Assume that the potential energy is a function of the generalized coordinates as in Equation (5.4.2). Lagrange's equations can be written as

$$\sum_j m_{kj} \ddot{q}_j + \sum_{i,j} \Gamma_{ijk} \dot{q}_i \dot{q}_j + \frac{\partial V}{\partial q_k} = Q_k$$

for $k = 1, 2, \dots, N$ where m_{kj} is the (kj) entry of the generalized mass matrix, Q_k is the k^{th} generalized force, and Γ is defined as

$$\Gamma_{ijk} := \frac{\partial m_{kj}}{\partial q_i} - \frac{1}{2} \frac{\partial m_{ij}}{\partial q_k},$$

for $i, j, k = 1, \dots, N$.

Proof. The terms that arise from the kinetic energy are considered first, starting with

$$\begin{aligned} \frac{d}{dt} \left(\frac{\partial T}{\partial \dot{q}_k} \right) &= \frac{d}{dt} \left(\frac{1}{2} \sum_{i,j}^N \frac{\partial(\dot{q}_i m_{ij} \dot{q}_j)}{\partial \dot{q}_k} \right) = \frac{d}{dt} \left(\frac{1}{2} \sum_{i,j}^N \left(\frac{\partial \dot{q}_i}{\partial \dot{q}_k} m_{ij} \dot{q}_j + \dot{q}_i m_{ij} \frac{\partial \dot{q}_j}{\partial \dot{q}_k} \right) \right), \\ &= \frac{d}{dt} \left(\frac{1}{2} \sum_{i,j}^N (\delta_{i,k} m_{ij} \dot{q}_j + \dot{q}_i m_{ij} \delta_{j,k}) \right) = \frac{d}{dt} \left(\frac{1}{2} \left(\sum_j^N m_{kj} \dot{q}_j + \sum_i^N \dot{q}_i m_{ik} \right) \right). = \frac{d}{dt} \left(\sum_j^N m_{kj} \dot{q}_j \right) \end{aligned}$$

The last line above follows from the symmetry of the matrix \mathbf{M} . When the total time derivative is taken,

$$\frac{d}{dt} \left(\frac{\partial T}{\partial \dot{q}_k} \right) = \sum_j^N \left(m_{kj} \ddot{q}_j + \sum_i^N \frac{\partial m_{kj}}{\partial q_i} \dot{q}_i \dot{q}_j \right).$$

When this total time derivative is combined with the term

$$\frac{\partial T}{\partial q_k} = \frac{1}{2} \sum_{i,j}^N \dot{q}_i \frac{\partial m_{ij}}{\partial q_k} \dot{q}_j,$$

the equations of motion for the robotic system can be written

$$\begin{aligned} \frac{d}{dt} \left(\frac{\partial T}{\partial \dot{q}_k} \right) - \frac{\partial T}{\partial q_k} + \frac{\partial V}{\partial q_k} &= Q_k, \\ &= \sum_j^N m_{kj} \ddot{q}_j + \sum_{i,j}^N \left(\frac{\partial m_{kj}}{\partial q_i} - \frac{1}{2} \frac{\partial m_{ij}}{\partial q_k} \right) \dot{q}_i \dot{q}_j + \frac{\partial V}{\partial q_k} = Q_k. \end{aligned}$$

A common form for the equations of motion of a robotic system are then obtained by noting that

$$\begin{aligned} \sum_{i,j}^N \frac{\partial m_{kj}}{\partial q_i} \dot{q}_i \dot{q}_j &= \frac{1}{2} \sum_{i,j}^N \frac{\partial m_{kj}}{\partial q_i} \dot{q}_i \dot{q}_j + \frac{1}{2} \sum_{j,i}^N \frac{\partial m_{ki}}{\partial q_i} \dot{q}_j \dot{q}_i, \\ &= \frac{1}{2} \sum_{i,j}^N \left(\frac{\partial m_{kj}}{\partial q_i} + \frac{\partial m_{ki}}{\partial q_j} \right) \dot{q}_i \dot{q}_j. \end{aligned}$$

The Christoffel symbols Γ_{ijk} of the first kind are defined as

$$\Gamma_{ijk} := \frac{1}{2} \left(\frac{\partial m_{kj}}{\partial q_i} + \frac{\partial m_{ki}}{\partial q_j} - \frac{\partial m_{ij}}{\partial q_k} \right).$$

One of the most common forms for the equations of motion for robotic systems that are also *natural systems* is then

$$\sum_j^N m_{kj} \ddot{q}_j + \sum_{i,j}^N \Gamma_{ijk} \dot{q}_i \dot{q}_j + \frac{\partial V}{\partial q_k} = Q_k, \quad (5.4.3)$$

for $k = 1, \dots, N$. These equations can be rewritten in terms of vector notation

$$\mathbf{M}(\mathbf{q}(t))\ddot{\mathbf{q}}(t) + \dot{\mathbf{q}}^T \boldsymbol{\Gamma}(\mathbf{q}(t))\dot{\mathbf{q}} + \frac{\partial V}{\partial \mathbf{q}} = \mathbf{Q},$$

where

$$\mathbf{q} = \begin{pmatrix} q_1 \\ q_2 \\ \vdots \\ q_n \end{pmatrix}, \quad \frac{\partial V}{\partial \mathbf{q}} = \begin{pmatrix} \frac{\partial V}{\partial q_1} \\ \vdots \\ \frac{\partial V}{\partial q_n} \end{pmatrix}, \quad \mathbf{Q} = \begin{pmatrix} Q_1 \\ Q_2 \\ \vdots \\ Q_n \end{pmatrix}.$$

The term $\dot{\mathbf{q}}^T \boldsymbol{\Gamma}(\mathbf{q})\dot{\mathbf{q}}$ is a symbolic expression for the vector

$$\dot{\mathbf{q}}^T \boldsymbol{\Gamma}(\mathbf{q})\dot{\mathbf{q}} = \begin{pmatrix} \dot{\mathbf{q}}^T \boldsymbol{\Gamma}_1 \dot{\mathbf{q}} \\ \dot{\mathbf{q}}^T \boldsymbol{\Gamma}_2 \dot{\mathbf{q}} \\ \vdots \\ \dot{\mathbf{q}}^T \boldsymbol{\Gamma}_n \dot{\mathbf{q}} \end{pmatrix},$$

with each of the $N \times N$ matrices $\boldsymbol{\Gamma}_k$ for $k = 1, 2, \dots, N$ defined so that its i^{th} row and j^{th} column is given by $\boldsymbol{\Gamma}_k := [\Gamma_{ijk}]$. \square

Example 5.4.1. Derive the equations of motion of the two link robotic arm in Example 5.2.1 using the representation of Lagrange's equations in terms of Christoffel symbols.

Solution: Direct calculation of the Christoffel symbols yields

$$\begin{aligned} \Gamma_{111} &= 0, \\ \Gamma_{211} &= -\frac{1}{2}m_2L_1L_2 \sin(\theta_2 - \theta_1), \\ \Gamma_{121} &= \frac{1}{2}m_2L_1L_2 \sin(\theta_2 - \theta_1), \\ \Gamma_{221} &= -m_2L_1L_2 \sin(\theta_2 - \theta_1), \\ \Gamma_{112} &= m_2L_1L_2 \sin(\theta_2 - \theta_1), \\ \Gamma_{212} &= -\frac{1}{2}m_2L_1L_2 \sin(\theta_2 - \theta_1), \\ \Gamma_{122} &= \frac{1}{2}m_2L_1L_2 \sin(\theta_2 - \theta_1), \\ \Gamma_{222} &= 0. \end{aligned}$$

For this two degree of freedom robot, the nonlinear vector \mathbf{n} can be written as

$$\mathbf{n} = - \left\{ \begin{array}{l} \dot{\mathbf{q}}^T \boldsymbol{\Gamma}_1 \dot{\mathbf{q}} + \frac{\partial V}{\partial \theta_1} \\ \dot{\mathbf{q}}^T \boldsymbol{\Gamma}_2 \dot{\mathbf{q}} + \frac{\partial V}{\partial \theta_2} \end{array} \right\},$$

where the 2×2 matrices $\boldsymbol{\Gamma}_1, \boldsymbol{\Gamma}_2$ are defined as

$$\boldsymbol{\Gamma}_1 = \begin{bmatrix} \Gamma_{111} & \Gamma_{121} \\ \Gamma_{211} & \Gamma_{221} \end{bmatrix} = \begin{bmatrix} 0 & \frac{1}{2}m_2L_1L_2 \sin(\theta_2 - \theta_1) \\ -\frac{1}{2}m_2L_1L_2 \sin(\theta_2 - \theta_1) & -m_2L_1L_2 \sin(\theta_2 - \theta_1) \end{bmatrix},$$

$$\boldsymbol{\Gamma}_2 = \begin{bmatrix} \Gamma_{112} & \Gamma_{122} \\ \Gamma_{212} & \Gamma_{222} \end{bmatrix} = \begin{bmatrix} m_2L_1L_2 \sin(\theta_2 - \theta_1) & \frac{1}{2}m_2L_1L_2 \sin(\theta_2 - \theta_1) \\ -\frac{1}{2}m_2L_1L_2 \sin(\theta_2 - \theta_1) & 0 \end{bmatrix}.$$

When the products above are calculated, \mathbf{n} becomes

$$\mathbf{n} = \begin{Bmatrix} m_2L_1L_2\dot{\theta}_2^2 \sin(\theta_2 - \theta_1) - (m_1 + m_2)gL_1 \cos\theta_1 \\ -m_2L_1L_2\dot{\theta}_1^2 \sin(\theta_2 - \theta_1) - m_2gL_2 \cos\theta_2 \end{Bmatrix}.$$

The solution of this problem can also be found in Example ?? of the MATLAB Workbook for DCRS.

Before concluding this section, one more common form used to represent the governing equations for a *natural system* is presented. The matrix $\mathbf{C} := \mathbf{C}(\mathbf{q}, \dot{\mathbf{q}})$ is defined by the vector expression

$$\mathbf{C}\dot{\mathbf{q}} := \dot{\mathbf{q}}^T \boldsymbol{\Gamma}(\mathbf{q}(t)) \dot{\mathbf{q}}, \quad (5.4.4)$$

where the entry of \mathbf{C} in the k th row and j th column

$$c_{kj} := \sum_{i=1}^N \Gamma_{ijk} \dot{q}_i. \quad (5.4.5)$$

The governing system in Equation (5.4.3) can now be written as

$$\sum_{j=1}^N m_{kj} \ddot{q}_i + \sum_j c_{k,j} + \frac{\partial V}{\partial q_k} = Q_k$$

for $k = 1, \dots, N$, or in the matrix form

$$\mathbf{M}\ddot{\mathbf{q}} + \mathbf{C}\dot{\mathbf{q}} + \frac{\partial V}{\partial \mathbf{q}} = \mathbf{Q}. \quad (5.4.6)$$

An important motivation for introducing the form shown in Equation (5.4.4) is that it can be used to illustrate some typical *conservation of energy* principles and proofs of stability. These technical conclusions are derived from the fact that the matrix $\dot{\mathbf{M}} - 2\mathbf{C}$ is *skew symmetric*.

Theorem 5.9. If the generalized inertia matrix \mathbf{M} is a symmetric matrix that is a function of the generalized coordinates \mathbf{q} so that

$$\mathbf{M}^T(\mathbf{q}) = \mathbf{M}(\mathbf{q}),$$

and \mathbf{C} is the Coriolis-Centripetal Matrix defined in Equations (5.4.4) and (5.4.5), then the matrix $\dot{\mathbf{M}} - 2\mathbf{C}$ is skew-symmetric,

$$(\dot{\mathbf{M}} - 2\mathbf{C})^T = -(\dot{\mathbf{M}} - 2\mathbf{C}).$$

Proof. The theorem itself stems directly from expanding the definitions of $\dot{\mathbf{M}}$ and \mathbf{C} to obtain

$$\dot{m}_{kj} = \frac{d}{dt}(m_{kj}) = \sum_{i=1}^N \frac{\partial m_{kj}}{\partial q_i} \dot{q}_i$$

for $k, j = 1 \dots N$. From Equation (5.4.6) the entry in row k and column j of $\dot{\mathbf{M}} - 2\mathbf{C}$ is therefore given by

$$\dot{m}_{kj} - 2c_{kj} = \sum_{i=1}^N \frac{\partial m_{kj}}{\partial q_i} \dot{q}_i - 2 \sum_{i=1}^N \frac{1}{2} \left(\frac{\partial m_{kj}}{\partial q_i} + \frac{\partial m_{ki}}{\partial q_j} - \frac{\partial m_{ij}}{\partial q_k} \right) = \sum_{i=1}^N \left(\frac{\partial m_{ki}}{\partial q_i} - \frac{\partial m_{ij}}{\partial q_k} \right).$$

If row k and column j are interchanged, it is concluded that

$$\dot{m}_{jk} - 2c_{jk} = \sum_{i=1}^N \left(\frac{2m_{ji}}{\partial q_k} - \frac{\partial m_{ik}}{\partial q_i} \right) = - \sum_{i=1}^N \left(\frac{\partial m_{ki}}{\partial q_i} - \frac{\partial m_{ij}}{\partial q_k} \right) = -(\dot{m}_{kj} - 2c_{kj}),$$

using the symmetry of the matrix \mathbf{M} . Therefore, $\dot{\mathbf{M}} - 2\mathbf{C}$ is skew symmetric. \square

5.4.2 Lagrange's Equations and the Denavit-Hartenberg Convention

The equations of motion derived in Section (5.4.1) can be used whenever the kinetic energy has the form $T = \dot{\mathbf{q}}^T \mathbf{M}(\mathbf{q}) \dot{\mathbf{q}}$ and the potential energy $V = V(\mathbf{q})$ depends only on the generalized coordinates. In problems concerned with deriving the equations of motion of robotic systems, the components making up the mechanical system will typically be collections of rigid bodies. Recall that a general expression for the kinetic energy of a rigid body was derived in Section (5.1.4) and has the form

$$T = \frac{1}{2} M \mathbf{v}_{0,c} \cdot \mathbf{v}_{0,c} + \frac{1}{2} \boldsymbol{\omega}_{\mathbb{X},\mathbb{B}} \cdot \mathbf{I}_c \boldsymbol{\omega}_{\mathbb{X},\mathbb{B}},$$

where $\mathbf{v}_{0,c}$ is the velocity of the center of mass, $\boldsymbol{\omega}_{\mathbb{X},\mathbb{B}}$ is the angular velocity vector of the rigid body in the ground frame, and \mathbf{I}_c is the inertia tensor about the mass center. Any set of generalized coordinates can be used in this expression for the kinetic energy. However, Chapter (3) showed that the Denavit-Hartenberg convention is often used to define the kinematics of robotic systems.

This section will focus on the specific form of the equations of motion for robotic systems defined using the Denavit-Hartenberg convention. Chapter (3), Section (3.3.5) is particularly relevant to this analysis since it provides a general method to relate the velocity and angular velocity of bodies that appear in a kinematic chain to the derivatives of the joint variables defined via the Denavit-Hartenberg convention. first, the Jacobian matrix will be defined that relates the velocity of the center of mass and angular velocity of a body to the joint variables.

Theorem 5.10. Suppose that the Denavit-Hartenberg convention is used to represent a robotic system that consists of N rigid bodies that form a kinematic chain. The components relative to the frame k of the velocity of the center of mass and angular velocity of the k^{th} body in the kinematic chain can be written as

$$\begin{Bmatrix} \mathbf{v}_{c_k}^k \\ \boldsymbol{\omega}_{0,k}^k \end{Bmatrix} = \begin{bmatrix} \mathbf{J}_{v,k}^k \\ \mathbf{J}_{\boldsymbol{\omega},k}^k \end{bmatrix} \dot{\mathbf{q}} = \begin{bmatrix} \mathbf{R}_0^k \mathbf{J}_{v,k}^0 \\ \mathbf{R}_0^k \mathbf{J}_{\boldsymbol{\omega},k}^0 \end{bmatrix} \dot{\mathbf{q}},$$

where the $3 \times N$ matrices $\mathbf{J}_{v,k}^0$ and $\mathbf{J}_{\boldsymbol{\omega},k}^0$ are defined as in Theorem (3.3).

Proof. The proof of the equation

$$\begin{Bmatrix} \mathbf{v}_{c_k}^k \\ \boldsymbol{\omega}_{0,k}^k \end{Bmatrix} = \begin{bmatrix} \mathbf{J}_{v,k}^k \\ \mathbf{J}_{\boldsymbol{\omega},k}^k \end{bmatrix} \dot{\mathbf{q}}$$

in this theorem follows directly from the proof of Theorem (3.3). The only change in the argument is the focus on the velocity of the center of mass $\mathbf{v}_{0,c}$ which is not in general equal to the velocity of the origin of frame k . That is, the origin of frame k does not coincide with the center of mass of link k in general. The vector $\mathbf{r}_{0,k}^k$ is replaced with the vector \mathbf{r}_{0,c_k}^0 in Theorem (3.3) to obtain the desired form of the Jacobian matrix associated with the center of mass of link k . The alternative form provided for the Jacobian matrix $\mathbf{J}_{v,k}^k$ and $\mathbf{J}_{\boldsymbol{\omega},k}^k$ are immediate when it is noted that the components of the velocity \mathbf{v}_{0,c_k}^k and angular velocity $\boldsymbol{\omega}_{0,k}^k$ are obtained from \mathbf{v}_{0,c_k}^0 and $\boldsymbol{\omega}_{0,k}^0$ by multiplication by the rotation matrix \mathbf{R}_0^k . \square

Theorem (5.10) summarizes how the Jacobian matrix can be used to represent the velocity of the center of mass and the angular velocity of a link in a kinematic chain that is described using the Denavit-Hartenberg convention. The following theorem shows how the Jacobian matrix can be incorporated into a calculation of the kinetic energy of a robotic system.

Theorem 5.11. Suppose that the Denavit-Hartenberg convention is used to represent a robotic system consists of N rigid bodies that form a kinematic chain. The kinetic energy of the system can be written in the form

$$T = \frac{1}{2} \sum_{k=1}^N \dot{\mathbf{q}}^T \mathbf{M}_k \dot{\mathbf{q}},$$

where

$$\mathbf{M}_k := \mathbf{M}_{v,k} + \mathbf{M}_{\omega,k}.$$

The matrix $\mathbf{M}_{v,k}$ can be written in either of the forms

$$\mathbf{M}_{v,k} = m_k (\mathbf{J}_{v,k}^0)^T \mathbf{J}_{v,k}^0 = m_k (\mathbf{J}_{v,k}^k)^T \mathbf{J}_{v,k}^k,$$

where m_k is the mass of link k . Suppose that $\mathbf{I}_{c_k}^k$ is the inertia matrix relative to a set of axes that are parallel to the frame k fixed in body k , but whose origin is located at the center of mass of body k . The matrix $\mathbf{M}_{\omega,k}$ can be written as

$$\mathbf{M}_{\omega,k} = (\mathbf{J}_{\omega,k}^k)^T \mathbf{I}_{c_k}^k \mathbf{J}_{\omega,k}^k.$$

Example 5.4.2. Use the DH convention to describe the kinematics of the two arm robot studied in Example 5.2.1 and derive the equations of motion using Lagrange's equations.

Solution: Example 5.2.1 employs two *global* angles of rotation θ_1 and θ_2 to describe the kinematics of the system: each angle is measured from the \mathbf{x}_0 axis. Figure 5.14 depicts the 0, 1 and 2 frames and the relative angles Θ_1 and Θ_2 that comply with the DH convention. The relative angles Θ_1, Θ_2 are related to the global angles θ_1, θ_2 by the equations

$$\begin{Bmatrix} \Theta_1 \\ \Theta_2 \end{Bmatrix} = \begin{bmatrix} 1 & 0 \\ -1 & 1 \end{bmatrix} \begin{Bmatrix} \theta_1 \\ \theta_2 \end{Bmatrix} \quad (5.4.7)$$

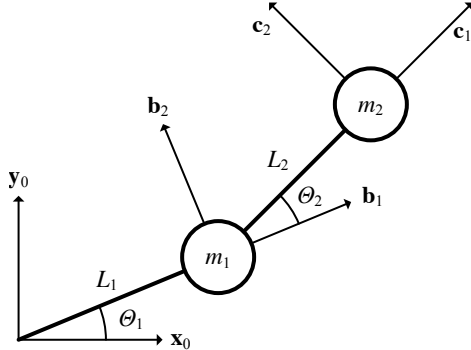
The DH parameters for this two link robotic arm are summarized in the table below.

Link	Displacement d_i	Rotation θ_i	Offset a_i	Twist α_i
1	0	Θ_1	L_1	0
2	0	Θ_2	L_2	0

The velocities of each of the masses m_1 and m_2 are given by

$$\begin{aligned} \mathbf{v}_{0,1} &= L_1 \dot{\Theta}_1 \mathbf{y}_1, \\ \mathbf{v}_{0,2} &= L_1 \dot{\Theta}_1 \mathbf{y}_1 + L_2 (\dot{\Theta}_1 + \dot{\Theta}_2) \mathbf{y}_2. \end{aligned}$$

The kinetic and potential energies are

Fig. 5.14: Two Link Robotic Arm with Relative Angles θ_1, θ_2

$$T = \frac{1}{2}m_1L_1^2\dot{\theta}_1^2 + \frac{1}{2}m_2(L_1^2\dot{\theta}_1^2 + L_2^2(\dot{\theta}_1 + \dot{\theta}_2)^2 + 2L_1L_2\dot{\theta}_1(\dot{\theta}_1 + \dot{\theta}_2)\cos\theta_2),$$

$$V = m_1gL_1\sin\theta_1 + m_2g(L_1\sin\theta_1 + L_2\sin(\theta_1 + \theta_2)).$$

By invoking Lagrange's equations, the generalized mass matrix and nonlinear right hand side are determined to be, respectively,

$$\mathbf{M} = \begin{bmatrix} (m_1 + m_2)L_1^2 + m_2L_2^2 + 2m_2L_1L_2\cos\theta_2 & m_2L_2(L_2 + L_1\cos\theta_2) \\ m_2L_2(L_2 + L_1\cos\theta_2) & m_2L_2^2, \end{bmatrix}$$

and

$$\mathbf{n} = \left\{ \begin{pmatrix} m_2L_1L_2\dot{\theta}_2^2\sin\theta_2 + 2m_2L_1L_2\dot{\theta}_1\dot{\theta}_2\sin\theta_2 \\ -m_2gL_2\cos(\theta_1 + \theta_2) - (m_1 + m_2)gL_1\cos\theta_1 \\ -m_2L_2(L_1\dot{\theta}_1^2\sin\theta_2 + g\cos(\theta_1 + \theta_2)) \end{pmatrix} \right\}.$$

The solution procedure outlined above can also be found in Example ?? of the MATLAB Workbook for DCRS.

5.5 Constrained Systems

Up to this point, the functionals under consideration have been required to be defined in terms of generalized coordinates, which by definition in this book are minimal or independent. In many applications it is not feasible, or at least not a straightforward task, to create such a minimal set of time varying parameters. Recall that the definition of generalized coordinates requires that the expression for the position of each point p in the mechanical system can be written uniquely in the form

$$\mathbf{r}_{\mathbb{X},p}(t) = \mathbf{r}_{\mathbb{X},p}(q_1(t), q_2(t), \dots, q_N(t), t).$$

The requirement that this expression be unique is relaxed in the following definition of *redundant generalized coordinates*.

Definition 5.7. A collection of n time varying parameters $\mathbf{q}(t) = \{q_1(t), q_2(t), \dots, q_N(t)\}^T$ is a set of *redundant generalized coordinates* for a mechanical system if for any point p in the mechanical system the position $\mathbf{r}_{\mathbb{X},p}(t)$ of the point p at any time t with respect to the inertial frame \mathbb{X} can be written in terms of these functions and (if necessary) time t , but this expression is not unique. If the redundant generalized coordinates satisfy D independent algebraic equations that have the form

$$\phi_i(q_1(t), q_2(t), \dots, q_N(t), t) = 0 \quad (5.5.1)$$

for $i = 1 \dots D$, the mechanical system is said to be subject to D *holonomic constraints*.

Sometimes Equation (5.5.1) is written in the matrix form

$$\mathbf{0} = \Phi(\mathbf{q}(t), t) = \begin{Bmatrix} \phi_1(\mathbf{q}(t), t) \\ \vdots \\ \phi_D(\mathbf{q}(t), t) \end{Bmatrix}$$

where $\Phi \in \mathbb{R}^{D \times 1}$. In principle, if a system is subject to D independent holonomic constraints that relate a set of N redundant generalized coordinates, it is possible to use the constraints to eliminate D of the time-varying parameters $\{q_1(t), q_2(t), \dots, q_N(t)\}$. The remaining $N - D$ variables would be independent, and therefore constitute a set of generalized coordinates. In practice this is not a trivial exercise, and it is often simpler to formulate the problem in terms of the redundant generalized coordinates. This will become evident in several of the examples and problems.

If the redundant generalized coordinates are subject to D independent holonomic constraints, then the properties of the virtual variation operator $\delta(\bullet)$ imply that the virtual variations $\delta\mathbf{q}^T = \{\delta q_1, \delta q_2, \dots, \delta q_N\}$ are not independent. This can be shown by taking the variation of the holonomic constraints

$$\delta\Phi(\mathbf{q}(t), t) = \begin{Bmatrix} \delta\phi_1(\mathbf{q}(t), t) \\ \vdots \\ \delta\phi_D(\mathbf{q}(t), t) \end{Bmatrix} = \mathbf{0}.$$

Since the variation operator acts like the differential operator, and the variation of time is zero by definition, the variation of the constraints yield

$$\delta\phi(\mathbf{q}(t), t) = \sum_R^N \frac{\partial\phi}{\partial q_k}(q(t), t)\delta q_k(t),$$

or

$$\delta\phi(q(t), t) = \frac{\partial\Phi}{\partial\mathbf{q}}(\mathbf{q}(t), t)\delta\mathbf{q}(t) = 0. \quad (5.5.2)$$

This last expression is a matrix equation. The Jacobian matrix associated with the constraints is defined as the matrix

$$\frac{\partial\Phi}{\partial\mathbf{q}}(\mathbf{q}(t), t) = \left[\frac{\partial\phi_i}{\partial q_j} \right]_{i=1\dots D, j=1\dots N} \in \mathbb{R}^{D \times N}$$

Equation (5.5.2) is a nonlinear equation among the redundant generalized coordinates and their variations, but it is linear in the variations $\delta\mathbf{q}$. When the D constraint equations are independent, the rank of this matrix is equal to D . In principle, the D equations can be used to express D of the variations in terms of the remaining $N - D$ variations and all of the redundant generalized coordinates.

It is possible to modify Lagrange's Equations so that they apply when a set of redundant generalized coordinates are used to describe the system. The following theorem describes this case.

Theorem 5.12. Let $\mathbf{q}(t) := \{q_1(t), q_2(t), \dots, q_N(t)\}^T$ be a collection of redundant generalized coordinates for a conservative mechanical system that satisfy the independent holonomic constraints

$$\phi_i(\mathbf{q}, t) = 0 \quad (5.5.3)$$

for $i = 1 \dots D$. Suppose that $T = T(\dot{\mathbf{q}}, \mathbf{q}, t)$ and $V = V(\mathbf{q}, t)$. If the action functional $A(\mathbf{q})$ is stationary, an actual motion of such a system satisfies Lagrange's Equations with multipliers

$$\frac{d}{dt} \left(\frac{\partial T}{\partial \dot{\mathbf{q}}} \right) - \frac{\partial T}{\partial \mathbf{q}} + \frac{\partial V}{\partial \mathbf{q}} = \frac{\partial \Phi^T}{\partial \mathbf{q}} \boldsymbol{\lambda}(t) \quad (5.5.4)$$

and the holonomic constraints in Equation (5.5.3).

Proof. By following the same steps taken in the proof of Theorems (5.5) or (5.7), it can be shown that

$$\delta \int_{t_0}^{t_f} (T - V) dt = \int_{t_0}^{t_f} \left\{ -\frac{d}{dt} \left(\frac{\partial T}{\partial \dot{\mathbf{q}}} \right) + \frac{\partial T}{\partial \mathbf{q}} - \frac{\partial V}{\partial \mathbf{q}} \right\} \cdot \delta \mathbf{q}(t) dt. \quad (5.5.5)$$

In the case at hand, this equation must hold for all variations that are consistent with the constraints on the mechanical system. However, in contrast to the case in either Theorem (5.5) or (5.7), the variations are not independent in the constrained

problem, and it cannot be simply concluded that the term multiplying $\delta\mathbf{q}$ is zero. The variations $\delta\mathbf{q} = \{\delta q_1, \delta q_2, \dots, \delta q_n\}^T$ must satisfy the matrix equation

$$\frac{\partial\Phi}{\partial\mathbf{q}}(\mathbf{q}(t), t)\delta\mathbf{q} = 0. \quad (5.5.6)$$

The full rank matrix equation implies that out of the N variations $\delta\mathbf{q} = \{\delta q_1, \delta q_2, \dots, \delta q_N\}^T$, it is possible to express D of the variations in terms of the remaining $N - D$ variations and the N redundant generalized coordinates. Since Equation (5.5.6) holds, it is also true that

$$\boldsymbol{\lambda}^T \frac{\partial\Phi}{\partial\mathbf{q}}(\mathbf{q}(t), t)\delta\mathbf{q} = 0 \quad (5.5.7)$$

for any choice of the vector of time-varying functions $\boldsymbol{\lambda}(t) \in \mathbb{R}^D$. The vector $\boldsymbol{\lambda}$ is known as the vector of Lagrange multipliers for the constrained system. Equations (5.5.5) and (5.5.7) can then be combined into a single equation,

$$\delta \int_{t_0}^{t_f} (T - V) dt = \int_{t_0}^{t_f} \left\{ -\frac{d}{dt} \left(\frac{\partial T}{\partial \dot{\mathbf{q}}} \right) + \frac{\partial T}{\partial \mathbf{q}} - \frac{\partial V}{\partial \mathbf{q}} - \frac{\partial \Phi^T}{\partial \mathbf{q}} \boldsymbol{\lambda} \right\} \cdot \delta\mathbf{q}(t) dt. \quad (5.5.8)$$

Suppose that the set of redundant generalized coordinates are ordered so that the first $N - D$ coordinates correspond to the independent variations $\{\delta q_1, \dots, \delta q_{N-D}\}$, and the last D correspond to the dependent variations $\{\delta q_{N-D+1}, \delta q_{N-D+2}, \dots, \delta q_N\}$. Up until this point, a specific set of Lagrange multipliers has not been selected: Equation (5.5.8) holds for any choice of $\boldsymbol{\lambda}(t) \in \mathbb{R}^D$. Now, the D Lagrange multipliers $\boldsymbol{\lambda}$ are chosen so that the following equations hold

$$-\frac{d}{dt} \left(\frac{\partial T}{\partial \dot{q}_i} \right) + \frac{\partial T}{\partial q_i} - \frac{\partial V}{\partial q_i} + \frac{\partial \Phi^T}{\partial q_i} \boldsymbol{\lambda} = 0$$

for $i = N - D + 1, \dots, N$. This is always possible owing to the fact that these equations are linear in the Lagrange multipliers, there are D unknown Lagrange multipliers, there are D equations, and the rank of the constraint Jacobian matrix is D . In other words, the Lagrange multipliers $\boldsymbol{\lambda}$ have been chosen so that the coefficients that multiply the dependent variations $\delta q_{N-D+1}, \dots, \delta q_N$ are all equal to zero. With the Lagrange multipliers determined in this way, Equation (5.5.8) can be written

$$\mathbf{0} = \int_{t_0}^{t_f} \left\{ \begin{array}{l} -\frac{d}{dt} \left(\frac{\partial T}{\partial \dot{q}_1} \right) + \frac{\partial T}{\partial q_1} - \frac{\partial V}{\partial q_1} + \frac{\partial \Phi^T}{\partial q_1} \boldsymbol{\lambda} \\ -\frac{d}{dt} \left(\frac{\partial T}{\partial \dot{q}_2} \right) + \frac{\partial T}{\partial q_2} - \frac{\partial V}{\partial q_2} + \frac{\partial \Phi^T}{\partial q_2} \boldsymbol{\lambda} \\ \vdots \\ -\frac{d}{dt} \left(\frac{\partial T}{\partial \dot{q}_{N-D}} \right) + \frac{\partial T}{\partial q_{N-D}} - \frac{\partial V}{\partial q_{N-D}} + \frac{\partial \Phi^T}{\partial q_{N-D}} \boldsymbol{\lambda} \end{array} \right\} \cdot \begin{Bmatrix} \delta q_1(t) \\ \delta q_2(t) \\ \vdots \\ \delta q_{N-D}(t) \end{Bmatrix} dt. \quad (5.5.9)$$

With the above choice of Lagrange multipliers, the Equations (5.5.9) do not contain any of the dependent variations. Since all of the variations appearing in Equation

(5.5.9) are independent, each of the coefficients that multiply δq_i for $i = 1 \dots N - D$ must be equal to zero. The proof is complete. \square

Example 5.5.1. The planar robot depicted in Figure (5.15) is actuated at the revolute joint about the $\mathbf{z}_0 = \mathbf{z}_1$ axis and at the prismatic joint along the $\mathbf{x}_1 = \mathbf{x}_2$ axis. Suppose that the $x_2(t)$ and $y_2(t)$ are the coordinates of the center of mass of link 2. Derive Lagrange's Equations in terms of the redundant generalized coordinates $\theta(t), x_2(t)$, and $y_2(t)$ assuming that the mass and inertia of the links may be represented by a pair of point masses at the defined link mass centers.

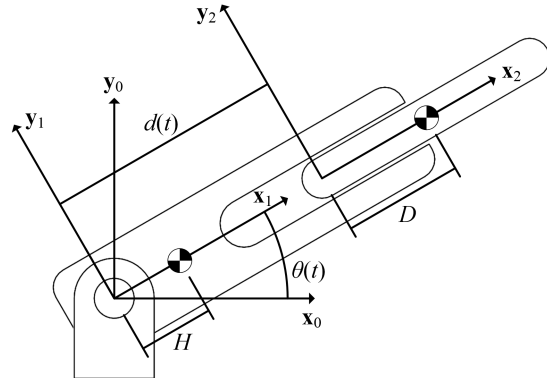


Fig. 5.15: Two Link Revolute-Prismatic Robot

Solution: Since it is known that this is a two degree of freedom system, there must exist one constraint among the redundant generalized coordinates θ, x_2, y_2 . It is known that

$$\begin{aligned} x_2 &= (d + D) \cos \theta, \\ y_2 &= (d + D) \sin \theta. \end{aligned}$$

Solving for $(d + D)$ in each of these equations and setting the results equal results in

$$\frac{x_2}{\cos \theta} = \frac{y_2}{\sin \theta}.$$

This equation can be written in the standard form required in Lagrange's Equation for constrained systems by defining

$$\phi_1(\theta, x_2, y_2) = x_2 \sin \theta - y_2 \cos \theta = 0.$$

In this problem, the are $N = 3$ redundant variables and $D = 1$ constraints. The matrix Φ has dimension $D \times 1 = 1 \times 1$. The Jacobian matrix $\frac{\partial \Phi}{\partial q}$ has dimension $D \times N = 1 \times 3$

and is given by

$$\frac{\partial \Phi}{\partial \mathbf{q}} = \begin{bmatrix} \frac{\partial \phi_1}{\partial q_1} & \frac{\partial \phi_1}{\partial q_2} & \frac{\partial \phi_1}{\partial q_3} \end{bmatrix} = \begin{bmatrix} (x_2 \cos \theta + y_2 \sin \theta), \sin \theta, -\cos \theta \end{bmatrix}.$$

Since it is assumed that these rigid bodies can be approximated as point masses, the kinetic energy of the two mass system in terms of the redundant variables is

$$T = \frac{1}{2}m_1H^2\dot{\theta}^2 + \frac{1}{2}m_2(\dot{x}_2^2 + \dot{y}_2^2) = \frac{1}{2}\left\{\dot{\theta} \ \dot{x}_2 \ \dot{y}_2\right\}^T \begin{bmatrix} m_1H^2 & 0 & 0 \\ 0 & m_2 & 0 \\ 0 & 0 & m_2 \end{bmatrix} \begin{Bmatrix} \dot{\theta} \\ \dot{x}_2 \\ \dot{y}_2 \end{Bmatrix} = \frac{1}{2}\dot{\mathbf{q}}^T \mathbf{M} \dot{\mathbf{q}},$$

where \mathbf{M} is a constant mass matrix. The potential energy is $V = m_1gH \sin \theta + m_2gy_2$. Lagrange's Equations for the redundant system can be written as

$$\begin{aligned} \frac{d}{dt}\left(\frac{\partial T}{\partial \dot{\mathbf{q}}}\right) - \frac{\partial T}{\partial \mathbf{q}} + \frac{\partial V}{\partial \mathbf{q}} - \left(\frac{\partial \Phi}{\partial \mathbf{q}}\right)^T \boldsymbol{\lambda}(t) &= 0, \\ \mathbf{M} \begin{Bmatrix} \ddot{\theta} \\ \ddot{x}_2 \\ \ddot{y}_2 \end{Bmatrix} - \mathbf{0} + \begin{Bmatrix} m_1gH \cos \theta \\ 0 \\ m_2g \end{Bmatrix} - \begin{Bmatrix} \frac{\partial \phi}{\partial \theta} \\ \frac{\partial \phi}{\partial x_2} \\ \frac{\partial \phi}{\partial y_2} \end{Bmatrix} \lambda &= \mathbf{0}, \end{aligned}$$

where $\boldsymbol{\lambda} \in \mathbb{R}^{D \times 1} = \mathbb{R}^{1 \times 1}$. We can substitute the Jacobian matrix above and find the final form of Lagrange's Equations for the constrained system to be

$$\begin{bmatrix} m_1H^2 & 0 & 0 \\ 0 & m_2 & 0 \\ 0 & 0 & m_2 \end{bmatrix} \begin{Bmatrix} \ddot{\theta} \\ \ddot{x}_2 \\ \ddot{x}_3 \end{Bmatrix} + \begin{Bmatrix} m_1gH \cos \theta \\ 0 \\ m_2g \end{Bmatrix} - \begin{Bmatrix} x_2 \cos \theta + y_2 \sin \theta \\ \sin \theta \\ -\cos \theta \end{Bmatrix} \lambda = \begin{Bmatrix} 0 \\ 0 \\ 0 \end{Bmatrix}.$$

The solution of this example can also be found in Example ?? of the MATLAB Workbook for DCRS.

5.6 Problems for Chapter 5, Analytical Mechanics

5.6.1 Problems on Hamilton's Principle

Problem 5.1 (Solution ??). A planar rigid link with mass m and length L is pinned at one end to the origin of the inertial frame as shown in Figure (5.16). Use Hamilton's Principle to derive the equations of motion for this mechanical system.

Problem 5.2 (Solution ??). The two degree of freedom manipulator shown in Figure (5.17) is constructed from two rigid links having length L and negligible mass.

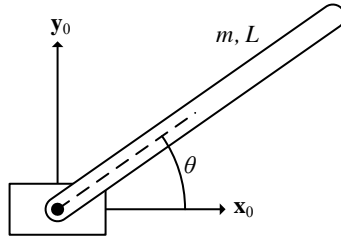


Fig. 5.16: Rigid Link Pinned to Inertial Frame Origin

Concentrated masses m_1 and m_2 are located at the ends of the links. Use Hamilton's Principle to derive the equations of motion for this mechanical system. Note that unlike Example (5.1.5), θ_2 is defined as the relative angle between links 1 and 2.

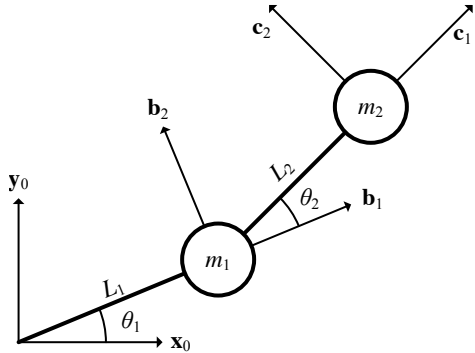


Fig. 5.17: Two Link Robotic Arm with Point Masses, Relative Joint Angles

Problem 5.3 (Solution ??). A rigid link having mass m and length L is pinned to a mass M that can translate along the horizontal direction as shown in Figure (5.18). Use Hamilton's Principle to derive the equations of motion for this mechanical system.

Problem 5.4 (Solution ??). A point mass m is constrained so that its motion follows the surface of a cylinder, as shown in Figure (5.19). Use Hamilton's Principle to derive the equations of motion for this mechanical system.

Problem 5.5 (Solution ??). A point mass m is constrained so that its motion follows the surface of a cone, as shown in Figure (5.20). Use Hamilton's Principle to derive the equations of motion for this mechanical system.

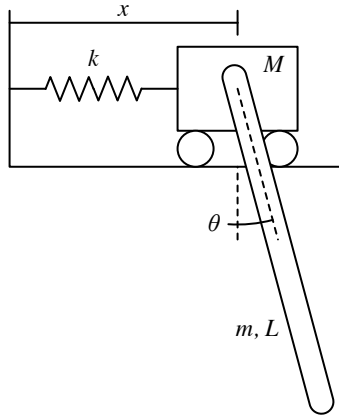


Fig. 5.18: Translating Mass with Rotating Pendulum

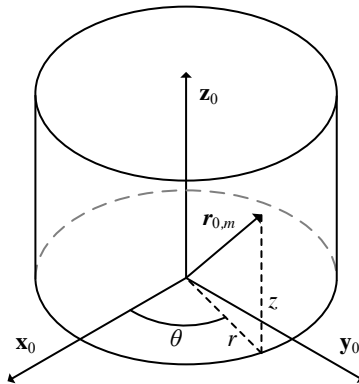


Fig. 5.19: Point Mass on Solid Cylinder

Problem 5.6 (Solution ??). A point mass m is constrained so that its motion follows the surface of hemispherical solid, as shown in Figure (5.21). Use Hamilton's Principle to derive the equations of motion for this mechanical system utilizing the spherical coordinates and frames shown in Figure (5.21).

Problem 5.7 (Solution ??). Two spring loaded pistons with masses m_1 and m_2 and stiffness k_1 and k_2 are connected via revolute joints to a rigid coupler with negligible mass and length L , as shown in Figure (5.22). Use Hamilton's Principle to derive the equations of motion for this mechanical system in terms of the single generalized coordinate x .

Problem 5.8 (Solution ??). Two point masses m_1 and m_2 are connected by a light, inextensible cable having negligible mass and fixed length L , as shown in Figure (5.23). Mass m_2 lies on the surface of the $x_0 - y_0$ plane, and the mass m_1 is suspended

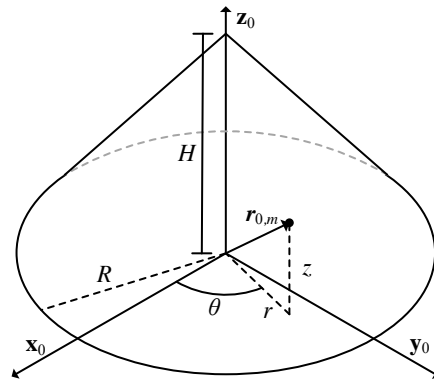


Fig. 5.20: Point Mass on Solid Cone

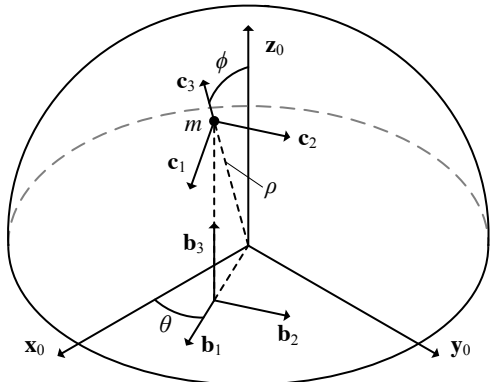


Fig. 5.21: Point Mass on Hemispherical Solid, Spherical Coordinates

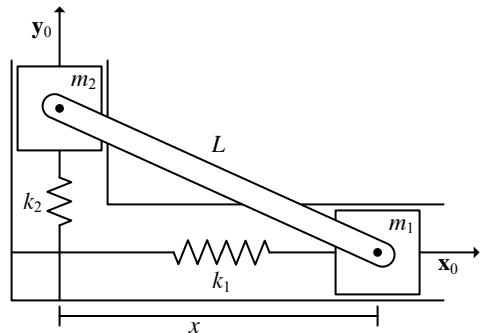


Fig. 5.22: Two Spring-Loaded Pistons Connected by a Massless Coupler

by the cable through a hole located at the origin of frame 0. Use Hamilton's Principle to derive the equations of motion for this mechanical system in terms of the two generalized coordinates r and θ .

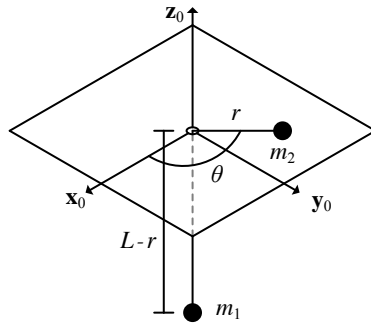


Fig. 5.23: Point Mass on Plane and Suspended Point Mass

5.6.2 Problems on Lagrange's Equations

Problem 5.9 (Solution ??). Consider the mechanical system described in Problem (5.1). Derive the equations of motion for this system using Lagrange's Equations.

Problem 5.10 (Solution ??). Consider the mechanical system described in Problem (5.2). Derive the equations of motion for this system using Lagrange's Equations.

Problem 5.11 (Solution ??). Consider the mechanical system described in Problem (5.3). Derive the equations of motion for this system using Lagrange's Equations.

Problem 5.12 (Solution ??). Consider the mechanical system described in Problem (5.4). Derive the equations of motion for this system using Lagrange's Equations.

Problem 5.13 (Solution ??). Consider the mechanical system described in Problem (5.5). Derive the equations of motion for this system using Lagrange's Equations.

Problem 5.14 (Solution ??). Consider the mechanical system described in Problem (5.6). Derive the equations of motion for this system using Lagrange's Equations.

Problem 5.15 (Solution ??). Consider the mechanical system described in Problem (5.7). Derive the equations of motion for this system using Lagrange's Equations.

Problem 5.16 (Solution ??). Consider the mechanical system described in Problem (5.8). Derive the equations of motion for this system using Lagrange's Equations.

Problem 5.17 (Solution ??). A two link robot is shown in Figure (5.24). The inertial frame has basis $\mathbf{x}_0, \mathbf{y}_0, \mathbf{z}_0$, and the frame 1 has basis $\mathbf{x}_1, \mathbf{y}_1, \mathbf{z}_1$ is fixed in the rotating base body. The base body is actuated about the revolute joint along the $\mathbf{z}_0 = \mathbf{z}_1$ axis, and the extensional arm is actuated by a linear motor along the \mathbf{x}_1 axis. The mass distribution of the base body is approximated by a point mass m_1 located at the center of mass of the base body, and the mass distribution of the extensional arm is approximated by a point mass m_2 located at the center of mass of the arm. Use

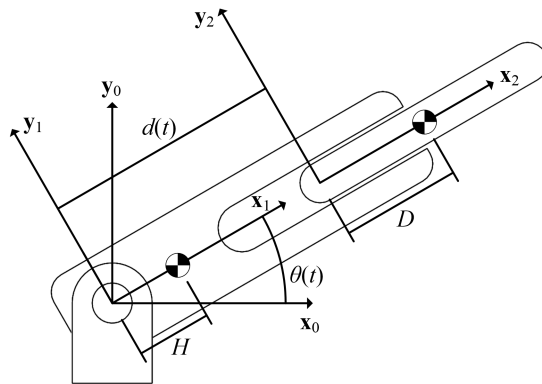


Fig. 5.24: Two Link Revolute-Prismatic Robot

Lagrange's Equations for nonconservative systems to show that the equations of motion for this system are given by

$$\begin{aligned} & \begin{bmatrix} m_2 & 0 \\ 0 & m_1H^2 + m_2(D+d)^2 \end{bmatrix} \begin{Bmatrix} \ddot{d} \\ \ddot{\theta} \end{Bmatrix} \\ &= \begin{Bmatrix} -m_2g\sin\theta + m_2(D+d)\dot{\theta}^2 \\ -g(m_1H + m_2(d+D))\cos\theta - 2m_2(d+D)\dot{d}\dot{\theta} \end{Bmatrix} + \begin{bmatrix} 1 & 0 \\ 0 & 1 \end{bmatrix} \begin{Bmatrix} F \\ M \end{Bmatrix}, \end{aligned}$$

where M is the actuating moment for revolute joint and F is the actuating force for the prismatic joint.

Problem 5.18 (Solution ??). Suppose that an actuator is added to the revolute joint between the ground and the link for the system discussed in Problems (5.1) and (5.9). A motor generates a moment m about the revolute joint axis that acts on the link, while $-m$ acts on the ground. What is the total virtual work performed by the actuation torque? What is the generalized force associated with the generalized coordinate θ ?

Problem 5.19 (Solution ??). Suppose that a pair of actuators is added to the two link manipulator discussed in Problems (5.2) and (5.10) that actuate its joints. The first motor generates a moment m_1 acting on link 1 about the axis of the revolute joint between ground and link 1. The second motor generates a moment m_2 acting

on the link 2 about the revolute joint between links 1 and 2. What is the total virtual work performed by the actuating moments? What are the generalized forces Q_1 and Q_2 associated with the generalized coordinates θ_1 and θ_2 ?

Problem 5.20 (Solution ??). Suppose that the revolute joint between the cart and the rod for the system discussed in Problems (5.3) and (5.11) is actuated by a motor. The motor generates a torque τ that acts on the rod and a torque $(-\tau)$ that acts on the mass. What is the total virtual work performed by the moment? What are the generalized forces associated with the generalized coordinates x and θ ?

5.6.3 Problems on Hamilton's Extended Principle

Problem 5.21 (Solution ??). Derive a simplified dynamic model of the PUMA robot in Figures (5.25) and (5.26) that assumes the mass and inertia of links 1 and 2 can be approximated as concentrated point masses m_1 and m_2 and that the mass and inertia of link 3 is negligible. Assume that the mass m_1 is concentrated at point q , and that that the mass m_2 is concentrated at point r . The actuating torques M_1 and M_2 drive joints 1 and 2 about the \mathbf{z}_0 and \mathbf{z}_1 axes, respectively.

Use the joint variables θ_1 and θ_2 as generalized coordinates and formulate the equations of motion for this system using Lagrange's equations.

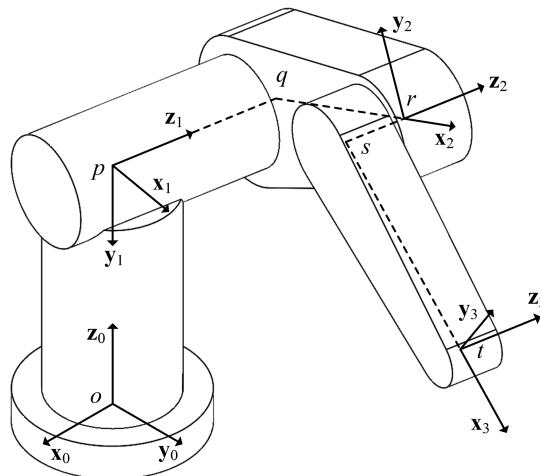


Fig. 5.25: PUMA Robot Frames

Problem 5.22 (Solution ??). Derive a simplified dynamic model of the PUMA robot in Figures (5.25) and (5.26) and studied in Problem (5.21) that assumes the mass and inertia of links 1 and 2 are negligible and that the mass and inertia of link

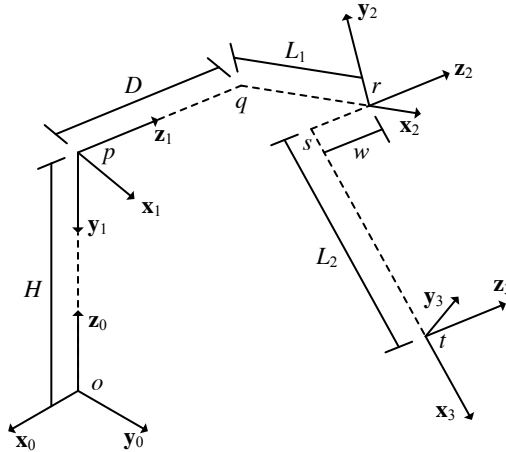


Fig. 5.26: PUMA Robot Frame Offsets

3 can be approximated as concentrated point mass m_3 . Assume that the mass m_3 is concentrated at point t . The actuating torques M_1 , M_2 , and M_3 drive joints 1, 2, and 3 about the \mathbf{z}_0 , \mathbf{z}_1 , and \mathbf{z}_2 axes, respectively.

Use the joint variables θ_1 , θ_2 , and θ_3 as generalized coordinates and formulate the equations of motion for this system using Lagrange's equations.

Problem 5.23 (Solution ??). Derive a simplified dynamic model of the PUMA robot in Figures (5.25) and (5.26) and studied in Problems (5.21) and (5.22) that represents the mass and inertia of links 1 and 2 as simplified rigid bodies and assumes the mass and inertia of link 3 is negligible. To simplify analysis, for link 1, assume that the mass is distributed along the shoulder in the cylindrical solid between points p and q . The center of mass for link 1 is halfway between points p and q , and the center of mass for link 2 is halfway between points q and r . The inertia matrix $\mathbf{I}_{c_i}^i$ for each body $i = \{1, 2\}$ is defined in Equation 5.6.1 at the center of mass c_i with respect to frame i . The actuating torques M_1 and M_2 drive joints 1 and 2 about the \mathbf{z}_0 and \mathbf{z}_1 axes, respectively.

Derive the equations of motion of the system using Lagrange's equations for nonconservative systems.

$$\mathbf{I}_{c_i}^i = \begin{bmatrix} I_{11,i} & 0 & 0 \\ 0 & I_{22,i} & 0 \\ 0 & 0 & I_{33,i} \end{bmatrix}. \quad (5.6.1)$$

Problem 5.24 (Solution ??). A three degree of freedom Cartesian robot is shown in Figure (5.27). The system is comprised of a frame that moves along the \mathbf{z}_0 direction, a crossbar that moves relative to the frame in the \mathbf{z}_1 direction, and a tool assembly that moves relative to the the crossbar in the \mathbf{z}_2 direction. The masses of the frame, crossbar and tool assembly are m_1, m_2 and m_3 , respectively. The motion of the frame

relative to the ground is measured by the coordinate $z(t)$, the motion of the crossbar relative to the frame is measured by $x(t)$, and the motion of the tool assembly relative to the crossbar is measured by $y(t)$. The actuation forces F_z , F_x and F_y act between the ground and the frame, the frame and the crossbar, and the crossbar and the tool assembly, respectively. Use Lagrange's equations for nonconservative systems to derive the equations of motion of the robot.

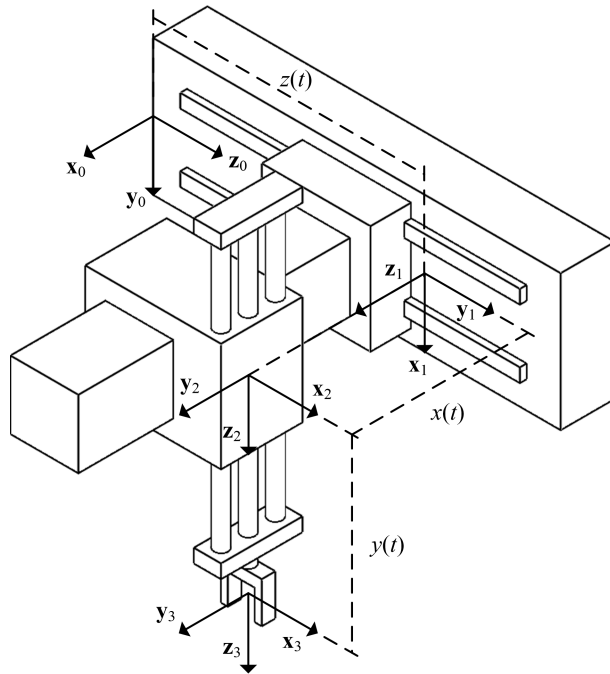


Fig. 5.27: Cartesian Robot with Frames and Coordinates

Problem 5.25 (Solution ??). Consider the spherical wrist shown in Figures (5.28) and (5.29). Let m_1, m_2 and m_3 be the masses of links 1, 2 and 3, respectively, with positions as shown in Figure (5.29). Let t_1, t_2 and t_3 be the actuation torques that drive the joints in the spherical wrist. Use Lagrange's equations for nonconservative systems to derive the equations of motion of this system by approximating each link as a point mass.

Problem 5.26 (Solution ??). The SCARA robot studied in Problem (4.4) and Problem (4.5) of Chapter (4) and shown in Figures (5.30) and (5.31). Derive a dynamic model for this robot assuming that the links can be represented as point masses whose locations are depicted in Figure (5.31). Derive the equations of motion using Lagrange's equations for nonconservative systems.

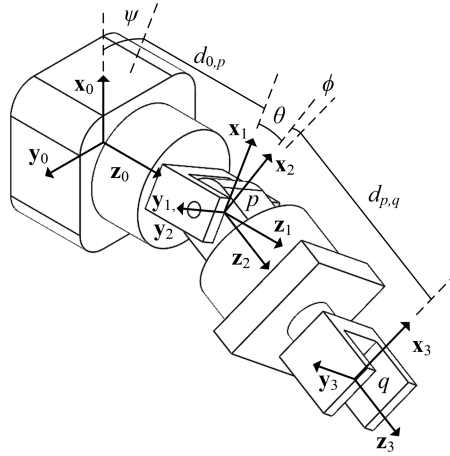


Fig. 5.28: Spherical Wrist Frames and Coordinates

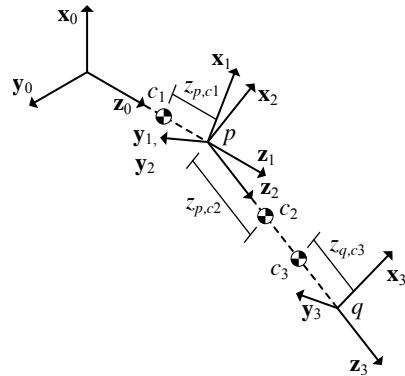


Fig. 5.29: Spherical Wrist Center of Mass Positions

Problem 5.27 (Solution ??). Derive the equations of motion for the SCARA robot analyzed in Problem (5.26), but now assume that the mass distributions of the links 1, 2 and 3 are uniform. The mass centers are still located as shown in Figure (5.31). Assume that the inertia matrix for each link $i = 1, 2, 3$ relative to the frame $\mathbf{x}_i, \mathbf{y}_i, \mathbf{z}_i$ at the the center of mass of each link has the form

$$\mathbf{I}_{cm_i}^i = \begin{bmatrix} I_{11,i} & 0 & 0 \\ 0 & I_{22,i} & 0 \\ 0 & 0 & I_{33,i} \end{bmatrix}.$$

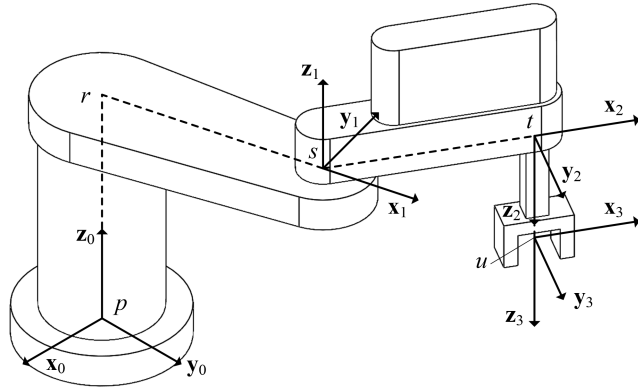


Fig. 5.30: SCARA Robot Frames

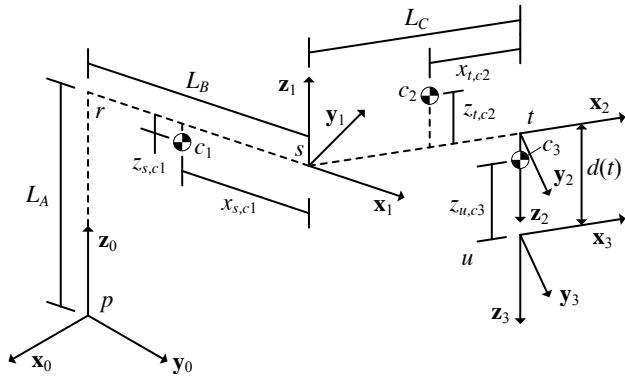


Fig. 5.31: SCARA Robot Joint and Mass Center Offsets

Could it be deduced that the inertia matrices have the diagonal structure shown based on the symmetry arguments? If the density were uniform over each link, what structure of the inertia matrices could be inferred by symmetry arguments? Derive the equations of motion of the system using Lagrange's equations for nonconservative systems.

Problem 5.28 (Solution ??). Derive a dynamic model for the cylindrical robot shown in Figures (5.32) and (5.33) assuming the mass and inertia of each link may be represented by a point mass m_i for each link $i = 1, 2, 3$. The locations of the center of mass of each link relative to its body fixed frame are depicted in Figure (5.33). Derive the equations of motion using Lagrange's equations for nonconservative systems.

Problem 5.29 (Solution ??). Derive the equations of motion for the cylindrical robot analyzed in Problem (5.28) assuming that the mass distributions of links 1,

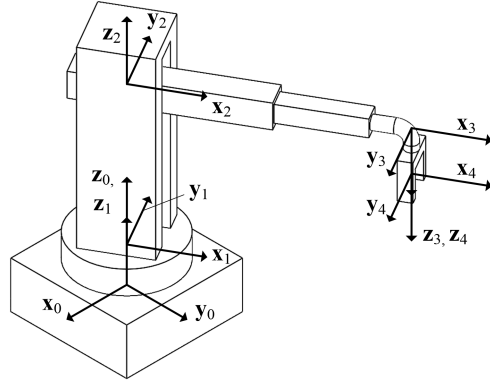


Fig. 5.32: Cylindrical Robot Frames

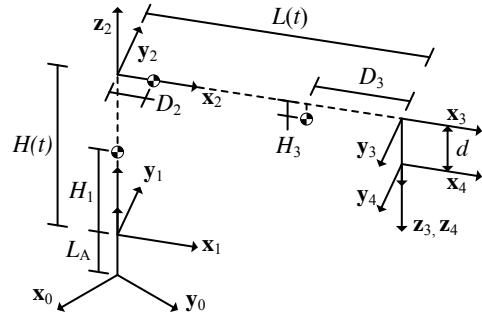


Fig. 5.33: Cylindrical Robot Joint and Mass Center Offsets

2 and 3 are uniform. Derive the equations of motion using Lagrange's equations for nonconservative systems.

Problem 5.30 (Solution ??). Derive a dynamic model of the spherical robot shown in Figures (5.34) and (5.35). The robot is modeled by defining frames 1, 2 and 3 that are fixed in links 1, 2 and 3, respectively. The ground frame is the 0 frame in the figure. The angle θ_i that measures the rotation of frame i relative to frame $i-1$ is defined from axis \mathbf{x}_{i-1} to axis \mathbf{x}_i about the \mathbf{z}_{i-1} axis for $i = 1, 2$. The variable $d_{p,q}(t)$ measures the distance from point p to q . Use a lumped mass approximation of the links where the location of the mass centers are shown Figure (5.35).

Use the variables θ_1, θ_2 and $d_{q,r}$ as generalized coordinates and formulate the equations of motion using Lagrange's Equations.

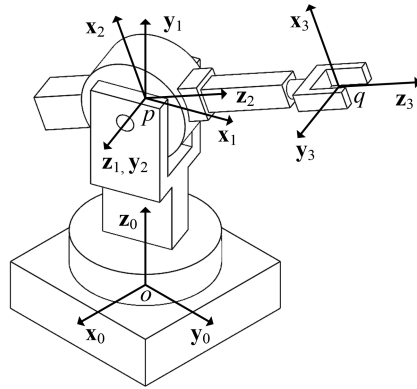


Fig. 5.34: Spherical Robot Frames

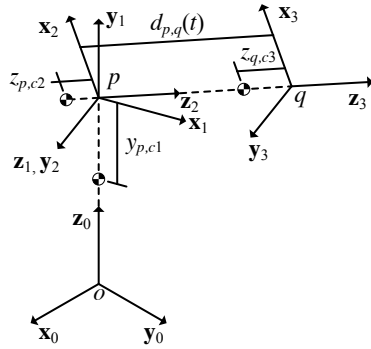


Fig. 5.35: Spherical Robot Joint and Mass Center Offsets

5.6.4 Problems on Constrained Systems

Problem 5.31 (Solution ??). Let $(x(t), y(t))$ denote the location of the center of mass in the inertial frame of the link depicted in Figure (5.16). The collection of variables

$$\mathbf{q}(t) = \{x(t) \ y(t) \ \theta(t)\}^T$$

defines a set of redundant generalized coordinates for the single rigid link in Problem (5.1). Derive Lagrange's Equations for this choice of redundant generalized coordinates.

Problem 5.32 (Solution ??). Let $(x_1(t), y_1(t))$ and $(x_2(t), y_2(t))$ denote the location in the inertial frame of the center of mass of the links 1 and 2, respectively, in Figure (5.13). The collection of variables

$$\mathbf{q}(t) = \{x_1(t) \ x_2(t) \ \theta_1(t) \ x_2(t) \ y_2(t) \ \theta_2(t)\}^T$$

defines a set of redundant generalized coordinates for the two arm robot in Problem (5.2). Derive Lagrange's equations for this choice of redundant coordinates.

Problem 5.33 (Solution ??). Let x be the location in the inertial frame of the block M and (x_2, y_2) be the location of the center of mass of the bar. The set of variables

$$\mathbf{q} = \{x_1 \ x_2 \ y_2 \ \theta\}$$

is a set of redundant generalized coordinates for the robot in Figure (5.3). Derive Lagrange's Equations for this choice of redundant generalized coordinates.

Chapter 6

Control of Robotic Systems

Abstract Chapters (2), (3), (4) and (5) have described a large collection of tools that can be used to study the kinematics and derive the equations of motion of robotic systems. This chapter poses and solves several classical problems that arise in the control of robotic systems. This is a vast topic, and one with a long history. An overview of some of the most commonly encountered robotic control problems is presented. This chapter derives *joint space, full state feedback control* strategies, while Chapter (7) discusses *task space feedback control* methods. The latter class is well-suited to applications in vision-based control of robots. Upon completion of this chapter, the student should be able to

- Define the essential ingredients of a control problem for a robotic system.
- State various definitions of stability and apply them to robotic systems.
- State Lyapunov's direct method and apply it to study the stability of robots.
- Formulate computed torque or inverse dynamics controllers for robotic systems.
- Discuss the structure of inner and outer loop controllers for robotic systems.
- Formulate controllers based on passivity principles for robotic systems.

6.1 The Structure of Control Problems

Many of the common robotic systems encountered in this book have been shown to be governed by equations that have the form

$$\mathbf{M}(\mathbf{q}(t))\ddot{\mathbf{q}}(t) = \mathbf{n}(\mathbf{q}(t), \dot{\mathbf{q}}(t)) + \boldsymbol{\tau}(t) \quad (6.1.1)$$

where $\mathbf{q}(t)$ is an N -vector of generalized coordinates, $\mathbf{M}(\mathbf{q}(t))$ is the $N \times N$ generalized mass or inertia matrix, $\mathbf{n}(\mathbf{q}(t), \dot{\mathbf{q}}(t))$ is the N -vector of nonlinear functions of the generalized coordinates and their derivatives, and $\boldsymbol{\tau}(t)$ is an N -vector of actuation torques or forces. If \mathbf{M} is invertible, it always possible to rewrite these second order governing equations as a system of first order ordinary differential equations. First define

$$\mathbf{x}(t) = \begin{Bmatrix} \mathbf{q}(t) \\ \dot{\mathbf{q}}(t) \end{Bmatrix} = \begin{Bmatrix} \mathbf{x}_1(t) \\ \mathbf{x}_2(t) \end{Bmatrix} \quad \text{and} \quad \mathbf{f}(t, \mathbf{x}(t)) = \begin{Bmatrix} \mathbf{x}_1(t) \\ \mathbf{M}^{-1}(\mathbf{x}_1(t))(\mathbf{n}(\mathbf{x}_1(t), \mathbf{x}_2(t)) + \boldsymbol{\tau}(t)) \end{Bmatrix}.$$

The resultant governing equations can then be written as

$$\begin{aligned} \dot{\mathbf{x}} &= \mathbf{f}(t, \mathbf{x}(t)), \\ \mathbf{x}(t_0) &= \mathbf{x}_0. \end{aligned} \tag{6.1.2}$$

This system is the desired set of first order nonlinear ordinary differential equations subject to the initial condition \mathbf{x}_0 at the time $t = t_0$.

Control methods for robotic systems will be studied using both the second order form in Equation (6.1.1) and the first order form in Equation (6.1.2). The first order form is particularly useful in the analysis of *stability*, a topic covered in Section (6.2). The expression of the equations of motion in second order form is convenient in deriving some specific control laws. The discussions of *computed torque controllers* in Section (6.6) or controllers based on *passivity principles* in Section (6.8) are based on Equation (6.1.1).

The ultimate goal in Chapters (4) and (5) was to derive the governing equations of motion in the general form shown in Equations (6.1.1) or (6.1.2). In applications numerical or analytical methods are used to solve for the trajectory of the generalized coordinates $\mathbf{q}(t)$ for $t \in \mathbb{R}^+$, given a prescribed set of input functions $\boldsymbol{\tau}(t)$ for $t \in \mathbb{R}^+$. Completion of this task solves the classical *forward dynamics* problem of robotics. Problems of control theory seek the solution to a different problem: given some desired goal, can the input $\boldsymbol{\tau}(t)$ be chosen for $t \in \mathbb{R}^+$ so that the system achieves that goal? Many different control problems have been studied over the years. Control strategies are usually categorized depending on (1) the goal the control strategy seeks to attain, and (2) the method used to reach that goal. Common goals include disturbance rejection, error minimization, trajectory tracking, or system stabilization.

6.1.1 Setpoint and Tracking Feedback Control Problems

Two types of goals will be considered in this chapter. The first type is *position control* or *setpoint control* which seeks to drive the robotic system to a desired state. The goal in setpoint control is to find the actuation input $\boldsymbol{\tau}(t)$ for $t \in \mathbb{R}^+$ such that the state approaches some fixed, desired state

$$\mathbf{x}(t) \rightarrow \mathbf{x}_d \tag{6.1.3}$$

as $t \rightarrow \infty$. A typical problem in setpoint control might seek to find the controls $\boldsymbol{\tau}(t)$ that position and orient the end effector of a robotic arm in some prescribed configuration in the workspace. The second type of control problem studied in this chapter is that of *tracking control*. The goal of a trajectory tracking controller is to find a control input $\boldsymbol{\tau}(t)$ such that

$$\mathbf{x}(t) \rightarrow \mathbf{x}_d(t)$$

as $t \rightarrow \infty$. The mapping $t \mapsto \mathbf{x}_d(t)$ is a vector of desired, time-varying trajectories. As the name suggests, a problem in tracking control might seek to find the control inputs that steer a radar antenna or camera so that it always points at some moving target. It is possible to view a setpoint control law as a special case of a tracking control law. However, it can be easier to state conditions that guarantee that the setpoint control objective is achieved, and for this reason these two problems are studied independently.

6.1.2 Open Loop and Closed Loop Control

In addition to the goal that defines a particular control strategy, the means for achieving that goal differentiates control techniques. One of the most fundamental differences among control strategies distinguishes between *open loop control* and *closed loop control* methods. This distinction is based on the structure of the control input $\boldsymbol{\tau}$. An open loop control method is one that chooses the control input $\boldsymbol{\tau}$ to be some explicit function of the time t alone. If, on the other hand, the actuation input $\boldsymbol{\tau}$ is given as some function of the states $\mathbf{x}(t)$ and perhaps time t ,

$$\boldsymbol{\tau}(t) := \boldsymbol{\tau}(t, \mathbf{x}(t)),$$

the vector $\boldsymbol{\tau}$ defines a closed loop control or feedback control strategy. Feedback controllers have many desirable properties. Two important reasons that they are attractive include the fact that they are amenable to real-time implementations using measurements of output, and they reduce the sensitivity of systems to disturbances. This book will only study feedback controllers. Sections (6.6), (6.7), and (6.8) discuss several approaches for deriving setpoint or tracking feedback controllers.

6.1.3 Linear and Nonlinear Control

It has been emphasized in this book that the governing equations for most robotic systems are nonlinear: it is an unusual case when they happen to be linear. Chapter (4) showed that Newton-Euler formulations can yield systems of nonlinear ODEs or DAEs. Chapter (5) demonstrated that Hamilton's Principle or Lagrange's Equations also yield systems of nonlinear ODEs or DAEs. In most undergraduate curricula, the first, and often only, discussion of control theory is restricted to *linear systems*. A powerful and comprehensive theory of linear control theory has been developed over the past several decades. The focus on *linear control theory* during undergraduate program is justified: it enables the study of linear ODEs that arise in numerous

problems from applications in mechanical design, heat transfer, electrical circuits, and fluid flow.

The development of control strategies for *nonlinear systems*, such as those studied in robotics, is significantly more difficult than that for linear systems. One source of trouble is the fact that the study of the stability is much more complicated for nonlinear systems than linear systems. In addition, the underlying structure of linear control systems is easier to describe than that for nonlinear systems. Each of these issues will be discussed briefly.

The concepts of *stability* and *asymptotic stability* (introduced in Definitions (6.2) and (6.3)) for general nonlinear systems are *local definitions*. This means that the assurances that trajectories that start close to an equilibrium remain nearby for all time are guaranteed to be true only when the initial conditions reside in some neighborhood of the equilibrium under consideration. It can be the case that the neighborhood in which the stability guarantees hold is a very small set. If the initial conditions are too far from the equilibrium, and are outside this neighborhood, the guarantee of stability does not hold. In contrast, for linear systems, the neighborhood of the equilibrium is always the whole space. This fact means that for linear systems, local stability implies *global stability*. It can be a formidable task to prove that a nonlinear system satisfies conditions of global stability. When designing controllers, assurances of global stability and convergence are most desired.

Discussions of stability, including the considerations above, are central in the synthesis of control strategies. The question of whether a system can be rendered stable through the introduction of feedback control is made rigorous via the definition of *stabilizability* of dynamic systems. In addition to stabilizability, there are other qualitative properties of dynamic systems that have been defined that are essential to understanding the feasibility of certain control design tasks. For example, the definition of *controllability* makes clear when it is possible to drive or steer a system to certain configurations. The definition of *observability* describes the ability to reconstruct the state from a specific set of system observations or measurements. There is a rich theory that has been developed for linear systems that provides practical means for determining stabilizability, controllability and observability. These techniques can be applied to many realistic problems and are now standard tools available in control synthesis software. For certain smooth nonlinear systems the corresponding notions of stabilizability, controllability and observability have been defined, but the application of these principles to a specific nonlinear system can be exceptionally difficult. The interested student can consult [21] for a detailed discussion.

For the reasons above, the derivation of a control strategy for a nonlinear system, such as a typical robotic system, can be significantly more challenging than that for a linear system.

Fortunately, the structure of the governing equations for many robotic systems is such that it is often possible to define a feedback control law that transforms the set of *nonlinear ODEs* into a system of *linear ODEs*. This is possible, as will be shown, for robotic manipulators that constitute a kinematic or serial chain that is ground based. It is important to realize that this transformation, that chooses a feedback

control to change or modify a set of governing nonlinear ODEs into a system of linear ODEs, cannot be carried out for an arbitrary nonlinear system. It is the special form of certain robotic systems that makes this approach feasible. The question of when this strategy is possible for general systems is studied systematically in the control theory community as the problem of *feedback linearization*. A good treatment of the problem can be found in [21]. This approach is also known as the *method of dynamic inversion* or as *computed torque control* in the robotics literature. Overviews of these approaches for robotic systems are found in [15] and [30]. Most descriptions of feedback linearization cast the theory in terms of systems of first order ODEs, while descriptions of computed torque control or dynamic inversion retain the structure of second order ODEs that appear directly in either Newton-Euler or analytical mechanic formulations of dynamics. This observation makes it possible to view the approaches derived within the context of dynamic inversion or computed torque control as special cases of the theory of feedback linearization.

6.2 Fundamentals of Stability Theory

This chapter discusses the fundamentals of how to construct and analyze methods of feedback control for robotic systems. The single most important requirement of any control strategy is that the dynamic system that results from the use of the control law is stable. While the relative merit of different control strategies can be quantified via different measures of performance, any viable control technique must yield a stable system.

Stability theory can be framed using different levels of abstraction, as well as under various operating hypotheses. Stability in metric spaces is studied in [40], for example, whereas a stochastic framework is employed in [32]. The stability of infinite dimensional systems is considered in [13], and finite dimensional systems are studied in [19]. Popular treatments that develop stability theory as it is applied to the control of systems of ordinary differential equations can be found in [42], [28], or [44]. These last three references provide a good background for the material in this section, as well as additional advanced material of general interest to robotics control. Finally, the textbooks [30, 3] discuss how the general techniques in stability theory can be tailored to specific classes of robotic systems. The discussion of stability here begins by introducing a few background definitions.

Definition 6.1. A motion or trajectory \mathbf{x} of the system defined by Equations (6.1.2) starting at $\mathbf{x}_0 \in \mathbb{R}^N$ is a vector valued function of time $\mathbf{x} : [t_0, \infty) \rightarrow \mathbb{R}^N$ that satisfies Equation (6.1.2) for each $t \in [t_0, \infty)$. An *equilibrium* is a constant trajectory that satisfies Equation (6.1.2).

It is important to note in this definition that a motion or trajectory associated with the *nonautonomous system* in Equation 6.1.2 depends parametrically on the initial time t_0 and initial condition \mathbf{x}_0 . Sometimes this dependency is emphasized by writing

$$\mathbf{x}(t) := \mathbf{x}(t; t_0, \mathbf{x}_0) \quad t_0 \leq t < \infty$$

An equilibrium $\mathbf{x}_e \in \mathbb{R}^N$ of the system, being a constant trajectory that does not depend on time, must satisfy the equations $\mathbf{0} = \mathbf{f}(t, \mathbf{x}_e)$ and $\mathbf{x}_e = \mathbf{x}_0$. That is, the trajectory associated with an equilibrium starts at \mathbf{x}_0 and remains at \mathbf{x}_0 for all time $t \geq t_0$. The following theorem makes precise the notion of stability for an equilibrium: it takes the form of a standard $\delta - \epsilon$ proof.

Definition 6.2. Suppose \mathbf{x}_e is an equilibrium of the system in Equation (6.1.2). The trajectory \mathbf{x}_e is a *stable equilibrium* if for any $\epsilon > 0$, there is a $\delta := \delta(\epsilon, \mathbf{x}_0) > 0$ such that

$$\|\mathbf{x}_0 - \mathbf{x}_e\| < \delta \implies \|\mathbf{x}(t) - \mathbf{x}_e\| < \epsilon \quad \text{for all } t \geq t_0,$$

where $\mathbf{x}(t) := \mathbf{x}(t; t_0, \mathbf{x}_0)$ is the trajectory starting at (t_0, \mathbf{x}_0) of the system governed by Equation (6.1.2)

Definition (6.2) imposes requirements only in some neighborhood of the equilibrium under consideration, and for this reason it is sometimes said to define the *local stability of an equilibrium*. If the radius δ in the definition can be selected to be arbitrarily large, the equilibrium is said to be *globally stable*. In this book, any discussion of stability may be assumed to be a discussion of local stability, and any discussion of global stability will be explicitly labeled as such.

Figure (6.1) illustrates a graphical interpretation of the definition of stability. As shown in the figure, the equilibrium \mathbf{x}_e can be visualized as a trajectory that starts at the fixed point \mathbf{x}_e in the space of initial conditions and is extended as a constant function for all time t . The parameter ϵ defines a tube of radius ϵ centered about the constant trajectory \mathbf{x}_e that is extruded along the time axis. The system is stable if for any $\epsilon > 0$ it is possible to find a disk of radius δ about the initial condition \mathbf{x}_e such that any trajectory starting in the disk remains inside the tube of radius ϵ for all time. It follows that if the neighborhood of the equilibrium is chosen to be small enough, all trajectories starting in the neighborhood remain bounded for all time.

The application of this definition becomes more clear in the following example.

Example 6.2.1. Consider the two link robot depicted in Figure (5.24) and studied in Problem (5.17) of Chapter (5). Suppose that the second link is locked in position where

$$d(t) = \bar{d} = \text{constant}.$$

Discuss the stability of this system when the control torque $M \equiv 0$.

Solution:

The governing equation of motion for the revolute joint may be extracted from Problem (5.17) as

$$\left(m_1 H^2 + m_2 (\bar{d})^2 \right) \ddot{\theta} + g(m_1 H + m_2 D) \cos \theta + m_2 \bar{d} g \cos \theta = 0$$

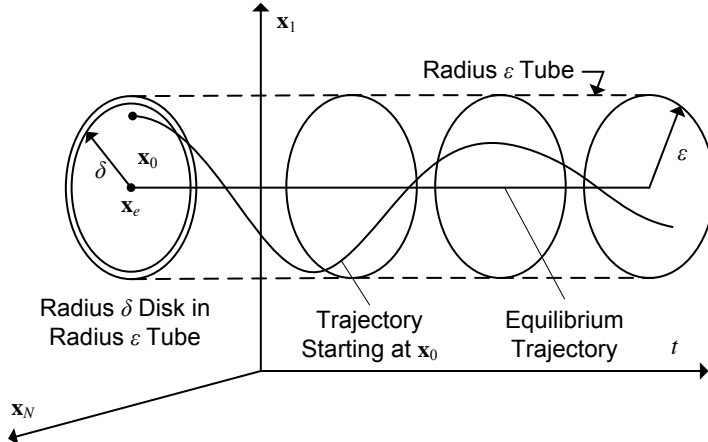


Fig. 6.1: Graphic Representation of Stability

under the assumptions of this example. It can be further simplified to emphasize the essential features of the stability analysis. The location of the mass center along the arm may be defined as

$$d_c = \frac{1}{m_1 + m_2} (m_1 H + m_2 (\bar{d} + D)),$$

and the total mass and the inertia about the point 0 may be defined as via the equations

$$\begin{aligned} M_T &= m_1 + m_2, \\ J_0 &= m_1 H^2 + m_2 (D + \bar{d})^2. \end{aligned}$$

Using these parameters, the governing equation can be rewritten as shown in Equation (6.1.1)

$$J_0 \ddot{\theta} + M_T g d_c \cos \theta = 0. \quad (6.2.1)$$

Next, this equation can be cast in the form of a first order ODE as in Equation (6.1.2). Define $l := J_0 / M_T d_c$ and choose the definition of the state variables to be

$$\mathbf{x} = \begin{Bmatrix} x_1 \\ x_2 \end{Bmatrix} = \begin{Bmatrix} \theta + \frac{\pi}{2} \\ \dot{\theta} \end{Bmatrix}.$$

Therefore,

$$\dot{\mathbf{x}}(t) = \begin{Bmatrix} \dot{x}_1 \\ \dot{x}_2 \end{Bmatrix} = \begin{Bmatrix} \dot{\theta} \\ \ddot{\theta} \end{Bmatrix} = \begin{Bmatrix} x_2 \\ -\frac{g}{l} \cos(x_1 - \frac{\pi}{2}) \end{Bmatrix} = \begin{Bmatrix} x_2 \\ -\frac{g}{l} \sin x_1 \end{Bmatrix} = \mathbf{f}(\mathbf{x}(t))$$

The equilibria for the system satisfy

$$\begin{Bmatrix} 0 \\ 0 \end{Bmatrix} = \mathbf{f}(\mathbf{x}_e) = \begin{Bmatrix} x_{2,e} \\ -\frac{g}{l} \sin x_{1,e} \end{Bmatrix},$$

or

$$\begin{Bmatrix} x_{1,e} \\ x_{2,e} \end{Bmatrix} = \begin{Bmatrix} k\pi \\ 0 \end{Bmatrix} \quad \text{for } k \in \mathbb{Z},$$

where \mathbb{Z} is the set of integers. The stability of the equilibria may be studied by multiplying the governing Equation (6.2.1) by $\dot{\theta}$ and employing the identity

$$J_0 \dot{\theta} \ddot{\theta} + M_T g d_c \dot{\theta} \cos \theta = J_0 \frac{d}{dt} \left(\frac{1}{2} \dot{\theta}^2 + \frac{g}{l} \sin \theta \right) = 0.$$

Integrating this identity in time shows that the total mechanical energy $E(t) := T + V$ in the system is a constant,

$$E(t) = E(0) = \frac{1}{2} J_0 \dot{\theta}^2 + M_T g d_c \sin \theta = J_0 \left(\frac{1}{2} x_2^2 + \frac{g}{l} \sin \left(x_1 - \frac{\pi}{2} \right) \right). \quad (6.2.2)$$

Figure (6.2) depicts the constant value contours of this integral of motion projected onto the $x_1 - x_2$ plane as a function of the trajectories $\mathbf{x}(t) = \begin{Bmatrix} x_1(t) & x_2(t) \end{Bmatrix}^T$. The equilibria in this figure are located on the x_1 axis where $x_1 = \pm k\pi$ for $k \in \mathbb{Z}$. This figure shows that the equilibria for odd values of k are unstable. To visualize this, imagine a tube of radius ϵ centered about any of these equilibria and extruded out of the page along the time axis. Any disk, having any radius $\delta > 0$, centered about the equilibrium \mathbf{x}_e associated with an odd value of k will contain some trajectories that leave the ϵ -tube for t large enough. For example, one such disk is depicted that has radius δ and is centered at the initial condition for the equilibrium at $x_1 = \pi$. No matter how small of a value of δ is chosen in the figure, some of the initial conditions inside the disk generate trajectories that depart the ϵ -tube. Analogous reasoning also shows that the equilibria associated with even values of k are stable.

The solution of this example using MATLAB can be found in ?? of the MATLAB workbook for DCRS.

The analysis carried out in Example (6.2.1) is typical of the reasoning employed in studying the stability of a nonlinear system. In particular, the example shows that the concept of stability is associated with a specific trajectory or equilibrium. The ODE representing the robot in Example (6.2.1) has an infinite number of stable equilibria, as well as an infinite number of unstable equilibria. If the state space of the dynamical system representing the robot is selected to be a manifold, then there are a finite number of equilibria. See [10]. The following definition introduces two stronger forms of stability, *asymptotic stability* and *exponential stability*. These notions of stability are used in the design of both setpoint and tracking controllers and play an important role in this discussion.

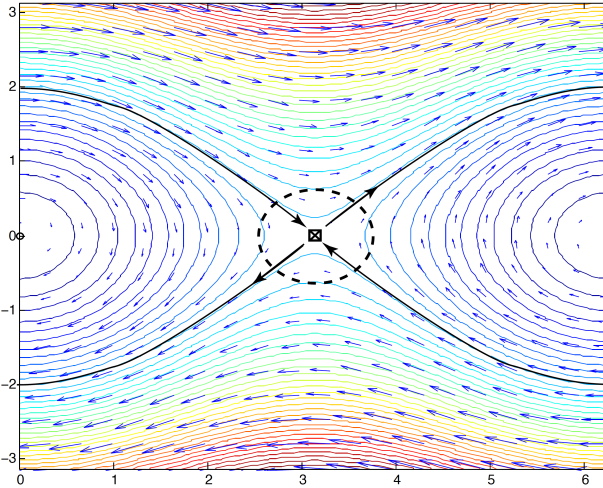


Fig. 6.2: Plot of $\frac{1}{2}x_2^2 + \frac{g}{l} \sin\left(x_1 - \frac{\pi}{2}\right)$ for $\frac{g}{l} = 1$, stable equilibrium marked with \circ , unstable equilibrium marked with \times . Disc of radius δ around $(x_1, x_2) = (\pi, 0)$ shown with dashed line.

Definition 6.3. A stable equilibrium \mathbf{x}_e of the system in Equation (6.1.2) is asymptotically stable if there is a $\delta = \delta(\epsilon, \mathbf{x}_0) > 0$ such that

$$\|\mathbf{x}_0 - \mathbf{x}_e\| < \delta \quad \longrightarrow \quad \lim_{t \rightarrow \infty} \|\mathbf{x}(t) - \mathbf{x}_e\| = 0,$$

where $\mathbf{x}(t) := \mathbf{x}(t; t_0, \mathbf{x}_0)$ is the trajectory starting at (t_0, \mathbf{x}_0) . A stable equilibrium \mathbf{x}_0 is exponentially stable if there is a $\delta = \delta(\epsilon, \mathbf{x}_0) > 0$ such that

$$\|\mathbf{x}_0 - \mathbf{x}_e\| < \delta \quad \longrightarrow \quad \|\mathbf{x}(t) - \mathbf{x}_e\| \leq ce^{-at} \quad \forall t \in [0, \infty),$$

for two constants $c, a > 0$.

Note that the definitions of asymptotic and exponential stability of equilibria require that they be stable. Figure (6.3) depicts the trajectories of a system that satisfies $\lim_{t \rightarrow \infty} \|\mathbf{x}(t) - \mathbf{x}_e\| = 0$ for any initial condition. That is, all trajectories are attracted to the equilibrium at the origin. However, the equilibrium at the origin is not stable, hence it is not asymptotically stable. It should be emphasized that Definition (6.3) requires that an asymptotically equilibrium must be stable and attractive: attractivity alone is not enough.

A stable equilibrium is asymptotically stable if a disk of radius $\delta > 0$ can be found for which trajectories that start at any initial condition in that disk converge to the equilibrium as $t \rightarrow \infty$. An equilibrium is exponentially stable if it is asymptotically stable and converges to the equilibrium at an exponential rate. Again, it is

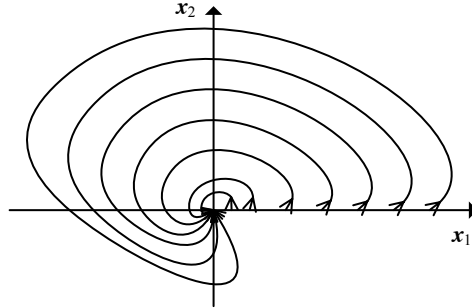


Fig. 6.3: A dynamical system that attracts to the origin, but is not stable at the origin.

emphasized that Definition (6.2) imposes conditions only in neighborhood of radius δ about the equilibrium, and for this it is sometimes said that the equilibrium is *locally asymptotically stable*. If the radius δ can be chosen to be arbitrarily large, the equilibrium is said to be *globally asymptotically stable*. In this book an asymptotically stable equilibrium is understood to mean a locally asymptotically stable, and globally asymptotically stable equilibria are explicitly labeled such.

The next example shows that these two types of stability appear naturally in typical control problems.

Example 6.2.2. The equations of motion for the control problem in Example (6.2.1) may be written in the form

$$\dot{\mathbf{x}}(t) = \begin{Bmatrix} \dot{x}_1(t) \\ \dot{x}_2(t) \end{Bmatrix} = \begin{Bmatrix} x_2 \\ -\frac{g}{l} \sin x_1 \end{Bmatrix} + \begin{Bmatrix} 0 \\ \frac{1}{J_0} \end{Bmatrix} m(t) \quad (6.2.3)$$

where $m(t) = 0$ is the control input.

Suppose now in this example that the control input torque in Example (6.2.1) is selected to be

$$m(t) = J_0 \left(\frac{g}{l} \sin x_1 - k_0 x_1 - k_1 \dot{x}_1 \right) = J_0 \left(\frac{g}{l} \sin x_1 - k_0 x_1 - k_1 x_2 \right)$$

where $k_1, k_2 > 0$ are constants. Discuss the stability of the system.

Solution: For this choice of feedback control law, the system equations of motion are equivalent to the second order ordinary differential equation

$$\ddot{x}_1 + k_1 \dot{x}_1 + k_0 x_1 = 0.$$

Note that this choice of feedback control exactly cancels the nonlinear term from the governing equation, and yields a linear ordinary differential equation as a result. This is a common strategy in many control synthesis problems for robotic systems.

We will study this approach in general terms in Section (6.6) where it is known as the method of *dynamic inversion* or *computed torque control*. This equation may be rewritten in terms of the natural frequency ω_n and damping ratio ξ by introducing the identities $k_1 = 2\xi\omega_n$ and $k_0 = \omega_n^2$ so that

$$\ddot{x}_1 + 2\xi\omega_n\dot{x}_1 + \omega_n^2 x_1 = 0. \quad (6.2.4)$$

The equilibrium of this system is given by

$$\begin{Bmatrix} x_1 \\ x_2 \end{Bmatrix}_e = \begin{Bmatrix} 0 \\ 0 \end{Bmatrix},$$

since

$$\dot{\mathbf{x}}_e = \begin{Bmatrix} \dot{x}_1 \\ \dot{x}_2 \end{Bmatrix}_e = \begin{Bmatrix} x_2 \\ -2\xi\omega_n x_2 - \omega_n^2 x_1 \end{Bmatrix}_e = \begin{Bmatrix} 0 \\ 0 \end{Bmatrix}.$$

Assuming that $\xi < 1$, the solution of Equation (6.2.4) can be written as

$$x_1(t) = e^{-\xi\omega_n t} \left(x_{1,0} \cos \omega_d t + \frac{x_{2,0} + \xi\omega_n x_{1,0}}{\omega_d} \sin \omega_d t \right)$$

with $\omega_d = \omega_n \sqrt{1 - \xi^2}$ the damped natural frequency. It is therefore evident that

$$\|\mathbf{x}(t) - \mathbf{x}_e\| = \|\mathbf{x}(t)\| \leq c e^{-\xi\omega_n t}$$

for some constant $c > 0$ that depends on the initial condition. From the solution for $x_1(t)$ above, the following bound exists

$$\begin{aligned} |x_1(t)| &\leq e^{-\xi\omega_n t} \left(|x_{1,0}| + \frac{1}{\omega_d} (|x_{2,0}| + (\xi\omega_n)|x_{1,0}|) \right), \\ &\leq e^{-\xi\omega_n t} \left(\left(1 + \frac{\xi\omega_n}{\omega_d} \right) |x_{1,0}| + \frac{1}{\omega_d} |x_{2,0}| \right), \\ &\leq \frac{1}{\omega_d} \sqrt{1 + (\omega_d + \xi\omega_n)^2} \|\mathbf{x}_0\| e^{-\xi\omega_n t}. \end{aligned}$$

Similarly,

$$|x_2(t)| = |\dot{x}_1(t)| \leq \frac{\xi\omega_n}{\omega_d} \sqrt{1 + (\omega_d + \xi\omega_n)^2} \|\mathbf{x}_0\| e^{-\xi\omega_n t},$$

and it follows that

$$\|\mathbf{x}(t)\| \leq \frac{\sqrt{1 + (\xi\omega_n)^2} \sqrt{1 + (\omega_d + \xi\omega_n)^2}}{\omega_d} \|\mathbf{x}_0\| e^{-\xi\omega_n t}.$$

Let $\mathbf{B}_\delta(\mathbf{0})$ be the open ball centered at the origin of radius δ , $\mathbf{B}_\delta(\mathbf{0}) = \{\mathbf{x} \in \mathbb{R}^2 \mid \|\mathbf{x}\| < \delta\}$. The bound (6.2.2) guarantees that if $\mathbf{x}_0 \in \mathbf{B}_\delta(\mathbf{0})$, then $\|\mathbf{x}\| \rightarrow 0$ as $t \rightarrow \infty$. The equilibrium at the origin of the closed loop system is therefore exponentially stable.

In fact, the origin is globally exponentially stable since the constant δ can be chosen to be arbitrarily large.

Example ?? in the MATLAB workbook for DCRS creates a phase portrait plot of a neighborhood of the equilibrium of the origin. The phase portrait provides a graphical illustration of stability; it illustrates which trajectories converge to the origin.

6.3 Advanced Techniques of Stability Theory

The previous section introduced the definitions of stability, asymptotic stability and exponential stability. These definitions were applied directly in Examples (6.2.1) and (6.2.2) to study a simple robotic system. In Example (6.2.2), the stability of the equilibrium at the origin was studied by explicitly solving for the solution of the closed loop governing equations. In Example (6.2.1), the equation of motion was multiplied by \dot{x}_1 and integrated in time to find a conserved quantity. The critical step wrote the time derivative of the total mechanical energy $E := T + V$ in the form

$$\frac{d}{dt}(E(t)) = J_0 \left(\ddot{x}_1 + \frac{g}{l} \sin\left(x_1 - \frac{\pi}{2}\right) \right) \dot{x}_1 = J_0 \frac{d}{dt} \left(\frac{1}{2} \dot{x}_1^2 + \frac{g}{l} \sin\left(x_1 - \frac{\pi}{2}\right) \right)$$

which was integrated in time to yield

$$E(t) = E(0) = J_0 \left(\frac{1}{2} \dot{x}_1^2 + \frac{g}{l} \sin\left(x_1 - \frac{\pi}{2}\right) \right) = \text{constant.} \quad (6.3.1)$$

The study of the stability of different equilibria is straightforward using this conserved or invariant quantity.

The study of the stability of control methods for realistic robotic systems can be sufficiently difficult that it is not feasible to analytically solve the closed loop governing equations. It therefore is not practical, or seldom even possible, to use the explicit analytical solution to design and study a feedback control law.

Fortunately, the strategy in which conserved quantities such as energy are identified to study stability can be generalized and applied to many practical robotic systems. These generalizations of energy principles are applied by invoking Lyapunov's Direct Method. It is now a standard practice in the study of robotic systems to use variants of Lyapunov's Direct Method to analyze their stability. The study of the finer points of this approach to stability theory extend beyond the scope of this book. This book will introduce only those definitions and theorems that find the most frequent use in applications; no proofs of the underlying theorems are given. The texts [44] or [28] can be consulted for the proofs and for an expanded discussion of Lyapunov theory as it is applied to systems of ordinary differential equations. It

is also worth observing that this framework has been extended to broader classes of abstract dynamic systems. A good overview can be found in [40].

6.4 Lyapunov's Direct Method

The theorems of Lyapunov's Direct Method introduce *Lyapunov functions*, which constitute the principal tools for the study of stability. The discussion begins by defining useful ways of describing the growth, or decay, of functions.

Definition 6.4. A continuous function $f : \mathbb{R}^+ \rightarrow \mathbb{R}^+$ belongs to class \mathcal{K} provided (i) $f(0) = 0$, (ii) $f(x) > 0$ for $x > 0$, and (iii) f is nondecreasing.

Examples of class \mathcal{K} functions are readily available. They are positive functions that pass through the origin and are nondecreasing. The functions $f(x) = x^2$ or $f(x) = \sqrt{x}$ are class \mathcal{K} functions, as are $f(x) = x^p$ for $0 < p < \infty$. Some of these functions are depicted in Figure (6.4).

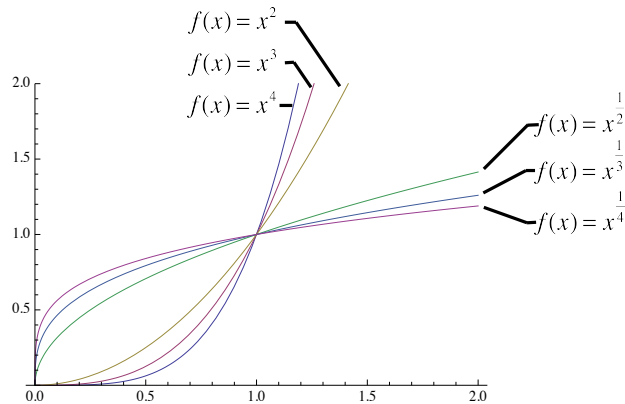


Fig. 6.4: Examples of Class \mathcal{K} Functions, $f(x) = x^p$ for $0 < p < \infty$

The collection of class \mathcal{K} functions are used to define notions of positivity and negativity that are suitable for the study of stability. It will be shown that stability and asymptotic stability are guaranteed if a Lyapunov function \mathcal{V} can be identified that is (*locally*) *positive definite* and whose time derivative $\dot{\mathcal{V}}$ is (*locally*) *negative definite*. The definitions below establish what is meant when a Lyapunov function is said to be positive and its derivative negative.

Definition 6.5. A continuous function $\mathcal{V} : \mathbb{R}^+ \times \mathbb{R}^N \rightarrow \mathbb{R}$ is a locally positive definite function on a neighborhood $\mathcal{N} \subseteq \mathbb{R}^N$ of the origin if there is a class \mathcal{K} function f such that

$$\mathcal{V}(t, \mathbf{x}) \geq f(\|\mathbf{x}\|)$$

for all $t \geq 0$ and $\mathbf{x} \in \mathcal{N}$. The function \mathcal{V} is positive definite if the neighborhood \mathcal{N} can be chosen to be all of \mathbb{R}^N . A function \mathcal{V} is negative definite if $-\mathcal{V}$ is positive definite.

A continuous function $\mathcal{V} : \mathbb{R}^+ \times \mathbb{R}^N \rightarrow \mathbb{R}$ is a *locally decreasing* function on a neighborhood $\mathcal{N} \subseteq \mathbb{R}^N$ of the origin if there is a class \mathcal{K} function g such that

$$\mathcal{V}(t, \mathbf{x}) \leq g(\|\mathbf{x}\|)$$

for all $t \geq 0$ and $\mathbf{x} \in \mathcal{N}$. A function \mathcal{V} is *decreasing* if the neighborhood \mathcal{N} can be chosen to be all of \mathbb{R}^N .

With this definition, one of the most common forms of Lyapunov stability theorems may be stated. This theorem will be the principal tool used in this book for the study of stability of robotic systems.

Theorem 6.1. Suppose that the origin $\mathbf{0} \in \mathbb{R}^N$ is an equilibrium of the system of equations

$$\begin{aligned}\dot{\mathbf{x}}(t) &= \mathbf{f}(t, \mathbf{x}(t)), \\ \mathbf{x}(0) &= \mathbf{x}_0.\end{aligned}$$

Let the function $\mathcal{V} : \mathbb{R}^+ \times \mathbb{R}^N \rightarrow \mathbb{R}$ have continuous partial derivatives and be locally positive definite on a neighborhood $\mathcal{N} \subseteq \mathbb{R}^N$ of the origin. If

$$\dot{\mathcal{V}}(t, \mathbf{x}) \leq 0 \quad \forall t \geq 0, \quad \forall \mathbf{x} \in \mathcal{N}$$

then the equilibrium at the origin is stable. If \mathcal{V} is also locally negative definite on the neighborhood \mathcal{N} , then the equilibrium is asymptotically stable.

It should be noted the above theorem is stated for an equilibrium located at the origin. This is not a restriction in practice. Analysis of nonzero equilibria begins with a change of variable to shift the equilibrium and define a new set of equations as required in Theorem (6.1).

In order to enforce *global asymptotic stability* (i.e., $\mathcal{N} = \mathbb{R}^N$), an additional condition on the Lyapunov function of radial unboundedness must be enforced. As the norm of the state approaches infinity, the Lyapunov function must also approach infinity. Additional details may be found in [28].

A function V that has the properties noted in Theorem (6.1) is a *Lyapunov function*. The most difficult task in using Lyapunov's direct method can be in determining a candidate Lyapunov function. Fortunately, for many robotic systems, there are

often good candidates. Researchers have derived, categorized and documented examples of Lyapunov functions for many classes of robotic systems. The reader can see [15] or [30] for examples. Many Lyapunov functions can be derived from, or related to, conserved or energy-like quantities. The following example is typical in that the Lyapunov function is chosen to be the total mechanical energy.

Example 6.4.1. Use Theorem (6.1) to show that the equilibrium at $\theta_e = -\frac{\pi}{2}$ for the robotic system studied in Example (6.2.1) is stable

Solution: The governing equation in Example (6.2.1) is the nonlinear second order ordinary differential equation

$$J_0\ddot{\theta} + M_T g d_c \cos \theta = 0,$$

which has an equilibrium of interest at $\theta_e = -\frac{\pi}{2}$. Theorem (6.1) is stated in terms of a system of first order nonlinear ordinary differential equations that have an equilibrium at the origin. Thus, the analysis begins by shifting the coordinates so that the equilibrium under investigation occurs at the origin. Defining the state to be

$$\mathbf{x} = \begin{Bmatrix} x_1 \\ x_2 \end{Bmatrix} = \begin{Bmatrix} \theta + \frac{\pi}{2} \\ \dot{\theta} \end{Bmatrix},$$

allows for the governing equation to be written as

$$\dot{\mathbf{x}} = \begin{Bmatrix} \dot{x}_1 \\ \dot{x}_2 \end{Bmatrix} = \begin{Bmatrix} \dot{\theta} \\ \ddot{\theta} \end{Bmatrix} = \begin{Bmatrix} x_2 \\ -\frac{g}{l} \cos(x_1 - \frac{\pi}{2}) \end{Bmatrix} = \begin{Bmatrix} x_2 \\ -\frac{g}{l} \sin x_1 \end{Bmatrix} = \mathbf{f}(\mathbf{x}(t)),$$

with $l := \frac{J_0}{M_T d_c}$. The equilibrium $\mathbf{x}_e = \begin{Bmatrix} 0 \\ 0 \end{Bmatrix}^T$ at the origin corresponds to the equilibrium $\theta_e = -\frac{\pi}{2}$, as desired. The total mechanical energy of the system is chosen as the Lyapunov function with

$$\begin{aligned} \mathcal{V} &= J_0 \left(\frac{1}{2} x_2^2 + \frac{g}{l} \left(\sin \left(x_1 - \frac{\pi}{2} \right) + 1 \right) \right), \\ &= J_0 \left(\frac{1}{2} x_2^2 + \frac{g}{l} (-\cos x_1 + 1) \right). \end{aligned}$$

The constant $m_2 g d_c$, which corresponds to a choice of the zero potential energy datum, has been added to ensure that

$$\mathcal{V}\left(\begin{Bmatrix} 0 \\ 0 \end{Bmatrix}\right) = 0.$$

It is also clear from the plot shown in Figure (6.5) that \mathcal{V} is a locally positive definite function on the neighborhood of the origin defined by

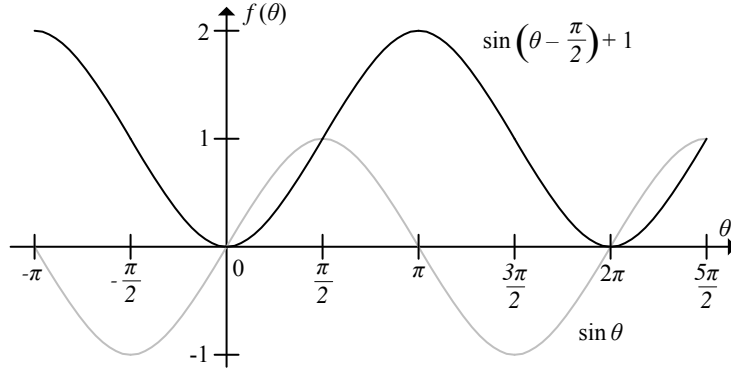


Fig. 6.5: Shifted sine function used in Lyapunov function

$$\mathcal{N} := \left\{ \begin{Bmatrix} x_1 \\ x_2 \end{Bmatrix} : -\pi < x_1 < \pi, x_2 \in \mathbb{R} \right\}.$$

The derivative of \mathcal{V} along the trajectories of the system is

$$\begin{aligned} \dot{\mathcal{V}} &:= \sum_{i=1}^2 \frac{\partial \mathcal{V}}{\partial x_i} \dot{x}_i + \frac{\partial \mathcal{V}}{\partial t} = \frac{\partial \mathcal{V}}{\partial \mathbf{x}} \cdot \dot{\mathbf{x}} = \left\{ \frac{\partial \mathcal{V}}{\partial x_1} \quad \frac{\partial \mathcal{V}}{\partial x_2} \right\} \cdot \mathbf{f}, \\ &= J_0 \left\{ \frac{g}{l} \sin x_1 \quad x_2 \right\} \left\{ \begin{array}{c} x_2 \\ -\frac{g}{l} \sin x_1 \end{array} \right\} = 0. \end{aligned}$$

Since $\dot{\mathcal{V}}(\mathbf{x}(t)) \leq 0$ for all $t \geq 0$ and $\mathbf{x} \in \mathcal{N}$, the equilibrium at the origin is stable. Note that the analysis yields only a local stability guarantee: the neighborhood \mathcal{N} is a proper subset of \mathbb{R}^2 .

Example ?? of the MATLAB workbook for DCRS depicts the Lyapunov function $\mathcal{V}(\mathbf{x})$ over a neighborhood of the origin. A trajectory whose initial condition resides in this neighborhood of the equilibrium at the origin is depicted, and it is illustrated that the the Lyapunov function evaluated over this trajectory, $\mathcal{V}(\mathbf{x}(t))$, is non increasing.

6.5 The Invariance Principle

The definitions and theorems introduced in the last section that constitute Lyapunov's Direct Method can be applied to many robotic systems. Several examples throughout this chapter will show that they can be employed directly for the derivation of stability results.

tion and study of control methods. For example, when seeking to design a controller for a robotic system, it is often desirable to establish some form of asymptotic stability. In the example of setpoint control, a controller is desired such that the joint variables and their derivatives approach some desired constant value as $t \rightarrow \infty$,

$$\mathbf{x}(t) := \begin{Bmatrix} \mathbf{q}(t) \\ \dot{\mathbf{q}}(t) \end{Bmatrix} \rightarrow \begin{Bmatrix} \mathbf{q}_d \\ 0 \end{Bmatrix} := \mathbf{x}_d.$$

This condition might correspond to the task of positioning the end effector of a kinematic chain at a prescribed location and orientation. The problem of tracking control seeks a feedback function that causes the joint variables or their derivatives to track some desired trajectories as $t \rightarrow \infty$,

$$\mathbf{x}(t) := \begin{Bmatrix} \mathbf{q}(t) \\ \dot{\mathbf{q}}(t) \end{Bmatrix} \rightarrow \begin{Bmatrix} \mathbf{q}_d(t) \\ \dot{\mathbf{q}}_d(t) \end{Bmatrix} := \mathbf{x}_d(t).$$

In both of these problems, the goal of the control strategy can be cast as a requirement in terms of the asymptotic stability of the error $\mathbf{e} := \mathbf{q} - \mathbf{q}_d$ and its derivative $\dot{\mathbf{e}}$; namely, that

$$\begin{Bmatrix} \mathbf{e}(t) \\ \dot{\mathbf{e}}(t) \end{Bmatrix} \rightarrow \begin{Bmatrix} 0 \\ 0 \end{Bmatrix}$$

as $t \rightarrow \infty$ in both cases.

The technique for establishing asymptotic stability via Lyapunov's Direct Method requires that the Lyapunov function \mathcal{V} is positive, and that the derivative $\dot{\mathcal{V}}$ is negative, for all states in some neighborhood of the equilibrium under consideration. Moreover, the most useful control designs would reach such conclusions for all states, and not just in some neighborhood of the equilibrium. It is always preferable to obtain global, as opposed to local, guarantees of stability in control design. It is usually not difficult to guarantee that \mathcal{V} is locally positive definite. Energy or energy-like quantities often exist for robotic systems that are positive and non-decreasing, and these are often used in constructing Lyapunov functions for the system. However, it is frequently the case that \mathcal{V} is *negative semidefinite*, with

$$\dot{\mathcal{V}}(t, \mathbf{x}) \leq 0$$

for all $\mathbf{x} \in \mathcal{N}$, but not locally negative definite. In such cases Lyapunov's Direct Method only guarantees stability of an equilibrium and makes no claim regarding asymptotic stability. The following example is typical of this situation and is a common occurrence in realistic applications.

Example 6.5.1. Show that

$$\mathcal{V} = \frac{1}{2}x_1^2 + \frac{1}{2}k_0x_1^2$$

is a Lyapunov function for the closed loop system studied in Example (6.2.2) that is positive definite. Show that the derivative $\dot{\mathcal{V}}$ along the system trajectories is negative

semidefinite and use Lyapunov's direct method to conclude that the equilibrium at the origin is stable.

Can this Lyapunov function and Theorem (6.1) be used to conclude that the equilibrium at the origin is asymptotically stable?

Solution: First, it can be seen that

$$\begin{aligned}\mathcal{V}(\mathbf{0}) &= 0, \\ \mathcal{V}(\mathbf{x}) &\geq c\|\mathbf{x}\|^2 \quad \forall \mathbf{x} \in \mathcal{N}\end{aligned}$$

for the constant $c := \frac{1}{2}\min\{J_0, k_0\}$. The function \mathcal{V} is positive definite since the neighborhood can be chosen as $\mathcal{N} = \mathbb{R}^2$ in the inequality above. The derivative of \mathcal{V} along the trajectories is calculated as

$$\dot{\mathcal{V}} = \frac{d}{dt} \left(\frac{1}{2} \dot{x}_1^2 + \frac{1}{2} k_0 x_1^2 \right) = \dot{x}_1 (\ddot{x}_1 + k_0 x_1).$$

Substituting the equation of motion results in $\dot{\mathcal{V}} = -k_1 \dot{x}_1^2 = -k_1 x_2^2$. Therefore,

$$\dot{\mathcal{V}}(t, \mathbf{x}) \leq 0 \quad \forall \mathbf{x} \in \mathcal{N} = \mathbb{R}^2$$

and the equilibrium at the origin is globally stable by Theorem (6.1). However, Theorem (6.1) cannot be applied to conclude that the equilibrium at the origin is asymptotically stable since the function $\dot{\mathcal{V}} = -k_1 x_2^2$ is not locally negative definite for all \mathbf{x} in an open neighborhood $\mathcal{N} \in \mathbb{R}^2$ of the origin $(0, 0)$. For example, for any state $\mathbf{x} = \{x_1, 0\}^T$ with $x_1 \neq 0$, it is evident that $\dot{\mathcal{V}}(t, \mathbf{x}) = 0$. But $\mathbf{x} = 0$, so $\dot{\mathcal{V}}$ is not locally negative definite in any neighborhood of the origin. Example (6.2.2) already established that the origin is globally asymptotically stable by explicitly solving the governing equations. In this case it is clear that the application of Lyapunov's Direct Method, in the form of Theorem (6.1), does not yield the strongest conclusions possible regarding the stability of the equilibrium at the origin.

There are various techniques to overcome the difficulties associated with a Lyapunov function that has a derivative that is negative semidefinite but not negative definite. The most popular method is based on LaSalle's Invariance Principle, which requires the definitions of a *positive invariant set*, a *weakly invariant set* and an *invariant set*.

Definition 6.6. Let $\mathbf{x}(t; \mathbf{s})$ be the solution of the system of nonlinear ordinary differential equations

$$\dot{\mathbf{x}}(t) = \mathbf{f}(t, \mathbf{x}(t)) \quad \forall t \in \mathbb{R}^+ \quad (6.5.1)$$

generated by the initial condition $\mathbf{x}(0) = \mathbf{s} \in \mathbb{R}^N$. A set of states $\mathcal{S} \subseteq \mathbb{R}^N$ is positive invariant with respect to the system in Equation (6.5.1) if

$$\mathbf{s} \in \mathcal{S} \rightarrow \mathbf{x}(t; \mathbf{s}) \in \mathcal{S} \quad (6.5.2)$$

for all $t \geq 0$ and for all $\mathbf{s} \in \mathcal{S}$.

Definition (6.6) stipulates that a set \mathcal{S} is positive invariant if every trajectory that starts in \mathcal{S} stays in \mathcal{S} for all time $t \in \mathbb{R}^+$. The set $\{\mathbf{x}_e\}$ where \mathbf{x}_e is an equilibrium is one example of a positive invariant set. A set \mathcal{S} is weakly invariant if for each $\mathbf{s} \in \mathcal{S}$ there is a trajectory $\{\mathbf{x}(\tau)\}_\tau \in \mathbb{R}$ (defined over all time $-\infty < \tau < \infty$) that passes through \mathcal{S} . A set \mathcal{S} is invariant with respect to the system in Equation 6.5.1 if both \mathcal{S} and the complement of \mathcal{S} are positive invariant. See Figure (6.6) for a graphic interpretation of positive invariance, weak invariance, and invariance.

Theorem 6.2 (La Salle's Principle). Let the origin $\mathbf{0} \in \mathbb{R}^N$ be an equilibrium of the system of autonomous ordinary differential equations

$$\begin{aligned} \dot{\mathbf{x}}(t) &= \mathbf{f}(\mathbf{x}(t)), \\ \mathbf{x}(0) &= \mathbf{x}_0. \end{aligned}$$

Suppose that the function $\mathcal{V} : \mathbb{R}^N \rightarrow \mathbb{R}$ has continuous partial derivatives, satisfies $\mathcal{V}(\mathbf{0}) = \mathbf{0}$, and is locally positive definite

$$\mathcal{V}(\mathbf{x}) > 0 \quad \forall \mathbf{x} \neq \mathbf{0} \text{ and } \mathbf{x} \in \mathcal{N}$$

on some neighborhood \mathcal{N} of the origin. Suppose that the derivative of \mathcal{V} along the system trajectories $\dot{\mathcal{V}}$ satisfies $\dot{\mathcal{V}}(\mathbf{0}) = 0$ and is locally negative semi-definite

$$\dot{\mathcal{V}}(\mathbf{x}(t)) \leq 0 \quad \forall \mathbf{x} \in \mathcal{N}.$$

If the trajectories of Equation (6.5.1) remain in a closed and bounded subset of \mathcal{N} , then they are attracted to the largest weakly invariant subset \mathcal{S} contained in \mathcal{M} where

$$\mathcal{S} \subseteq \mathcal{M} = \left\{ \mathbf{x} : \dot{\mathcal{V}}(\mathbf{x}) = 0, t \in \mathbb{R}^+ \right\}.$$

It is important to observe that LaSalle's Theorem holds for systems of autonomous ordinary differential equations, ones that do not depend explicitly on time. The conclusion of LaSalle's Principle is that trajectories are attracted to the largest weakly invariant subset contained in

$$\mathcal{M} = \left\{ \mathbf{x} : \dot{\mathcal{V}}(\mathbf{x}) = 0, t \in \mathbb{R}^+ \right\}$$

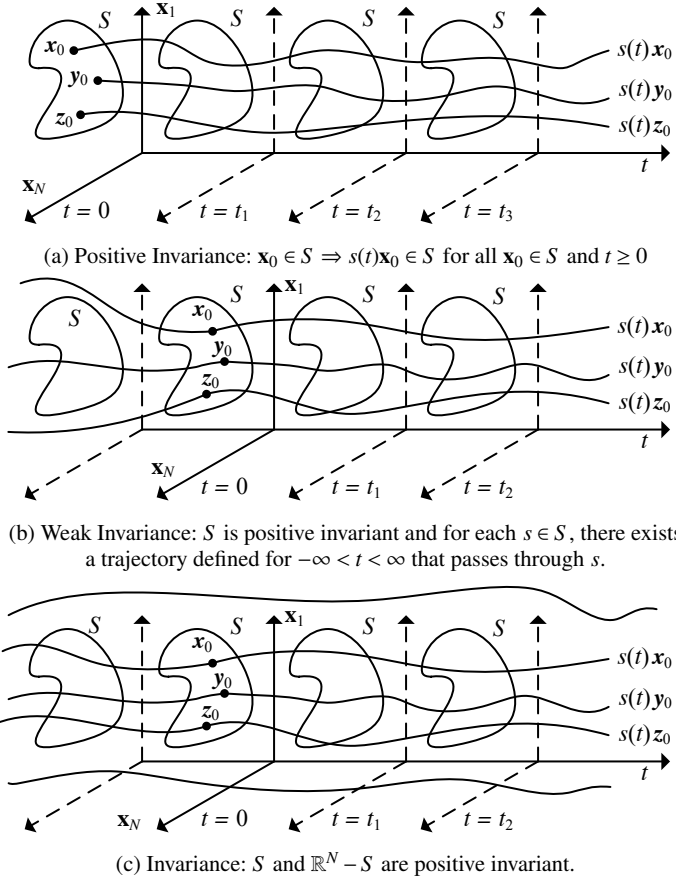


Fig. 6.6: Graphical Interpretation of Positive Invariance, Weak Invariance, and Invariance

Suppose that $S \subseteq \mathcal{M}$ is the largest weakly invariant subset contained in \mathcal{M} . A trajectory is attracted to S provided

$$d(\mathbf{x}(t), S) \rightarrow 0$$

as $t \rightarrow \infty$ where $d(\mathbf{x}(t), S)$ is the distance from $\mathbf{x}(t)$ to the set S

$$d(\mathbf{x}(t), S) = \inf_{\mathbf{s} \in S} \|\mathbf{x}(t) - \mathbf{s}\|.$$

While the conclusions of LaSalle's Principle is of interest in its own right, it is usually employed in control applications by showing that the largest invariant subset S contains a single element $\{\mathbf{s}\} = S$. Then the invariance principle implies that

$$\lim_{t \rightarrow \infty} \mathbf{x}(t) = \mathbf{s}.$$

The conclusion is precisely what is required to show that a stable equilibrium is in fact asymptotically stable. Example (6.5.2) applies this strategy in a typical robotics problem.

Example 6.5.2. Show that LaSalle's Invariance Principle can be used to conclude that the equilibrium at the origin is asymptotically stable in Example (6.5.1).

Solution: It has already been established that the derivative satisfies $\dot{\mathcal{V}} = -\frac{1}{2}k_1x_2^2$ when the Lyapunov function is selected to be $\mathcal{V} = \frac{1}{2}x_2^2 + \frac{1}{2}k_0x_1^2$. These identities hold over any open ball $\mathcal{B}_r(0)$ of radius r that contains the origin. In fact, if the closed and bounded set $C_{\mathbf{x}_0} = \{\mathbf{x} | \mathcal{V}(\mathbf{x}) < \mathcal{V}(\mathbf{x}_0)\}$ such that it is contained in $\mathcal{B}_r(0)$, then all the trajectories that start in $\mathcal{V}_{\mathbf{x}_0}$ stay in $\mathcal{V}_{\mathbf{x}_0}$. This fact follows since $\dot{\mathcal{V}}(\mathbf{x}(t)) \leq 0$, and therefore $\mathcal{V}(\mathbf{x}(t))$ is nonincreasing as a function of time $t \geq 0$. It is always true that $\mathcal{V}(\mathbf{x}(t)) \leq \mathcal{V}(\mathbf{x}_0)$, and therefore $\mathbf{x}_0 \in C_{\mathbf{x}_0}$ implies $\mathbf{x}(t) \in C_{\mathbf{x}_0}$. Hence, all the hypotheses of LaSalle's Principle hold. It is known therefore that trajectories are attracted to the largest weakly invariant subset $\mathcal{N} = \{\mathbf{x} | \dot{\mathcal{V}}(\mathbf{x}) = 0\}$. A set \mathcal{S} is weakly invariant provided it is positive invariant and there is a full trajectory $\mathbf{x}(t)$ for $t \in \mathbb{R}$ that passes through each element $\mathbf{s} \in \mathcal{S}$. So $\mathbf{s} \in \mathcal{S}$ if and only if $\mathbf{x}(t) \in \mathcal{S}$ for $t \in \mathbb{R}$ and $\mathbf{x}(0) = \mathbf{s}$. It is known that

$$\dot{\mathcal{V}}(\mathbf{x}(t)) = 0$$

if and only if $x_2(t) = 0$ for $t \in \mathbb{R}^+$. The equation of motion

$$J_0\dot{x}_2(t) + k_1x_2(t) + k_0x_1(t) = 0,$$

shows that

$$\dot{\mathcal{V}}(\mathbf{x}(t)) = 0 \leftrightarrow \mathbf{x}(t) = \begin{Bmatrix} x_1(t) \\ x_2(t) \end{Bmatrix} = \begin{Bmatrix} 0 \\ 0 \end{Bmatrix}$$

The equilibrium at the origin is the only element in the largest positive invariant subset $S \subseteq \mathcal{M} = \{\mathbf{x}(t) : \dot{\mathcal{V}}(\mathbf{x}(t)) = 0, t \in \mathbb{R}^+\}$. Therefore,

$$\begin{Bmatrix} x_1(t) \\ x_2(t) \end{Bmatrix} = \begin{Bmatrix} \theta(t) \\ \dot{\theta}(t) \end{Bmatrix} \rightarrow \begin{Bmatrix} 0 \\ 0 \end{Bmatrix}$$

as $t \rightarrow \infty$, and asymptotic stability of the equilibrium at the origin is proved.

6.6 Dynamic Inversion or Computed Torque Control

Chapters (4) and (5) showed that the governing equations for a natural system can be written in the form

$$\mathbf{M}(\mathbf{q}(t))\ddot{\mathbf{q}} = \mathbf{n}(\mathbf{q}(t), \dot{\mathbf{q}}(t)) + \boldsymbol{\tau}(t) \quad (6.6.1)$$

where \mathbf{q} is an N -vector of generalized coordinates, \mathbf{M} is an $N \times N$ generalized mass or inertia matrix, \mathbf{n} is an N -vector of nonlinear contributions to the equations of motion and $\boldsymbol{\tau}$ is an N -vector of actuation torques or forces. The vector \mathbf{n} contains contributions from the potential energy V of the system as well as the Coriolis and centripetal terms. The vector \mathbf{n} has been shown in Chapter 5 to have the specific structure

$$\mathbf{n} = -\left(\mathbf{C}\dot{\mathbf{q}} + \frac{\partial V}{\partial \mathbf{q}}\right), \quad (6.6.2)$$

where \mathbf{C} is an $N \times N$ generalized damping matrix. Since the generalized inertia matrix \mathbf{M} is symmetric and positive definite, it is always invertible. Therefore, it is possible to solve for the vector of second derivatives

$$\ddot{\mathbf{q}} = \mathbf{M}^{-1}(\mathbf{n} + \boldsymbol{\tau}).$$

The *computed torque control law* selects the actuation torques to be

$$\boldsymbol{\tau} = \mathbf{M}\mathbf{v} - \mathbf{n}, \quad (6.6.3)$$

where \mathbf{v} is a new, as of yet undetermined, control input vector. With this choice of the actuation torques, the governing equations become

$$\ddot{\mathbf{q}} = \mathbf{v}. \quad (6.6.4)$$

Equation (6.6.4) is a linear system that has been obtained from the nonlinear Equations (6.6.1). A nonlinear control law is defined in Equation (6.6.3) that transforms the system of governing nonlinear ODEs in Equation (6.6.1) into a system of linear ODEs in Equation (6.6.4). All of the rich theory that has been developed in linear control theory can now be brought to bear on the system in Equation (6.6.4). There are a wide collection of control functions \mathbf{v} that can be selected in Equation (6.6.4) that yield specific desirable behavior in the unknown generalized coordinates \mathbf{q} . The next theorem discusses one popular feedback strategy that achieves tracking control. The control \mathbf{v} is selected so that the generalized coordinates and their derivatives asymptotically track some desired variables \mathbf{q}_d and their derivatives $\dot{\mathbf{q}}_d$.

Theorem 6.3. Let the equations of motion for a robotic system have the form of Equations (6.6.1) and (6.6.2), and suppose that the input τ is selected to be the computed torque control law $\tau := \mathbf{M}\mathbf{v} - \mathbf{n}$ where

$$\mathbf{v} := \ddot{\mathbf{q}}_d - \mathbf{G}_1(\dot{\mathbf{q}} - \dot{\mathbf{q}}_d) - \mathbf{G}_0(\mathbf{q} - \mathbf{q}_d), \quad (6.6.5)$$

for which \mathbf{q}_d is a twice differentiable N vector of desired generalized coordinate trajectories $\mathbf{q}_d(t) := \{q_{d,1}(t) \dots q_{d,N}(t)\}^T$ for $t \in \mathbb{R}^+$, and $\mathbf{G}_1, \mathbf{G}_0$ are constant symmetric positive definite gain matrices. It is the generalized mass or inertia matrix $\mathbf{M}(\mathbf{q})$ is \mathbf{q} -uniformly elliptic and $\mathbf{n}(\mathbf{q}, \dot{\mathbf{q}})$ is a continuous, bounded function on $\mathbb{R}^N \times \mathbb{R}^N$, then the origin is a globally asymptotically stable equilibrium for the generalized coordinate tracking error $\{\mathbf{e}^T \dot{\mathbf{e}}^T\}$ where for $t \in \mathbb{R}^+$

$$\mathbf{e}(t) := \mathbf{q}(t) - \mathbf{q}_d(t).$$

Proof. The requirement that $\mathbf{M}(\mathbf{q})$ is \mathbf{q} -uniformly elliptic means that there exist two constants $c_1, c_2 > 0$ such that for any vector $\mathbf{z} \in \mathbb{R}^N$, then

$$c_1 \|\mathbf{z}\|^2 \leq \mathbf{z}^T \mathbf{M} \mathbf{z} \leq \|\mathbf{z} c_2\|^2$$

for all $\mathbf{q} \in \mathbb{R}^N$. Among other things, this condition ensures that the inverse of \mathbf{M} exists and is not singular for any configuration \mathbf{q} . Likewise, the assumption that $\mathbf{n}(\mathbf{q}, \dot{\mathbf{q}})$ is a continuous, bounded function on $\mathbb{R}^N \times \mathbb{R}^N$ precludes the possibility that there exist "singular" states of velocities for which $\mathbf{n}(\mathbf{q}, \dot{\mathbf{q}})$ is unbounded.

First note that the feedback law above is exactly the computed torque control in Equation (6.6.3) for which

$$\mathbf{v} = \ddot{\mathbf{q}}_d - \mathbf{G}_1(\dot{\mathbf{q}} - \dot{\mathbf{q}}_d) - \mathbf{G}_0(\mathbf{q} - \mathbf{q}_d), \quad (6.6.6)$$

$$= \ddot{\mathbf{q}}_d - \mathbf{G}_1 \dot{\mathbf{e}} - \mathbf{G}_0 \mathbf{e}. \quad (6.6.7)$$

The control \mathbf{v} is said to contain the *feedforward control* $\ddot{\mathbf{q}}_d$, the *position feedback* $-\mathbf{G}_0 \mathbf{e}$ and the *derivative feedback* $-\mathbf{G}_1 \dot{\mathbf{e}}$. When the feedback is substituted into the governing equation, a new set of equations is obtained for the tracking error,

$$\ddot{\mathbf{e}} + \mathbf{G}_1 \dot{\mathbf{e}} + \mathbf{G}_0 \mathbf{e} = \mathbf{0}. \quad (6.6.8)$$

Define the Lyapunov function

$$\mathcal{V}\left(\begin{Bmatrix} \mathbf{e} \\ \dot{\mathbf{e}} \end{Bmatrix}\right) := \frac{1}{2} \dot{\mathbf{e}}^T \dot{\mathbf{e}} + \frac{1}{2} \mathbf{e}^T \mathbf{G}_0 \mathbf{e}$$

for the closed loop error in Equations (6.6.8). The function $\mathcal{V}\left(\begin{Bmatrix} \mathbf{e} \\ \dot{\mathbf{e}} \end{Bmatrix}\right)$ is positive everywhere except at the origin, where it is equal to zero. If the derivative of the

Lyapunov function is computed along the trajectories of the closed loop system, it is found that

$$\dot{\mathcal{V}}\left(\begin{Bmatrix} \mathbf{e}(t) \\ \dot{\mathbf{e}}(t) \end{Bmatrix}\right) = \dot{\mathbf{e}}^T (\ddot{\mathbf{e}} + \mathbf{G}_0 \mathbf{e}) = -\dot{\mathbf{e}}^T \mathbf{G}_1 \dot{\mathbf{e}} \leq 0$$

Thus, $\dot{\mathcal{V}}$ is negative semidefinite on any neighborhood of the origin. Therefore, the origin is stable. To show that the origin is asymptotically stable, LaSalle's Principle can be used. It states that the trajectories of the system are attracted to the largest invariant subset \mathcal{S} of the set

$$\mathcal{S} \subseteq \mathcal{M} := \left\{ \begin{Bmatrix} \mathbf{e} \\ \dot{\mathbf{e}} \end{Bmatrix} : \dot{\mathcal{V}}\left(\begin{Bmatrix} \mathbf{e} \\ \dot{\mathbf{e}} \end{Bmatrix}\right) = 0 \right\}.$$

But $\dot{\mathcal{V}}$ is identically equal to zero if and only if $\dot{\mathbf{e}}$ is identically equal to zero since \mathbf{G}_1 is positive definite. That is,

$$\dot{\mathcal{V}} = -\dot{\mathbf{e}}^T \mathbf{G}_1 \dot{\mathbf{e}} \equiv 0 \quad \leftrightarrow \quad \dot{\mathbf{e}} \equiv 0.$$

It can be concluded from the equation of motion that the only states in the set \mathcal{S} are those (that have a trajectory) $\begin{Bmatrix} \mathbf{e}(t) & \dot{\mathbf{e}}(t) \end{Bmatrix}^T$ for which

$$\mathbf{G}_0 \mathbf{e}(t) = \underbrace{(-\ddot{\mathbf{e}}(t) + \mathbf{G}_1 \dot{\mathbf{e}}(t))}_0$$

for all $t \in \mathbb{R}^+$. Since \mathbf{G}_0 is symmetric positive definite, the tracking error is identically equal to zero, so that

$$\mathbf{e}(t) \equiv 0$$

for all $t \in \mathbb{R}^+$. In other words, this shows that $\dot{\mathcal{V}}(t) = 0$ if and only if $\dot{\mathbf{e}}(t) = \mathbf{e}(t) = \mathbf{0}$. It follows that the only invariant subset of \mathcal{M} is $\mathcal{S} = \{\mathbf{0}\}$. Hence, the origin of the closed loop error equations is a globally, asymptotically stable equilibrium. \square

If the physical system is instrumented so that \mathbf{q} and $\dot{\mathbf{q}}$ can be measured, it is possible to calculate the actuator forces and moments in $\boldsymbol{\tau}$ via Equation (6.6.3) in the implementation of the closed loop feedback control law. It is for this reason that this feedback equation is called the computed torque control law. The choice of control in Equation (6.6.3) is also said to be derived from *dynamic inversion* since the control input $\boldsymbol{\tau}$ can be interpreted as the solution of a classical inverse dynamics problem. This description will be explained.

The forward dynamics problem associated with the governing equations in Equation (6.6.1) is the same problem studied in Chapters (4) and (5). In this problem the actuation forces $\boldsymbol{\tau}$ are given, and Equation (6.6.1) is solved for the second derivatives of the generalized coordinates $\ddot{\mathbf{q}}$. In other words, the problem of forward dynamics uses Equation (6.6.1) to define a mapping from inputs to outputs

$$\boldsymbol{\tau} \rightarrow \ddot{\mathbf{q}}.$$

If the control in Equation (6.6.3) is chosen, $\ddot{\mathbf{q}} = \mathbf{v}$ is obtained. When the result is substituted into Equation (6.6.1),

$$\mathbf{M}(\mathbf{q}(t))\mathbf{v}(t) = \mathbf{n}(\mathbf{q}(t), \dot{\mathbf{q}}(t)) + \boldsymbol{\tau}(t). \quad (6.6.9)$$

Now Equation (6.6.9) is solved for the actuation torques from the vector \mathbf{v} . The inverse mapping is defined consequently as

$$\mathbf{v} \rightarrow \boldsymbol{\tau}.$$

The computed torque control is also known as the control determined by dynamic inversion.

This methodology admits an implementation of the control strategy in terms of a well-known architecture. The architecture combines a nonlinear compensator and outer loop controller in a natural way. The structure of the overall system is depicted in Figure (6.7). In this figure the governing equations of the robot are embodied in

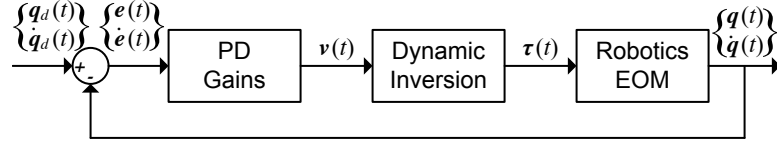


Fig. 6.7: Architecture of Computed Torque Control

the block labeled “Robotics EOM”. The input to this block is the actuation inputs $\boldsymbol{\tau}$ and the outputs of the block are the generalized coordinates \mathbf{q} and their derivatives $\dot{\mathbf{q}}$. The nonlinear compensator in the block labeled “dynamic inversion” calculates actuator inputs given the input \mathbf{v} using Equation (6.6.9). This nonlinear transformation is achieved via the solution of the inverse dynamics problem. Finally, the outer loop controller takes as feedback the desired trajectories \mathbf{q}_d and their derivatives $\dot{\mathbf{q}}_d$ and the generalized coordinates \mathbf{q} and their derivatives $\dot{\mathbf{q}}$, and from these calculates the control input \mathbf{v} . In Theorem (6.4) the outer loop controller calculates \mathbf{v} from Equation 6.6.5. This calculation is carried out in terms of a linear gain matrix acting on the tracking and tracking rate error, $\mathbf{v} = \ddot{\mathbf{q}}_d - [\mathbf{G}_0 \ \mathbf{G}_1] \begin{Bmatrix} \mathbf{e} \\ \dot{\mathbf{e}} \end{Bmatrix}$. In general, this matrix multiplication can be replaced by a suitable transfer function to implement more general classes of outer loop control.

Example 6.6.1. Consider the spherical robotic manipulator shown in Figures (6.8) and (6.9). Derive a controller for this robot that uses the exact computed torque in Theorem (6.3) with proportional-derivative feedback in the outer loop to achieve setpoint control. Select the system parameters to be $m_1 = m_2 = m_3 = 10 \text{ kg}$, $d_{p,q} = 0.1$

m and $y_{q,c_2} = 0.05$ m. Choose the gain matrices \mathbf{G}_0 and \mathbf{G}_1 in Theorem (6.3) to have the form $\mathbf{G}_0 = g_0\mathbb{I}$ and $\mathbf{G}_1 = g_1\mathbb{I}$, where the gains are selected to be $(g_0, g_1) = (1, 1), (5, 5), (10, 10)$ or $(100, 100)$, and suppose the desired state is

$$\mathbf{x}_d = \begin{Bmatrix} \mathbf{q}_d \\ \dot{\mathbf{q}}_d \end{Bmatrix} = \left\{ \begin{Bmatrix} 1 & 1 & 1 \end{Bmatrix} \begin{Bmatrix} 0 & 0 & 0 \end{Bmatrix} \right\}^T.$$

The initial and final configurations of the robotic manipulator in this example are shown in Figures (6.10) (a) and (b). Evaluate the performance of this controller by plotting the state trajectories, set point error, and control inputs as a function of time.

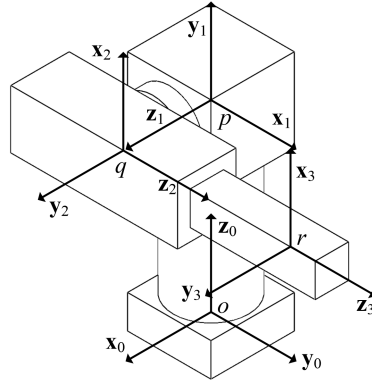


Fig. 6.8: Spherical Robot Frames

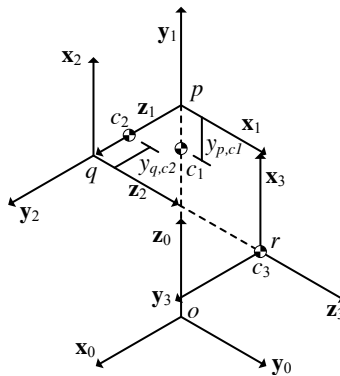


Fig. 6.9: Spherical Robot Center of Mass Offsets

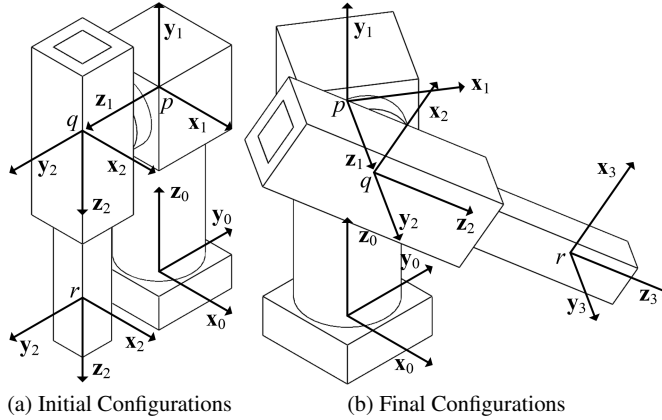


Fig. 6.10: Initial and Final Configurations

Solution: The computed torque control law in Theorem (6.3) has the form in Equation (6.6.3) $\tau = \mathbf{M}\mathbf{v} - \mathbf{n}$, where

$$\mathbf{M} = \begin{bmatrix} m_3(d_{p,q}^2 + \sin^2 \theta_2 d_{q,r}^2) + m_2(d_{p,q} - y_{q,c_2})^2 & m_3 \cos \theta_2 d_{p,q} d_{q,r} & m_3 \sin \theta_2 d_{p,q} \\ m_3 \cos \theta_2 d_{p,q} d_{q,r} & m_3 d_{q,r}^2 & 0 \\ m_3 \sin \theta_2 d_{p,q} & 0 & m_3 \end{bmatrix},$$

$$\mathbf{n} = \left\{ \begin{array}{l} -m_3(d_{q,r}(2 \sin \theta_2 \dot{\theta}_1 \dot{d}_{q,r} - d_{p,q} \dot{\theta}_2^2) \sin \theta_2 + 2d_{p,q} \dot{\theta}_2 \dot{d}_{q,r} \cos \theta_2 + \dot{\theta}_1 \dot{\theta}_2 d_{q,r}^2 \sin 2\theta_2) \\ \frac{1}{2} m_3 d_{q,r} (-4\dot{\theta}_2 \dot{d}_{q,r} + \dot{\theta}_1^2 d_{q,r} \sin 2\theta_2 - 2g \sin \theta_2) \\ m_3(d_{q,r}(\dot{\theta}_2^2 + \dot{\theta}_1^2 \sin^2 \theta_2) + g \cos \theta_2) \end{array} \right\},$$

and the outer loop control signal \mathbf{v} is given by

$$\begin{aligned} \mathbf{v} &= \ddot{\mathbf{q}}_d - \mathbf{G}_1(\dot{\mathbf{q}} - \dot{\mathbf{q}}_d) - \mathbf{G}_0(\mathbf{q} - \mathbf{q}_d), \\ &= \begin{Bmatrix} \ddot{\theta}_{1,d} \\ \ddot{\theta}_{2,d} \\ \ddot{d}_{q,r,d} \end{Bmatrix} - \mathbf{G}_1 \begin{Bmatrix} \dot{\theta}_1 - \dot{\theta}_{1,d} \\ \dot{\theta}_2 - \dot{\theta}_{2,d} \\ \dot{d}_{q,r} - \dot{d}_{q,r,d} \end{Bmatrix} - \mathbf{G}_0 \begin{Bmatrix} \theta_1 - \theta_{1,d} \\ \theta_2 - \theta_{2,d} \\ d_{q,r} - q_{q,r,d} \end{Bmatrix}. \end{aligned}$$

When this feedback law is substituted into the equations of motion, the closed loop system is governed by the equations

$$(\ddot{\theta}_1 - \ddot{\theta}_{1,d}) + g_1(\dot{\theta}_1 - \dot{\theta}_{1,d}) + g_0(\theta_1 - \theta_{1,d}) = 0, \quad (6.6.10)$$

$$(\ddot{\theta}_2 - \ddot{\theta}_{2,d}) + g_1(\dot{\theta}_2 - \dot{\theta}_{2,d}) + g_0(\theta_2 - \theta_{2,d}) = 0, \quad (6.6.11)$$

$$(\ddot{d}_{q,r} - \ddot{d}_{q,r,d}) + g_1(\dot{d}_{q,r} - \dot{d}_{q,r,d}) + g_0(d_{q,r} - d_{q,r,d}) = 0. \quad (6.6.12)$$

This last set of equations has been obtained using the fact that $\mathbf{G}_1 = g_1 \mathbb{I}$ and $\mathbf{G}_2 = g_0 \mathbb{I}$. Each of these ordinary differential equations have the exact same form since the gain matrices are chosen to be diagonal matrices with the same value on the diagonal. The

Equations (6.6.10), (6.6.11), and (6.6.12) can be written as

$$\ddot{\mathbf{e}} + g_1 \dot{\mathbf{e}} + g_0 \mathbf{e} = \mathbf{0},$$

where $\mathbf{e} = \{e_1 \ e_2 \ e_3\}^T$ and e_k is the error in degree of freedom k for $k = 1, 2, 3$. The solutions of the error equation have identical structure and differ only in their initial conditions. Figures (6.11) (a), (b) and (c) depict the trajectories of $\theta_1(t)$, $\theta_2(t)$ and $d_{q,r}(t)$ when the initial condition has been selected as

$$\mathbf{x}(0)^T := \{\mathbf{q}(0)^T \ \dot{\mathbf{q}}(0)^T\} = \{\{0 \ 0 \ 1\} \ \{0 \ 0 \ 0\}\},$$

and the target is given by

$$\mathbf{x}_d^T := \{\mathbf{q}_d^T \ \dot{\mathbf{q}}_d^T\} = \{\{1 \ 1 \ 1\} \ \{0 \ 0 \ 0\}\}.$$

Since the initial conditions for $(\theta_1, \dot{\theta}_1)$ and $(\theta_2, \dot{\theta}_2)$ are equal in this simulation, the solutions for $\theta_1(t)$ and $\theta_2(t)$ are identical functions of time, as shown in Figures (6.11) (a) and (b). The trajectories do approach the desired target values, as guaranteed in Theorem (6.3); however, some choices of the feedback gains g_0 and g_1 result in rather slow convergence. The convergence of the end effector to the desired terminal location when $g_0 = g_1 = 1$ requires roughly 50 seconds. Since the initial condition $(d_{q,r}(0), \dot{d}_{q,r}(0))$ matches the desired values $(d_{q,r,d}, \dot{d}_{q,r,d})$, the trajectory for $d_{q,r}(t)$ is the constant trajectory as depicted in Figure (6.11)(c). This response is expected because the solution of Equation (6.6.10) for the tracking error, when the initial condition of the tracking error and its derivative are equal to zero, is just the function $d_{q,r}(t) - d_{q,r,d} = 0$. Whenever the performance of a setpoint controller is studied, the convergence of the states and the actuation forces required to achieve convergence must also be analyzed. It would serve no purpose to design a controller that requires an actuation authority that exceeds the capabilities of the available actuators. Figure (6.12) (a) depicts the actuation torque that is required to drive revolute joint 1 in this simulation over the time period $t \in [0, 0.5]$ seconds, and Figure (6.12) (b) depicts the actuation torque for joint 2 over the same period. These two plots illustrate a common feature of feedback linearization techniques: the exactly canceling feedback often induces large transient actuation forces and torques. The figures show that these transient, or startup, input actuation histories can be quite large when the gains are large.

The steady state behavior of the actuation torques acting at the 1 and 2 joints is depicted in Figures (6.11) (d) and (e). Note that the steady state responses are at least an order of magnitude less than the peak transient, for large values of the gain. It should also be noted that actuation torque 1, since it does not need to counter the force of gravity, approaches zero as time increases. The torque m_2 must counteract the torque generated by gravity and approaches a finite static value as time increases. The actuation force for the prismatic joint is shown in Figure (6.11) (f). Again, this force approaches a nonzero value since it must counter the force due to gravity on link 3. A key observation from these results that is true across many

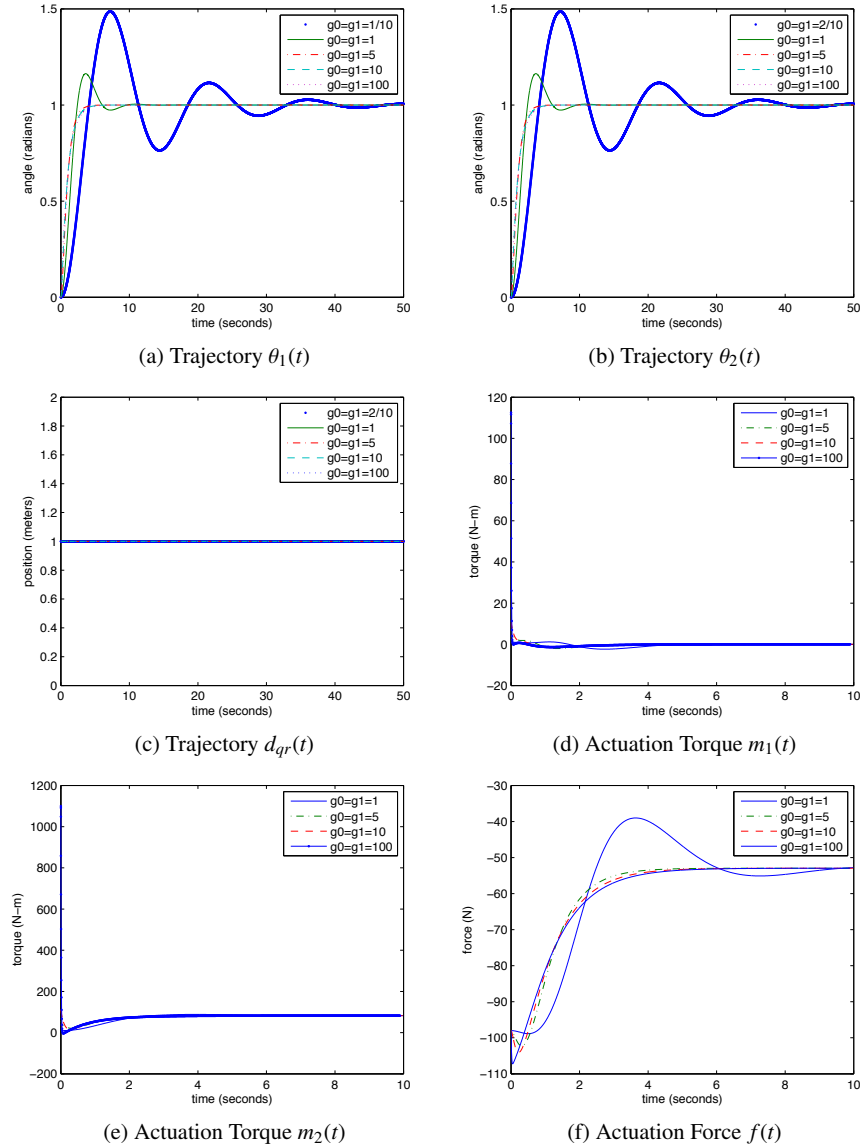


Fig. 6.11: Time Histories of Generalized Coordinates and Actuation Inputs

control problems is that “high gain” controllers that achieve improved convergence induce larger actuation inputs. Finding the optimal balance between performance in error, required actuation authority, actuation bandwidth, and system stability makes control synthesis a challenging task.

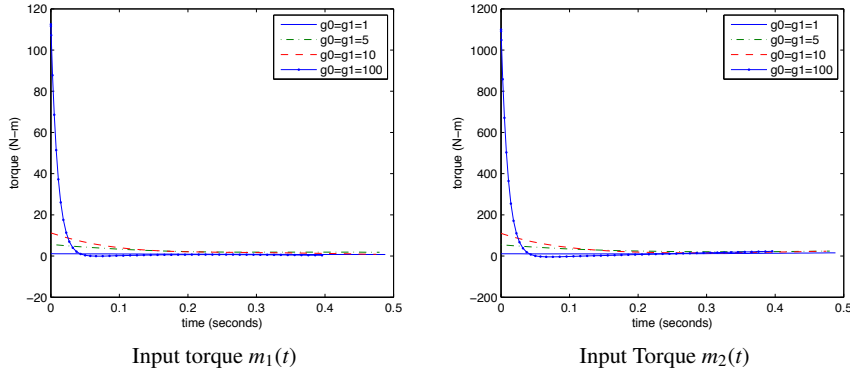


Fig. 6.12: Input Torque Transients

Example 6.6.2. Consider the spherical robotic manipulator studied in Example (6.6.1). Derive a controller that uses the exact computed torque in Theorem (6.3) with proportional-derivative feedback in the outer loop to achieve tracking control. Select the system parameters to be $m_1 = m_2 = m_3 = 10\text{kg}$, $d_{p,q} = 0.1\text{m}$ and $y_{q,c_2} = 0.05\text{m}$, identical to those in Example (6.6.1). Choose the gain matrices \mathbf{G}_0 and \mathbf{G}_1 in Theorem (6.3) again to have the form $\mathbf{G}_0 = g_0 \mathbb{I}$ and $\mathbf{G}_1 = g_1 \mathbb{I}$, where the gains are selected to be $(g_0, g_1) = (1, 1), (5, 5), (10, 10)$ or $(100, 100)$. Suppose that the desired trajectory is now

$$\mathbf{q}_d(t) = \begin{Bmatrix} A_1 \sin(\Omega_1 t) \\ A_2 \sin(\Omega_2 t) \\ A_3 \sin(\Omega_3 t) + 1 \end{Bmatrix}$$

where $(A_1, A_2, A_3) = (-\frac{1}{16}, -1, -\frac{1}{4})$ and $(\Omega_1, \Omega_2, \Omega_3) = (4, 1, 2)$. Evaluate the performance of this controller by plotting the state trajectories, tracking errors and control inputs as a function of time for the closed loop system.

Solution: This example has been included to emphasize the fact that the setpoint control law is essentially identical to the exactly canceling computed torque tracking controller. Just as in Example (6.6.1), the closed loop equations that govern the error in tracking are

$$\begin{aligned} (\ddot{\theta}_1 - \ddot{\theta}_{1,d}) + g_1(\dot{\theta}_1 - \dot{\theta}_{1,d}) + g_0(\theta_1 - \theta_{1,d}) &= 0, \\ (\ddot{\theta}_2 - \ddot{\theta}_{2,d}) + g_1(\dot{\theta}_2 - \dot{\theta}_{2,d}) + g_0(\theta_2 - \theta_{2,d}) &= 0, \\ (\ddot{d}_{q,r} - \ddot{d}_{q,r,d}) + g_1(\dot{d}_{q,r} - \dot{d}_{q,r,d}) + g_0(d_{q,r} - d_{q,r,d}) &= 0, \end{aligned}$$

which may be consolidated into

$$\ddot{\mathbf{e}} + g_1 \dot{\mathbf{e}} + g_0 \mathbf{e} = \mathbf{0}.$$

The tracking error in each degree of freedom satisfies the same linear ordinary differential equation, subject to perhaps different initial conditions in the tracking error and its derivative. Figure (6.13) (a), (b) and (c) depict the state trajectories for θ_1, θ_2 and $d_{q,r}$, respectively, for the different choices of the gains g_0 and g_1 .

All approach their desired trajectories at an exponential rate as $t \rightarrow \infty$, as predicted in theory. The actuation inputs m_1, m_2 and f are depicted in Figures (6.13) (d), (e) and (f), respectively. The required actuation moments and torques vary periodically with the frequency of the desired trajectories. As in Example (6.6.1), the exactly canceling control laws result in transient peaks that far exceed the steady state input values. Figures (6.14)(a) and (b) show that the highest gain, which corresponds to the best tracking performance, yields peak actuation torques that occur over a very brief period. The oscillatory steady state trajectories of the torque and force inputs in Figure (6.13)(d),(e) and (f) have magnitudes that are only a small fraction of the startup transient values.

6.7 Approximate Dynamic Inversion and Uncertainty

Section (6.6) presented the fundamentals of *dynamic inversion* or *computed torque control*. This approach to the control of robotic systems is one of the most popular starting points for control design. The methodology is applicable to a reasonably large collection of systems, and can also be used to motivate and understand alternative control schemes. Still, one notable drawback of this approach is that the exact cancellation of unwanted terms requires knowledge of the explicit form of the nonlinearities that appear in the governing equations. Since these nonlinear terms depend parametrically on the link mass, moments of inertia, and products of inertia, the approach also requires exact knowledge of these constants. In practice, the exact values for these constants are not known and the introduction of a *computed control torque* never achieves the desired exact cancellation. Just as importantly, some applied forces to which the robotic system is subject are very difficult to determine in principle or in practice. Friction, dissipative forces and moments, and nonlinear effects like backlash and hysteresis fall in this category.

The lack of knowledge of the exact form of the nonlinearities is one reason that the analysis described in Section (6.6) for the *computed control torques* is at best an idealization. There is always some mismatch in practice among the terms to be canceled using a computed torque control law. This section will extend the analysis and allow for the possibility that the actuation vector in Equation (6.6.3) is only approximately equal to the *computed torque control*. Suppose now that the control

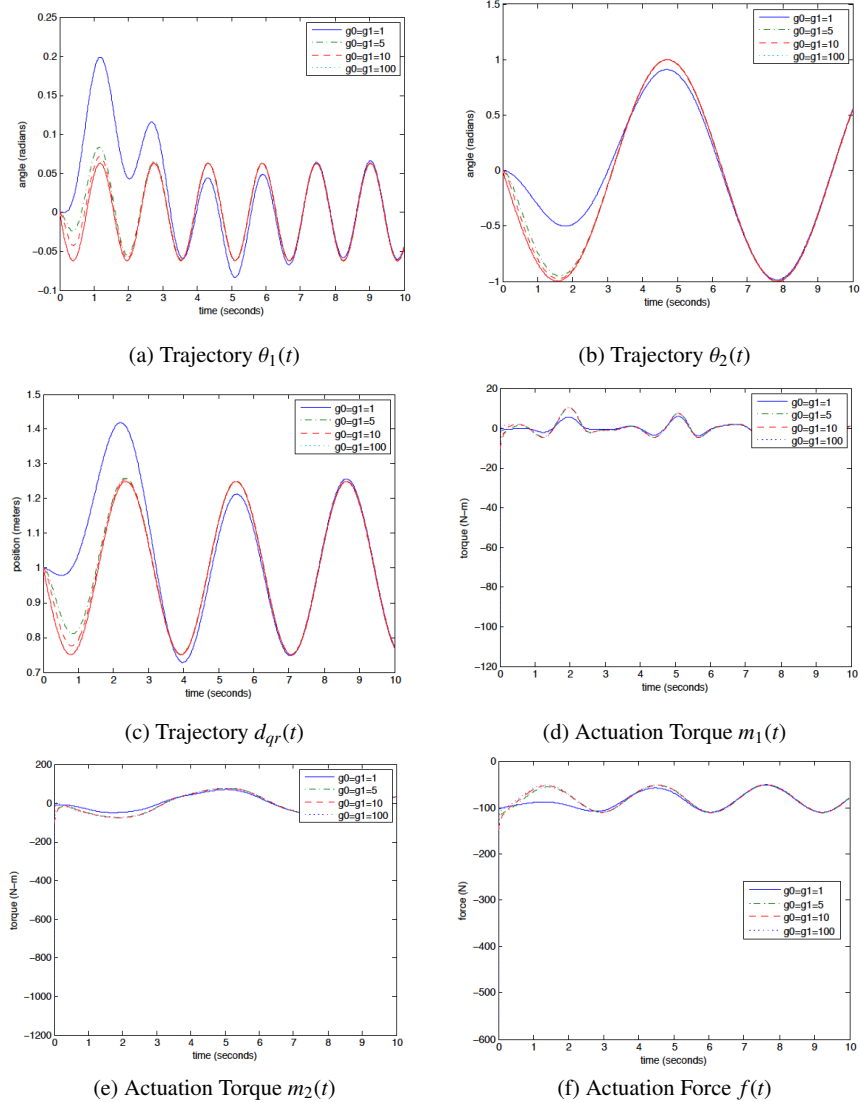


Fig. 6.13: Time Histories of Generalized Coordinates and Actuation Inputs

input is given by

$$\boldsymbol{\tau} = \mathbf{M}_a \mathbf{v} - \mathbf{n}_a, \quad (6.7.1)$$

where \mathbf{M}_a and \mathbf{n}_a are approximations to the generalized mass or inertia matrix \mathbf{M} and nonlinear term \mathbf{n} , respectively, in Equation (6.6.3). The form of the governing

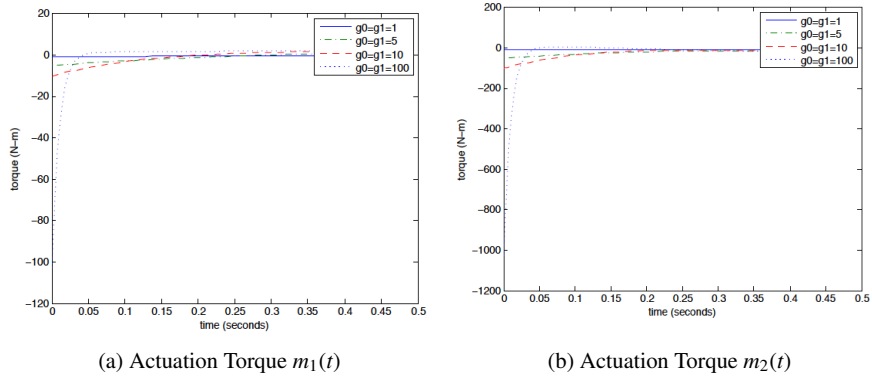


Fig. 6.14: Actuation Input Transient Response

equations will also be generalized; suppose that the equations of motion for the robot are

$$\mathbf{M}\ddot{\mathbf{q}} = \mathbf{n} + \boldsymbol{\tau}_d + \boldsymbol{\tau} \quad (6.7.2)$$

and that τ_d denotes an unknown disturbance torque. The governing equations can be rewritten using the controller (6.7.1) derived from *approximate dynamic inversion* as

$$\mathbf{M}\ddot{\mathbf{q}} = \mathbf{M}_a \mathbf{v} + \mathbf{n} - \mathbf{n}_a + \boldsymbol{\tau}_d. \quad (6.7.3)$$

Equation (6.7.3) can be written in the compact form $\bar{\mathbf{q}} = \mathbf{v} + \mathbf{d}$, where \mathbf{d} is a measure of the mismatch in exact cancellation

$$\mathbf{d} = \mathbf{M}^{-1} \mathcal{A} \mathbf{M} \mathbf{v} - \mathbf{M}^{-1} \mathcal{A} \mathbf{n} + \mathbf{M}^{-1} \boldsymbol{\tau}_d,$$

and $\Delta\mathbf{M}$ and $\Delta\mathbf{n}$ measure the approximation error for the generalized inertia matrix and nonlinear vector $\Delta\mathbf{M} = \mathbf{M}_a - \mathbf{M}$ and $\Delta\mathbf{n} = \mathbf{n}_a - \mathbf{n}$. Equations (6.7.3) reduce to the form achieved via exact cancellation in Equation (6.6.4) when $\mathbf{M}_a = \mathbf{M}$, $\mathbf{n}_a = \mathbf{n}$ and $\tau_d = 0$, as expected.

Many controllers can be derived using the framework described above. One frequently used controller cancels the gravity terms only, approximates the generalized inertia matrix as the identity, and uses *proportional-derivative (PD) control* for the outer loop. This controller is able to drive the robot so that it approaches a desired final constant pose as $t \rightarrow \infty$. This is another simple example of *setpoint control*.

Theorem 6.4. Let the equations of motion for a robotic system have the form in Equation (6.7.2) where the disturbance torque $\tau_d = \mathbf{0}$. Suppose that the control input τ is selected using the approximate dynamic inversion law in Equation (6.7.1) where it is assumed

$$\mathbf{M}_a = \mathbb{I}, \quad \mathbf{n}_a = -\frac{\partial V}{\partial \mathbf{q}}, \quad \mathbf{v} = -\mathbf{G}_1 \dot{\mathbf{q}} - \mathbf{G}_0(\mathbf{q} - \mathbf{q}_d),$$

with \mathbf{q}_d an N -vector of constant desired generalized coordinates and $\mathbf{G}_1, \mathbf{G}_0$ constant symmetric positive definite gain matrices. The origin is an asymptotically stable equilibrium for the generalized coordinate tracking error $\{\mathbf{e}^T, \dot{\mathbf{q}}^T\}^T$ where $\mathbf{e}(t) := \mathbf{q}(t) - \mathbf{q}_d$.

Proof. Define the Lyapunov function to be

$$\mathcal{V} = \frac{1}{2} \dot{\mathbf{q}}^T \mathbf{M} \dot{\mathbf{q}} + \frac{1}{2} \mathbf{e}^T \mathbf{G}_0 \mathbf{e}$$

It can be seen that $\mathcal{V}(\mathbf{0}) = 0$ and \mathcal{V} is positive definite on any neighborhood of the origin. The derivative of \mathcal{V} along the trajectories of the system is

$$\dot{\mathcal{V}} = \dot{\mathbf{q}}^T \{\mathbf{M} \ddot{\mathbf{q}} + \mathbf{G}_0 \mathbf{e}\} + \frac{1}{2} \dot{\mathbf{q}}^T \dot{\mathbf{M}} \dot{\mathbf{q}}, \quad (6.7.4)$$

and closed loop equations of motion are

$$\mathbf{M} \ddot{\mathbf{q}} = -\underbrace{\mathbf{C} \dot{\mathbf{q}} - \frac{\partial V}{\partial \mathbf{q}}}_{\mathbf{n}} - \mathbf{G}_1 \dot{\mathbf{q}} - \mathbf{G}_0(\mathbf{q} - \mathbf{q}_d) + \underbrace{\frac{\partial V}{\partial \mathbf{q}}}_{-\mathbf{n}_a}.$$

This equation can be rearranged and written as the identity

$$\mathbf{M} \ddot{\mathbf{q}} + \mathbf{G}_0 \mathbf{e} = -\mathbf{C} \dot{\mathbf{q}} - \mathbf{G}_1 \dot{\mathbf{q}}.$$

Substituting this equation into Equation (6.7.4) results in

$$\dot{\mathcal{V}} = -\dot{\mathbf{q}}^T \mathbf{C} \dot{\mathbf{q}} - \dot{\mathbf{q}}^T \mathbf{G}_1 \dot{\mathbf{q}} + \frac{1}{2} \dot{\mathbf{q}}^T \dot{\mathbf{M}} \dot{\mathbf{q}} = \frac{1}{2} \dot{\mathbf{q}}^T (\dot{\mathbf{M}} - 2\mathbf{C}) \dot{\mathbf{q}} - \dot{\mathbf{q}}^T \mathbf{G}_1 \dot{\mathbf{q}}.$$

It has been shown in Chapter (4) that the matrix $\dot{\mathbf{M}} - 2\mathbf{C}$ is skew-symmetric; therefore, $\dot{\mathcal{V}} = -\dot{\mathbf{q}}^T \mathbf{G}_1 \dot{\mathbf{q}}$. The derivative of the Lyapunov function is negative semidefinite

$$\dot{\mathcal{V}} \left(\begin{Bmatrix} \mathbf{e}(t) \\ \dot{\mathbf{q}}(t) \end{Bmatrix} \right) \leq 0,$$

for all $\{\mathbf{e}^T \dot{\mathbf{q}}^T\}^T$. Lyapunov's Direct Method thus ensures that the equilibrium at the origin $\{\mathbf{0} \mathbf{0}\}^T$ is stable. LaSalle's Principle stipulates that trajectories will be attracted to the largest *positive invariant set* S contained in \mathcal{M} where

$$\mathcal{M} = \left\{ \begin{Bmatrix} \mathbf{e}(t) \\ \dot{\mathbf{q}}(t) \end{Bmatrix} : \dot{\mathcal{V}}\left(\begin{Bmatrix} \mathbf{e}(t) \\ \dot{\mathbf{q}}(t) \end{Bmatrix}\right) = 0, t \in \mathbb{R}^+ \right\}.$$

Since \mathbf{G}_1 is *symmetric positive definite*, it is known that

$$\dot{\mathcal{V}}\left(\begin{Bmatrix} \mathbf{e}(t) \\ \dot{\mathbf{q}}(t) \end{Bmatrix}\right) = -\dot{\mathbf{q}}^T(t)\mathbf{G}_1\dot{\mathbf{q}}(t) = 0 \iff \dot{\mathbf{q}}(t) = \mathbf{0},$$

for each $t \in \mathbb{R}^+$. The equations of motion reduce to

$$\underbrace{\mathbf{M}\ddot{\mathbf{q}} + (\mathbf{C} + \mathbf{G}_1)\dot{\mathbf{q}}}_{0} = -\mathbf{G}_0\mathbf{e}$$

when $\dot{\mathbf{q}}(t) \equiv 0$. Since \mathbf{G}_0 is *symmetric positive definite*, it is invertible. These equations of motion therefore show that

$$\dot{\mathcal{V}}\left(\begin{Bmatrix} \mathbf{e}(t) \\ \dot{\mathbf{q}}(t) \end{Bmatrix}\right) = 0 \iff \begin{Bmatrix} \mathbf{e}(t) \\ \dot{\mathbf{q}}(t) \end{Bmatrix} = \mathbf{0}.$$

It follows that the only invariant set in \mathcal{M} is $\{\mathbf{0}^T \mathbf{0}^T\}^T$. Therefore, the trajectories $\{\mathbf{e}^T(t) \dot{\mathbf{q}}^T(t)\}^T$ are attracted to the origin, and the theorem is proved. \square

Theorem (6.3) shows that the method of *approximate dynamic inversion* can be used to achieve setpoint control when only the nonlinear term due to $\frac{\partial V}{\partial q}$ is canceled and a PD controller is employed in the outer loop. Many other controllers based on *approximate dynamic inversion* appear in the literature. The next example provides one technique for achieving a stabilizing controller in the presence of disturbances and uncertainty using a discontinuous control law. This control law is written in a simple form, one that emphasizes that an asymptotically stable response is achieved if the unknown uncertainty $\mathbf{d}(t)$ is small enough. Practical versions of the theorem, that establish *a priori* bounds on the uncertainty \mathbf{d} , can be found in the literature. See for example [15].

Theorem 6.5. Let the equations of motion of a robotic system have the form in Equation (6.7.2), suppose $\mathbf{q}_d(t)$ is an N -vector of desired trajectories, define the tracking error to be $\mathbf{e}(t) := \mathbf{q}(t) - \mathbf{q}_d(t)$, and define $\mathbf{x}(t) = \begin{Bmatrix} \mathbf{e}(t) \\ \dot{\mathbf{e}}(t) \end{Bmatrix}$. Suppose that the following three conditions hold:

- (1) The $N \times N$ matrix \mathbf{P} is a symmetric positive definite solution of the Lyapunov equation

$$\mathbf{A}^T \mathbf{P} + \mathbf{P} \mathbf{A} = -\mathbf{Q}, \quad (6.7.5)$$

where

$$\mathbf{A} = \begin{bmatrix} 0 & \mathbb{I} \\ -\mathbf{G}_0 & -\mathbf{G}_1 \end{bmatrix} \in \mathbb{R}^{2N \times 2N},$$

\mathbf{Q} is an $N \times N$ symmetric positive definite matrix, and $\mathbf{G}_1, \mathbf{G}_0$ are symmetric positive definite gain matrices.

- (2) The control input $\mathbf{u}(t)$ is defined to be

$$\mathbf{u}(t) = \begin{cases} -k \frac{\mathbf{B}^T \mathbf{P} \mathbf{x}}{\|\mathbf{B}^T \mathbf{P} \mathbf{x}\|} & \text{if } \mathbf{B}^T \mathbf{P} \mathbf{x} \neq 0, \\ 0 & \text{if } \mathbf{B}^T \mathbf{P} \mathbf{x} = 0, \end{cases} \quad (6.7.6)$$

where k is a positive constant and $\mathbf{B} = [\mathbf{0}^T, \mathbb{I}^T]^T \in \mathbb{R}^{2N \times N}$.

- (3) The input $\boldsymbol{\tau}$ in Equation (6.7.2) is selected to be the approximate dynamic inversion control in Equation (6.7.1) where

$$\boldsymbol{\tau} = \mathbf{M}_a(\ddot{\mathbf{q}}_d - \mathbf{G}_1(\dot{\mathbf{q}} - \dot{\mathbf{q}}_d) - \mathbf{G}_0(\mathbf{q} - \mathbf{q}_d) + \mathbf{u}) - \mathbf{n}_a. \quad (6.7.7)$$

If the uncertainty \mathbf{d} satisfies $\|\mathbf{d}\| < k$ for all $t \in \mathbb{R}^+$, then the equilibrium at the origin of the tracking error dynamics $\begin{Bmatrix} \mathbf{e} \\ \dot{\mathbf{e}} \end{Bmatrix}$ is asymptotically stable

Proof. Strictly speaking, the introduction of a discontinuous control input as in Equation (6.7.6) requires the introduction of *chattering solutions* or *measure valued solutions* of the governing equations. An interested reader can consult [13] for the details. It turns out that the analysis via Lyapunov's Direct Method can be extended to this case. Substitution of Equation (6.7.7) into Equation (6.7.2) results in the closed loop equations of motion

$$\ddot{\mathbf{q}} = \ddot{\mathbf{q}}_d - \mathbf{G}_1(\dot{\mathbf{q}} - \dot{\mathbf{q}}_d) - \mathbf{G}_0(\mathbf{q} - \mathbf{q}_d) + \mathbf{u} + \mathbf{d},$$

with

$$\mathbf{d} = \mathbf{M}^{-1} \Delta \mathbf{M} \mathbf{v} - \mathbf{M}^{-1} \Delta \mathbf{n} + \mathbf{M}^{-1} \boldsymbol{\tau}_d.$$

These equations can be written in state space form by introducing the states

$$\mathbf{x} = \begin{Bmatrix} \mathbf{q} - \mathbf{q}_d \\ \dot{\mathbf{q}} - \dot{\mathbf{q}}_d \end{Bmatrix} = \begin{Bmatrix} \mathbf{e} \\ \dot{\mathbf{e}} \end{Bmatrix} \Rightarrow \dot{\mathbf{x}} = \underbrace{\begin{bmatrix} 0 & I \\ -\mathbf{G}_0 & -\mathbf{G}_1 \end{bmatrix}}_{\mathbf{A}} \mathbf{x} + \underbrace{\begin{bmatrix} 0 \\ \mathbb{I} \end{bmatrix}}_{\mathbf{B}} (\mathbf{u} + \mathbf{d}).$$

Define the Lyapunov function $\mathcal{V} = \frac{1}{2}\mathbf{x}^T \mathbf{P} \mathbf{x}$ for the \mathbf{P} defined in Equation (6.7.5). When the Lyapunov function is differentiated along the system trajectories,

$$\begin{aligned} \dot{\mathcal{V}} &= \frac{1}{2} (\mathbf{x}^T \mathbf{P} \dot{\mathbf{x}} + \dot{\mathbf{x}}^T \mathbf{P} \mathbf{x}), \\ &= \frac{1}{2} \left\{ \mathbf{x}^T \mathbf{P} (\mathbf{A} \mathbf{x} + \mathbf{B}(\mathbf{u} + \mathbf{d})) + (\mathbf{A} \mathbf{x} + \mathbf{B}(\mathbf{u} + \mathbf{d}))^T \mathbf{P} \mathbf{x} \right\}, \\ &= \mathbf{x}^T \underbrace{(\mathbf{P} \mathbf{A} + \mathbf{A}^T \mathbf{P})}_{-\mathbf{Q}} \mathbf{x} + \mathbf{x}^T \mathbf{P} \mathbf{B}(\mathbf{u} + \mathbf{d}). \end{aligned}$$

The derivative of the Lyapunov function equals $\dot{\mathcal{V}} = -\mathbf{x}^T \mathbf{Q} \mathbf{x}$ when $\mathbf{B}^T \mathbf{P} \mathbf{x}(t) = 0$. If $\mathbf{B}^T \mathbf{P} \mathbf{x}(t) \neq 0$, the derivative becomes

$$\dot{\mathcal{V}} = -\mathbf{x}^T \mathbf{Q} \mathbf{x} + \mathbf{x}^T \mathbf{P} \mathbf{B} \mathbf{d} - k \|\mathbf{B}^T \mathbf{P} \mathbf{x}\|$$

The last two terms on the right in this case can be bounded such that

$$\mathbf{x}^T \mathbf{P} \mathbf{B} \mathbf{d} - k \|\mathbf{B}^T \mathbf{P} \mathbf{x}\| \leq \|\mathbf{B}^T \mathbf{P} \mathbf{x}\| \|\mathbf{d}\| - k \|\mathbf{B}^T \mathbf{P} \mathbf{x}\| = \|\mathbf{B}^T \mathbf{P} \mathbf{x}\| (\|\mathbf{d}\| - k) < 0$$

Therefore, the derivative along the system trajectories satisfies $\dot{\mathcal{V}} \leq -\mathbf{x}^T \mathbf{Q} \mathbf{x}$. It has been shown that \mathcal{V} is a *positive definite* function and $\dot{\mathcal{V}}$ is a *negative definite* function on any open neighborhood of the origin. Therefore, the origin of the tracking error dynamics $\mathbf{x} = \{\mathbf{e} \ \dot{\mathbf{e}}\}^T$ is asymptotically stable. \square

Theorem (6.5) shows that one means of constructing a tracking controller that accommodates uncertainty in the system dynamics is to introduce the switching feedback signal $\mathbf{u}(t)$ defined in Equation (6.7.6). Such a controller achieves good performance, in principle. If the disturbance or unknown dynamics that gives rise to the mismatch \mathbf{d} satisfies $\mathbf{d}(t) \leq k$ for all $t \in \mathbb{R}^+$, then the tracking error and its derivative converge to zero asymptotically. Still, there are a couple of troublesome issues with such a “hard” switching controller. One difficulty is theoretical in nature. As mentioned earlier, when the right hand side of the governing system of ordinary differential equations is discontinuous, the rigorous justification for the Lyapunov stability argument must be expressed in terms of generalized solutions. Such an analysis is beyond the scope of this text. See [13, 3, 30] for a discussion of the details in this case. In addition to such theoretical considerations, there are practical reasons why the “hard” switching controller can be problematic in applications. It is common that this controller exhibits high-frequency oscillation as the actuation varies. Moreover, it is not simple to predict when a particular system will exhibit such a pathological response regime because the closed loop system is nonlinear.

The following theorem illustrates that it is possible to address some of these problems by using a “smoothed” switching control. The smoothed switching controller

introduces another parameter $\epsilon > 0$ that defines a region over which the control input varies in a smooth way between the large output amplitudes of the “hard” switching controller. The right hand side of the resulting closed loop system is continuous, and the system can be described by a conventional, continuous Lyapunov function. As a result, more esoteric notions of generalized solutions are not required for the analysis or interpretation of this control law. In practical terms, the introduction of the parameter $\epsilon > 0$ gives an explicit bound on the size of the set over which the switching control varies in amplitude. It is possible as a consequence to eliminate the high-frequency oscillation associated with chattering control input signals.

Theorem 6.6. Suppose that the hypotheses of Theorem (6.5) hold, but instead of Equation (6.7.6), choose the control signal $\mathbf{u}(t)$ such that

$$\mathbf{u}(t) = \begin{cases} -k \frac{\mathbf{B}^T \mathbf{P} \mathbf{x}}{\|\mathbf{B}^T \mathbf{P} \mathbf{x}\|} & \text{if } \|\mathbf{B}^T \mathbf{P} \mathbf{x}\| \geq \epsilon, \\ -k \frac{\mathbf{B}^T \mathbf{P} \mathbf{x}}{\epsilon} & \text{if } \|\mathbf{B}^T \mathbf{P} \mathbf{x}\| < \epsilon. \end{cases} \quad (6.7.8)$$

Then the tracking error dynamics $\mathbf{x}^T := \{\mathbf{e}^T \ \dot{\mathbf{e}}^T\}$ of the closed loop system approaches the largest weakly invariant subsets of the set

$$\mathcal{S} \subseteq \{\mathbf{x} | \dot{\mathcal{V}}(\mathbf{x}) = 0\} \subseteq \left\{ \mathbf{x} \left| \frac{1}{2} \mathbf{x}^T \mathbf{Q} \mathbf{x} = \epsilon k \right. \right\}.$$

The closed loop tracking error dynamics is uniformly ultimately bounded with a magnitude of the order $O(\epsilon)$.

Proof. Consider the Lyapunov function $\mathcal{V}(\mathbf{x}) := \frac{1}{2} \mathbf{x}^T \mathbf{P} \mathbf{x}$ where $\mathbf{x}^T := \{\mathbf{e}^T \ \dot{\mathbf{e}}^T\}$, and \mathbf{P} is the solution of the Lyapunov Equation (6.7.5). The derivative of the Lyapunov function \mathcal{V} along the trajectories of the closed loop system yields the same expression obtained in Theorem (6.5) $\dot{\mathcal{V}}(\mathbf{x}) = -\frac{1}{2} \mathbf{x}^T \mathbf{Q} \mathbf{x} + \mathbf{x}^T \mathbf{P} \mathbf{B}(\mathbf{u} + \mathbf{d})$. If it is the case that $\|\mathbf{B}^T \mathbf{P} \mathbf{x}\| \geq \epsilon$, the upper bound on the derivative can be derived as

$$\dot{\mathcal{V}} \leq -\frac{1}{2} \mathbf{x}^T \mathbf{Q} \mathbf{x} + \|\mathbf{B}^T \mathbf{P} \mathbf{x}\| (\|\mathbf{d}\| - k)$$

As in the proof of Theorem (6.5), $\dot{\mathcal{V}} < 0$ as long as $\|\mathbf{d}\| < k$. If, however, $\|\mathbf{B}^T \mathbf{P} \mathbf{x}\| < \epsilon$, the derivative along the trajectories is evaluated as

$$\begin{aligned} \dot{\mathcal{V}} &= -\frac{1}{2} \mathbf{x}^T \mathbf{Q} \mathbf{x} - \frac{k}{\epsilon} \|\mathbf{B}^T \mathbf{P} \mathbf{x}\|^2 + \mathbf{x}^T \mathbf{P} \mathbf{B} \mathbf{d} \\ &\leq -\frac{1}{2} \mathbf{x}^T \mathbf{Q} \mathbf{x} + \|\mathbf{B}^T \mathbf{P} \mathbf{x}\| \left(\|\mathbf{d}\| - \frac{k}{\epsilon} \|\mathbf{B}^T \mathbf{P} \mathbf{x}\| \right) \leq -\frac{1}{2} \mathbf{x}^T \mathbf{Q} \mathbf{x} + \epsilon k. \end{aligned}$$

It is known that $\dot{\mathcal{V}}(\mathbf{x}) \leq -\frac{1}{2} \mathbf{x}^T \mathbf{Q} \mathbf{x} + \epsilon k$. The right hand side of this equation may be visualized using Figure (6.15). From this figure, it is clear that

$$\left\{ \mathbf{x} \mid \dot{V}(\mathbf{x}) = 0 \right\} \subseteq \left\{ \mathbf{x} \mid -\frac{1}{2} \mathbf{x}^T \mathbf{Q} \mathbf{x} + \epsilon k = 0 \right\} = \left\{ \mathbf{x} \mid \frac{1}{2} \mathbf{x}^T \mathbf{Q} \mathbf{x} = \epsilon k \right\}.$$

This completes the proof. \square

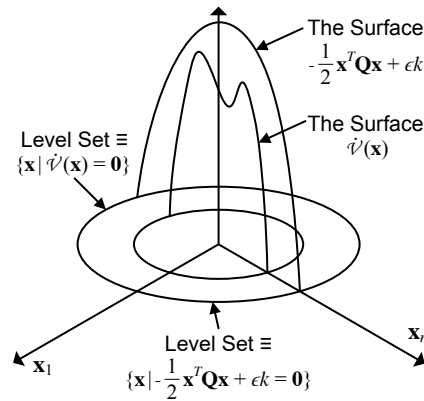


Fig. 6.15: Visualization of Uniform Ultimate Boundedness

The next two examples study controllers based on approximate dynamic inversion for typical robotic systems.

Example 6.7.1. Consider once again the spherical robotic manipulator studied in Examples (6.6.1) and (6.6.2). Derive the controller that uses the proportional-derivative (PD) feedback and gravity compensation as described in Theorem (6.4) to achieve setpoint control for the spherical robot. Select the system parameters to be $m_1 = m_2 = m_3 = 10$ kg, $d_{p,q} = 0.1$ m, and $y_{q,c_2} = 0.05$ m. Choose the gain matrices \mathbf{G}_0 and \mathbf{G}_1 in Theorem (6.4) to have the form $\mathbf{G}_0 = g_0 \mathbb{I}$ and $\mathbf{G}_1 = g_1 \mathbb{I}$, where the gains are selected to be $(g_0, g_1) = (1, 1), (5, 5), (10, 10)$ or $(100, 100)$, and the desired state is

$$\mathbf{x}_d = \begin{Bmatrix} \mathbf{q}_d \\ \dot{\mathbf{q}}_d \end{Bmatrix} = \left\{ \begin{Bmatrix} 1 & 1 & 1 \end{Bmatrix} \begin{Bmatrix} 0 & 0 & 0 \end{Bmatrix} \right\}^T.$$

Evaluate the performance of this controller by plotting the state trajectories, set point error and control inputs as a function of time.

Solution: The controller for the spherical robot based on PD feedback and gravity compensation chooses the control torque τ in Equation (6.7.1) to be

$$\boldsymbol{\tau} = \begin{Bmatrix} m_1 \\ m_2 \\ f \end{Bmatrix} = -g_1 \begin{Bmatrix} \dot{\theta}_1 \\ \dot{\theta}_2 \\ \dot{d}_{q,r} \end{Bmatrix} - g_0 \begin{Bmatrix} \theta_1 - \theta_d \\ \theta_2 - \theta_d \\ d_{q,r} - d_{q,r,d} \end{Bmatrix} + \begin{Bmatrix} 0 \\ m_3 g d_{q,r} \sin \theta_2 \\ -m_3 g \cos \theta_2 \end{Bmatrix}.$$

Figures (6.16) (a), (b) and (c) depict state trajectories for the specified choices of gains, and Figures (6.16)(d), (e) and (f) depict actuation inputs m_1, m_2 and f as function of time for these gains. As expected, all state trajectories approach their respective desired values as $t \rightarrow \infty$. A comparison of the qualitative behavior of these trajectories in comparison to those trajectories obtained using the exactly canceling computed torque yields some important observations. The trajectories for $\theta_1(t)$ and $\theta_2(t)$ in this example are indeed different functions of time, even though the initial conditions for these two variables are identical. The closed loop governing equations for θ_1 and θ_2 are different coupled nonlinear equations when the approximate dynamic inversion in Theorem (6.4) is used. In contrast, when the exact computed torque in Example (6.6.1) is used, the closed loop equations for θ_1 and θ_2 are identical. In that case the feedback linearization yields the same function of time, $\theta_1(t) = \theta_2(t)$ in Example (6.6.1) whenever the initial conditions for θ_1 and θ_2 are the same.

The differences in the axial displacement $d_{q,r}(t)$ in Example (6.6.1) and the current case shown in Figure (6.16)(c) are also striking. In Example (6.6.1) the initial condition for the axial displacement matches the target state, and the closed loop governing equation is a linear ODE. The solution in Example (6.6.1) for the error dynamics is just the function that is equal to zero for all time. In contrast, the error dynamic associated with $d_{q,r}(t)$ in Figure (6.16)(c) is not identically equal to zero in the current example, even though the initial conditions and target states are identical. The closed loop equations for all of the unknowns are coupled when using the PD and gravity compensation controller. Even though the tracking error in the variable $d_{q,r}(t)$ starts at zero for the controller in this example, it quickly becomes nonzero due to its coupling to the θ_1 and θ_2 states. With regards to the actuation loading, the controller exhibits large transient variations at startup, particularly for large gains. This is a typical problem of many controllers when abrupt or instantaneous changes in the system states are required, as is the case for the setpoint controller in this example. The states are initially $\theta_1(t_0) = \theta_2(t_0) = 0$, and it is desired to have $\theta_1(t), \theta_2(t) \rightarrow 1$ as t increases.

Example 6.7.2. Construct a set point controller based on approximate feedback linearization with a sliding mode term to drive the spherical robotic manipulator studied in Examples 6.6.1, 6.6.2 and 6.7.1 to the desired final configuration where $\mathbf{q}_d := \{1 \ 1\}^T$ and $\dot{\mathbf{q}}_d := \{0 \ 0\}^T$. Suppose that the true values of the physical parameters are identical to those in Example 6.7.1. Let m denote the common, true value of the mass links $m := m_1 = m_2 = m_3$. Suppose that the physical parameters $y_{q,c2}$ and $d_{p,q}$ are known exactly, but that the mass m of the links is approximated

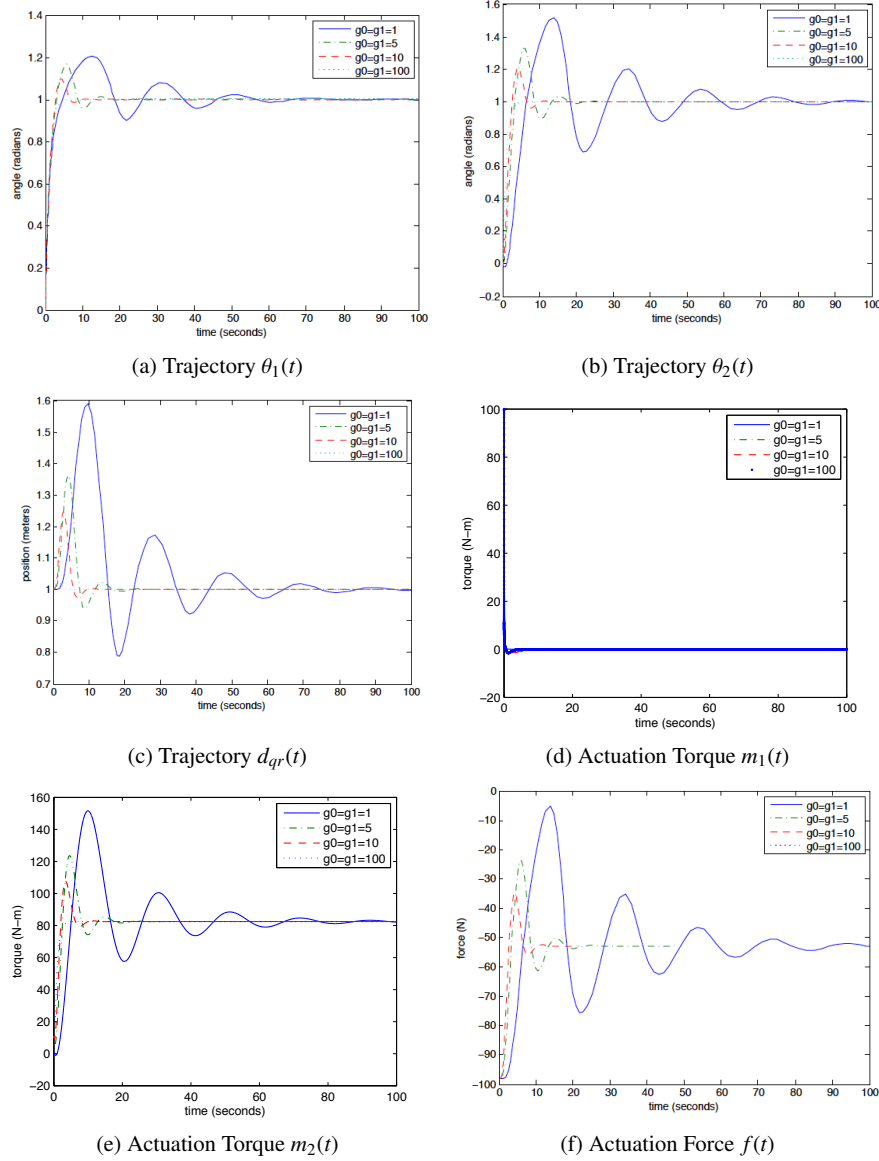


Fig. 6.16: Time Histories of Generalized Coordinates and Actuation Inputs

by m_a . Design a controller to drive the robotic arm to the desired state when the approximate mass estimate m_a may be in error up to 20% of the true mass m .

Solution: By inspection, the generalized mass matrix \mathbf{M} and nonlinear vector \mathbf{n} can be factored into the expressions

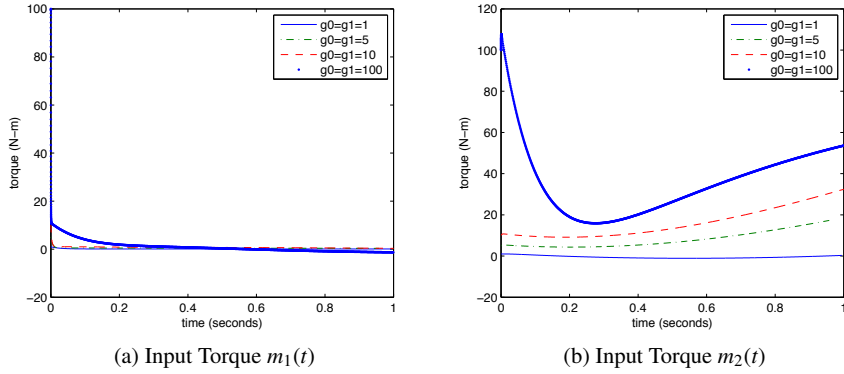


Fig. 6.17: Actuator Inputs Transients Response

$$\mathbf{M}(\mathbf{q}) = m\bar{\mathbf{M}}(\mathbf{q}), \\ \mathbf{n}(\mathbf{q}, \dot{\mathbf{q}}) = m\bar{\mathbf{n}}(\mathbf{q}, \dot{\mathbf{q}}),$$

where $\bar{\mathbf{M}}$ and $\bar{\mathbf{n}}$ are known functions. The approximations \mathbf{M}_a and \mathbf{n}_a of \mathbf{M} and \mathbf{n} , respectively, are chosen to be

$$\mathbf{M}_a := m_a \bar{\mathbf{M}} = \frac{m_a}{m} \mathbf{M} = \alpha \mathbf{M} \\ \mathbf{n}_a := m_a \bar{\mathbf{n}} = \frac{m_a}{m} \mathbf{n} = \alpha \mathbf{n}$$

where $\alpha := m/m_a$ is the ratio of the exact mass m to the approximate mass m_a . With these definitions of the approximate generalized mass matrix \mathbf{M}_a and the approximate nonlinear vector \mathbf{n}_a , the errors $\Delta \mathbf{M}$ and $\Delta \mathbf{n}$ that approximate the nonlinear terms and the resulting disturbance \mathbf{d} can be written as

$$\Delta \mathbf{M} = (m_a - m) \bar{\mathbf{M}}, \quad \Delta \mathbf{n} = (m_a - m) \bar{\mathbf{n}}, \\ \mathbf{d} = \mathbf{M}^{-1} \Delta \mathbf{M} \mathbf{w} - \mathbf{M}^{-1} \Delta \mathbf{n} = \frac{m_a - m}{m} (\mathbf{w} - \mathbf{M}^{-1} \mathbf{n}) = (\alpha - 1) (\mathbf{w} - \mathbf{M}^{-1} \mathbf{n}),$$

where $\mathbf{w} := \ddot{\mathbf{q}}_d - \mathbf{G}_1(\dot{\mathbf{q}} - \dot{\mathbf{q}}_d) - \mathbf{G}_0(\mathbf{q} - \mathbf{q}_d) + \mathbf{v}$ and \mathbf{v} is the sliding mode control term. Note that the feedback control term $\boldsymbol{\tau} := \mathbf{M}_a(\mathbf{q})\mathbf{w} - \mathbf{n}_a(\mathbf{q}, \dot{\mathbf{q}})$ can be implemented without explicit knowledge of the true mass m .

The control law is first implemented with a discontinuous sliding mode controller for \mathbf{v} . In this case,

$$\mathbf{v} = \begin{cases} -k \frac{\mathbf{B}^T \mathbf{P} \mathbf{x}}{\|\mathbf{B}^T \mathbf{P} \mathbf{x}\|} & \text{whenever } \|\mathbf{B}^T \mathbf{P} \mathbf{x}\| > \epsilon, \\ \mathbf{0} & \text{otherwise.} \end{cases} \quad (6.7.9)$$

Figures 6.18 depict the trajectories in time of the generalized coordinates, input forces and torques, Lyapunov function $\mathcal{V}(\mathbf{x}(t))$ and disturbance $\mathbf{d}(t)$ when the gains $g_0 = 40$ and $g_1 = 4$, the sliding mode control gain $k = 7$, the value of $\epsilon = 1e-12$, and the matrix \mathbf{P} is the solution of Lyapunov's equation $\mathbf{A}^T \mathbf{P} + \mathbf{P} \mathbf{A} = -\mathbf{Q}$ with $\mathbf{Q} = \mathbb{I}$,

$$\mathbf{P} = \begin{bmatrix} 5.175 & 0 & 0 & 0.0125 & 0 & 0 \\ 0 & 5.175 & 0 & 0 & 0.0125 & 0 \\ 0 & 0 & 5.175 & 0 & 0 & 0.0125 \\ 0.0125 & 0 & 0 & 0.128125 & 0 & 0 \\ 0 & 0.0125 & 0 & 0 & 0.128125 & 0 \\ 0 & 0 & 0.0125 & 0 & 0 & 0.128125 \end{bmatrix}. \quad (6.7.10)$$

The trajectories depicted in Figure (6.18) are typical in several respects of results obtained with discontinuous sliding mode controllers. In (6.18) (a) and (b), the generalized coordinates quickly converge to the sliding surface at approximately $t = 0.5$ seconds, but thereafter converge rather slowly towards their desired values. Figure 6.18(c) illustrates the input forces and torques. The control inputs exhibit chattering as the controls drive the system response repeatedly across the sliding surface after $t = 0.5$ seconds. The controller also requires a linear actuator that can deliver up to 150 Newtons of force and motors that generate over 150 Newton-meters of torque. Even if the actuators have the authority to deliver the input forces and torques shown in the figure, the bandwidth is prohibitively high during the chattering regime.

Figure 6.18(d) and (e) show the value of the Lyapunov function $\mathcal{V}(\mathbf{x}(t))$ and the disturbance $\mathbf{d}(t)$ evaluated along the system trajectory. The gain $k = 7$ has been selected appropriately in that it is always true that $k > \|\mathbf{d}(t)\|$ during this simulation, and it is expected that the theoretical guarantees of stability convergence should hold. Finally, Figure 6.18(f) illustrates several contributions to the derivative of the Lyapunov function. This graph is based on the fact that the derivative $\frac{d\mathcal{V}}{dt}$ can be computed from the equation

$$\frac{d\mathcal{V}}{dt}(\mathbf{x}(t)) = -\frac{1}{2}\mathbf{x}^T(t)\mathbf{Q}\mathbf{x}(t) + \mathbf{x}^T(t)\mathbf{P}\mathbf{B}(\mathbf{v}(t) + \mathbf{d}(t)). \quad (6.7.11)$$

The figure shows that the black line representing $\frac{d\mathcal{V}}{dt}$ is always negative, as required in the proof of stability. The contribution due to the uncertainty is equal to $\mathbf{x}^T(t)\mathbf{P}\mathbf{B}\mathbf{d}(t)$ and may be positive, but it is always dominated by the negative sliding mode term $\mathbf{x}^T(t)\mathbf{P}\mathbf{B}\mathbf{v}(t)$.

Next, consider the regularized sliding mode controller which is given by

$$\mathbf{v} = \begin{cases} -k \frac{\mathbf{B}^T \mathbf{P} \mathbf{x}}{\|\mathbf{B}^T \mathbf{P} \mathbf{x}\|} & \text{whenever } \|\mathbf{B}^T \mathbf{P} \mathbf{x}\| > \epsilon, \\ -k \frac{\mathbf{B}^T \mathbf{P} \mathbf{x}}{\epsilon} & \text{otherwise.} \end{cases} \quad (6.7.12)$$

Figure 6.19 depicts the corresponding system trajectories when all the controller gains are identical, except that the boundary layer variable is chosen to be $\epsilon = 0.01$. Qualitatively, the trajectories of the generalized coordinates depicted in Figures 6.19(a) and (b) are similar to those shown in Figures 6.18 (a) and (b) that are

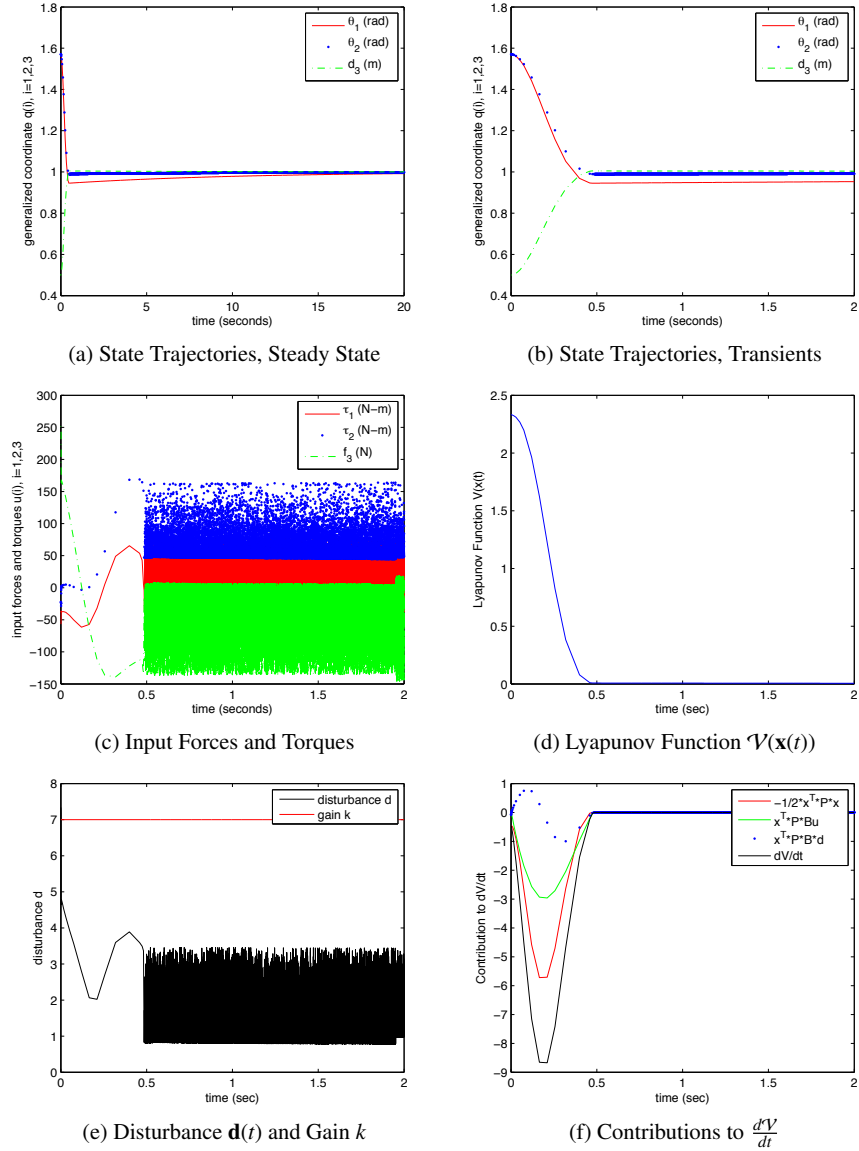


Fig. 6.18: Time Histories Generated by Discontinuous Sliding Mode Controller

obtained with the discontinuous sliding mode controller. However, while the trajectories obtained with the discontinuous controller are guaranteed to converge to their desired values, the trajectories generated by the continuous controller are only guaranteed to converge to some neighborhood of the desired values. The size of this

neighborhood is guaranteed to be $O(k\epsilon)$ in size and can be made smaller by reducing the size of the boundary layer ϵ .

The most drastic difference between the two controllers is illustrated by contrasting Figures 6.18(c) and 6.19(c). While the discontinuous controller exhibits a significant chattering regime, the control inputs generated by the regularized sliding mode controller do not. As a result, the continuous controller is physically realizable, whereas the discontinuous controller is not. However, as the boundary layer ϵ is decreased further and further, the control inputs will become increasingly similar to those of the discontinuous system and will exhibit increasing degrees of chattering.

6.8 Controllers Based on Passivity

The derivation of controllers based on *approximate dynamic inversion* leads to a family of practical control strategies, ones that are designed for a number of different performance metrics. Another class of popular controllers have been derived that rely on the *skew symmetry* of the matrix $\dot{\mathbf{M}} - 2\mathbf{C}$ and associated *passivity properties* of the governing equations. It has been shown in Chapter (4) that the governing equations for a *natural system* can be written in the form

$$\mathbf{M}(\mathbf{q})\ddot{\mathbf{q}}(t) + \mathbf{C}(\mathbf{q}(t), \dot{\mathbf{q}}(t))\dot{\mathbf{q}} + \frac{\partial V}{\partial \mathbf{q}}(\mathbf{q}(t)) = \boldsymbol{\tau}(t). \quad (6.8.1)$$

For this equation of motion the matrix $\dot{\mathbf{M}} - 2\mathbf{C}$ is *skew symmetric*. That is, the identity

$$\mathbf{y}^T(\dot{\mathbf{M}} - 2\mathbf{C})\mathbf{y} = 0$$

holds for any vector \mathbf{y} . As before, define the tracking error to be $\mathbf{e}(t) := \mathbf{q}(t) - \mathbf{q}_d(t)$.

The construction of controllers based on *passivity* can be carried out by introducing the filtered tracking error \mathbf{r} and the auxiliary variables \mathbf{v} and \mathbf{a} as

$$\mathbf{r}(t) := \dot{\mathbf{e}}(t) + \Lambda \mathbf{e}(t), \quad (6.8.2)$$

$$\mathbf{v}(t) := \dot{\mathbf{q}}_d(t) - \Lambda \mathbf{e}(t), \quad (6.8.3)$$

$$\mathbf{a}(t) := \dot{\mathbf{v}}(t) = \ddot{\mathbf{q}}_d(t) - \Lambda \dot{\mathbf{e}}(t), \quad (6.8.4)$$

where Λ is a positive diagonal matrix. The controller based on *passivity* chooses the control input

$$\boldsymbol{\tau} = \mathbf{M}(\mathbf{q})\mathbf{a} + \mathbf{C}(\mathbf{q}, \dot{\mathbf{q}})\mathbf{v} + \frac{\partial V}{\partial \mathbf{q}}(\mathbf{q}) - \mathbf{K}\mathbf{r} \quad (6.8.5)$$

where \mathbf{K} is a positive, diagonal gain matrix. With this choice of control input $\boldsymbol{\tau}$, the closed loop system dynamics are governed by the equations

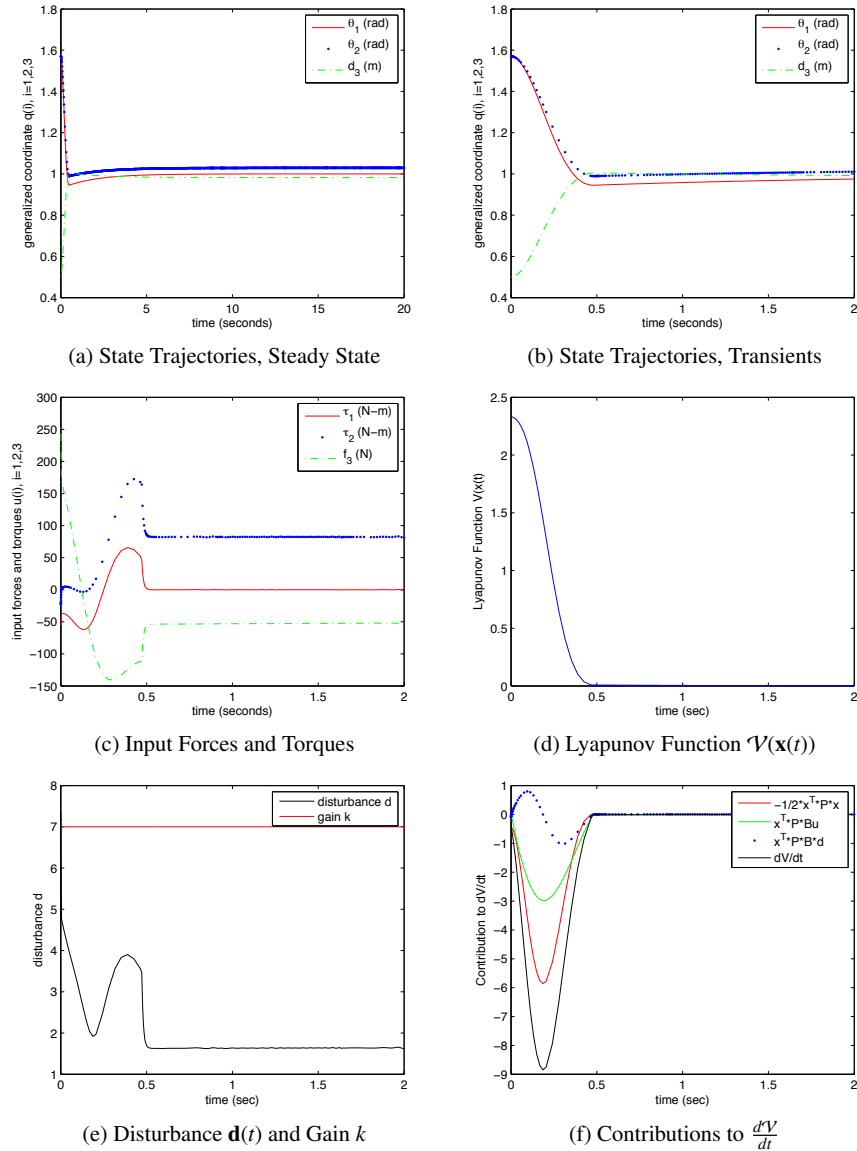


Fig. 6.19: Time Histories Generated by Regularized Sliding Mode Controller

$$\underbrace{\mathbf{M}(\ddot{\mathbf{q}} - \ddot{\mathbf{q}}_d + \boldsymbol{\Lambda}(\dot{\mathbf{q}} - \dot{\mathbf{q}}_d))}_{\mathbf{r}} + \underbrace{\mathbf{C}(\dot{\mathbf{q}} - \dot{\mathbf{q}}_d + \boldsymbol{\Lambda}(\mathbf{q} - \mathbf{q}_d))}_{\mathbf{r}} + \mathbf{K}\mathbf{r} = \mathbf{0},$$

or

$$\mathbf{M}\dot{\mathbf{r}} + \mathbf{C}\mathbf{r} + \mathbf{K}\mathbf{r} = \mathbf{0}.$$

Theorem 6.7. Let the equations of motion of a robotic system have the form in Equation (6.8.1). Suppose \mathbf{q}_d is an N -vector of desired trajectories and define \mathbf{r}, \mathbf{v} and \mathbf{a} as in Equations (6.8.2), (6.8.3), (6.8.4), respectively. Then the feedback control in Equation (6.8.5) renders the equilibrium at the origin of the tracking error dynamics $\begin{Bmatrix} \mathbf{e} \\ \dot{\mathbf{e}} \end{Bmatrix}$ asymptotically stable.

Proof. The critical step, as in each of the cases studied in this chapter, relies on an appropriate choice of a Lyapunov function. Choose \mathcal{V} to be

$$\mathcal{V} = \frac{1}{2}\mathbf{r}^T \mathbf{M}\mathbf{r} + \mathbf{e}^T \boldsymbol{\Lambda} \mathbf{K} \mathbf{e}.$$

Note that the product $\boldsymbol{\Lambda} \mathbf{K}$ in this expression is a symmetric, positive definite matrix since $\boldsymbol{\Lambda}$ and \mathbf{K} are both positive diagonal matrices. The calculation of the derivative along the trajectories of the system yields

$$\dot{\mathcal{V}} = \mathbf{r}^T \mathbf{M}\dot{\mathbf{r}} + \frac{1}{2}\mathbf{r}^T \dot{\mathbf{M}}\mathbf{r} + 2\mathbf{e}^T \boldsymbol{\Lambda} \mathbf{K} \dot{\mathbf{e}}.$$

A negative definite derivative $\dot{\mathcal{V}}$ is obtained when the closed loop equations are substituted into this equation,

$$\dot{\mathcal{V}} = \frac{1}{2}\underbrace{\mathbf{r}^T (\dot{\mathbf{M}} - 2\mathbf{C})\mathbf{r}}_0 - \mathbf{r}^T \mathbf{K}\mathbf{r} + 2\mathbf{e}^T \boldsymbol{\Lambda} \mathbf{K} \dot{\mathbf{e}}.$$

The first term on the right is equal to zero since the matrix $\dot{\mathbf{M}} - 2\mathbf{C}$ is skew symmetric. The remaining expression can be simplified to

$$\begin{aligned} \dot{\mathcal{V}} &= -(\dot{\mathbf{e}} + \boldsymbol{\Lambda} \mathbf{e})^T \mathbf{K}(\dot{\mathbf{e}} + \boldsymbol{\Lambda} \mathbf{e}) + 2\mathbf{e}^T \boldsymbol{\Lambda} \mathbf{K} \dot{\mathbf{e}}, \\ &= -\dot{\mathbf{e}}^T \mathbf{K} \dot{\mathbf{e}} - \mathbf{e}^T \boldsymbol{\Lambda} \mathbf{K} \boldsymbol{\Lambda} \mathbf{e} - 2\mathbf{e}^T \boldsymbol{\Lambda} \mathbf{K} \dot{\mathbf{e}} + 2\mathbf{e}^T \boldsymbol{\Lambda} \mathbf{K} \dot{\mathbf{e}}, \\ &= -\dot{\mathbf{e}}^T \mathbf{K} \dot{\mathbf{e}} - \mathbf{e}^T \boldsymbol{\Lambda} \mathbf{K} \boldsymbol{\Lambda} \mathbf{e}. \end{aligned}$$

This expression shows that $\dot{\mathcal{V}}$ is a negative definite function of the state $\begin{Bmatrix} \mathbf{e} \\ \dot{\mathbf{e}} \end{Bmatrix}^T$. The equilibrium at the origin of the tracking error dynamics is asymptotically stable. \square

Example 6.8.1. Consider the spherical robotic manipulator studied in Examples (6.6.1), (6.6.2) and (6.7.1). Derive a controller based on passivity as described in

Theorem (6.7) to achieve tracking control. Select the system parameters to be $m_1 = m_2 = m_3 = 10 \text{ kg}$, $d_{p,q} = 0.1 \text{ m}$ and $y_{q,c_2} = 0.05 \text{ m}$. Choose the gain matrices \mathbf{A} and \mathbf{K} in Theorem (6.7) to have the form $\mathbf{A} = \lambda \mathbb{I}$ and $\mathbf{K} = k \mathbb{I}$, where the gains are selected to be $(\lambda, k) = (1, 10), (2, 10), (4, 10)$ or $(20, 100)$. Assume that the desired trajectory is

$$\mathbf{q}_d = \begin{Bmatrix} A_1 \sin(\Omega_1 t) \\ A_2 \sin(\Omega_2 t) \\ A_3 \sin(\Omega_3 t) + 1 \end{Bmatrix},$$

with $(A_1, A_2, A_3) = (-\frac{1}{16}, -1, -\frac{1}{4})$ and $(\Omega_1, \Omega_2, \Omega_3) = (4, 1, 2)$. Write a program to simulate the performance of the controller for the control gains and desired trajectories. Plot the state trajectories, the tracking error and the control inputs as a function of time.

Solution: The controller for the spherical robotic manipulator based on passivity principles in Theorem (6.7) has the form in Equation (6.8.5)

$$\boldsymbol{\tau} = \mathbf{Ma} + \mathbf{Cv} + \frac{\partial V}{\partial \mathbf{q}} - \mathbf{Kr}$$

where \mathbf{r}, \mathbf{v} and \mathbf{a} are defined in Equations (6.8.2), (6.8.3), (6.8.4), and

$$\mathbf{M} = \begin{bmatrix} m_3(d_{p,q}^2 + \sin^2 \theta_2 d_{q,r}^2) + m_2(d_{p,q} - y_{q,c_2})^2 & m_3 \cos \theta_2 d_{p,q} d_{q,r} & m_3 \sin \theta_2 d_{p,q} \\ m_3 \cos \theta_2 d_{p,q} d_{q,r} & m_3 d_{q,r}^2 & 0 \\ m_3 \sin \theta_2 d_{p,q} & 0 & m_3 \end{bmatrix},$$

$$\frac{\partial V}{\partial \mathbf{q}} = \begin{Bmatrix} 0 \\ m_3 g d_{q,r} \sin \theta_2 \\ -m_3 g \cos \theta_2 \end{Bmatrix},$$

$$\mathbf{C} = \begin{bmatrix} \sin \theta_2 m_3 d_{q,r} (\cos \theta_2 d_{q,r} \dot{\theta}_2 + \sin \theta_2 d_{q,r} \dot{\theta}_1) & m_3 (\sin \theta_2 d_{q,r} (\cos \theta_2 d_{q,r} \dot{\theta}_1 - d_{p,q} \dot{\theta}_2) + \cos \theta_2 d_{p,q} d_{q,r}) & m_3 (d_{q,r} \dot{\theta}_1 \sin^2 \theta_2 + \cos \theta_2 d_{p,q} \dot{\theta}_2) \\ -\frac{1}{2} \sin 2\theta_2 m_3 d_{q,r}^2 \dot{\theta}_1 & m_3 d_{q,r} d_{q,r} & m_3 d_{q,r} \dot{\theta}_2 \\ -\sin^2 \theta_2 m_3 d_{q,r} \dot{\theta}_1 & -m_3 d_{q,r} \dot{\theta}_2 & 0 \end{bmatrix}.$$

In contrast to the case when exact cancellation of nonlinearities is achieved using the ideal *computed torque control*, the resulting equations that govern the closed loop system are neither decoupled nor linear. It is not possible to obtain a simple closed form solution of the governing closed loop equations as in Examples (6.6.1) or (6.6.2). Figures (6.20) (a) through (f) depict the state trajectories and control input time histories for the closed loop system when the initial condition has been selected to be

$$\mathbf{x}(0)^T = \{ \mathbf{q}(0)^T \quad \dot{\mathbf{q}}(0)^T \} = \{ \{ 0 \ 0 \ 1 \} \ \{ 0 \ 0 \ 0 \} \}.$$

Figures (6.20)(a), (b) and (c) depict the state trajectories $\theta_1(t), \theta_2(t)$ and $d_{q,r}(t)$, respectively, for the various choices of feedback gains λ and k . Good tracking performance is evident for $\theta_1(t)$ and $\theta_2(t)$, while the asymptotic convergence of $d_{p,q}(t)$ to its desired trajectory is rather slow. Figures (6.20)(d), (e) and (f) depict the control input time histories. The input authority required for this controller is similar in magnitude to that encountered in Examples (6.6.1) or (6.6.2). The steady state magnitude of the input torque m_2 oscillates between $\pm 50 \text{ N-m}$, and the actuation force

varies from -50 N and -100 N as $t \rightarrow \infty$. The magnitudes of the startup transient actuation forces and moments are several times their steady state magnitudes.

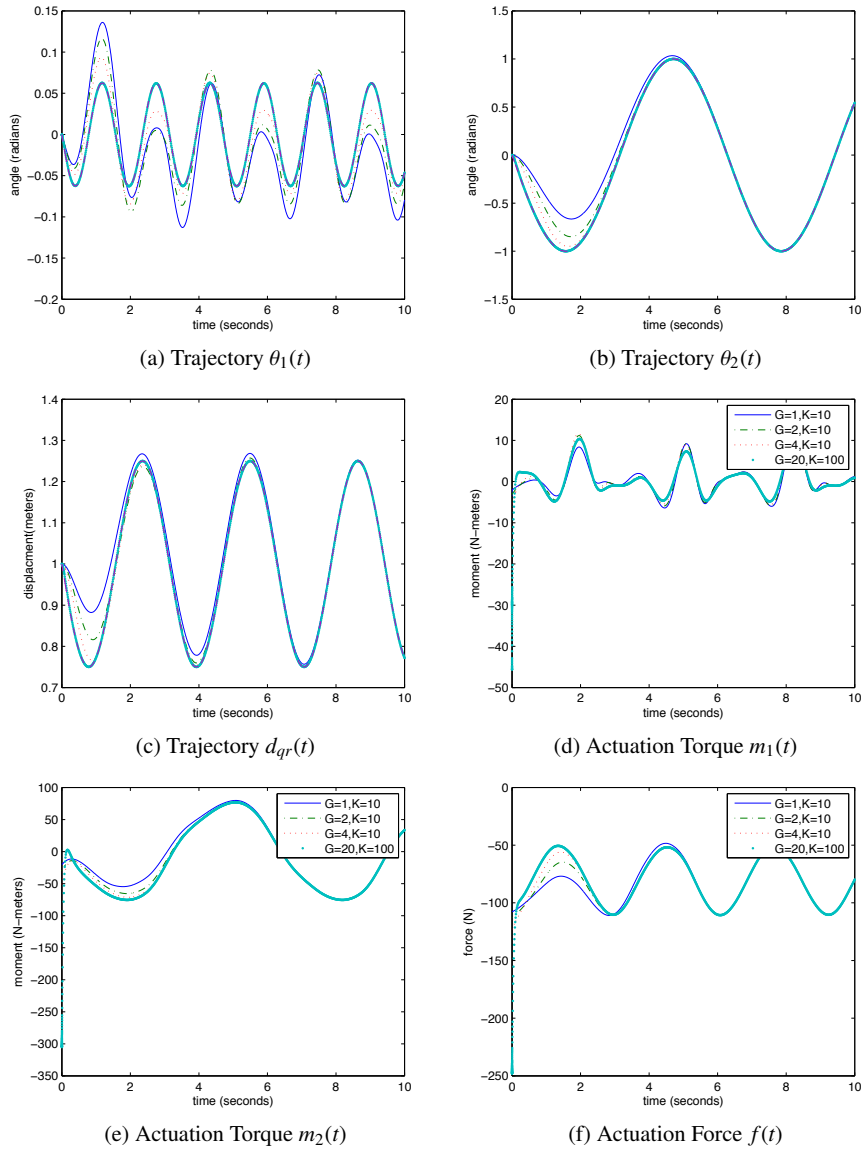


Fig. 6.20: Time Histories of Generalized Coordinates and Actuation Inputs

6.9 Actuator Models

Modern robotic systems, including the diverse array described in Chapter (1), utilize a wide array of actuators. The actuators may include conventional electric motors, hydraulic cylinders, or pneumatic pistons. These common actuation systems have numerous variants and individual designs, each having specific advantages and drawbacks. They may require models with tailored governing equations to represent the physics of their operation. Each may exhibit its own characteristic nonlinearities, which must be accounted for in modeling and control synthesis. Moreover, ever increasing numbers of novel and unconventional actuators appear in robotics applications each year. These include actuators based on shape memory alloys, biomaterials, electrochemicals, electrostructural materials, and magnetostructural materials. The research into alternative systems is driven by the need for more compact, lightweight, high authority, and high bandwidth actuation systems.

6.9.1 Electric Motors

Of all the possible actuation devices, the electric motor is the most common in robotic systems. Nearly all electric motors operate based on the principles of *electromagnetic induction* whereby a current carrying wire immersed in a magnetic field undergoes a force. Electric motors operate by passing a current through loops of wire that are aligned relative to an external magnetic field so that the force turns the rotor. Electric motors are popular owing to their relative simplicity, fast response, and large startup torque output. There are many different types of electric motors including direct current (DC), induction, synchronous, brushless, and stepper motors. This section focuses on the fundamentals of electric motors and stresses those aspects of electric motor architecture that are common to many electric motors.

This section presents the physical foundations and derives the governing equations for a *permanent magnet, direct current (DC) motor* shown schematically in Figure (6.21). A DC motor works by virtue of the Lorentz force law. This law can be used to show that the force \mathbf{f} acting on a conductor of length l that carries current i in the magnetic field having magnetic flux \mathbf{B} is given by $\mathbf{f} = il\mathbf{n} \times \mathbf{B}$, where \mathbf{n} is a unit vector along the length of the wire. Consider a loop of wire that rotates in the magnetic field having magnetic flux $\mathbf{B} = B\mathbf{y}$ along the unit vector \mathbf{y} as shown in Figure (6.22). In this case the force on the wire from c to d is given by

$$\mathbf{f} = (il\mathbf{x}) \times (B\mathbf{y}) = ilB\mathbf{z}$$

A similar calculation shows that the force acting on the wire from a to b is $\mathbf{f} = -ilB\mathbf{z}$. The net torque applied on the wire loop in the configuration shown is therefore

$$\mathbf{t} = (2rlB)\mathbf{i}\mathbf{x} = t\mathbf{x}$$

This torque will cause the loop to rotate counterclockwise about the \mathbf{x} axis until the loop passes the $\mathbf{x} - \mathbf{z}$ plane.

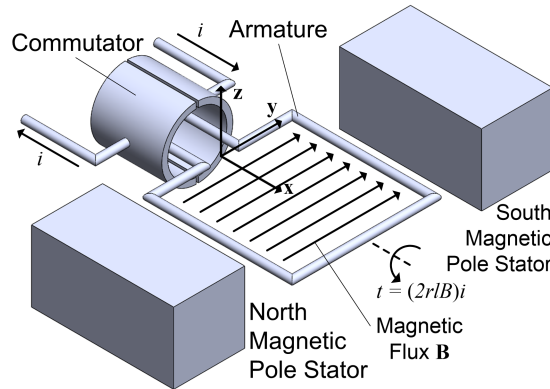


Fig. 6.21: Permanent Magnet Direct Current (DC) motor

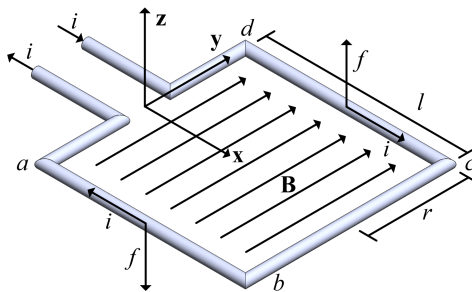


Fig. 6.22: Loop of Wire Carrying a Current in the Magnetic Field Having Flux \mathbf{B}

If the loop rotates and passes the vertical plane in Figure (6.22), the sign of the moment about the \mathbf{x} axis changes. A DC motor as depicted in Figure (6.21) utilizes a *commutator* to avoid the reversal in sign of the torque generated in this example of a rotating loop of wire. The primary components of the DC motor depicted in Figure (6.21) include a *stator* that contains the north and south magnetic poles, the *armature* that rotates relative to the stator, and the *commutator* that is fixed to the armature. The *brushes* maintain a sliding contact between the *commutator* and the

power source that drives the motor. The *commutator* is made of segments that are electrically isolated from each other and are fixed to the rotating *armature*. The ends of the wire loops are connected to the *commutator* segments. The commutator segments rotate relative to the *stator* and maintain contact to the external power supply through the *brushes*. Practical motors have windings that contain many loops, instead of the single loop shown in Figure (6.21). The resultant torque generated by a winding having N loops is

$$\mathbf{t} = \underbrace{(2NBrI)}_{k_t} \mathbf{x} = tx$$

This expression may be re-cast in terms of a single torque constant $k_t = (2NrI/B)$ that collects the electromechanical properties of the motor into a single term, such that

$$t = k_t i \quad (6.9.1)$$

Equation (6.9.1) provides a characterization of how the applied torque varies with the input current, but it does not describe how the current varies as a function of time. Whenever a conductor moves in a magnetic field, a voltage develops across that conductor. This induced potential difference is the *back electromotive force (EMF)*. Faraday's law states that the back EMF is equal to the time derivative of the *magnetic flux linkage* λ in the winding

$$e_b = -\frac{d}{dt}(\lambda).$$

The *magnetic flux linkage* λ in the winding that contains N turns is

$$\lambda = N\phi,$$

where the *magnetic flux linkage* ϕ in a single loop is defined as

$$\phi = \int \mathbf{B} \times \mathbf{n} dA.$$

In this equation \mathbf{B} is the *magnetic flux*, \mathbf{n} is a unit vector perpendicular to the loop of wire, and the integral is carried out over the area enclosed by the wire. The linkage ϕ is computed to be

$$\begin{aligned} \phi &= \int (By) \times (-\sin\theta\mathbf{y} + \cos\theta\mathbf{z}) dA \\ &= 2BrI \cos\theta \end{aligned}$$

where θ is the angle between the y axis and the loop of wire ($\theta = \frac{\pi}{2}$ for the example under consideration). The voltage that develops across the ends of the winding is consequently

$$e_b = (2NBrI \sin\theta)\dot{\theta} = \underbrace{(2NBrI)}_{k_b} \dot{\theta} = k_b \dot{\theta}$$

The constant k_b is the *back EMF constant* of the electric motor. Kirchoff's voltage law can now be applied around the circuit formed by the power supply, brushes, commutator and armature windings to show that

$$\begin{aligned} e_i - L \frac{di}{dt} - Ri - e_b &= 0, \\ L \frac{di}{dt} + Ri + k_b \dot{\theta} &= e_i, \end{aligned}$$

where L is the armature inductance and R is the armature resistance. These results in the following theorem.

Theorem 6.8. Let e_i be the voltage input and θ be the rotation of the DC motor shown Figure (6.21) which has armature inductance L and resistance R . The equation governing the armature circuit is

$$L \frac{di}{dt} + Ri + k_b \dot{\theta} = e_i,$$

where the back EMF is $e_b = k_b \dot{\theta}$. The torque that acts on the armature is $t = k_t i$.

Example 6.9.1. Suppose that the θ_1 constraint that drives link 1 of the spherical robotic manipulator is actuated by a DC motor. What are the changes to the resulting equations of motion for the system?

Solution: As shown in Problem (5.25), the equations of motion for the spherical robotic manipulator can be written in the form

$$\mathbf{M}(\mathbf{q}(t))\ddot{\mathbf{q}} = \mathbf{n}(\mathbf{q}(t), \dot{\mathbf{q}}(t)) + \boldsymbol{\tau}, \quad (6.9.2)$$

where $q = \{\theta_1 \ \theta_2 \ d_{q,r}\}^T$ is the vector of generalized coordinates, $\boldsymbol{\tau} = \{t_1 \ t_2 \ f\}^T$ are the actuator inputs, and the generalized mass matrix and nonlinear right hand side are

$$\begin{aligned} \mathbf{M}(\mathbf{q}) &= \\ &\begin{bmatrix} m_3(d_{p,q}^2 + \sin^2 \theta_2 d_{q,r}^2) + m_2(d_{p,q} - y_{q,c_2})^2 & m_3 \cos \theta_2 d_{p,q} d_{q,r} & m_3 \sin \theta_2 d_{p,q} \\ m_3 \cos \theta_2 d_{p,q} d_{q,r} & m_3 d_{q,r}^2 & 0 \\ m_3 \sin \theta_2 d_{p,q} & 0 & m_3 \end{bmatrix}, \\ \mathbf{n}(\mathbf{q}, \dot{\mathbf{q}}) &= \\ &\left\{ \begin{array}{l} -m_3(\sin \theta_2 d_{q,r}(2 \sin \theta_2 \dot{\theta}_1 \dot{d}_{q,r} - d_{p,q} \dot{\theta}_2^2) + 2 \cos \theta_2 d_{p,q} \dot{\theta}_2 \dot{d}_{q,r} + \sin 2\theta_2 \dot{\theta}_1 \dot{\theta}_2 d_{q,r}^2) \\ \frac{1}{2} m_3 d_{q,r}(-4 \dot{\theta}_2 \dot{d}_{q,r} + \sin 2\theta_2 \dot{\theta}_1^2 d_{q,r} - 2g \sin \theta_2) \\ m_3(d_{q,r}(\dot{\theta}_2^2 + \sin^2 \theta_2 \dot{\theta}_1^2) + g \cos \theta_2) \end{array} \right\}. \end{aligned}$$

This example determines the torque t_1 when the joint 1 is driven by a DC motor. Figure (6.23) provides a free body diagram of link 1. The torque t_1 is applied on the link by the motor shaft, the torque t_{a1} is the torque applied to the armature that is connected to the rotating shaft, and the torque t_r is the reaction torque applied on the stator by the ground. Applying Euler's Second Law about the \mathbf{z}_0 axis for the armature results in

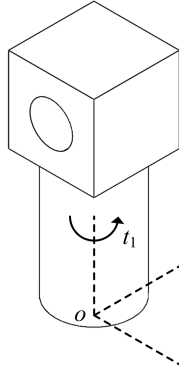


Fig. 6.23: Free Body Diagram of Link 1

$$J_1 \ddot{\theta}_1 = t_{a1} - t_1, \quad (6.9.3)$$

where J_1 is the inertia of the armature about the \mathbf{z}_0 axis. From Theorem (6.8) it is known that the circuit through the armature satisfies

$$L_1 \frac{di_1}{dt} + R_1 i_1 + k_{b1} \dot{\theta}_1 = e_1, \quad (6.9.4)$$

$$t_{a1} = k_{t1} i_1. \quad (6.9.5)$$

The following observations are made regarding the full system of governing equations.

1. The most general form of the governing equations, when J_{a1}, L_1, R_1 are non-negligible, is obtained by solving the Equation (6.9.3) for the torque t_1 and substituting the result into Equation (6.9.2). When Equation (6.9.4) is appended to the resulting system of equations, four differential equations are obtained:

$$\left\{ \mathbf{M}(\mathbf{q}) + \begin{bmatrix} J_1 & 0 & 0 \\ 0 & 0 & 0 \\ 0 & 0 & 0 \end{bmatrix} \right\} \ddot{\mathbf{q}} = \mathbf{n}(\mathbf{q}, \dot{\mathbf{q}}) + \begin{Bmatrix} k_{t1} i_1 \\ t_2 \\ f \end{Bmatrix},$$

$$L_1 \frac{di_1}{dt} + R_1 i_1 + k_{b1} \dot{\theta}_1 = e_1.$$

- These equations can be cast as a system of 7 nonlinear, first order equations where the state $\mathbf{x} = \{\theta_1 \ \theta_2 \ d_{q,r} \dot{\theta}_1 \ \dot{\theta}_2 \ \dot{d}_{q,r} \ i_1\}^T$ and the input is the voltage e_1 .
2. If the inductance L_1 is negligible, it is possible to solve for the current in Equation (6.9.4). In this case the system of governing equations can be reduced to the form

$$\left\{ \mathbf{M}(\mathbf{q}) + \begin{bmatrix} J_1 & 0 & 0 \\ 0 & 0 & 0 \\ 0 & 0 & 0 \end{bmatrix} \right\} \ddot{\mathbf{q}} = \mathbf{n}(\mathbf{q}, \dot{\mathbf{q}}) + \begin{Bmatrix} -\frac{1}{R_1} k_{t_1} k_b \dot{\theta}_1 \\ t_2 \\ f \end{Bmatrix} + \begin{Bmatrix} \frac{1}{R} k_{t_1} \\ 0 \\ 0 \end{Bmatrix} e_1.$$

3. If the inertia of the armature is negligible, the torque applied by the magnetic field on the armature is equal to the torque applied on the link 1 by the motor. That is,

$$t_1 = t_{a_1} = k_{t_1} i_1.$$

In this case the governing equations are

$$\begin{aligned} \mathbf{M}(\mathbf{q}) \ddot{\mathbf{q}} &= \mathbf{n}(\mathbf{q}, \dot{\mathbf{q}}) + \begin{Bmatrix} k_{t_1} i_1 \\ t_2 \\ f \end{Bmatrix}, \\ L_1 \frac{di_1}{dt} + R_1 i_1 + k_{b_1} \dot{\theta}_1 &= e_1. \end{aligned}$$

The analysis in Example (6.9.1) is based on the application of the Newton-Euler equations for individual bodies that make up the robotic system and the application of Kirchoff's Voltage Law for the electrical circuit. This approach can be used to study any robotic system. Often it can be advantageous to deduce the form of the equations of motion that include actuator physics for the robotic system using principles of analytic mechanics. This strategy simply adds the appropriate additional terms to the kinetic and potential energy that are introduced by the physics of the actuator. In such a strategy it is often possible to derive the equations of motion without an actuator model, and then to add terms subsequently that account for actuator physics. The following example illustrates the utility of this method.

Example 6.9.2. Suppose that link 2 of the spherical robotic manipulator is actuated by a DC motor. What are the changes to the resulting equations of motion?

Solution: The governing equations for the spherical robotic manipulator have been derived as

$$\mathbf{M}(\mathbf{q}(t)) \ddot{\mathbf{q}}(t) = \mathbf{n}(\mathbf{q}(t), \dot{\mathbf{q}}(t)) + \boldsymbol{\tau},$$

where

$$\mathbf{M}(\mathbf{q}) = \begin{bmatrix} m_3(d_{p,q}^2 + \sin^2 \theta_2 d_{q,r}^2) + m_2(d_{p,q} - y_{q,c_2})^2 & m_3 \cos \theta_2 d_{p,q} d_{q,r} & m_3 \sin \theta_2 d_{p,q} \\ m_3 \cos \theta_2 d_{p,q} d_{q,r} & m_3 d_{q,r}^2 & 0 \\ m_3 \sin \theta_2 d_{p,q} & 0 & m_3 \end{bmatrix},$$

$$\mathbf{n}(\mathbf{q}, \dot{\mathbf{q}}) = \begin{Bmatrix} -m_3(\sin \theta_2 d_{q,r}(2 \sin \theta_2 \dot{\theta}_1 \dot{d}_{q,r} - d_{p,q} \dot{\theta}_2^2) + 2 \cos \theta_2 d_{p,q} \dot{\theta}_2 \dot{d}_{q,r} + \sin 2\theta_2 \dot{\theta}_1 \dot{\theta}_2 d_{q,r}^2) \\ \frac{1}{2} m_3 d_{q,r}(-4 \dot{\theta}_2 \dot{d}_{q,r} + \sin 2\theta_2 \dot{\theta}_1^2 d_{q,r} - 2g \sin \theta_2) \\ m_3(d_{q,r}(\dot{\theta}_2^2 + \sin^2 \theta_2 \dot{\theta}_1^2) + g \cos \theta_2) \end{Bmatrix},$$

$$\boldsymbol{\tau} = \begin{Bmatrix} \tau_1 \\ \tau_2 \\ f \end{Bmatrix}.$$

The calculation of the generalized force $\mathbf{Q} = \boldsymbol{\tau}$ has been carried out assuming that the actuator torque τ_2 is applied to link 2 and the equal and opposite torque ($-\tau_2$) is applied to link 1 about the horizontal revolute joint. A DC motor is introduced that actuates joint 2 by fixing the stator and motor casing to link 1 and by fixing the armature and drive shaft to link 2. Because of these additions, the mass and inertia matrices for both links should be updated to include the additional contributions to each rigid body,

$$\begin{aligned} m_1 &= m_{1,\text{link}} + \Delta m_{1,\text{stator}}, \\ m_2 &= m_{2,\text{link}} + \Delta m_{2,\text{armature}}, \\ \mathbf{I}_1 &= \mathbf{I}_{1,\text{link}} + \Delta \mathbf{I}_{1,\text{stator}}, \\ \mathbf{I}_2 &= \mathbf{I}_{2,\text{link}} + \Delta \mathbf{I}_{2,\text{armature}}. \end{aligned}$$

The forces and moments that act between the two links, which now include the rigidly attached stator and rotor, are depicted in Figure (6.24). The reaction forces g_1, g_2, g_3 and moments m_1 and m_2 enforce the constraints associated with the revolute joint and perform no virtual work. They do not contribute to the equations of motion obtained via Lagrange's equations. The actuation moment τ_2 is precisely the torque applied to the armature about the revolute joint axis. Therefore,

$$\begin{aligned} L_2 \frac{di_2}{dt} + R_2 i_2 + k_{b_2} \dot{\theta}_2 &= e_2, \\ \tau_2 &= k_{t_2} i_2, \end{aligned}$$

where R_2 and L_2 are the armature resistance and inductance in the motor. The governing equations, including the model for the electric motor that drives joint 1 studied in Example (6.9.1), can be written in the form

$$\mathbf{M}(\mathbf{q})\ddot{\mathbf{q}} = \mathbf{n}(\mathbf{q}, \dot{\mathbf{q}}) + \begin{Bmatrix} 0 \\ 0 \\ f \end{Bmatrix} + \begin{bmatrix} k_{t_1} & 0 \\ 0 & k_{t_2} \\ 0 & 0 \end{bmatrix} \begin{Bmatrix} i_1 \\ i_2 \end{Bmatrix},$$

$$\begin{bmatrix} L_1 & 0 \\ 0 & L_2 \end{bmatrix} \begin{Bmatrix} \frac{di_2}{dt} \\ \frac{di_2}{dt} \end{Bmatrix} + \begin{bmatrix} R_1 & 0 \\ 0 & R_2 \end{bmatrix} \begin{Bmatrix} i_1 \\ i_2 \end{Bmatrix} + \begin{bmatrix} k_{b_1} & 0 \\ 0 & k_{b_2} \end{bmatrix} \begin{Bmatrix} \dot{\theta}_1 \\ \dot{\theta}_2 \end{Bmatrix} = \begin{Bmatrix} e_1 \\ e_2 \end{Bmatrix}.$$

It is important to note that the generalized mass matrix $\mathbf{M}(\mathbf{q})$ in the above equation is the *new* mass matrix obtained with the addition of the motor components to each of the links. Just as in Example (6.9.1), it is possible to derive special forms of these equations if it happens that armature inertias or motor inductances are negligible.

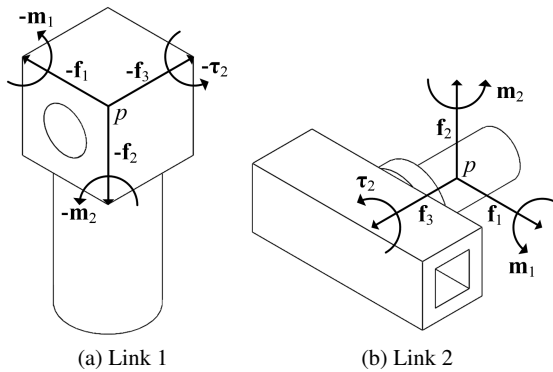


Fig. 6.24: Free Body Diagrams

6.9.2 Linear Actuators

This book focuses on constructing robotic systems primarily through the introduction of either revolute or prismatic joints, or a superposition of these joints. The previous section introduced the fundamental underlying principles by which a DC motor converts electrical energy into rotational motion. These systems can be applied directly to drive revolute joints in robotic systems. Actuators that are used commonly to drive prismatic joints include hydraulic cylinders, pneumatic pistons, and electromechanical linear motors. Hydraulic and pneumatic actuation can be attractive in applications that require large loads and stroke. Earth moving machinery, such as an excavator or bulldozer, makes use of hydraulic cylinders. Electrical linear motors are used in applications that require rapid response and portability, and they

are common components used for actuation of robotic systems. This section focuses on the class of *electromechanical linear motors*.

An *electromechanical linear motor* is an actuator that combines a conventional electric motor and a mechanical subsystem to convert the rotational motion of the motor into translational motion. The mechanical subsystem may consist of a screw mechanism or gears, for example. Figure (6.25) illustrates the primary components of a typical electromechanical linear motor. The electric motor rotates the lead screw which translates the linear stage along the guide rails. The drive nut embedded in the linear stage is prevented from rotating by the guide rails of the drive casing as it travels along the lead screw.

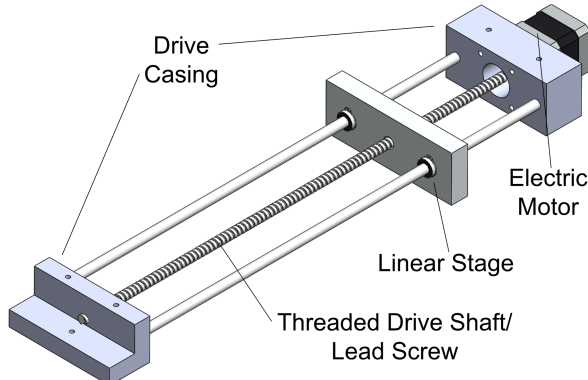


Fig. 6.25: Schematic of an Electromechanical Linear Motor

Example 6.9.3. Derive the equations of motion for the electromechanical linear motor shown in Figure (6.25) when the motor is fixed in the inertial frame and a force f is applied to the linear stage.

Solution: The kinetic energy of the system can be written

$$T = \frac{1}{2}m_T\dot{x}^2 + \frac{1}{2}J\dot{\theta}^2$$

where m_T is the mass of the linear stage, J is the moment of inertia of the armature and drive shaft, x is the displacement of the linear stage and θ is the rotation of the armature. The displacement x and rotation θ satisfy the kinematic equation

$$x = c\theta$$

where c is the pitch constant of the lead screw that has units of m/rad. The virtual work performed by the applied external force f acting on the linear stage and by the torque τ applied to the armature is

$$\begin{aligned}\delta W &= (\mathbf{f}\mathbf{x}_0) \cdot \delta \mathbf{r}_p + \tau \delta \theta, \\ &= (\mathbf{f}\mathbf{x}_0) \cdot \delta x \mathbf{x}_0 + \tau \delta \theta, \\ &= (cf + \tau) \delta \theta = Q_\theta \delta \theta.\end{aligned}$$

Lagrange's equations yield

$$\begin{aligned}\frac{d}{dt} \left(\frac{\partial T}{\partial \dot{\theta}} \right) - \frac{\partial T}{\partial \theta} + \frac{\partial V}{\partial \theta} &= Q_\theta, \\ (J + m_T c^2) \ddot{\theta} &= cf + \tau.\end{aligned}$$

The combined set of electrical and mechanical domain equations for the linear motor are

$$\begin{aligned}(J + m_T c^2) \ddot{\theta} &= cf + k_t i, \\ L \frac{di}{dt} + Ri + k_b \dot{\theta} &= e.\end{aligned}$$

where L is the armature inductance, R is the armature resistance, k_b is the back EMF constant, k_t is the motor torque constant, and e is the input voltage. The mechanical subsystem equation can be written in terms of the displacement of the motor as

$$\left(m_T + \frac{J}{c^2} \right) \ddot{x} = f + \frac{1}{c} k_t i$$

Example 6.9.4. Suppose that link 3 of the spherical robot manipulator is actuated using an electromechanical linear motor as depicted in Figure (6.25). Assume that the inertia matrix of the armature and drive shaft assembly is negligible and that the links can be modeled as lumped masses located at their mass centers. Find the complete set of governing equations when actuator dynamics discussed in Examples 6.9.1 and 6.9.2 are included in the model of the robotic system.

Solution: Suppose that the linear actuator in Figure (6.25) is mounted in the robotic arm such that the electric motor housing and stator are fixed to the link 2 and the linear stage is rigidly attached to link 3, the telescoping arm. In this case the mass and inertia matrix of link 2 are modified so that they include the additional terms due to the actuator. Let $\Delta m_2, \Delta \mathbf{I}_2$ be the mass and inertia matrix of all of the components of the linear actuator that are rigidly attached to link 2.

$$\begin{aligned}m_2 &= m_{2, \text{link}} + \Delta m_2, \\ \mathbf{I}_2 &= \mathbf{I}_{2, \text{link}} + \Delta \mathbf{I}_2.\end{aligned}$$

Likewise, the mass and inertia matrices for link 3 are modified to include contributions of additional terms for the attached actuator. Let $\Delta m_3, \Delta \mathbf{I}_3$ be the mass and

inertia matrix of the components of the electromechanical actuator that are rigidly attached to link 3,

$$\begin{aligned} m_3 &= m_{3, \text{link}} + \Delta m_3, \\ \mathbf{I}_3 &= \mathbf{I}_{3, \text{link}} + \Delta \mathbf{I}_2. \end{aligned}$$

The distance $d_{q,r}(t)$ that has been used to locate the center of mass of link 3 as a function of time is related to the displacement $x(t)$ in the actuator via

$$d_{q,r}(t) = x(t) + z_{c_3}$$

where z_{c_3} is a constant. The addition of mass to link 2 and link 3 will alter the locations of the mass centers of the links, and it is assumed that y_{q,c_2} and z_{c_3} reflect these updated center of mass positions. The rotation θ_a of the armature relative to the motor casing is related to the displacement of the linear actuator $x = c\theta_a$, where c is the screw pitch having units of meters per radian. The kinetic energy of the armature and drive shaft can be written as

$$T_a = \frac{1}{2}m_a \mathbf{v}_{0,c_a} \cdot \mathbf{v}_{0,c_a} + \frac{1}{2}\boldsymbol{\omega}_{0,a} \cdot \mathbf{I}_a \boldsymbol{\omega}_{0,a}$$

where \mathbf{v}_{0,c_a} is the velocity of the mass center of the armature and drive shaft assembly, and $\boldsymbol{\omega}_{0,a}$ is the angular velocity of the armature

$$\boldsymbol{\omega}_{0,a} = \boldsymbol{\omega}_{0,2} + \dot{\theta}_a \mathbf{z}_3 = \boldsymbol{\omega}_{0,2} + \frac{1}{c} \dot{x} \mathbf{z}_3.$$

With all of these changes, the kinetic energy of the robot can be written as

$$\begin{aligned} T &= T_1 + T_2 + T_3 + T_a, \\ &= \frac{1}{2}m_1 \mathbf{v}_{0,1} \cdot \mathbf{v}_{0,1} + \frac{1}{2}\boldsymbol{\omega}_{0,1} \cdot \mathbf{I}_1 \boldsymbol{\omega}_{0,1}, \\ &\quad + \frac{1}{2}m_2 \mathbf{v}_{0,2} \cdot \mathbf{v}_{0,2} + \frac{1}{2}\boldsymbol{\omega}_{0,2} \cdot \mathbf{I}_2 \boldsymbol{\omega}_{0,2}, \\ &\quad + \frac{1}{2}m_3 \mathbf{v}_{0,3} \cdot \mathbf{v}_{0,3} + \frac{1}{2}\boldsymbol{\omega}_{0,3} \cdot \mathbf{I}_3 \boldsymbol{\omega}_{0,3}, \\ &\quad + \frac{1}{2}m_a \mathbf{v}_{0,c_a} \cdot \mathbf{v}_{0,c_a} + \frac{1}{2}\boldsymbol{\omega}_{0,a} \cdot \mathbf{I}_a \boldsymbol{\omega}_{0,a}. \end{aligned}$$

The kinetic energy has been written explicitly in this form to emphasize that the armature and drive shaft make contributions to the total kinetic energy. It has been assumed that these terms are negligible in the remainder of this example. The final form of the kinetic energy, using a lumped mass approximation, assuming the armature mass and inertia are negligible becomes, and observing that the link 1 center of mass does not translate, becomes

$$T = \frac{1}{2}m_2 \mathbf{v}_{0,2} \cdot \mathbf{v}_{0,2} + \frac{1}{2}m_3 \mathbf{v}_{0,3} \cdot \mathbf{v}_{0,3}.$$

The potential energy has the form $V = m_3 g(d_{o,p} - d_{q,r} \cos \theta_2)$, where the mass m_3 and definition of $d_{q,r}$ account for the actuator mass contributions. The virtual work performed by the electromagnetic torque τ_3 acting on the armature is equal to $\delta W = \tau_3 \delta \theta_a = \tau_3 \frac{1}{c} \delta x = \frac{1}{c} \tau_3 \delta d_{q,r}$.

Kirchoff's voltage law for the armature circuit is

$$L_3 \frac{di_3}{dt} + R_3 i_3 + k_{b_3} \dot{\theta}_a = e_3,$$

$$\tau_3 = k_{t_3} i_3,$$

where L_3 and R_3 are the armature inductance and resistance, respectively, k_{b_3} is the motor back EMF constant, i_3 is the armature current and e_3 is the input voltage. The final system of governing equations is therefore

$$\mathbf{M}(\mathbf{q})\ddot{\mathbf{q}} = \mathbf{n}(\mathbf{q}, \dot{\mathbf{q}}) + \begin{Bmatrix} \tau_1 \\ \tau_2 \\ \frac{1}{c} k_{t_3} i_3 \end{Bmatrix},$$

$$L_3 \frac{di_3}{dt} + R_3 i_3 + \frac{1}{c} k_{b_3} \dot{d}_{q,r} = e_3.$$

The generalized mass matrix \mathbf{M} and nonlinear right hand side \mathbf{n} have the same form as derived in previous problems for this robotic structure, but with the coefficients m_2 and m_3 modified for the addition of mass of the linear actuator.

If the equations are collected from Examples 6.9.1 and 6.9.2 for the joint 1 and 2 actuators, along with these equations for the linear actuator, the following equations can be constructed to represent the robotic system with actuator dynamics

$$\mathbf{M}(\mathbf{q}(t))\ddot{\mathbf{q}}(t) = \mathbf{n}(\mathbf{q}(t), \dot{\mathbf{q}}(t)) + \begin{bmatrix} K_{b_1} & 0 & 0 \\ 0 & K_{t_2} & 0 \\ 0 & 0 & \frac{1}{c} K_{t_3} \end{bmatrix} \begin{Bmatrix} i_1 \\ i_2 \\ i_3 \end{Bmatrix},$$

$$\begin{bmatrix} L_1 & 0 & 0 \\ 0 & L_2 & 0 \\ 0 & 0 & L_3 \end{bmatrix} \begin{Bmatrix} \frac{di_1}{dt} \\ \frac{di_2}{dt} \\ \frac{di_3}{dt} \end{Bmatrix} + \begin{bmatrix} R_1 & 0 & 0 \\ 0 & R_2 & 0 \\ 0 & 0 & R_3 \end{bmatrix} \begin{Bmatrix} i_1 \\ i_2 \\ i_3 \end{Bmatrix} + \begin{bmatrix} K_{b_1} & 0 & 0 \\ 0 & K_{b_2} & 0 \\ 0 & 0 & \frac{1}{c} K_{b_3} \end{bmatrix} \begin{Bmatrix} \dot{\theta}_1 \\ \dot{\theta}_2 \\ \dot{d}_{qr} \end{Bmatrix} = \begin{Bmatrix} e_1 \\ e_2 \\ e_3 \end{Bmatrix}.$$

In this equation, \mathbf{M} and \mathbf{n} are modified from their nominal values without actuators to account for the mass and inertia of the two rotational and one linear actuator. The next section will show that these equations are one example of a general form for the equations of motion of robotic systems that include actuator dynamics.

6.10 Backstepping Control and Actuator Dynamics

This chapter has discussed several methods for deriving feedback controllers having the structure $\tau(t) := \tau(\mathbf{q}(t), \dot{\mathbf{q}}(t))$ for robotic systems that take the form

$$\mathbf{M}(\mathbf{q}(t))\ddot{\mathbf{q}}(t) = \mathbf{n}(\mathbf{q}(t), \dot{\mathbf{q}}(t)) + \boldsymbol{\tau}. \quad (6.10.1)$$

Stability and convergence of the controlled system is based on analysis of a Lyapunov function that is tailored to the form of the governing Equation (6.10.1) and the specific feedback input $\boldsymbol{\tau} := \boldsymbol{\tau}(\mathbf{q}(t), \dot{\mathbf{q}}(t))$. As noted in the previous section, it is rare for actuation torques or forces to be directly controlled in practice. It is much more common that commanded inputs take the form of voltages or currents that drive motors, which in turn generate forces or moments that act on the robot. It has been shown that one of the general models that include actuator dynamics arising from DC motors or electromechanical linear actuators consist of a set of coupled mechanical and electrical subsystems

$$\mathbf{M}(\mathbf{q}(t))\ddot{\mathbf{q}}(t) = \mathbf{n}(\mathbf{q}(t), \dot{\mathbf{q}}(t)) + \mathbf{K}_t \mathbf{i}(t), \quad (6.10.2)$$

$$\mathbf{L} \frac{d\mathbf{i}}{dt}(t) + \mathbf{R}\mathbf{i}(t) + \mathbf{K}_b \dot{\mathbf{q}}(t) = \mathbf{e}(t), \quad (6.10.3)$$

where \mathbf{L} is the diagonal $N \times N$ inductance matrix, \mathbf{R} is the diagonal $N \times N$ resistance matrix, \mathbf{K}_b is the diagonal $N \times N$ back EMF constant matrix, and \mathbf{K}_t is the diagonal $N \times N$ torque constant matrix. Equations (6.10.2) and (6.10.3) can also be rewritten in first order form as a pair of equations

$$\dot{\mathbf{x}}_1(t) = \mathbf{f}(\mathbf{x}_1(t)) + \mathbf{G}(\mathbf{x}_1(t))\mathbf{x}_2(t), \quad (6.10.4)$$

$$\dot{\mathbf{x}}_2(t) = \mathbf{h}(\mathbf{x}_1(t), \mathbf{x}_2(t), \mathbf{u}(t)). \quad (6.10.5)$$

Suppose that an ideal feedback law $\mathbf{x}_2(t) := \mathbf{k}(\mathbf{x}_1(t))$ could be imposed directly in Equation (6.10.4). Also suppose that the stability of the motion of \mathbf{x}_1 that would result when this ideal feedback is substituted into Equation (6.10.4) is guaranteed by a Lyapunov function that satisfies

$$\begin{aligned} \mathcal{V}_1 &:= \mathcal{V}_1(\mathbf{x}_1) > 0 && \text{for all } \mathbf{x}_1 \neq 0, \\ \dot{\mathcal{V}}_1 &:= \frac{\partial \mathcal{V}}{\partial \mathbf{x}_1} \cdot (\mathbf{f}(\mathbf{x}_1) + \mathbf{G}(\mathbf{x}_1)\mathbf{k}(\mathbf{x}_1)) < 0 && \text{for all } \mathbf{x}_1 \neq 0. \end{aligned} \quad (6.10.6)$$

However, when the coupled pair of Equations (6.10.4) and (6.10.5) are considered together, it is the input $\mathbf{u}(t)$ for $t \in \mathbb{R}^+$ that is imposed, and it cannot be guaranteed that the desired control law $\mathbf{x}_2(t) \equiv \mathbf{k}(\mathbf{x}_1(t))$ holds for each $t \in \mathbb{R}^+$. Define a new state \mathbf{z} as

$$\mathbf{z}(t) := \mathbf{x}_2(t) - \mathbf{k}(\mathbf{x}_1(t))$$

that measures how closely the evolution of the coupled system comes to satisfying the ideal control law. With the introduction of the new state \mathbf{z} , the governing

equations in first order form can now be expressed as

$$\begin{aligned}\dot{\mathbf{x}}_1(t) &= \mathbf{f}(\mathbf{x}_1) + \mathbf{G}(\mathbf{x}_1(t))\mathbf{k}(\mathbf{x}_1(t)) + \mathbf{G}(\mathbf{x}_1)\mathbf{z}(t) \\ \dot{\mathbf{z}}(t) &= \mathbf{h}(t) - \dot{\mathbf{k}}(t) := \mathbf{v}(t)\end{aligned}$$

By using the assumption that the control law $\mathbf{k}(\mathbf{x}_1)$ corresponds to the Lyapunov function \mathcal{V}_1 that satisfies the conditions in Equation (6.10.6), it is possible to define a feedback controller for the coupled pair of equations. Choose the Lyapunov function

$$\mathcal{V}_2\left(\begin{Bmatrix} \mathbf{x}_1 \\ \mathbf{z} \end{Bmatrix}\right) := \mathcal{V}_1(\mathbf{x}_1) + \frac{1}{2}\mathbf{z}^T\mathbf{z}$$

When the derivative of the Lyapunov function \mathcal{V}_2 is calculated along the trajectories of the coupled pair of equations,

$$\begin{aligned}\dot{\mathcal{V}}_2 &= \frac{\partial \mathcal{V}_1}{\partial \mathbf{x}_1} \cdot \{(\mathbf{f}(\mathbf{x}_1) + \mathbf{G}(\mathbf{x}_1)\mathbf{k}(\mathbf{x}_1)) + \mathbf{G}(\mathbf{x}_1)\mathbf{z}\} + \mathbf{z}^T \dot{\mathbf{z}}, \\ &= \underbrace{\frac{\partial \mathcal{V}_1}{\partial \mathbf{x}_1} \cdot \{\mathbf{f}(\mathbf{x}_1) + \mathbf{G}(\mathbf{x}_1)\mathbf{k}(\mathbf{x}_1)\}}_{<0 \text{ for all } \mathbf{x}_1 \neq 0} + \mathbf{z}^T \left\{ \mathbf{G}(\mathbf{x}_1)^T \frac{\partial \mathcal{V}_1}{\partial \mathbf{x}_1} + \mathbf{v} \right\}.\end{aligned}$$

Now suppose \mathbf{v} is chosen to be

$$\mathbf{v} := -\kappa \mathbf{z} - \mathbf{G}(\mathbf{x}_1)^T \frac{\partial \mathcal{V}_1}{\partial \mathbf{x}_1}^T. \quad (6.10.7)$$

For this case, it follows that

$$\begin{aligned}\mathcal{V}_2\left(\begin{Bmatrix} \mathbf{x}_1 \\ \mathbf{z} \end{Bmatrix}\right) &> 0 \quad \text{for all } \begin{Bmatrix} \mathbf{x}_1 \\ \mathbf{z} \end{Bmatrix} \neq 0, \\ \dot{\mathcal{V}}_2\left(\begin{Bmatrix} \mathbf{x}_1 \\ \mathbf{z} \end{Bmatrix}\right) &< 0 \quad \text{for all } \begin{Bmatrix} \mathbf{x}_1 \\ \mathbf{z} \end{Bmatrix} \neq 0.\end{aligned}$$

Therefore, the equilibrium at the origin of the coupled dynamics governing $\{\mathbf{x}_1^T \mathbf{x}_1^T\}^T$ is asymptotically stable. The use of *backstepping control* is shown in the following example.

Example 6.10.1. Design a setpoint controller for the robotic system studied in Example (6.9.4) using a backstepping controller by using the Lyapunov function and feedback controller based on ideal dynamic inversion.

Solution: Define the state

$$\mathbf{x}_1 := \begin{Bmatrix} \mathbf{e} \\ \dot{\mathbf{e}} \end{Bmatrix}$$

where $\mathbf{e} := \mathbf{q} - \mathbf{q}_d$. The “ideal feedback law” that consists of a feedforward component that achieves dynamic inversion and a proportional-derivative outer loop is

defined as

$$\begin{aligned}\mathbf{k}(\mathbf{x}_1) &:= \mathbf{K}_t^{-1} \{ \mathbf{M}(-\mathbf{G}_1(\dot{\mathbf{q}} - \dot{\mathbf{q}}_d) - \mathbf{G}_0(\mathbf{q} - \mathbf{q}_d)) - \mathbf{n} \}, \\ &= \mathbf{K}_t^{-1} \{ \mathbf{M}(-\mathbf{G}_1 \dot{\mathbf{e}} - \mathbf{G}_0 \mathbf{e}) - \mathbf{n} \}.\end{aligned}$$

When the state $\mathbf{z} := \mathbf{i} - \mathbf{k}(\mathbf{x}_1)$ that measures how well the state \mathbf{i} follows that ideal dynamic inversion control law is defined, the mechanical equations of motion can be written as

$$\begin{aligned}\dot{\mathbf{x}}_1(t) &:= \begin{bmatrix} \mathbf{0} & \mathbb{I} \\ -\mathbf{G}_0 & -\mathbf{G}_1 \end{bmatrix} \mathbf{x}_1(t) + \begin{bmatrix} \mathbf{0} \\ \mathbf{M}^{-1} \mathbf{K}_t \end{bmatrix} \mathbf{z}(t), \\ &= \mathbf{A} \mathbf{x}_1(t) + \mathbf{B} \mathbf{z}(t).\end{aligned}$$

Define the Lyapunov function associated with the state \mathbf{x}_1 to be $\mathcal{V}_1(\mathbf{x}_1) := \frac{1}{2} \mathbf{x}_1^T \mathbf{P} \mathbf{x}_1$ where \mathbf{P} is a symmetric, positive definite solution of Lyapunov's equation

$$\mathbf{P} \mathbf{A} + \mathbf{A}^T \mathbf{P} = -\mathbf{Q},$$

for some symmetric, positive matrix \mathbf{Q} . Such a matrix \mathbf{P} is guaranteed to exist since \mathbf{A} is Hurwitz. \mathcal{V}_1 may be verified as a Lyapunov function for the uncoupled equation in \mathbf{x}_1 that is obtained when $\mathbf{z}(t) \equiv 0$, or $\mathbf{i}(t) \equiv \mathbf{k}(\mathbf{x}_1(t))$, for all $t \in \mathbb{R}^+$.

The electrical domain equations, expressed in terms of the new state, become

$$\begin{aligned}\dot{\mathbf{z}} &= \frac{d\mathbf{i}}{dt} - \dot{\mathbf{k}}, \\ &= \mathbf{L}^{-1} (-\mathbf{R}\mathbf{i} - \mathbf{K}_b \dot{\mathbf{q}} + \mathbf{e}) - \dot{\mathbf{k}}.\end{aligned}$$

Next, the derivative $\dot{\mathbf{k}}$ of the feedback is expanded as

$$\begin{aligned}\dot{\mathbf{k}} &= \mathbf{K}_t^{-1} \mathbf{M} \begin{bmatrix} -\mathbf{G}_0 & -\mathbf{G}_1 \end{bmatrix} \dot{\mathbf{x}}_1 - \mathbf{K}_t^{-1} \frac{\partial \mathbf{n}}{\partial \mathbf{x}_1} \dot{\mathbf{x}}_1, \\ &= \underbrace{\left\{ \mathbf{K}_t^{-1} \mathbf{M} \begin{bmatrix} -\mathbf{G}_0 & -\mathbf{G}_1 \end{bmatrix} - \mathbf{K}_t^{-1} \frac{\partial \mathbf{n}}{\partial \mathbf{x}_1} \right\}}_{\mathbf{G}_2} \{ \mathbf{A} \mathbf{x}_1 + \mathbf{B} \mathbf{z} \}.\end{aligned}$$

The electrical subsystem governing equation can therefore be written as

$$\dot{\mathbf{z}} = \underbrace{\mathbf{L}^{-1} (-\mathbf{R}\mathbf{i} - \mathbf{K}_b \dot{\mathbf{q}} + \mathbf{e}) - \mathbf{G}_2 (\mathbf{A} \mathbf{x}_1 + \mathbf{B} \mathbf{z})}_{\mathbf{v}}$$

As derived in Equation (6.10.7), $\mathbf{v} := -\frac{1}{2} k \mathbf{z} - \mathbf{G}^T \frac{\partial \mathcal{V}_1}{\partial \mathbf{x}_1}^T$. This requires that

$$\mathbf{v} = -\frac{1}{2} k \mathbf{z} - \mathbf{G}^T \frac{\partial \mathcal{V}_1}{\partial \mathbf{x}_1}^T = \mathbf{L}^{-1} (\mathbf{R}\mathbf{i} - \mathbf{K}_b \dot{\mathbf{q}} + \mathbf{e}) - \mathbf{G}_2 (\mathbf{A} \mathbf{x}_1 + \mathbf{B} \mathbf{z}).$$

This identity holds when the input voltages \mathbf{e} to the actuators are prescribed as

$$\mathbf{e} = \mathbf{L} \left(-\frac{1}{2}k\mathbf{z} - \mathbf{B}^T \mathbf{P} \mathbf{x}_1 + \mathbf{G}_2 [\mathbf{A} \mathbf{x}_1 + \mathbf{B} \mathbf{z}] \right) - \mathbf{R} \dot{\mathbf{i}} + \mathbf{K}_b \dot{\mathbf{q}} \quad (6.10.8)$$

Now, the ability of the control input voltages \mathbf{e} to generate the desired asymptotic behavior will be verified. With the actuator voltages \mathbf{e} in Equation (6.10.8), the vector \mathbf{v} becomes

$$\mathbf{v} = -\frac{1}{2}k\mathbf{z} - \mathbf{B}^T \mathbf{P} \mathbf{x}_1.$$

Calculating the derivative of the Lyapunov function $\mathcal{V}_2 := \mathcal{V}_1 + \frac{1}{2}\mathbf{z}^T \mathbf{z}$ along the trajectories of the coupled mechanical-electrical system results in

$$\begin{aligned} \dot{\mathcal{V}}_2 &:= \frac{1}{2} \left[(\mathbf{A} \mathbf{x}_1 + \mathbf{B} \mathbf{z})^T \mathbf{P} \mathbf{x}_1 + \mathbf{x}_1^T \mathbf{P}^T (\mathbf{A} \mathbf{x}_1 + \mathbf{B} \mathbf{z}) \right] + \mathbf{z}^T \dot{\mathbf{z}}, \\ &= \frac{1}{2} \left[\mathbf{x}_1^T (\mathbf{A}^T \mathbf{P} + \mathbf{P} \mathbf{A}) \mathbf{x}_1 + \mathbf{z}^T \mathbf{B}^T \mathbf{P} \mathbf{x}_1 + \mathbf{z}^T \left(-\frac{1}{2}k\mathbf{z} - \mathbf{B}^T \mathbf{P} \mathbf{x}_1 \right) \right], \\ &= -\frac{1}{2} \mathbf{x}_1^T \mathbf{Q} \mathbf{x}_1 - \frac{1}{2} k \mathbf{z}^T \mathbf{z}. \end{aligned}$$

This shows that $\mathcal{V}_2 > 0$ and $\dot{\mathcal{V}}_2 < 0$ for $\mathbf{x} := \{\mathbf{x}_1^T \mathbf{z}^T\}^T \neq \mathbf{0}^T$. Therefore, the origin of the coupled dynamics is asymptotically stable.



6.11 Problems for Chapter (6), control of Robotic Systems

6.11.1 Problems on Gravity Compensation and PD setpoint control

Problem 6.1. A two degree of freedom PUMA model has been derived in Problem (5.21) for the robot depicted in Figures (5.25) and (5.26). The generalized coordinates for this robot have been selected to be

$$\mathbf{q}(t) := \begin{Bmatrix} \theta_1(t) \\ \theta_2(t) \end{Bmatrix},$$

where θ_1 and θ_2 are the angles for revolute joints 1 and 2, respectively. The generalized forces are

$$\boldsymbol{\tau}(t) := \begin{Bmatrix} \tau_1(t) \\ \tau_2(t) \end{Bmatrix},$$

where τ_1 and τ_2 are the actuation torques that act about the revolute joints 1 and 2, respectively. Let the system parameters for this robot be $m_1 = m_2 = 2$ kg and $L_1 = 0.25$ meters. Derive the controller that uses PD feedback with gravity compensation as described in Theorem (6.4) for this robot to achieve setpoint control. Write a program to simulate the performance of the controller. Plot the state trajectories, setpoint error, and control inputs as a function of time for various choices of the initial conditions, the target state and the choice of feedback gains.

Problem 6.2. A three degree of freedom model has been derived in Problem (5.22) for the PUMA robot depicted in Figures (5.25) and (5.26). The generalized coordinates for this robot have been selected to be

$$\mathbf{q}(t) := \begin{Bmatrix} \theta_1(t) \\ \theta_2(t) \\ \theta_3(t) \end{Bmatrix},$$

where θ_1, θ_2 and θ_3 are the angles for revolute joints 1, 2 and 3, respectively. The generalized forces are

$$\boldsymbol{\tau}(t) := \begin{Bmatrix} \tau_1(t) \\ \tau_2(t) \\ \tau_3(t) \end{Bmatrix},$$

where τ_1, τ_2 and τ_3 are the actuation torques that act at revolute joints 1, 2 and 3, respectively. Let the system parameters for this robot be $W = 0.5$ meters, $D = 0.5$ meters, $L_1 = 1$ meter, $L_2 = 1$ meter, and $m_3 = 20$ kg. Derive the controller that uses PD feedback with gravity composition as described in Theorem (6.4) for this robot to achieve setpoint control. Write a program to simulate the performance of the controller. Plot the state trajectories, setpoint error, and control inputs as a function of time for various choices of the initial conditions, the target state and the choice of feedback gains.

Problem 6.3. A two degree of freedom model has been derived in Problem (5.23) for the PUMA robot depicted in Figures (5.25) and (5.26). The generalized coordinates for this robot have been selected to be

$$\mathbf{q}(t) := \begin{Bmatrix} \theta_1(t) \\ \theta_2(t) \end{Bmatrix},$$

where θ_1 and θ_2 are the angles for revolute joints 1 and 2, respectively. The generalized forces are

$$\boldsymbol{\tau}(t) = \begin{Bmatrix} \tau_1(t) \\ \tau_2(t) \end{Bmatrix},$$

where τ_1 and τ_2 are the actuation torques that act at the revolute joints 1 and 2, respectively. Let the system parameters for this robot be $m_1 = m_2 = 25$ kg, $I_{11,2} = 20$ kg-m², $I_{22,2} = 25$ kg-m², $I_{33,2} = 10$ kg-m², $D = 0.25$ m and $L_1 = 0.5$ m. Derive the controller that uses PD feedback with gravity composition as described in Theorem (6.4) for this robot to achieve setpoint control. Write a program to simulate the performance of the controller. Plot the state trajectories, setpoint error, and control inputs as a function of time for various choices of the initial conditions, the target state and the choice of feedback gains.

Problem 6.4. A three degree of freedom model has been derived in Problem (5.24) for the Cartesian robot depicted in Figure (5.27). The generalized coordinates for this robot have been selected to be

$$\mathbf{q}(t) := \begin{Bmatrix} x(t) \\ y(t) \\ z(t) \end{Bmatrix},$$

where $x(t)$, $y(t)$ and $z(t)$ are the translations in the inertial $\mathbf{x}_0, \mathbf{y}_0, \mathbf{z}_0$ directions, respectively. The generalized forces are

$$\boldsymbol{\tau}(t) := \begin{Bmatrix} f_x \\ f_y \\ f_z \end{Bmatrix},$$

where f_x , f_y and f_z are the actuation forces acting along the prismatic joints along the inertial $\mathbf{x}_0, \mathbf{y}_0$ and \mathbf{z}_0 directions, respectively. Let the system parameters for this robot be $m_1 = 20$ kg, $m_2 = 10$ kg, $m_3 = 5$ kg. Derive the controller that uses PD feedback with gravity compensation as described in Theorem (6.4) for this robot to achieve setpoint control. Write a program to simulate the performance of the controller. Plot the state trajectories, setpoint error, and control inputs as a function of time for various choices of the initial conditions, the target state and the choice of feedback gains.

Problem 6.5. A three degree of freedom model has been derived in Problem (5.25) for the spherical wrist depicted in Figures (5.28) and (5.29). The generalized coordinate for this robot have been selected to be

$$\mathbf{q}(t) := \begin{Bmatrix} \psi(t) \\ \theta(t) \\ \phi(t) \end{Bmatrix},$$

where ψ, θ and ϕ are the angles for joints 1, 2 and 3, respectively. The generalized forces are

$$\boldsymbol{\tau}(t) = \begin{Bmatrix} \tau_1 \\ \tau_2 \\ \tau_3 \end{Bmatrix},$$

where τ_1, τ_2 and τ_3 are the actuation torques that act at joints 1, 2 and 3, respectively. Let the system parameters for this robot be $m_1 = 5 \text{ kg}$, $m_2 = 5 \text{ kg}$, $m_3 = 2 \text{ kg}$, $I_{33,1} = 5 \text{ kg}\cdot\text{m}^2$, $I_{33,2} = 4 \text{ kg}\cdot\text{m}^2$, $I_{33} = 2 \text{ kg}\cdot\text{m}^2$, $I_{11,3} = 3 \text{ kg}\cdot\text{m}^2$, $I_{22,2} = 1 \text{ kg}\cdot\text{m}^2$, $z_{p,c2} = 0.1 \text{ m}$, and $z_{q,c3} = 0.1 \text{ m}$. Derive the controller that uses PD feedback with gravity composition as described in Theorem (6.4) for this robot to achieve setpoint control. Write a program to simulate the performance of the controller. Plot the state trajectories, setpoint error, and control inputs as a function of time for various choices of the initial conditions, the target state and the choice of feedback gains.

Problem 6.6. A three degree of freedom model has been derived in Problem (5.26) for the SCARA robot depicted in Figures (5.30) and (5.31). The generalized coordinates for this robot have been selected to be

$$\mathbf{q}(t) := \begin{Bmatrix} \theta_1(t) \\ \theta_2(t) \\ d(t) \end{Bmatrix},$$

where θ_1, θ_2 are the joint variables for revolute joints 1, 2, respectively, and d is the joint variable for prismatic joint 3. The generalized forces are

$$\boldsymbol{\tau}(t) = \begin{Bmatrix} \tau_1 \\ \tau_2 \\ f \end{Bmatrix},$$

where τ_1, τ_2 are the actuation moments that drive revolute joints 1, 2, respectively and f is the actuation force that drives prismatic joint 3. Let the system parameters for this robot be $m_1 = 10 \text{ kg}$, $m_2 = 10 \text{ kg}$, $m_3 = 2 \text{ kg}$, $L_1 = 0.25 \text{ meters}$, $D_1 = 0.2 \text{ meters}$, $L_2 = 0.2 \text{ meters}$, $D_2 = 0.1 \text{ meters}$. Derive the controller that uses PD feedback with gravity composition as described in Theorem (6.4) for this robot to achieve setpoint control. Write a program to simulate the performance of the controller. Plot the state trajectories, setpoint error, and control inputs as a function of time for various choices of the initial conditions, the target state and the choice of feedback gains.

Problem 6.7. A three degree of freedom model has been derived in Problem (5.27) for the robot depicted in Figures (5.30) and (5.31). The generalized coordinates for this robot have been selected to be

$$\mathbf{q}(t) := \begin{Bmatrix} \theta_1(t) \\ \theta_2(t) \\ d(t) \end{Bmatrix},$$

where θ_1, θ_2 are the joint variables for revolute joints 1,2, respectively, and d is the displacement along prismatic joint 3. The generalized forces are

$$\boldsymbol{\tau}(t) = \begin{Bmatrix} \tau_1 \\ \tau_2 \\ f \end{Bmatrix},$$

where τ_1, τ_2 are the joint torques for revolute joints 1,2, respectively, and f is the joint force for prismatic joint 3. Let the system parameters for this robot be $m_1 = 5$ kg, $m_2 = 4$ kg, $m_3 = 2$ kg, $L_1 = 0.1$ meters, $L_2 = 0.2$ meters, $I_{33,1} = 2$ kg-m², $I_{33,2} = 3$ kg-m², $I_{33,3} = 4$ kg-m². Derive the controller that uses PD feedback with gravity composition as described in Theorem (6.4) for this robot to achieve setpoint control. Write a program to simulate the performance of the controller. Plot the state trajectories, setpoint error, and control inputs as a function of time for various choices of the initial conditions, the target state and the choice of feedback gains.

Problem 6.8. A three degree of freedom model has been derived in Problem (5.28) for the robot depicted in Figures (5.32) and (5.33). The generalized coordinates for this robot have been selected to be

$$\mathbf{q}(t) := \begin{Bmatrix} \theta(t) \\ H(t) \\ L(t) \end{Bmatrix},$$

where θ is the joint angle for revolute joint 1 and $H(t), L(t)$ are the displacements for prismatic joints 2,3, respectively. The generalized forces are

$$\boldsymbol{\tau}(t) := \begin{Bmatrix} \tau(t) \\ f_1(t) \\ f_2(t) \end{Bmatrix},$$

where τ is the actuation torque that acts on revolute joint 1 and f_1, f_2 are the actuation forces that act along prismatic joints 2,3, respectively. Let the system parameters for this robot be $m_1 = 10$ kg, $m_2 = 10$ kg, $m_3 = 3$ kg, $L_A = 0.2$ m, $H_1 = 0.3$ m, $D_2 = 0.2$ m, $H_3 = 0.1$ m and $D_3 = 0.2$ m. Derive the controller that uses PD feedback with gravity composition as described in Theorem (6.4) for this robot to achieve setpoint control. Write a program to simulate the performance of the controller. Plot the state trajectories, setpoint error, and control inputs as a function of time for various choices of the initial conditions, the target state and the choice of feedback gains.

Problem 6.9. A three degree of freedom model has been derived in Problem (5.29) for the robot depicted in Figures (5.32) and (5.33). The generalized coordinates for this robot have been selected to be

$$\mathbf{q}(t) := \begin{Bmatrix} \theta(t) \\ H(t) \\ L(t) \end{Bmatrix},$$

where θ is the angle revolute joint 1 and $H(t), L(t)$ are the displacements for prismatic joints 2,3, respectively. The generalized forces are

$$\boldsymbol{\tau}(t) := \begin{Bmatrix} m(t) \\ f_1(t) \\ f_2(t) \end{Bmatrix},$$

where m is the actuation torque for revolute joint 1 and f_1, f_2 are the actuation forces that act at along the prismatic joints 2,3, respectively. Let the system parameters for this robot be $m_1 = 10$ kg, $m_2 = 10$ kg, $m_3 = 3$ kg, $I_{33,1} = 2$ kg-m², $I_{33,3} = 10$ kg-m², $L_A = 0.2$ m, $H_1 = 0.3$ m, $D_2 = 0.2$ m, $H_3 = 0.1$ m and $D_3 = 0.2$ m. Derive the controller that uses PD feedback with gravity composition as described in Theorem (6.4) for this robot to achieve setpoint control. Write a program to simulate the performance of the controller. Plot the state trajectories, setpoint error, and control inputs as a function of time for various choices of the initial conditions, the target state and the choice of feedback gains.

6.11.2 Problems on Computed Torque Tracking Control

Problem 6.10. Consider the robot studied in Problem (6.1). Derive a tracking controller that uses the exact computed torque control with the outer loop selected to be PD feedback as in Theorem (6.3). Write a program to simulate the performance of the controller. Plot the state trajectories, tracking error, and control inputs as a function of time for various choices of the initial conditions, desired trajectories and the choice of feedback gains.

Problem 6.11. Consider the robot studied in Problem (6.2). Derive a tracking controller that uses the exact computed torque control with the outer loop selected to be PD feedback as in Theorem (6.3). Write a program to simulate the performance of the controller. Plot the state trajectories, tracking error, and control inputs as a function of time for various choices of the initial conditions, desired trajectories and the choice of feedback gains.

Problem 6.12. Consider the robot studied in Problem (6.3). Derive a tracking controller that uses the exact computed torque control with the outer loop selected to be PD feedback as in Theorem (6.3). Write a program to simulate the performance of the controller. Plot the state trajectories, tracking error, and control inputs as a function of time for various choices of the initial conditions, desired trajectories and the choice of feedback gains.

Problem 6.13. Consider the robot studied in Problem (6.4). Derive a tracking controller that uses the exact computed torque control with the outer loop selected to be PD feedback as in Theorem (6.3). Write a program to simulate the performance of the controller. Plot the state trajectories, tracking error, and control inputs as a function of time for various choices of the initial conditions, desired trajectories and the choice of feedback gains.

Problem 6.14. Consider the robot studied in Problem (6.5). Derive a tracking controller that uses the exact computed torque control with the outer loop selected to be PD feedback as in Theorem (6.3). Write a program to simulate the performance of the controller. Plot the state trajectories, tracking error, and control inputs as a function of time for various choices of the initial conditions, desired trajectories and the choice of feedback gains.

Problem 6.15. Consider the robot studied in Problem (6.6). Derive a tracking controller that uses the exact computed torque control with the outer loop selected to be PD feedback as in Theorem (6.3). Write a program to simulate the performance of the controller. Plot the state trajectories, tracking error, and control inputs as a function of time for various choices of the initial conditions, desired trajectories and the choice of feedback gains.

Problem 6.16. Consider the robot studied in Problem (6.7). Derive a tracking controller that uses the exact computed torque control with the outer loop selected to be PD feedback as in Theorem (6.3). Write a program to simulate the performance of the controller. Plot the state trajectories, tracking error, and control inputs as a function of time for various choices of the initial conditions, desired trajectories and the choice of feedback gains.

Problem 6.17. Consider the robot studied in Problem (6.8). Derive a tracking controller that uses the exact computed torque control with the outer loop selected to be PD feedback as in Theorem (6.3). Write a program to simulate the performance of the controller. Plot the state trajectories, tracking error, and control inputs as a function of time for various choices of the initial conditions, desired trajectories and the choice of feedback gains.

Problem 6.18. Consider the robot studied in Problem (6.9). Derive a tracking controller that uses the exact computed torque control with the outer loop selected to be PD feedback as in Theorem (6.3). Write a program to simulate the performance of the controller. Plot the state trajectories, tracking error, and control inputs as a function of time for various choices of the initial conditions, desired trajectories and the choice of feedback gains.

6.11.3 Problems on Dissipativity Based Tracking Control

Problem 6.19. Consider the robot studied in Problem (6.1). Derive a tracking controller that uses the controller based on dissipativity principles in Theorem (6.7).

Write a program to simulate the performance of the controller. Plot the state trajectories, tracking error, and control inputs as a function of time for various choices of the initial conditions, desired trajectories and the choice of feedback gains.

Problem 6.20. Consider the robot studied in Problem (6.2). Derive a tracking controller that uses the controller based on dissipativity principles in Theorem (6.7). Write a program to simulate the performance of the controller. Plot the state trajectories, tracking error, and control inputs as a function of time for various choices of the initial conditions, desired trajectories and the choice of feedback gains.

Problem 6.21. Consider the robot studied in Problem (6.3). Derive a tracking controller that uses the controller based on dissipativity principles in Theorem (6.7). Write a program to simulate the performance of the controller. Plot the state trajectories, tracking error, and control inputs as a function of time for various choices of the initial conditions, desired trajectories and the choice of feedback gains.

Problem 6.22. Consider the robot studied in Problem (6.4). Derive a tracking controller that uses the controller based on dissipativity principles in Theorem (6.7). Write a program to simulate the performance of the controller. Plot the state trajectories, tracking error, and control inputs as a function of time for various choices of the initial conditions, desired trajectories and the choice of feedback gains.

Problem 6.23. Consider the robot studied in Problem (6.5). Derive a tracking controller that uses the controller based on dissipativity principles in Theorem (6.7). Write a program to simulate the performance of the controller. Plot the state trajectories, tracking error, and control inputs as a function of time for various choices of the initial conditions, desired trajectories and the choice of feedback gains.

Problem 6.24. Consider the robot studied in Problem (6.6). Derive a tracking controller that uses the controller based on dissipativity principles in Theorem (6.7). Write a program to simulate the performance of the controller. Plot the state trajectories, tracking error, and control inputs as a function of time for various choices of the initial conditions, desired trajectories and the choice of feedback gains.

Problem 6.25. Consider the robot studied in Problem (6.7). Derive a tracking controller that uses the controller based on dissipativity principles in Theorem (6.7). Write a program to simulate the performance of the controller. Plot the state trajectories, tracking error, and control inputs as a function of time for various choices of the initial conditions, desired trajectories and the choice of feedback gains.

Problem 6.26. Consider the robot studied in Problem (6.8). Derive a tracking controller that uses the controller based on dissipativity principles in Theorem (6.7). Write a program to simulate the performance of the controller. Plot the state trajectories, tracking error, and control inputs as a function of time for various choices of the initial conditions, desired trajectories and the choice of feedback gains.

Problem 6.27. Consider the robot studied in Problem (6.9). Derive a tracking controller that uses the controller based on dissipativity principles in Theorem (6.7).

Write a program to simulate the performance of the controller. Plot the state trajectories, tracking error, and control inputs as a function of time for various choices of the initial conditions, desired trajectories and the choice of feedback gains.

Chapter 7

Image-Based Control of Robotic Systems

Abstract Chapter (6) introduced some of the fundamental *joint space feedback control* methods. Many variants of these control strategies have been derived in the literature. This chapter focuses on the derivation of feedback controllers that utilize measurements or observations collected from cameras or in the form of *CCD imagery* in the *task space*. The *image based visual servo* control problem is defined, and its stability and convergence are discussed. General methods to achieve asymptotic stability of *task space controllers* that utilize the computed torque control strategy are introduced. It is shown that camera and CCD imagery measurements can be employed in *task space control formulations*. Upon completion of this chapter the student should be able to

- Define the *image plane coordinates* and *pixel coordinates* associated with *camera measurements* of robotic system location and orientation.
- Derive the *interaction matrix* relating the derivatives of *image plane coordinates* to the velocity of the origin of the camera frame and the angular velocity of the *camera frame* in the *inertial frame*.
- State the *Image-Based Visual Servo* control problem and discuss its *stability*.
- Derive computed torque controllers in terms of task space coordinates.
- Derive task space controllers for visual servoing problems.

7.1 The Geometry of Camera Measurements

Modern *robotic control systems* utilize a wide variety of *sensors* to measure the configuration and motion of a *robotic system* during its operation. These sensors may include *accelerometers*, *rate gyros*, *magnetometers*, *angle encoders* or *global positioning system (GPS)* sensors, to name a few. This section will discuss a basic *camera model* that can be used to represent many of the cameras that are used in robotics for various control tasks. The simplest *camera model* that is applicable to many of the commercially available cameras is based on the *pinhole camera* or *perspective projection camera*.

7.1.1 Perspective Projection and Pinhole Camera Models

As shown in Figure (7.1), when a classical pinhole camera creates an image of a point p , a ray is traced from the point p through the pinhole located at the origin of the *camera frame* \mathbb{C} onto the *focal plane*. The *focal length* f is the distance from the origin of the *camera frame* to the *focal plane*. This chapter denotes the basis for the *camera frame* \mathbb{C} as by $\mathbf{x}_c, \mathbf{y}_c, \mathbf{z}_c$. By convention the *line-of-sight* of the camera is along the \mathbf{z}_c axis. The *camera coordinates* (X, Y, Z) of a *feature point* p viewed from a camera are defined in terms of the *position vector* $\mathbf{r}_{\mathbb{C},p}$ of the point p in the *camera frame* \mathbb{C} ,

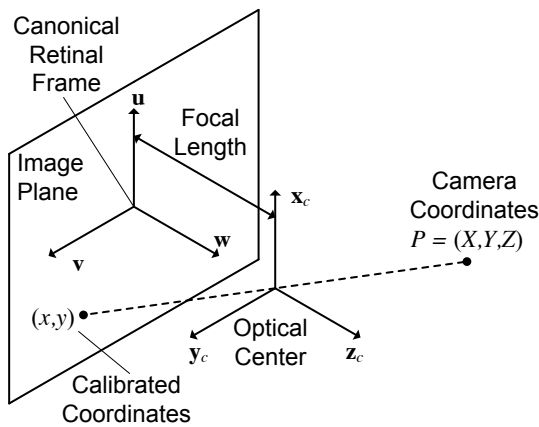


Fig. 7.1: Perspective Pinhole Camera, Rear Projected

$$\mathbf{r}_{\mathbb{C},p} = X\mathbf{x}_c + Y\mathbf{y}_c + Z\mathbf{z}_c.$$

The coordinates (u, v) of the *image point* in the *focal plane* are known as the the *canonical image plane coordinates*, *retinal coordinates*, or *calibrated coordinates*. As shown in Figure (7.1), the location of the the *focal plane* on the opposite side of the point p being viewed implies that the image in the *focal plane* is inverted. Figure (7.2) shows a full view of the $u - w$ plane in this case. The relationship between the camera coordinates X, Y, Z and the *focal plane* coordinates (u, v) can be derived by considering similar triangles in Figure (7.2). Knowing the *focal length* f between the *focal plane* and *camera frame*, the relationship is

$$u = -f \frac{X}{Z}, \quad v = -f \frac{Y}{Z}. \quad (7.1.1)$$

It is common practice to replace the physically motivated geometry in Figure (7.1) with a mathematical model that places the *focal plane* between the origin of the *camera frame* and point p being viewed as shown in Figure (7.3). While this ar-

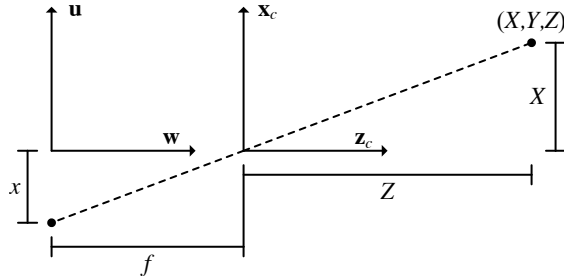


Fig. 7.2: Perspective Pinhole Camera, Coordinate Calculation

arrangement is not physically realizable, it is used so that the image is not inverted in the focal plane. In this mathematical model, the negative signs in Equation (7.1.2) do not appear, and the relationship between the focal plane coordinates (u, v) and the camera coordinates (X, Y, Z) is simply $u = fX/Z$ and $v = fY/Z$. These equations

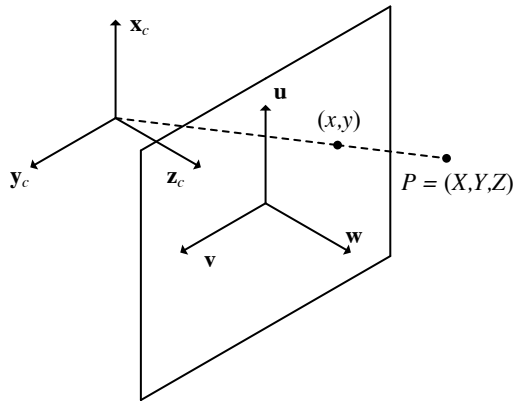


Fig. 7.3: Perspective Pinhole Camera, Front Projected

can be rewritten in terms of the *homogeneous coordinates* of the *image point* in the *focal plane* and the *camera frame coordinates* as

$$Z \begin{Bmatrix} u \\ v \\ 1 \end{Bmatrix} = \begin{bmatrix} f & 0 & 0 & 0 \\ 0 & f & 0 & 0 \\ 0 & 0 & 1 & 0 \end{bmatrix} \begin{Bmatrix} X \\ Y \\ Z \\ 1 \end{Bmatrix} \quad (7.1.2)$$

Equation (7.1.2) relates the *focal plane coordinates* (u, v) to the *camera coordinates* (X, Y, Z) , but it is often desired to understand how the coordinates of the point p

in the inertial 0 frame are related to the *focal plane coordinates*. The tools derived in Chapters (2) and (3) can be used to obtain the desired expression. Recall that the *homogeneous coordinates* of the point with respect to the camera C-frame are defined as $\mathbf{p}^C = \{X, Y, Z, 1\}^T$. These coordinates are related to the inertial frame 0 using the *homogeneous transform* $\mathbf{p}^C = \mathbf{H}_0^C \mathbf{p}^0$,

$$\begin{Bmatrix} X \\ Y \\ Z \\ 1 \end{Bmatrix} = \begin{bmatrix} \mathbf{R}_0^C & \mathbf{d}_{C,0}^C \\ 0 & 1 \end{bmatrix} \begin{Bmatrix} X_0 \\ Y_0 \\ Z_0 \\ 1 \end{Bmatrix}. \quad (7.1.3)$$

The final *homogeneous transformation* that relates the *inertial frame 0 coordinates* and the *focal plane* coordinates is achieved by combining Equations (7.1.2) and (7.1.3),

$$Z \begin{Bmatrix} u \\ v \\ 1 \end{Bmatrix} = \begin{bmatrix} f & 0 & 0 \\ 0 & f & 0 \\ 0 & 0 & 1 \end{bmatrix} \begin{bmatrix} 1 & 0 & 0 & 0 \\ 0 & 1 & 0 & 0 \\ 0 & 0 & 1 & 0 \end{bmatrix} \begin{bmatrix} \mathbf{R}_0^C & \mathbf{d}_{C,0}^C \\ 0 & 1 \end{bmatrix} \begin{Bmatrix} X_0 \\ Y_0 \\ Z_0 \\ 1 \end{Bmatrix}. \quad (7.1.4)$$

7.1.2 Pixel Coordinates and CCD Cameras

Most modern cameras are comprised of sensors that make measurements using *charge coupled device*, or *CCD*, arrays. Cameras based on *CCD arrays* return a two-dimensional matrix of intensity values, in contrast to the mathematical abstraction used in the last section that considers the image as a continuously varying intensity over the *focal plane*. The *pixel coordinates* are used to represent the locations of the entries in the *CCD array* of intensity values. The *pixel coordinates* are introduced in a two step process. First, because the individual pixel elements in the *CCD array* can have different dimensions in the horizontal and vertical directions, the *scaled coordinates* (u_s, v_s) are defined in terms of the *focal coordinates* (u, v) via the simple diagonal matrix equation

$$\begin{Bmatrix} u_s \\ v_s \end{Bmatrix} = \begin{bmatrix} s_u & 0 \\ 0 & s_v \end{bmatrix} \begin{Bmatrix} u \\ v \end{Bmatrix}, \quad (7.1.5)$$

where the parameters s_u, s_v are *scale factors* in the u and v directions, respectively.

In addition to scaling, it is also common that the *pixels* in a *CCD array* are numbered from left to right, starting at the upper left corner of the *pixel array*. We account for this offset and define the *pixel coordinates* by shifting the origin with respect to the scaled coordinates,

$$\begin{Bmatrix} \xi \\ \eta \end{Bmatrix} = \begin{Bmatrix} u_s \\ v_s \end{Bmatrix} + \begin{Bmatrix} o_u \\ o_v \end{Bmatrix}, \quad (7.1.6)$$

where (o_u, o_v) is the location of the *principal point* or the image of the *line-of-sight* of the camera in the *CCD array*. The process of scaling and translating to obtain the *pixel coordinates* in terms of the *focal plane coordinates* can be written by combining Equations (7.1.5) and (7.1.6) in terms of a single transformation

$$\begin{Bmatrix} \xi \\ \eta \\ 1 \end{Bmatrix} = \begin{bmatrix} s_u & 0 & o_u \\ 0 & s_v & o_v \\ 0 & 0 & 1 \end{bmatrix} \begin{Bmatrix} u \\ v \\ 1 \end{Bmatrix}. \quad (7.1.7)$$

Before closing this section, several variants of the equations that relate the *camera coordinates*, *inertial coordinates*, *focal plane coordinates*, and *pixel coordinates* are derived. These equations introduce the *intrinsic* or *calibration parameter matrix*. With Equation (7.1.7), Equation (7.1.4) can be used to relate the *pixel coordinates* and *inertial coordinates* of the *image point* p in

$$Z \begin{Bmatrix} \xi \\ \eta \\ 1 \end{Bmatrix} = \begin{bmatrix} s_u & s_\theta & o_u \\ 0 & s_v & o_v \\ 0 & 0 & 1 \end{bmatrix} \begin{bmatrix} f & 0 & 0 \\ 0 & f & 0 \\ 0 & 0 & 1 \end{bmatrix} \begin{bmatrix} 1 & 0 & 0 & 0 \\ 0 & 1 & 0 & 0 \\ 0 & 0 & 1 & 0 \end{bmatrix} \begin{Bmatrix} X \\ Y \\ Z \\ 1 \end{Bmatrix}.$$

Note that these equations have introduced another scalar parameter, s_θ , that measures how *pixels* in the *CCD array* are sheared relative to the vertical and horizontal directions. Combining the *focal length* with the *calibration constants* $s_x, s_y, s_\theta, o_u, o_v$ results in

$$Z \begin{Bmatrix} \xi \\ \eta \\ 1 \end{Bmatrix} = \begin{bmatrix} fs_u & fs_\theta & o_u \\ 0 & fs_v & o_v \\ 0 & 0 & 1 \end{bmatrix} \begin{bmatrix} 1 & 0 & 0 & 0 \\ 0 & 1 & 0 & 0 \\ 0 & 0 & 1 & 0 \end{bmatrix} \begin{Bmatrix} X \\ Y \\ Z \\ 1 \end{Bmatrix},$$

in which the *camera intrinsic parameter matrix* or *calibration matrix* may be defined as \mathbf{K} ,

$$\mathbf{K} = \begin{bmatrix} fs_u & fs_\theta & o_u \\ 0 & fs_v & o_v \\ 0 & 0 & 1 \end{bmatrix}.$$

By defining the *projection matrix*

$$\boldsymbol{\Pi}_0 = \begin{bmatrix} 1 & 0 & 0 & 0 \\ 0 & 1 & 0 & 0 \\ 0 & 0 & 1 & 0 \end{bmatrix}$$

that extracts the first three coordinates from any 4 – vector of *homogeneous coordinates*, a succinct rule that defines the *pixel coordinates* in terms of the *camera coordinates* is written as

$$Z \begin{Bmatrix} \xi \\ \eta \\ 1 \end{Bmatrix} = \mathbf{K} \boldsymbol{\Pi}_0 \begin{Bmatrix} X \\ Y \\ Z \\ 1 \end{Bmatrix}.$$

For completeness the relationships that use the *intrinsic parameter matrix* \mathbf{K} to express the *pixel coordinates* in terms of the *inertial coordinates* are summarized,

$$Z \begin{Bmatrix} \xi \\ \eta \\ 1 \end{Bmatrix} = \mathbf{K} \boldsymbol{\Pi}_0 \mathbf{H}_0^C \begin{Bmatrix} X_0 \\ Y_0 \\ Z_0 \\ 1 \end{Bmatrix} = \mathbf{K} \boldsymbol{\Pi}_0 \begin{bmatrix} \mathbf{R}_0^C & \mathbf{d}_{C,0}^C \\ 0 & 1 \end{bmatrix} \begin{Bmatrix} X_0 \\ Y_0 \\ Z_0 \\ 1 \end{Bmatrix},$$

$$Z \begin{Bmatrix} u \\ v \\ 1 \end{Bmatrix} = Z \mathbf{K}^{-1} \begin{Bmatrix} \xi \\ \eta \\ 1 \end{Bmatrix} = \boldsymbol{\Pi}_0 \mathbf{H}_0^C \begin{Bmatrix} X_0 \\ Y_0 \\ Z_0 \\ 1 \end{Bmatrix}.$$

7.1.3 The Interaction Matrix

This section derives the *interaction matrix* or *image Jacobian matrix* that plays a critical role in the development of control strategies that use camera measurements for feedback. The *interaction matrix* relates the derivatives of the *focal plane coordinates* to the velocity and angular velocity of the *camera frame* in the *inertial frame*.

Definition 7.1. Let $\mathbf{u}(t) := (u(t), v(t))^T$ be the time varying *image plane coordinates* of a point that is fixed in the *inertial frame* or 0 frame. The *interaction matrix* \mathbf{L} relates the time derivative $\dot{\mathbf{u}} := (\dot{u}(t), \dot{v}(t))^T$ of the *image plane coordinates*, the velocity in the inertial frame $\mathbf{v}_{0,c}$ of the origin of the *camera frame* C and the *angular velocity* of the *camera frame* in the *inertial frame* via the equation

$$\dot{\mathbf{u}}(t) = \begin{Bmatrix} \dot{u}(t) \\ \dot{v}(t) \end{Bmatrix} = \mathbf{L} \begin{Bmatrix} \mathbf{v}_{0,c}^C \\ \boldsymbol{\omega}_{0,C}^C \end{Bmatrix}. \quad (7.1.8)$$

The following theorem specifies an explicit representation of the *interaction matrix* \mathbf{L} when the *focal length* is equal to 1.

Theorem 7.1. If the focal length is equal to 1, interaction matrix $\mathbf{L} = \mathbf{L}(u, v, Z)$ satisfies

$$\begin{Bmatrix} \dot{u} \\ \dot{v} \end{Bmatrix} = \underbrace{\begin{bmatrix} -\frac{1}{Z} & 0 & \frac{u}{Z} & uv & -(1+u^2) & v \\ 0 & -\frac{1}{Z} & \frac{v}{Z} & (1+v^2) & -uv & -u \end{bmatrix}}_{\mathbf{L}(u,v,Z)} \begin{Bmatrix} \mathbf{r}_{0,c}^C \\ \boldsymbol{\omega}_{0,C}^C \end{Bmatrix} \quad (7.1.9)$$

Proof. There are several ways to derive the identity in Equation (7.1.9). This proof will use the *Derivative Theorem* (2.12) that relates the calculation of time derivatives when the basis for the *camera frame* and the *inertial frame* are held fixed. By

definition, the position vectors can be related via $\mathbf{r}_{0,p} = \mathbf{r}_{\mathbb{C},p} + \mathbf{d}_{0,c}$, where $\mathbf{r}_{0,p}$ is the position of the *feature point* p in the 0 frame, $\mathbf{r}_{\mathbb{C},p}$ is the position of the *feature point* p in the \mathbb{C} frame, and $\mathbf{d}_{0,c}$ is the vector that connects the origin of the 0 frame to the origin c of the \mathbb{C} frame. When the derivative is taken of this vector equation while holding the basis for the 0 frame fixed, it becomes

$$\underbrace{\frac{d}{dt}\Big|_0(\mathbf{r}_{0,p})}_{\mathbf{v}_{0,p}=0} = \frac{d}{dt}\Big|_0(\mathbf{r}_{\mathbb{C},p}) + \underbrace{\frac{d}{dt}\Big|_0(\mathbf{d}_{0,c})}_{\mathbf{v}_{0,c}}.$$

Note that the definition of the velocity of the point p in the 0 frame and the velocity of the origin c of the \mathbb{C} frame in the inertial frame is used in this equation. The troublesome term is the derivative $\frac{d}{dt}\Big|_0(\mathbf{r}_{\mathbb{C},p})$ which is not known *a priori*. However, the Derivative Theorem (2.12) provides a method of relating the derivatives of an arbitrary vector \mathbf{a} with respect to any two frames \mathbb{F}, \mathbb{G} as

$$\frac{d}{dt}\Big|_{\mathbb{F}}(\mathbf{a}) = \frac{d}{dt}\Big|_{\mathbb{G}}(\mathbf{a}) + \boldsymbol{\omega}_{\mathbb{F},\mathbb{G}} \times \mathbf{a}. \quad (7.1.10)$$

By assumption, the *camera frame coordinates* are $(X(t), Y(t), Z(t))^T$, so the position $\mathbf{r}_{\mathbb{C},p}$ is $\mathbf{r}_{\mathbb{C},p} = X\mathbf{x}_{\mathbb{C}} + Y\mathbf{y}_{\mathbb{C}} + Z\mathbf{z}_{\mathbb{C}}$, where $\mathbf{x}_{\mathbb{C}}, \mathbf{y}_{\mathbb{C}}, \mathbf{z}_{\mathbb{C}}$ is the basis for frame \mathbb{C} . Define the velocity of the origin c of the camera frame \mathbb{C} and the *angular velocity* of the *camera frame* \mathbb{C} in the inertial 0-frame as $\mathbf{v}_{0,c} = v_x\mathbf{x}_{\mathbb{C}} + v_y\mathbf{y}_{\mathbb{C}} + v_z\mathbf{z}_{\mathbb{C}}$ and $\boldsymbol{\omega}_{0,\mathbb{C}} = \omega_x\mathbf{x}_{\mathbb{C}} + \omega_y\mathbf{y}_{\mathbb{C}} + \omega_z\mathbf{z}_{\mathbb{C}}$. Applying the *Transport Theorem* in Equation (7.1.10) for frames $\mathbb{F} = 0$ and $\mathbb{G} = \mathbb{C}$ results in

$$\frac{d}{dt}\Big|_0(\mathbf{r}_{\mathbb{C},p}) = \frac{d}{dt}\Big|_{\mathbb{C}}(\mathbf{r}_{\mathbb{C},p}) + \boldsymbol{\omega}_{0,\mathbb{C}} \times \mathbf{r}_{\mathbb{C},p} = \dot{X}\mathbf{x}_{\mathbb{C}} + \dot{Y}\mathbf{y}_{\mathbb{C}} + \dot{Z}\mathbf{z}_{\mathbb{C}} + \begin{vmatrix} \mathbf{x}_{\mathbb{C}} & \mathbf{y}_{\mathbb{C}} & \mathbf{z}_{\mathbb{C}} \\ \omega_x & \omega_y & \omega_z \\ X & Y & Z \end{vmatrix}.$$

If this expression is substituted for $\frac{d}{dt}\Big|_0(\mathbf{r}_{\mathbb{C},p})$ in Equation (7.1.3), and the result is solved for $(\dot{X}, \dot{Y}, \dot{Z})^T$, the matrix equation becomes

$$\begin{Bmatrix} \dot{X} \\ \dot{Y} \\ \dot{Z} \end{Bmatrix} = \underbrace{\begin{bmatrix} -1 & 0 & 0 & 0 & -Z & Y \\ 0 & -1 & 0 & Z & 0 & -X \\ 0 & 0 & -1 & -Y & X & 0 \end{bmatrix}}_{\mathbf{D}(X,Y,Z)} \begin{Bmatrix} \mathbf{v}_{0,c}^{\mathbb{C}} \\ \boldsymbol{\omega}_{0,\mathbb{C}}^{\mathbb{C}} \end{Bmatrix}. \quad (7.1.11)$$

This relationship will be used in several of the proofs that follow. It is written in compact form as

$$\dot{\mathbf{X}} = \mathbf{D}(X, Y, Z) \begin{Bmatrix} \mathbf{v}_{0,c}^{\mathbb{C}} \\ \boldsymbol{\omega}_{0,\mathbb{C}}^{\mathbb{C}} \end{Bmatrix} \quad (7.1.12)$$

Next, a relationship between u, v, \dot{X}, \dot{Y} and \dot{Z} will be determined. By definition, $u = fX/Z$ and $v = fY/Z$. Suppose that the *focal length* $f = 1$. Differentiating $u(t)$ and $v(t)$

yields

$$\begin{Bmatrix} \dot{u} \\ \dot{v} \end{Bmatrix} = \frac{1}{Z} \begin{Bmatrix} \dot{X} \\ \dot{Y} \end{Bmatrix} - \frac{1}{Z^2} \dot{Z} \begin{Bmatrix} X \\ Y \end{Bmatrix} = \frac{1}{Z} \begin{Bmatrix} \dot{X} \\ \dot{Y} \end{Bmatrix} - \frac{\dot{Z}}{Z} \begin{Bmatrix} u \\ v \end{Bmatrix}$$

When the identity above is simplified using the definition of the *image plane coordinates*, it is possible to obtain a matrix equation that relates the derivatives (\dot{u}, \dot{v}) of the *image plane coordinates* to the derivatives $(\dot{X}, \dot{Y}, \dot{Z})$ of the *camera frame coordinates* in

$$\begin{Bmatrix} \dot{u} \\ \dot{v} \end{Bmatrix} = \frac{1}{Z} \begin{bmatrix} 1 & 0 & -u \\ 0 & 1 & -v \end{bmatrix} \begin{Bmatrix} \dot{X} \\ \dot{Y} \\ \dot{Z} \end{Bmatrix}. \quad (7.1.13)$$

The final expression for the *interaction matrix* is obtained when Equation (7.1.11) is substituted into Equation (7.1.13)

$$\begin{aligned} \begin{Bmatrix} \dot{u} \\ \dot{v} \end{Bmatrix} &= \frac{1}{Z} \begin{bmatrix} 1 & 0 & -u \\ 0 & 1 & -v \end{bmatrix} \begin{Bmatrix} \dot{X} \\ \dot{Y} \\ \dot{Z} \end{Bmatrix}, \\ &= \frac{1}{Z} \begin{bmatrix} 1 & 0 & -u \\ 0 & 1 & -v \end{bmatrix} \begin{bmatrix} -1 & 0 & 0 & 0 & -Z & Y \\ 0 & -1 & 0 & Z & 0 & -X \\ 0 & 0 & -1 & -Y & X & 0 \end{bmatrix} \begin{Bmatrix} \mathbf{v}_{0,c}^C \\ \boldsymbol{\omega}_{0,C}^C \end{Bmatrix}, \\ &= \underbrace{\begin{bmatrix} -\frac{1}{Z} & 0 & \frac{u}{Z} & \frac{uY}{Z} & -(1 + \frac{uX}{Z}) & \frac{Y}{Z} \\ 0 & -\frac{1}{Z} & \frac{v}{Z} & (1 + \frac{vY}{Z}) & -\frac{vX}{Z} & -\frac{X}{Z} \end{bmatrix}}_{\mathbf{L}} \begin{Bmatrix} \mathbf{v}_{0,c}^C \\ \boldsymbol{\omega}_{0,C}^C \end{Bmatrix}, \\ &= \underbrace{\begin{bmatrix} -\frac{1}{Z} & 0 & \frac{u}{Z} & uv & -(1 + u^2) & v \\ 0 & -\frac{1}{Z} & \frac{v}{Z} & (1 + v^2) & -uv & -u \end{bmatrix}}_{\mathbf{L}} \begin{Bmatrix} \mathbf{v}_{0,c}^C \\ \boldsymbol{\omega}_{0,C}^C \end{Bmatrix}. \end{aligned}$$

□

Equation (7.1.9) shows that the matrix \mathbf{L} is a 2×6 matrix for a single feature point. In general, Theorem (7.1) will be employed for several feature points. Suppose there are feature points $i = 1, \dots, N_p$. Introduce the $(2 \times N_p)$ vector \mathbf{u} and the $(3 \times N_p)$ vector \mathbf{X} that are obtained by stacking the *image plane coordinates* $\mathbf{u}_i(t) = (u(t), v(t))^T$ and by stacking the *camera coordinates* $\mathbf{X}_i(t) = (X(t), Y(t), Z(t))^T$ for all the feature points $i = 1, \dots, N_p$ as

$$\mathbf{u}(t) := \begin{Bmatrix} \mathbf{u}_1(t) \\ \mathbf{u}_2(t) \\ \vdots \\ \mathbf{u}_{N_p}(t) \end{Bmatrix}, \quad \mathbf{X}(t) = \begin{Bmatrix} \mathbf{X}_1(t) \\ \mathbf{X}_2(t) \\ \vdots \\ \mathbf{X}_{N_p}(t) \end{Bmatrix}. \quad (7.1.14)$$

The *system interaction matrix* is obtained by applying Theorem (7.1) for each feature point $i = 1, \dots, N_p$,

$$\begin{Bmatrix} \dot{u} \\ \dot{v} \end{Bmatrix}_i = \begin{bmatrix} -\frac{1}{Z} & 0 & \frac{u}{Z} & uv & -(1+u^2) & v \\ 0 & -\frac{1}{Z} & \frac{v}{Z} & (1+v^2) & -uv & -u \end{bmatrix}_i \begin{Bmatrix} \mathbf{v}_{0,c}^C \\ \boldsymbol{\omega}_{0,C}^C \end{Bmatrix},$$

or more concisely as,

$$\dot{\mathbf{u}}_i = \mathbf{L}(u_i, v_i, Z_i) \begin{Bmatrix} \mathbf{v}_{0,c}^C \\ \boldsymbol{\omega}_{0,C}^C \end{Bmatrix}. \quad (7.1.15)$$

When we stack these equations, we obtain the *system interaction matrix* \mathbf{L}_{sys}

$$\dot{\mathbf{u}}(t) = \begin{Bmatrix} \dot{\mathbf{u}}_1(t) \\ \dot{\mathbf{u}}_2(t) \\ \vdots \\ \dot{\mathbf{u}}_{N_p}(t) \end{Bmatrix} = \underbrace{\begin{bmatrix} \mathbf{L}(u_1, v_1, Z_1) \\ \mathbf{L}(u_2, v_2, Z_2) \\ \vdots \\ \mathbf{L}(u_{N_p}, v_{N_p}, Z_{N_p}) \end{bmatrix}}_{\mathbf{L}_{sys}} \begin{Bmatrix} \mathbf{v}_{0,c}^C \\ \boldsymbol{\omega}_{0,C}^C \end{Bmatrix}, \quad (7.1.16)$$

or

$$\dot{\mathbf{u}}(t) = \mathbf{L}_{sys} \begin{Bmatrix} \mathbf{v}_{0,c}^C \\ \boldsymbol{\omega}_{0,C}^C \end{Bmatrix}. \quad (7.1.17)$$

Just as the *system interaction matrix* \mathbf{L}_{sys} is defined, an equation is also needed for the system of N_p feature points that is analogous to Equation (7.1.12). For $i = 1, \dots, N_p$

$$\begin{Bmatrix} \dot{X} \\ \dot{Y} \\ \dot{Z} \end{Bmatrix}_i = \begin{bmatrix} -1 & 0 & 0 & 0 & -Z & Y \\ 0 & -1 & 0 & Z & 0 & -X \\ 0 & 0 & -1 & -Y & X & 0 \end{bmatrix}_i \begin{Bmatrix} \mathbf{v}_{0,c}^C \\ \boldsymbol{\omega}_{0,C}^C \end{Bmatrix},$$

$$\dot{\mathbf{X}}_i = \mathbf{D}(X_i, Y_i, Z_i) \begin{Bmatrix} \mathbf{v}_{0,c}^C \\ \boldsymbol{\omega}_{0,C}^C \end{Bmatrix}.$$

Stacking these equations for $i = 1, \dots, N_p$ results in

$$\dot{\mathbf{X}}(t) := \begin{Bmatrix} \dot{\mathbf{X}}_1(t) \\ \dot{\mathbf{X}}_2(t) \\ \vdots \\ \dot{\mathbf{X}}_{N_p}(t) \end{Bmatrix} = \underbrace{\begin{bmatrix} \mathbf{D}(X_1, Y_1, Z_1) \\ \mathbf{D}(X_2, Y_2, Z_2) \\ \vdots \\ \mathbf{D}(X_{N_p}, Y_{N_p}, Z_{N_p}) \end{bmatrix}}_{\mathbf{D}_{sys}} \begin{Bmatrix} \mathbf{v}_{0,c}^C \\ \boldsymbol{\omega}_{0,C}^C \end{Bmatrix}, \quad (7.1.18)$$

or more succinctly,

$$\dot{\mathbf{X}}(t) = \mathbf{D}_{sys} \begin{Bmatrix} \mathbf{v}_{0,c}^C \\ \boldsymbol{\omega}_{0,C}^C \end{Bmatrix}. \quad (7.1.19)$$

7.2 Image-Based Visual Servo Control

With the construction of the matrices \mathbf{L}_{sys} and \mathbf{D}_{sys} in Equations (7.1.17) and (7.1.19) for a system that includes *feature points* $i = 1, \dots, N_p$ that are fixed in the inertial 0 frame, it is straightforward to pose and solve a number of standard problems in the control of robotic systems using camera-based measurements. This section will discuss one such control problem, the *Image-Based Visual Servo* (IBVS) control problem.

7.2.1 Control Synthesis and Closed Loop Equations

The *Image-Based Visual Servo* control problem is a specific example of a *tracking control problem*. First, the *Image-Based Visual Servo* control problem will be defined to specify the goals of the strategy and the measurements that will be used for feedback control.

Definition 7.2. Suppose a set of *feature points* for $i = 1, \dots, N_p$ are given that are fixed in the *inertial frame*, and let $(u_1^*, v_1^*), (u_2^*, v_2^*), \dots, (u_{N_p}^*, v_{N_p}^*)$ denote N_p *desired image point locations* that are fixed in the *image plane*. the *tracking error in the image plane* for the i^{th} feature point is defined to be

$$\mathbf{e}_i(t) := \begin{Bmatrix} u_i(t) \\ v_i(t) \end{Bmatrix} - \begin{Bmatrix} u_i^* \\ v_i^* \end{Bmatrix}, \quad (7.2.1)$$

and the *image plane tracking error* for the system is given by

$$\mathbf{e}(t) := \begin{Bmatrix} \mathbf{u}_1(t) - \mathbf{u}_1^* \\ \mathbf{u}_2(t) - \mathbf{u}_2^* \\ \vdots \\ \mathbf{u}_{N_p}(t) - \mathbf{u}_{N_p}^* \end{Bmatrix}. \quad (7.2.2)$$

The *Image-Based Visual Servo* control problem seeks to find the *control input* vector $\mathbf{U}(t)$ that consists of the velocity $\mathbf{v}_{0,c}^C$ of the origin of the *camera frame* and *angular velocity* $\boldsymbol{\omega}_{0,C}^C$ of the *camera frame* in the inertial 0-frame,

$$\mathbf{U}(t) := \begin{Bmatrix} \mathbf{v}_{0,c}^C(t) \\ \boldsymbol{\omega}_{0,C}^C(t) \end{Bmatrix} \quad (7.2.3)$$

so that

- (i) the control input $\mathbf{U}(t)$ is a *feedback function* given in terms the *tracking error* $\mathbf{e}(t)$ and perhaps *camera extrinsic parameters*,
- (ii) the dynamics of the closed loop system is *stable*, and
- (iii) the tracking error approaches zero as $t \rightarrow \infty$.

The derivation of the *visual servo control* strategy to solve the problem statement in Definition (7.2) is not difficult given the derivation of the matrices \mathbf{L}_{sys} and \mathbf{D}_{sys} . Since the *tracking error* should approach zero asymptotically, the *control law* can be defined so that the *closed loop system* has a *tracking error* that satisfies the equation

$$\dot{\mathbf{e}}(t) = -\lambda \mathbf{e}(t), \quad (7.2.4)$$

where λ is some positive scalar. The solution of Equation (7.2.4) is given in terms of exponential function

$$\mathbf{e}(t) = e^{-\lambda t} \mathbf{e}(0).$$

Consequently, if the *closed loop tracking error* satisfies Equation (7.2.4), it will approach zero at an exponential rate. The definition of the *tracking error* can be combined with Equation (7.2.4) to obtain

$$\dot{\mathbf{e}}(t) = \frac{d}{dt}(\mathbf{u}(t) - \mathbf{u}^*) = \dot{\mathbf{u}}(t) = \mathbf{L}_{sys} \begin{Bmatrix} \mathbf{v}_{0,c}^C \\ \boldsymbol{\omega}_{0,C}^C \end{Bmatrix} = -\lambda \mathbf{e}(t). \quad (7.2.5)$$

Ideally, Equation (7.2.5) would be uniquely solvable for the velocity $\mathbf{v}_{0,c}^C$ and angular velocity $\boldsymbol{\omega}_{0,C}^C$. However, the *system interaction matrix* is not square in general since

$$\mathbf{L}_{sys} \in \mathbb{R}^{(2N_p) \times 6},$$

and it may be that $2N_p \neq 6$. Depending on the number of *system feature points*, the matrix equation

$$\mathbf{L}_{sys} \begin{Bmatrix} \mathbf{v}_{0,c}^C \\ \boldsymbol{\omega}_{0,C}^C \end{Bmatrix} = -\lambda \mathbf{e}(t) \quad (7.2.6)$$

can be *underdetermined*, *overdetermined* or *exactly determined*. If the matrix \mathbf{L}_{sys} has fewer rows than columns, $2N_p < 6$, the system is said to be *underdetermined*. If the matrix \mathbf{L}_{sys} has more rows than columns, $2N_p > 6$, the system is said to be *overdetermined*. If the matrix \mathbf{L}_{sys} has equal numbers of rows and columns, $2N_p = 6$, the system is said to be *exactly determined*.

Even if the system is not *exactly determined*, it is possible to obtain an expression for the control input $\{\mathbf{v}_{0,c}^C, \boldsymbol{\omega}_{0,C}^C\}^T$ by using the *pseudo-inverse*

$$\mathbf{L}_{sys}^+ := (\mathbf{L}_{sys}^T \mathbf{L}_{sys})^{-1} \mathbf{L}_{sys}^T.$$

When both sides of Equation (7.2.6) are multiplied by \mathbf{L}_{sys}^+ , an expression for the *control input* vector is obtained as

$$\begin{Bmatrix} \mathbf{v}_{0,c}^C \\ \boldsymbol{\omega}_{0,C}^C \end{Bmatrix} = -\lambda \mathbf{L}_{sys}^+ \mathbf{e}(t). \quad (7.2.7)$$

Before proceeding to the discussion of the *closed loop system* and its *stability*, it is important to make several observations about the construction thus far.

- The *pseudo-inverse* \mathbf{L}_{sys}^+ is not a square matrix. It has dimension $6 \times (2N_p)$
- The *pseudo-inverse* expression

$$\mathbf{L}_{sys}^+ = (\mathbf{L}_{sys}^T \mathbf{L}_{sys})^{-1} \mathbf{L}_{sys}^T$$

only makes sense provided that the matrix $(\mathbf{L}_{sys}^T \mathbf{L}_{sys})$ is *invertible*. While the expression given for \mathbf{L}_{sys}^+ assumes that $(\mathbf{L}_{sys}^T \mathbf{L}_{sys})$ is invertible, the *pseudo-inverse* always exists for any matrix. The form of the *pseudo-inverse* for an arbitrary matrix can be expressed in terms of the *singular value decomposition* of the matrix. While this topic is beyond the scope of this book, the interested reader is referred to [18] for a discussion.

- The *pseudo-inverse* is a nonlinear function of the image plane coordinates and the range of each the *system feature points*. That is,

$$\mathbf{L}_{sys}^+ = \mathbf{L}_{sys}^+(u_1, v_1, Z_1, \dots, u_{N_p}, v_{N_p}, Z_{N_p}).$$

This implies that the expression in Equation (7.2.6) is a nonlinear equation.

- The set of equations in (7.2.6) is not a *closed set of ordinary differential equations*. The left hand side of Equation (7.2.6) contains the derivatives of the tracking error \mathbf{e} , while the right hand side of these same equations contains the *image plane coordinates and ranges* $(u_1, v_1, Z_1, \dots, u_{N_p}, v_{N_p}, Z_{N_p})$. To put this set of equations in the standard form for a system of *ordinary differential equations*, it must be rewritten as

$$\dot{\mathbf{x}}(t) = \mathbf{f}(t, \mathbf{x}(t)) \quad (7.2.8)$$

for some set of *state variables* \mathbf{x} .

The following theorem derives the set of *coupled, nonlinear ordinary differential equations* that characterizes the dynamics of the *closed loop system* associated with the *feedback control law* embodied in Equation (7.2.6).

Theorem 7.2. Suppose that the Image Based Visual Servo control law in Equation (7.2.6) is used to control a robotic system. The dynamics of the closed loop system is governed by the following closed set of coupled, nonlinear ordinary differential equations

$$\dot{\mathbf{e}}(t) = -\lambda \mathbf{L}_{sys} \mathbf{L}_{sys}^+ \mathbf{e}(t), \quad (7.2.9)$$

$$\dot{\mathbf{u}}(t) = -\lambda \mathbf{L}_{sys} \mathbf{L}_{sys}^+ \mathbf{e}(t), \quad (7.2.10)$$

$$\dot{\mathbf{X}}(t) = -\lambda \mathbf{D}_{sys} \mathbf{L}_{sys}^+ \mathbf{e}(t). \quad (7.2.11)$$

Proof. These equations follow from the derivation of the closed loop control law in Equation (7.2.6). From Equation (7.2.7),

$$\begin{Bmatrix} \mathbf{v}_{0,C}^C \\ \boldsymbol{\omega}_{0,C}^C \end{Bmatrix} = -\lambda \mathbf{L}_{sys}^+ \mathbf{e}(t), \quad (7.2.12)$$

which when combined with Equation (7.2.5) yields

$$\dot{\mathbf{e}}(t) = -\lambda \mathbf{L}_{sys} \mathbf{L}_{sys}^+ \mathbf{e}(t).$$

Moreover, it is known that

$$\mathbf{e}(t) := \begin{Bmatrix} \mathbf{e}_1(t) \\ \mathbf{e}_2(t) \\ \vdots \\ \mathbf{e}_n(t) \end{Bmatrix} = \begin{Bmatrix} \mathbf{u}_1(t) \\ \mathbf{u}_2(t) \\ \vdots \\ \mathbf{u}_n(t) \end{Bmatrix} - \begin{Bmatrix} \mathbf{u}_1^* \\ \mathbf{u}_2^* \\ \vdots \\ \mathbf{u}_n^* \end{Bmatrix}.$$

When this equation is differentiated with respect to time $\dot{\mathbf{e}}(t) = \dot{\mathbf{u}}(t)$, and it follows that $\dot{\mathbf{u}}(t) = -\lambda \mathbf{L}_{sys} \mathbf{L}_{sys}^+ \mathbf{e}(t)$. Finally, Equation (7.1.19) shows that

$$\dot{\mathbf{X}}(t) = \mathbf{D}_{sys} \begin{Bmatrix} \mathbf{v}_{0,c}^C \\ \boldsymbol{\omega}_{0,C}^C \end{Bmatrix},$$

which results in

$$\dot{\mathbf{X}}(t) = -\lambda \mathbf{D}_{sys} \mathbf{L}_{sys}^+ \mathbf{e}(t)$$

when Equation (7.2.12) is substituted into Equation (7.1.19). Thus, each of the equations in Theorem (7.2) holds. It remains to show that this collection of three vector equations constitutes a *closed system of ordinary differential equations*. Recall from the discussion of Equation (7.2.8) that this collection of equations must be able to be written in the form $\dot{\mathbf{x}} = \mathbf{f}(t, \mathbf{x}(t))$ for some N_s -vector $\mathbf{x}(t)$ of *state variables* and some function $f : \mathbb{R} \times \mathbb{R}^{N_s} \rightarrow \mathbb{R}^{N_s}$. Define the *state variable* vector to be

$$\mathbf{x}(t) := \begin{Bmatrix} \mathbf{e}(t) \\ \mathbf{u}(t) \\ \mathbf{X}(t) \end{Bmatrix}.$$

Then the left hand side of the collection of governing equations

$$\begin{aligned} \dot{\mathbf{e}}(t) &= -\lambda \mathbf{L}_{sys} \mathbf{L}_{sys}^+ \mathbf{e}(t), \\ \dot{\mathbf{u}}(t) &= -\lambda \mathbf{L}_{sys} \mathbf{L}_{sys}^+ \mathbf{e}(t), \\ \dot{\mathbf{X}}(t) &= -\lambda \mathbf{D}_{sys} \mathbf{L}_{sys}^+ \mathbf{e}(t). \end{aligned}$$

is simply $\dot{\mathbf{x}}(t)$, and the right hand side of this set of 3 vector equations depends on $\mathbf{e}(t), \mathbf{u}(t), \mathbf{X}(t)$, which are the entries of $\mathbf{x}(t)$. Thus, the system is a closed set of ordinary differential equations. \square

7.2.2 Calculation of Initial Conditions

The actual simulation of the collection of nonlinear *ordinary differential equations* written in the form $\dot{\mathbf{x}}(t) = \mathbf{f}(t, \mathbf{x}(t))$, where the vector of *state variables* \mathbf{x} is given by

$$\mathbf{x}(t) := \begin{Bmatrix} \mathbf{e}(t) \\ \mathbf{u}(t) \\ \mathbf{X}(t) \end{Bmatrix},$$

can use any of a number of standard *numerical integration methods* for *systems of ordinary differential equations*. These numerical methods include the family of *linear multistep methods*. The *linear multistep methods* include many popular *predictor-corrector methods*, such as the Adams-Bashforth-Moulton method. Another popular family of numerical integration methods include the self-starting *Runge-Kutta methods*. The reader is referred to [2] for a discussion of these methods, as well as other popular alternatives.

To use such a numerical algorithm to obtain an approximate solution of these equations, it is necessary to specify the *initial condition*

$$\mathbf{x}(t_0) = \begin{Bmatrix} \mathbf{e}(t_0) \\ \mathbf{u}(t_0) \\ \mathbf{X}(t_0) \end{Bmatrix}.$$

To describe a general procedure to solve for the *initial condition* $\mathbf{x}(t_0)$, the initial and final orientation of the *camera frame* will need to be described. The basis for the *initial camera frame* $\mathbb{C}(t_0)$ will be denoted by $\mathbf{x}_{\mathbb{C}}(t_0), \mathbf{y}_{\mathbb{C}}(t_0), \mathbf{z}_{\mathbb{C}}(t_0)$, and the basis for the *final camera frame* $\mathbb{C}(t_f)$ will be denoted by $\mathbf{x}_{\mathbb{C}}(t_f), \mathbf{y}_{\mathbb{C}}(t_f), \mathbf{z}_{\mathbb{C}}(t_f)$. The position of a point p relative to the *camera frame* in its initial configuration is then

$$\mathbf{r}_{\mathbb{C},p}(t_0) = X(t_0)\mathbf{x}_{\mathbb{C}}(t_0) + Y(t_0)\mathbf{y}_{\mathbb{C}}(t_0) + Z(t_0)\mathbf{z}_{\mathbb{C}}(t_0),$$

and the position of the point p relative to the camera frame in its final configuration is

$$\mathbf{r}_{\mathbb{C},p}(t_f) = X(t_f)\mathbf{x}_{\mathbb{C}}(t_f) + Y(t_f)\mathbf{y}_{\mathbb{C}}(t_f) + Z(t_f)\mathbf{z}_{\mathbb{C}}(t_f).$$

The following steps can be used to calculate the initial condition $\mathbf{x}(t_0)$.

- (i) Find the *coordinates of the offset* $\mathbf{d}_{0,f}^0$ between the origin of the *final camera frame* and the origin of the *initial camera frame*, and find the *rotation matrix* \mathbf{R}_f^0 that maps coordinates with respect to the *final camera frame* into coordinates with respect to the *initial camera frame*. Create the *homogeneous transformation* \mathbf{H}_f^0 that maps the *homogeneous coordinates* with respect to the *final camera frame* into the *homogeneous coordinates* with respect to the *initial coordinate frame*.

$$\mathbf{H}_f^0 = \begin{bmatrix} \mathbf{R}_f^0 & \mathbf{d}_{0,f}^0 \\ \mathbf{0}^T & 1 \end{bmatrix}. \quad (7.2.13)$$

- (ii) Calculate the *camera coordinates* with respect to the *initial camera frame* from the *camera coordinates* with respect to the *final camera frame* for each of the points $i = 1, \dots, n_p$,

$$\begin{Bmatrix} X(t_0) \\ Y(t_0) \\ Z(t_0) \\ 1 \end{Bmatrix}_i = \begin{bmatrix} \mathbf{R}_f^0 & \mathbf{d}_{0,f}^0 \\ \mathbf{0}^T & 1 \end{bmatrix} \begin{Bmatrix} X(t_f) \\ Y(t_f) \\ Z(t_f) \\ 1 \end{Bmatrix}_i. \quad (7.2.14)$$

This equation can also be written more compactly as

$$\begin{Bmatrix} \mathbf{X}_i(t_0) \\ 1 \end{Bmatrix} = \begin{bmatrix} \mathbf{R}_f^0 & \mathbf{d}_{0,f}^0 \\ \mathbf{0}^T & 1 \end{bmatrix} \begin{Bmatrix} \mathbf{X}_i(t_f) \\ 1 \end{Bmatrix}. \quad (7.2.15)$$

- (iii) Use the *camera coordinates* with respect to the *initial camera frame* ($\mathbf{X}_1(t_0), \mathbf{X}_2(t_0), \dots, \mathbf{X}_{n_p}(t_0)$) to calculate the *initial focal plane coordinates* for $i = 1, \dots, n_p$

$$\mathbf{u}_i(t_0) = \begin{Bmatrix} u(t_0) \\ v(t_0) \end{Bmatrix}_i = \begin{Bmatrix} X_i(t_0)/Z_i(t_0) \\ Y_i(t_0)/Z_i(t_0) \end{Bmatrix}. \quad (7.2.16)$$

- (iv) Use the *initial focal plane coordinates* $\mathbf{u}_1(t_0), \mathbf{u}_2(t_0), \dots, \mathbf{u}_{n_p}(t_0)$ to calculate the *initial focal plane tracking error* for each point $i = 1, \dots, n_p$.

$$\mathbf{e}_i(t_0) = \begin{Bmatrix} e_x(t_0) \\ e_y(t_0) \end{Bmatrix}_i = \begin{Bmatrix} u_i(t_0) - u_i^* \\ v_i(t_0) - v_i^* \end{Bmatrix}. \quad (7.2.17)$$

Once these steps have been completed, the initial condition $\mathbf{x}(t_0)$ is constructed by stacking the vectors $\mathbf{e}_i(t_0), \mathbf{u}_i(t_0), \mathbf{X}_i(t_0)$ for $i = 1, \dots, N_p$ to form the vectors $\mathbf{e}(t_0), \mathbf{u}(t_0), \mathbf{X}(t_0)$,

$$\mathbf{e}(t_0) = \begin{Bmatrix} \mathbf{e}_1(t_0) \\ \mathbf{e}_2(t_0) \\ \vdots \\ \mathbf{e}_{N_p}(t_0) \end{Bmatrix}, \quad \mathbf{u}(t_0) = \begin{Bmatrix} \mathbf{u}_1(t_0) \\ \mathbf{u}_2(t_0) \\ \vdots \\ \mathbf{u}_{N_p}(t_0) \end{Bmatrix}, \quad \mathbf{X}(t_0) = \begin{Bmatrix} \mathbf{X}_1(t_0) \\ \mathbf{X}_2(t_0) \\ \vdots \\ \mathbf{X}_{N_p}(t_0) \end{Bmatrix},$$

and subsequently assembling

$$\mathbf{x}(t_0) = \begin{Bmatrix} \mathbf{e}(t_0) \\ \mathbf{u}(t_0) \\ \mathbf{X}(t_0) \end{Bmatrix}.$$

Example 7.2.1. Derive an *Image-Based Visual Servo controller* using camera measurements of four *feature points* that are fixed in the *inertial frame*. Consider the orientation of the camera frame, focal plane and camera coordinates of the feature points as shown in Figure (7.4). For this problem the *focal length* $f = 1$. Note that the figure depicts the desired or final configuration of the camera frame.

Solution:

The desired *focal plane coordinates* shown in the figure are given by

$$\begin{Bmatrix} u^* \\ v^* \end{Bmatrix}_1 = \begin{Bmatrix} \frac{1}{2} \\ \frac{1}{2} \end{Bmatrix}, \quad \begin{Bmatrix} u^* \\ v^* \end{Bmatrix}_2 = \begin{Bmatrix} \frac{1}{2} \\ -\frac{1}{2} \end{Bmatrix}, \quad \begin{Bmatrix} u^* \\ v^* \end{Bmatrix}_3 = \begin{Bmatrix} -\frac{1}{2} \\ -\frac{1}{2} \end{Bmatrix}, \quad \begin{Bmatrix} u^* \\ v^* \end{Bmatrix}_4 = \begin{Bmatrix} -\frac{1}{2} \\ \frac{1}{2} \end{Bmatrix}.$$

The coordinates of the *feature points* relative to the final orientation of the *camera frame* are given by

$$\begin{Bmatrix} X(t_f) \\ Y(t_f) \\ Z(t_f) \end{Bmatrix}_1 = \begin{Bmatrix} 4 \\ 4 \\ 8 \end{Bmatrix}, \quad \begin{Bmatrix} X(t_f) \\ Y(t_f) \\ Z(t_f) \end{Bmatrix}_2 = \begin{Bmatrix} 4 \\ -4 \\ 8 \end{Bmatrix}, \quad \begin{Bmatrix} X(t_f) \\ Y(t_f) \\ Z(t_f) \end{Bmatrix}_3 = \begin{Bmatrix} -4 \\ -4 \\ 8 \end{Bmatrix}, \quad \begin{Bmatrix} X(t_f) \\ Y(t_f) \\ Z(t_f) \end{Bmatrix}_4 = \begin{Bmatrix} -4 \\ 4 \\ 8 \end{Bmatrix}.$$

The initial condition will be chosen so that

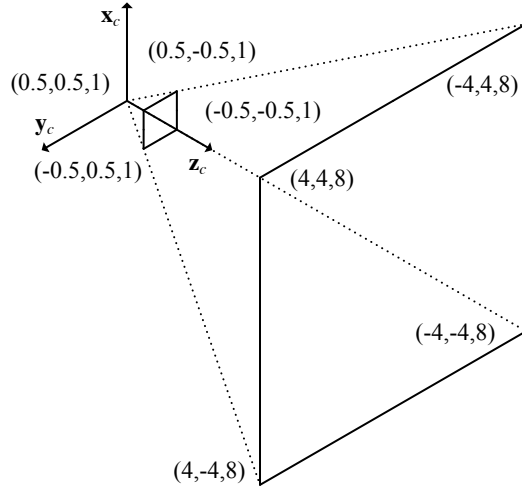


Fig. 7.4: Final Configuration of Camera Frame and Feature Points

1. the origin of the *initial camera frame* coincides with the origin of the *final camera frame*, and
2. the orientation of the *initial camera frame* is obtained by rotating the *final camera frame* by $\pi/4$ about the $\mathbf{z}_C(t_f) = \mathbf{z}_C(t_0)$ axis.

The system of *ordinary differential equations* in Theorem (7.2) is used to simulate the behavior of the control scheme. The calculation of the initial condition for these governing equations is carried out using the Steps (i) through (iv) above. In this example,

$$\mathbf{d}_{0,f}^0 = \begin{Bmatrix} 0 \\ 0 \\ 0 \end{Bmatrix},$$

and the rotation matrix that maps the *final camera coordinates* to the *initial camera coordinates* is simply

$$\mathbf{R}_f^0 = \begin{bmatrix} \frac{1}{\sqrt{2}} & \frac{1}{\sqrt{2}} & 0 \\ -\frac{1}{\sqrt{2}} & \frac{1}{\sqrt{2}} & 0 \\ 0 & 0 & 1 \end{bmatrix}.$$

Figure (7.5) depicts the performance of the closed-loop system by plotting the trajectories of the *focal plane coordinates*. The *focal plane coordinates* of each *feature point* start at the corners of the red square, which represents the image of the *feature points* viewed from the *initial camera configuration*. The *visual servo image-based control law* drives the camera so that the *focal plane coordinates* of each of the feature points approaches the desired locations in the *focal plane*.

Figure (7.6) illustrates the trajectories taken by the *camera coordinates* as a function of time when the camera is driven by the *image-based visual servo control law*.

Note that in Figure (7.6) the camera moves in the \mathbf{z}_C direction as it is driven by the control law. Even though the *target camera configuration* is related to the *initial camera configuration* by a simple rotation about the \mathbf{z}_C basis vector, the set of *closed loop equations* induce a motion in the \mathbf{z}_C direction: the rotation about the \mathbf{z}_C direction is coupled with the rotation about the \mathbf{z}_C direction.

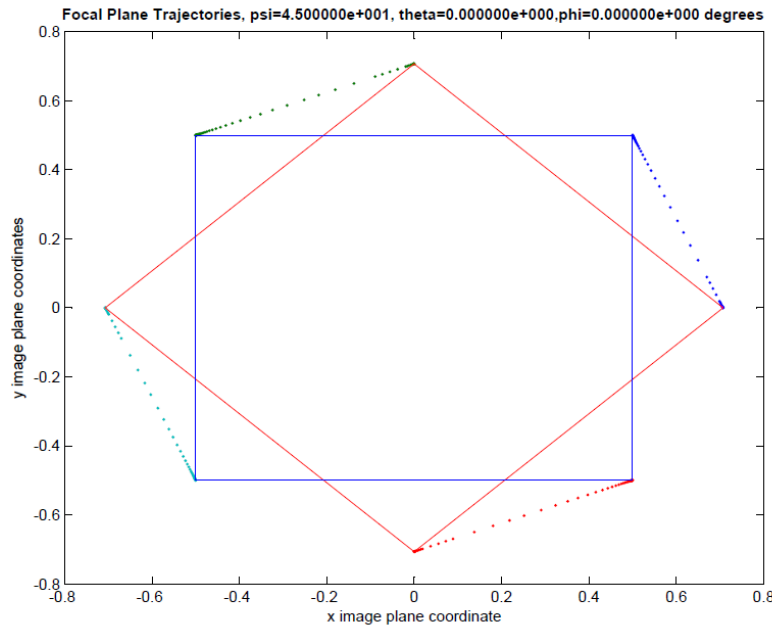


Fig. 7.5: Rotation About Z-axis, $\psi = \pi/4$, Focal Plane Trajectories

Example 7.2.2. As in Example (7.2.1), derive an *Image-Based Visual Servo controller* using camera measurements of four *feature points* that are fixed in the *inertial frame*. The feature points have the same relative geometry with respect to the *final camera frame*, but the *initial camera frame* is defined as shown in Figure (7.7).
Solution: As shown in Figure (7.7), the position and orientation of the *initial camera frame* are defined to satisfy two conditions.

1. The origin of the *initial camera frame* is offset from the origin of the *final camera frame* by

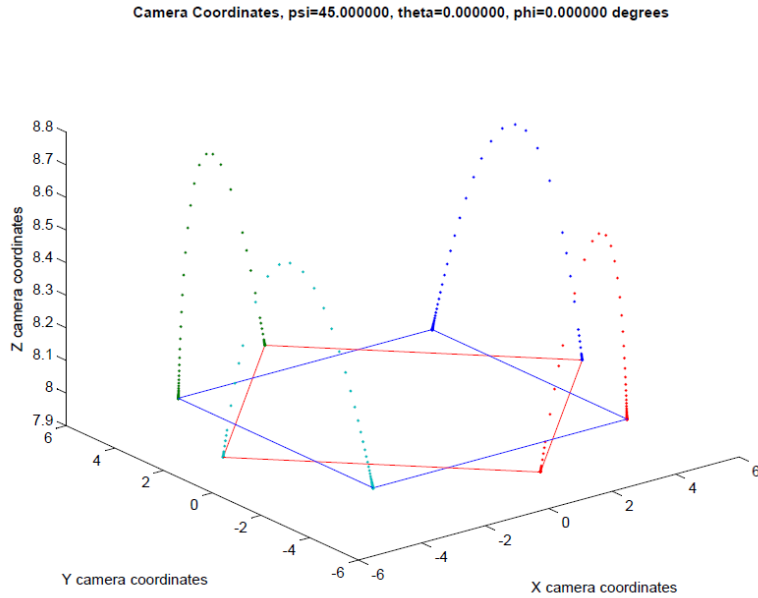


Fig. 7.6: Rotation About Z-axis, $\psi = \pi/4$, Camera Coordinate Trajectories

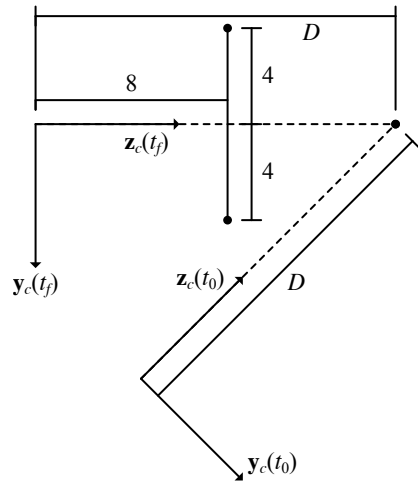


Fig. 7.7: Initial Condition Configuration

$$\mathbf{d}_{f,0}^f = \begin{Bmatrix} 0 \\ \frac{1}{\sqrt{2}}D \\ D - \frac{1}{\sqrt{2}}D \end{Bmatrix}. \quad (7.2.18)$$

2. The orientation of the *initial camera frame* is obtained via a rotation of the *final camera frame* about the $\mathbf{x}_c(t_f)$ axis by an angle of $\pi/4$, so that

$$\mathbf{R}_f^0 = \begin{bmatrix} 1 & 0 & 0 \\ 0 & \frac{1}{\sqrt{2}} & \frac{1}{\sqrt{2}} \\ 0 & -\frac{1}{\sqrt{2}} & \frac{1}{\sqrt{2}} \end{bmatrix}. \quad (7.2.19)$$

As before, the *initial condition* $\mathbf{x}(t_0)$ are calculated using the updated rotation matrix \mathbf{R}_f^0 and the *origin offset* $\mathbf{d}_{0,f}^0 = -\mathbf{R}_f^0 \mathbf{d}_{f,0}^f$ in Equations (7.2.19) and (7.2.18).

Figures (7.8) and (7.9) illustrate the results of the numerical simulation in these cases. Note that in contrast to the last example, the image of the feature points viewed from the *initial camera configuration* is significantly skewed. The red polygons in Figures (7.8) and (7.9) denotes the image of the *feature points* viewed from the *initial camera configuration*. The controller drives the trajectories of the *feature points* in the *focal plane* to the desired locations, as shown in Figures (7.8) and (7.9). The trajectories of the *camera coordinates* are shown in Figure (7.9). Again, the *camera coordinates* of all the *feature points* converge to the desired locations as a function of time.

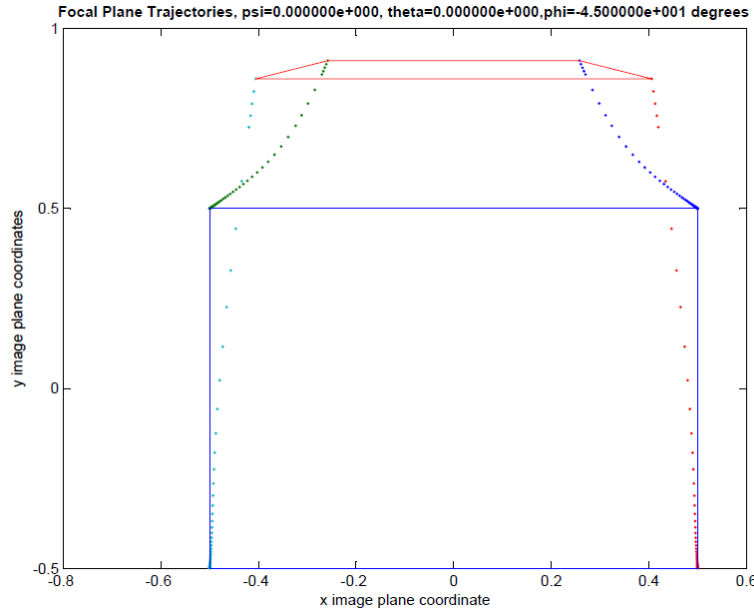


Fig. 7.8: Rotation About x-axis, $\phi = \pi/4$, Focal Plane Trajectories

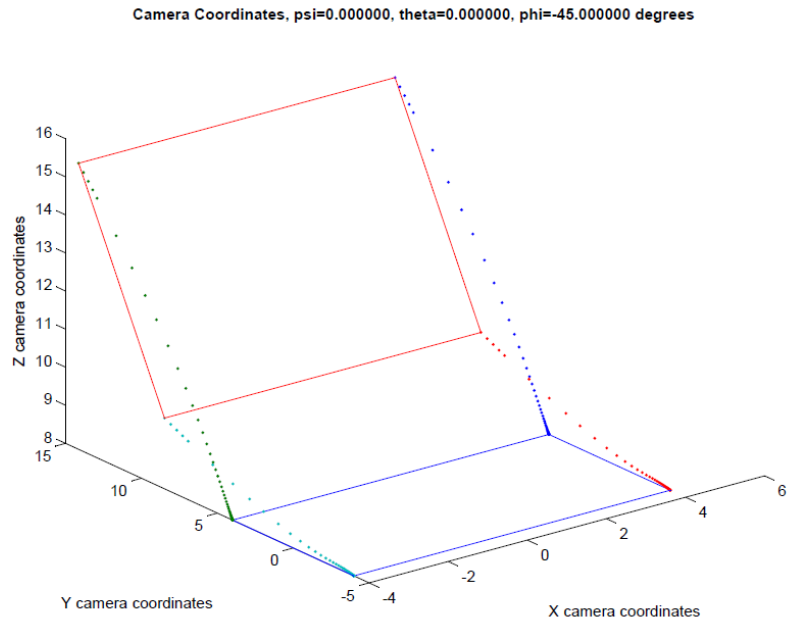


Fig. 7.9: Rotation About x-axis, $\phi = \pi/4$, Camera Coordinate Trajectories

Example 7.2.3. Consider again the case studied in Example (7.2.1) where the origin of the *initial camera frame* coincides with the origin of the *final camera frame*, and the *initial camera frame* is obtained by rotating the *final camera frame* by $\pi/4$ about the \mathbf{z}_C axis. This example utilizes this same setup but chooses the rotation angle to be $\pi/2, 3\pi/4, 7\pi/8$, and $99\pi/100$.

Solution: Figures (7.11) through (7.18) depict the *focal plane trajectories* and *camera coordinate trajectories* for these four test cases. Figures (7.11), (7.13), (7.15) and (7.17) show that the *focal plane trajectories* behave exactly as expected in these four cases. The *focal plane trajectories* start at the corners of the red polygon associated with the image of the *feature points* viewed from the *initial camera frame*, and they end at the corners of the blue polygon corresponding to the view of the *feature points* from the *final camera frame*. However, Figures (7.12), (7.14), (7.16) and (7.18) exhibit striking behavior. As the rotation angle approaches π , the range of motion along the \mathbf{z}_C direction increases dramatically. The following short table summarizes these results.

Rotation Angle	Maximum Range	Minimum Singular Value
$\pi/4$	8.8	$O(10^{-3})$
$\pi/2$	11.5	$O(10^{-4})$
$3\pi/4$	22	$O(10^{-6})$
$7\pi/8$	45	$O(10^{-9})$
$99\pi/100$	600	$O(10^{-15})$

Fig. 7.10: Table Comparing Rotation Angle, Range of Motion, and Singular Value

Recall that the origin of the *final camera frame* is required to be located at a z -axis distance of 8 units from all of the feature points. Consider in particular the case when the rotation angle is $99\pi/100$. It is clear in this case that the performance of the control method is entirely unsatisfactory. The control law drives the camera so that its maximum range is 600 units from the feature points.

The reason for this aberrant behavior can be deduced from the last column in the table. This column lists the *minimum singular value* of the *system interaction matrix* \mathbf{L}_{sys} over the entire range of motion. A plot of these *minimum singular values* is given for simulations associated with the various rotation angles in Figures (7.19) through (7.22). This *minimum singular value* can be viewed as a measure of how close the matrix $\mathbf{L}_{sys}^T \mathbf{L}_{sys}$ is to being singular. The *image Jacobian* is said to be rank deficient, or singular, in the neighborhood of the configuration associated with the rotation angle π . This difficulty is well-understood and has counterparts in many robotic control problems.

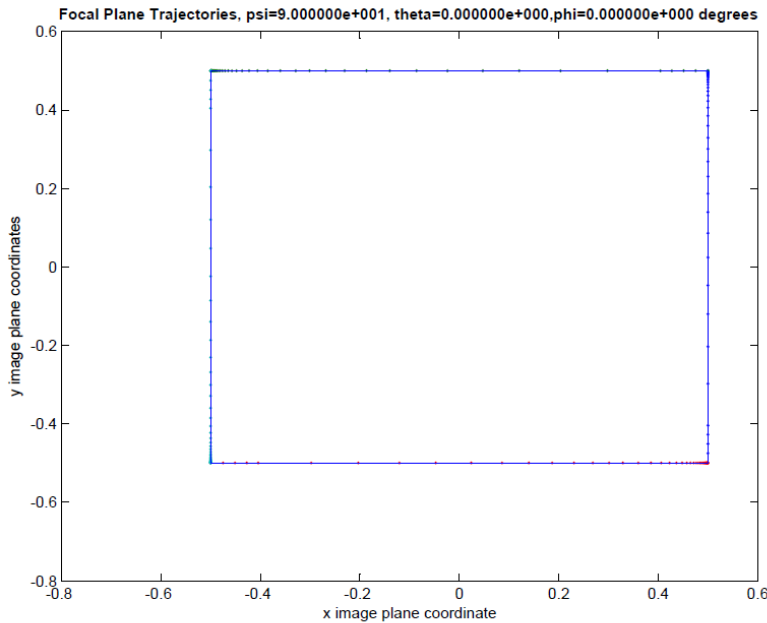


Fig. 7.11: Rotation About z-axis, $\psi = \pi/2$, Focal Plane Trajectories

7.3 Task Space Control

Chapter (6) describes several techniques for deriving feedback controllers for fully actuated robotic systems. All of these control strategies are derived so that the generalized coordinates \mathbf{q} and their derivatives $\dot{\mathbf{q}}$ approach a desired trajectory as $t \rightarrow \infty$, $\mathbf{q}(t) \rightarrow \mathbf{q}_d(t)$ and $\dot{\mathbf{q}}(t) \rightarrow \dot{\mathbf{q}}_d(t)$. For setpoint controllers the desired trajectory is a constant trajectory for which $\dot{\mathbf{q}}_d(t) \equiv \mathbf{0}$, while trajectory tracking controllers consider time-varying desired trajectories. Since all of the formulations in this book have selected the generalized coordinates to be either joint angles or joint displacements, the techniques derived in Chapter (6) are sometimes referred to as methods of *joint space control*. That is, the performance criteria or objective of the controllers discussed in Chapter (6) is the minimization of an error expressed explicitly in terms of the joint degrees of freedom.

Frequently the goal or objective to be achieved via feedback control is naturally expressed in terms of variables associated with the problem at hand, but are not easily written in terms of the joint variables. For example, designing a controller that locates the tool or end effector at some position in the workspace. In this case suppose that the position p of the tip of the tool is given by the vector

$$\mathbf{r}_{0,p}(t) = x_1(t)\mathbf{x}_0 + x_2(t)\mathbf{y}_0 + x_3(t)\mathbf{z}_0.$$

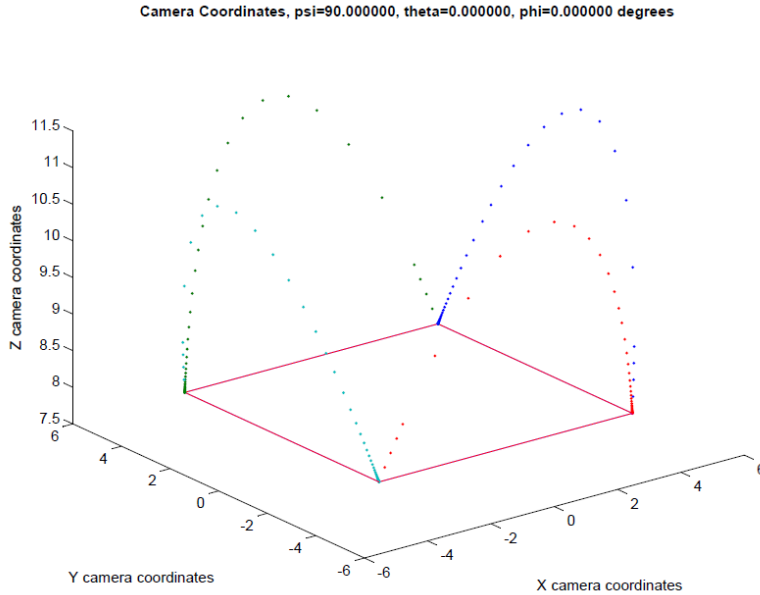


Fig. 7.12: Rotation About z-axis, $\psi = \pi/2$, Camera Coordinate Trajectories

The control strategy should guarantee that $x_1(t) \rightarrow x_{1,d}$, $x_2(t) \rightarrow x_{2,d}$, $x_3(t) \rightarrow x_{3,d}$ as $t \rightarrow \infty$. However, the coordinates (x_1, x_2, x_3) are not the joint variables for the robotic manipulator, and the strategies discussed in Chapter (6) are not directly applicable. In principle, it is usually possible to reformulate the equations of motion in terms of the task space variables, but this can be a tedious problem for a realistic robotic system. The set of variables (x_1, x_2, x_3) are an example of a collection of *task space variables* for the problem at hand. Fortunately, there are many techniques that can be used to derive *task space controllers*. One approach employs the *task space Jacobian matrix* and is summarized in the following theorem.

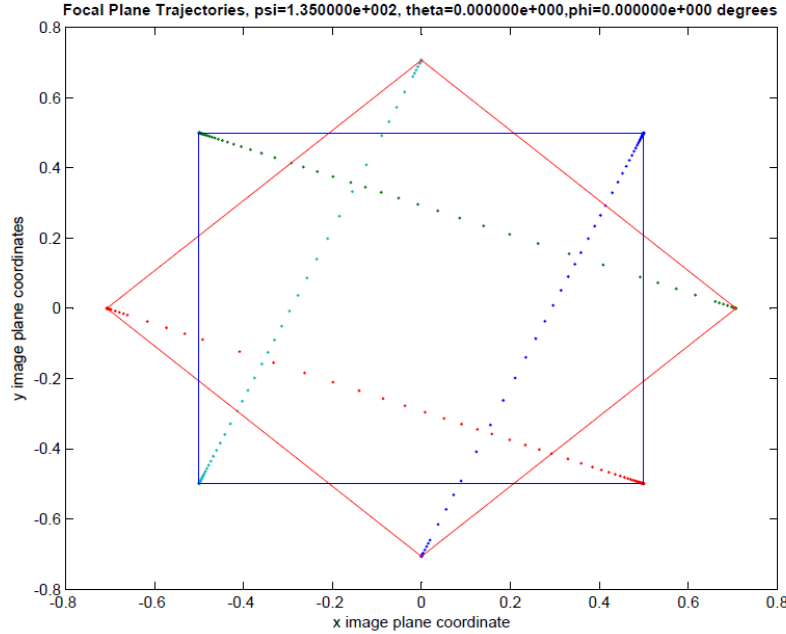


Fig. 7.13: Rotation About z-axis, $\psi = 3\pi/4$, Focal Plane Trajectories

Theorem 7.3. Suppose that $\{q_1 \dots q_N\}$ are the N generalized coordinates of a robotic system whose governing equations have the form in Equation (6.1.1). Suppose further that N task space coordinates $\{x_1 \dots x_N\}$ are given. The $(i, j)^{\text{th}}$ entry of the task space Jacobian matrix $\mathbb{J} = \frac{\partial \mathbf{x}}{\partial \mathbf{q}}$ is defined to be

$$\mathbb{J}_{ij} := \frac{\partial x_i}{\partial q_j} \quad i, j = 1, \dots, N,$$

and the task space tracking error is defined to be $\mathbf{e}_x(t) = \mathbf{x}(t) - \mathbf{x}_d(t)$ with $\mathbf{x}_d(t)$ the desired task space trajectory. Assume the following

1. The generalized mass matrix $\mathbf{M}(\mathbf{q})$ and nonlinear right hand side $\mathbf{n}(\mathbf{q}, \dot{\mathbf{q}})$ satisfy the hypothesis of Theorem (6.1).
2. The task space Jacobian $\mathbb{J} = \mathbb{J}(\mathbf{q})$ and its derivative $\dot{\mathbb{J}} = \dot{\mathbb{J}}(t, \mathbb{R}^N)$ are continuous functions on \mathbb{R}^N and $\mathbb{R}^+ \times \mathbb{R}^N$, respectively.
3. The task space Jacobian is uniformly invertible in the sense that there exists constants c_1 and c_2 such that

$$c_1 \|\mathbf{w}\|^2 \leq \mathbf{w}^T \mathbb{J}(\mathbf{q}) \mathbf{w} \leq c_2 \|\mathbf{w}\|^2$$

for all $\mathbf{w} \in \mathbb{R}^N$ and $\mathbf{q} \in \mathbb{R}^N$.

Then the computed torque control law $\boldsymbol{\tau} = \mathbf{M}\mathbf{v} - \mathbf{n}$ with

$$\mathbf{v} = \mathbb{J}^{-1}(\ddot{\mathbf{x}}_d - \dot{\mathbb{J}}\dot{\mathbf{q}} - \mathbf{G}_1(\mathbf{J}\dot{\mathbf{q}} - \dot{\mathbf{x}}_d) - \mathbf{G}_0(\mathbf{x} - \mathbf{x}_d))$$

yields a closed loop system for which the origin of the task space tracking error and its derivative are asymptotically stable.

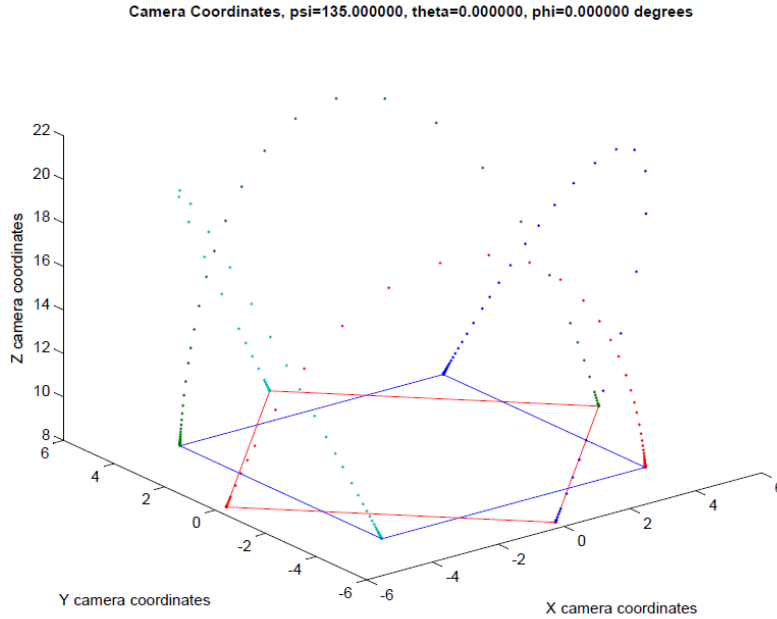


Fig. 7.14: Rotation About z-axis, $\psi = 3\pi/4$, Camera Coordinate Trajectories

Proof. When the computed torque control law is substituted into the governing equations of motion, we obtain

$$\ddot{\mathbf{q}} = \mathbf{v} = \mathbb{J}^{-1}(\ddot{\mathbf{x}}_d - \dot{\mathbb{J}}\dot{\mathbf{q}} - \mathbf{G}_1(\mathbb{J}\dot{\mathbf{q}} - \dot{\mathbf{x}}_d) - \mathbf{G}_0(\mathbf{x} - \mathbf{x}_d)).$$

Rearranging this equation yields

$$((\mathbb{J}\dot{\mathbf{q}} + \dot{\mathbb{J}}\dot{\mathbf{q}}) - \dot{\mathbf{x}}_d) + \mathbf{G}_1(\mathbb{J}\dot{\mathbf{q}} - \dot{\mathbf{x}}_d) + \mathbf{G}_0(\mathbf{x} - \mathbf{x}_d) = \mathbf{0}.$$

By the chain rule,

$$\begin{aligned}\dot{\mathbf{x}} &= \frac{d}{dt}(\mathbf{x}(\mathbf{q})) = \frac{\partial \mathbf{x}}{\partial \mathbf{q}} \dot{\mathbf{q}} = \mathbb{J}\dot{\mathbf{q}}, \\ \ddot{\mathbf{x}} &= \mathbb{J}\ddot{\mathbf{q}} + \dot{\mathbb{J}}\dot{\mathbf{q}}.\end{aligned}$$

It follows that the closed loop governing equation may be represented in the form

$$(\ddot{\mathbf{x}} - \ddot{\mathbf{x}}_d) + \mathbf{G}_1(\dot{\mathbf{x}} - \dot{\mathbf{x}}_d) + \mathbf{G}_0(\mathbf{x} - \mathbf{x}_d) = \mathbf{0},$$

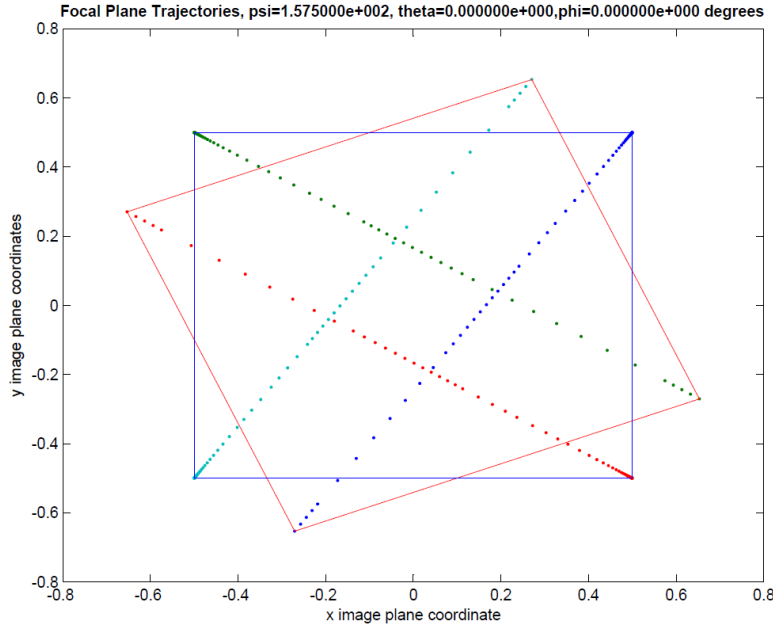


Fig. 7.15: Rotation About Z-axis, $\phi = 7\pi/8$, Focal Plane Trajectories

or

$$\ddot{\mathbf{e}}_x + \mathbf{G}_1 \dot{\mathbf{e}}_x + \mathbf{G}_0 \mathbf{e}_x = \mathbf{0},$$

where $\mathbf{e}_x(t) := \mathbf{x}(t) - \mathbf{x}_d(t)$. The origin $\{\mathbf{0} \ \mathbf{0}\} = \{\mathbf{e}_x^T \ \dot{\mathbf{e}}_x^T\}$ is consequently asymptotically stable. \square

Example 7.3.1. Consider the spherical robotic manipulator studied in Examples (6.6.1), (6.6.2), (6.7.1), and (6.8.1) in Chapter (6). Derive a *task space controller* based on Theorem (7.3) where the task space coordinates (x_1, x_2, x_3) are defined as the coordinates in the 0 frame of the origin r of frame 3. In other words, define

$$\mathbf{r}_{0,r}(t) := x_1(t)\mathbf{x}_0 + x_2(t)\mathbf{y}_0 + x_3(t)\mathbf{z}_0.$$

The controller must be designed so that the task space coordinates track the desired trajectories

$$\begin{aligned} x_{1,d}(t) &= 1 + A_1 \sin \Omega_1 t, \\ x_{2,d}(t) &= 1 + A_2 \sin \Omega_2 t, \\ x_{3,d}(t) &= 1 + A_3 \sin \Omega_3 t, \end{aligned} \tag{7.3.1}$$

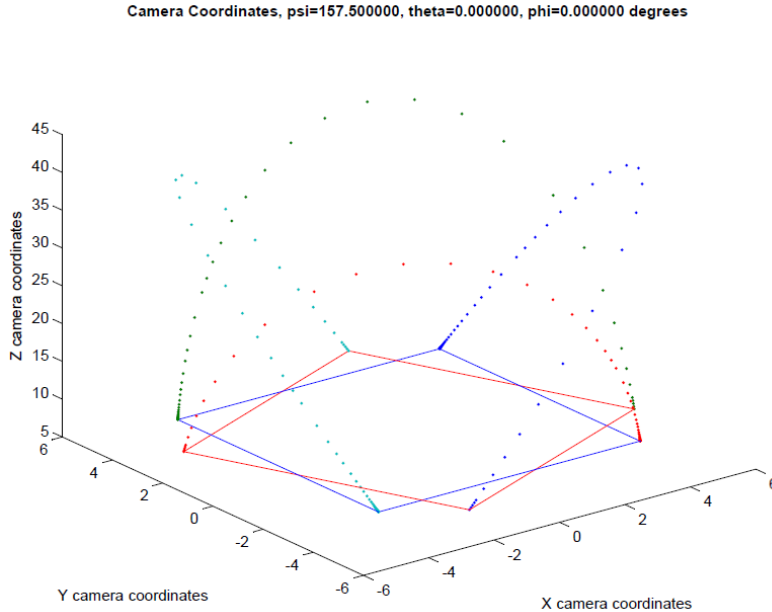


Fig. 7.16: Rotation About Z-axis, $\phi = 7\pi/8$, Camera Coordinate Trajectories

where $A_i = \frac{1}{10}$ and $\Omega_i = 2\text{rad/s}$. Choose the gain matrices to be $\mathbf{G}_0 = g_0\mathbb{I}$ and $\mathbf{G}_1 = g_1\mathbb{I}$, where $(g_0, g_1) = (1, 1), (5, 5), (10, 10)$, or $(100, 100)$. Assume the robot's initial configuration is as shown in Figure (7.23). Evaluate the performance of this controller by plotting the state trajectories, tracking error and control inputs as a function of time.

Solution: The change of coordinates $x_i = x_i(q_1, \dots, q_N)$ for $i = 1, \dots, N$ is needed that defines the task space coordinates (x_1, x_2, x_3) in terms of the generalized coordinates $(q_1, q_2, q_3) := (\theta_1, \theta_2, d_{q,r})$. From kinematic analysis of the robot,

$$\begin{Bmatrix} x_1 \\ x_2 \\ x_3 \end{Bmatrix} = \begin{Bmatrix} d_{p,q} \sin \theta_1 + d_{q,r} \cos \theta_1 \sin \theta_2 \\ -d_{p,q} \cos \theta_1 + d_{q,r} \sin \theta_1 \sin \theta_2 \\ d_{o,p} - d_{q,r} \cos \theta_2 \end{Bmatrix}.$$

The task space Jacobian matrix can be calculated either by taking partial derivatives of this expression, or by involving the tools developed in Chapter (3) for the evaluation of Jacobian matrices. In either case, the Jacobian is found to be

$$\begin{Bmatrix} \dot{x}_1 \\ \dot{x}_2 \\ \dot{x}_3 \end{Bmatrix} = \underbrace{\begin{bmatrix} (d_{p,q} \cos \theta_1 - d_{q,r} \sin \theta_1 \sin \theta_2) & d_{q,r} \cos \theta_1 \cos \theta_2 & \cos \theta_1 \sin \theta_2 \\ (d_{p,q} \sin \theta_1 + d_{q,r} \cos \theta_1 \sin \theta_2) & d_{q,r} \sin \theta_1 \cos \theta_2 & \sin \theta_1 \sin \theta_2 \\ 0 & d_{q,r} \sin \theta_2 & -\cos \theta_2 \end{bmatrix}}_{\mathbf{J}} \begin{Bmatrix} \dot{\theta}_1 \\ \dot{\theta}_2 \\ \dot{d}_{q,r} \end{Bmatrix}.$$

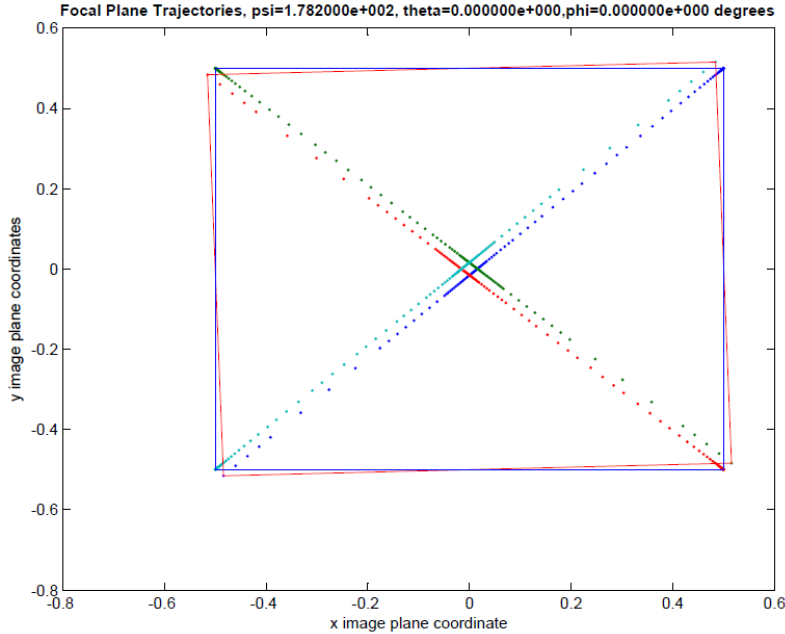


Fig. 7.17: Rotation About Z-axis, $\psi = 99\pi/100$, Focal Plane Trajectories

For this specific choice of the task space coordinates, the Jacobian matrix is precisely equal to the velocity Jacobian matrix \mathbf{J}_v introduced in Chapter (2). The time derivative $\dot{\mathbf{J}}$ of the task space Jacobian matrix is straightforward, although lengthy, to evaluate; its derivation is omitted here. Figures (7.24) and (7.25) depict the tracking errors e_{x_1} and e_{x_2} , respectively, when the initial condition is selected to be

$$\{\mathbf{q}^T(0) \ \dot{\mathbf{q}}^T(0)\} = \left\{ \left\{ \frac{\pi}{2} \ \frac{\pi}{2} \ 1 \right\} \left\{ 0 \ 0 \ 0 \right\} \right\}$$

and the configuration of the robot initially is depicted in Figure (7.23). The graph of the tracking error e_{x_3} is identical to that of e_{x_1} and is not shown. It is evident from Figures (7.24) and (7.29) that the tracking error converges to zero at an exponential rate, as predicted by the theory. The trajectory of the point r in the inertial coordinates is depicted in Figure (7.26). The trajectory converges to the straight line described parametrically by Equations (7.3.1). The actuation force and moments required to drive the robot are shown in Figures (7.27), (7.28) and (7.29). It is clear from the figures that there is a substantial transient torque required at startup as the gains are increased.

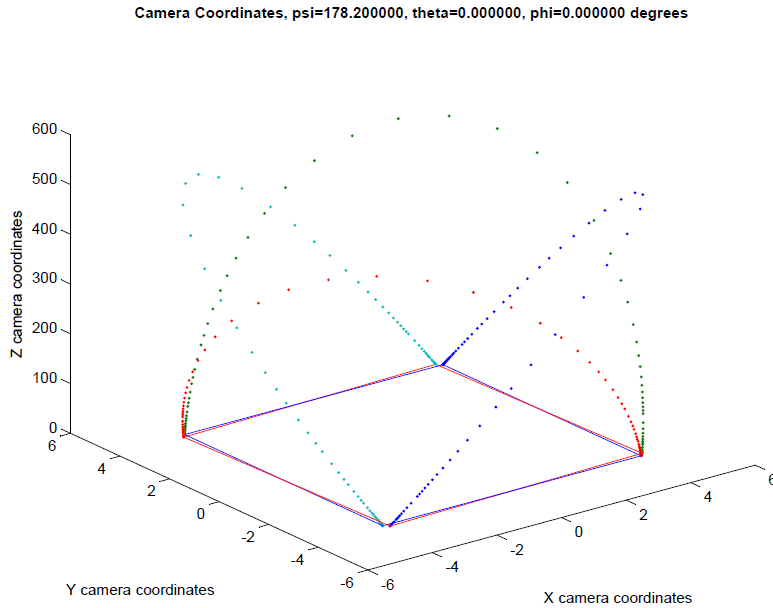


Fig. 7.18: Rotation About Z-axis, $\psi = 99\pi/100$, Camera Coordinate Trajectories

7.4 Task Space and Visual Control

The previous section has discussed how the inner loop-outer loop architecture of the computed torque control strategy introduced in Section (6.6) of Chapter (6) can be used to derive tracking or setpoint controllers in task space variables. This section will illustrate that this approach can be used to design controllers based on typical camera observations. The design of controllers based on *task space coordinates* associated with camera measurements yields stability and convergence results that are more realistic than those described in Section (7.3) of this chapter. Recall that Section (7.3) discusses the visual servo control problem where it is assumed that the input to the controller is the vector of velocities and angular velocities of the camera frame. The value of this input vector is selected so that

$$\mathbf{u}(t) := \left\{ \begin{array}{l} \mathbf{v}_{0,c}^C \\ \boldsymbol{\omega}_{0,C}^C \end{array} \right\} = -\lambda \mathbf{L}_{sys}^+ \mathbf{e}(t), \quad (7.4.1)$$

where \mathbf{e} is the tracking error in the image plane of the feature points. However, the velocities and angular velocities of the camera frame are not the output of an actuator: they are response variables. Their values depend on the forces and moments delivered by the actuators. If the input torques and forces can be chosen such that the velocities and angular velocities satisfy Equation (7.4.1) exactly, then the the

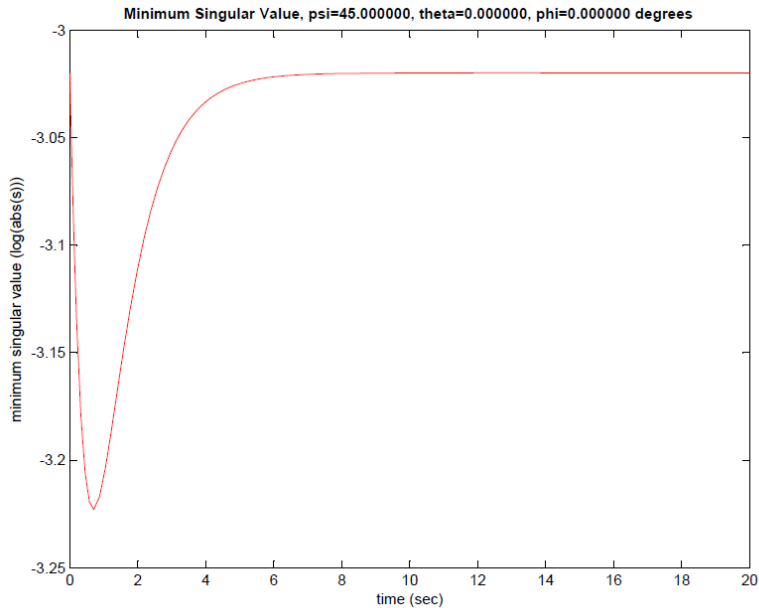


Fig. 7.19: Rotation About Z-axis, $\psi = \pi/4$, Minimum Singular Value

discussion of stability and convergence in Section (7.3) applies. In practice, it is not possible to achieve the exact specification of the velocities and angular velocities in Equation (7.4.1).

Example 7.4.1. Suppose that the spherical robot manipulator studied in Example (7.2.2) is equipped with a camera and laser ranging system. The camera is mounted on the robot so that the camera frame coincides with the 3 frame. The camera focal length may be taken as $f = 1$. A reflective target t is located as depicted in Figure (7.30), having coordinates in the 0 frame given by

$$\mathbf{r}_{0,t}^0 = \begin{Bmatrix} d_{p,q} \\ d_{q,r} + f + D_p \\ d_{o,p} \end{Bmatrix}.$$

Let (X, Y, Z) denote the coordinates relative to the camera frame of the point t so that $\mathbf{r}_{3,t}^3 = X\mathbf{x}_3 + Y\mathbf{y}_3 + Z\mathbf{z}_3$. Assume that the laser ranging system enables the real-time measurement of the range Z of the point t . Derive a controller that will orient the robot so that the image of point t approaches the origin of the image plane and the range Z approaches some desired constant value Z_d as $t \rightarrow \infty$. Evaluate the performance of the controller through simulation. Discuss potential limitations or

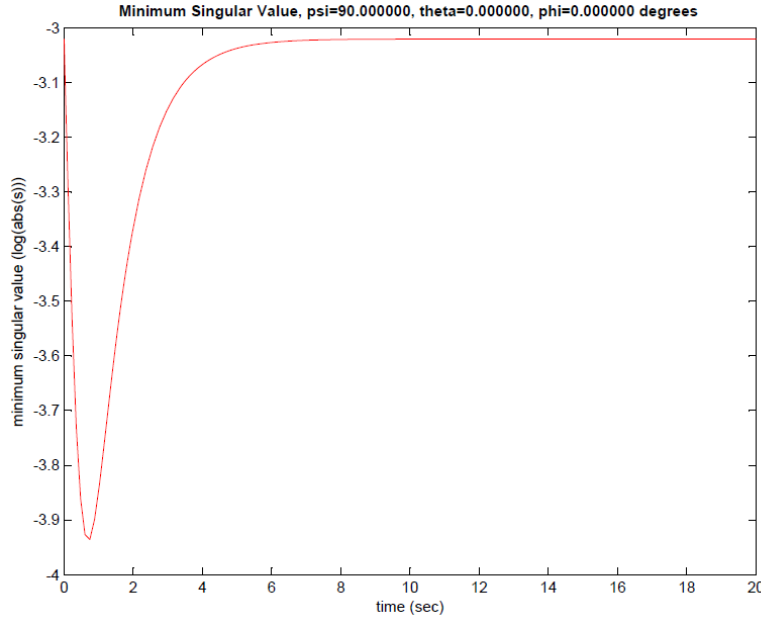


Fig. 7.20: Rotation About Z-axis, $\psi = \pi/2$, Minimum Singular Value

drawbacks of the proposed controller.

Solution: The controller will be designed using the computed torque $\tau = \mathbf{M}\mathbf{v} - \mathbf{n}$, where the vector \mathbf{v} is given in terms of task space coordinates

$$\mathbf{v} = \mathbb{J}^{-1}(\dot{\mathbf{x}}_d - \dot{\mathbb{J}}\dot{\mathbf{q}} - \mathbf{G}_1(\mathbb{J}\dot{\mathbf{q}} - \dot{\mathbf{x}}_d) - \mathbf{G}_0(\mathbf{x} - \mathbf{x}_d)), \quad (7.4.2)$$

as specified in Theorem (7.3). The task space coordinates are chosen as $\mathbf{x} = \{u, v, Z\}^T$, where the image plane coordinates (u, v) of the point p are $u = fX/Z$ and $v = fY/Z$. The task space Jacobian \mathbb{J} and its time derivative $\dot{\mathbb{J}}$ are required to implement the control law in Equation (7.4.2). Note that the Jacobian \mathbb{J} in Equation (7.4.2) is defined to be

$$\mathbb{J} = \frac{\partial \mathbf{x}}{\partial \mathbf{q}},$$

and can be identified from the equation $\dot{\mathbf{x}} = \mathbb{J}\dot{\mathbf{q}}$.

It will be shown that the matrix \mathbb{J} can be written as a product of two matrices, $\mathbb{J} = \mathbf{L}\mathbf{J}$, where \mathbf{L} and \mathbf{J} are defined in the equations

$$\dot{\mathbf{x}} = \mathbf{L} \begin{Bmatrix} \mathbf{v}_{0,r}^3 \\ \boldsymbol{\omega}_{0,3}^3 \end{Bmatrix} \quad \text{and} \quad \begin{Bmatrix} \mathbf{v}_{0,r}^3 \\ \boldsymbol{\omega}_{0,3}^3 \end{Bmatrix} = \mathbf{J}\dot{\mathbf{q}}$$

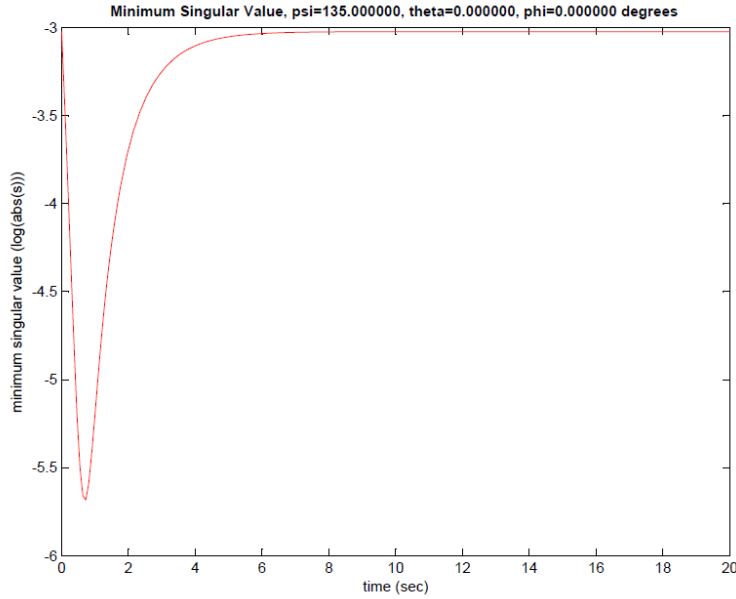


Fig. 7.21: Rotation About Z-axis, $\psi = 3\pi/4$, Minimum Singular Value

The matrix \mathbf{J} is by definition the joint space Jacobian matrix studied in Chapter (3). It is possible to derive this matrix from first principles by calculating the velocity and angular velocity directly, or by using the specialized procedures derived in Chapter (3). Using either approach, this is found to be

$$\mathbf{J} = \begin{bmatrix} d_{q,r} \cos \theta_2 & d_{q,r} 0 \\ -d_{q,r} \sin \theta_2 & 0 0 \\ d_{p,q} \sin \theta_2 & 0 1 \\ \sin \theta_2 & 0 0 \\ 0 & 1 0 \\ -\cos \theta_2 & 0 0 \end{bmatrix}.$$

The determination of the matrix \mathbf{L} is also direct using the interaction matrix \mathbf{L} and the matrix \mathbf{D} introduced in Section (7.2) of this chapter. Since

$$\begin{aligned} \begin{Bmatrix} \dot{u} \\ \dot{v} \end{Bmatrix} &= \mathbf{L} \begin{Bmatrix} \mathbf{v}_{0,r}^3 \\ \boldsymbol{\omega}_{0,3}^3 \end{Bmatrix} = \begin{bmatrix} -\frac{1}{Z} & 0 & \frac{u}{Z} & uv & -(1+u^2) & v \\ 0 & -\frac{1}{Z} & \frac{v}{Z} & (1+v^2) & -uv & -u \end{bmatrix} \begin{Bmatrix} \mathbf{v}_{0,r}^3 \\ \boldsymbol{\omega}_{0,3}^3 \end{Bmatrix}, \\ \begin{Bmatrix} \dot{X} \\ \dot{Y} \\ \dot{Z} \end{Bmatrix} &= \mathbf{D} \begin{Bmatrix} \mathbf{v}_{0,r}^3 \\ \boldsymbol{\omega}_{0,3}^3 \end{Bmatrix} = \begin{bmatrix} -1 & 0 & 0 & 0 & -Z & Y \\ 0 & -1 & 0 & Z & 0 & -X \\ 0 & 0 & -1 & -Y & X & 0 \end{bmatrix} \begin{Bmatrix} \mathbf{v}_{0,r}^3 \\ \boldsymbol{\omega}_{0,3}^3 \end{Bmatrix}, \end{aligned}$$

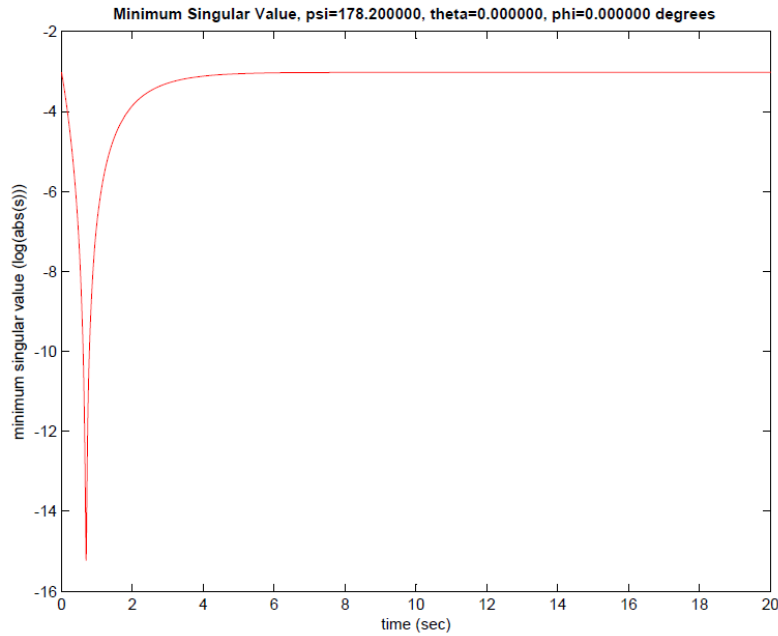


Fig. 7.22: Rotation About Z-axis, $\psi = 99\pi/100$, Minimum Singular Value

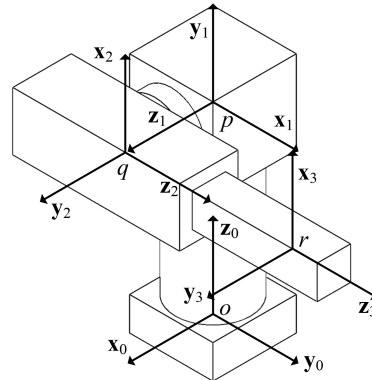
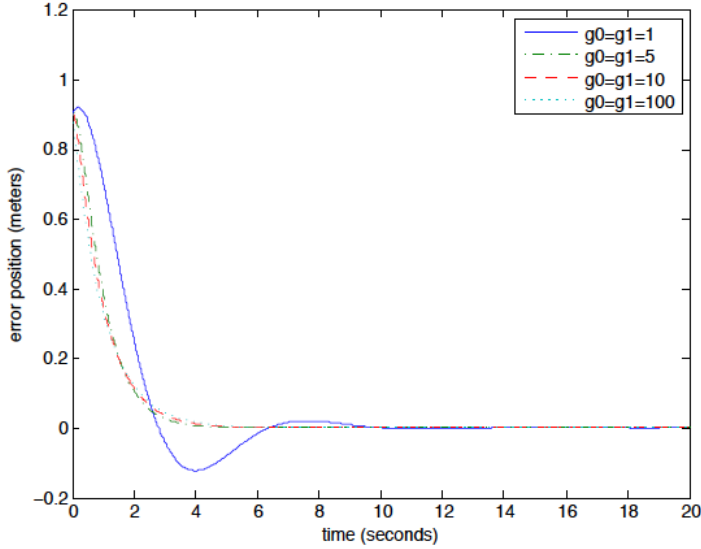


Fig. 7.23: Initial Configuration: $\theta_1 = \frac{\pi}{2}$ rad, $\theta_2 = \frac{\pi}{2}$ rad, $d_{p,q} = 1$ m

the matrix \mathbf{L} is given by

$$\mathbf{L} = \begin{bmatrix} -\frac{1}{Z} & 0 & \frac{u}{z} & uv & -(1+u^2) & v \\ 0 & -\frac{1}{Z_1} & \frac{v}{Z} & (1+v^2) & -uv & -u \\ 0 & 0 & -1 & -vz & uZ & 0 \end{bmatrix}.$$

Fig. 7.24: Tracking error, $e_{x_1}(t)$, Example (7.3.1)

The time derivative of the Jacobian in task space variables is now computed via

$$\dot{\mathbf{J}} = \frac{d}{dt}(\mathbf{L} \cdot \mathbf{J}) = \dot{\mathbf{L}}\mathbf{J} + \mathbf{L}\dot{\mathbf{J}}$$

where

$$\dot{\mathbf{L}} = \begin{bmatrix} \frac{1}{z^2}\dot{z} & 0 & (\frac{1}{z}\dot{u} - \frac{u}{z^2}\dot{z}) & (\dot{u}v + u\dot{v}) & -2u\dot{u} & \dot{v} \\ 0 & \frac{1}{z^2}\dot{z} & (\frac{1}{z}\dot{v} - \frac{v}{z^2}\dot{z}) & 2v\dot{v} & -(\dot{u}v + u\dot{v}) & -\dot{u} \\ 0 & 0 & 0 & -(\dot{v}z + v\dot{z}) & (\dot{u}z + u\dot{z}) & 0 \end{bmatrix}$$

and

$$\dot{\mathbf{J}} = \begin{bmatrix} (\dot{d}_{q,r}\cos\theta_2 - d_{q,r}\dot{\theta}_2\sin\theta_2) & \dot{d}_{q,r} & 0 \\ (-\dot{d}_{q,r}\sin\theta_2 - d_{q,r}\dot{\theta}_2\cos\theta_2) & 0 & 0 \\ d_{p,q}\dot{\theta}_1\cos\theta_2 & 0 & 0 \\ \dot{\theta}_2\cos\theta_2 & 0 & 0 \\ 0 & 0 & 0 \\ \dot{\theta}_2\sin\theta_2 & 0 & 0 \end{bmatrix}.$$

Two sets of initial conditions have been used to evaluate the controller designed in this example. Figures (7.33) through (7.37) depict the results obtained when the initial condition is selected to be

$$\{\mathbf{q}^T(\mathbf{0}), \dot{\mathbf{q}}^T(\mathbf{0})\} = \left\{ \left\{ \frac{\pi}{4}, \frac{\pi}{2}, 1 \right\} \left\{ 0 \ 0 \ 0 \right\} \right\}.$$

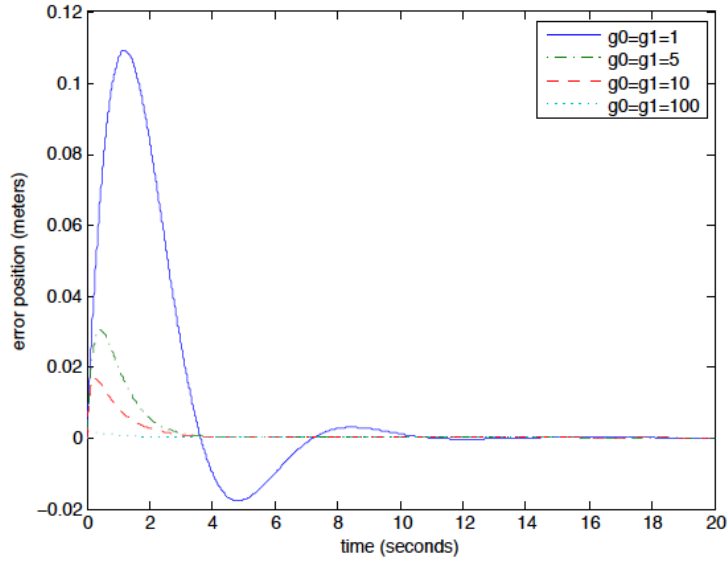


Fig. 7.25: Tracking error, $e_{x_2}(t)$, Example (7.3.1)

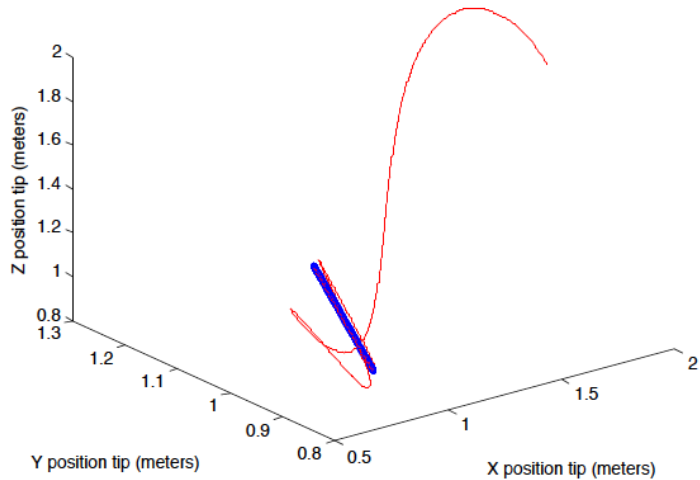
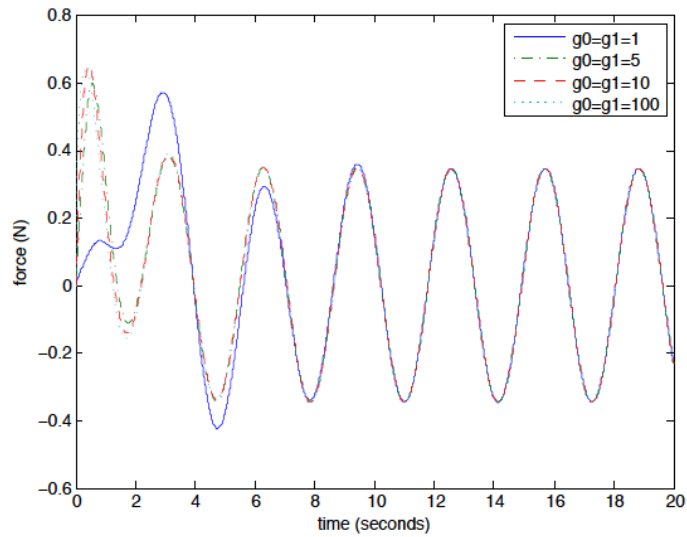
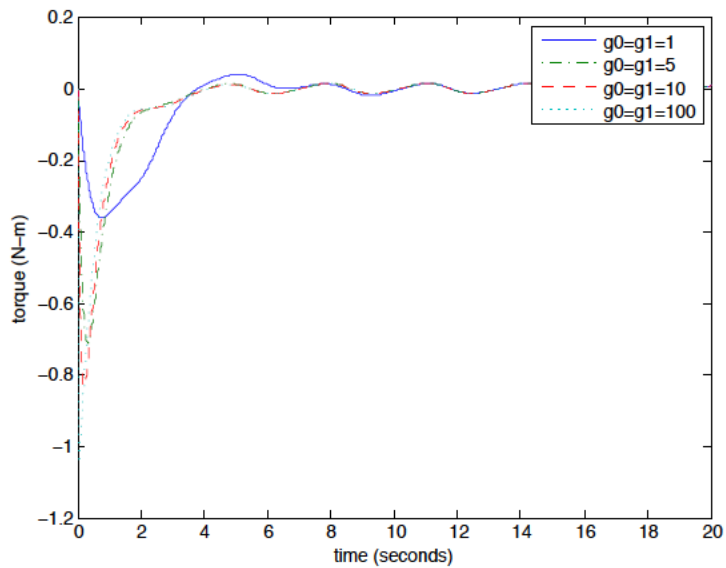
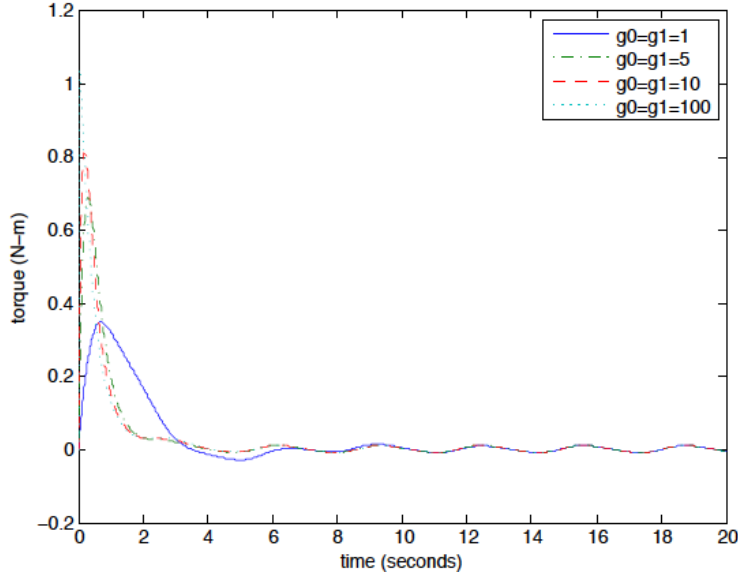
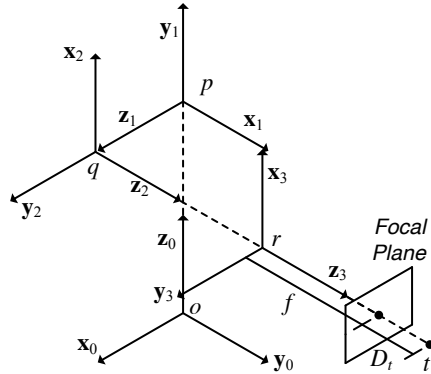


Fig. 7.26: Tip trajectory in inertial coordinates, $(x_1(t), x_2(t), x_3(t))$, Example (7.3.1)

Fig. 7.27: Actuation force, $f(t)$, Example (7.3.1)Fig. 7.28: Actuation moment, $m_1(t)$, Example (7.3.1)

Fig. 7.29: Actuation moment, $m_2(t)$, Example (7.3.1)Fig. 7.30: Spherical robot configuration $(\theta_1, \theta_2, d_{q,r}) = (\frac{\pi}{2}, \frac{\pi}{2}, d_{q,r})$ and inertially fixed feature point t

The configuration of the robot for this initial condition is depicted in Figures (7.31) and (7.32).

Figures (7.33), (7.34) and (7.35) depict the trajectories of $\theta_1(t), \theta_2(t)$ and $d_{q,r}(t)$ starting with this initial condition. It is seen that

$$\theta_1(t) \rightarrow \frac{\pi}{2}, \quad \theta_2(t) \equiv \frac{\pi}{2}, \quad d_{q,r}(t) \rightarrow 1$$

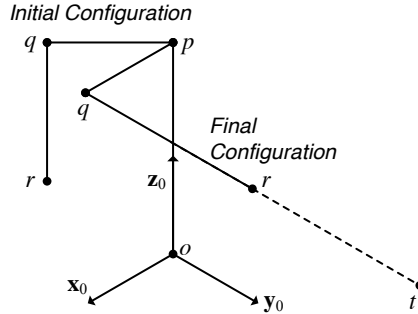


Fig. 7.31: Schematic of Initial Configuration of Robot for Case 1

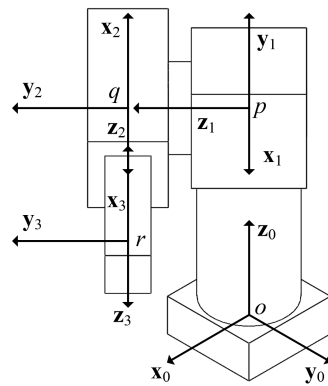


Fig. 7.32: Isometric View of Initial Configuration of Robot for Case 1

as $t \rightarrow \infty$, which implies that the task coordinates must satisfy

$$u(t) \rightarrow 0, \quad v(t) \rightarrow 0, \quad z(t) \rightarrow 2$$

as $t \rightarrow \infty$. Figures (7.36) and (7.37) illustrate the corresponding tracking errors for e_v and e_z , respectively, which converge asymptotically to zero. The tracking error e_u has a magnitude on the order of the numerical accuracy $O(10^{-16})$ of the simulation and is not shown. Figures (7.38) and (7.39) show the actuation force and moment that drives joint 1. The magnitude of the actuation moment about joint 2 is numerically equal to zero and is also not shown.

The results of the simulation when the initial condition is selected to be

$$\{\mathbf{q}^T(\mathbf{0}), \dot{\mathbf{q}}^T(\mathbf{0})\} = \left\{\left\{\frac{\pi}{2}, \frac{\pi}{4}, 1\right\}\left\{0, 0, 0\right\}\right\}$$

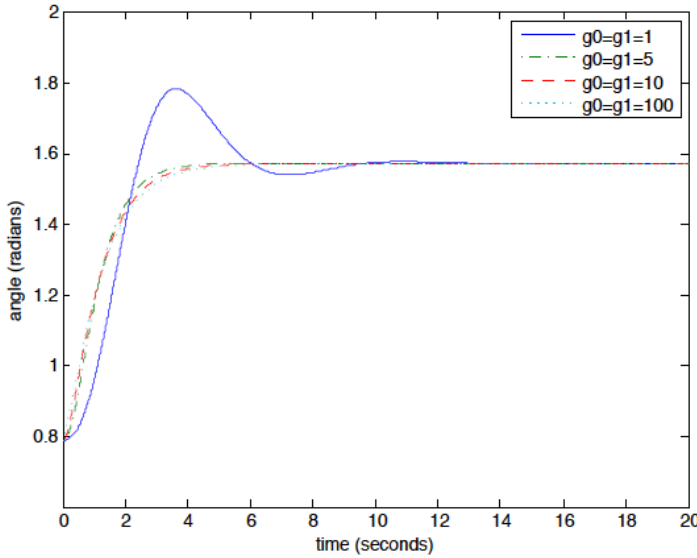
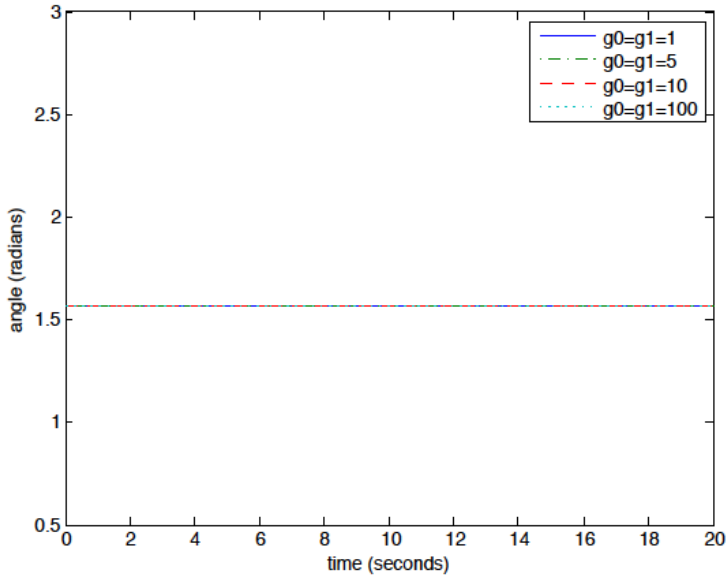
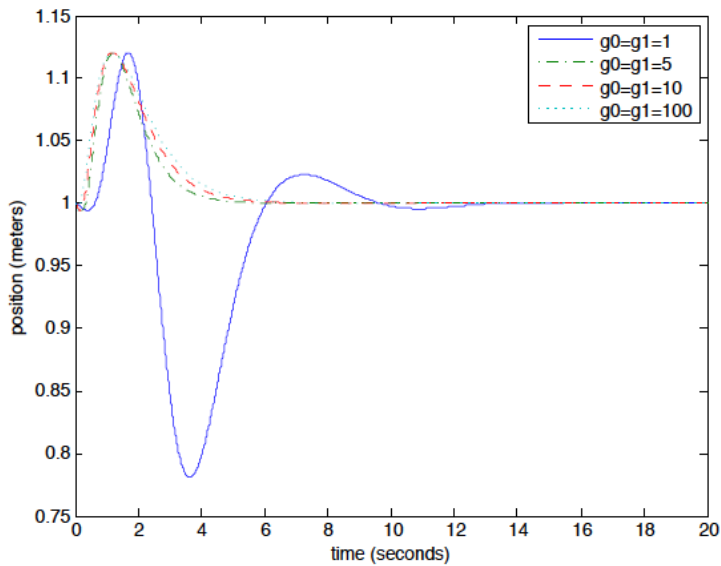


Fig. 7.33: Trajectory $\theta_1(t)$, Example (7.4.1), Case 1

are depicted in Figures (7.42) through (7.49). The configuration of the spherical robotic manipulator associated with this initial condition is depicted in Figures (7.40) and (7.41).

Figures (7.42), (7.43) and (7.44) depict the state trajectories $\theta_1(t), \theta_2(t)$, and $d_{q,r}(t)$, respectively, generated by this initial condition. In contrast to test case 1, it is the angle θ_1 that remains at $\frac{\pi}{2}$, while $\theta_2(t)$ and $d_{q,r}(t)$ vary substantially before they reach steady state. Figures (7.45) and (7.46) illustrate that $\theta_u(t)$ and $\theta_z(t)$ approach zero asymptotically, as expected. The tracking error $e_u(t)$ likewise approaches zero, but its amplitude is less than $O(10^{-10})$ for the duration of the simulation and it is not shown. The actuation force is plotted in Figure (7.47), and the actuation torque that drives joint 2 is shown in Figure (7.49). The magnitude of the torque that drives joint 1 never exceeds $O(10^{-9})$ N-m and is therefore not shown.



Fig. 7.34: Trajectory $\theta_2(t)$, Example (7.4.1), Case 1Fig. 7.35: Trajectory $d_{q,r}(t)$, Example (7.4.1), Case 1

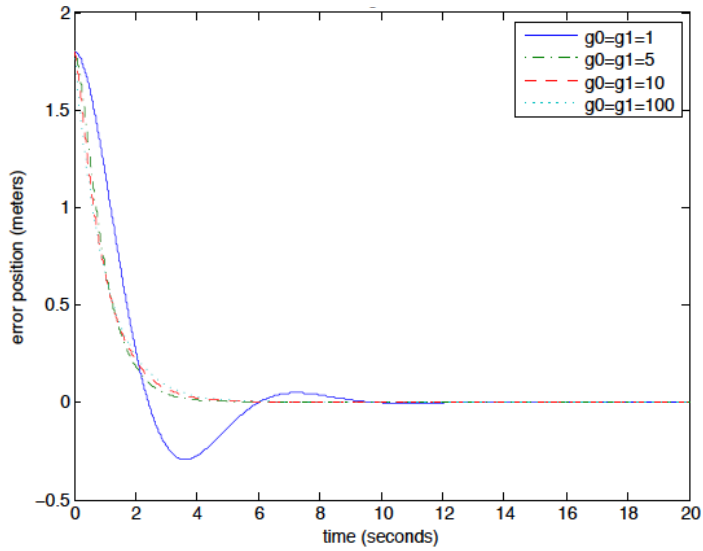


Fig. 7.36: Tracking Error $e_v(t)$, Example (7.4.1), Case 1

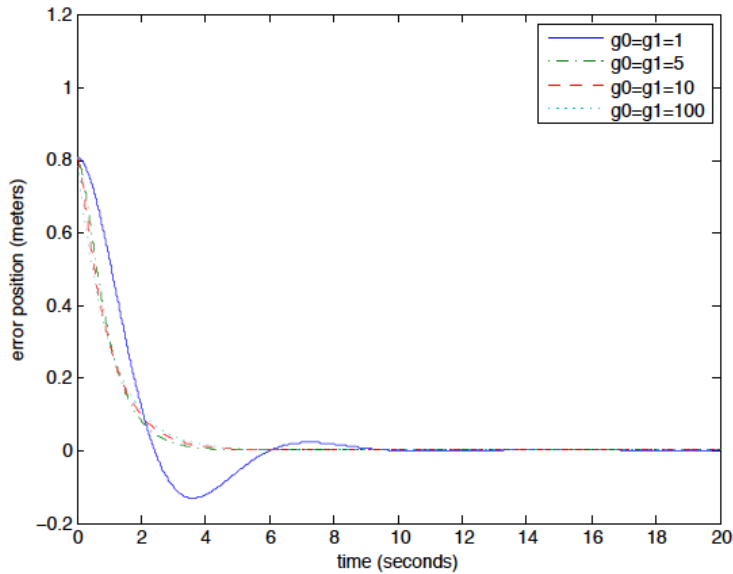
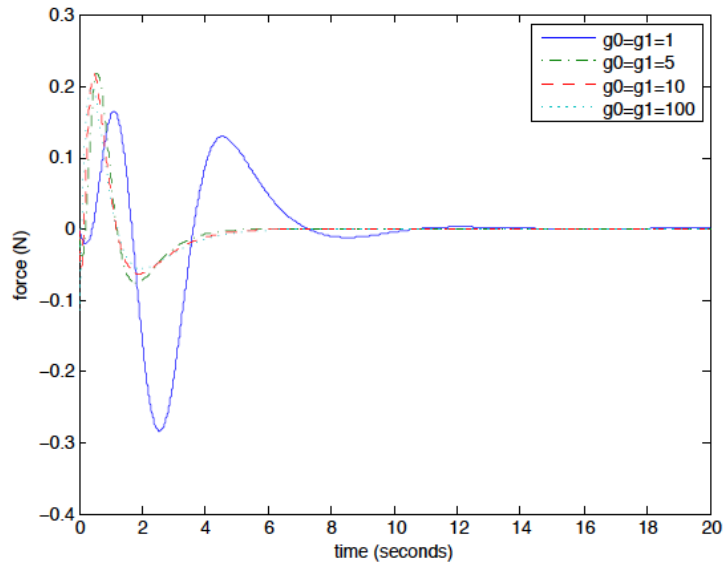
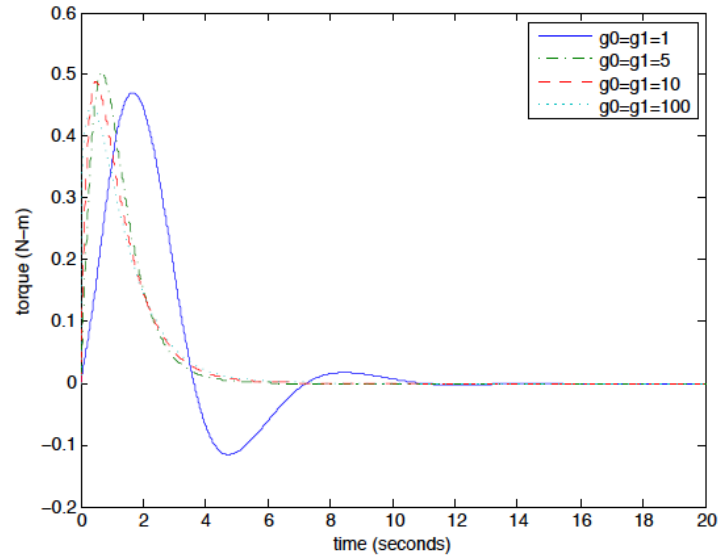


Fig. 7.37: Tracking Error $e_Z(t)$, Example (7.4.1), Case 1

Fig. 7.38: Actuation force $f(t)$, Example (7.4.1), Case 1Fig. 7.39: Actuation moment $m_1(t)$, Example (7.4.1), Case 1

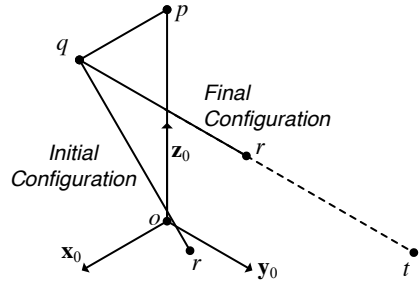


Fig. 7.40: Schematic of Initial Configuration of Robot for Case 1

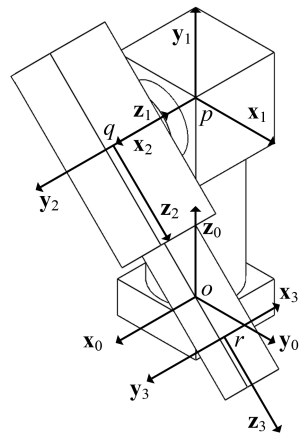
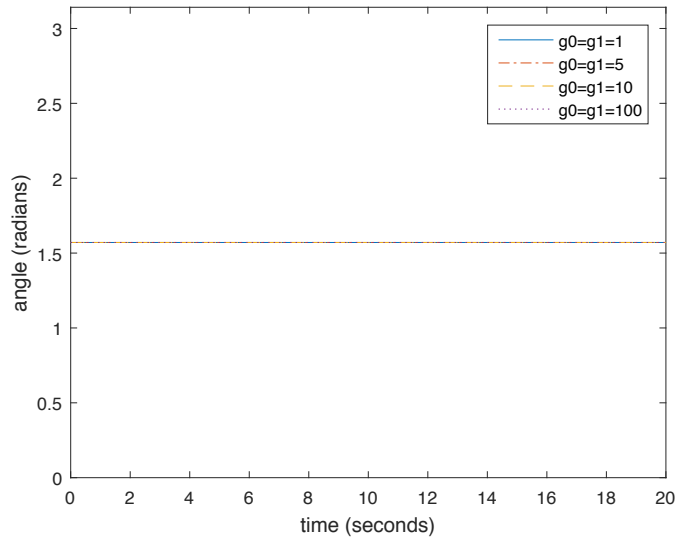
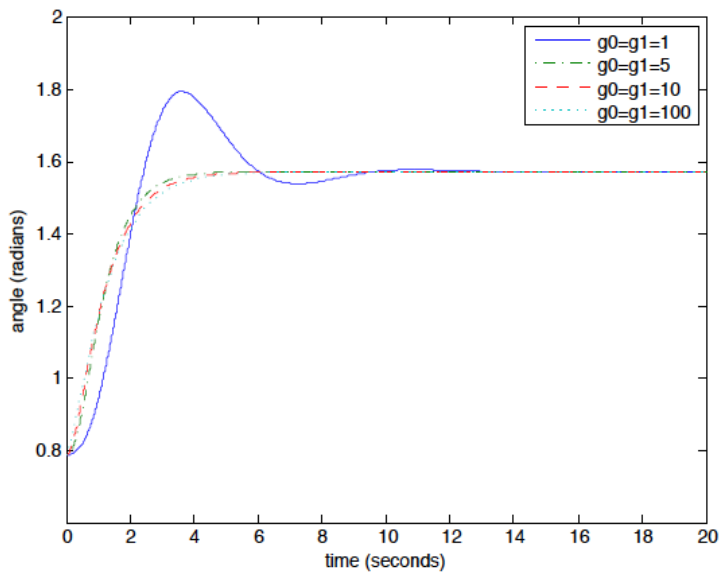


Fig. 7.41: Isometric View of Initial Configuration of Robot for Case 1

Fig. 7.42: Trajectory $\theta_1(t)$, Example (7.4.1), Case 2Fig. 7.43: Trajectory $\theta_2(t)$, Example (7.4.1), Case 2

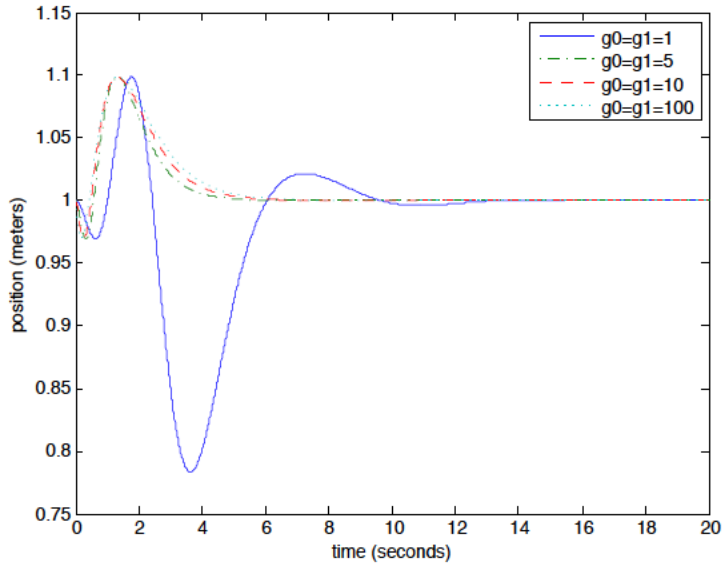


Fig. 7.44: Trajectory $d_{q,r}(t)$, Example (7.4.1), Case 2

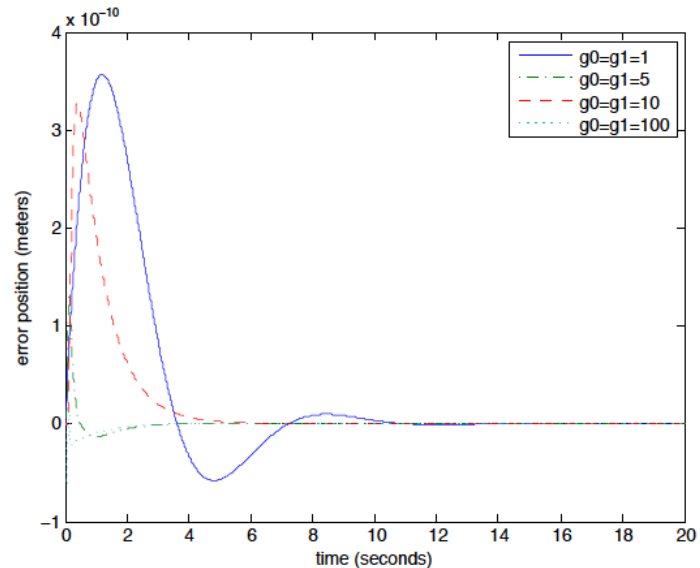
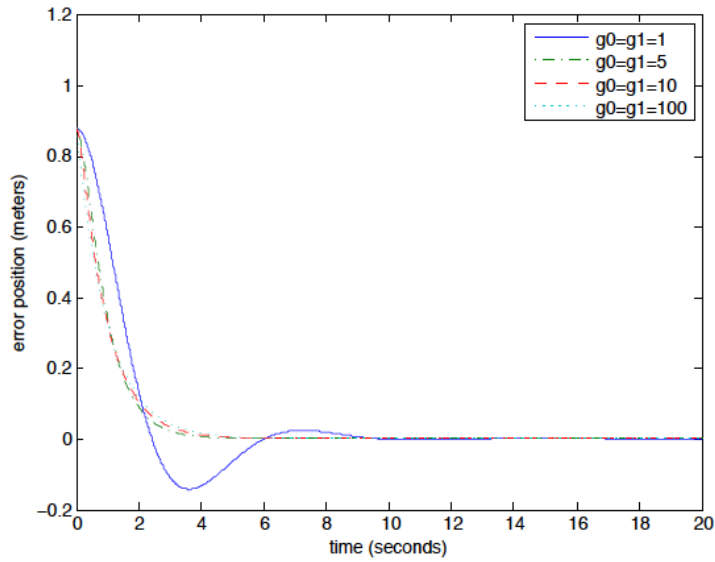
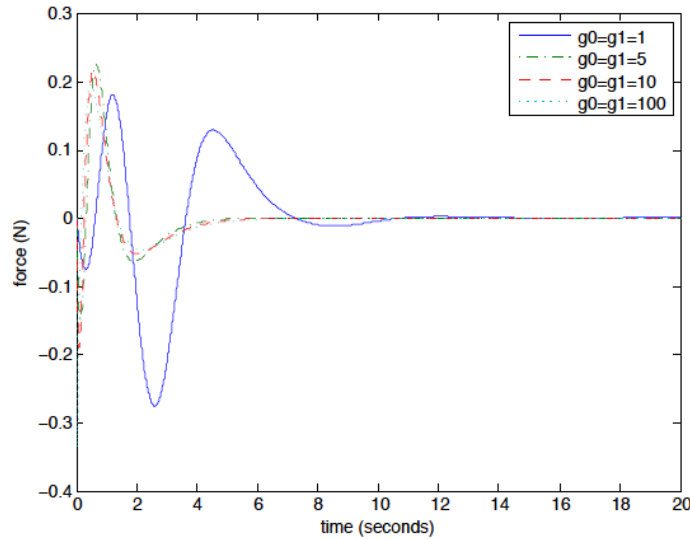


Fig. 7.45: Tracking error $e_v(t)$, Example (7.4.1), Case 2

Fig. 7.46: Tracking error $e_Z(t)$, Example (7.4.1), Case 2Fig. 7.47: Actuation force $f(t)$, Example (7.4.1), Case 2

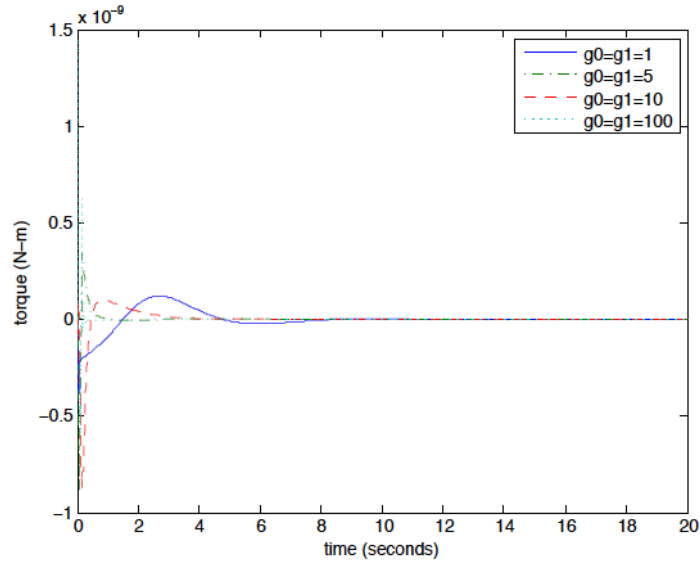


Fig. 7.48: Actuation moment $m_1(t)$, Example (7.4.1), Case 2

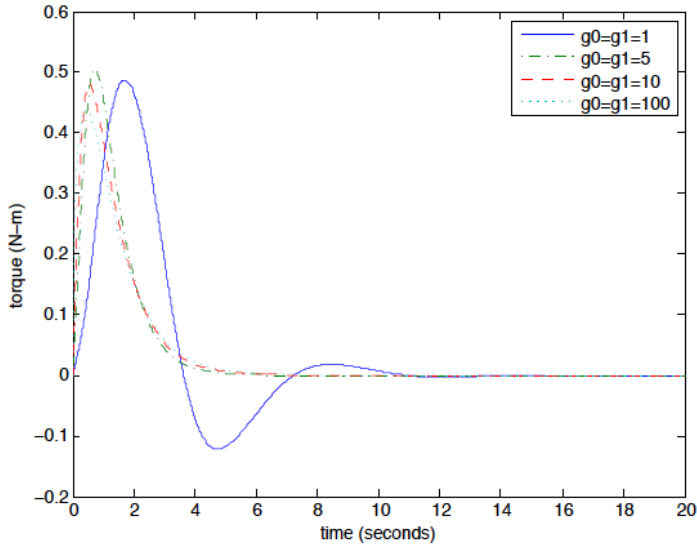


Fig. 7.49: Actuation moment $m_2(t)$, Example (7.4.1), Case 2

7.5 Problems for Chapter (7)

Problem 7.1. Figure (7.50a) depicts the configuration of a camera and a calibration pattern. Assume the the z-axis of the camera is perpendicular to the plane of the calibration pattern and that it intersects the exact center of the calibration pattern. Further assume that the x- and y-axes of the camera are parallel to the x- and y-axes of the retinal plane. The image produced by this configuration is shown in Figure (7.50b). Given a focal length of 2.98 mm, an image resolution of 1080×1920 pixels, and a imaging sensor size of $3.514\text{mm} \times 6.248\text{mm}$, determine the calibration matrix that relates the pixel coordinates (η, ν) to retinal coordinates for this image.

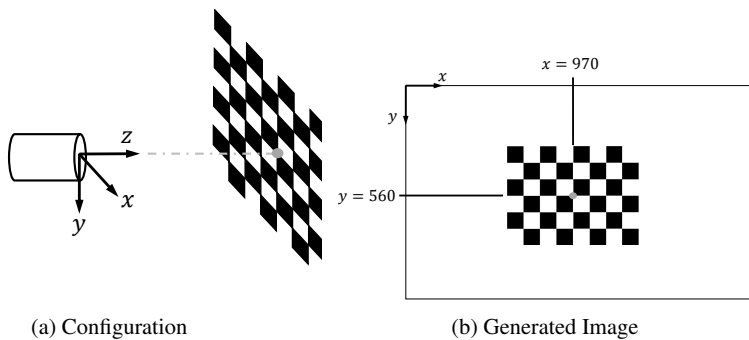


Fig. 7.50: Camera Calibration Pattern Configuration and Generated Image

Problem 7.2. Suppose that a camera is mounted so that its camera frame is rigidly fixed to link 3 of the PUMA robot as shown in Figure (7.51). Assume that the location and orientation of the camera relative to the 3 frame of the PUMA robot is given by the constant homogeneous transformation $\mathbf{p}^C = \mathbf{H}_3^C \mathbf{p}^3$,

$$\begin{Bmatrix} X \\ Y \\ Z \end{Bmatrix} = \begin{bmatrix} B_3^C & \mathbf{d}_{3,C}^C \\ 0 & 1 \end{bmatrix} \begin{Bmatrix} x^3 \\ y^3 \\ z^3 \end{Bmatrix}.$$

For the following two problems let the PUMA robot be configured with

$$\theta_1 = 0, \quad \theta_2 = 0, \quad \theta_3 = -\frac{\pi}{2}$$

(a) Suppose that \mathbf{R}_3^C is the rotation matrix in which the C frame is rotated by 45° about the \mathbf{z}_3 axis, and that

$$\mathbf{d}_{3,C}^3 = \left\{ 0 \ 0 \ \frac{1}{10} d_{s,t} \right\}^T \text{ m.}$$

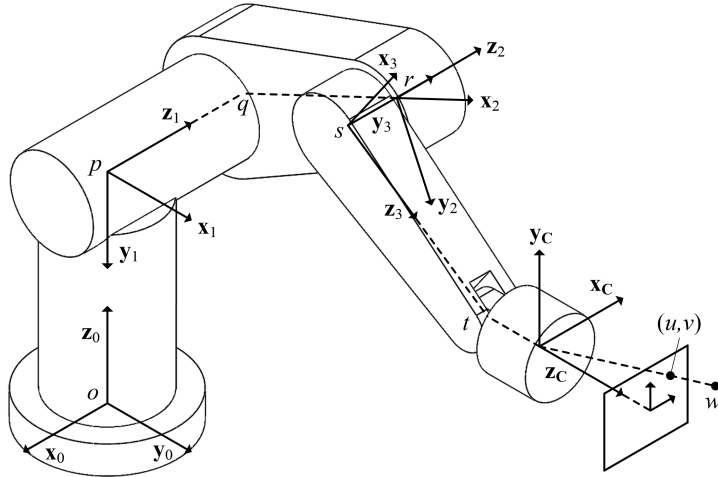


Fig. 7.51: PUMA robot with attached camera

Which points in the world are mapped to the point $(u, v) = (2, 4)$ in the canonical focal plane?

(b) Suppose that \mathbf{R}_3^C is the rotation matrix in which the C frame is rotated by 30° about the x_3 axis, and that

$$\mathbf{d}_{3,C}^3 = \left\{ \frac{1}{10}d_{s,t}, \frac{1}{10}d_{s,t}, 0 \right\}^T.$$

To what point (u, v) in the canonical image plane is the point w having inertial coordinates

$$\mathbf{r}_{o,w}^o = \left\{ (d_{q,r} + d_{s,t} + 5d_{s,t}, d_{p,q} - d_{r,s} + \frac{1}{10}d_{r,s}, d_{o,p} - \frac{1}{10}d_{o,p}) \right\}$$

mapped?

Problem 7.3. Suppose that a camera is mounted so that the camera frame is fixed rigidly to link 3 of the spherical wrist as shown in Figure (7.52).

Suppose that the location and orientation of the camera relative to the 3 frame of the spherical wrist is given by the constant homogenous transformation $\mathbf{p}^C = \mathbf{H}_3^C \mathbf{p}^3$,

$$\begin{Bmatrix} X \\ Y \\ Z \\ 1 \end{Bmatrix} = \begin{bmatrix} \mathbf{R}_3^C & \mathbf{d}_{3,C}^C \\ 0 & 1 \end{bmatrix} \begin{Bmatrix} x^3 \\ y^3 \\ z^3 \\ 1 \end{Bmatrix}.$$

(a) Suppose that \mathbf{R}_0^C is the rotation matrix parametrized by the $3 - 2 - 1$ Euler angles that is used with \mathbf{R}_3^C to map frame 0 into the C frame, where the yaw ψ , pitch θ and roll ϕ are

$$\psi = \frac{\pi}{4} \text{ rad}, \quad \theta = 0, \quad \phi = \frac{\pi}{2} \text{ rad}$$

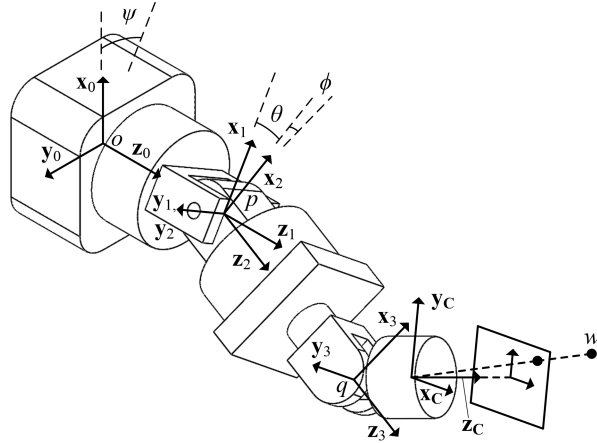


Fig. 7.52: Spherical wrist with mounted camera

Suppose further that $d_{3,\mathbb{C}}^3 = \left\{ 0, 0, \frac{1}{20} \right\} m$. Which points in the are mapped to the point $(u, v) = (1, 1)$ in the canonical retinal plane?

(b) Suppose that $\mathbf{R}_0^{\mathbb{C}}$ is the rotation matrix parametrized by the 3 – 2 – 1 Euler angles used to map frame 0 into the \mathbb{C} frame, where the yaw ψ , pitch θ and roll ϕ are

$$\psi = 0, \quad \theta = \frac{\pi}{4} \text{ rad}, \quad \phi = 0$$

Suppose further that $d_{3,\mathbb{C}}^3 = \left\{ 0, 0, \frac{1}{20} \right\} m$. To what point (u, v) in the canonical retinal plane is the point w having inertial coordinates

$$\mathbf{r}_{o,w}^o = \begin{Bmatrix} 0 \\ 0 \\ d_{o,p} \end{Bmatrix} + \mathbf{R}_0^{\mathbb{C}} \begin{Bmatrix} \frac{1}{20} \\ \frac{1}{10} \\ d_{p,q} + \frac{1}{10} \end{Bmatrix} \quad m$$

mapped?

Problem 7.4. An ideal pinhole camera is mounted on the SCARA robot shown in Figure (7.53) so that the camera axes coincide with the 3 frame and the optical center is located at point u . Find the transformation that maps the inertial coordinates $(x_1(t), x_2(t), x_3(t))$ of point w , $\mathbf{r}_{0,w}(t) := x_1(t)\mathbf{x}_0 + x_2(t)\mathbf{y}_0 + x_3(t)\mathbf{z}_0$, to the canonical focal plane coordinates $(u(t), v(t))$. Find the transformation that maps the inertial coordinates of w to the pixel coordinates $(3, 2)$.

Problem 7.5. An ideal pinhole camera is mounted on the cylindrical robot shown in Figure (7.54) so that the camera axes coincide with the 4 frame and the optical center is located at point t . Find the transformation that map the inertial coordinates $(x_1(t), x_2(t), x_3(t))$ of the point w , $\mathbf{r}_{0,w}(t) := x_1(t)\mathbf{x}_0 + x_2(t)\mathbf{y}_0 + x_3(t)\mathbf{z}_0$, to the canon-

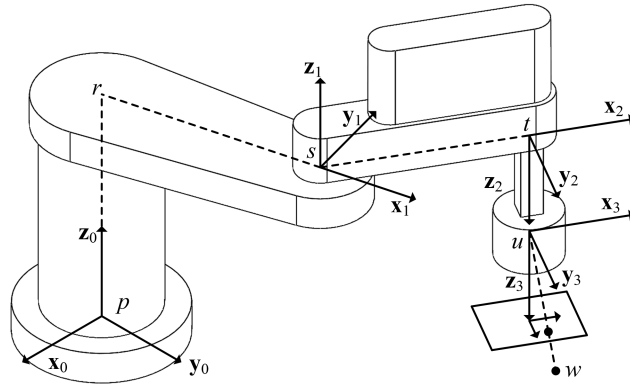


Fig. 7.53: SCARA Robot with Mounted Camera

cal focal plane coordinates $(u(t), v(t))$. Find the transformation that maps the inertial coordinates of w to the pixel coordinates (ξ, η) .

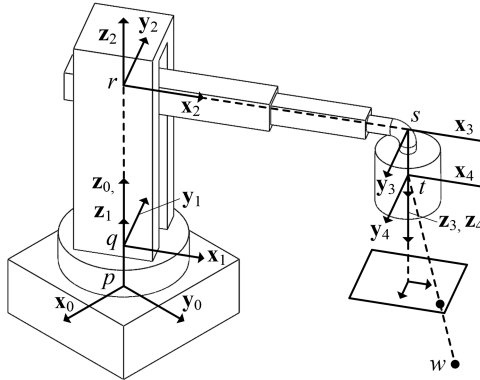


Fig. 7.54: Cylindrical robot with mounted camera

Problem 7.6. Derive a controller so that the point t on the cylindrical robot depicted in Figure (7.55) tracks the trajectory of the point w . The point w has coordinates $(x_{1,d}(t), x_{2,d}(t), x_{3,d}(t))$ relative to the inertial frame 0, $\mathbf{r}_{0,w}(t) := x_{1,d}(t)\mathbf{x}_0 + x_{2,d}(t)\mathbf{y}_0 + x_{3,d}(t)\mathbf{z}_0$. Base the controller on the task space computed torque control law studied in Theorem (7.3).

Problem 7.7. Derive a controller so that the point u on the SCARA robot depicted in Figure (7.56) tracks the trajectory of the point v . The point v has coordinates $(x_{1,d}(t), x_{2,d}(t), x_{3,d}(t))$ relative to the inertial frame 0, $\mathbf{r}_{0,v}(t) := x_{1,d}(T)\mathbf{x}_0 + x_{2,d}(t)\mathbf{y}_0 + x_{3,d}(t)\mathbf{z}_0$. Base the controller on the task space computed torque control law studied in Theorem (7.3).

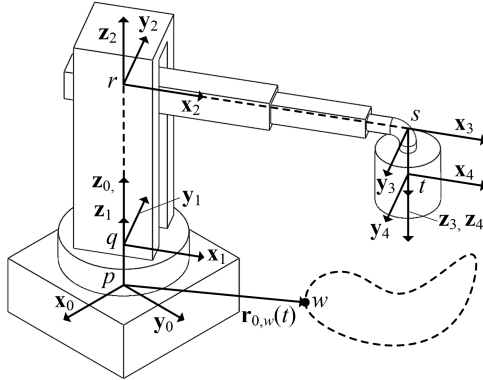


Fig. 7.55: Cylindrical Robot and Task Space Trajectory Tracking

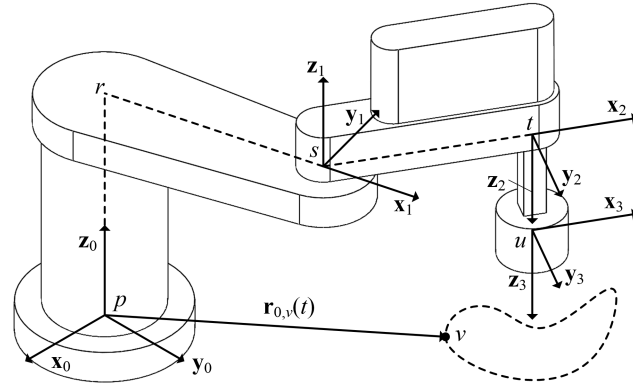


Fig. 7.56: SCARA Robot and Task Space Trajectory Tracking

Problem 7.8. Suppose that the robot depicted in Figure (7.53) is equipped with a camera whose axes coincide with the 3 frame and laser ranging system. Let \$(X, Y, Z)\$ denote the coordinates relative to the camera frame of the point \$w\$ so that \$\mathbf{r}_{3,w} := X\mathbf{x}_3 + Y\mathbf{y}_3 + Z\mathbf{z}_3\$. Assume the laser ranging system enables the measurement of the \$Z\$ coordinate of the point \$w\$. Derive a controller that will actuate the robot so that the canonical focal plane coordinates \$(u(t), v(t))\$ of the point \$w\$ approach the origin of the focal plane and the depth \$z(t)\$ approaches some fixed value \$Z\$.

Problem 7.9. Suppose that the robot depicted in Figure (7.54) is equipped with a camera whose axes coincide with the 4-frame and a laser ranging system. Let \$(X, Y, Z)\$ denote the coordinates relative to the camera frame of point \$w\$, \$\mathbf{r}_{4,w} := X\mathbf{x}_3 + Y\mathbf{y}_3 + Z\mathbf{z}_3\$. Assume the laser ranging system enables the measurement of the \$Z\$ coordinate of the point \$w\$. Derive a controller that will actuate the robot so that the canonical retinal plane coordinates \$(u(t), v(t))\$ of point \$w\$ approach the origin of the focal plane and (2) the depth \$Z(t)\$ approaches some fixed value \$Z\$.

Problem 7.10. Show that the *interaction matrix* for *focal length* f is given by

$$\mathbf{L} = \begin{bmatrix} -\frac{f}{Z} & 0 & \frac{u}{Z} & \frac{uv}{f} & -\frac{f^2+u^2}{f} & v \\ 0 & -\frac{f}{Z} & \frac{v}{Z} & \frac{f^2+v^2}{f} & -\frac{uv}{f} & -u \end{bmatrix}.$$

Chapter 8

Appendices

8.1 Fundamentals of Linear Algebra

This section presents some of the most common concepts from linear algebra that have direct application to robotics and autonomous systems. The interested reader is referred to the numerous excellent texts on this topic, such as [18], for a detailed discussion. This book will restrict its attention to linear algebra over the *vector space* of M -tuples of real numbers \mathbb{R}^M . The operations of *vector addition* and *multiplication of vectors by scalars* are defined intuitively in terms of componentwise operations. If $\mathbf{x}^T = \{x_1 \ x_2 \ \dots \ x_M\}$, $\mathbf{y}^T = \{y_1 \ y_2 \ \dots \ y_M\}$, and $\mathbf{z}^T = \{z_1 \ z_2 \ \dots \ z_M\}$, for addition,

$$\mathbf{z} = \mathbf{x} + \mathbf{y} \quad \text{if and only if} \quad \begin{Bmatrix} z_1 \\ z_2 \\ \vdots \\ z_M \end{Bmatrix} = \begin{Bmatrix} x_1 + y_1 \\ x_2 + y_2 \\ \vdots \\ x_M + y_M \end{Bmatrix}.$$

Multiplication of a vector \mathbf{x} by a scalar α is likewise defined componentwise as

$$\mathbf{z} = \alpha \mathbf{x} \quad \text{if and only if} \quad \begin{Bmatrix} z_1 \\ z_2 \\ \vdots \\ z_M \end{Bmatrix} = \begin{Bmatrix} \alpha x_1 \\ \alpha x_2 \\ \vdots \\ \alpha x_M \end{Bmatrix}.$$

Definition 8.1. A subset S of \mathbb{R}^M is a *vector subspace* of \mathbb{R}^M if and only if it is closed under the operations of *vector addition* and multiplication of vectors by a real scalar. In other words, it must be true that $(\mathbf{x} + \mathbf{y}) \in S$ whenever $\mathbf{x}, \mathbf{y} \in S$, and that $(\alpha \mathbf{x}) \in S$ for any scalar $\alpha \in \mathbb{R}$ when $\mathbf{x} \in S$.

One of the implications of this definition is that for a subset S to be a *vector subspace* of \mathbb{R}^M , the *zero vector* must be contained in S . Since the scalar $\alpha = 0$ can

always be chosen, the requirement that S be closed with respect to multiplication of vectors by a scalar means that $\alpha\mathbf{x} = \mathbf{0x} = \mathbf{0} \in S$ for any vector $\mathbf{x} \in S$. The most common way to define *vector subspaces* is by considering the *span* of a fixed finite set of vectors.

Definition 8.2. Suppose that $\mathbf{a}_1, \mathbf{a}_2, \dots, \mathbf{a}_N$ is a collection of N vectors contained in \mathbb{R}^M . The vector \mathbf{z} is a *finite linear combination* of the these vectors if it can be written in the form

$$\mathbf{z} = \alpha_1 \mathbf{a}_1 + \alpha_2 \mathbf{a}_2 + \dots + \alpha_N \mathbf{a}_N$$

for some real constants $\alpha_1, \alpha_2, \dots, \alpha_N \in \mathbb{R}$. The *span* of the vectors $\mathbf{a}_1, \mathbf{a}_2, \dots, \mathbf{a}_N$ is the *vector subspace* that consists of all *finite linear combinations* of these vectors,

$$\begin{aligned} & \text{span}\{\mathbf{a}_1, \mathbf{a}_2, \dots, \mathbf{a}_N\} \\ &= \left\{ \mathbf{z} \in \mathbb{R}^M \mid \mathbf{z} = \alpha_1 \mathbf{a}_1 + \dots + \alpha_N \mathbf{a}_N \text{ for some scalars } \alpha_1, \dots, \alpha_N \in \mathbb{R} \right\} \end{aligned}$$

The definition above asserts that the *span* of a set of vectors is in fact a *vector subspace*. This is not difficult to see. A *vector subspace* must be closed with respect to the operations of *vector addition* and multiplication of a vector by a scalar. Suppose that \mathbf{x}, \mathbf{y} are two arbitrary vectors in the *span* of the vectors $\mathbf{a}_1, \mathbf{a}_2, \dots, \mathbf{a}_N$. By definition there must be two sets of coefficients $\alpha_1, \alpha_2, \dots, \alpha_N$ and $\beta_1, \beta_2, \dots, \beta_N$ such that the finite linear combinations of these vectors may be defined as

$$\mathbf{x} = \mathbf{A}\boldsymbol{\alpha} = \mathbf{a}_1\alpha_1 + \mathbf{a}_2\alpha_2 + \dots + \mathbf{a}_N\alpha_N$$

and

$$\mathbf{y} = \mathbf{A}\boldsymbol{\beta} = \mathbf{a}_1\beta_1 + \mathbf{a}_2\beta_2 + \dots + \mathbf{a}_N\beta_N.$$

But if this is the case, the sum can be written as

$$\mathbf{x} + \mathbf{y} = \mathbf{a}_1(\alpha_1 + \beta_1) + \mathbf{a}_2(\alpha_2 + \beta_2) + \dots + \mathbf{a}_N(\alpha_N + \beta_N),$$

and it follows that the vector $\mathbf{x} + \mathbf{y}$ lies in the *span* of this set of vectors. Similarly, if \mathbf{x} lies in the *span* of the set of vectors $\mathbf{a}_1, \mathbf{a}_2, \dots, \mathbf{a}_N$ and c is any real number, it can be written that

$$c\mathbf{x} = \mathbf{a}_1(c\alpha_1) + \mathbf{a}_2(c\alpha_2) + \dots + \mathbf{a}_N(c\alpha_N).$$

Thus, the vector $c\mathbf{x}$ also lies in the *span* of these vectors. The *span* of the set of vectors is therefore closed with respect to *vector addition* and multiplication of vectors by scalars, so it is a *vector subspace* of \mathbb{R}^M .

Definition 8.3. Let \mathbf{A} be an $M \times N$ matrix that is partitioned into its columns

$$\mathbf{A} = [\mathbf{a}_1 \ \mathbf{a}_2 \ \dots \ \mathbf{a}_N].$$

The *range* of the matrix \mathbf{A} is the *span* of its columns,

$$\text{range}(\mathbf{A}) = \text{span}\{\mathbf{a}_1, \mathbf{a}_2, \dots, \mathbf{a}_N\} \subseteq \mathbb{R}^M.$$

The *nullspace* of the matrix \mathbf{A} is the *vector subspace* of \mathbb{R}^N that consists of all vectors that the matrix \mathbf{A} maps into the zero vector

$$\text{nullspace}(\mathbf{A}) = \{\mathbf{v} : \mathbf{Av} = \mathbf{0}\} \subseteq \mathbb{R}^N.$$

The reader should carefully note that the above definition states that the *range* and *nullspace* of a matrix \mathbf{A} are *vector subspaces* of \mathbb{R}^M and \mathbb{R}^N , respectively. Since the *range* of a matrix \mathbf{A} is defined to be the *span* of its column vectors, it is closed under the operations of *vector addition* and multiplication of vectors by scalars, following the reasoning after Definition (8.2).

The definitions of the *range* and *nullspace* of a matrix \mathbf{A} have been introduced because they are immediately useful in the analysis of numerous problems in robotics. The following theorem shows that the *range* of a matrix \mathbf{A} and the *nullspace* of the *transposed matrix* \mathbf{A}^T induces an *orthogonal decomposition*. This decomposition is useful in applications where a matrix equation must be solved; it enables a geometric interpretation.

Theorem 8.1. Any $M \times N$ matrix \mathbf{A} induces the orthogonal decomposition of \mathbb{R}^M ,

$$\mathbb{R}^M = \text{range}(\mathbf{A}) \oplus \text{nullspace}(\mathbf{A}^T). \quad (8.1.1)$$

This theorem is interpreted as follows. For any vector \mathbf{v} in \mathbb{R}^M , \mathbf{v} can be written in the form

$$\mathbf{v} = \mathbf{v}_R + \mathbf{v}_N$$

where \mathbf{v}_R lies in the *range* of \mathbf{A} , \mathbf{v}_N lies in the *nullspace* of \mathbf{A}^T , and $\mathbf{v}_R^T \mathbf{v}_N = 0$.

8.1.1 Solution of Matrix Equations

Now consider the matrix equation

$$\mathbf{Ax} = \mathbf{b} \quad (8.1.2)$$

where \mathbf{A} is an $M \times N$ matrix, \mathbf{x} is an $N \times 1$ vector, and \mathbf{b} is an $M \times 1$ vector. With the fundamental definition of the *range* of a matrix given in the previous section, an alternative way to express the fact that matrix Equation (8.1.2) has at least one

solution may be defined.

Theorem 8.2. *There exists a solution of the matrix equation in Equation (8.1.2) if and only if \mathbf{b} lies in the range of the matrix \mathbf{A} .*

Proof. The proof of this theorem follows from recalling the definition of the *range* of a matrix. First, partition the matrix \mathbf{A} in Equation (8.1.2) into its columns so that

$$\left[\mathbf{a}_1 \ \mathbf{a}_2 \ \dots \ \mathbf{a}_N \right] \begin{Bmatrix} x_1 \\ x_2 \\ \vdots \\ x_N \end{Bmatrix} = \mathbf{b}.$$

This equation can be rewritten as

$$\mathbf{a}_1 x_1 + \mathbf{a}_2 x_2 + \dots + \mathbf{a}_N x_N = \mathbf{b}.$$

By earlier definition, this equation states that the vector \mathbf{b} lies in the span of the vectors $\mathbf{a}_1, \dots, \mathbf{a}_N$. \square

Theorem (8.2) summarized the fact that the existence of a solution to the matrix Equation (8.1.2) can be interpreted as a requirement that vector \mathbf{b} lies in the *range* of the matrix \mathbf{A} . The next theorem shows that multiple solutions to the matrix equation exist if and only if the nullspace of the matrix \mathbf{A} contains some non-zero vector.

Theorem 8.3. *Suppose that \mathbf{x}^* is a solution of the matrix equation in (8.1.2). Then $\mathbf{x} = \mathbf{x}^* + \mathbf{n}$ is also a solution of the matrix equation (8.1.2) where \mathbf{n} is any vector that is contained in the nullspace of the matrix \mathbf{A} ,*

$$\mathbf{n} \in \text{nullspace}(\mathbf{A}).$$

Proof. If $\mathbf{x}^* + \mathbf{n}$ is substituted into the governing matrix Equation (8.1.2),

$$\mathbf{A}(\mathbf{x}^* + \mathbf{n}) = \underbrace{\mathbf{A}\mathbf{x}^*}_{\mathbf{b}} + \underbrace{\mathbf{A}\mathbf{n}}_0.$$

In fact, it is not difficult to see that if \mathbf{x}^* is a solution to Equation (8.1.2), then *any solution* to the equation has the form $\mathbf{x}^* + \mathbf{n}$ where $\mathbf{n} \in \text{nullspace}(\mathbf{A})$. Suppose that \mathbf{y} is also a solution to Equation (8.1.2). Then, it can be written

$$\mathbf{A}(\mathbf{x}^* - \mathbf{y}) = \mathbf{A}\mathbf{x}^* - \mathbf{A}\mathbf{y} = \mathbf{b} - \mathbf{b} = \mathbf{0}.$$

But this equation is nothing more than a statement that

$$\mathbf{x}^* - \mathbf{y} \in \text{nullspace}(\mathbf{A}),$$

and it follows that the arbitrary solution \mathbf{y} has the form

$$\mathbf{y} = \mathbf{x}^* + \mathbf{n}$$

for some vector $\mathbf{n} \in \text{nullspace}(\mathbf{A})$. □

8.1.2 Linear Independence and Rank

It has been shown that the existence of a solution of the matrix Equation (8.1.2) can be couched in terms of the *range* of the matrix \mathbf{A} in Theorem (8.2). The characterization of multiple solutions of this equation is given in terms of the *nullspace* of the matrix \mathbf{A} in Theorem (8.3). While these two theorems provide a geometric interpretation of the solution of the matrix Equation (8.1.2), it is also common to discuss solutions of this equation in terms of *rank* conditions on the matrix \mathbf{A} . The definition of the *rank* of a matrix \mathbf{A} is prepared for by introducing the notion of *linear independence* of a set of vectors and a *basis* for a *vector subspace* of \mathbb{R}^M .

Definition 8.4. A set of N vectors $\mathbf{v}_1, \dots, \mathbf{v}_N$ in \mathbb{R}^M is *linearly independent* if and only if the sum

$$\alpha_1 \mathbf{v}_1 + \alpha_2 \mathbf{v}_2 + \dots + \alpha_N \mathbf{v}_N = \mathbf{0}$$

holds only when the coefficients $\alpha_1, \alpha_2, \dots, \alpha_N$ are identically zero

$$\alpha_1 = \alpha_2 = \dots = \alpha_N = 0.$$

The set of vectors is *linearly dependent* if it is not *linearly independent*.

If a set of vectors $\mathbf{v}_1, \mathbf{v}_2, \dots, \mathbf{v}_N$ is *linearly dependent* it is possible to express at least one of the vectors in terms of the remaining vectors in the set. To see why this is the case, suppose that the set of vectors is not *linearly independent*. This means that there is some set of coefficients, not all equal to zero, such that

$$\alpha_1 \mathbf{v}_1 + \alpha_2 \mathbf{v}_2 + \dots + \alpha_N \mathbf{v}_N = \mathbf{0}.$$

Suppose, without loss of generality, that the coefficient $\alpha_N \neq 0$ in this summation. In this case \mathbf{v}_N can be solved for in the form

$$\mathbf{v}_N = -\frac{1}{\alpha_N} (\alpha_1 \mathbf{v}_1 + \alpha_2 \mathbf{v}_2 + \dots + \alpha_{N-1} \mathbf{v}_{N-1}).$$

Collections of vectors that are *linearly independent* play a critical role in determining *bases* for *vector subspaces*.

Definition 8.5. A set of vectors $\mathbf{v}_1, \mathbf{v}_2, \dots, \mathbf{v}_N$ contained in a *vector subspace* $S \subseteq \mathbb{R}^M$ is a *basis* for the *vector subspace* if the following two conditions hold.

- (i) The set of vectors is *linearly independent*.
- (ii) The *vector subspace* S does not contain a larger collection of *linearly independent* vectors.

If the set of vectors $\mathbf{v}_1, \mathbf{v}_2, \dots, \mathbf{v}_N$ is a basis for the *vector subspace* S , the dimension of the *vector subspace* is equal to N .

The definition of a *basis* for a *vector subspace*, as well as its *dimension*, will make it possible to give a precise description the existence and multiplicity of solutions to the matrix Equation (8.1.2). This description will be given in terms of the *rank* of a matrix \mathbf{A} .

Definition 8.6. The *column rank* (*row rank*) of an $M \times N$ matrix \mathbf{A} is the *dimension* of the *vector subspace spanned by the columns (rows)* of \mathbf{A} .

The *column rank* of a matrix \mathbf{A} is the *dimension* of the *range* of \mathbf{A} . The following theorem notes that these two values are equal for a given matrix.

Theorem 8.4. The column rank and row rank of any matrix \mathbf{A} are equal. The rank of the matrix \mathbf{A} is this shared value of the row rank and column rank.

One implication of the above theorem is that the largest possible dimension of any subspace S contained in \mathbb{R}^M is the *dimension M* of the ambient space.

Theorem 8.5. Any set of $M + 1$ vectors in \mathbb{R}^M is linearly dependent.

Proof. The proof of this theorem follows from Theorem (8.4). Suppose a set of vectors $\mathbf{a}_1, \mathbf{a}_2, \dots, \mathbf{a}_{M+1}$ are given that are contained in \mathbb{R}^M . Create the matrix \mathbf{A} by taking these vectors as its columns. Thus, the matrix \mathbf{A} is an $M \times (M + 1)$ matrix. Since the *row rank* is equal to the *column rank*, it must be the case that the number of *linearly independent* columns is equal to the number of *linearly independent* rows. But the number of *linearly independent* rows must be less than or equal to M . It follows that the number of *linearly independent* columns is equal to $M < M + 1$. Thus, the $M + 1$ columns are *linearly dependent*. \square

8.1.3 Invertibility and Rank

It has been shown that the existence and uniqueness of solutions to the linear matrix equations $\mathbf{Ax} = \mathbf{b}$ can be described in terms of the range and nullspace of the matrix

\mathbf{A} when $\mathbf{A} \in \mathbb{R}^{M \times N}$. When \mathbf{A} is a square matrix, the existence and uniqueness of the solutions to this equation can be discussed in terms of the *invertibility* of \mathbf{A} .

Theorem 8.6. *A square matrix \mathbf{A} is invertible if there exists a matrix \mathbf{B} such that*

$$\mathbf{BA} = \mathbf{AB} = \mathbf{I}.$$

The inverse of the matrix \mathbf{A} is denoted by $\mathbf{A}^{-1} := \mathbf{B}$.

The following theorem summarizes several well-known facts relating the inverse, rank, range, nullspace, and determinant of the matrix \mathbf{A} to the existence and uniqueness of solutions to the linear matrix equation $\mathbf{Ax} = \mathbf{b}$.

Theorem 8.7. *Suppose \mathbf{A} is an $M \times M$ matrix. The following conditions are equivalent:*

- (i) *The matrix \mathbf{A} is invertible.*
- (ii) *There is a unique solution to the equation $\mathbf{Ax} = \mathbf{b}$.*
- (iii) *The $\det(\mathbf{A}) \neq 0$.*
- (iv) *The $\text{range}(\mathbf{A}) = \mathbb{R}^M$.*
- (v) *The $\text{nullspace}(\mathbf{A}) = \{\mathbf{0}\}$.*
- (vi) *The $\text{rank}(\mathbf{A}) = M$.*

The proof of all of these properties can be carried out using the definitions and theorems developed thus far, but in some cases they can be lengthy. With the use of the *Singular Value Decomposition*, introduced in Section (8.1.4), it is straightforward to show the equivalence of these properties. Therefore, the proof of this theorem is deferred until the next section.

8.1.4 Least Squares Approximation

Some of the common, fundamental theorems that describe the matrix Equation (8.1.2) have been discussed in Sections (8.1.1) and (8.1.2). It is often the case that the matrix equation $\mathbf{Ax} = \mathbf{b}$ cannot be solved exactly. It may be that the information given is *inconsistent* with the form of the matrix equation. This often occurs if the data in the coefficient matrix \mathbf{A} or the right hand side \mathbf{b} is obtained via experiment. Even if the data is known precisely or analytically, it can also happen that the solution \mathbf{x} to this equation is desired if it exists, but it is sufficient if it is merely “close to satisfying” the equation. This occurs often in the synthesis of control laws, for example.

No matter the motivation, vectors \mathbf{x} that only approximately solve the matrix Equation (8.1.2) can be found by replacing Equation (8.1.2) with an optimization problem. A vector \mathbf{x} should minimize the norm of the *residual* or *defect* $\mathbf{Ax} - \mathbf{b}$

$$\min_{\mathbf{x}} \|\mathbf{Ax} - \mathbf{b}\|. \quad (8.1.3)$$

The norm $\|\mathbf{Ax} - \mathbf{b}\|$ is greater than or equal to zero for all possible choices of \mathbf{x} , and it can only equal zero when $\mathbf{Ax} - \mathbf{b}$ equals zero. Thus, if the matrix Equation (8.1.2) has an exact solution, then it exactly solves the optimization problem in Equation (8.1.3). However, it is always possible to solve Equation (8.1.3), even if Equation (8.1.2) does not have an exact solution. This fact enables us to define approximate solutions of the matrix Equation (8.1.2).

The solution of the alternative optimization problem in Equation (8.1.3) uses a property of *orthogonal matrices* derived in Chapter (2). The norm of a vector does not change when acted upon by a *rotation matrix*. For the problem at hand, consider the norm of the *residual* $\mathbf{Ax} - \mathbf{b}$ when this vector is premultiplied by some orthogonal matrix \mathbf{O} ,

$$\begin{aligned} \|\mathbf{Ax} - \mathbf{b}\|^2 &= (\mathbf{Ax} - \mathbf{b})^T (\mathbf{Ax} - \mathbf{b}), \\ &= (\mathbf{Ax} - \mathbf{b})^T \mathbf{O}^T \mathbf{O} (\mathbf{Ax} - \mathbf{b}), \\ &= \|\mathbf{O}(\mathbf{Ax} - \mathbf{b})\|. \end{aligned}$$

The minimization in Equation (8.1.3) is equivalent then to the minimization problem

$$\min_{\mathbf{x}} \|\mathbf{O}(\mathbf{Ax} - \mathbf{b})\|. \quad (8.1.4)$$

The *orthogonal matrix* \mathbf{O} can be chosen to simplify the computational task.

In practice there are many reasonable choices for the construction of the matrix \mathbf{O} . Methods based on Givens transformations, Householder transformations, and Jacobi rotations are just a few of the *orthogonal matrices* that can be used in this approach. The interested reader should consult [18] for a complete summary. This book will only discuss one such method based on the *Singular Value Decomposition* of a matrix.

Theorem 8.8. Any real, $M \times N$ matrix \mathbf{A} has a Singular Value Decomposition in the form

$$\mathbf{A} = \mathbf{U}\Sigma\mathbf{V}^T \quad (8.1.5)$$

where \mathbf{U} is an $M \times M$ orthogonal matrix, Σ is a $M \times N$ diagonal matrix and \mathbf{V} is an $N \times N$ orthogonal matrix. By convention the diagonal singular values are arranged in non-increasing order on the diagonal of Σ .

Suppose that $M \geq N$, so that the problem is *overdetermined* or *exactly determined*. Partition the matrix \mathbf{U} so that \mathbf{U}_1 corresponds to the first N columns of the matrix \mathbf{U} and \mathbf{U}_2 corresponds to the next $M - N$ columns of \mathbf{U} in

$$\mathbf{U} = \begin{bmatrix} \mathbf{U}_1 & \mathbf{U}_2 \end{bmatrix},$$

and conformally partition the matrix Σ into the $N \times N$ diagonal matrix σ and the $(M - N) \times N$ zero matrix

$$\Sigma = \begin{bmatrix} \sigma \\ \mathbf{0} \end{bmatrix}.$$

This decomposition is applied to the *optimization problem* in Equation (8.1.4) by choosing \mathbf{O} to be equal to \mathbf{U}^T .

$$\|\mathbf{U}^T(\mathbf{Ax} - \mathbf{b})\|^2 = \|\mathbf{U}^T\mathbf{Ax} - \mathbf{U}^T\mathbf{b}\|^2 = \|\Sigma\mathbf{V}^T\mathbf{x} - \mathbf{U}^T\mathbf{b}\|^2, \quad (8.1.6)$$

$$= \left\| \begin{bmatrix} \sigma \\ \mathbf{0} \end{bmatrix} \mathbf{V}^T \mathbf{x} - [\mathbf{U}_1 \ \mathbf{U}_2]^T \mathbf{b} \right\|^2, \quad (8.1.7)$$

$$= \left\| \begin{bmatrix} \sigma \\ \mathbf{0} \end{bmatrix} \mathbf{V}^T \mathbf{x} - \begin{bmatrix} \mathbf{U}_1^T \\ \mathbf{U}_2^T \end{bmatrix} \mathbf{b} \right\|^2, \quad (8.1.8)$$

$$= \|\sigma \mathbf{V}^T \mathbf{x} - \mathbf{U}_1^T \mathbf{b}\|^2 + \|\mathbf{U}_2 \mathbf{b}\|^2. \quad (8.1.9)$$

The term $\mathbf{U}_2^T \mathbf{b}$ is independent of the choice of vector \mathbf{x} . The first term, however, can be solved using the following theorem.

Theorem 8.9. Suppose that the dimensions of the $M \times N$ matrix \mathbf{A} satisfy $M \geq N$, and that the rank of the matrix \mathbf{A} is N . The solution of the least squares optimization problem is given by

$$\mathbf{x} = \mathbf{V} \sigma^{-1} \mathbf{U}_1^T \mathbf{b},$$

and the norm of the residual for this choice of the vector \mathbf{x} is given by

$$\|\mathbf{Ax} - \mathbf{b}\| = \|\mathbf{U}_2^T \mathbf{b}\|.$$

Next, the proof of Theorem (8.7) will be reconsidered using the singular value decomposition of the matrix \mathbf{A}

Proof. First, it is clear that property (i) is equivalent to property (ii) by the definition of the matrix inverse. Next, it will be shown that property (i) is equivalent to property (iii). The *singular value decomposition* of the square matrix \mathbf{A} is given by

$$\mathbf{A} = \mathbf{U} \Sigma \mathbf{V}^T$$

where \mathbf{U} , \mathbf{V} and Σ are all $M \times M$ matrices. Suppose that \mathbf{A} is invertible. We will show that Σ is invertible. Since it can be written that

$$\Sigma = \mathbf{U}^T \mathbf{A} \mathbf{V},$$

and \mathbf{A} is assumed to be invertible, the inverse of the term on the right is equal to

$$(\mathbf{U}^T \mathbf{A} \mathbf{V})^{-1} = \mathbf{V}^T \mathbf{A}^{-1} \mathbf{U}.$$

Therefore, Σ is a diagonal, nonnegative matrix for which the inverse exists. The inverse of a diagonal matrix Σ is obtained by inverting the diagonal elements of Σ , and because of this there are no zeros on the diagonal of Σ . Therefore, $\det(\Sigma) \neq 0$,

as the determinant of a diagonal matrix is equal to the product of the terms on the diagonal. Therefore, if \mathbf{A} is invertible, then $\det(\mathbf{A}) \neq 0$ since

$$\det(\mathbf{A}) = \det(\mathbf{U}\Sigma\mathbf{V}^T) = \det(\mathbf{U})\det(\Sigma)\det(\mathbf{V}) = \det(\Sigma) \neq 0.$$

In addition, this sequence of steps can be reversed, starting with the assumption that $\det(\mathbf{A}) \neq 0$, next deducing that $\det(\Sigma) \neq 0$, proceeding to argue that Σ is invertible, and finally concluding that \mathbf{A} is invertible. Therefore, property (i) holds if and only if property (iii) holds.

Next, the matrix \mathbf{U} will be partitioned according to the number of nonzero singular values in Σ for which

$$\mathbf{A} = [\mathbf{U}_1 \ \mathbf{U}_2] \begin{bmatrix} \boldsymbol{\sigma} & \mathbf{0} \\ \mathbf{0} & \mathbf{0} \end{bmatrix} \begin{bmatrix} \mathbf{V}_1^T \\ \mathbf{V}_2^T \end{bmatrix} = \mathbf{U}_1 \boldsymbol{\sigma} \mathbf{V}_1^T.$$

In this equation it is assumed that there are $J \leq M$ nonzero singular values, so that $\boldsymbol{\sigma}$ is a $J \times J$ matrix, \mathbf{U}_1 and \mathbf{V}_1 are $M \times J$ matrices, and \mathbf{U}_2 and \mathbf{V}_2 are $M \times (M - J)$ matrices. By inspection, $\text{range}(\mathbf{A}) = \text{range}(\mathbf{U}_1)$ and $\text{nullspace}(\mathbf{A}) = \text{span}(\mathbf{V}_2)$. From the proof that properties (i) and (iii) are equivalent, it is known that \mathbf{A}^{-1} exists if and only if Σ has no zeros on the diagonal. This is equivalent to saying that $J = M$. It follows that

$$\text{range}(\mathbf{A}) = \mathbb{R}^M \iff \text{nullspace}(\mathbf{A}) = \{0\} \iff \mathbf{A}^{-1} \text{ exists},$$

which states that property (i), (iv), and (v) are equivalent.

Finally, it is known that $\text{rank}(\mathbf{A})$ is equal to the number of linearly independent columns of \mathbf{A} , which is the same as the dimension of $\text{range}(\mathbf{A})$. Since $\text{range}(\mathbf{A}) = \text{span}(\mathbf{V}_2)$, and all of the columns of \mathbf{V}_2 are orthogonal and therefore linearly independent, $\text{rank}(\mathbf{A}) = J$. This shows that property (vi) is equivalent to property (i). \square

Example 8.1.1. Consider the matrix equation

$$\begin{bmatrix} 1 & 2 \\ 0 & 1 \\ 1 & 0 \end{bmatrix} \mathbf{x} = \mathbf{b}. \quad (8.1.10)$$

Use Theorem (8.2) to give a geometric interpretation of the existence of solutions to Equation (8.1.10).

Solution: By definition, the matrix \mathbf{A} can be partitioned into its columns \mathbf{a}_1 and \mathbf{a}_2 with

$$\mathbf{A} = [\mathbf{a}_1 \ \mathbf{a}_2] = \left[\begin{Bmatrix} 1 \\ 0 \\ 1 \end{Bmatrix} \begin{Bmatrix} 2 \\ 1 \\ 0 \end{Bmatrix} \right].$$

This equation can be rewritten in the form

$$\mathbf{a}_1 \mathbf{x}_1 + \mathbf{a}_2 \mathbf{x}_2 = \begin{Bmatrix} 1 \\ 0 \\ 1 \end{Bmatrix} \mathbf{x}_1 + \begin{Bmatrix} 2 \\ 1 \\ 0 \end{Bmatrix} \mathbf{x}_2 = \mathbf{b}.$$

This expansion shows that the matrix Equation (8.1.10) has a solution if and only if the vector \mathbf{b} lies in the plane spanned by \mathbf{a}_1 and \mathbf{a}_2 .



Example 8.1.2. Consider again the matrix Equation (8.1.10) in Example (8.1.1). That example stated that the matrix Equation (8.1.10) has at least one solution if \mathbf{b} lies in the *range* of the matrix \mathbf{A} . Derive a simple condition that can be used to check the *consistency* of the matrix equation for a given right hand side \mathbf{b} .

Solution: First, there are many computational tools that can be used to construct a basis for the *range* of a matrix \mathbf{A} , such as the QR decomposition or Singular Value Decomposition [18]. However, a simple test is desired that can be used for the problem at hand. Theorem (8.1) provides one relatively easy way to check the *consistency* of the matrix equation for a specific right hand side. Theorem (8.1) states that any vector \mathbf{v} in \mathbb{R}^m can be decomposed into the sum of a vector \mathbf{v}_R that lies in the *range* of a matrix \mathbf{A} and a vector \mathbf{v}_N that lies in the nullspace of the transposed matrix \mathbf{A}^T . Moreover, the vectors \mathbf{v}_R and \mathbf{v}_N are orthogonal. It is not difficult to calculate the *nullspace* of the matrix \mathbf{A}^T in this problem. As before, partition the matrix \mathbf{A} into its columns $\mathbf{a}_1, \mathbf{a}_2$. This partitioning of \mathbf{A} into columns also partitions \mathbf{A}^T into rows via

$$\mathbf{A}^T = \begin{bmatrix} \mathbf{a}_1^T \\ \mathbf{a}_2^T \end{bmatrix} = \begin{bmatrix} \begin{Bmatrix} 1 & 0 & 1 \end{Bmatrix} \\ \begin{Bmatrix} 2 & 1 & 0 \end{Bmatrix} \end{bmatrix}. \quad (8.1.11)$$

The *nullspace* of \mathbf{A}^T is defined to be the *vector subspace*

$$\text{nullspace}(\mathbf{A}^T) = \left\{ \mathbf{z} \in \mathbb{R}^3 : \mathbf{A}^T \mathbf{z} = 0 \right\}.$$

The set of vectors that are perpendicular to $\begin{Bmatrix} 1 & 0 & 1 \end{Bmatrix}$ and $\begin{Bmatrix} 2 & 1 & 0 \end{Bmatrix}$ can be defined as any multiple of the cross product $\mathbf{a}_1 \times \mathbf{a}_2 = \begin{Bmatrix} 1 & -2 & -1 \end{Bmatrix}$. This shows that

$$\text{nullspace}(\mathbf{A}^T) = \text{span} \begin{Bmatrix} 1 \\ -2 \\ -1 \end{Bmatrix}.$$

Suppose Theorem (8.1) is used to decompose the vector \mathbf{b} into two such perpendicular components $\mathbf{b} = \mathbf{v}_R + \mathbf{v}_N$. The matrix equation has a solution if and only if \mathbf{b} lies in the *range* of the matrix \mathbf{A} , which holds only if $\mathbf{v}_N = 0$. In other words, a solution exists if and only if $\mathbf{b} = \mathbf{v}_R$. Because \mathbf{v}_R is perpendicular to the *nullspace* of \mathbf{A}^T , it must be true that

$$\mathbf{b} \cdot \begin{Bmatrix} -1 \\ 2 \\ 1 \end{Bmatrix} = 0.$$

Given the right hand side vector \mathbf{b} , this equation is simple to check.

8.1.5 Rank Conditions and the Interaction Matrix

The derivation of the *image-based visual servo control* law required a solution to the matrix equation

$$\mathbf{L}_{\text{sys}} \begin{Bmatrix} \mathbf{v}_{0,C}^C \\ \omega_{0,C}^C \end{Bmatrix} = -\lambda \mathbf{e}$$

for the velocity of the origin and angular velocity of the *camera frame* in the *inertial frame*. The matrix \mathbf{L}_{sys} was shown to have dimension $2n_p \times 6$ where n_p is the number of *system feature points*. This matrix is not square in general which complicates the discussion of the solution of the associated matrix equation. Rewrite the equation above in the form

$$\mathbf{A}\mathbf{x} = \mathbf{b}$$

where \mathbf{A} is an $M \times N$ matrix, \mathbf{x} is an $N \times 1$ vector of unknowns and \mathbf{b} is a $M \times 1$ vector of given right hand side values.

8.2 The Algebraic Eigenvalue Problem

The *algebraic eigenvalue problem* appears in many contexts in the study of dynamics and control of robotic systems. It is used to define *spectral decompositions* that are important in understanding the stability of linear systems, and it is used to construct diagonalizations of real symmetric matrices. This latter construction is important in the definition of *principal axes* for the *inertia matrix* of a rigid body.

Definition 8.7. A nontrivial M -vector ϕ is an *eigenvector* of the $M \times M$ matrix \mathbf{A} corresponding to the *eigenvalue* λ if it satisfies

$$\mathbf{A}\phi = \lambda\phi.$$

It is essential to note that the definition of the *eigenvector* requires that ϕ is a *nontrivial* vector. In other words, ϕ cannot identically equal zero. This definition also shows that an *eigenvector* is a direction that is *invariant* under the application of the matrix \mathbf{A} . It is also evident that if ϕ is an *eigenvector* of the matrix \mathbf{A} , then so is $c\phi$ for any scalar $c \in \mathbb{R}$. The *eigenvectors* of \mathbf{A} are said to be determined only up to a scalar multiple.

One of the most common descriptions of solutions to the *algebraic eigenvalue problem* can be inferred by applying the theory from the last few sections about the solvability of linear systems.

Theorem 8.10. *The scalar λ is an eigenvalue of the matrix \mathbf{A} if and only if*

$$\det(\mathbf{A} - \lambda\mathbf{I}) = 0.$$

Every $M \times M$ matrix \mathbf{A} has M eigenvalues.

Proof. The definition of the *eigenvectors* ϕ and *eigenvalues* λ in Definition (8.7) requires that

$$(\mathbf{A} - \lambda\mathbf{I})\phi = \mathbf{0} \quad (8.2.1)$$

for some scalar λ and a vector ϕ that is not identically equal to the zero vector. It is known from the discussion in Section (8.1.2) that if the matrix $\mathbf{A} - \lambda\mathbf{I}$ is invertible, there is a unique solution to the system of equations

$$(\mathbf{A} - \lambda\mathbf{I})\mathbf{x} = \mathbf{b}$$

for any choice of the right hand side \mathbf{b} . Therefore, if the matrix $(\mathbf{A} - \lambda\mathbf{I})$ is invertible, there is a unique solution to Equation (8.2.1), and it must be that $\phi = \mathbf{0}$. However, this case is not of interest for the solution of the *algebraic eigenvalue problem*. Therefore, the matrix $(\mathbf{A} - \lambda\mathbf{I})$ must not be invertible to allow for multiple solutions, and to permit a nontrivial ϕ that satisfies Equation (8.2.1). Section (8.1.2) has shown that the matrix $(\mathbf{A} - \lambda\mathbf{I})$ is invertible if and only if $\det(\mathbf{A} - \lambda\mathbf{I}) \neq 0$. Thus λ is an *eigenvalue* of the matrix \mathbf{A} if and only if

$$\det(\mathbf{A} - \lambda\mathbf{I}) = 0.$$

If \mathbf{A} is an $M \times M$ matrix, the equation $\det(\mathbf{A} - \lambda\mathbf{I}) = 0$ yields an M^{th} order polynomial in λ that must be equal to zero. This polynomial equation is called the *characteristic equation* of the *algebraic eigenvalue problem*. Every M^{th} order polynomial has M (complex) roots, and it is concluded that every $M \times M$ matrix has M eigenvalues. \square

This theorem shows that the *eigenvalues* of the $M \times M$ matrix \mathbf{A} are defined from the roots of the characteristic polynomial $\det(\mathbf{A} - \lambda\mathbf{I}) = 0$. Even if \mathbf{A} is a real matrix, so that the coefficients in the characteristic polynomial are real, the roots of the characteristic polynomial can still be complex. Also, while every $M \times M$ matrix has M eigenvalues, it is not always the case that there are M distinct eigenvectors. This phenomenon is studied in more detail in Section (8.2.2).

8.2.1 Self-Adjoint Matrices

For an important class of matrices, those matrices that are *self-adjoint*, a full set of M eigenvectors can be found. A matrix \mathbf{A} is *self-adjoint* whenever

$$\mathbf{A} = \mathbf{A}^* = \overline{\mathbf{A}}^T$$

where $\overline{\mathbf{A}}$ is the complex conjugate of the matrix \mathbf{A} . In the applications under consideration, only real matrices will be considered, and a real matrix is *self-adjoint* when it is *symmetric*. The following theorem shows that it is possible to construct an *orthonormal basis* for \mathbb{R}^M in terms of the *eigenvectors* of \mathbf{A} in this case. This result is a special case of the *spectral theory* associated with *self-adjoint matrices*.

Theorem 8.11. Suppose that \mathbf{A} is an $M \times M$ real, symmetric matrix. Then

- (i) The eigenvalues of \mathbf{A} are real.
- (ii) The eigenvectors of \mathbf{A} corresponding to distinct eigenvalues are orthogonal.
- (iii) The eigenvectors of \mathbf{A} corresponding to distinct eigenvalues are \mathbf{A} -orthogonal, so that

$$\phi^T \mathbf{A} \psi = 0$$

for eigenvectors ϕ and ψ corresponding to distinct eigenvalues.

- (iv) It is possible to construct an $M \times M$ modal matrix Φ whose columns are eigenvectors of \mathbf{A} such that

$$\Phi^* \Phi = \mathbf{I},$$

$$\Phi^* \mathbf{A} \Phi = \begin{bmatrix} \lambda_1 & 0 & \cdots & 0 \\ 0 & \lambda_2 & \cdots & 0 \\ \vdots & \vdots & \ddots & \vdots \\ 0 & 0 & \cdots & \lambda_M \end{bmatrix},$$

where λ_i is the i^{th} eigenvalue of \mathbf{A} for $i = 1, 2, \dots, M$.

Proof. First, (i) will be shown to hold. Suppose that λ is an *eigenvalue* and ϕ is an *eigenvector* of \mathbf{A} with

$$\mathbf{A}\phi = \lambda\phi. \quad (8.2.2)$$

If λ is an *eigenvalue* of \mathbf{A} , it is also an *eigenvalue* of $\mathbf{A}^* = \overline{\mathbf{A}}^T$. Let ψ be the *eigenvector* of \mathbf{A}^* corresponding to λ ,

$$\mathbf{A}^* \psi = \lambda \psi. \quad (8.2.3)$$

Premultiply Equation (8.2.2) by ψ^* and Equation (8.2.3) by ϕ^* to attain

$$\begin{aligned}\boldsymbol{\psi}^* \mathbf{A} \boldsymbol{\phi} &= \lambda \boldsymbol{\psi}^* \boldsymbol{\phi}, \\ \boldsymbol{\phi}^* \mathbf{A}^* \boldsymbol{\psi} &= \lambda \boldsymbol{\phi}^* \boldsymbol{\psi}.\end{aligned}$$

The conjugate transpose of the second equation is taken and subtracted from the first to obtain

$$\begin{aligned}0 &= (\boldsymbol{\psi}^* \mathbf{A} \boldsymbol{\phi} - (\boldsymbol{\phi}^* \mathbf{A}^* \boldsymbol{\psi})^*) = (\boldsymbol{\psi}^* \mathbf{A} \boldsymbol{\phi} - \boldsymbol{\psi}^* \mathbf{A} \boldsymbol{\phi}), \\ &= \lambda \boldsymbol{\psi}^* \boldsymbol{\phi} - (\lambda \boldsymbol{\phi}^* \boldsymbol{\psi})^* = (\lambda - \bar{\lambda}) \boldsymbol{\psi}^* \boldsymbol{\phi}.\end{aligned}$$

In general $\boldsymbol{\psi}^* \boldsymbol{\phi}$ is not equal to zero, which implies that $\lambda = \bar{\lambda}$. Therefore, the eigenvalue λ must be real.

Next, (ii) will be shown to hold. Suppose that $\lambda_1, \boldsymbol{\phi}_1$ and $\lambda_2, \boldsymbol{\phi}_2$ are distinct *eigenpairs* of the matrix \mathbf{A} . That is, assume that $\lambda_1 \neq \lambda_2$. The following two equations are satisfied for these *eigenpairs*,

$$\begin{aligned}\mathbf{A} \boldsymbol{\phi}_1 &= \lambda_1 \boldsymbol{\phi}_1, \\ \mathbf{A} \boldsymbol{\phi}_2 &= \lambda_2 \boldsymbol{\phi}_2.\end{aligned}$$

Similar to the discussion of (i), premultiply the first equation above by $\boldsymbol{\phi}_2^T$, premultiply the second equation above by $\boldsymbol{\phi}_1^T$, and subtract the transpose of the resulting second equation from the first to obtain

$$\begin{aligned}0 &= (\boldsymbol{\phi}_2^T \mathbf{A} \boldsymbol{\phi}_1 - (\boldsymbol{\phi}_1^T \mathbf{A} \boldsymbol{\phi}_2)^T) = (\boldsymbol{\phi}_2^T \mathbf{A} \boldsymbol{\phi}_1 - \boldsymbol{\phi}_2^T \mathbf{A} \boldsymbol{\phi}_1) \\ &= \lambda_1 \boldsymbol{\phi}_2^T \boldsymbol{\phi}_1 - (\lambda_2 \boldsymbol{\phi}_1^T \boldsymbol{\phi}_2)^T = (\lambda_1 - \lambda_2) \boldsymbol{\phi}_2^T \boldsymbol{\phi}_1\end{aligned}$$

Since the *eigenvalues* are distinct, $\lambda_1 - \lambda_2 \neq 0$. Therefore, $\boldsymbol{\phi}_2^T \boldsymbol{\phi}_1 = 0$, or $\boldsymbol{\phi}_1$ is orthogonal to $\boldsymbol{\phi}_2$.

For the proof of (iii), it is known that

$$\boldsymbol{\phi}_2^T \mathbf{A} \boldsymbol{\phi}_1 = \lambda_1 \boldsymbol{\phi}_2^T \boldsymbol{\phi}_1 = 0,$$

which shows directly that $\boldsymbol{\phi}_1$ and $\boldsymbol{\phi}_2$ are \mathbf{A} -orthogonal.

For the proof of (iv), if the *eigenvalues* are distinct and the *eigenvectors* are assumed to each have magnitudes equal to 1 (a common choice for systematically defining eigenvectors), the two properties of the modal matrix Φ may be directly evaluated as

$$\boldsymbol{\Phi}^T \boldsymbol{\Phi} = \begin{bmatrix} \boldsymbol{\phi}_1^T \\ \boldsymbol{\phi}_2^T \\ \vdots \\ \boldsymbol{\phi}_M^T \end{bmatrix} \begin{bmatrix} \boldsymbol{\phi}_1 & \boldsymbol{\phi}_2 & \cdots & \boldsymbol{\phi}_M \end{bmatrix} = \begin{bmatrix} \boldsymbol{\phi}_1^T \boldsymbol{\phi}_1 & \boldsymbol{\phi}_1^T \boldsymbol{\phi}_2 & \cdots & \boldsymbol{\phi}_1^T \boldsymbol{\phi}_M \\ \boldsymbol{\phi}_2^T \boldsymbol{\phi}_1 & \boldsymbol{\phi}_2^T \boldsymbol{\phi}_2 & \cdots & \boldsymbol{\phi}_2^T \boldsymbol{\phi}_M \\ \vdots & \vdots & \ddots & \vdots \\ \boldsymbol{\phi}_M^T \boldsymbol{\phi}_1 & \boldsymbol{\phi}_M^T \boldsymbol{\phi}_2 & \cdots & \boldsymbol{\phi}_M^T \boldsymbol{\phi}_M \end{bmatrix} \begin{bmatrix} 1 & 0 & \cdots & 0 \\ 0 & 1 & \cdots & 0 \\ \vdots & \vdots & \ddots & \vdots \\ 0 & 0 & \cdots & 1 \end{bmatrix},$$

and

$$\Phi^T \mathbf{A} \Phi = \begin{bmatrix} \boldsymbol{\phi}_1^T \mathbf{A} \boldsymbol{\phi}_1 & \boldsymbol{\phi}_1^T \mathbf{A} \boldsymbol{\phi}_2 & \cdots & \boldsymbol{\phi}_1^T \mathbf{A} \boldsymbol{\phi}_M \\ \boldsymbol{\phi}_2^T \mathbf{A} \boldsymbol{\phi}_1 & \boldsymbol{\phi}_2^T \mathbf{A} \boldsymbol{\phi}_2 & \cdots & \boldsymbol{\phi}_2^T \mathbf{A} \boldsymbol{\phi}_M \\ \vdots & \vdots & \ddots & \vdots \\ \boldsymbol{\phi}_M^T \mathbf{A} \boldsymbol{\phi}_1 & \boldsymbol{\phi}_M^T \mathbf{A} \boldsymbol{\phi}_2 & \cdots & \boldsymbol{\phi}_M^T \mathbf{A} \boldsymbol{\phi}_M \end{bmatrix} = \begin{bmatrix} \lambda_1 & 0 & \cdots & 0 \\ 0 & \lambda_2 & \cdots & 0 \\ \vdots & \vdots & \ddots & \vdots \\ 0 & 0 & \cdots & \lambda_M \end{bmatrix},$$

using the analysis already presented. If the eigenvalues are not distinct, it is possible to show that the dimension of any eigenspace is finite and has a basis of mutually perpendicular eigenvectors. \square

8.2.2 Jordan Canonical Form

The spectral theory for self-adjoint matrices in the last section provides a way to diagonalize a self-adjoint matrix in terms of its eigenvectors. As already noted, not all $M \times M$ matrices have a full set of M linearly independent eigenvectors. A nearly diagonal factorization that is qualitatively similar to the spectral factorization can be achieved by employing the *Jordan Canonical Form* of a general $M \times M$ matrix. This factorization is particularly useful for the study of the stability of linear systems, as studied in Chapter (6) utilizing feedback linearization to compensate for non-linear terms.

Theorem 8.12. Let \mathbf{A} be an $M \times M$ matrix. There exists a matrix \mathbf{P} such that \mathbf{A} has the block diagonal decomposition

$$\mathbf{A} = \mathbf{P} \begin{bmatrix} \mathbf{J}_1 & \mathbf{0} & \cdots & \mathbf{0} \\ \mathbf{0} & \mathbf{J}_2 & \cdots & \mathbf{0} \\ \vdots & \vdots & \ddots & \vdots \\ \mathbf{0} & \mathbf{0} & \cdots & \mathbf{J}_K \end{bmatrix} \mathbf{P}^{-1},$$

where each $n_k \times n_k$ block \mathbf{J}_k for $k = 1, \dots, K$ has the form

$$\mathbf{J}_k = \begin{bmatrix} \lambda_k & 1 & 0 & \cdots & 0 \\ 0 & \lambda_k & 1 & \cdots & 0 \\ 0 & 0 & \lambda_k & \cdots & 0 \\ \vdots & \vdots & \vdots & \ddots & \vdots \\ 0 & 0 & 0 & \cdots & \lambda_k \end{bmatrix}.$$

The scalar λ_k is the k^{th} eigenvalue and has multiplicity n_k .

Note that the columns of the matrix \mathbf{P} , in contrast to the matrix Φ for the self-adjoint case, is not necessarily constructed from the *eigenvectors* of the matrix \mathbf{A} . The columns of \mathbf{P} are sometimes denoted the *generalized eigenvectors* of the matrix \mathbf{A} . The interested reader is referred to [18] for a discussion.

8.3 Gauss Transformations and LU Factorizations

It is often the case in the study of the dynamics of robotic systems that a matrix system of equations that have the form

$$\mathbf{Ax} = \mathbf{b} \quad (8.3.1)$$

must be solved, where \mathbf{A} is an $M \times M$ matrix, \mathbf{x} is an $M \times 1$ vector of unknowns and \mathbf{b} is a known $M \times 1$ vector. In some cases, these equations must be solved symbolically, while in other cases a numerical solution suffices. Several conditions in Sections (8.1.1), (8.1.3) and (8.1.4) guarantee the existence and uniqueness of solutions to systems of equations having the form shown in Equation (8.3.1). In particular, it has been shown that if there is a unique solution \mathbf{x} to Equation (8.3.4), the solution of these equations is equivalent to the calculation of the inverse \mathbf{A}^{-1} of the matrix \mathbf{A} . The proof of Theorem (8.7) following Theorem (8.9) shows that the *Singular Value Decomposition* can be used to calculate the inverse of a matrix when it exists. Unfortunately, the *Singular Value Decomposition* is computationally expensive compared to several alternative numerical algorithms; thus, other methods are often preferred in robotic system applications. This section will discuss one such choice that uses sequences of Gauss transformations to derive the inverse of a matrix \mathbf{A} , or equivalently, to solve equations having the form shown in Equation (8.3.1).

The strategy underlying the use of Gauss transformations to solve Equation (8.3.1) is easy to describe. Suppose two sequences can be found such that

$$\mathbf{L}_{i,j} \quad j = 1, \dots, M-1, \quad i = j+1, \dots, M$$

and

$$\mathbf{U}_{i,j} \quad i = 1, \dots, M-1, \quad j = i+1, \dots, M$$

of $M \times M$ invertible matrices such that premultiplication of \mathbf{A} by the product of the $\mathbf{L}_{i,j}$ and postmultiplication of \mathbf{A} by the product of the $\mathbf{U}_{i,j}$ is equal to the identity matrix, as in the equation

$$\mathbb{I} = \mathbf{L}_{N,N-1} \mathbf{L}_{N,N-2} \cdots \mathbf{L}_{4,1} \mathbf{L}_{3,1} \mathbf{L}_{2,1} \mathbf{A} \mathbf{U}_{N-1,N} \mathbf{U}_{N-2,N} \mathbf{U}_{1,3} \mathbf{U}_{1,2}. \quad (8.3.2)$$

If this is the case, the inverse of the matrix \mathbf{A} can be written as

$$\mathbf{A} = \mathbf{L}_{2,1}^{-1} \mathbf{L}_{3,1}^{-1} \cdots \mathbf{L}_{N-1,N-2}^{-1} \mathbf{L}_{N,N-1}^{-1} \mathbf{U}_{1,2}^{-1} \mathbf{U}_{1,3}^{-1} \cdots \mathbf{U}_{N-2,N}^{-1} \mathbf{U}_{N-1,N}^{-1}. \quad (8.3.3)$$

Note that it is critical in this construction that each of the matrices $\mathbf{L}_{i,j}$ or $\mathbf{U}_{i,j}$ in the sequence is invertible for each i and j . The principle conclusion discussed in this section is that such a product can be constructed provided certain *pivot elements* of the matrix \mathbf{A} are not equal to zero. The construction is carried out using *Gauss transformations*.

A *Gauss transformation* is a matrix that is equal to the identity matrix except for a single off-diagonal entry. Such a matrix has either the lower triangular form shown

in Figure (8.1) where l_{ij} is the off-diagonal entry located at row i and column j , or it has the upper triangular form shown in Figure (8.2) where u_{ij} is the off-diagonal entry located at row i and column j .

$$\mathbf{L}_{i,j} = \begin{bmatrix} 1 & & & \\ & 1 & & \\ \vdots & \ddots & & \\ l_{ij} & \cdots & 1 & \\ \uparrow & & & \\ & & & 1 \end{bmatrix} \quad \begin{array}{l} \text{row } i \\ \text{column } j \end{array}$$

Fig. 8.1: Gauss Transformation, Lower Triangular Form

$$\mathbf{U}_{i,j} = \begin{bmatrix} 1 & & & u_{ij} & \\ & 1 & \cdots & \vdots & \\ & \ddots & \ddots & & \\ & & 1 & & \\ \uparrow & & & & 1 \end{bmatrix} \quad \begin{array}{l} \text{row } i \\ \text{column } j \end{array}$$

Fig. 8.2: Gauss Transformation, Upper Triangular Form

It is clear that each of these matrices has an inverse, and it is simple to calculate the inverse as

$$\mathbf{L}_{ij}^{-1} = \begin{bmatrix} 1 & & & \\ & 1 & & \\ \vdots & \ddots & & \\ -l_{ij} & \cdots & 1 & \\ & & & 1 \end{bmatrix}$$

or

$$\mathbf{U}_{ij}^{-1} = \begin{bmatrix} 1 & & & -u_{ij} & \\ & 1 & \cdots & \vdots & \\ & \ddots & \ddots & & \\ & & 1 & & \\ & & & & 1 \end{bmatrix}$$

A *Gauss transformation* has several properties that can be attributed to its highly structured form that are crucial in applications. Lower triangular matrices $\mathbf{L}_{i,j}$ will be discussed first and several properties of these matrices will be derived. It will be shown how to select such a matrix so that premultiplication of \mathbf{A} by the matrix will zero out a specific entry in \mathbf{A} below the main diagonal. If a matrix \mathbf{A} is premultiplied by a judiciously selected sequence of such matrices, it is possible to make all of the entries below the main diagonal of the resulting matrix equal to zero. In other words, the product

$$\mathbf{L}_{N,N-1}\mathbf{L}_{N,N-2}\cdots\mathbf{L}_{4,1}\mathbf{L}_{3,1}\mathbf{L}_{2,1}\mathbf{A}$$

can be made upper triangular.

Then, it will be argued that similar constructions based on the upper triangular matrices $\mathbf{U}_{i,j}$ can be achieved. Postmultiplication of the matrix \mathbf{A} by a carefully constructed $\mathbf{U}_{i,j}$ can be made to zero out a specific entry above the main diagonal. Postmultiplication of \mathbf{A} by a suitably crafted collection of these matrices will result in all entries above the main diagonal set equal to zero. In other words, the product

$$\mathbf{A}\mathbf{U}_{N-1,N}\mathbf{U}_{N-2,N}\mathbf{U}_{1,3}\mathbf{U}_{1,2}$$

can be made lower triangular.

Finally, both types of matrices will be used together to achieve the **LU Decomposition** of a matrix \mathbf{A} into the product of a lower triangular and an upper triangular matrix. Consider first the *Gauss transformation* $\mathbf{L}_{i,j}$. It is crucial to the understanding of Gauss transforms to observe that premultiplication of a matrix \mathbf{A} by $\mathbf{L}_{i,j}$ only changes row i and leaves the rest of the matrix \mathbf{A} unchanged. In fact, it is straightforward to observe that the only terms that are modified by premultiplication by $\mathbf{L}_{i,j}$ are denoted by b_{ik} for $k = 1, \dots, M$ in the product below

$$\mathbf{L}_{i,j}\mathbf{A} = \begin{bmatrix} 1 & & & a_{11} & \cdots & a_{1M} \\ & 1 & & \vdots & & \vdots \\ & & 1 & & & \\ l_{ij} & & & a_{M1} & \cdots & a_M \\ & & 1 & & & \end{bmatrix}, \quad (8.3.4)$$

$$= \begin{bmatrix} a_{11} & a_{12} & \cdots & & a_{1M} \\ \vdots & & & & \\ b_{i1} & b_{i2} & \cdots & b_{ij} & b_{i,j+1} \cdots b_{i,M-1} & b_{i,M} \\ \vdots & & & & & \\ a_{M,1} & a_{M,2} & \cdots & \cdots & & a_{M,M} \end{bmatrix}. \quad (8.3.5)$$

Each newly modified term in row i denoted b_{ik} in Equation (8.3.4) is given by

$$b_{ik} = l_{ij}a_{jk} + a_{ik} \quad (8.3.6)$$

for $k = 1, \dots, M$. Consider this equation for the choice of $k = j$,

$$b_{ij} = l_{ij}a_{jj} + a_{ij}.$$

If the diagonal term $a_{jj} \neq 0$, it is possible to choose l_{ij} so that the Gauss transformation \mathbf{L}_{ij} introduces a zero at the entry (i, j) of the matrix \mathbf{A} . The condition $b_{ij} = 0$ can be enforced by choosing $l_{ij} = \frac{-a_{ij}}{a_{jj}}$ since

$$b_{ij} = l_{ij}a_{jj} + a_{ij} = \left(\frac{-a_{ij}}{a_{jj}} \right) a_{jj} + a_{ij} = 0.$$

The diagonal entry a_{jj} is known as the *pivot term*, and the success of this strategy relies on the fact that a_{jj} is not equal to zero. The observations that premultiplication by \mathbf{L}_{ij} affects only row i , and that l_{ij} can be chosen so that $b_{ij} = 0$, leads to a general procedure for constructing a sequence of matrices \mathbf{L}_{ij} that drives the matrix \mathbf{A} to a lower triangular form. The matrices \mathbf{L}_{ij} can be successively chosen to zero out entries while progressing down each column below the main diagonal. That is, entries are zeroed out as depicted in Figure (8.3). It is left as an exercise to show that

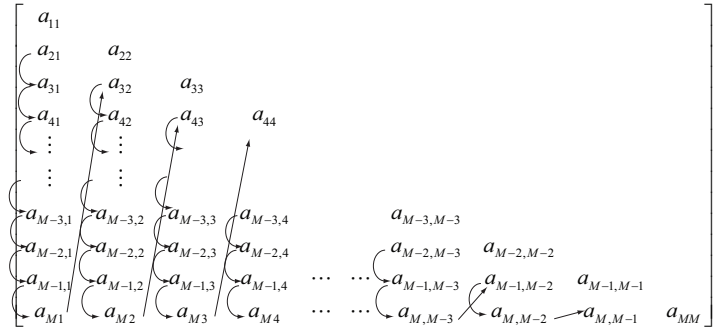


Fig. 8.3: Progression of Zeros Below Diagonal

this algorithm is guaranteed to zero out all the sub-diagonal entries of the matrix \mathbf{A} , provided that the *pivot elements* a_{jj} for $j = 1, \dots, M$ are non-zero. These steps are summarized in Figure (8.4).

- (1) Loop for all the columns except the last: $j = 1, \dots, (M - 1)$
- (2) Loop for all the rows below the diagonal: $i = (j + 1), \dots, M$
- (3) Calculate the Gauss transform that will zero element i, j : $l_{ij} = \frac{-a_{ij}}{a_{jj}}$

Fig. 8.4: Gauss Transformations to Zero Subdiagonal Entries of \mathbf{A}

All of the observations made thus far regarding the lower triangular Gauss transformations \mathbf{L}_{ij} can be extended to the upper triangular Gauss transformations \mathbf{U}_{ij}

with some minor modifications. Postmultiplication of \mathbf{A} by \mathbf{U}_{ij} modifies only the entries of the column j . Equation (8.3.7) depicts the elements b_{kj} for rows $k = 1, \dots, M$ in column j that are modified when we compute the product \mathbf{AU}_{ij}

$$\mathbf{A} = \begin{bmatrix} a_{11} & \cdots & a_{1M} \\ \vdots & & \vdots \\ a_{1M} & \cdots & a_{MM} \end{bmatrix} \begin{bmatrix} 1 & & & \\ & 1 & u_{ij} & \\ & & 1 & \\ & & & 1 \end{bmatrix} \quad (8.3.7)$$

$$= \begin{bmatrix} a_{11} & a_{12} & \cdots & a_{1,j-1} & b_{1,j} & a_{1,j+1} & \cdots & a_{1M} \\ a_{21} & a_{22} & & a_{2,j-1} & b_{2,j} & a_{2,j+1} & & a_{2,M} \\ \vdots & \vdots & & \vdots & \vdots & \vdots & & \vdots \\ a_{M,1} & a_{M,2} & & a_{M,j-1} & b_{M,j} & a_{M,j+1} & \cdots & a_{M,M} \end{bmatrix} \quad (8.3.8)$$

As in the case of \mathbf{L}_{ij} , it is possible to introduce a zero at location i, j provided that the *pivot term* a_{jj} on the diagonal is not zero. Each term b_{kj} for rows $k = 1, \dots, M$ in column j satisfies the equation

$$b_{kj} = a_{ki}u_{ij} + a_{kj}.$$

For the specific choice of $k = i$,

$$b_{ij} = a_{ii}u_{ij} + a_{ij}. \quad (8.3.9)$$

If u_{ij} is defined as $-a_{ij}/a_{ii}$,

$$b_{ij} = u_{ij}a_{ij} + a_{ij} = \frac{-a_{ij}}{a_{ii}}a_{ii} + a_{ij} = 0. \quad (8.3.10)$$

Analogous to the strategy summarized in Figure (8.4), the sequence of upper triangular Gauss transformations can be used to make the product

$$\mathbf{AU}_{N-1,N}\mathbf{U}_{N-2,N} \cdots \mathbf{U}_{1,3}\mathbf{U}_{1,2}, \quad (8.3.11)$$

lower triangular. Figure (8.6) summarizes the sequence of entries that are successively set to zero in this strategy

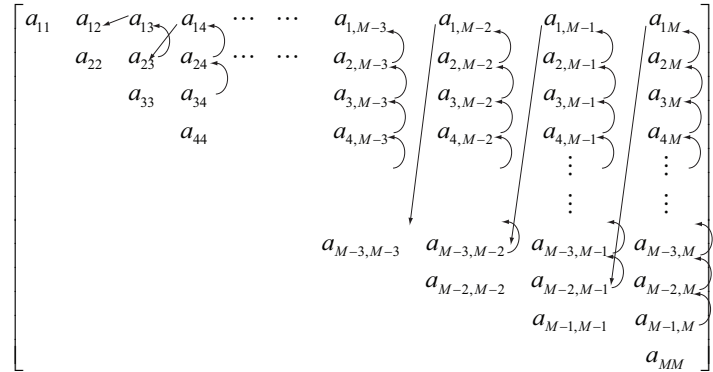


Fig. 8.5: Progression of Zeros Above Diagonal

- (1) Loop backwards for all the columns except the first: $j = M, \dots, 3, 2$
 - (2) Loop for all the rows above the diagonal: $i = (j-1), \dots, 2, 1$
 - (3) Calculate the Gauss transform that will zero element i, j : $u_{ij} = \frac{-a_{ij}}{a_{ii}}$

Fig. 8.6: Gauss Transformations for Upper Triangular Factorization of A

References

1. ALCIATORE, D. G., AND HISTAND, M. B. *Introduction to Mechatronics and Measurement Systems*. McGraw-Hill, New York, 2002.
2. ASCHER, U. M., AND PETZOLD, L. R. *Computer Methods for Ordinary Differential Equations and Differential-Algebraic Equations*. Society for Industrial and Applied Mathematics, 1998.
3. B. SICILIANO, L. SCIavicco, L. V., AND ORIOLO, G. *Robotics: Modeling, Planning and Control*. Springer Verlag, London, 2009.
4. BEN-TZVI, P. Experimental validation and field performance metrics of a hybrid mobile robot mechanism. *Journal of Field Robotics* 27, 3 (May 2010), 250–267.
5. BEN-TZVI, P., GOLDENBERG, A. A., AND ZU, J. W. Design and analysis of a hybrid mobile robot mechanism with compounded locomotion and manipulation capability. *Transactions of the ASME, Journal of Mechanical Design* 130, 7 (July 2008), 1–13.
6. BEN-TZVI, P., GOLDENBERG, A. A., AND ZU, J. W. Articulated hybrid mobile robot mechanism with compounded mobility and manipulation and on-board wireless sensor/actuator control interfaces. *Mechatronics Journal* 20, 6 (September 2010), 627–639.
7. BISHOP, R. *Tensor Analysis on Manifolds*. Dover Publications, 1980.
8. BOLTON, W. *Mechatronics: Electronic Control Systems in Mechanical and Electrical engineering*. Pearson Education Limited, United Kingdom, 2015.
9. BOWEN, R. M. *Introduction to Vectors and Tensors*. Plenum Press, New York, 1976.
10. BULLO, F., AND LEWIS, A. *Geometric Control of Mechanical Systems*. Springer-Verlag New York, 2005.
11. CETYINKUNT, S. *Mechatronics*. John Wiley & Sons, Inc., 2007.
12. CRAIG, R. R., AND KURDILA, A. J. *Fundamentals of Structural Dynamics*. John Wiley and Sons, 2006.
13. FAITTORINI, H. *Infinite Dimensional Optimization and Control Theory*. Cambridge University Press, 1999.
14. FEATHERSTONE, R. *Rigid Body Dynamics Algorithms*. Springer, 2008.
15. F.L. LEWIS, D. D., AND ABDALLAH, C. *Robot Manipulator Control: Theory and Practice*. Marcel Dekker, Inc., 1993.
16. G. RODRIGUEZ, A. J., AND KREUTZ-DELGADO, K. Spatial operator algebra for multibody system dynamics. *Journal of the Astronautical Sciences* 40, 1 (1992), 27–50.
17. GINSBERG, J. *Engineering Dynamics*. Cambridge University Press, 2008.
18. GOLUB, G. H., AND LOAN, C. F. V. *Matrix Computations*. Johns Hopkins University Press, 1996.
19. GUCKENHEIMER, J., AND HOLMES, P. *Nonlinear Oscillations, Dynamical Systems and Bifurcations of Vector Fields*. Springer Verlag, New York, 1983.
20. HERBERT GOLDSTEIN, C. P., AND SAFKO, J. *Classical Mechanics*. Addison Wesley, 2002.
21. ISIDORI, A. *Nonlinear Control Systems*. Springer Verlag, New York, 1995.
22. JAIN, A. Spatially recursive dynamics for flexible manipulators. In *Proceedings of the IEEE International Conference on Robotics and Automation* (1991), vol. 3, IEEE, Piscataway, N.J., United States, pp. 2350–2355.
23. JAIN, A. Unified formulation of dynamics for serial rigid multibody systems. *Journal of Guidance, Control and Dynamics* 14, 3 (May-June 1991), 531–542.
24. JAIN, A. *Robot and Multibody Dynamics: Analysis and Algorithms*. Springer, New York, 2011.
25. JAIN, A., AND RODRIGUEZ, G. Diagonalized lagrangian robot dynamics. *IEEE Transactions on Robotics and Automation* 11, 4 (1995), 571–584.
26. JAIN, A., AND RODRIGUEZ, G. Computational robot dynamics using spatial operators. In *Proceedings of the IEEE International Conference on Robotics and Automation* (2000), vol. 1, IEEE, Piscataway, N.J., United States, pp. 843–849.
27. K.E. BRENAN, S.L. CAMPBELL, L. P. *Numerical Solution of Initial-Value Problems in Differential-Algebraic Equations*. North-Holland Publishing Company, 1989.
28. KHALIL, H. *Nonlinear Systems*. Prentice-Hall, 2002.
29. KURDILA, A. J., AND ZABARANKIN, M. *Convex Functional Analysis*. Birkhauser Verlag, 2005.

30. M. SONG, S. H., AND VIDYASAGAR, M. *Robot Modeling and Control*. John Wiley & Sons, Inc., 2006.
31. MEIROVITCH, L. *Methods of Analytical Dynamics*. McGraw-Hill, 1970.
32. MEYN, S. *Markov Chains and Stochastic Stability*. Cambridge University Press, 2009.
33. NIJMEIJER, H., AND VAN DER SCHAFT, A. *Nonlinear Dynamical Control Systems*. Springer New York, 1990.
34. ODEN, J. T. *Applied Functional Analysis*. Prentice-Hall, 1979.
35. POLAK, E. *Optimization: Algorithms and Consistent Approximations*. Springer, 1997.
36. RICHARD M. MURRAY, Z. L., AND SAstry, S. S. *A Mathematical Introduction to Robotic Manipulation*. CRC Press, Boca Raton, 1994.
37. RODRIGUEZ, G. Kalman filtering, smoothing, and recursive robot arm forward and inverse dynamics. *IEEE Journal of Robotics and Automation* 3, 6 (1987), 624–639.
38. RODRIGUEZ, G. Spatially random models, estimation theory and robot arm dynamics. In *Proceedings of the IEEE International Symposium on Intelligent Control* (1987), U. IEEE, New York, Ed., pp. 27–30.
39. RODRIGUEZ, G., AND KREUTZ-DELGADO, K. Spatial operator factorization and inversion of the manipulator mass matrix. *IEEE Transactions on Robotics and Automation* 8, 1 (1992), 65–76.
40. SAPERSTONE, S. *Semidynamical Systems in Infinite Dimensional Spaces*. Springer Verlag, New York, 1981.
41. SAstry, S. S. *Nonlinear Systems: Analysis, Stability, and Control*. Springer New York, 1999.
42. SAstry, S. S., AND BODSON, M. *Adaptive Control: Stability, Convergence, and Robustness*. Prentice-Hall, 1989.
43. TROUTMAN, J. L. *Variational Calculus and Optimal Control*. Springer Verlag, New York, 1996.
44. VIDYASAGAR, M. *Nonlinear Systems Analysis*. Prentice-Hall, 1993.
45. WITTENBURG, J. *Dynamics of Multibody Systems*. North-Holland Publishing Company, 1980.
46. WITTENBURG, J. *Dynamics of Multibody Systems*. Springer Verlag, New York, 2008.
47. ZEIDLER, E. *Nonlinear Functional Analysis and its Applications III: Variational Methods and Optimization*. Springer, 1984.